53BP1 and double-strand break repair pathway choice in cancer

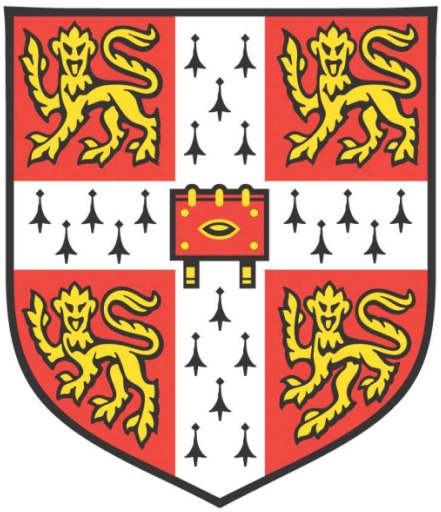

Harveer S. Dev

Gurdon Institute

University of Cambridge

This dissertation is submitted for the degree of Doctor of Philosophy

St John's College

June 2019

DECLARATION

This dissertation is the result of my own work and includes nothing, which is the outcome of work done in collaboration except where specifically indicated in the text. It has not been previously submitted, in part or whole, to any university or institution for any degree, diploma, or other qualification.

In accordance with the Biology Degree Committee guidelines, this thesis does not exceed 60,000 words.

Harveer S. Dev

June 2019

ABSTRACT 53BP1 AND DOUBLE-STRAND BREAK REPAIR PATHWAY CHOICE IN CANCER.

HARVEER S. DEV.

The cellular response to DNA double-strand breaks (DSB) is principally the result of two competing repair pathways. The Tumour Protein P53 Binding Protein 1 (TP53BP1) gene product plays a central role in DSB repair pathway choice, promoting non-homologous end-joining (NHEJ) and counteracting homologous recombination (HR). As with all DNA damage response (DDR) proteins, cell-cycle regulation of 53BP1 is critical to its function. The inappropriate activity of 53BP1 in mitosis, during which most of the DDR is inactivated to preserve genome stability, has been shown to have adverse effects on cell division that are characteristic of cancers. We explored the consequences of replication stress, associated with oncogene activity, and the impact of aberrantly active 53BP1 in mitosis. This work reveals interference with normal mitotic mechanisms for detecting and resolving stalled replication intermediates; most evidently manifest as reduced mitotic DNA synthesis (MiDAS), and increased accumulation of acentric micronuclei and G1 nuclear bodies. We propose that the functional sequestration of TOPBP1 may be responsible for these chromosomal mis-segregation defects.

The mechanism by which 53BP1 (together with RIF1 and MAD2L2) promote NHEJ remains elusive. Genome instability in HR-defective cancers, principally those harbouring a mutation in BRCA1, can be rescued by the concomitant loss of either 53BP1, RIF1 or MAD2L2. This phenomenon has relevance for the development of PARP (Poly(ADP-ribose) polymerase) inhibitor resistance, now being used in BRCA1-deficient breast, ovarian and prostate cancers based on the principle of 'synthetic lethality'. As part of a search for other resistance mechanisms, we identified the shieldin complex (SHLD1/C20orf196 and SHLD2/FAM35A) that when lost suppressed PARP inhibitor sensitivity in BRCA1-deficient cancer cells. We demonstrate that SHLD1/2 represent the terminal end-effectors of the 53BP1-RIF1-MAD2L2 axis, supporting NHEJ activity. We identified three OB-fold domains in SHLD2/FAM35A, that bind single-stranded DNA and are necessary for NHEJ. Loss of SHLD1 or SHLD2 (SHLD1/2)

caused a hyper-resection phenotype, and which, in the absence of BRCA1 was associated with rescuing RAD51 loading. Downregulation in SHLD1/2 expression was also associated with intrinsic and acquired resistance across a panel of BRCA1-deficient patient-derived xenograft models. Promisingly, this mechanism may impart an acquired vulnerability to cisplatin or radiotherapy. Thus, we have characterised a critical component of the 53BP1 axis which is deterministic in repair pathway choice and carries implications for the treatment of cancers.

For Kiran and Dilan

"What can be asserted without evidence can also be dismissed without evidence"

Christopher Hitchens

Slate Magazine (20 October 2003)

"Science is a bit like the joke about the drunk who is looking under a lamppost for a key that he has lost on the other side of the street, because that's where the light is. It has no other choice."

Noam Chomsky

Letter to Robert F. Barsky (14 June 1993)

"We will never know until we try, so go and do the fucking experiment"

Professor Gerard Evan

Gurdon Institute Anniversary Lecture (circa early 2000's)

ACKNOWLEDGEMENTS

I owe a huge debt of gratitude to many individuals and organisations, both in my personal and professional life, who have helped me to complete this degree to the best of my ability over the last four years.

Thanks in the first instance, to the National Institute for Health Research (NIHR), and my former mentor Emeritus Professor David Neal, for supporting me in my early academic urology career and stimulating my interest in cancer research. I would also like to thank the Wellcome Trust, and the Cambridge PhD Program for clinicians programme director Krish Chatterjee, for allowing me to join a highly supportive doctoral programme which has facilitated this research.

I am grateful to the Royal College of Surgeons, and the US-UK Fulbright Commission for awarding me with funding to complete the first year of my PhD at the Dana-Farber Cancer Institute (Boston, USA) working in the laboratory of Harvard University Professor Dipanjan Chowdhury. Dipanjan was incredibly generous in accepting me into his laboratory between 2015 and 2016, providing a stimulating setting in which to build on my knowledge of DNA repair biology, and develop technical capabilities in his laboratory. I would like to thank Xiao-Feng Zheng and other members of the Chowdhury group, as well as Neil Umbreit and David Pellman, for their collaboration during this time. Dipanjan and his department played a fundamental role in establishing this foundation for my research, and I am appreciative of his support and friendship during this personally and professionally defining year in the USA.

I have spent the subsequent three years up until 2019 in the group of Steve Jackson, to whom I must also declare my sincere appreciation. During this time I have had the privilege of working with many wonderful individuals in the group, engaging in exciting scientific discussion and discovery. It has been a tremendous opportunity to have had the chance to work alongside so many enthusiastic and experienced scientists and support staff, and it has been a highlight of my career to date. This is in large part, a credit to my supervisor Steve, who not only supported all of my scientific ideas and project plans (no matter how ambitious!), but managed to create this positive working environment which has made attending the laboratory each day a pleasure

rather than a chore. I will be forever indebted for his support, and I am delighted to have been able to call him a supervisor, mentor and friend.

I am also grateful to the many lab members who worked with me to explore the role of shieldin in DNA repair. This was an exciting (and demanding) time for us, but we benefitted from a unity of purpose that helped us to achieve our goals. Particular thanks to Yaron Galanty, Julia Coates and Matylda Sczaniecka-Clift for their efforts and patience, with my bold experimental plans and for tolerating somewhat unorthodox working practices. It was a pleasure to supervise Jonathan Lam (BBSRC PhD student) during his placement at the lab. I would like to thank Will Chiang and Mareike Herzog for their initial efforts with performing and analysing the CRISPR-Cas9 screen, which allowed us to embark upon this exciting work. Inigo Ayesteran and John Thomas have since been integral to our bioinformatic assessments and I thank you both for your willingness to help me understand these efforts. Muku Demir, Linda Baskcomb and Helen Reed, together with our core support staff at the Gurdon Institute have provided essential assistance to make all these scientific efforts a success. I would also like to thank Kate-Dry for her critical reading of far too many documents to mention. Thanks to Gabriel Balmus and the Sanger Institute for their contributions, as well as Rimma Belotserkovskaya, Francisco Muñoz Martínez and Israel Salguero for their input and helpful discussions over the years. I am also grateful to Luca Pellegrini and Qian Wu for their insights and efforts. The shieldin project received the input of various external collaborators, and I thank Ludovic Deriano (Institut Pasteur, Paris), Jacqueline Jacobs (NCI, Amsterdam), Petra Beli (IMB, Mainz), Mark O'Connor (AstraZeneca, Cambridge), Carlos Caldas (CRUK CI, Cambridge) and their teams.

It has been a joy to work alongside PhD colleagues Rebecca Lloyd, Ramsay Bowden and Domenic Pilger. We have shared many a late evening together in tissue culture, or at the microscope, and the pleasure of stress-testing scientific hypothesis has only been surpassed by the good humour and comradery that we have developed over the years.

Thanks to St John's College Cambridge for their collegiate support, the Department of Biochemistry, and to Julian Sale (Cambridge) and Madalena Tarsounas (Oxford) for examining my dissertation.

None of this would have been possible without the familial support of my wife Jas, mum, dad and brother, especially for their tolerance and understanding of the occasional(/frequent) disruptive scheduling of lab-based experiments. The long weekdays and weekends of work, have however, been made infinitely more tolerable by a continuous stream of videos of Kiran and Dilan, and the excitement of coming home to see them both. Boys; I look forward to being able to share with you some of the contents of this thesis, and my experiences of the last four years when you are a little older.

Finally, I am grateful to the NHS and our patients, who support these projects, and offer the freedom for academic clinicians like myself to take time out of training to gain essential research skills and experience. On return to practice, I hope that this will enable me to positively contribute to cutting-edge translational cancer research, and ultimately improve treatments and patient outcomes.

CONTENTS

Abstract *iii*

Contents *x*

1. Chapter 1 Introduction 1

1.1. The DNA damage response 1

1.1.1. DNA damage 1

1.1.2. Damage detection and single-strand break repair 2

1.2. Double strand break repair pathways 3

1.2.1. Homologous recombination 4

1.2.2. Non-homologous end-joining 7

1.2.3. DSB repair pathway choice 12

1.3. DDR in mitosis 14

1.3.1. DSB repair is attenuated in mitosis 14

1.3.2. Ectopic recruitment of 53BP1 to chromatin can generate mitotic defects 16

1.3.3. Replication stress induces mitotic defects in the absence of recombination factors 16

1.4. Targeting the DDR in cancer 20

1.4.1. DDR dysfunction in disease 20

1.4.2. Targeting DDR in the clinic 21

1.4.3. PARP inhibitors and resistance 22

2. Chapter 2 Material & Methods 28

2.1. Nucleic Acid Methods 28

2.1.1. Guide RNA design and cloning methods 28

2.1.2. Polymerase chain reaction (PCR), agarose gel electrophoresis and site-directed mutagenesis 30

2.1.3. Reverse transcription – quantitative polymerase chain reaction (RT-qPCR) 31

2.2. Protein Methods 32

2.2.1. Cell lysis and Immunoblotting 32

2.2.2. Immunoprecipitation 33

2.2.3. In-vitro GST pull-down 34

2.2.4. DNA oligo pull-downs 34

2.2.5. Mass spectrometric analysis 35

2.3. Mammalian cell culture techniques 35
2.3.1. Cell culture, propagation and cell stock freezing 35
2.3.2. Plasmid transfection and electroporation in mammalian cells 36
2.3.3. Performing siRNA mediated knockdowns 37
2.3.4. Generating stable cell lines 37
2.3.5. Generating knockout cell lines 38
2.3.6. Cell viability assays 39
2.3.7. DNA damaging agents and laser micro-irradiation 40
2.4. Mammalian cell analysis methods 40
2.4.1. Immunofluorescence 40
2.4.2. Flow cytometry 42
2.4.3. Cellular reporter assays 43
2.5. CRISPR-Cas9 screen 44
2.6. Statistics and analyses 45
2.6.1. Reproducibility of experiments. 45
3. Chapter 3 Results: Genome instability and 53BP1 in mitosis 46
3.1. Introduction 46
3.2. Results 48
3.2.1. 53BP1^{AA} induces micronuclei formation with aphidicolin treatment 48
3.2.2. Aphidocolin induced G1 nuclear bodies with mitotic 53BP1^{AA} 50
3.2.3. 53BP1^{AA} impairs unscheduled DNA synthesis in mitosis. 52
3.2.4. 53BP1^{AA} impairs unscheduled DNA synthesis in mitosis following reduced replication origin firing 53
3.2.5. 53BP1^{AA} interacts with TOPBP1 in a replication-stress dependent manner in mitosis. 54
3.3. Discussion 56
4. Chapter 4 Results: Shieldin interacts with 53BP1 to promote NHEJ and counter HR in BRCA1-deficient cells 60
4.1. Introduction 60
4.2. Results 61
4.2.1. CRISPR-Cas9 screens identify suppressors of PARP-inhibitor sensitivity in BRCA1-mutant cells. 61
4.2.2. FAM35A and C20orf196 domains, interactions and IRIF formation. 65
4.2.3. FAM35A and C20orf196 promote NHEJ and immunoglobulin class-switch recombination. 75

4.2.4. FAM35A and C20orf196 promote telomere-mediated fusions and limit DNA end-resection. ..76
4.2.5. FAM35A OB folds mediate ssDNA interaction and is required for IR resistance.....79
4.2.6. FAM35A or C20orf196 loss restores HR in BRCA1-deficient cells. 83
4.2.7. FAM35A or C20orf196 loss correlates with PARP inhibitor resistance in cancers.....91

4.3. Discussion 97

5. Future directions 106

6. Supplementary information 109

6.1. List of figures 109

6.2. Commonly used abbreviations 115

6.3. Antibodies, plasmids, primers, siRNA, gRNA and knockout sequencing..... 116

6.4. Control blots of siRNA used in study 118

6.5. Top 1000 gene enrichments from CRISPR-Cas9 screen 119

6.6. FAM35A SILAC interactomes 131

6.7. C20orf196 SILAC interactomes 162

6.8. Paper: Shieldin complex promotes DNA end-joining and counters homologous recombination in BRCA1-null cells (2018) 193

7. References.....230

1. Chapter 1 Introduction

1.1. The DNA damage response

Cells are under constant exposure to endogenous and exogenous sources of DNA damage which may compromise genome stability. Accurate replication and genome maintenance are essential for cellular homeostasis, faithful transmission of genetic material, and organism survival. The complex interconnected signal transduction pathways that cells mount in response to DNA damage are known as the DNA damage response (DDR). This network of sensors, mediators and effectors is necessary for the effective remodelling and repair of DNA, along with checkpoint activation to stall cell cycle progression and facilitate these processes. The DDR also involves chromatin remodelling, transcriptional changes, and interactions with DNA replication machinery, at both a local and global level (Blackford and Jackson, 2017). The recruitment and activation of various DDR factors is temporally and spatially regulated in a lesion-specific manner. This ensures the safe coordinated action of a plethora of enzymatic activities, which if left unchecked could themselves generate cytotoxic DNA damage (Ciccia and Elledge, 2010). Furthermore, the dysregulation of these pathways can have a profound impact on human health and disease.

1.1.1. DNA damage

DNA damage can originate from sources endogenous and exogenous to the cell. Internal sources of DNA damage are varied, and can include spontaneous nucleotide misincorporation or interconversion leading to abasic or mismatched DNA, or SAM (S-adenosyl methionine)-induced alkylation (Ciccia and Elledge, 2010). Cellular metabolism can also lead to the generation of single-strand breaks via reactive oxygen species (ROS), as well as vis-à-vis gaps formed by unligated Okazaki fragments (Hanzlikova et al., 2018). These form an important substrate that is relevant to our understanding of the DDR, as are inappropriately embedded genomic ribonucleotides which represent one of the most frequent DNA lesions (Zimmermann et al., 2018). Endogenous stressors including R-loops and transcription collisions can also result in the

collapse of replication forks and hence the generation of DNA breaks. Physiological processes can also lead to the purposeful generation of double-strand breaks, such as programmed V(D)J recombination and immunoglobulin class switching in lymphocytes (see 1.2.2.2 below).

Exogenous DNA damaging agents encompass the gamut of external physical or chemical sources. The former is exemplified by ultraviolet (UV) and ionising irradiation (IR), either from environmental or therapeutic sources; UV generates pyrimidine adducts, while IR can induce a range of single-strand and double-strand breaks (SSB and DSB respectively), particularly generating complex DNA ends, along with oxidative stress and proteomic damage. Clastogenic chemicals include traditional pharmacological agents and currently utilised clinical compounds, which may alkylate, cross-link or enzymatically inhibit, as typified by methyl methanesulfonate (MMS), cisplatin and the topoisomerase I inhibitor camptothecin respectively. The response to any of these DNA lesions, begins with their detection for the purposes of activating a specific repair pathway to resolve the precise type of abnormal DNA structure which has been generated.

1.1.2. Damage detection and single-strand break repair

Three single-stranded DNA damage repair pathways exist. Nucleotide mismatches i.e. A:T or T:C, are initially recognised by MSH2-MSH6, which are digested by EXO1 and resynthesised by a DNA polymerase, during *mismatch repair*.

Small non-distorted base modifications such as alkylation, oxidation or deamination are flipped out of the double helix by DNA glycosylases to generate an abasic site, which after cleavage by AP endonucleases generates a SSB; the process of *base excision repair* can subsequently involve end-processing, (e.g. PNKP), DNA polymerase for synthesis, before flap endonuclease cleavage (e.g. FEN1) and DNA ligation (e.g. LIG1/LIG3 and XRCC1).

In contrast, bulkier helix-distorting lesions require the *nucleotide excision repair* pathway, which involves various complexes to detect damage in a transcription dependent or independent manner, via transcription-coupled or global genomic NER. Dual incision for nucleotide removal is followed by the action of DNA polymerases prior to ligation of the remaining nicks. This pathway, along with components of homologous recombination, also contribute to interstrand

cross-link (ICL) repair that centres around the Fanconi anaemia pathway (see 1.2.1 below). While SSBs represent the more abundant of lesions, DSBs represent the most cytotoxic lesions to a cell.

1.2. Double strand break repair pathways

There are four principal repair pathways for dealing with DSBs. Classical non-homologous end-joining (cNHEJ), alternative end-joining (or microhomology-mediated end-joining) alt-EJ, homologous recombination (HR) and single-strand annealing (SSA). While all of these repair pathways employ unique combinations of signal transducers and effectors, they all start with the common lesion of a gap across both strands of the DNA duplex.

The DSB is a competitive substrate, which is initially targeted by at least three proteins with rapid binding kinetics; PARP1/PARP2, Ku70/80 (XRCC5/XRCC6) and the MRN (MRE11-RAD50-NBS1) complex. PARP1 can detect both SSB and DSBs (Langelier et al., 2012) via its Zn-finger related domains, and through a conformational change unfolds the ADP-ribosyl transferase catalytic domain leading to auto-PARylation and the establishment of a PARylated platforms on surrounding chromatin, which can serve as a docking site for proteins with PAR-binding motifs (Lord and Ashworth, 2017, Ray Chaudhuri and Nussenzweig, 2017). PARP1 and the Ku70/80 heterodimer are likely to be the fastest-acting primary sensors (in part related to their high expression levels), which compete directly with each other for mutually exclusive access to the DNA ends on which they 'cap' or 'slide' onto respectively (Yang et al., 2018). Binding of the Ku70/80 heterodimer facilitates subsequent activation of DNA-PK, which initiates the NHEJ repair pathway (see 1.2.2 below).

The MRN complex consists of a heterotrimer of MRE11 nuclease (harbouring endo- and exo-nuclease activities), and structural proteins RAD50 and NBS1. NBS1 appears to initiate the binding of the complex to DSBs (Williams et al., 2007). Similar to the actions of Ku on DNA-PKc (PRKDC), MRN has an important role in the recruitment and activation of the related kinase ATM (Blackford and Jackson, 2017). It is possible for MRN and Ku to simultaneously occupy a single DSB site within a cell (Britton et al., 2013), and the net effect of competing sensors on the specific

underlying DNA lesion contributes to a cellular commitment to homologous recombination or an end-joining repair pathway.

In the first instance, the ATM activation mediates a signalling cascade on chromatin surrounding the break site, which via a series of post-translational modifications and protein recruitments serves to amplify the initial damage signal. ATM activation leads to phosphorylation of the histone variant H2AX (H2AFX, comprising ~10% histones in human fibroblasts) at Ser139, also known as γH2AX; this provides the docking site for MDC1, which recruits additional MRN and ATM, as well as the E3 ubiquitin ligase RNF8. RNF8 mediates widespread chromatin decondensation (Luijsterburg et al., 2012), and K-63 linked poly-ubiquitination of L3MBTL2 (Nowsheen et al., 2018) and/or the histone linker H1 (Thorslund et al., 2015), to recruit the E3 ligase RNF168, which ubiquitinates H2AK13,15 (Mattiroli et al., 2012), and potentially other proteins. This activity may itself be regulated by sumoylations via the SUMO ligases PIAS1/4 (Galanty et al., 2009). The ubiquitination platform serves to recruit proteins such as 53BP1, RAP80 (UIMC1) for the purpose of BRCA1 loading, RAD18 and RNF169, which is auto-propagated by RNF168's own ubiquitin binding domain (Schwertman et al., 2016). RNF169 may promote resection mediated repair such as SSA, by competing with 53BP1 for H2AK13,15ub binding (An et al., 2018, Hu et al., 2017, Kitevski-LeBlanc et al., 2017, Panier et al., 2012). Additional chromatin-associated protein modifications in the form of methylations and acetylations also play a critical role in establishing a histone code which facilitates the recruitment of individual proteins, and tailors the specific DDR that is mounted. The removal of such signals by deubiquitinases, demethylases and deacetylases offers further opportunities to regulate the cellular response to DNA damage, along with other post-translational modifications including sumoylation and ufmylation (Schwertman et al., 2016, Qin et al., 2019). The balance of these competing processes can for example, determine 53BP1 or BRCA1 recruitment, and play important roles in determining repair pathway choice, as discussed in 1.2.3 below.

1.2.1. Homologous recombination

Homologous recombination (HR) describes a form of DNA recombination used to repair DSBs in an error-free manner. Its high-fidelity stems from the use of a homology template, which is

typically the replicated sister chromatid and hence is restricted to use during S and G2 phases of the cell cycle. The failure to utilise the homologous chromosome likely reflects the spatial proximity of the sister chromatid, and inhibitory mechanisms which operate on HR components outside of these phases.

After DNA damage detection, DNA end-resection must occur to generate a 3' overhang for the purpose of recombination. Control of DNA end-resection is an obligatory step toward commitment to a repair pathway that requires strand annealing, effectively blocking cNHEJ, and is therefore an important step in repair pathway choice (see 1.2.3 below). CtIP (RBBP8) and MRN are likely to conform to the minimal resection machinery (Anand et al., 2016, Sartori et al., 2007), with MRE11's *endo*nuclease activity beginning the process with an internal nick which facilitates its 3'→5' *exo*nuclease action generating a short 3' overhang. The HR protein BRCA1 is known to form a complex with CtIP and MRN (BRCA1-C complex) (Chen et al., 2008), and likely plays a modulatory role in accelerating end-resection (Cruz-Garcia et al., 2014). In contrast, the BRCA1-A complex (which associates with MERIT40/BRCC3/BABAM1/2/ABRAXAS1 via RAP80) is thought to restrict end-resection (Hu et al., 2011), and clearly the interplay between different complexes will be important in determining this outcome. BRCA1 is a 1863aa protein with an N-terminal RING domain required for heterodimerisation with another RING-containing protein, BARD1; it contains a central region encoded by exon 11; a coiled-coil domain mediating its interaction with PALB2; and C-terminal BRCT repeats that are phosphorylated to enable its interaction with phosphorylated CtIP.

Long-range DNA end-resection by BLM/DNA2 and EXO1 helicase/nucleases generates extensive tracts of transiently exposed single-stranded DNA (ssDNA) which are rapidly coated by the ssDNA-binding heterotrimer RPA complex (RPA1-RPA2-RPA3). This eliminates secondary structures and serves to protect DNA from degradation (Chen et al., 2013), and acts as substrate for exchange with the RAD51 recombinase, preventing spontaneous annealing between regions of microhomology (Deng et al., 2014). RPA turnover can also be mediated by ubiquitination via RFWD3 and PRP19 which can act to activate ATR and HR at stalled replication forks (Dubois et al., 2017). The sumoylation of RPA following SENP6 dissociation, can also

promote SUMO-targeted ubiquitination and degradation of RPA by RNF4, and/or the recruitment of CtIP to facilitate RAD51 exchange (Galanty et al., 2012, Yin et al., 2012).

RAD51 loading onto DNA is thought to be brought about by the coordinated actions of the BRCA1-PALB2-BRCA2 complex. Specifically, BRCA2s C-terminal BRCT repeats disrupt RAD51 oligomers and facilitates RPA exchange and RAD51-ssDNA loading as monomers, forming a nucleofilament for the purposes of strand invasion into the homologous template (Carreira and Kowalczykowski, 2011). This invasion step is also likely to be stimulated by the action of BRCA1-BARD1 binding to RAD51, and the branched DNA D-loop structure which forms during recombination (Zhao et al., 2017). This D-loop is generated for synthesis dependent strand annealing (SDSA), or can form a double Holliday Junction (HJ) via second-end capture, which facilitates branch migration. Dissolution of the latter can also lead to non-crossover products as a result of the action of the BLM-TOPOIII-RMI1/2 (BTR complex); in contrast HJ resolution by GEN1 or the MUS81-EME1/SLX1-SLX4 nuclease complex generates crossovers. There are various anti-recombinases which can act at various stages of this process to reverse these processes and favour alternative repair mechanisms, including PARI and the helicases RECQL5 and RTEL-1 (Ceccaldi et al., 2016a). RADX appears to restrict the recombinogenic function of RAD51 by opposing HR and contributes to the cytotoxicity of the PARP inhibitor olaparib and the TOP1 poison camptothecin in BRCA2 deficiency (see 1.4.3 below) (Bhat et al., 2018, Dungrawala et al., 2017, Schubert et al., 2017). BRCA1 and CtIP are also likely to process the second end of a DSB, facilitating its capture in order to achieve SDSA, hence suppressing more error-prone long-tract gene conversions; these also suppress small tandem duplications which form after aberrant repair of stalled replication forks generating genomic rearrangements (Chandramouly et al., 2013, Willis et al., 2017).

The proteins involved in HR are also employed in the terminal steps of the more complex Fanconi anemia pathway for interstrand crosslink (ICL) repair. In brief, the detection of an ICL by FANCM-MHF1-MHF2 and UHRF1 recruit the FA core complex and FANCD2-I respectively (Rodriguez and D'Andrea, 2017). The core complex serves to ubiquitinate FANCD2-I, which is required for recruiting various endonucleases, for the purpose of NER-type DNA incision and

unhooking by MUS81-SLX1-SLX4. This generates a DNA adduct which can be bypassed by RAD18/PCNA-mediated translesion DNA polymerase ζ (REV3 with REV1 and REV7) recruitment and synthesis, and which then serves as a template for HR repair of the remaining DSB (Ceccaldi et al., 2016b).

In contrast to HR, the two alternative lower fidelity homology-based repair pathways are alternative end-joining (alt-EJ) and single-strand annealing (SSA) which are discussed in 1.2.2.4 below.

1.2.2. Non-homologous end-joining

1.2.2.1. Classical NHEJ and core NHEJ machinery

The main DSB repair pathway which can operate throughout the cell cycle, is classical (or canonical) NHEJ (Beucher et al., 2009). This involves peripheral factors which promote the pathway but are not an absolute requirement for effective repair, and the core end-joining machinery which operates in close proximity to the DNA break ends (Ciccia and Elledge, 2010). Single molecule fluorescence imaging studies, suggest a two stage model, in which 'long-range' tethering is mediated by Ku70/80 and DNA-PK bridging the two ends of DNA. This facilitates direct ligation by XRCC4-LIG4 and XLF/PAXX co-factors (Ochi et al., 2015) with the formation of a short-range complex, sterically blocking access of processing factors in order to prioritise rapid direct DNA end-ligation (Graham et al., 2016, Graham et al., 2018). If direct end-joining cannot occur, then DNA processing by accessory factors such as Artemis (DCLRE1C) and PNKP may be required to generate compatible ends for DNA end-ligation (Ciccia and Elledge, 2010, Blackford and Jackson, 2017). It has recently been proposed that the deliberate incorporation of ribonucleotides into the DNA ends by DNA Nucleotidylexotransferase (DNTT) and Polμ facilitate rapid and effective NHEJ repair (Pryor et al., 2018), albeit ultimately requiring removal by RNASEH2A. In this regard, it is noteworthy that while cNHEJ can lead to insertions or deletions, it is mostly accurate (Betermier et al., 2014).

1.2.2.2. 53BP1 promotes cNHEJ

We have considered the effects of the DDR in modifying chromatin to create a permissive environment for supporting the recruitment of double-strand break repair factors (see 1.2 above). Central to promoting NHEJ is the recruitment and retention of p53-binding protein 1 (53BP1; see Figure 3.2). 53BP1 is recruited to the chromatin via two principal motifs, a tudor domain that facilitates interaction with a dimethylated histone (H4K20me2) and a ubiquitin-dependent recruitment (UDR) motif which facilitates interaction with the H2AK13,15ub site (Fradet-Turcotte et al., 2013, Lee et al., 2014, Orthwein et al., 2014). Constitutive methylation of H4K20me2 in the pre-damaged state is bound by the polycomb group proteins L3MBTL1 and JMJD2A (KDM4A) which preclude 53BP1 tudor domain binding, in addition to interaction of this domain with the TIRR (NUDT16L1) chaperone protein (Her and Bunting, 2018, Drane et al., 2017). This interaction is further regulated by the acetylation status of the neighbouring H4K16 residues as determined by KAT5 and HDAC1/2 (Hsiao and Mizzen, 2013, Tang et al., 2013). The damage dependent re-localisation of 53BP1 from undamaged chromatin, to localise on ~1Mb chromatin surrounding a DSB (Clouaire et al., 2018), leads to the formation of microscopically visible subnuclear foci, to which the recruitment of downstream partners can be identified. The minimal focus-forming region (FFR) of 53BP1 required to facilitate accumulation of 53BP1 foci, encompasses the oligomerisation domain, the Gly-Arg-rich (GAR) motif, and the tandem Tudor and UDR domains. The N-terminus 28 Ser/Thr-Gln sites are important for downstream interactions with RIF1 and PTIP (PAXIP1), while the C-terminus harbours a BRCT domain which together with USP28 facilitates p53-mediated transcription independent of its role in DSB repair (Panier and Boulton, 2014, Cuella-Martin et al., 2016); see Figure 3.2.

Central to the function of 53BP1 in promoting NHEJ appears to be its role as a chromatin barrier to DNA end-resection which channels repair away from HR. 53BP1 recruits the downstream effectors RIF1 to its N-terminal S/T-Q motif in an ATM (and/or ATR) dependent fashion (Chapman et al., 2013, Di Virgilio et al., 2013, Escribano-Diaz et al., 2013, Feng et al., 2013, Zimmermann et al., 2013), which itself has been shown to be necessary for the recruitment of MAD2L2 (or REV7; a subunit of the heterotrimer REV1-REV3-REV7 which has an unrelated

function in translesion DNA synthesis as the DNA polymerase ζ) (Boersma et al., 2015, Xu et al., 2015). The recruitment of the trimeric complex of 53BP1-RIF1-MAD2L2 (Simonetta et al., 2018) to sites of damage demonstrates a mutually antagonistic relationship with BRCA1; discussed further in 1.2.2.3 below.

Loss of 53BP1 (Bunting et al., 2010, Bouwman et al., 2010), RIF1 (Chapman et al., 2013, Di Virgilio et al., 2013, Escribano-Diaz et al., 2013, Feng et al., 2013, Zimmermann et al., 2013) or MAD2L2 (Boersma et al., 2015, Xu et al., 2015) is associated with increased DNA end-resection and a failure to perform cNHEJ. The latter can be evaluated in physiological contexts, notably for immune cell functions. The processing of RAG1-mediated DSBs for V(D)J recombination, necessary for antibody diversification, appears to require the core end-joining machinery, but the role of 53BP1, if relevant, is limited to recombination between RAG cleavage sites that are separated by large distances (Difilippantonio et al., 2008, Bothmer et al., 2010, Dimitrova et al., 2008), and may be functionally redundant with XLF (Oksenych et al., 2012). In contrast, 53BP1 appears integral for the process of class switch recombination (CSR); this involves activation-induced deaminase (AID) mediated DSBs at immunoglobulin switch regions to facilitate cNHEJ between the two DSBs, resulting in class switching from IgM to different antibody isotypes (Ward et al., 2004, Bunting et al., 2010). A similar dependency of CSR on RIF1 (Chapman et al., 2013, Di Virgilio et al., 2013, Escribano-Diaz et al., 2013, Feng et al., 2013, Zimmermann et al., 2013) or MAD2L2 (Boersma et al., 2015, Xu et al., 2015) has also been described. Furthermore, the end-resection that results from I-SceI induced CSR in the absence of 53BP1 is ATM and CtIP dependent, suggesting a general mechanism in negatively regulating these processes on DNA ends to facilitate end-joining. 53BP1 has also been suggested to assist with chromatin mobilisation and the formation of long range synapses, and may also contribute to these functions, by for example, restricting nuclease access (Bothmer et al., 2011, Difilippantonio et al., 2008, Dimitrova et al., 2008); and RIF1 has also been shown to repress the chromatin loading of BLM (Feng et al., 2013).

In a pathological context, the deprotection of linear telomeric ends exposes DSBs which can fuse via cNHEJ in a 53BP1-RIF1-MAD2L2 dependent manner. This fusion of deprotected telomeres can occur when component(s) of the shelterin complex which normally caps the telomeric ends

(preventing damage signalling via ATM activation) are lost e.g. experimentally via TRF2 silencing (Zimmermann and de Lange, 2014, Palm and de Lange, 2008). It is important to note that the phenotypes described for loss of 53BP1, RIF1 or MAD2L2 do not consistently phenocopy loss of core end-joining factors (see (Bunting et al., 2010) and below).

The 53BP1 effector protein PTIP, may also contribute to some of these processes, possibly via its downstream engagement with ABRAXAS. *Nussenzweig* and colleagues proposed separate regions of the 53BP1 N-terminal S/T-Q motif as mediating its recruitment, compared to RIF1; although 53BP1-independent recruitment has also been described (Jowsey et al., 2004, Gong et al., 2009, Munoz et al., 2007). PTIP does not appear to contribute to CSR, although one study suggests its loss can rescue HR in BRCA1 depleted cells, in contrast to the partial rescue of this phenotype which they describe for RIF1 depletion (Callen et al., 2013); see below. This partial effect may in part reflect the contribution of RIF1 to replication fork stabilisation and origin firing (Buonomo et al., 2009, Xu et al., 2010). Hence PTIP's functions may be complicated by a degree of competition with RIF1 for 53BP1 binding, as well cell line differences, exemplified by a HR-promoting role for PTIP in chicken DT-40 cells (Wang et al., 2010).

1.2.2.3. Interplay between 53BP1 and BRCA1

As well as the contribution of the 53BP1-RIF1-MAD2L2 complex to cNHEJ, these components also appear to be important in the HR defect that is brought about by BRCA1 deficiency, as seen in familial and sporadic cancers (see 1.4 below). This mutual antagonism may operate at several levels of BRCA1 function.

The BRCA1-C complex involving CtIP generates the 3' DNA overhang which may be countered by a cell cycle dependent regulatory circuit of reciprocal inhibition centred around RIF1 (Escribano-Diaz et al., 2013) and MAD2L2. In keeping with this idea, BRCA1/CtIP depletion appears to de-repress RIF1 IRIF in S/G2 phases of the cell cycle (with a minimal effect on 53BP1); which may involve ubiquitination via BRCA1-UHRF1 (Zhang et al., 2016). Conversely, 53BP1 and RIF1 together prevent the ectopic formation of BRCA1 foci (independently of CtIP) in response to damage during G1. The G1 mediated exclusion of BRCA1 from chromatin is likely to be driven by the cell cycle (see below), while progress into S phase is associated with the CDK mediated

interaction between BRCA1 and CtIP (Sartori et al., 2007, Huertas and Jackson, 2009) which likely contributes to the displacement of RIF1 (Escribano-Diaz et al., 2013) and MAD2L2.

The interplay between BRCA1 and 53BP1 and their associated proteins, appears to be more important than direct competition with core components of cNHEJ or DNA end-resection; this is reflected by the partial suppression of radial chromosome aberrations in $BRCA1^{ko}$/$LIG4^{ko}$ cells (without rescuing HR) (Bunting et al., 2010), and the partial/minimal defect in end-resection of BRCA1 loss compared with say, CtIP (Zhou et al., 2014, Cruz-Garcia et al., 2014, Escribano-Diaz et al., 2013, Polato et al., 2014). During S/G2, 53BP1 surrounds a central core focus of BRCA2 (Chapman et al., 2012), and this might help to promote heterochromatic relaxation, and even facilitate HR during G2 (Noon et al., 2010, Kakarougkas et al., 2013), as well as by limiting DNA hyper-resection and SSA (see 1.2.2.4 below; (Ochs et al., 2016)).

BRCA1 also functions with PALB2 and BRCA2 promoting RAD51 loading, an effect which is almost entirely abolished in the absence of BRCA1. Concomitant loss of either 53BP1, RIF1 or MAD2L2 restores RAD51 IRIF and rescues HR, which can be explained as an indirect effect of restoring 3' ssDNA overhangs (above), or more directly by de-repressing RAD51 loading (e.g. by facilitating PALB2 mediated chromatinisation (Zong et al., 2019)). This rescue is evidenced by reporter assays, as well as the suppression of PARP-inhibitor (see 1.4.3 below) induced toxic chromosome fusions and cell death in BRCA1-deficient cells (Bunting et al., 2010).

See 1.2.3 below for repair pathway choice.

1.2.2.4. Alternative end-joining and single-strand annealing

Alternative end-joining represents a less well-understood subpathway of NHEJ, which can utilise small regions (ranging between 2 and 20bp, but typically 4-6nt) of microhomology to facilitate DNA annealing between two ends of a DSB, in the absence of classical NHEJ components (which instead utilises 0-4nt homology (Chang et al., 2016)). Microhomology mediated end-joining describes this same effect and occurs via existing DNA or template-independent nucleotides that are added by DNA Polθ (POLQ) (Chang et al., 2017, Wood and Doublie, 2016). DNA Polθ can serve to tether DNA ends with minimal microhomology, minimising large deletions, and utilising

terminal transferase activity to provide insertions for microhomology (Kent et al., 2016, Yu and McVey, 2010). While this pathway can contribute to chromosomal translocations and rearrangements, inactivation of factors like DNA Polθ supports its positive contribution to genome stability (Yousefzadeh et al., 2014). The DNA damage sensing and/or signalling likely involves PARP1 (Robert et al., 2009), followed by MRN/CtIP processing, and potentially flap processing and gap filling; concluding with ligation via DNA LIG1/LIG3. A recent study by Markus Löbrich and colleagues challenges this model by proposing that slow G1 resection may accommodate cNHEJ-mediated repair of resected DNA ends, with Artemis and DNA-PKcs engagement for end-processing (Biehs et al., 2017).

In contrast to cNHEJ which involves DNA end protection by 53BP1 and Ku to minimise DNA end-resection, both alt-EJ and SSA (like HR) require some DNA end-resection; this is likely to be initiated by MRN/CtIP. Single strand annealing (SSA) requires longer tracts of ssDNA resulting from extended lengths of DNA end-resection, typically >20nt of sequence homology and larger deletions (but less than the >100bp required for HR) (Bhargava et al., 2016). BLM/DNA2 and EXO1 appear to contribute to this longer tract resection to facilitate RPA binding and RAD52 exchange, for the purpose of annealing large regions of homology. It is suggested that the anti-resection function of 53BP1 may, when limiting, be overcome and favour SSA (Ochs et al., 2016). Furthermore, negative regulators of RAD51 nucleofilament formation, are also likely to promote these more mutagenic repair pathways; e.g. PARI (PARBP), RECQL5, BLM (Ceccaldi et al., 2016a, Grabarz et al., 2013). It is noteworthy that RAD52 loss produces a minimal phenotype but is synthetic lethal with BRCA1, PALB2 or BRCA2 loss, suggesting a dependence on this back-up pathway upon HR-deficiency (Lok et al., 2013). SSA is also more likely to necessitate the removal of large unannealed non-homologous stretches of 3' ssDNA, utilising components of the NER (e.g. XPF-ERCC1) and MMR (MSH2-MSH3) machinery for this flap processing (Bhargava et al., 2016, Chang et al., 2017).

1.2.3.DSB repair pathway choice

The relationship between BRCA1 and 53BP1 represents an important regulatory partnership that integrates various cellular signals and helps to determine the correct repair of DNA DSBs. We

have discussed how this interplay is likely to be deterministic in the control of DNA end-resection and RAD51 loading, and as a consequence, repair pathway 'choice'. The cell cycle plays a key role in these processes (Hustedt and Durocher, 2016), including the general suppression of DSB repair processes that occurs during mitosis (see 1.3.1 below).

CDK activity not only acts directly on CtIP to regulate its contribution to resection, but may also coordinate its BRCA1 interaction to promote end-resection (Cruz-Garcia et al., 2014, Huertas and Jackson, 2009, Huertas et al., 2008) and hence HR; while PLK3 phosphorylations of CtIP at overlapping residues may play a role in G1 mediated resection for alt-EJ (Barton et al., 2014, Biehs et al., 2017). Both direct effects on mediators of resection such as NBS1 (Falck et al., 2012), and indirect effects on expression levels e.g. MRE11 (Kanakkanthara et al., 2016), are required to ensure adequate cell cycle control. As previously outlined, the CDK dependent phosphorylation of Ser327 on CtIP is important for BRCA1's antagonism of RIF1 recruitment to sites of damage. Clearly there are other regulators of end-resection factors, such as DNA-PK phosphorylations reducing Ku-DNA binding during S-phase, and RNF138 facilitating Ku removal and/or promoting CtIP's recruitment to DSB sites (Schmidt et al., 2015, Ismail et al., 2015). The ssDNA translocase HELB, interacts with RPA and appears to restrict further end-resection, in a manner which is countered by CDK2 activity that reduces its nuclear import during S-phase (Tkac et al., 2016). Meanwhile, the S/G2 specific expression of the NHEJ inhibitor CYREN (cell cycle regulator of NHEJ) appears to interfere with Ku binding, with loss promoting toxic end-joining at deprotected telomeres (Arnoult et al., 2017).

G1 is also the phase during which BRCA1 and PALB2 are prevented from interacting, by CRL3-KEAP1 mediated ubiquitination, which is countered in S-phase by its deubiquitination due to upregulation of the DUB USP11, facilitating formation of the BRCA1-PALB2-BRCA2 complex for HR (Orthwein et al., 2015). ATR mediated phosphorylation of PALB2 in response to resected DNA also promotes this BRCA1-PALB2 interaction, favouring RAD51 loading in S-phase (Buisson et al., 2017).

Another important dimension of pathway choice is the chromatin state and its 'permissiveness'. Dynamic chromatin changes via post-translational modifications, constituted histone variants,

and DNA methylations can alter flexibility and mobility and hence accessibility of DNA to different repair factors. For example a widespread DSB-induced ubiquitination to acetylation switch on H2BK120, which 'cross-talks' with other chromatin modifications (e.g. H3K79me2 and H3K4me3 demethylation) appears to occur specifically at HR-prone sites (Clouaire and Legube, 2019, Clouaire et al., 2018). The histone code has been shown to have a role in directing DSB repair pathway choice toward HR in actively transcribed genes (Aymard et al., 2014). There also appears to be complex contributions of nuclear position and the role of F-actin/myosin relocalisation of breaks to facilitate specific repair pathways (Caridi et al., 2018, Chiolo et al., 2011, Lemaitre et al., 2014).

A model can be put forward to define the relationship between HR and the onset of S phase, whereby HR promoting factors appear behind replication forks resulting in local activation (Hustedt and Durocher, 2016). The incorporation of H4K20me0 impairs 53BP1 binding through a dilutional effect of methylated histones after replication (Pellegrino et al., 2017). It also results in the recruitment of chromatin readers such as MMS22L-TONSL (Saredi et al., 2016) and the BRCA1-BARD1 (Nakamura et al., 2019) complex, which likely promote RAD51 loading through chromatin remodelling and via BRCA1 localisation at DSBs (in an E3-independent manner but necessitating BARD1 binding) respectively. This latter finding suggested that the E3 ligase activity of BRCA1-BARD1 complex is dispensable, contradicting other work suggesting a role for BRCA1 mediated ubiquitination of H2A at K127 which promotes activity of the chromatin remodeller SMARCARD1 and repositioning of 53BP1 to drive long-range end-resection (Densham et al., 2016). Regardless, there is clearly a complex interplay between DDR factors which regulate pathway choice in a context-specific manner.

1.3. DDR in mitosis

1.3.1. DSB repair is attenuated in mitosis

Mitosis is the shortest stage of the cell cycle, characterised by chromatin condensation and the equal segregation of sister chromatids into two separate daughter cells. It has long been established that mitotic cells tolerate DNA damage, without activating the complete canonical

checkpoint and signaling events that characterise the DDR during interphase (Zirkle and Bloom, 1953, Rieder and Cole, 1998). As in interphase, γH2AX foci appear following primary detection by MRN and MDC1, with concomitant amplification of the ATM signaling cascade (Giunta et al., 2010). This early phase of the DDR can be mounted in response to damage, but the following downstream mediators – RNF8 and RNF168 E3 ligases – are excluded from damaged sites until the later stages of mitosis (telophase/cytokinesis) (Giunta and Jackson, 2011, Giunta et al., 2010). DSBs are therefore likely to be detected and contained in mitosis, but further processing appears to occur in the following G1 phase, when large 2-3μm 'nuclear bodies' containing 53BP1 can assemble (Lukas et al., 2011). It is tempting to speculate that in mitosis the condensed state of the chromatin makes DSB repair difficult, and infer a cost-benefit balance favouring the rapid progression through mitosis for cells which have already passed the G2/M and mitotic spindle assembly (SAC) checkpoints.

The *Chowdhury* and *Durocher* groups have uncovered how the next layer of the DDR is kept inactive during mitosis (Lee et al., 2014, Orthwein et al., 2014): the mitotic kinases (CDK1 and PLK1) mediate hyperphosphorylations which inactivate RNF8 (T198) and the ubiquitin-dependent recruitment motif (UDR) of 53BP1 (T1609/S1618), with these sites being re-'primed' prior to G1 entry via the phosphatase complex PPP4C/PPP4R3B. The phospho-null mutant $RNF8^{T198A}$ can form IRIF in mitosis, and recruits BRCA1, but fails to recruit 53BP1 without it being dephosphorylated (Orthwein et al., 2014).

The $53BP1^{ED}$ phospho-mimic mutant failed to interact with ubiquitinated H2A K13/15 residues, the first of a two-part recognition motif proposed for its recruitment to a DSB (the second requires an interaction between 53BP1's Tudor domain with dimethylated H4K20) (Orthwein et al., 2014, Fradet-Turcotte et al., 2013). In contrast, cells expressing the phospho-null mutant ($53BP1^{AA}$) were able to form IRIF and resolve γH2AX to the same extent as the wild-type ($53BP1^{WT}$) during interphase. Expressing 53BP1 and RNF8 phospho-null alanine mutants restores their recruitment to sites of damage in mitosis, but paradoxically exacerbates the sensitivity of these mitotic cells to radiation (Orthwein et al., 2014).

1.3.2. Ectopic recruitment of 53BP1 to chromatin can generate mitotic defects

The deleterious nature of damage-responsive RNF8^{T198A}/53BP1^{AA} expression in mitosis was further demonstrated after 0.5Gy irradiation in nocodazole-arrested cells, which led to anaphase bridges, lagging chromosomes and whole-chromosome mis-segregation into (kinetochore-positive) micronuclei (Lee et al., 2014, Orthwein et al., 2014). These effects could be suppressed by inhibiting DNA-PKc, silencing RNF168 (which potentiates 53BP1's recruitment to chromatin) PTIP and RIF1 (53BP1 effector proteins), thus reflecting a deleterious role for activating the NHEJ axis in mitosis. Furthermore, stress-induced telomere deprotection following prolonged mitosis and genotoxic stress was suggested as one potential mechanism for the observation of telomere fusions (Orthwein et al., 2014).

Hence, the aberrant activation of NHEJ in mitosis interferes with the normal process of chromosome segregation and can lead to aneuploidy. It is not understood why ectopic activation of the RNF8-53BP1 axis in mitosis should cause this range of defects.

1.3.3. Replication stress induces mitotic defects in the absence of recombination factors

The cytologically toxic effect of NHEJ activation is reminiscent of recent work identifying the role of HR and HJ mediators in resolving stress-induced replication intermediates, which when silenced produced similar mitotic defects. The recruitment of 53BP1^{AA} to damaged DNA was induced by low-dose radiation (0.5Gy), and it will be important to establish its relevance to endogenous oncogene-induced replication stress. This cellular stress can also generate DSBs as well as stalled replication intermediates, and these DNA structures may serve as additional substrates for the recruitment of 53BP1 (Halazonetis et al., 2008, Costantino et al., 2014, Lukas et al., 2011, Schmidt et al., 2014).

Low levels of cellular stress can remain undetected allowing cells to enter mitosis in an 'under-replicated' state, particularly at telomeric and centromeric sequences and common fragile sites (CFSs). These under-replicated regions may contain stalled or collapsed forks, post-replicative gaps or recombination intermediates; and these structures can be fully processed in mitosis by

HR-mediated stalled replication fork pathways involving endonucleases and unscheduled DNA synthesis (see 1.3.3.4 below).

1.3.3.1. Common fragile sites

Chromosomal rearrangements have a predilection for common fragile sites (CFS) (Glover et al., 1984) which describe over 200 loci within the genome that with replication stress (experimentally-induced using low-dose aphidicolin), can be visualised as chromosome gaps or breaks on metaphase spreads. These regions are inherently difficult to replicate by virtue of their sequence (and structure), dormant replication origins, hypoacetylated chromatin, and/or interference with active transcriptional machinery or RNA (Lukas et al., 2011). The inability to complete replication of these sites during S-phase can lead to fork stalling and generate abnormal intermediates which can persist into mitosis.

1.3.3.2. Replication fork stalling and restart

The stalling of a replication fork (RF) in S phase is an important cellular event, that likely occurs with frequency in response to a variety of endogenous and exogenous stressors. Replication stress (RS) is an important early driver of tumourigenesis and is associated with the activation of various oncogenes (Kotsantis et al., 2018). It can be defined as anything which impairs the progression of the replisome, and the signalling events that follow are known as the replication stress response (RSR). The RSR can result from a variety of DNA structures (e.g. hairpins, G-quadruplexes, R-loops), nucleotide pool depletion, as well as transcription machinery collisions which can interfere with progression of the RF. The RSR begins with a response that results from helicase-polymerase uncoupling, which via ssDNA-coated RPA signals to ATR via TOPBP1/RHNO1/RAD17/RAD9-RAD1-HUS1 or ETAA1 (Bass et al., 2016, Haahr et al., 2016). This leads to γH2AX formation and downstream activation of CHK1, resulting in cell cycle arrest, dormant origin firing (and late origin suppression) for the purpose of stabilising the stalled RF for repair (Dungrawala et al., 2015). ATR suppression of late origin firing is also important for preventing nuclear RPA exhaustion which if derepressed can lead to replication catastrophe (Toledo et al., 2013). These signalling events may be accompanied by fork reversal; regression of the fork structure to reanneal parental strands and allow binding of the newly synthesised strands

in a 'chicken foot' structure, which are likely to play a role in protecting the fork from collapse (Kotsantis et al., 2018). Many proteins involved in the DDR have moonlighting functions at replication forks, including PARP1 (Ray Chaudhuri et al., 2012), SMARCAL1 (Betous et al., 2013), RAD51 (Zellweger et al., 2015) and BRCA1/2 (Schlacher et al., 2011, Schlacher et al., 2012), as well as recent reports for 53BP1 itself (Her et al., 2018, Byrum et al., 2019). These work together to ensure fork stabilisation and restart, although when this does not happen the concerted actions of nucleases can result in the formation of a collapsed RF and single-ended DSBs (seDSB) which can only be repaired by HR, and without which leads to toxic end-joining and chromatid fusions (Dehe and Gaillard, 2017, Balmus et al., 2019). Fanconi anemia proteins, generally attributed to interstrand crosslink repair (as well as alternative lengthening of telomeres), also play a role in replication fork stability. This includes the core complex, monoubiquitinated FANCD2-I, with FANCD2 specifically limiting ssDNA accumulation by restraining the replication fork (Ceccaldi et al., 2016b, Kais et al., 2016).

The precise contributions of DNA endonucleases and their timing are complex, and not universally degradative: CtIP may have an important role in limiting long range resection and the collapse of replication forks (Przetocka et al., 2018), as well as MRE11 nuclease activity itself which may be necessary to prepare DNA ends for further repair (Mohiuddin et al., 2019).

BRCA1/BRCA2 appear to have critical roles in countering MRE11-mediated fork degradation, which is independent of their effects in HR. Indeed, loss of the proteins PTIP, CHD4 and PARP1 but not 53BP1, appear to suppress this phenotype, and may play in a role in chemoresistance to agents such as PARP inhibitors (see 1.4.3 below) (Ray Chaudhuri et al., 2016).

Restoration of stalled forks can therefore involve replisome repriming or fork regression, while collapsed forks or fork reversions with MUS81-cleavage generate single-ended DSBs for DSB repair. The gene conversion process can involves HJ formation, which are eventually disassembled by BLM-mediated 'dissolution' (in complex with BLM-TopoIIIα-RMI1-RMI2 or the BTR complex), or structure-specific endonuclease-mediated 'resolution' in G2/M by GEN1 or SLX1-SLX4-MUS81-EME1 complexes (Sarbajna and West, 2014, Sarbajna et al., 2014). The failure to resolve these intermediates can lead to various mitotic defects.

1.3.3.3. Anaphase bridges

DNA that remains intertwined within an unresolved HJ (catenanes) will impair sister chromatid disjunction, and can generate anaphase bridges, which may eventually rupture, and form chromosomal breaks. These 'bulky' bridges are DAPI- (and BTR complex) positive strands which join separating chromatin masses in anaphase and are distinct from thin DAPI-negative ultrafine bridges (UFBs) which lack histones and are experimentally visualised by their bound proteins (e.g. PICH (ERCC6L) and BLM). UFBs have been identified at the centromeres, telomeres and CFSs (Chan and Hickson, 2009). Centromeric UFBs predominate, and are likely to be physiological, anchored by kinetochores and the result of intertwined dsDNA catenanes. Alternatively both centromeric and telomeric UFBs may arise from recombined DNA due to repetitive satellite elements within these regions (Liu et al., 2014). CFS-UFBs are associated with a pair of FANCD2/I foci on each sister chromatid, and can bind RPA which may reflect an underlying stress-induced gap on the DNA (Chan et al., 2009, Naim and Rosselli, 2009). These sites can develop into 53BP1 nuclear bodies in G1 if they are not fully resolved in mitosis (Harrigan et al., 2011).

1.3.3.4. A model for resolving DNA intermediates in mitosis

A model is emerging in which cell stress can generate interlinked sister chromatids, due to stalled replication intermediates (containing HJs), unreplicated regions or post-replicative gaps. Chromosome condensation appears to prime some of these structures for processing. This enables MUS81-mediated cleavage of HJs and/or the resolution of any under-replicated/post-replicative gaps (Lai et al., 2017) possibly by break-induced replication (BIR) (see Figure 3.1 taken from (Pedersen et al., 2015)). This can prevent the formation of anaphase bridges and hence avoids their breakage and potential for fusion (Costantino et al., 2014, Minocherhomji et al., 2015). In chicken DT-40 cells, TOPBP1, which co-localises with FANCD2 'twin foci', may recruit SLX4 and help to facilitate this mitotic DNA synthesis (MiDAS) at CFSs (Pedersen et al., 2015). Following replication stress, MiDAS appears to require RAD52 which is necessary for the timely recruitment of MUS81 and (non-catalytic subunit Polδ-3 (POLD3)), but ATR, BRCA2 and RAD51 appears dispensable for the process of MiDAS (Bhowmick et al., 2016). Defective chromosome condensation, silenced MUS81, or inhibited Polδ-3 all reduce CFS 'expression', and produce a

familiar pattern of anaphase bridges and chromosome non-disjunctions which also increase 53BP1 nuclear body formation at CFSs in G1, and can be lethal (Minocherhomji et al., 2015, Costantino et al., 2014, Naim et al., 2013).

1.4. Targeting the DDR in cancer

1.4.1. DDR dysfunction in disease

The DNA Damage Response (DDR) is critical for genomic stability and cellular survival, and its perturbation contributes to premature ageing, neurodevelopmental disorders, immunodeficiencies and cancer (Jackson and Bartek, 2009). Repair pathways can be linked to specific biological processes within organisms, that explain the consequences of their dysregulation in diseased states. We have already considered some of the physiological roles of NHEJ with respect to generating immune cell diversity. Furthermore, meiosis involving SPO11-mediated DSBs and HR is essential in maintaining genetic diversity for the purpose of gamete production. These functions may be relevant to the immune deficiencies and sterility observed in patients with defects in DDR genes; indeed mutations in cNHEJ genes can be associated with radiosensitive severe combined immunodeficiency disorders (Ciccia and Elledge, 2010).

HR also has a role in some cancers, in ensuring telomere length is maintained by the process of alternative lengthening of telomeres (ALT). While the shelterin complex exists to dampen DDR activity at telomeric ends, the dysfunctional recruitment of NHEJ components can result in telomere shortening and fusion events, generating chromosomal instability during mitosis. The natural attrition of telomeric ends over time is associated with the ageing process and some DDR defective mouse models demonstrate hallmarks of accelerated ageing (Niedernhofer et al., 2006).

Neurons are particularly sensitive to DNA damage, as these cells generate large amounts of ROS in part due to their high mitochondrial activity. Their inability to replicate also limits their capacity to utilise template-mediated repair, and this may explain some of the neurodegenerative

features observed in diseases defined by DDR gene mutations, e.g. microcephaly associated with the RF stabiliser DONSON (Reynolds et al., 2017).

The predisposition to cancer is generally accepted based on the contribution of genome instability to its development (Hanahan and Weinberg, 2011). Gross structural rearrangements which characterise cancers, and more subtle effects of mutagenesis result from impairments in repair pathways like HR. As one possible mechanistic explanation, HR-deficient cancers often upregulate backup alt-EJ pathways such as via Polθ (Ceccaldi et al., 2015, Mateos-Gomez et al., 2015). The dependency on these repair pathways is also likely to contribute to the HR-deficient genetic mutation signatures (Nik-Zainal et al., 2012).

The inheritance of mutations in critical repair genes can generate a 'mutator phenotype', which enables cells to tolerate an accumulation of genome instability, reflecting an inability to detect, transduce or repair in response to endogenous DNA damage accumulated over the lifetime of an organism (Jackson and Bartek, 2009). In the first instance, the DDR serves as a barrier to uncontrolled growth, hence most tumours will evolve some deficiency to overcome this effect (Halazonetis et al., 2008). BRCA1 mutations are an exemplar, which when mutated, greatly increase the risk of developing breast, ovarian, prostate and pancreatic cancer in particular. The penetrance for mutation carriers is variable across tissues, but can be as high as 57% for breast cancer by the age of 70 (Chen and Parmigiani, 2007). However, the tissue-specificity of this predisposition is very unclear and an area of ongoing investigation.

1.4.2.Targeting DDR in the clinic

Not only can mutations in DNA repair genes predispose to cancer development, but the cellular response to DNA damage is critical in order to understand how tumours react to treatments such as radiotherapy and chemotherapy. These generate DNA damage, and traditional selectivity has relied upon the higher proliferation rates (S-phase indices) of tumour cells relative to surrounding healthy tissues. In this regard, cancers with deficiencies in critical DNA repair factors often have greater sensitivity to such agents.

The preferential toxicity toward cancer (relative to normal cells) is being tested with the clinical trials of various DDR enzyme inhibitors. This principle of targeting nononcogene addiction is premised on cancer cells relying on 'backup pathways' which are essential to their survival (Luo et al., 2009, Lord and Ashworth, 2017). The exemplar is PARP inhibition described below, but other therapies are also being explored which can exploit key differences in cancer DDR, not just the loss of specific repair pathways, but also increased levels of endogenous DNA damage, including replication stress, that are uniquely exhibited by cancer cells (O'Connor, 2015).

The latter has driven the targeting of the ATR-CHEK1-WEE1 axis which plays an important role in stabilisation and repair of replication forks, preventing the early entry of under-replicated genomes in mitosis (O'Connor, 2015). The principle of RPA exhaustion and sensitivity of cancers with high replication stress to ATR inhibitors has been described in vitro (Toledo et al., 2017, Toledo et al., 2013). Similarly WEE1 inhibition which leads to disinhibition of CDK1 can also promote mitotic entry and catastrophe (Aarts et al., 2012). These therapies are being explored in clinical trials as monotherapies, and it remains to be seen whether a clinical use can be established as a radiosensitiser or other combination regime. As our understanding of DDR and RSR pathways and their interconnectivity improves, it will be important to identify the optimal patient cohorts in which to use these and other emerging inhibitors including Polθ, and FEN1 inhibitors currently in development.

1.4.3.PARP inhibitors and resistance

PARP inhibitors have been developed based on mimicry of the NAD+ core, with a view to inhibit the catalytic site of the PARP enzyme. In doing so, this prevents its PARylation activity, impairing chromatin relaxation and PARP dissociation from DNA by competitively inhibiting NAD+ utility and hence generating replication fork blockade, which eventually leads to seDSBs (Murai et al., 2012).

1.4.3.1. The paradigm of PARP inhibition

The paradigm for cancer selectivity and pharmacological 'synthetic lethality', is represented by PARP inhibitors in HR-deficient cancers (e.g. familial BRCA1 mutations) (Lord and Ashworth,

2017). Two genes are synthetic lethal when the inactivation of either one is compatible with survival, but the combined loss results in cell death (Lord and Ashworth, 2017, Lord and Ashworth, 2016). Loss of the second allele as per the 'two hit hypothesis' results in the complete absence of BRCA1, and the predisposition to cancer. However, such cancer cells are exquisitely sensitive to the formation of lesions which can only be repaired by HR; PARP inhibition and replication fork collapse generates such a single-ended DSB, which in the absence of HR causes cell death. In contrast, surrounding BRCA1 heterozygous cells proficient in HR, tolerate PARP inhibition, thus explaining the cancer-selective effect of the drug and limited toxicity to surrounding healthy cells, and the clinical efficacy observed in a range of HR defective cancers (Moore et al., 2018, Robson et al., 2017, Mateo et al., 2015).

1.4.3.2. The mode of action of PARP inhibition

Early models suggested that the inhibition of PARP impairs the capacity of base excision repair, leading to single-stranded nicks which are converted into DSBs following RF progression (Farmer et al., 2005, Bryant et al., 2005). Since this time, the contribution of PARP trapping has been suggested to play a central role, providing a physical obstruction to the progressing replisome, and leading to collision, replication fork stalling, and ultimately collapse after processing to generate the single-ended DSB which necessitates repair by HR (Murai et al., 2012). In keeping with this hypothesis, the potency of PARP inhibitors in terms of their ability to induce trapping on DNA (rather than catalytic inhibition per se), appears to correlate strongly with their toxicity in HR defective cells (Murai et al., 2012). The utility of lower fidelity repair mechanisms accentuates genomic instability and most likely results in a critical accumulation of DSBs which is incompatible with cell survival (Patel et al., 2011, Ceccaldi et al., 2015, Balmus et al., 2019). The role of PARP1 in alt-EJ may also contribute to the lethality of its inhibition, epistatic to Polθ (POLQ) inhibition (Ceccaldi et al., 2015). Furthermore, the generation of seDSBs, and activation of NHEJ, may act in concert to promote toxic NHEJ and chromosome fusions, which may contribute to the tumouricidal effects in certain contexts (Balmus et al., 2019, D'Andrea, 2018).

Bartek and colleagues have proposed that inhibition of PARP prevents the detection of replication stress and instead increases RF speed rather than collapse, but this in of itself is

sufficient to cause DNA damage via an unspecified mechanism (Maya-Mendoza et al., 2018). PARP inhibition is known to prevent fork reversal which is necessary for efficient fork restart (Ray Chaudhuri et al., 2012). If this fork reversal is necessary to enable the adequate processing of unligated Okazaki fragments (a potential endogenous substrate of PARP trapping (Hanzlikova et al., 2018)), the increase in RF speed due to PARP inhibition may reflect a failure in RF reversal and impaired SSB repair at these sites (Maya-Mendoza et al., 2018, Hanzlikova et al., 2018). Persistent SSBs at Okazaki sites are likely to form a replication barrier during the subsequent S-phase, whereupon they lead to RF stalling (and/or collapse). In addition to this contribution, PARP inhibitors are also likely to benefit from the misincorporation of ribonucleotides, which appears to require the action of TOP1 as a backup pathway for RNaseH2 based ribonucleotide excision repair pathway (Zimmermann et al., 2018). In the absence of RNaseH2, the accumulated ribonucleotides are substrates for TOP1-mediated cleavage, and this generates many single-strand breaks for PARP trapping and subsequent RF blockade (Zimmermann et al., 2018).

1.4.3.3. Mechanisms of resistance to PARP inhibition

Since its FDA approval for use in breast and ovarian cancer patients, PARP inhibitors have been used as a monotherapy to great effect in patients harbouring BRCA1 and BRCA2 mutations. Unfortunately, as with all chemotherapeutic agents, a significant fraction of non-responders or transient responders have been identified, reflecting innate or acquired resistance respectively.

The simplest mechanisms of PARP inhibitor resistance, are those which lead to the re-expression of the BRCA1/BRCA2 protein. Genetic reversion of an inherited mutation can restore full length wild type protein, while other events can simply cancel a frameshift and restore the open reading frame, restoring function by expression of near-full length proteins (Edwards et al., 2008, Sakai et al., 2008). Certain truncation mutants can be tolerated, while other mutations will vis-à-vis nonsense mediated decay fail to be translated, or else through protein misfolding lead to proteasomal degradation e.g. BRCT domain mutations (Johnson et al., 2013). BRCA1 promoter methylation is also a well-documented aetiology of HR deficiency, and similarly this can be reversed, by active demethylation, or more likely, positive selection from a heterogenous group of tumour cells with less promoter methylation. Mutations in PARP1 can also account for PARP

inhibitor resistance in patients, due to the inability of PARP1 (the major target) to bind the drug (Pettitt et al., 2018) or else decreased/loss of expression of PARP1 itself. Similarly, efflux proteins (e.g. P-glycoprotein efflux pump) have been implicated in modifying PARP inhibitor responses (D'Andrea, 2018).

Given the general mechanism of BRCA1 and BRCA2 in terms of promoting HR and RF protection, PARP inhibitor resistance can also come about by decreases or loss of protein expression which result in restoration of these pathways. We have already outlined the antagonistic relationship between BRCA1 and 53BP1, and indeed loss of 53BP1 (Bunting et al., 2010, Bouwman et al., 2010), RIF1 (Chapman et al., 2013, Di Virgilio et al., 2013, Escribano-Diaz et al., 2013, Feng et al., 2013, Zimmermann et al., 2013) or MAD2L2 (Boersma et al., 2015, Xu et al., 2015) and PTIP (Callen et al., 2013) have been shown to restore HR function. In the case of PTIP, its loss has also been shown to rescue the RF defect observed in both BRCA1 and BRCA2-deficient cells (Ray Chaudhuri et al., 2016). Such a rescue at the level of RF stability appears to be independent of restoration of HR, as also demonstrated for PARP1 and CHD4 loss (Ray Chaudhuri et al., 2016), which appear to mitigate MRE11 mediated recruitment and RF degradation. Similarly, loss of the methyltransferase EZH2, reduces H3K27 methylation and impairs recruitment of the MUS81 nuclease to the stalled forks due to BRCA2 loss, and indeed EZH2 levels appear to correlate with poor outcomes in patients (Rondinelli et al., 2017).

Recent genetic screens by *Elledge* and colleagues have revealed synthetic lethal relationships between BRCA1 or BRCA2 and FEN1 or APEX2, highlighting the contribution of BER and alt-EJ to Okazaki fragment processing, SSB repair, and backup repair of DSBs in cells which are HR-deficient (Mengwasser et al., 2019). This screen also suggested a dominant negative role involving BRCA2 truncation mutants (terminating near BRC repeat 5, compared to those with intact BRC repeats) acting in concert with PALB2 and RAD51 paralogues. The expression of hypomorphic mutants appears to be a minimum requirement for the restoration of HR function following loss of 53BP1 or its related members, and truly null BRCA1 cells may be entirely incapable of restoring HR function despite the concomitant loss of an antagonistic protein (Nacson et al., 2018).

The loss or chemical inhibition of PARG as a mechanism of PARP inhibitor resistance, suggests a degree of catalytic activity is retained even in the presence of the drug. PARG loss/inhibition can result in restoring PARP1 signalling and PAR chain stabilisation, reducing PARP1-DNA complex formation thus preventing unrestrained RF progression and allowing the recruitment of DDR factors to survive the effects of PARP inhibition (Gogola et al., 2018).

Various strategies are being suggested to target these resistance mechanisms, including inhibitors of HSP90 to reduce BRCA1 hypomorph protein stability; PI3K/AKT (Ibrahim et al., 2012), HDAC (Adimoolam et al., 2007, Kachhap et al., 2010), CDK1 (Johnson et al., 2011) and CDK12 (Dubbury et al., 2018) to downregulate HR gene expression; EZH2 to restore MUS81 recruitment to BRCA2-deficient replication forks (Rondinelli et al., 2017); USP1 which appears to have a role in BRCA1-deficient RF stabilization (Lim et al., 2018); Polθ and FEN1 to impair backup alt-EJ pathways (Ceccaldi et al., 2015, Mateos-Gomez et al., 2015). There also appears to be a reliance in BRCA-deficient cells on ATR signalling, and therefore ATR inhibition may provide an additional strategy for overcoming treatment resistance (Yazinski et al., 2017). The G4 quadruplex stabilising compound pyridostatin has also been shown to cause DNA damage, potentiating replication stress and causing cytotoxicity in olaparib resistant Brca1/53bp1 or Brca1/Mad2l2 double-deficient cells (Zimmer et al., 2016). Establishing reliable techniques to define HR defects clinically, and identifying therapeutic vulnerabilities that may result, will be critical for the management of these patient cohorts.

In this thesis we will seek to explore 53BP1 and its contribution double-strand break repair in physiological settings and the pathological context of cancer. Chapter 3 explores the contribution of aberrantly active 53BP1 during mitosis, and how this process leads to genomic instability due to replication stress, reminiscent of cancer. Chapter 4 reveals insights into novel partners of 53BP1, and how these promote NHEJ. We also demonstrate the antagonistic relationship between these NHEJ factors and HR, highlighting clinical implications of PARP inhibitor utility in BRCA1-deficient cancers, and new therapeutic opportunities which may be appropriate in resistant settings. Finally, we consider how our approach for exploring DNA repair

networks and treatment resistance may be extended using developments in CRISPR-Cas9 technology, and translated into clinical settings for future studies.

2. Chapter 2 Material & Methods

2.1. Nucleic Acid Methods

2.1.1. Guide RNA design and cloning methods

Standardised NEB protocols were used for cloning and site-directed mutagenesis. Cloning for guide RNA insertion is exemplified below. For individual primers see appendix 6.3 below.

Guide RNAs were identified using http://crispr.mit.edu (site now closed) and https://chopchop.cbu.uib.no (Labun et al., 2019) webtools for selecting target sites for CRISPR/Cas9-directed mutagenesis. Guides receiving highest rankings based on specificity, upstream exon targeting and the presence of neighbouring restriction enzyme and primer sites for diagnostic digests and PCR were selected. The 3'NGG PAM motif is removed, and 20bp guide sequence (along with its reverse complement) are used along with overhangs to enable gRNAs to be cloned within the BsaI/BbsI sites. Hence the following arrangements are synthesised (Sigma):

5'-ACCG-20nucleotides-GTTT-3'

3'-TGGC-20nucleotides-CAAA-5'

An annealing reaction is performed using 1µl of 100µM stock of each forward and reverse oligo, along with 98µl of annealing buffer (100µl = 2µl 1M Tris-HCl pH 8.0 (20mM final), 1µl 5M NaCl (50mM final), 97µl nuclease-free water). The oligo suspension is placed in a microcentrifuge tube and holder allowed to sit in a beaker of boiling water, and allowed to cool down to room temperature over several hours. The oligo duplex is then phosphorylated using 5µl of duplexed oligo mix (with 5µl 10x PNK buffer (NEB), 5µl 10mM ATP, 1µl T4 PNK (NEB), 34µl water); this mixture is incubated for 30min at 37°C prior to heat inactivation for 20min at 65°C.

For cloning of gRNAs into a modified version of the Cas9 containing plasmid pSpCas9(BB)-2A-GFP (PX458; Addgene plasmid #48138), which contains a BamH1 digestion site within the BbsI dual sites before the guide scaffold. This protocol involves vector digestion and ligation with the

duplexed oligo as follows: 5µl phosphorylated oligos, 100 ng plasmid, 2µl NEB 1.1 (BbsI on pAIO-WT), 1µl BbsI/BsaI-HF, 1µl ATP 10mM, 0.5µl NEB T4 DNA ligase, made up to 20µl total reaction with water. This is followed by T4 ligase heat inactivation (10min at 65°C) and then plasmid digestion with 0.5µl BamHI-HF for 30min at 37°C to linearise any empty vectors which do not contain the guide. Finally, 5µl is transformed in 50µl of chemically competent Xl1-Blue bacteria for 30min (thawed from -80°C on ice for 30min). Heat shock is performed with incubation in a 42°C water-bath for 45s before returning the DNA-bacteria mixture to ice for 2min. Cells are then allowed to recover by transferring mixture to 1ml of antibiotic-free prewarmed SOC media at 37°C with shaking at 225rpm for 1h. After growing the cell-SOB mix is then pelleted by centrifugation 5min at 600g, and resuspending in 150µl volume for plating on LB agar with the relevant antibiotics, prior to spreading with 4mm autoclaved glass beads. The plate is allowed to dry before incubating inverted overnight at 37°C. Bacterial colonies can then be selected with 10µl sterile pipette tips for growth in 4ml LB media containing antibiotic at 37°C with shaking at 225rpm. The following day, DNA can be extracted isolated for PCR/cloning/sequencing using QIAprep Spin Miniprep kit (Qiagen) or transfection purposes via QIAGEN Plasmid Plus Midi or Maxi Kits (Qiagen) as per the manufacturer's protocol.

A diagnostic restriction digest is then performed using BamHI-HF to exclude empty vector, with EcoRI to identify two bands by agarose gel electrophoresis (see 2.1.2 below) of ~9kb and ~0.8kb (empty vector demonstrates three bands of ~5,4 and 0.8kb). Vectors identified to have likely guide inserts are selected for Sanger sequencing to confirm correct guide insertion using the primer CAGAGATTTTGAGACACGGGCC. Sanger sequencing was performed at the Department of Biochemistry, University of Cambridge, by preparing 10µl of DNA plasmid samples at ~100ng/µl, alongside sequencing primers at 10µM. Sequence alignment was performed using SnapGene v.3.3.4 (GSL Biotech).

For other vector/ligase digests, restriction digests were followed by gel band isolation and DNA gel extraction via QIAquick Gel Extraction Kit (Qiagen) as per protocol. Digested vectors were routinely dephosphorylated (1pmol of DNA ends, 2µl 10X CutSmart buffer (NEB), 1µl quick CIP (NEB) made up to 20µl water; incubated 37°C 10min followed by heat-inactivation at 80°C for

2min. Vector:Insert ligations were performed at 1:3, 1:5 and 1:10 molarity ratios and ligation by incubation with 2µl 10X T4 DNA ligase buffer (NEB), 1µl T4 DNA ligase (NEB) made up to 20µl water; this was gently mixed by pipetting, incubated at room temperature for 10min (or for blunt ends 16°C overnight), followed by heat inactivation 65°C 10min and chill on ice prior to transformation of 1-5µl of reaction into 50µl chemically-competent cells (see above).

2.1.2. Polymerase chain reaction (PCR), agarose gel electrophoresis and site-directed mutagenesis

In general polymerase chain reaction (PCR) was performed using Phusion DNA polymerase (NEB) as follows:

Component	20µl reaction	50µl reaction	Final
Nuclease-free water	to 20µl	to 50µl	
5X Phusion HF or GC	4µl	10µl	1X
10 mM dNTPs	0.4µl	1µl	200µM
10 µM Forward Primer	1µl	2.5µl	0.5µM
10 µM Reverse Primer	1µl	2.5µl	0.5µM
Template DNA	Variable	Variable	<250ng
DMSO (optional)	(0.6µl)	(1.5µl)	3%
Phusion DNA	0.2µl	0.5µl	1.0units/50µl PCR

Step	Temperature	Time
Initial Denaturation	98°C	30s
25 to 30 cycles	98°C	5-10s
	45-72°C	10-30s
	72 °C	15-30s per kb
Final Extension	72°C	5-10 min

Hold	4-10 °C

GC buffer is utilised where high GC contents are anticipated, and temperature gradients of 55°C to 80°C are occasionally used to identify optimal empirical annealing temperatures for PCR.

Agarose gel electrophoresis is performed using an appropriate concentration of agarose as determined by the anticipated product sizes. For 1% gel, 1.5g agarose is added to 150ml 1X TAE solution in a 500ml conical flask, which is heated close to boiling prior to the addition of ~17.5µl SYBR safe stain (Invitrogen) and pouring into a casting tray containing a gel comb. When set, combs are removed, and the gel placed in a gel tank containing TAE solution. A DNA ladder (1kbp or 100bp is used (NEB)), for typical run-times of ~80-150V for 1-2h depending on %/voltage. The gel can then evaluated using an ultraviolet (UV) transilluminator prior to image capture (ChemiDoc MP Imaging System, Bio-rad) and/or fragment isolation.

For the purposes of site-directed mutagenesis, primers are designed with mutations in the middle of primers containing 24-45bp overhangs, and GC content ⩾40%. Melting temperatures should be ⩾78°C and the 3' end a C or G. Asymmetric oligonucleotides can be designed to avoid excess primer-dimers or hairpin structures. Following PCR using the parental plasmid PCR, clean-up can be performed using QIAquick PCR purification kit (Qiagen) as described in their protocol. DpnI (NEB) digestion is performed to remove parental vector prior to bacterial transformation and DNA extraction as above.

2.1.3.Reverse transcription – quantitative polymerase chain reaction (RT-qPCR)

Reverse transcription followed by quantitative polymerase chain reaction was performed as follows:

$1x10^7$ cells are harvested by direct lysis using 600µl RLT buffer (add 10µl β-mercaptoethanol to 1ml RLT buffer). Add 1 vol (approx 600µl) 70% EtOH to lysate and mix by pipetting (do not centrifuge). Transfer up to 700µl sample including precipitate to RNeasy mini spin column. Centrifuge 15s, discard flowthrough. Add 350µl RW1 buffer, spin 15s, discard flowthrough. Add 10µl stock DNaseI to 70µl buffer RDD, mix by gentle inversion, brief centrifuge. Add 80µl DNase I mix to column, place on benchtop for 15min (20-30°C). Add 350µl RW1 buffer, spin 15s, discard

flowthrough. Add 500µl RPE to column, spin 15s, discard flowthrough. Add 500µl RPE to column, spin 2min, discard flowthrough. Spin 1min to dry. Elute into new eppendorf with 30-50µl RNase-free water, spin 1min. Measure RNA concentration. Using SuperScriptIII reverse transcriptase (Invitrogen), 1µl 50µM oligo dT20, 1µg total RNA, 1µl 10mM dNTP, and 10µl RNase free water mixture is made, and heated to 65°C for 5min before transfer to ice for 1min. After a brief centrifuge, the following is added to the mixture by gently pipetting up and down: 2µl 10X RT buffer, 4µl 25mM MgCl, 2µl 0.1M DTT, 1µl SuperScriptIII Reverse Transcriptase, 1µl RNase Out. This is incubated for 50min at 50°C before heat-inactivation for 5min at 85°C. Finally, 1µl RNaseH is added for 20min at 37°C.

Quantitative PCR reaction mixture is obtained with the following: 10µl 2x Fast SYBR Green Master Mix (Thermo Fisher), 0.4µl 10µM Fwd primer, 0.4µl 10µM Rev primer, 2µl cDNA template, and made up to 20µl with RNase-free water. Serial dilutions of individual cDNA samples are obtained (e.g. 10^{-1}, 10^{-2}, 10^{-3}), and individual reactions are performed in technical triplicates per cDNA dilution. Finally, primers for house-keeping genes are included in separate reactions in order to evaluate normalise changes in transcript levels. The StepOne Plus Real time PCR System (ThermoFisher) is used to obtain raw Ct values, in order to quantitate using the comparative Ct method $2^{-\Delta\Delta CT}$. Melting curves of primers are assessed to help evaluate specificity of primer binding. This protocol was used to verify knockout generation prior to Topo-cloning.

2.2. Protein Methods

2.2.1.Cell lysis and Immunoblotting

Adherent cells were washed twice with ice-cold PBS, prior to collection in lysis buffer which contained: 50mM Tris-HCl pH 7.5, 2% SDS, serine/threonine phosphatase inhibitor cocktail (Sigma-Aldrich), protease inhibitor cocktail (Roche) and 10mM N-ethylmaleimide (Sigma-Aldrich). Lysates were boiled for 5min at 95°C, before brief vortex and centrifugation. Protein concentration was measured using Pierce™ BCA Protein Assay Kit (ThermoFisher Scientific) with absorbance readings measured at 595nm. Samples were equalised in terms of volume and concentration with the addition of SDS-PAGE loading buffer. SDS-PAGE was performed using

NuPAGE Novex 4-12% Bis/Tris gradient gels (Invitrogen) or 4-20% Tris/glycine gels including the PageRuler Plus protein ladder (ThermoFisher), and run in Mini-Cell electrophoresis system (ThermoFisher) for 100min at 120V in 1x MOPS SDS (ThermoFisher) or Tris-Glycine/SDS (25mM Tris base, 190mM glycine, 0.1% SDS) running buffer respectively. Wet protein transfer onto (methanol-activated) PVDF membranes (GE Healthcare) occurred by overnight transfer (membrane and gel between Whatman filter papers and sponges) in transfer solution (25mM Tris base, 190mM glycine, 20% methanol, 0.1% SDS) at 250mA at 4°C overnight. Effective transfer was confirmed with Ponceau S staining, before being blocked with 5% BSA in TBS-T (TBS containing 0.1% Tween-20) for 1h at RT, and then immunoblotting with the indicated primary antibodies at 4°C overnight. The membrane was washed three times with TBS-T. Secondary staining was performed with appropriate species of HRP-conjugated antibodies for 1h at RT, prior to incubation with chemiluminescent detection regents (GE Healthcare Amersham ECL reagents, GE healthcare) and detection by X-ray film (Fuji) in a dark room. Experiments were performed at least twice unless otherwise stated. Membrane stripping was performed where necessary, by incubating PVDF membranes in 19ml 7M Guanidine HCl and 1ml 1M DTT stripping solution at 60°C on a shaker at 60rpm for 1h. The membrane is washed twice prior to further TBS-T wash and re-probing with primary antibodies overnight.

2.2.2. Immunoprecipitation

Adherent cells were washed twice with ice-cold PBS, prior to collection in lysis buffer which contained: 20mM Tris-HCl pH 7.5, 40mM NaCl, 2mM $MgCl_2$, 10% glycerol and 0.5% IGEPAL, *N*-ethylmaleimide (NEM, 10mM, Sigma-Aldrich), EDTA-free protease inhibitor cocktail (cOmplete Tablets, Roche), EDTA-free serine/threonine phosphatase inhibitor cocktail (PhosSTOP, Roche) and Benzonase (10µl/ml lysis buffer, Novagen 70664-3). The NaCl concentration was subsequently increased to 250-500mM, before vortexing and incubation on ice for 15min, followed by 16,000*g* centrifugation for 45min at 4°C. For GFP immunoprecipitations, cellular extracts were rotated at 4°C overnight with GFP-Trap-A beads (ChromoTek, 10µL per milligram of protein). The next day, immunoprecipitation buffer was used to wash the cell-bead mixture

five times. This was followed by protein elution from the beads by incubating the mixture at 95°C for 5min in 1.5x SDS sample buffer and immunoblotted as in 2.2.1 above.

2.2.3. In-vitro GST pull-down

Glutathione sepharose (GE Healthcare) affinity chromatography resin was washed with ice-cold PBS and blocked for 30min with 10 % bacterial lysate (non-induced BL21 cells, lysed using PBS and lysozyme). The sepharose was then resuspended in binding buffer (10mM Tris pH7.5, 150mM NaCl, 0.5% IGEPAL, 0.5mM EDTA, 0.5% BSA). 2pmol of purified GST (bacterial expression) or GST-FAM35A (Novus Biologicus) with His-C20orf196 (Creative BioMart) proteins were added to the sepharose resin, and incubated for 30min at 4°C. The mixture was then washed five times with wash buffer (10mM Tris, pH 7.5, 250mM NaCl, 0.5 % NP40, 0.5mM EDTA) before eluting bound proteins with elution buffer (100mM Tris pH 8, 20mM reduced glutathione, 120mM NaCl) for 15min at 4°C. The eluates were boiled in lysis buffer prior to immunoblotting with the indicated antibodies.

2.2.4. DNA oligo pull-downs

HEK293 cells were cultured after transfecting the indicated GFP-tagged products. These were prepared for immunoprecipitation as described above. Cell extracts were prepared in 250mM NaCl, and after benzonase digestion, EDTA/EGTA added at 10mM to inactivate the nuclease. Extracts were pre-cleared by rotation with unconjugated magnetic streptavidin Dyanbeads to mitigate non-specific binding, for 1h on slow rotation (Dynal, M-280; 50uL per reaction). Prior to the use of Dynabeads, washing was performed with 1x Binding and Washing buffer (1x B&W, 5mM Tris-HCl pH 7.5, 0.5mM EDTA, 1M NaCl). Oligo annealing to a separate batch of washed Dynabeads was then performed by rotation for 15min at RT in 1x B&W with 10nmol 5'-biotinylated ssDNA oligo of the sequence: 5'BiosG/ATCGCATTGGCATTGGCAATGCGATACG ACTGATCGAGGGTACTCAGCTAGCTGATTCCGATCGGCTTATTCCGTGTACATACATCGGA T-3' (IDT), followed by three washes with 1x B&W. Beads conjugated with DNA were then rotated with pre-cleared cellular extracts for 1h at RT. Four washes were performed with lysis buffer, prior

to protein elution by boiling in 2x SDS sample buffer for 5min, and immunoblotting as per 2.2.1 above.

2.2.5. Mass spectrometric analysis

GFP-Trap pulldown was performed for GFP-FAM35A and GFP-C20orf196 expressing HEK293 cells, and mass spectrometric analysis performed as detailed in (Dev et al., 2018). For each bait, two replicates were performed with label-swap; please refer to appendix 6.6 and 6.7 for enriched candidates, which are identified by SILAC H/L ratios in columns 10 and 11 of >2 and <0.5 respectively.

2.3. Mammalian cell culture techniques

2.3.1.Cell culture, propagation and cell stock freezing

Mammalian cells were cultured at 37°C in a humidified atmosphere containing 5% CO_2 in Dulbecco's modified Eagle's medium (DMEM; Sigma-Aldrich; or Nutrient Mixture F-12 (Ham's F-12; Sigma-Aldrich supplemented with 17ml $NaHCO_3$ 7.5% per 500ml (Sigma-Aldrich). All media was supplemented with 10% (v/v) fetal bovine serum (FBS; BioSera), 100U/ml penicillin (Gibco, Life technologies), 100µg/ml streptomycin (Sigma-Aldrich) and 2mM L-glutamine. SUM149PT cells were cultured in Ham's F12 supplemented with 5% (v/v) fetal bovine serum, 10mM HEPES, 1µg/mL hydrocortisone, 5µg/mL insulin, 100U/ml penicillin and 100µg/ml streptomycin. For maintenance and selection of cells stably expressing GFP or GFP-tagged constructs by G418/Kan resistant plasmids, 0.5mg/ml G418 (Invitrogen) was used. U2OS T-rex cells were selected in 200µg/ml hygromycin (Sigma-Aldrich), while U2OS-TLR cells were supplemented with 2 µg/ml puromycin (Sigma-Aldrich). Doxycycline induction of RPE-1 p53-null FRT-derived cells, U20S Trex/FRT cells stably expressing inducible-constructs occurred following co-culture with 1-2µg/ml doxycycline (Sigma-Aldrich) for 24-48 h to induce expression of GFP constructs. All cells were originally obtained from the ATCC cell repository and routinely tested to be mycoplasma free.

Cells were propagated by removing media, washing cells with sterile PBS, prior to the addition of warmed 0.025% Trypsin (Gibco, Life technologies) and incubation at 37°C for ~5min. Cells are observed for dissociation under the microscope, prior to harvesting and neutralisation in fresh media. For standard propagation, confluent plates of cells can be split and re-seeded in fresh media at ratios of 1:4 to 1:10 depending on the cell types. In contrast, where specific numbers of cells need to be seeded, cells are pelleted (3min at 400g) prior to resuspension in a smaller volume and cell counting. This occurs by mixing an equal volume of cell suspension with 0.4% trypan blue dye which is added to a Countess counting chamber (ThermoFisher) and evaluated using a Countess Automated Cell Counter (Thermo). An appropriate dilution of cell suspension is established for cell propagation.

Cells are frozen for the purposes of longer-term storage, and to avoid accrual of genome instability by continuous culture. Following harvesting and centrifugation, cells are resuspended in freezing media which consists of FBS containing 10% dimethylsulfoxide (DMSO) and transferred to cryovials (ThermoFisher). Cryovials are immediately placed within a 'Mr Frosty' Freezing Container (ThermoFisher) in -80°C freezer for 24-48h prior to transfer to liquid nitrogen for long-term storage. In order to thaw cells, cryovials are placed in 37°C incubator and allowed to thaw for ~10min, prior to centrifugation to remove the freezing media and resuspension in fresh warm antibiotic-free media.

2.3.2. Plasmid transfection and electroporation in mammalian cells

Plasmid transfections were achieved using TransIT-LT1 transfection reagent (Mirus). For example, in a 6cm plate, 5µg DNA is added to 500µl Optimem media (Gibco, Life technologies) while 15µl TransIT-LT1 is added to 500µl Optimem, and allowed to incubate for 5min at RT. These two mixtures are combined to incubate for a further 20-30min prior to dropwise addition on cells.

In some instances where electroporation was preferred, we utilised the Neon transfection system (ThermoFisher). In brief, $1x10^7$ RPE-1 cells were obtained and resuspended in 120µl R-buffer, mixed with ~8µg DNA dissolved in 30µl water. 100µl of this mixture would be taken up

using Neon pipette tips, and inserted into the electroporator with the following settings: 30N, 1400V, 30ms. Cells were subsequently added dropwise onto warm media in a suitable plate.

2.3.3. Performing siRNA mediated knockdowns

The siRNA duplexes were obtained from IDT or MWG biotech; reverse transfection was performed using Lipofectamine RNAiMAX (Invitrogen) as per the manufacturer's instructions. For a 6cm plate: 10µl 20µM siRNA duplex was added to 250µl Optimem media (Gibco, Life technologies), and 10µl RNAiMAX (Invitrogen) was added to 250µl Optimem, prior to their combination and incubation for 15min at RT. The complex is subsequently added to cells that have been freshly seeded (at ~150-200% of normal seeding concentrations), prior to dropwise addition of siRNA-lipid complex. Media was subsequently changed after 12-16h, and cells treated or harvested 48-72h later. Where siRNA depletion is inefficient, dual transfection method is adopted whereby forward transfection is repeated ~36h after the first transfection. For siRNA-plasmid co-transfections, plasmids were transfected 8h after siRNA treatment. In knockdown experiments, siRNA targeting firefly luciferase was used as a negative control (see appendix 6.3 below).

2.3.4. Generating stable cell lines

Cells stably expressing inducible proteins were generated in U2OS Trex or RPE-1 p53 null FRT (Flip-In) derived cells. The pcDNA5/FRT/TO-neo plasmid containing the GFP-tagged construct and pOG44 were transfected in cells in a 1:4 ratio. After 48h, selection was performed with 0.5mg/ml G418 (Invitrogen) for 7-14 days, in order to generate clones with inducible expression of a GFP-tagged protein. This was either facilitated by clonal dilution and manual selection at day 14 of individual clones using a fluorescence microscope, or bulk sorting by flow cytometry (MoFlo cell sorter, Beckman Coulter), into 96-well plate format. Protein expression was confirmed by immunoblotting or immunofluorescence.

2.3.4.1. Generating Cas9-expressing cell lines

Stable Cas9 expressing cells were generated by lentiviral infection. Lentivirus was generated using 293T-LentiX cells grown in 15cm dish at 60% confluency prior to transfection. 18.5µg

psPAX2, 4µg pMD2.G and 7.5µg plasmid of interest are added to 800µl Optimem media, and 800µl Optimem containing 90µl TransIT-LT1, are both left for 5min at RT. These are combined for 30min at RT prior to dropwise addition on cells in a 15cm dish. 48h later media is harvested and passed through a 0.45µm filter to prevent cell-to-cell contamination. Aliquots are subsequently snap frozen on dry ice and stored at -80°C. Virus packaged with wild-type Cas9 vector was used to infect parental cell lines, with antibiotic selection of 7-14 days. Individual clones were isolated prior to checking the efficiency of Cas9 activity, by transfecting individual clones with a plasmid containing: BFP, GFP and a gRNA targeting GFP; in the presence of efficient cutting the GFP/BFP ratio fell to <0.1.

2.3.5. Generating knockout cell lines

One of two strategies were adopted; either cell lines stably expressing Cas9 were transfected with synthetic gRNA or gRNA-expressing plasmids, or plasmids were transfected which encoded gRNA as well as Cas9 protein.

2.3.5.1. Plasmid Cas9-gRNA transfection, sorting, selection and verification

Knockouts were generated by transfecting the GFP-Cas9 and gRNA containing plasmid into cells (as per the method in 2.3.2 above). Cells of moderate GFP expression were isolated and single-cell sorted into 96 well plate using the MoFlo cell sorter (Beckman Coulter), before being allowed to expand over 7-14 days in 15% serum-containing medium. Single clones were isolated for duplication across two 96-well plates, followed by genomic DNA extraction using 50µl of QuickExtract DNA solution (Illumina) per well of the 96-well plate, and incubation for 5min at 65°C then 2min at 98°C in a PCR plate. The DNA was then used for diagnostic PCR as described in 2.1.2 above. Final verification was performed using immunoblotting where antibodies were available, and/or TOPO-TA cloning (ThermoFisher): 0.5-4µl fresh PCR product, 1µl salt solution, 1µl Topo vector made up to 6µl with water; mixture incubated 5-30min at RT prior to transformation as above. DNA was extracted as above, and Sanger sequencing with M13 forward and reverse standard primers to confirm successful gene-editing.

2.3.5.2. YM155 gene knockout strategy

Synthesised gRNA complexes are purchased (IDT) and transfected alone (in Cas9-expressing cells) or in combination with recombinant Cas9 to form ribonucleoproteins. In a 6 well plate format, 24pmol total crRNA is used with 24pmol of tracRNA (IDT). If positive selection by co-transfection with SLC35F2-targeting gRNA is used then this is included in a 3:1 ratio, i.e. 6pmol SLC35F2-crRNA + 6pmol tracrRNA complex with 18pmol GOI (gene of interest)-crRNA + 18pmol tracrRNA complex; these complexes are then mixed with 19.2µl Lipofectamine RNAiMAX in 800µL final volume (in OptiMEM) and incubated for 20min at RT to form the RNA-liposomes. 800µL mix is added to cells in 1600µl of complete medium without antibiotics (final volume 2400µl) and incubate at 37°C overnight. Cells are washed the following day to avoid excessive toxicity and complete medium added with antibiotics. 3-6 days can be given to allow for gene-editing prior to the addition of the positive selection agent YM155 (Selleck Chemicals; at a titrated dose; beginning with final concentration of ~20nM). It is noteworthy that excess agent may cause DNA damage so this titrated dose is kept to a minimum. Non-edited cells die within 48h, and after clonal expansion, knockout verification was performed by Topo-cloning as described in 2.3.5.1 above.

2.3.6. Cell viability assays

2.3.6.1. MTT assay

This assay measure cell viability based on the conversion of MTT (3-(4,5-dimethylthiazol-2-yl)-2,5-diphenyltetrazolium bromide) compound to an insoluble formazan product, leading to the formation of a coloured signal which can be measured in proportion to the number of viable cells. Based on plating 150 cells per well in a 96-well format; MTT (Sigma) powder was prepared at 5mg/ml in PBS solution (vortexed, and filtered at 0.2µm, stored 4°C in foil). The solution should be diluted 1:10 in serum-free media, and 100µl added to each well prior to incubation for 4h (to overnight) at 37°C. A further 100µl of 10% SDS (in PBS) should then be added to each well, and left all day in the incubator at 37°C, prior to measuring absorbance with a microplate reader at OD595 with normalisation to background media-only measurements.

2.3.6.2. Clonogenic survival assay

Cells were seeded in 6-well culture dishes (Corning); (1000 cells per well) and 48h later were treated with relevant drugs or irradiation. Media and drugs were replenished bi-weekly where appropriate. After 14 days, plates were washed with PBS, and colonies were stained with 0.5% crystal Violet/20% ethanol followed by washing with water, and air-drying. Quantification was performed by manual counting in a blinded fashion.

2.3.7. DNA damaging agents and laser micro-irradiation

Camptothecin and cisplatin (Sigma-Aldrich); olaparib (AZD2281), AZD2461 and talazoparib (BMN673) were applied at the indicated doses (Stratech Scientific). These were prepared in diluents and stored according to the manufacturer's instructions. Ionising radiation was generated using a Faxitron-CellRad (Faxitron Bioptics, LLC) at the stated dose using a 0.5mm aluminium filter. Localised tracks of DNA damage were induced by laser micro-irradiation as described in (Schmidt et al., 2015).

2.4. Mammalian cell analysis methods

2.4.1.Immunofluorescence

Cells were plated on cover-slips in 6-well plates, in order to achieve a final confluency at fixation of 70-80%. Prior to fixation, cells were washed 3x in 0.1% Tween-20/PBS, before pre-extraction using ice-cold 'modified CSK buffer (25mM pH7.4 HEPES, 50mM NaCl, 3mM $MgCl_2$, 0.25% Triton X-100, 300mM sucrose). Cells were then gently washed 3x in 0.1% Tween-20/PBS prior to fixation in 2% PFA/PBS for 20min at RT. Cells were washed again 3x in 0.1% Tween-20/PBS, prior to blocking in 5% BSA/0.1% Tween-20/PBS. Primary antibody solution was prepared in blocking buffer, and 50µl is placed on a strip of parafilm in a humidification chamber, before inverting the coverslip onto the solution and leaving the chamber at 4˚C overnight. The coverslips are returned to 24-well plates, before washing them 3x in 0.1% Tween20/PBS and incubating them in a solution containing the appropriate secondary antibody (1:500) and DAPI (Sigma, 1µg/ml) for 1h at RT. Finally washing 3x in 0.1% Tween20/PBS occurred before removing excess moisture from

each cover slip and inverting it onto a glass slide containing vector shield mounting media and sealing the edges with clear nail varnish.

2.4.1.1. Microscopy and live-cell imaging

The Olympus confocal microscopy FluoView 1000 was used to acquire fluorescent images of fixed and live-cells, acquired using a 40x/60x UPlanSApo/1.35 oil objective lens. Representative areas were identified, acquired and quantified as either single-slice confocal images, or multiple images across a Z-stack. Representative images shown with scale bar representing 10μm length unless otherwise stated.

2.4.1.2. Super-resolution microscopy

High resolution microscopy was performed using the Deltavision OMX 3D-SIM system V3 BLAZE (Applied Precision, GE healthcare), which harboured 3 sCMOS camera, and 405/499/592.5nm diode laser illumination, and an Olympus PlanApoN 60x 1.52NA oil objective lens and standard excitation/emission filter sets. Imaging of each channel occurred sequentially via three angles and five phase shifts. Sections were acquired at 0.125μm Z-steps. Raw OMX data was reconstructed in SoftWoRx software (v6.5.2., Applied Precision, GE healthcare). Voxelwise nearest-neighbour distances were measured between 53BP1 and GFP-FAM35A signals using a custom script for Fiji (Richard Bulter, Microscopy Facility, Gurdon Institute; 2017). This enabled mapping of signal volumes and measuring of distances using 3D Euclidean distance transformation with internal distances set to zero as per the histogram presented in the results (see Figure 4.9).

2.4.1.3. FRAP and association kinetics

The Olympus confocal microscopy FluoView 1000 setup was used for laser micro-irradiation, and subject to a bleach plus (five scans using 488nm argon laser focused via the 60X UPlanSApo/1.35 oil objective); main scanner, 100% AOTF (acousto–optical tunable filter, slow scanning mode), followed by image acquisition at the fastest speed. Average fluorescent intensities of GFP-RPA1 in the bleached regions were normalised against background intensity of neighbouring undamaged area. Mathematical modelling of GFP-RPA1 protein mobility fluorescence changes

over time were performed as previously (Schmidt et al., 2015). $(It-I_0)/I_{pre}$ values were plotted as a function of time, where I_0 is the fluorescence intensity immediately after bleaching, and I_{pre} is the average of the three prebleach measurements. Estimation of mobile protein fraction (A) and residence time (t) was performed using Prism 6 software, assuming the existence of one protein population using the following equation: $y(t) = A[1 \exp^{(-t/)}]$. Plotted data are averaged values of a minimum of 20 cells accumulated over three independent experiments. To compare between different experimental conditions, data were normalised against the fluorescence intensity at the time of micro-irradiation.

2.4.2. Flow cytometry

Cells are harvested by washing cell pellet with 1mg/ml BSA/PBS, before centrifugation for 4min at 400g, aspiration. Cells are either immediately fixed or initially pre-extracted depending on the application. Analysis is performed using BD Fortessa, with the following settings:

Specificity	Fluorochrome	Excitation laser	Filter
DAPI (4′,6-diamidino-2-phenylindole)		405nm	450/50
	Alexa-Fluor 488	488nm	530/30
	Alexa-Fluor 564	594nm	610/20
EdU (Click-IT)	Alexa-Fluor 647	647nm	670/14

At least 10,000 cells are recorded per event of interest. Data is exported as FACS files for analysis using FlowJo (TreeStar) software for analysis.

2.4.2.1. Cell cycle profiles

After washing the cell pellet, cells are fixed in 2% PFA/PBS, and incubated for 15min in RT, before neutralising the PFA by dilution with 1mg/ml BSA/PBS, and centrifugation for 4min at 400g. Samples are subsequently resuspended in BSA buffer containing DAPI (1µg/ml). In addition, immunostaining was performed to highlight S-phase populations by EdU incorporation. For detecting EdU incorporation, cells are pulsed with 10µM EdU for 30-60min in cell culture prior to harvesting and fixation. After fixation and washing, cells are subsequently permeabilised with

0.2% Triton X-100/PBS for 15-30min at RT. Washing with BSA/PBS is then followed by centrifugation, aspiration, and resuspension with the Click-It cocktail reaction for 1-2h at RT (ThermoFisher); 43.75µl PBS, 1µl 100mM $CuSO_4$, 0.25µl 200µM Azide dye, 5µl sodium ascorbate; stable for 15min). Cells are washed, centrifuged, aspirated, and resuspended in BSA/PBS buffer containing 0.02% sodium azide, DAPI (0.5µg/ml) and 250µg/ml RNase.

2.4.2.2. Immunostaining

For cellular staining necessitating pre-extraction, cells were initially washed with BSA/PBS, before incubating for 10min on ice with 0.2% Triton X-100/PBS solution. The sample was then washed with excess of 1mg/ml BSA/PBS, before centrifugation/aspiration and resuspension in 2% PFA/PBS for 15min at RT. After a further wash with BSA/PBS, centrifugation/aspiration, the cells were resuspended in antibody solution, and the protocol continued as described above.

2.4.3. Cellular reporter assays

2.4.3.1. Traffic-light-reporter assay

The TLR assay has been described previously in detail (Schmidt et al., 2015). In brief, the assay involves co-transfection of a plasmid template and I-SceI restriction enzyme, which cuts a specific locus within the U2OS-TLR cell line. The template encodes a plasmid which leads to the production of a GFP containing plasmid if error-free HR repair is performed following the I-SceI induced DSB. Alternatively, if erroneous end-joining is used to repair the break an mCherry signal will result. U2OS-TLR cells are depleted with the indicated siRNA for 8h prior to co-transfection with the I-SceI expression and HR-Donor plasmids. After 72h the cells are collected and sorted using the BD LSR-Fortessa (BD Biosciences), to measure the percentage of positive events. In each experiment, 10,000 cells positive for donor (BFP) and I-SceI (IFP) are evaluated for GFP (HR) and mCherry (mutagenic end-joining). Analysis is performed as described above. See Figure 4.19c for schematic of the TLR assay.

2.4.3.2. Random plasmid integration assay

Performed as described in (Galanty et al., 2009). Briefly, between two rounds of siRNA transfection, U2OS cells were transfected with BamHI–XhoI-linearised pEGFP-C1 (Clontech);

this can not be simply self-ligated and NHEJ is required. 24h after DNA transfection, cells were collected, counted and plated at low confluency onto a 15cm dish and 6cm dish in complete medium, and a 15cm dish in complete medium with 0.5 mg/ml G418 (Gibco, Life technologies). The following day, transfection efficiency was calculated by determining the proportion of GFP-positive cells on the 6cm dish. Cells on the 15cm dishes were incubated at 37 °C for 10-14 days until colonies had formed. Colonies were stained with crystal violet and counted, and integration events were normalised to transfection and plating efficiencies. Random plasmid integration = (plating efficiency of +G418)/[(plating efficiency of -G418) x (transfection efficiency)]. The p-value was calculated using an unpaired Student's t-test.

2.5. CRISPR-Cas9 screen

A genome-wide CRISPR-Cas9 screen was performed using three different PARP inhibitors in the BRCA1-deficient breast cancer cell line SUM149, as outlined in (Dev et al., 2018). The GeCKO v2.0 pooled library was utilised at a MOI 0.3 maintaining 250-fold coverage; PARP inhibitor treatment commenced at day 7 for a further 14 days, with olaparib/AZD2281 and BMN673/talazoparib dose equivalent to IC95, and AZD2461 dose equivalent to IC70. Following library preparation and PCR, Illumina Next Generation Sequencing was performed. The sequencing was de-multiplexed and number of reads matching each gRNA present in the library was determined from the single-read Illumina sequence reads using a custom programming script. Genes enriched or depleted in the inhibitor-treated samples were determined by a comparison of gRNA counts from these samples with an untreated control using the software package MAGeCK version 0.5.5 (Li et al., 2014).

The MAGeCK commands used were:

mageck test -k counts.csv -c DMSO -t WC_2461 -n WC_2461

mageck test -k counts.csv -c DMSO -t WC-673 -n WC-673

mageck test -k counts.csv -c DMSO -t WC-2281 -n WC-2281

2.6. Statistics and analyses.

Unless stated otherwise Prism 6 (GraphPad Software Inc) was used to calculate *p-values* based on Anova analysis, adjusted for multiple comparisons. Quantifications are based on at least three independent experiments unless otherwise specified. Data were considered statistically significant for *p-values* < 0.05. Microscopy image analyses were performed using the open software packages ImageJ/FIJI or Volocity 6.3 (Perkin-Elmer). Nuclei were manually segmented using the DAPI channel and the resulting regions of interest transferred to the fluorescence channel of interest (e.g. GFP, 53BP1, RPA2). Mitotic DNA foci were evaluated with a bespoke Fiji script, in condensed Z-stacks; channel intensity was then evaluated after foci detection to estimate co-localisations (e.g. EdU channel intensity within a FANCD2 focus). Where appropriate all results were normalised to responses in siRNA targeting luciferase (siCTRL) or wildtype cells.

2.6.1.Reproducibility of experiments.

Excluding screening experiments that were performed only once, and immunoblots which were performed twice, all experiments were performed at least three times unless otherwise specified.

3. Chapter 3 Results: Genome instability and 53BP1 in mitosis

3.1. Introduction

Non-phosphorylatable mutations in the UDR domain of 53BP1 (53BP1^{AA}) prevent its interaction with chromatin in response to damage. We have already outlined previous work which demonstrates how the ectopic chromatin recruitment of 53BP1 in response to IR is associated with chromosome mis-segregation defects during mitosis (see 1.3.2 above; (Lee et al., 2014)). It remains unclear however, whether this applies to the more pathophysiological context of replication stress as seen in cancers.

During interphase, DSB repair pathway choice is determined by the balance of factors which favour NHEJ or HR (see 1.2.3 above). By extension, premature activation of NHEJ during mitosis may antagonise the mediators involved with recombination and resolution of intermediates that form in response to cellular stress. BRCA2 and HR deficiency have been shown to generate replication stress, leading to hyper-resected DNA in G2 (potentially for long tract gene conversion); this can not only be carried over into mitosis (necessitating mitotic DNA synthesis) but also into G1, increasing 53BP1 nuclear body formation (Feng and Jasin, 2017). Intact HR pathways may also be required for the subsequent resolution of the G1 nuclear body in the following S-phase. This is alongside previously described roles for BRCA2 specific to mitosis (Choi et al., 2012, Daniels et al., 2004).

Inappropriate 53BP1 activity during mitosis may interfere with the processing of stalled replication intermediates. Figure 3.1 outlines a current working model of the serial recruitment of repair factors, nucleases and DNA synthesis observed during mitosis in response to replication stress. We will use this model to explore the impact of 53BP1 recruitment in prometaphase and metaphase cells. We hypothesise that the ectopic recruitment of 53BP1^{AA} to sites of DNA damage may phenocopy the loss of critical HJ and mitotic replication components in mitosis. If

so, 53BP1^{AA} should interfere with this normal DDR during mitosis, and result in genome instability.

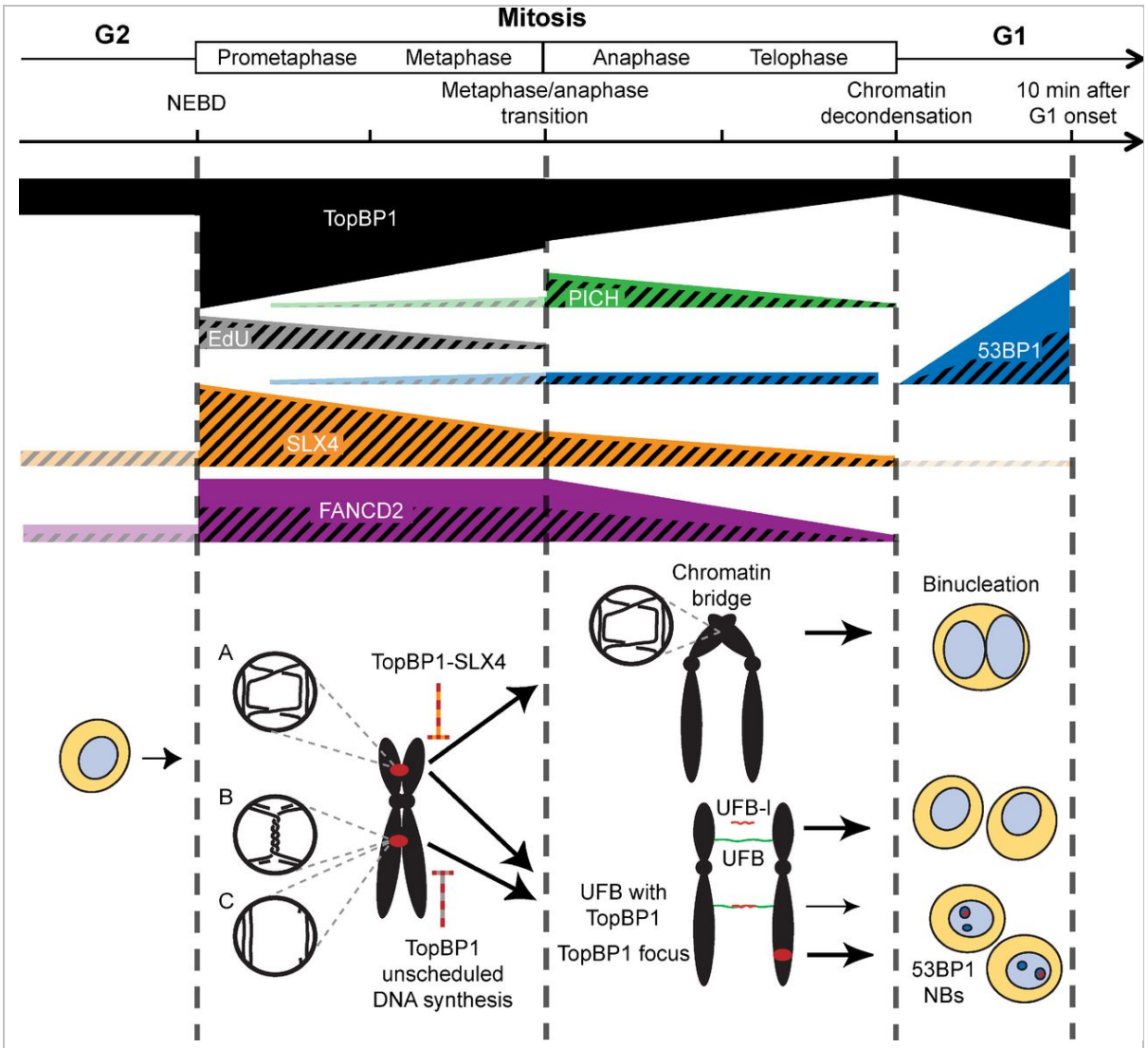

Figure 3.1 Model of resolving stalled replication intermediates carried over from S-phase during mitosis; taken from Pederson et al. 2015 (Pedersen et al., 2015). Recombination intermediates may interlink sister chromatids, or else post-replicative gaps may persist. TOPBP1 may be recruited to these sites to facilitate the resolution of HJ by SLX4 and if necessary complete replication via MiDAS. The persistence of unresolved interlinked intermediates can lead to the formation of DAPI-stained chromatin bridges or finer PICH-marked ultrafine bridges. Any or all of these, can manifest in the subsequent G1 as 53BP1 nuclear bodies.

In this chapter, we seek to develop a model system to explore the consequences of *short-term* expression of 53BP1^{AA}. While this protein should mimic wildtype 53BP1 during interphase and in response to damage, over-expression of any 53BP1 construct for a sustained period risks being deleterious to the cell and could impact the genome instability markers we are looking to measure. We will use confocal microscopy to image mitotic cells and identify DDR foci

(FANCD2) and DNA synthesis (by EdU incorporation); this will help to establish the effects of our 53BP1 mutant cell line on these well-characterised responses (Naim and Rosselli, 2009, Naim et al., 2013, Chan et al., 2009, Minocherhomji et al., 2015, Ying et al., 2013, Gallina et al., 2016, Pedersen et al., 2015). Finally we will attempt to explore the mechanism by which this leads to genome instability.

3.2. Results

3.2.1.53BP1^{AA} induces micronuclei formation with aphidicolin treatment

In order to study the impact of ectopic 53BP1 activity during mitosis, we generated Flag-tagged 53BP1 constructs which harbored wild-type or T1609A/S1618A ('AA') modifications in the UDR domain (Figure 3.2).

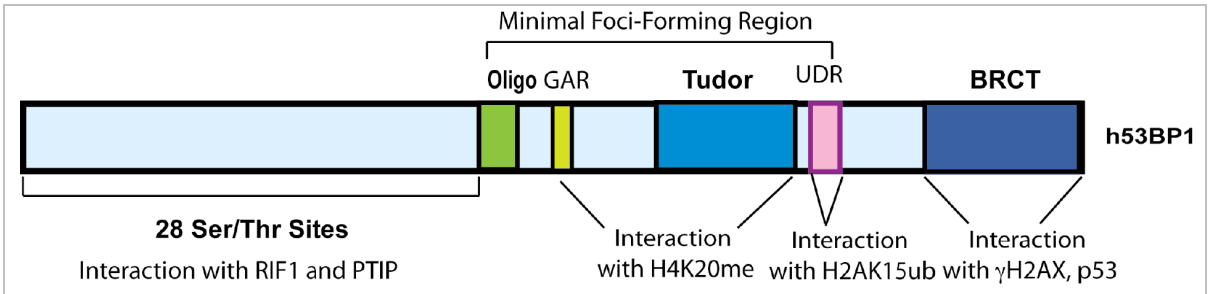

Figure 3.2 Schematic of 53BP1, demonstrating the major motifs of 53BP1, as well as the focus forming region (FFR) which represents the minimal length of protein necessary for IRIF formation. Importantly, the UDR motif contains T1609 and S1618 which are the sites normally phosphorylated during mitosis to prevent chromatinisation.

This was achieved by sub-cloning 53BP1 from lentiviral constructs into the pcDNA5/FRT-TO vector, performing site-directed mutagenesis and transfection to generate doxycycline-inducible U2OS cells (see materials and methods; 2.3.4); Figure 3.3a,b. By generating 'flip-in' cells expressing our protein of interest, we sought to minimise any unforeseen toxicity that might result from constitutive expression of our constructs. We also employed Flag-tagging for downstream purposes as outlined below.

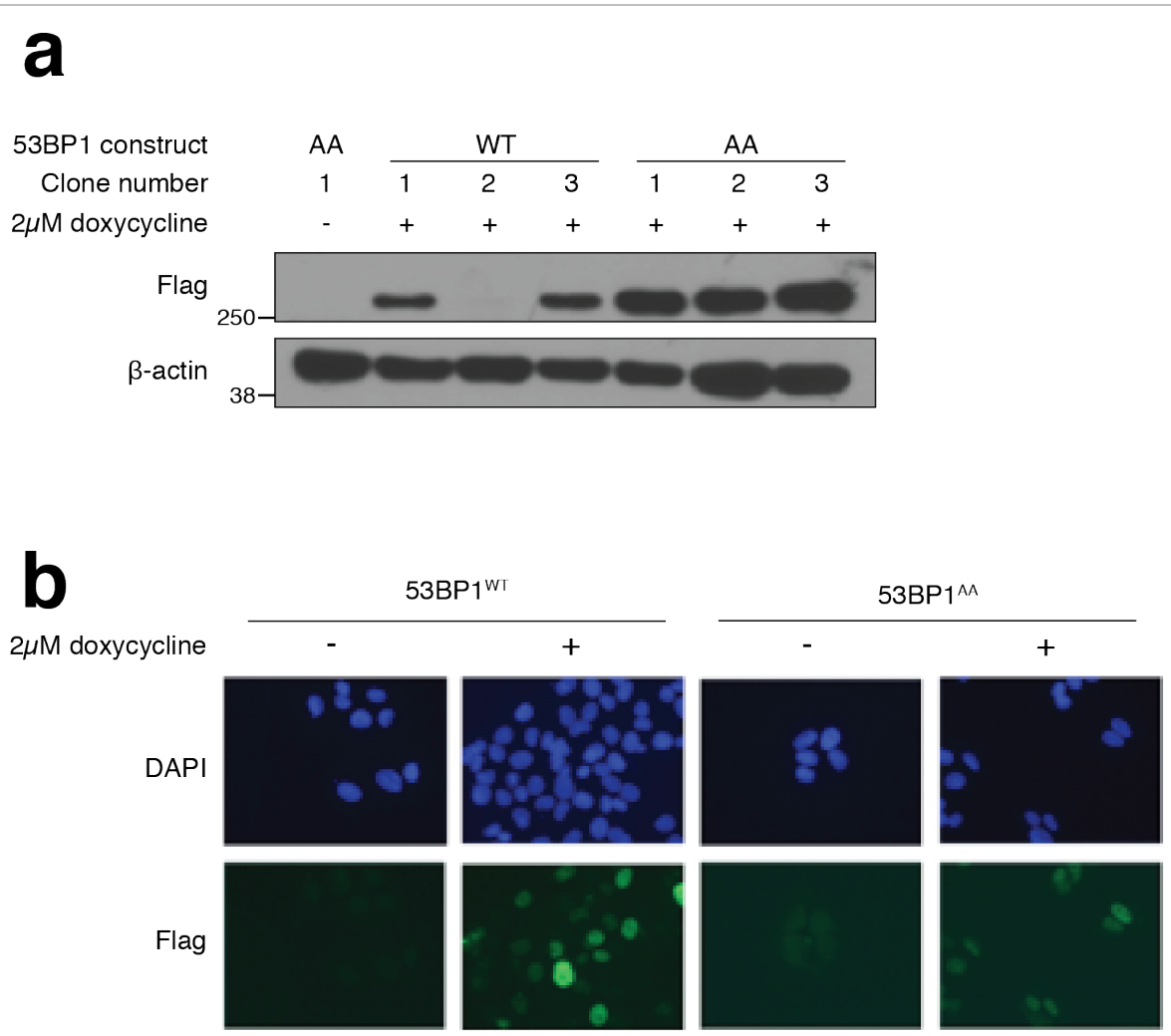

Figure 3.3 Generation of dox-inducible 53BP1 expressing U2OS cell lines. (a) Immunoblot demonstrating clones with dox-inducible expression of Flag-53BP1 harbouring WT or 'AA' residues at S1609 and T1618. (b) Immunofluorescence demonstrating dox-inducible expression of 53BP1 constructs in U2OS cells.

In the first instance, we sought to examine the impact of inappropriately active DDR during mitosis in cancer, when replication stress is used as a stimulus. There are a range of chromosome mis-segregation defects including anaphase bridges and micronuclei resulting from low-dose irradiation which can be mediated via NHEJ axis activity (Orthwein et al., 2014). We examined the impact of 0.2μM aphidicolin (APH, Sigma-Aldrich) on micronuclei formation; this was achieved by 8h of doxycycline-induction in the presence of 0.2μM APH treatment, followed by a further 16h of APH treatment in the presence of doxycycline and the CDK1 inhibitor R0-3306 (Sigma-Aldrich); Figure 3.4a. We observed an increase in a proportion of cells harbouring micronuclei when 53BP1^{AA} isoforms were expressed which could be ectopically recruited to the chromatin

during mitosis (Figure 3.4b). In addition, the majority of these micronuclei appeared acentric, as determined by anti-centromere antibody staining within micronuclei (Figure 3.4b).

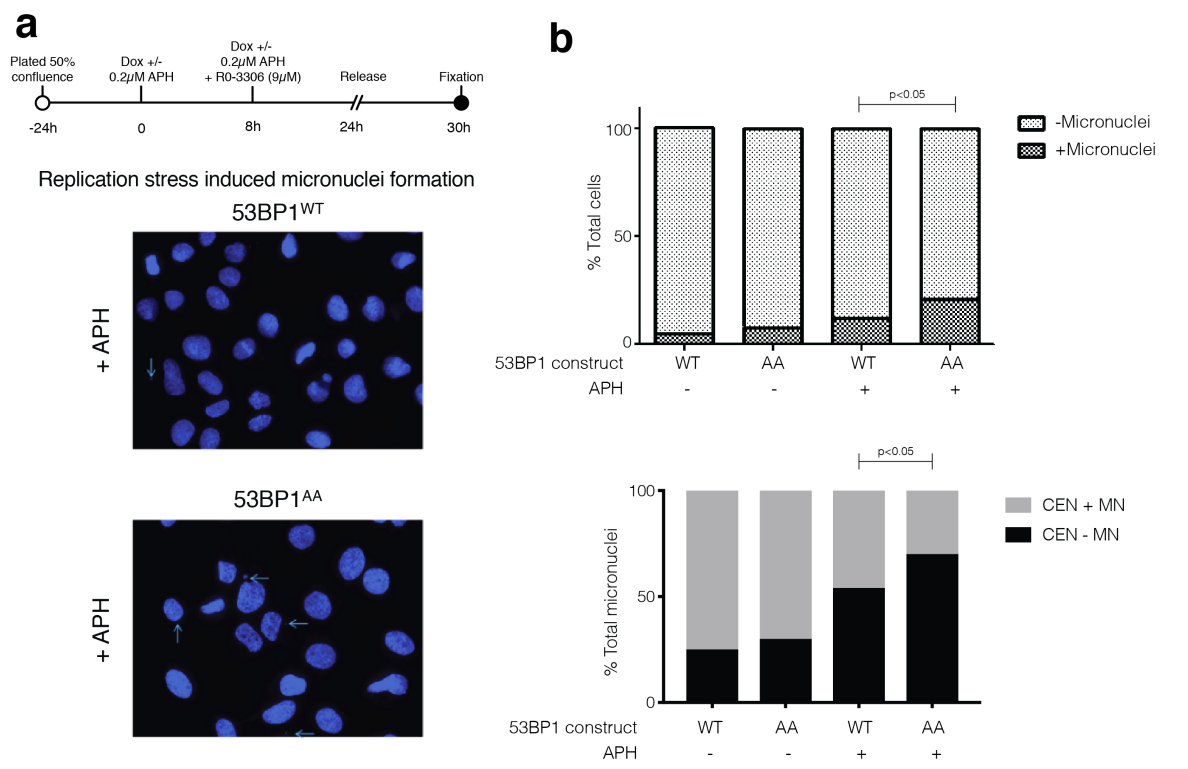

Figure 3.4 53BP1^{AA} promotes replication-stress induced acentromeric micronuclei formation. (a) Workflow for cell treatment prior to fixation, along with representative micrograph demonstrating DAPI-stained micronuclei. (b) Quantification showing (top) significant enrichment in APH-induced micronuclei in 53BP1^{AA} (compared to 53BP1^{WT}) expressing cells; and (bottom) a significant increase in APH-induced centromere negative micronuclei in 53BP1^{AA} (compared to 53BP1^{WT}) expressing cells.

3.2.2. Aphidocolin induced G1 nuclear bodies with mitotic 53BP1^{AA}

The accumulation of replication stress intermediates which remain unresolved during mitosis, have been suggested to manifest as large 53BP1 nuclear aggregations known as 53BP1 G1 nuclear bodies (Lukas et al., 2011, Harrigan et al., 2011). We performed a similar experiment as per Figure 3.4; in this instance evaluating Cyclin A negative cells (i.e. cells in G1) for 53BP1 nuclear bodies by immunofluorescence and microscopy (Figure 3.5a). Co-staining in the 594 channel with a 53BP1 antibody was used to functionally confirm anti-Flag accumulation of Flag-53BP1 constructs in nuclear bodies. This revealed 53BP1^{AA} was associated with a significantly greater proportion of G1 nuclear bodies, following replication stress (Figure 3.5b).

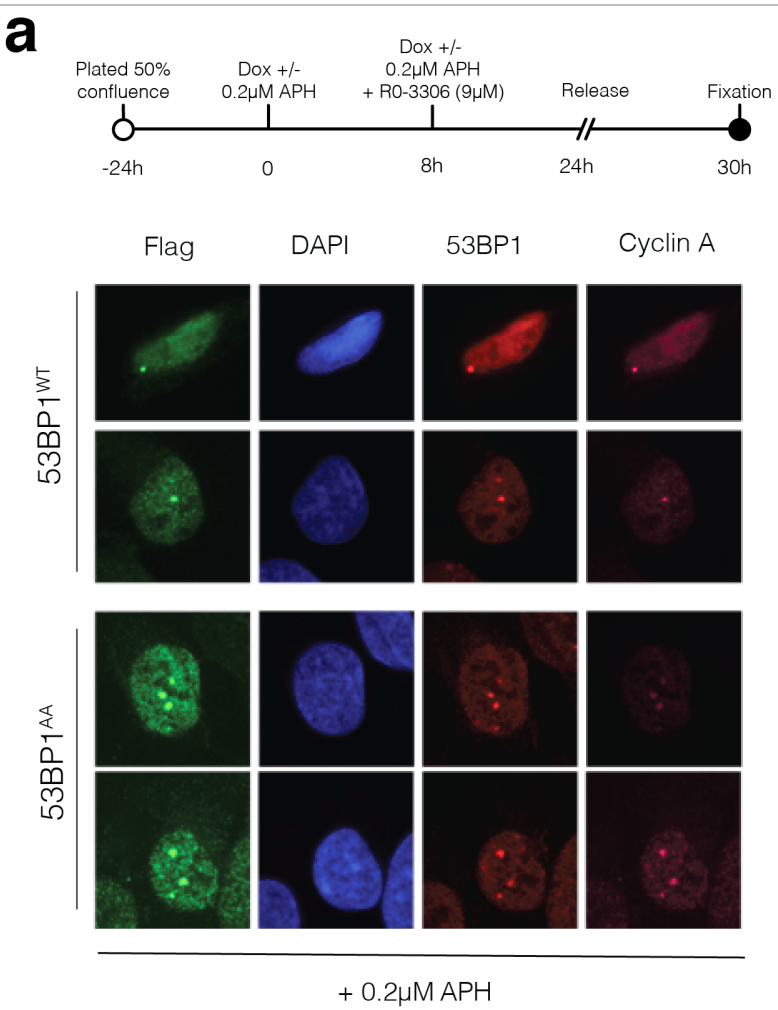

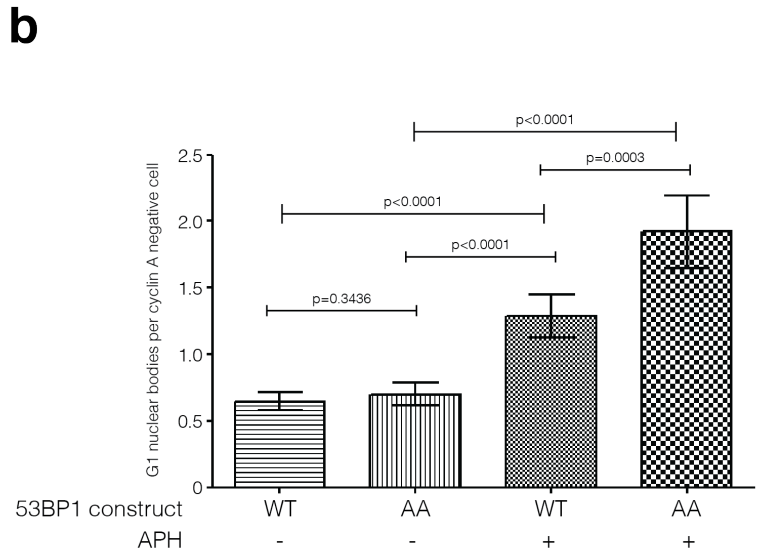

Figure 3.5 53BP1^{AA} promotes formation of G1 nuclear bodies in response to replication stress. (a) Workflow for cell treatment prior to fixation, with representative micrograph of 53BP1 nuclear body formation in response to APH. (b) Quantification of nuclear body formation in response to APH.

3.2.3. 53BP1^{AA} impairs unscheduled DNA synthesis in mitosis

It has recently been reported that replication stress is associated with DNA repair synthesis in mitosis (Minocherhomji et al., 2015). The incorporated nucleoside analogue EdU can be co-localised with FANCD2 foci, which themselves appear to correlate with Common Fragile Sites (CFS) i.e. regions of the genome that are difficult to replicate and may reach mitosis in an under-replicated state (Chan et al., 2009, Naim and Rosselli, 2009). We sought to evaluate mitotic DNA synthesis (Minocherhomji et al., 2015) as a result of replication stress and the expression of our 53BP1 derivatives. This followed a similar schema as described previously, except that after 16h CDK1 inhibition, cells were released into EdU containing media for 45min prior to fixation (see Figure 3.6a). In this experiment we examined prometaphase and metaphase spreads, excluding any cells at anaphase or beyond. EdU was coupled to Alexa-Fluor 647, and co-localisation of signal at FANCD2 foci was examined across 3-D imaging stacks, before utilising FIJI software to measure EdU signal intensity at these FANCD2 foci. We saw that despite both cell types demonstrating equivalent levels of damage (as indicated by FANCD2 foci per mitotic nucleus), each FANCD2 focus was approximately 50% less frequently associated with EdU incorporation (Figure 3.6b,c), and similarly each EdU focus was 50% less intense compared to wildtype conditions (Figure 3.6d). Arbitrary thresholds for EdU positivity were set in each experiment, but then maintained throughout the experiment and across the cell lines.

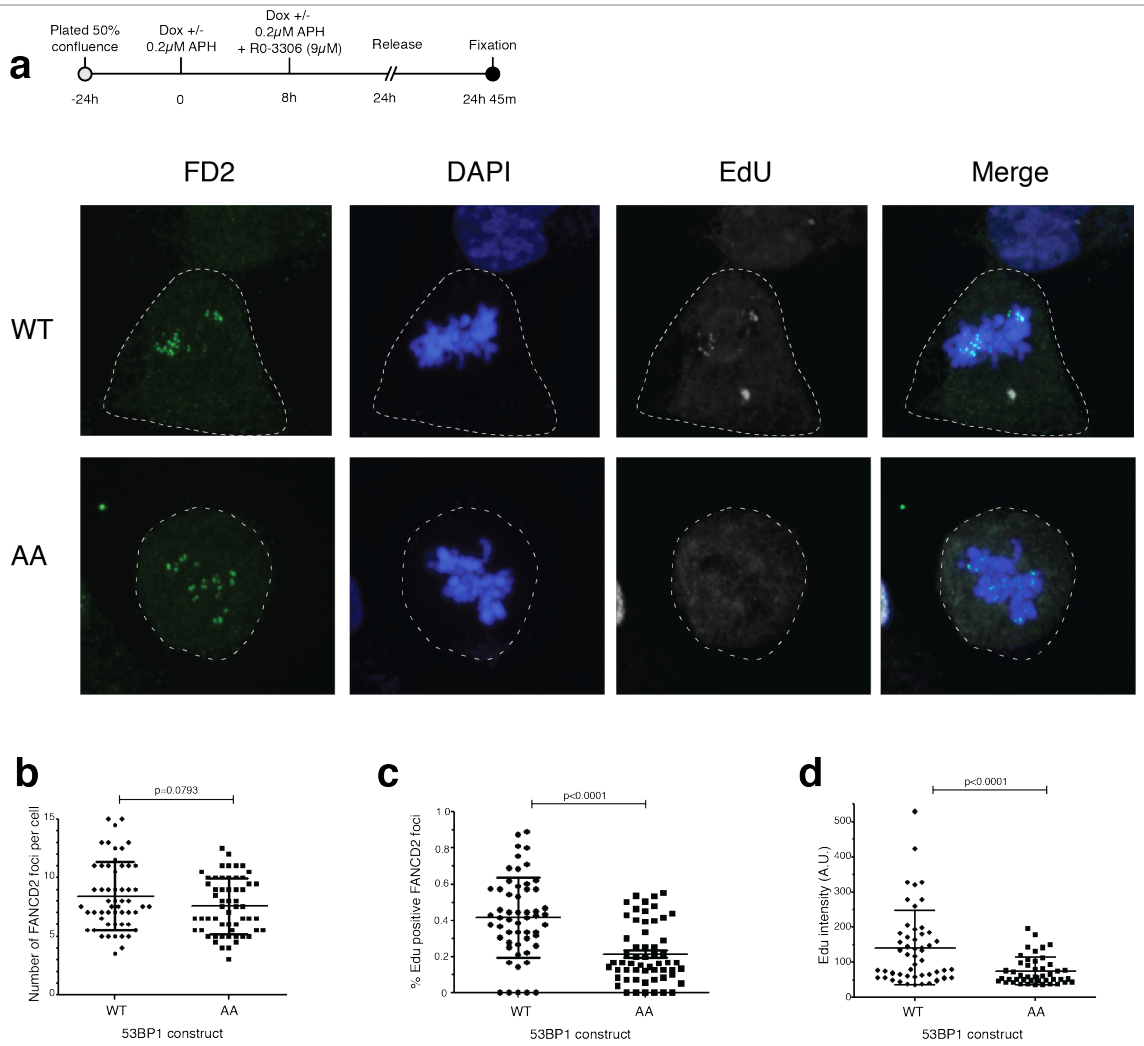

Figure 3.6 53BP1^{AA} impairs unscheduled DNA synthesis in mitosis. (a) Workflow for cell treatment prior to fixation, with representative micrograph demonstrating FANCD2 co-localisation with EdU signal on condensed chromosomes (DAPI) during mitosis. Quantification of (b) number of FANCD2 foci per cell; (c) % EdU positive FANCD2 foci; (d) mean EdU intensity per EdU focus (as defined by co-localisation with FANCD2).

3.2.4. 53BP1^{AA} impairs unscheduled DNA synthesis in mitosis following reduced replication origin firing

A general principle for this model suggests that under-replicated DNA can pass through mitosis for resolution in the subsequent daughter cells (Figure 3.1). The failure to complete conventional replication during S-G2 phases likely occurs following double fork stalling events. Indeed 53BP1 appears preferentially bound to larger replicons and its loss has been associated with the formation of anaphase UFBs, G1 nuclear bodies, as well as hypersensitivity to replication stress when replication origins were experimentally 'removed' by MCM5 depletion (Moreno et al., 2016). We used the reported technique of silencing of the origin licensing factor MCM5 as an

alternative source of more 'physiological' replication stress (Figure 3.7a), to evaluate the impact of 53BP1^{AA} on MiDAS (Moreno et al., 2016). Once again, results suggested that there was a significant, albeit smaller, reduction in EdU positive FANCD2 foci, which suggests a more subtle but significant reduction in EdU localisation at FANCD2 foci, and a significant reduction in EdU intensity per focus, despite equivalent induction of FANCD2 foci per cell; Figure 3.7b-d. We observed that MCM5 silencing, appeared to generate more EdU positive FANCD2 foci per cell across both conditions, likely reflecting a greater burden and hence carry-over of under-replicated regions from S-G2 into mitosis.

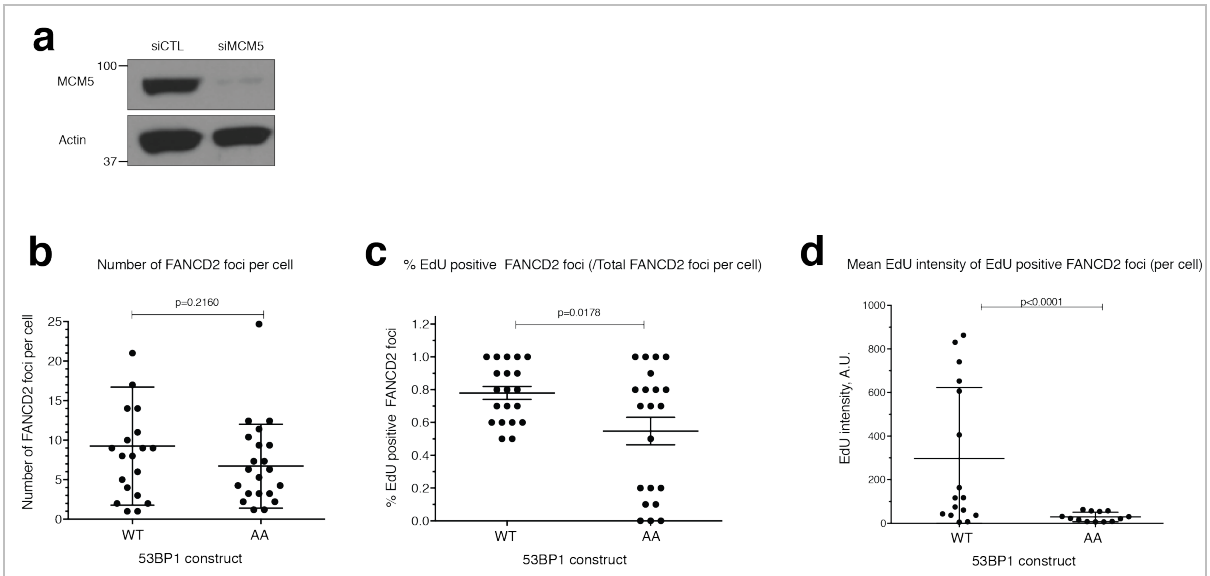

Figure 3.7 53BP1^{AA} impairs unscheduled DNA synthesis after reduced replication origin firing. (a) Immunoblot demonstrating effective MCM5 silencing. Quantification of (b) number of FANCD2 foci per cell; (c) % EdU positive FANCD2 foci; (d) mean EdU intensity per EdU focus (as defined by co-localisation with FANCD2).

3.2.5. 53BP1^{AA} interacts with TOPBP1 in a replication-stress dependent manner in mitosis

In addition to the formation of FANCD2 foci marking sites of replication stress carried into mitosis, it has recently been reported that TOPBP1 may also have a role co-localising with sites of mitotic DNA synthesis (Figure 3.1). *Lisby* and colleagues recently described a role for the multifunctional protein TOPBP1 in recruiting SLX4 and enabling EdU incorporation during mitosis (Pedersen et al., 2015). We performed immunoprecipitation of damaged mitotic U2OS cells expressing wildtype or 53BP1^{AA} derivatives.

Cells received doxycycline and CDK1 inhibitor as previously described to arrest cells at G2/M. Cells were then harvested upon release, this time into 0.1µg/ml nocodazole for 2h to ensure delay at mid-mitosis, while avoiding the DNA damaging effects of extended nocodazole treatment. This was to accommodate 'shake-off' of mitotic cells after 0.5Gy of irradiation (Figure 3.8a) or continued 0.2µM APH (Figure 3.8b). In the first instance, IR treatment of 53BP1^{AA} expressing U2OS cells appeared to be associated with a TOPBP1 interaction. This interaction was also seen to be damage-specific in response to APH; Figure 3.8b. This suggests that 53BP1^{AA} can interact with TOPBP1 during mitosis, potentially to the detriment of the normal role of TOPBP1 in tethering broken chromosomes until DNA repair can be reactivated in subsequent phases of the cell cycle (see discussion).

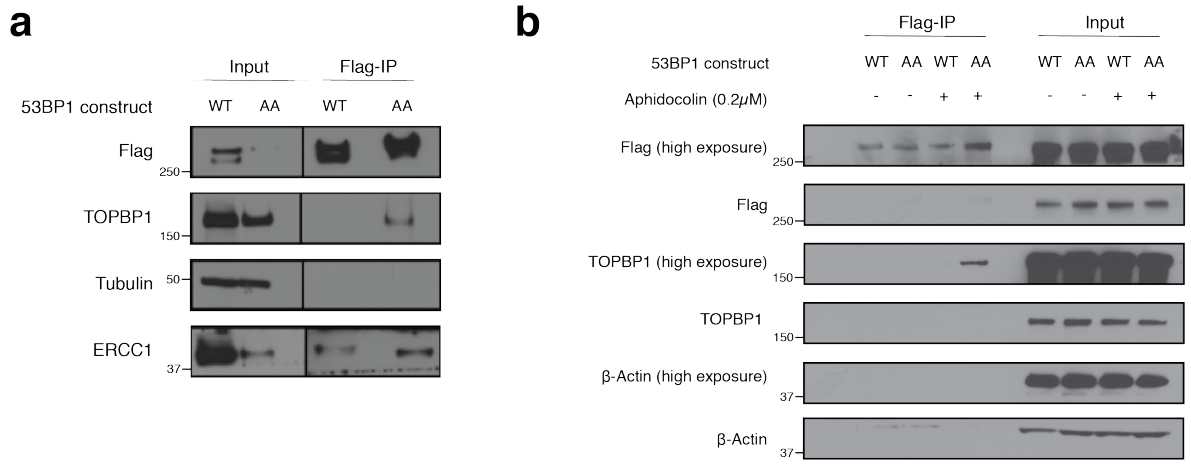

Figure 3.8 53BP1^{AA} interacts with TOPBP1 in a damage-dependent manner in mitosis. Flag immunoprecipitation in response to (a) IR or (b) APH treatment of U2OS cells.

To further extend this observation, mass spectrometry was performed using HeLa-S3 suspension cells expressing a tandem Flag-HA tagged focus forming region (FFR) of 53BP1 harbouring a wildtype or phospho-null mutation at the T1608/S1618 residues within the UDR; Figure 3.9a. HeLa-S3 cells were double thymidine synchronised and released into nocodazole for 6h prior to immunopurification. As would be expected, this 53BP1-FFR^{AA} mutant has been previously demonstrated to permit chromatin localization (Lee et al., 2014). These results demonstrate various interacting proteins are enriched for in the chromatin-bound fraction of 53BP1^{AA} (compared with 53BP1^{WT}), in particular CENPF, NUDT16L1 (the chaperone protein, TIRR (Drane et al., 2017)) and MDC1 (Figure 3.9b).

a

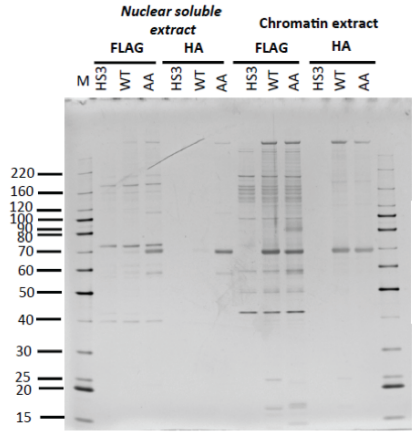

b

		Interacting proteins identified following TAP-MS analysis			
		53BP1-FFR^{WT}		53BP1-FFR^{AA}	
		Candidate	Unique peptides	Candidate	Unique peptides
Fraction	Nuclear-soluble	TP53BP1	15	TP53BP1	31
		LOR	2	NUDT16L1	15
		NUDT16L1	2	PYCRL	7
		S100A8	2	KPNA2	6
		HIST1H4A	2	HSPA9	5
		USP28	1	KPNB1	3
		HUST1H2AI	2		
		KIF11	1		
		HNRNPK	1		
	Chromatin-bound	TP53BP1	47	TP53BP1	47
		TPX2	8	MDC1	14
		HSPA9	7	CENPF	14
		LMNA	7	NUDT16L1	13
		DSG1	6	TPX2	10
		MDC1	6	LMNA	7

Figure 3.9 Mass spectrometry identifying differential interacting partners of 53BP1^{WT} and 53BP1^{AA} recombinants (tandem Flag HA tagged). (a) PAGE and silver staining of nuclear soluble and chromatin fractions was followed by tryptic digestion and mass spectrometry. (b) Unique interacting peptides identified by proteomic analysis of significance p>0.05 (experiment performed by Dipanjan Chowdhury Group; 2016).

3.3. Discussion

53BP1 exists in its dephosphorylated form throughout interphase, hence the expression of wildtype or phospho-null proteins should be functionally equivalent during S and G2 phases. However the expression of 53BP1^{AA} during mitosis is known to be able to facilitate its early ectopic recruitment to chromatin, visible as foci by live-cell imaging in metaphase or anaphase (Lee et al., 2014, Orthwein et al., 2014). In response to low dose IR of 0.5Gy, 53BP1^{AA} expression has been shown to be associated with increased lagging chromosomes and micronuclei formation, which appeared to be reversible after inhibition of DNA-PK (Lee et al., 2014). This effect was likely dominant negative since 53BP1^{AA} was co-expressed alongside the endogenous (phosphorylated) form of 53BP1. The persistent activation of 53BP1^{AA} in mitosis appeared to confer hypersensitivity to IR, which could also be reversed by DNA-PK inhibition (Orthwein et al., 2014).

The observed features of genome instability described, are found across various cancer types. It will be important to establish the contribution of mechanisms like mitotic 53BP1 activity in disease states, and the degree to which this specific aberration contributes to what is likely to be a general phenomenon of chromosomal mis-segregation defects. The overexpression of PPP4C and the regulatory subunit PPP4R3B in pancreatic, ovarian and gastric cancers (proteinatlas.org),

as well as the reduced expression of PLK1 across similar cancer types, may have an impact on the phosphorylation status of 53BP1 in mitosis, although this association will need to be verified.

Our work has demonstrated that the phenomenon of aberrant mitotic DDR activity may be relevant in the response to replication stress, a more cancer-relevant phenomenon that is likely to contribute to broader features of genome instability (Burrell et al., 2013). We have demonstrated that inappropriately 'active' 53BP1 during mitosis is sufficient to cause genome instability due to replication stress in the preceding S-phase. This was demonstrated in response to the DNA polymerase inhibitor APH, as well as MCM5 silencing, which can be used to suppress origin firing and reproduce double fork stalling events (Moreno et al., 2016). 53BP1 has been shown to associate with large replicons in G1, where the probability of stalling is greater, supporting a positive role for 53BP1's appropriately timed recruitment to chromatin to resolve under-replicated DNA during interphase (Moreno et al., 2016).

53BP1 nuclear bodies are thought to represent the sequestration of entangled/under-replicated DNA that persists when first attempts to mediate its repair (involving nucleases, TOPBP1, RAD52 and Polδ-3 in MiDAS etc. (Figure 3.1)) fail to resolve the underlying damage (Lukas et al., 2011, Harrigan et al., 2011, Pedersen et al., 2015, Bhowmick et al., 2016, Minocherhomji et al., 2015, Moreno et al., 2016). Recent work supports the theory that a second chance for repair is available, coordinated by 53BP1 in the following cell cycle, which confines the replication and repair of these lesions to the latter part of the subsequent S-phase, and utilise its downstream recruitment of RIF1 to control late origin firing (Spies et al., 2019). Furthermore, 53BP1's interaction with shieldin (see Chapter 4) appears to play an important role in inhibiting end-resection and in this instance, prevents inappropriate RAD51 recruitment in a replicative process that instead requires RAD52 for appropriate nuclear body dissolution (Spies et al., 2019). Our work describes the consequences of the mistimed utility of 53BP1 during mitosis, which is ordinarily dephosphorylated by PPP4C/R3β to permit its normal recruitment in the subsequent G1 (Lee et al., 2014). It is interesting to highlight the differences in regulation between first and second attempts at repair, whereby 53BP1-independent RAD52 recruitment for MiDAS may be appropriate for repair during mitosis, contrasting with the role of 53BP1 in facilitating the

mobilisation of RAD52 over RAD51 in the subsequent late S-phase replication-coupled repair. This interference with RAD52 loading during the process of MiDAS may explain our observation of 53BP1^{AA} reducing EdU incorporation at sites of damage after replication stress.

We observed an increase in the formation of acentric micronuclei with 53BP1^{AA} expression in response to APH, likely reflecting broken chromosome fragments. This contrasts with some observations of whole chromosome mis-segregations (lagging chromosomes) seen with concomitant IR treatment in mitosis in some studies (Orthwein et al., 2014, Lee et al., 2014), while comparable with others (Leimbacher et al., 2019). Our finding of increased acentric chromosome fragments within micronuclei fits with a model in which stalled replication intermediates fail to be adequately protected, and untethered chromatin fragments become separated from the mitotic spindle and undergo random segregation to daughter nuclei.

A recent study by *Stucki, Blackford* and colleagues in 2019 has observed that the interaction between MDC1 and TOPBP1 plays a critical role in the limited DDR which normally occurs in response to damage during mitosis (Leimbacher et al., 2019). The MDC1-TOPBP1 complex was suggested to stabilise spontaneous chromosome breaks in mitosis, possibly via a bridging role between tethered DNA ends. The finding that some DSBs remain unrepaired and co-localised with MDC1 and TOPBP1 up to 24h later, as well as the role for RNF8-RNF168-53BP1 in promoting TOPBP1 foci formation during interphase (but not mitosis), suggests a possible explanation for our results. The interaction of 53BP1^{AA} with TOPBP1 and possibly MDC1 during mitosis, may cause the sequestration of these factors away from the sites of damage. The BRCT0-2 and BRCT4/5 domains of TOPBP1 are responsible for its direct binding to phosphorylated MDC1 and 53BP1 respectively (Cescutti et al., 2010, Blackford et al., 2015, Leimbacher et al., 2019), hence there is the potential for sequestration and/or steric competition for binding between these proteins. Our findings are also in keeping with *Lisby's* work, phenocopying the impact of mitotic TOPBP1 depletion in terms of impairing MiDAS and leading to an increase in 53BP1 nuclear body formation in the following G1 (Pedersen et al., 2015).

It was interesting to note a preferential interaction of dephosphorylated 53BP1 FFR with its recently identified chaperone NUDT16L1 or TIRR (Drane et al., 2017), see Figure 3.9. The study

identifying this protein, posits a role for it in binding the tudor domain of 53BP1, and acting competitively with H4K20me2. While the majority of TIRR-bound 53BP1 is thought to be nucleoplasmic, it is possible some detergent-resistant fraction exists in dynamic equilibrium.

In this regard, it is noteworthy that we were unable to visualise 53BP1^{AA} foci at early stages of mitosis in response to replication stress, a finding which is consistent with the reported literature (Orthwein et al., 2014, Lee et al., 2014). We utilised 0.5% IGEPAL, 0.5M NaCl and benzonase for immunoprecipitation experiments (Figure 3.8), suggesting the chromatin-bound 53BP1 (its majority) is the fraction interacting with TOPBP1. The failure of 53BP1^{AA} to co-localise with FANCD2 foci in response to APH is perhaps not surprising, given the adverse contribution 53BP1^{AA} appears to play, which is likely spatially separated from sites of repair foci. It will be interesting to see whether downstream mediators of 53BP1, such as RIF1 and PTIP, are independent of this mitotic interaction, or contribute to this interaction.

Another notable finding was the mass-spectrometry interaction of the dephosphorylated 53BP1 FFR interacting specifically with the centromeric protein CENPF. A recent study has revealed a mitosis-specific R-loop driven ATR pathway which operates at centromeres to resolve catenations and suppress chromosome instability (Kabeche et al., 2018). RNAs have been implicated in mediating RNA binding at break sites (Francia et al., 2012) and serving as a trigger for 53BP1 transfer from TIRR to damage-associated chromatin (Botuyan et al., 2018). This distinct ATR-mediated mitotic signaling pathway centres around an interaction between ATR, Aurora A and CENPF to recruit RPA to centromeric R-loops for their dissolution; it is tempting to speculate that the preferential interaction of 53BP1^{AA} with CENPF could further contribute to the general phenomenon of genome instability which we have documented.

4. Chapter 4 Results: Shieldin interacts with 53BP1 to promote NHEJ and counter HR in BRCA1-deficient cells

4.1. Introduction

The discovery of 53BP1 and its two downstream mediators RIF1 and MAD2L2 contributing to the HR defect observed in BRCA1 deficiency, reveals an important axis involved in DSB repair pathway choice (see 1.2.3). However, it remains unclear whether there are any other members of the 53BP1-RIF1-MAD2L2 axis that may contribute to this function. It also remains to be seen how the NHEJ-promoting function of this complex is achieved, particularly in regard to any interaction between the chromatin and DNA compartments surrounding a DSB, and if there is any evidence of direct interaction with core end-joining machinery or whether the supportive function of the 53BP1 axis occurs indirectly.

BRCA1-deficient cancers represent a substantial fraction of germline and acquired genetic deficiencies defining various malignancies, including those affecting the breast, ovaries and prostate. While these are characterised by their responsiveness to therapies like platinum agents and PARP inhibitors, clinical trials also reveal intrinsic and acquired resistance, as discussed in 1.4.3 above. In order to manage these patients, it will be important to establish an exhaustive list of potential mechanisms which may bring about drug resistance.

One recent technological development which advances this effort is the utility of CRISPR-Cas9, in the setting of pooled forward genetic screening. The RNA-guided endonuclease Cas9 has emerged from the microbial CRISPR (clustered regular interspaced short palindromic repeat) immune system, and represents a transformational gene editing technology for performing precise programmable DNA modifications; these are targeted by short RNAs that hybridise with target DNA, allowing Cas9 to generate a precise DSB that can be repaired by NHEJ. This leads to the generation of indels which can create frameshift mutations and lead to nonsense mediated decay of transcripts and/or non-functional protein expression. Libraries of single guide RNAs (gRNA) can be generated by pooling together guides targeting any set of genes or non-coding

regions, and these can be used with Cas9 to perform high throughput screening of phenotypes of interest. For the purposes of identifying markers of drug resistance, genome-wide loss of function screens continue to provide valuable insights. We begin by using this method to identify suppressors of PARP inhibitor sensitivity in BRCA1-mutant cells.

4.2. Results

4.2.1. CRISPR-Cas9 screens identify suppressors of PARP-inhibitor sensitivity in BRCA1-mutant cells.

A CRISPR-Cas9 survival screen was used to identify suppressors of PARP-inhibitor sensitivity in a BRCA1-mutant cell line (performed by W-T Chiang, PhD student, Steve Jackson Group, 2016). In brief, the breast cancer cell line SUM149 (harbouring null and Δexon11 BRCA1 alleles) was infected with the whole-genome CRISPR-Cas9 gRNA library (Gecko v.2) at a multiplicity of infection of 0.3, prior to seven days of antibiotic selection with puromycin. Library-infected cells were then cultured for 14 days in the presence of DMSO or one of three PARP inhibitors (olaparib, AZD2461 and talozaporib/BMN673). Genomic DNA extraction, library preparation and next-generation sequencing was performed. Read counts were analysed using the MAGeCK algorithm and ranked plots of guide abundance were generated (by M Herzog, PhD student, Steve Jackson Group, 2016); Figure 4.1a. The screen identified known NHEJ factors which when lost restore HR in BRCA1-mutant cells, including TP53BP1, RIF1 and MAD2L2 (Figure 4.1b). The two genes which scored highest based on p-value and log-fold change, were two previously uncharacterised genes, FAM35A and C20orf196.

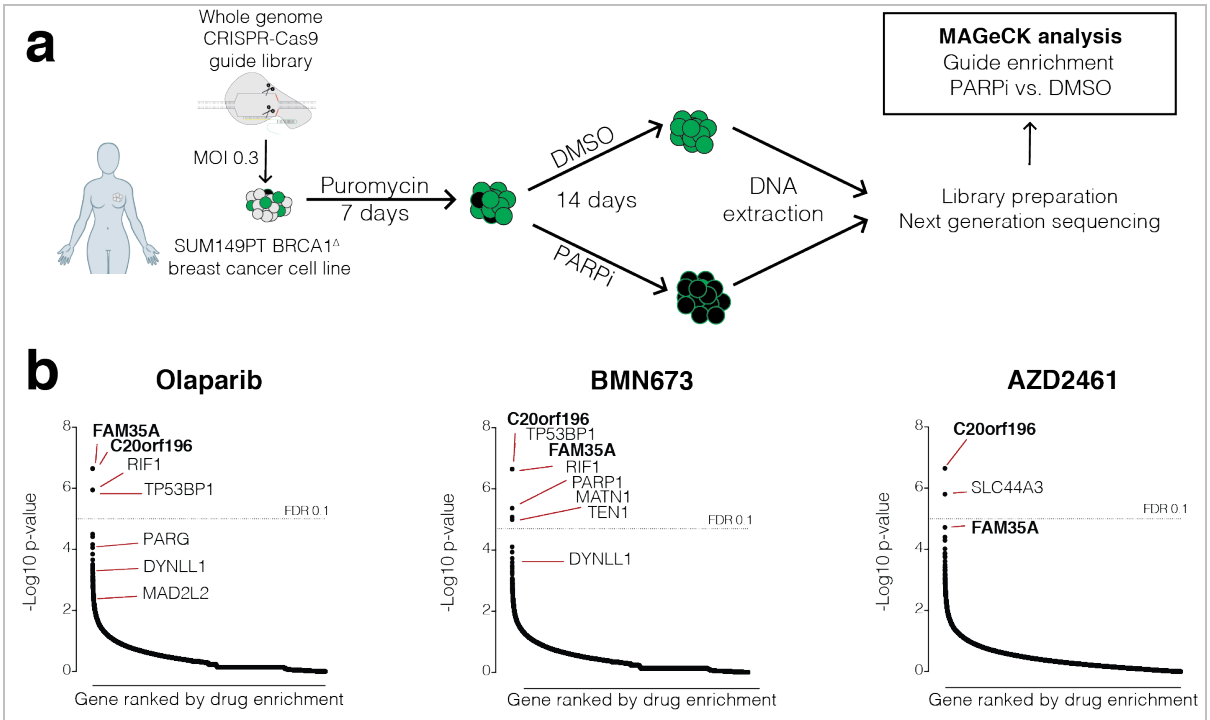

Figure 4.1 (a) Schematic of CRISPR-Cas9 screen for PARP-inhibitor resistance factors in BRCA1-mutant cancer cell line. (b) MAGeCK analysis of guide enrichments following PARP-inhibitor treatment; False Discovery Rate (FDR) of 0.1 shown on each plot.

These gene hits were subsequently validated (Figure 4.2). In the first instance, siRNAs were generated which were validated using cells transiently expressing GFP-tagged expression constructs of the respective gene products (Figure 4.2a,b,d). The human immortalised epithelial cell line RPE-1^{p53ko} were subsequently used as a parental cell line, along with a BRCA1-null version (generated by R. Belotserkovskaya, Postdoctoral scientist, Steve Jackson Group, 2015). These siRNAs were used to confirm rescue of olaparib-mediated cell death in BRCA1-null but not BRCA1-proficient cells (Figure 4.2a,b). Differences in cell survival did not appear to be mediated by differences in cell cycle profile (data not shown). CRISPR-Cas9 was used to generate FAM35A and C20orf196 de-novo gene knockouts in RPE-1^{p53ko} and RPE-1$^{p53ko/BRCA1ko}$ cell lines. This was particularly challenging in the latter, where polyploidy associated with BRCA1 deficiency reduced the probability of generating complete knockouts (Figure 4.2e). Complementations (generated by Flp-In of GFP-tagged constructs) demonstrated the specificity of FAM35A and C20orf196 loss to mediate olaparib sensitivity in the setting of BRCA1 deficiency (Figure 4.2c-e). It is noteworthy that C20orf196 overexpression caused a dominant-negative sensitisation of RPE-1$^{p53ko/BRCA1ko/C20orf196ko}$ cells to olaparib.

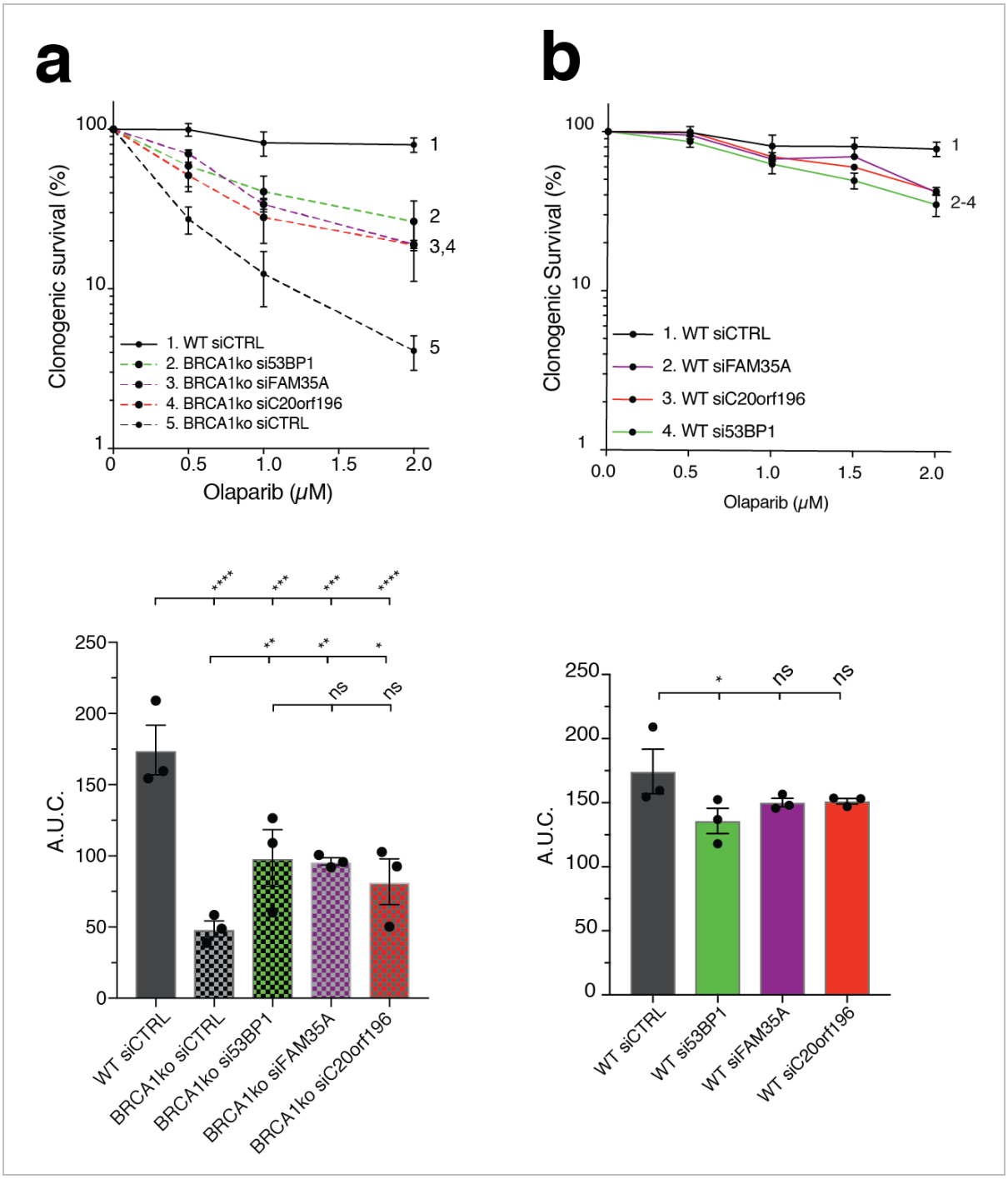
a
Clonogenic survival (%)
100
10
1
0
0.5
1.0
1.5
2.0
Olaparib (μM)
1
2
3,4
5
1. WT siCTRL
2. BRCA1ko si53BP1
3. BRCA1ko siFAM35A
4. BRCA1ko siC20orf196
5. BRCA1ko siCTRL
b
Clonogenic Survival (%)
100
10
1
0.0
0.5
1.0
1.5
2.0
Olaparib (μM)
1
2-4
1. WT siCTRL
2. WT siFAM35A
3. WT siC20orf196
4. WT si53BP1
A.U.C.
250
200
150
100
50
0
****
***
***
****
**
**
*
ns
ns
WT siCTRL
BRCA1ko siCTRL
BRCA1ko si53BP1
BRCA1ko siFAM35A
BRCA1ko siC20orf196
A.U.C.
250
200
150
100
50
0
*
ns
ns
WT siCTRL
WT si53BP1
WT siFAM35A
WT siC20orf196

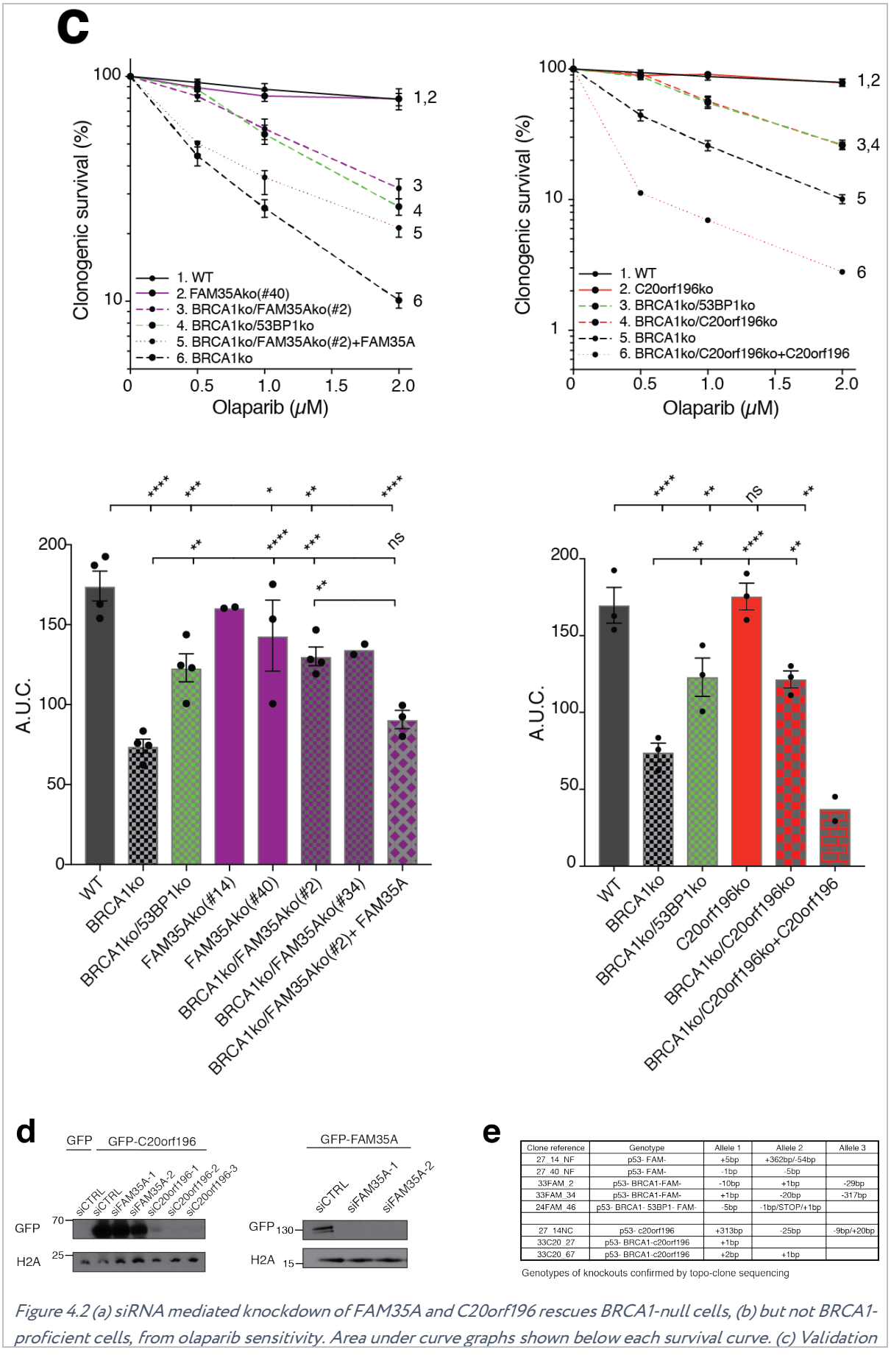

Clone reference	Genotype	Allele 1	Allele 2	Allele 3
27_14_NF	p53- FAM-	+5bp	+362bp/-54bp	
27_40_NF	p53- FAM-	-1bp	-5bp	
33FAM_2	p53- BRCA1-FAM-	-10bp	+1bp	-29bp
33FAM_34	p53- BRCA1-FAM-	+1bp	-20bp	-317bp
24FAM_46	p53- BRCA1- 53BP1- FAM-	-5bp	-1bp/STOP/+1bp	
27_14NC	p53- c20orf196	+313bp	-25bp	-9bp/+20bp
33C20_27	p53- BRCA1-c20orf196	+1bp		
33C20_67	p53- BRCA1-c20orf196	+2bp	+1bp	

Figure 4.2 (a) siRNA mediated knockdown of FAM35A and C20orf196 rescues BRCA1-null cells, (b) but not BRCA1-proficient cells, from olaparib sensitivity. Area under curve graphs shown below each survival curve. (c) Validation

of FAM35A (left) and C20orf196 (right) knockouts rescuing olaparib sensitivity, and complementations. (d) Validation of siRNA efficacy used in (a) by western blot. (e) Validation of CRISPR-Cas9 knockouts by Topo-cloning and sequencing.

4.2.2. FAM35A and C20orf196 domains, interactions and IRIF formation.

We sought to establish if any structural insights could be gained about FAM35A and C20orf196 genes, and whether there was any relationship between the two genes. FAM35A and C20orf196 genes arise relatively late in evolution, with conservation principally among vertebrates (Figure 4.3a,b). FAM35A encodes for two principle isoforms of 835 and 904 amino acids. Structure prediction modelling, by RaptorX, identified an unstructured N-terminal half, and a C-terminal half harbouring three highly-conserved oligonucleotide/oligosaccharide-binding (OB)-folds. One of these contained a pair of (CXXC) Zn-finger motifs, which were also identifiable in the following proteins: 1/ DNA damage-induced apoptosis suppressor protein (Q8IXT1); 2/ Meiosis-specific with OB domain-containing protein (Q8N635); 3/ DNA repair-scaffolding protein (Q14159); 4/ CTC1 and 5/ RPA70. The latter bind to single-stranded DNA, and these OB-folds were highly-suggestive of a DNA-interacting module.

C20orf196 encoded for a shorter protein of 201aa, with potentially one or two wing-helix (WH) domains in the C-terminus, similar to those in the yeast CST subunit Stn1 (Sun et al., 2009);Figure 4.3a. These structural similarities to two components of the CST complex were suggestive of functional similarities that will be discussed in 4.3 below.

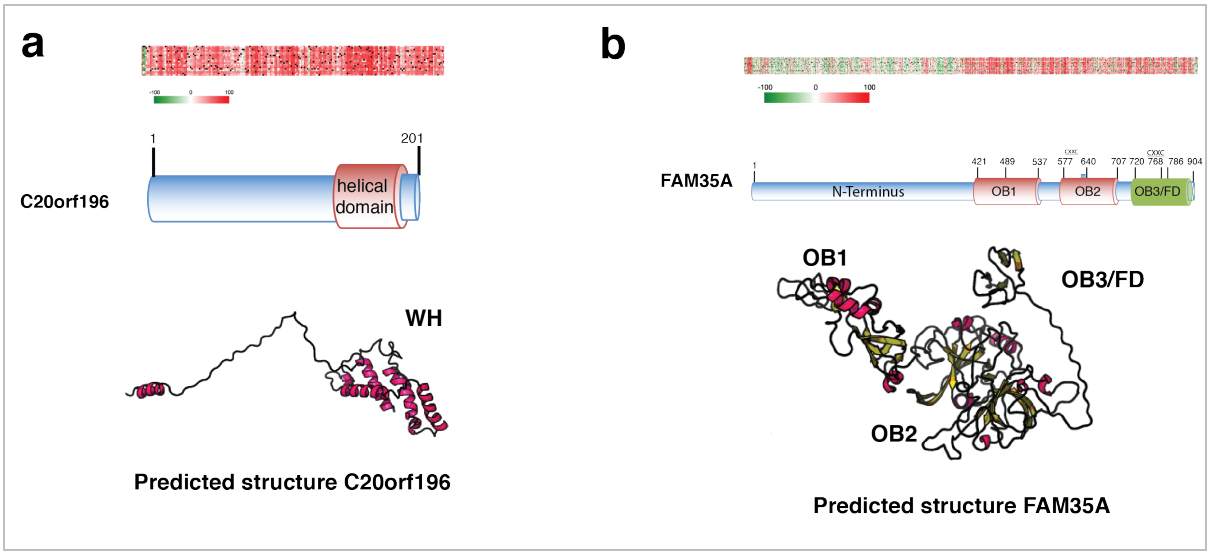

Figure 4.3 RaptorX modelling (raptorx.uchicago.edu; bottom), schematic (middle) and per-residue analysis of functional changes given a point mutation (predictprotein.org; top) for (a) C20orf196 and (b) FAM35A.

Given that FAM35A and C20orf196 demonstrate similar phenotypes, we hypothesised that they may act in concert. We investigated whether FAM35A and C20orf196 functionally interact, in the first instance by utilising a lacR/lacO co-localisation system in U2OS cells. In brief, mCherry-LacR tagged C20orf196 constructs were generated, and co-transfected in a U2OS cell line harbouring a series of lacO repeats, in conjunction with a GFP-tagged expression construct of various FAM35A derivatives (U2OS LacSceIII cell line gift from D. Durocher, Toronto). This revealed an interaction between FAM35A and C20orf196 mediated via the C-terminus and OB3/"FAM"-domain (Figure 4.4a-c). This was confirmed biochemically using cell extracts expressing GFP-FAM35A derivatives and HA-C20orf196, as well as by the observation that the latter appears to co-stabilise the expression of the former (Figure 4.4d-f).

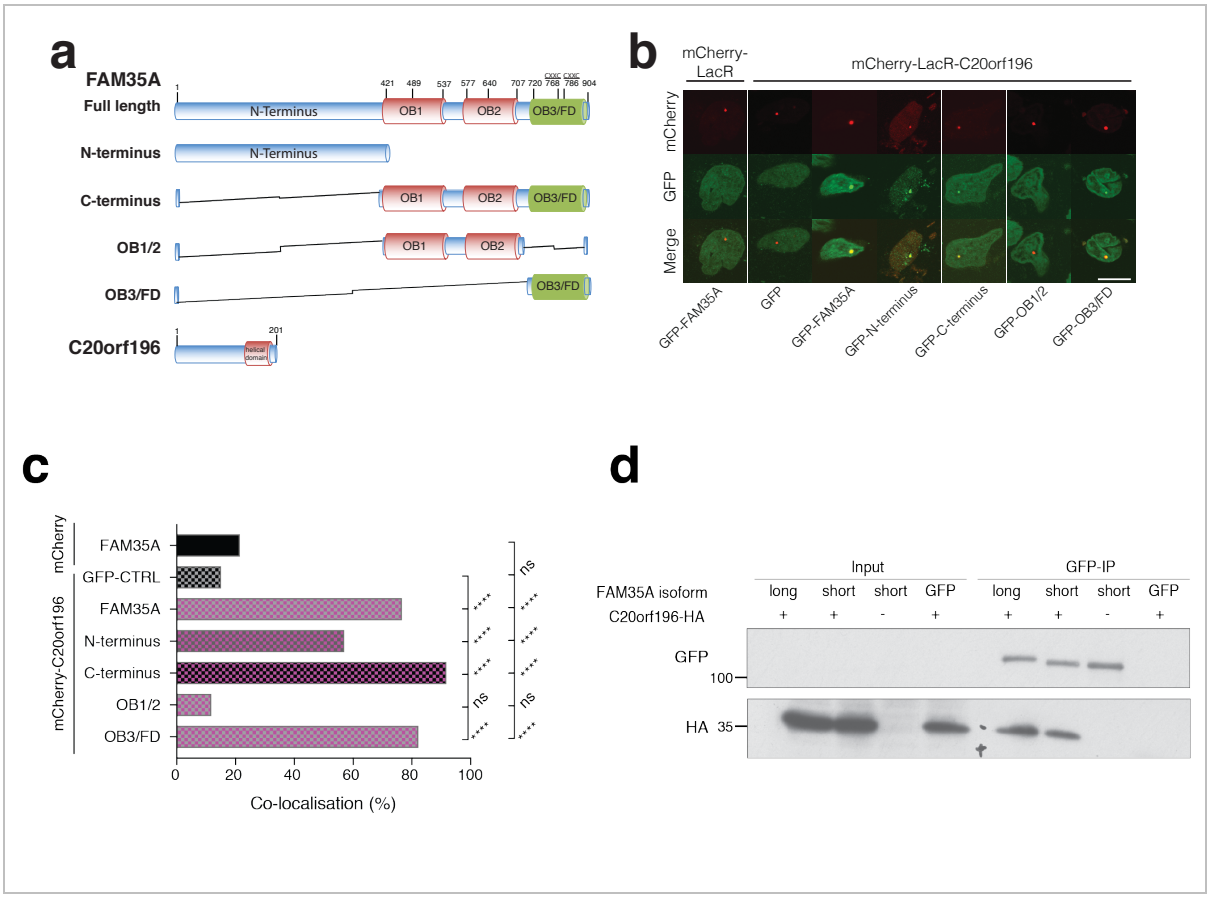

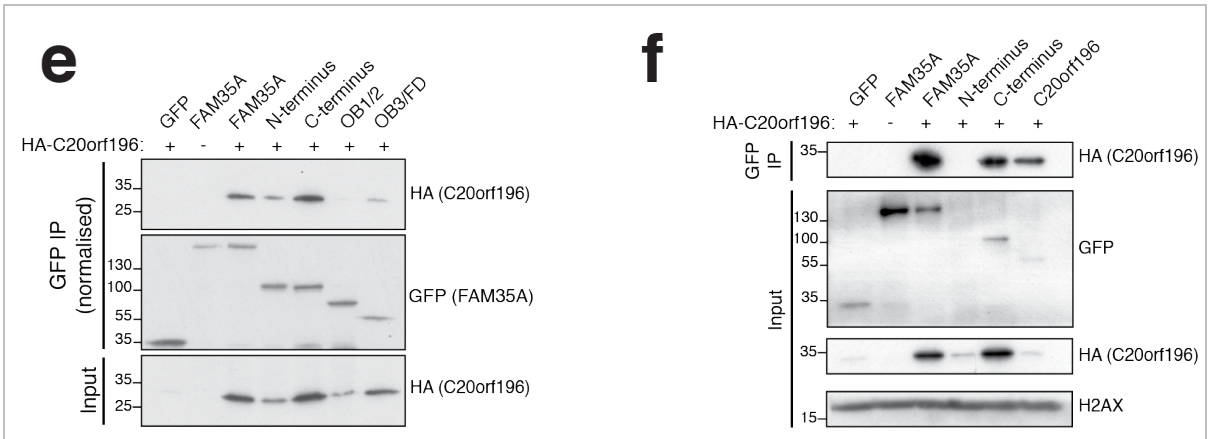

Figure 4.4 (a) FAM35A and C20orf196 constructs used in this study, (b) establish an interaction via FAM35A N-terminus and OB3/FAM-domain with C20orf196, quantified in (c). (d) Co-immunoprecipitation demonstrating both FAM35A isoforms interact with C20orf196. (e) Mapping the domains of interaction and (f) non-normalised co-immunoprecipitation assay showing the effects of co-stabilisation. GFP-tagged constructs used as bait for GFP co-immunoprecipitation experiments.

We sought to establish whether the interaction between FAM35A and C20orf196 was direct or indirect. In order to assess this, bacterial constructs were designed and synthesised within an RSF-duet plasmid vector, encoding for His-tagged C20orf196 in tandem with GST-tagged FAM35A for use with Rosetta bacteria and IPTG-mediated expression. We engineered this vector to express the proteins in tandem, based on their co-stabilisation. While these could be detected with harsh lysis conditions (Figure 4.5a), it was not possible to isolate the proteins with milder conditions (Figure 4.5b). Purified products of full-length GST-FAM35A (Novus Biologicus) and His-C20orf196 (Creative BioMart) were then commercially obtained, and in-vitro GST pulldown confirmed a direct interaction between the two proteins (Figure 4.5c).

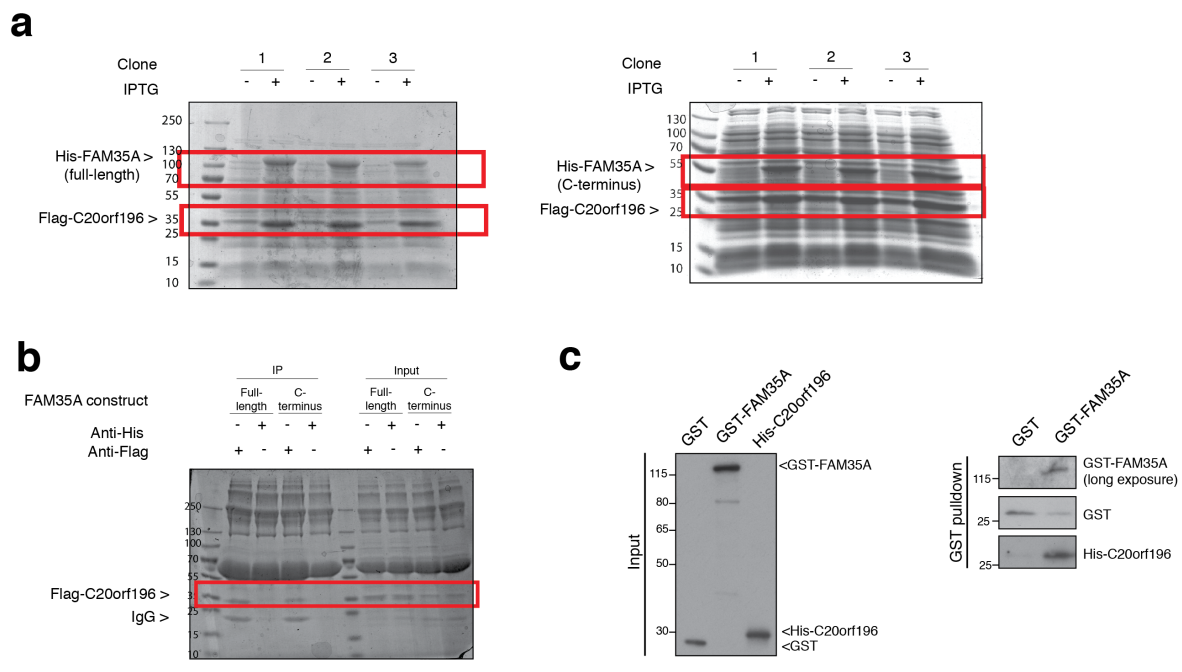

Figure 4.5 (a) Protein purification under (a) harsh (2% SDS) and (b) milder (sonication/1% Triton-X) conditions; (c) Recombinant GST-FAM35A and His-C20orf196 interact directly (experiment performed with M. Sczaniecka-Clift, Postdoctoral scientist, Steve Jackson Group, 2017)).

The screen results demonstrate genetic loss of FAM35A or C20orf196 phenocopies the effect already established due to loss of 53BP1, RIF1 or MAD2L2 on PARP inhibitor resistance in BRCA1-deficient cells. Having established the interaction between FAM35A and C20orf196, we speculated whether the interaction extended to these NHEJ accessory factors. Co-immunoprecipitation experiments were performed with GFP-tagged FAM35A or C20orf196 and HA-tagged C20orf196 or FAM35A respectively; Figure 4.6. This confirmed a constitutive interaction between our newly identified complex and established components of the 53BP1-RIF1-MAD2L2 cascade, which was unaffected by the addition of camptothecin. FAM35A was consistently more challenging to detect relative to C20orf196, suggestive of its lower endogenous abundance, which was subsequently confirmed via mass-spectrometry studies with collaborators (Petra Beli Group, Mainz, Germany; see appendix 6.6 and 6.7 for enrichments).

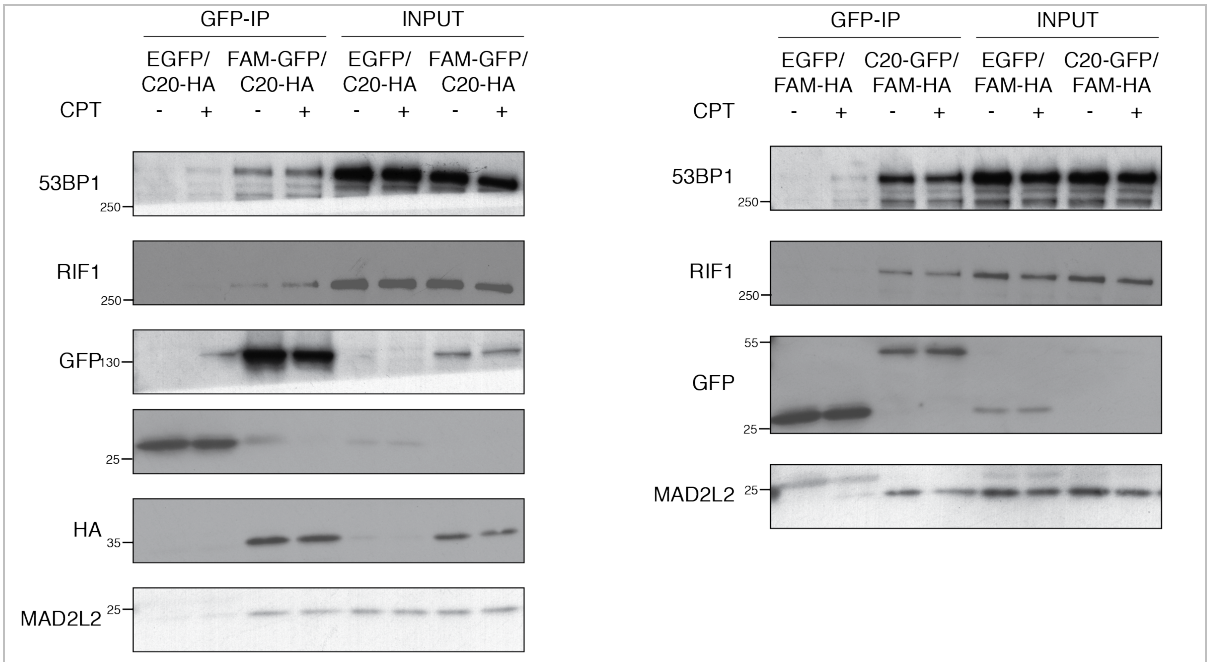

Figure 4.6 FAM35A and C20orf196 interact with 53BP1, RIF1 and MAD2L2, by GFP co-immunoprecipitation experiments in BRCA1-proficient HEK293 cells.

We next sought to establish whether FAM35A/C20orf196 is recruited to sites of DNA damage, and the nature of the relationship with the 53BP1-axis members. In the first instance, U2OS cells stably expressing RFP-53BP1 were transfected with GFP-tagged FAM35A or C20orf196 constructs, prior to live-cell imaging and generating localised DNA damage induced by laser micro-irradiation. 53BP1 could be readily detected within five minutes, and both FAM35A and C20orf196 localised to sites of damage in similar timeframes (Figure 4.7a). DNA repair factors demonstrate localisation to discrete 'foci' in response to damage, and we were able to detect these in response to camptothecin and irradiation (Figure 4.7b). Figure 4.7c demonstrates the ability to detect full-length and N-terminus FAM35A derivatives, but not the C-terminus of FAM35A, co-localising with γH2AX in response to irradiation (irradiation-induced foci, IRIF). We evaluated the dependence of 53BP1 axis members on the formation of FAM35A and C20orf196 IRIF. Depletion of 53BP1, RIF1 and MAD2L2 attenuated the formation of foci (relative to control conditions) by approximately 80% (Figure 4.7d-g). Notably, FAM35A depletion (and to a lesser extent C20orf196) attenuates the ability to detect the other foci, likely reflecting their co-stabilisation effect noted in Figure 4.4e,f. Hence, 53BP1-RIF1-MAD2L2 act upstream of

FAM35A/C20orf196, while depletion of the 53BP1-interacting protein PTIP has no effect (Figure 4.7h). As a general observation C20orf196 foci were notably smaller than those of FAM35A.

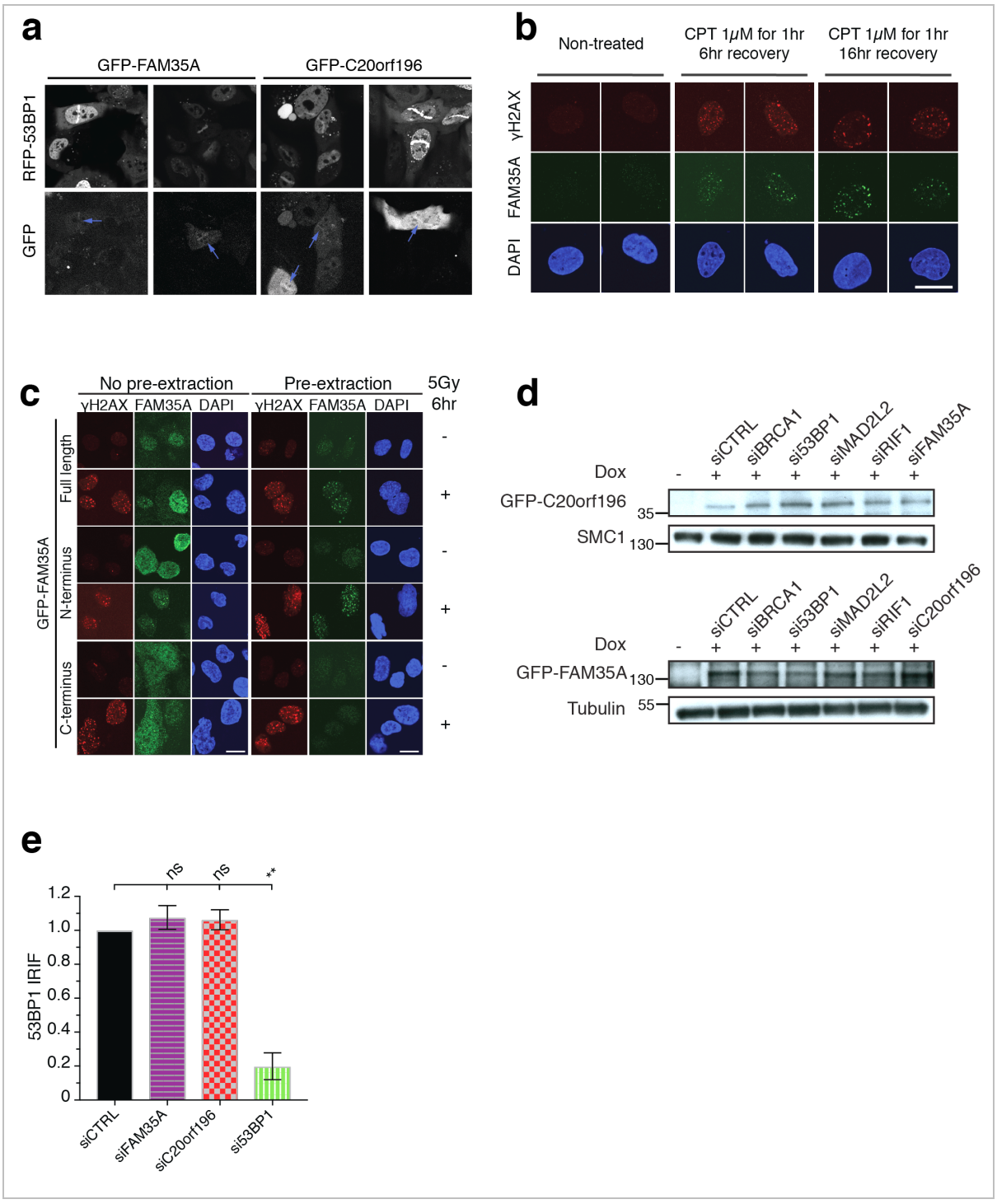

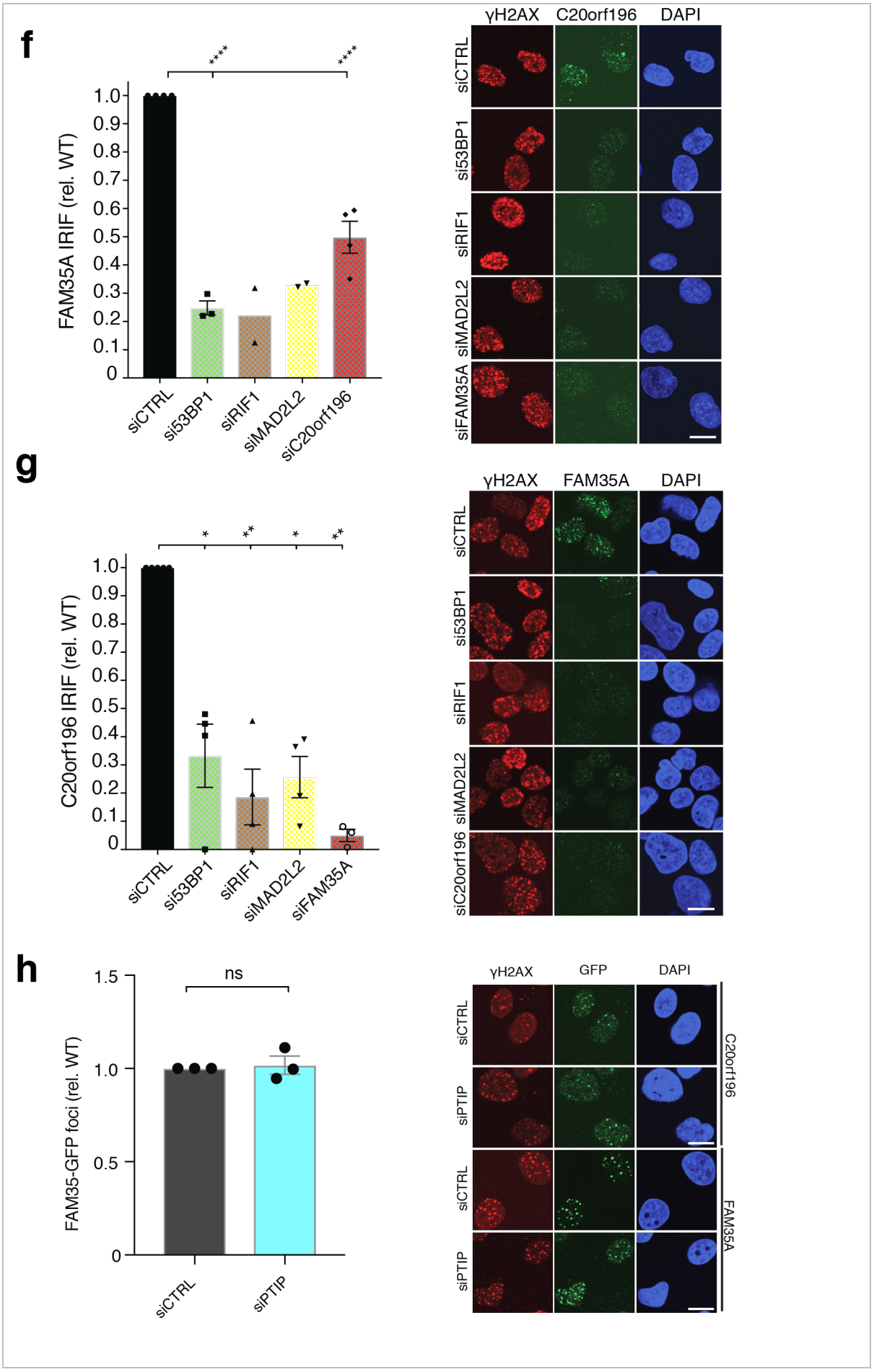
f
FAM35A IRIF (rel. WT)
siCTRL
si53BP1
siRIF1
siMAD2L2
siC20orf196
γH2AX
C20orf196
DAPI
siFAM35A
g
C20orf196 IRIF (rel. WT)
siFAM35A
FAM35A
h
FAM35-GFP foci (rel. WT)
ns
siPTIP
GFP

Figure 4.7 (a) FAM35A and C20orf196 are recruited to localised sites of damage induced by laser micro-irradiation (by live-cell imaging) and (b) camptothecin (immunofluorescence micrographs of fixed cells). (c) Full-length and N-terminus of FAM35A but not its C-terminus form IRIF which can be visualised by IF after pre-extraction. (d) FAM35A and C20orf196 expression levels are not affected by BRCA1/53BP1-axis depletion. (e) FAM35A/C20orf196 do not affect 53BP1 IRIF formation, but 53BP1, RIF1 and MAD2L2 depletions do attenuate (f) FAM35A, and (g) C20orf196 IRIF. (h) PTIP depletion did not affect FAM35A/C20orf196 IRIF. Representative micrographs shown adjacent to quantifications.

Since the N-terminus of FAM35A was able to form IRIF, we postulated whether its recruitment shared the same dependencies as the full-length FAM35A. We confirmed a similar effect on foci number when 53BP1, RIF1 or MAD2L2 were silenced, and further defined the interaction with MAD2L2 as occurring via this domain; Figure 4.8a,b.

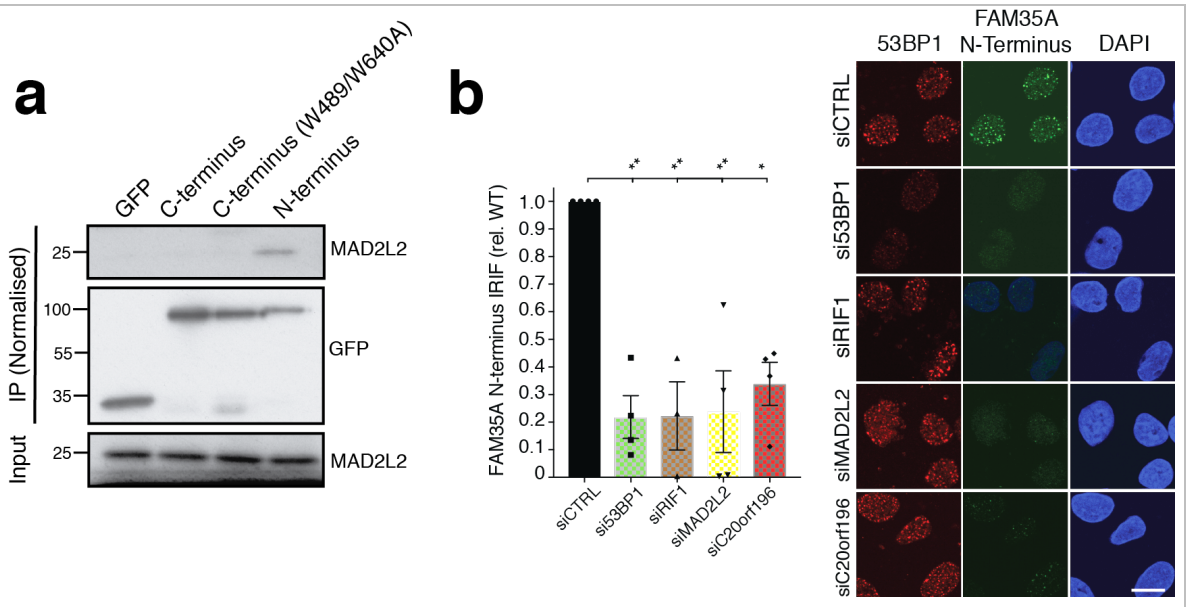

Figure 4.8 (a) Co-immunoprecipitation showing interaction between N-terminus of FAM35A and MAD2L2, and (b) similar dependencies of FAM35A N-terminus IRIF on 53BP1-RIF1-MAD2L2 axis (with representative micrographs on the right).

We performed super-resolution microscopy of both full-length and N-terminus of FAM35A (both harbouring an N' GFP tag), which were co-expressed with RFP-53BP1, in an effort to explore the spatial relationship between these proteins. If FAM35A oligomerised via its C-terminus we might expect larger filamentous complexes more spatially separated from a core of 53BP1, hence forming larger distances between detectible signals. However, we were able to establish that both full-length and N-terminal FAM35A lie within close proximity to chromatinised 53BP1, in a conformation that was not distinguishable by these super-resolution conditions, potentially supporting an association between the N-terminus of FAM35A and

chromatinised 53BP1, and less of an importance of the C-terminus for promoting any oligomerisation; Figure 4.9.

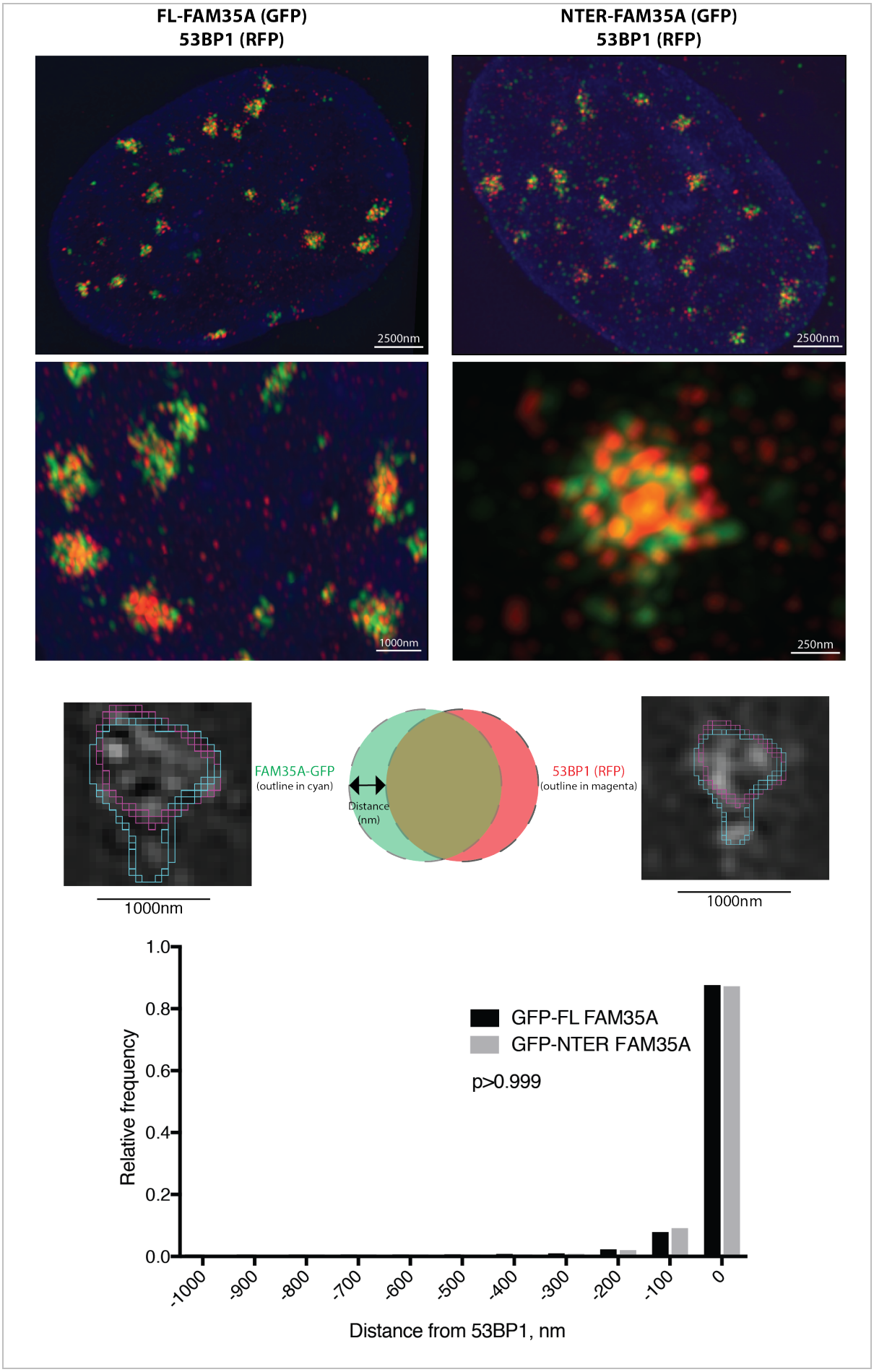
FL-FAM35A (GFP)
53BP1 (RFP)
NTER-FAM35A (GFP)
53BP1 (RFP)
2500nm
2500nm
1000nm
250nm
FAM35A-GFP
(outline in cyan)
Distance
(nm)
53BP1 (RFP)
(outline in magenta)
1000nm
1000nm
Relative frequency
1.0
0.8
0.6
0.4
0.2
0.0
GFP-FL FAM35A
GFP-NTER FAM35A
p>0.999
-1000
-900
-800
-700
-600
-500
-400
-300
-200
-100
0
Distance from 53BP1, nm

Figure 4.9 Super-resolution microscopy showing overlap of FAM35A N-terminus and 53BP1 in IRIF. Representative micrographs (top), representative approach of algorithm used to quantify spatial overlap (middle); histogram showing relative distance of FAM35A pixels from 53BP1 core (bottom).

4.2.3. FAM35A and C20orf196 promote NHEJ and immunoglobulin class-switch recombination.

Given the dependence of FAM35A/C20orf196 recruitment to sites of damage via the 53BP1-RIF1-MAD2L2 axis, we wanted to address whether this complex contributes to the process of NHEJ. In the first instance, we assessed the impact of depleting FAM35A or C20orf196 on the ability to randomly integrate a linearised transfected plasmid. Depletion of both genes individually reproduced the random plasmid integration defect observed with silencing 53BP1 or core end-joining machinery factors such as XRCC4 and LIG4; Figure 4.10a. This was supported by the cellular sensitivity to irradiation observed in FAM35A or C20orf196 knockout cells, generated using the parental cell line RPE-1^{p53ko} (Figure 4.10b; experiments performed with scientific technician Julia Coates, Steve Jackson group; 2017).

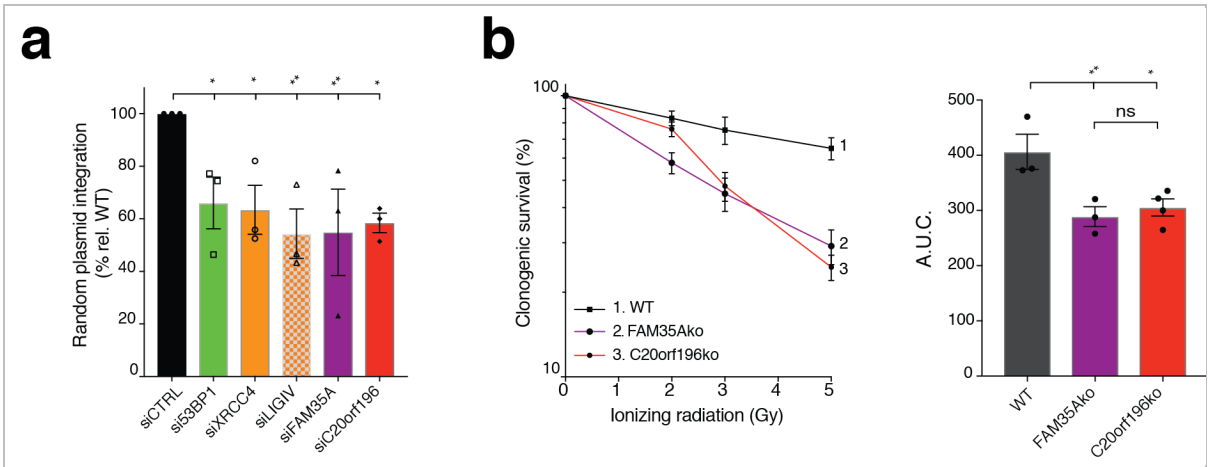

Figure 4.10 FAM35A and C20orf196 contribute to NHEJ as supported by effects of depletion or knockout on (a) random plasmid integration and (b) cellular sensitivity to irradiation; right graph shows area under curve.

We sought to establish whether FAM35A/C20orf196 contributed to the process of physiological NHEJ, by the assessment of class switch recombination (Figure 4.11a). We designed guides for mouse Fam35a and C20orf196 genes in order to generate knockouts in CH12-Cas9 clones. Cytokine stimulation led to comparable AID expression and cellular proliferation (data not shown), enabling the measurement of IgM to IgA switching via flow cytometry. Fam35a or C20orf196 knockout phenocopied the effect of 53bp1 or Mad2l2 knockout (CSR experiment

performed by Ludovic Deriano Group; 2017); Figure 4.11b (complementation experiments performed for C20orf196ko; data not shown).

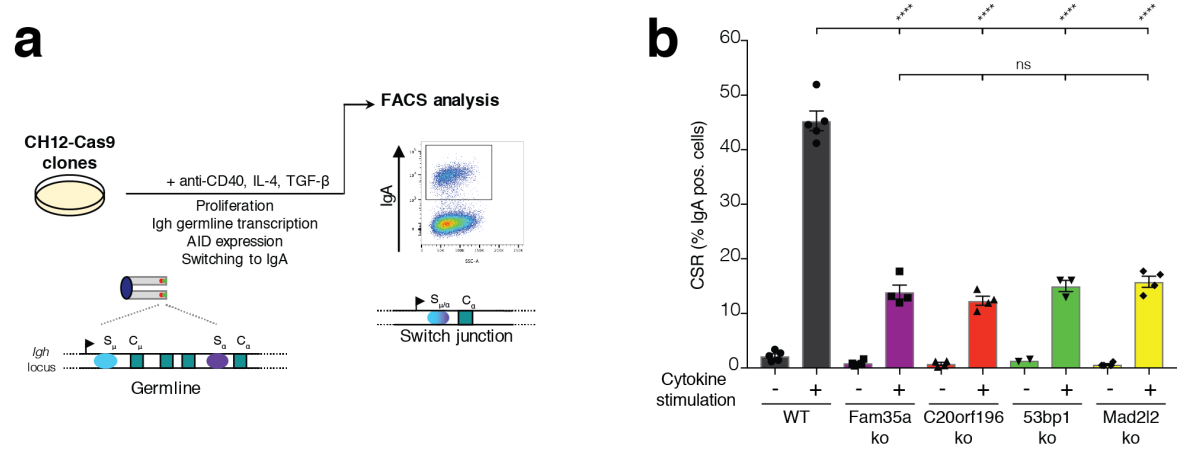

Figure 4.11 (a) Schematic of class switch recombination assay, demonstrating (b) CSR defect due to Fam35a or C20orf196 knockout in mouse B-cells (experiment performed by Ludovic Deriano Group; 2017).

4.2.4. FAM35A and C20orf196 promote telomere-mediated fusions and limit DNA end-resection.

In addition to the contribution of Fam35a/C20orf196 to class switch recombination, we also examined the impact of their depletion on telomere-mediated fusions after telomere-end deprotection. As has been demonstrated for 53bp1 (Martinez et al., 2012), Rif1 (Chapman et al., 2013) and Mad2l2 (Boersma et al., 2015), depletion of these NHEJ factors leads to telomere fusion following deprotection, which is experimentally achieved by TRF2 depletion using a thermo-sensitive allele system (TRF2ts) in MEF cells (Boersma et al., 2015) (Figure 4.12a). Fam35a and C20orf196 depletion phenocopied the effect of Mad2l2 depletion, abrogating telomere fusions by ½ to 2/3 (experiment performed by Jacqueline Jacobs Group; 2017), Figure 4.12b.

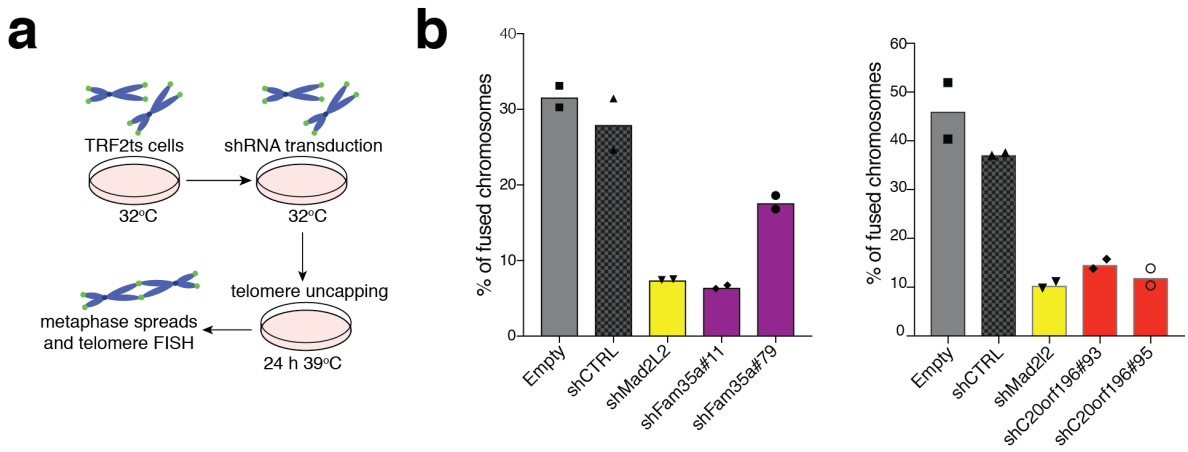

Figure 4.12 (a) Schematic of telomere fusion assay in MEFs, demonstrating (b) Fam35a/C20orf196 mediate telomere fusion upon deprotection by TRF2 depletion (experiment performed by Jacqueline Jacobs Group; 2017).

One suggested mechanism for blocking telomere fusion has been the dysregulation of DNA end-resection which leads to processing of DNA ends that renders the ends incompatible for end-joining. We tested this hypothesis by visualising ssDNA in FAM35A and C20orf196 knockout cells in response to camptothecin. This revealed a disinhibition of end-joining (Figure 4.13a). This result was reinforced by the effect of camptothecin-induced RPA2 loading as measured by cumulative RPA2 intensity (following pre-extraction; experiments performed with PhD student Dominic Pilger; Steve Jackson Group; 2018); Figure 4.13b. In the absence of FAM35A/C20orf196, the helicase BLM likely mediated our observation of hyperresection, as measured by RPA intensity in BLM depleted cells lacking FAM35A or C20orf196 (Figure 4.13b). This was supported by evidence of increased BLM accumulation at sites of laser micro-irradiation in FAM35A or C20orf196 knockout cells; Figure 4.13c. This effect of limiting resection did not appear to be a by-product of affecting RPA2 residency time at sites of resected double-strand breaks, as established by FRAP (Figure 4.13d).

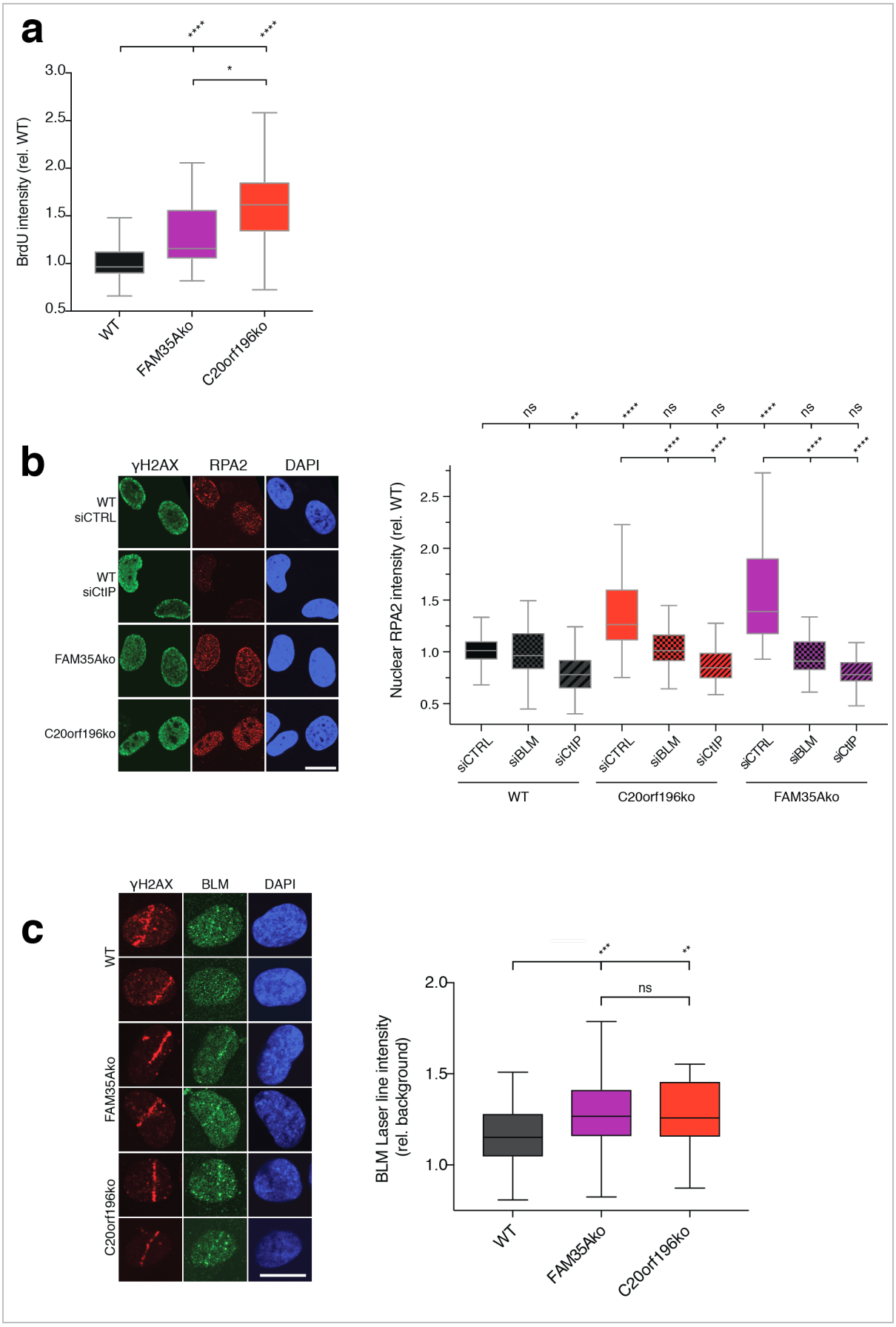
a
BrdU intensity (rel. WT)
3.0
2.5
2.0
1.5
1.0
0.5
****
****
*
WT
FAM35Ako
C20orf196ko
b
γH2AX
RPA2
DAPI
WT siCTRL
WT siCtIP
FAM35Ako
C20orf196ko
Nuclear RPA2 intensity (rel. WT)
ns
**
****
ns
ns
****
ns
ns
siCTRL
siBLM
siCtIP
WT
C20orf196ko
FAM35Ako
c
γH2AX
BLM
DAPI
WT
FAM35Ako
C20orf196ko
BLM Laser line intensity (rel. background)
***
**
ns
2.0
1.5
1.0
WT
FAM35Ako
C20orf196ko

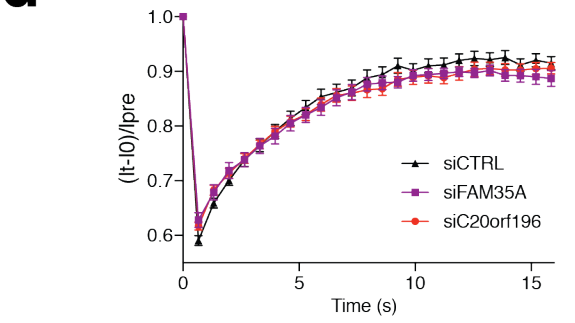

GFP-RPA1	siCTRL	siFAM35A	siC20orf196
Mean residence time (s)	4.74 +/- 0.30	4.89 +/- 0.45	4.67 +/- 0.24
R Square	0.98	0.96	0.96
number of cells, n	28	22	30

+/- 95% Confidence Intervals

Figure 4.13 FAM35A/C20orf196 knockout promotes (a) ssDNA and (b) RPA2 accumulation, likely resulting in disinhibition of end-resection mediated by (c) BLM accumulation at sites of damage (performed with PhD student D. Pilger, Jackson Group; 2018) (d) FRAP confirms equivalent RPA2 turnover after FAM35A or C20orf196 depletion.

4.2.5. FAM35A OB folds mediate ssDNA interaction and is required for IR resistance.

Given the effect of FAM35A/C20orf196 on limiting DNA end-resection, we postulated that the OB-folds of the C-terminus of FAM35A may serve a role in competing with resection promoted by BLM. Alignment of yeast RPA2 and the C-terminus of FAM35A revealed two tryptophan residues which likely played a critical role in DNA binding and could be mapped to within the OB1 and OB2 domains (evaluated with Luca Pellegrini, Department of Biochemistry, Cambridge; 2017); Figure 4.14a,b. We generated FAM35A derivatives harbouring W→A mutations which would be predicted to abrogate DNA binding, based on the domain's shared functional homology to the single-stranded DNA binding protein RPA2. Oligo-IP revealed binding to single-stranded DNA that appeared to be dependent on these two residues, while binding to dsDNA was less consistent and never affected by W→A point mutations (Figure 4.14b).

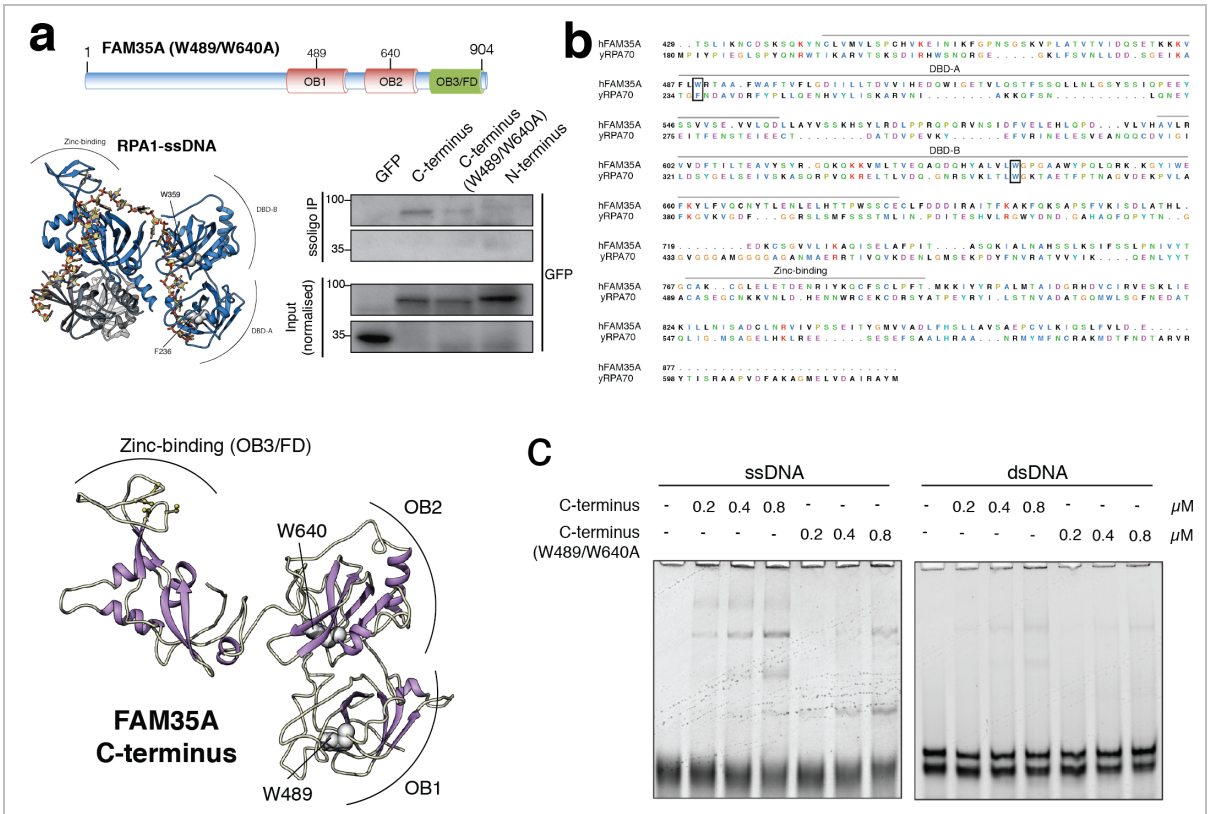

Figure 4.14 (a) Schematic structure of FAM35A, and similarity to RPA bound to ssDNA, highlighting two W residues predicted to be relevant for DNA binding; as demonstrated by cell lysate co-incubation and pulldown of biotinylated oligos, which revealed W489/W640 mediated binding to ssDNA (performed with PhD student Jonathan Lam, Steve Jackson Group; 2017). (b) Sequence homology to yRPA2 reveals potential residues critical for DNA binding. (c) EMSA confirms binding to ssDNA mediated via W489 and W640 (EMSA performed by Postdoctoral scientist Qian Wu, Tom Blundell Group; 2017).

Bacterial expression constructs were then modified to facilitate purified production of the C-terminal fragment of FAM35A, and a version harbouring mutations in W489/W640 →AA. EMSA on native (non-denaturing) gels confirmed binding specifically mediated by these two residues (performed by Postdoctoral scientist Qian Wu, Tom Blundell Group; 2017); Figure 4.14c.

While GFP-tagged FAM35A harbouring mutations in W489A/W640A were able to form foci in response to irradiation, a general observation was made of higher background intensity and lower foci intensity relative to a higher background in the mutant derivative cell line (Figure 4.15a). This likely reflects a reduced capacity to be able to mobilise from pre-damaged pan-chromatinised regions to sites of damage as readily as wild-type FAM35A. This supports a model whereby the N-terminus is necessary for damage-dependent localisation, while the C-terminal ssDNA binding domain merely assists (but is not an absolute requirement for) IRIF formation/retention.

Exploring the phenotypic consequences of abrogating DNA binding, these derivatives were unable to rescue FAM35A knockout cells' sensitivity to irradiation (Figure 4.15b). Notably overexpressing the N-terminus of FAM35A mediates a dominant negative effect on the IR sensitivity of both FAM35A knockout and wild-type cells, suggesting that interference of FAM35A C-terminus to bind to DNA impairs its ability to support end-joining (Figure 4.15b,c). In contrast, there was no discernible effect on the olaparib sensitivity of wild-type RPE-1^{p53ko} cells upon overexpression of these FAM35A derivatives (Figure 4.15d). Survival experiments were performed in conjunction with scientific technician Julia Coates, Steve Jackson Group; 2017).

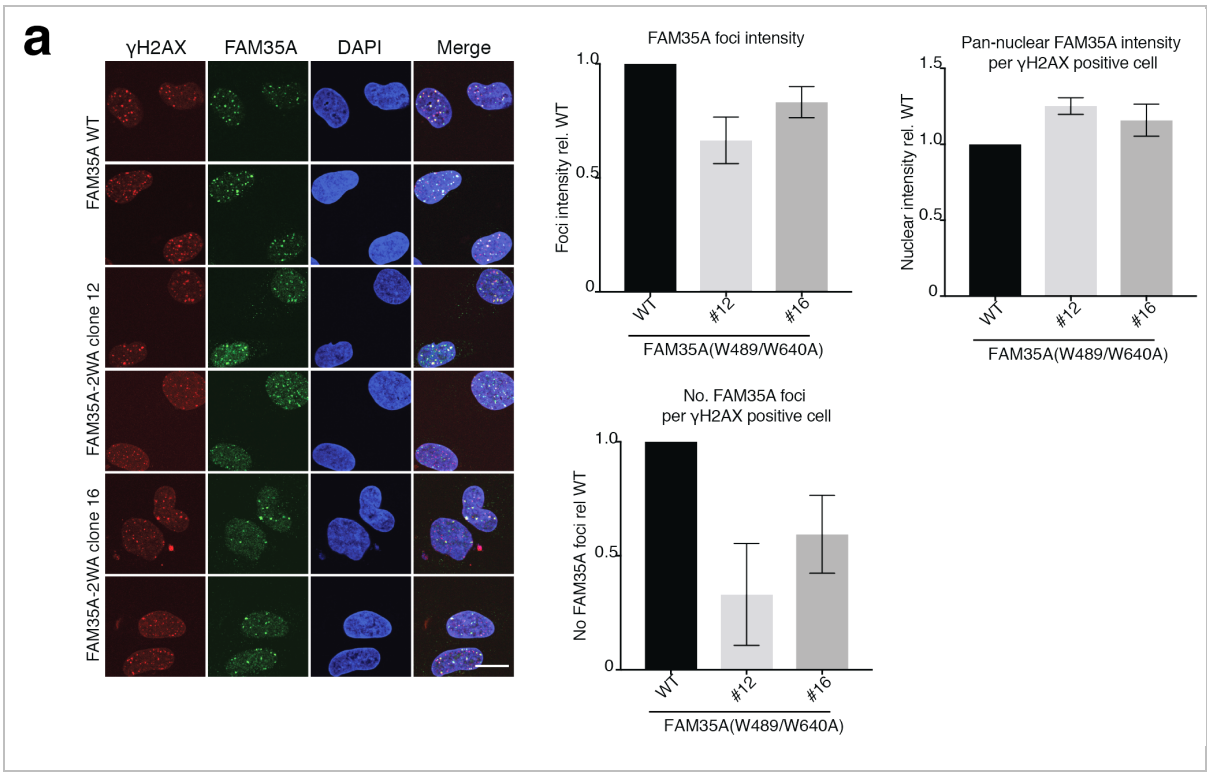

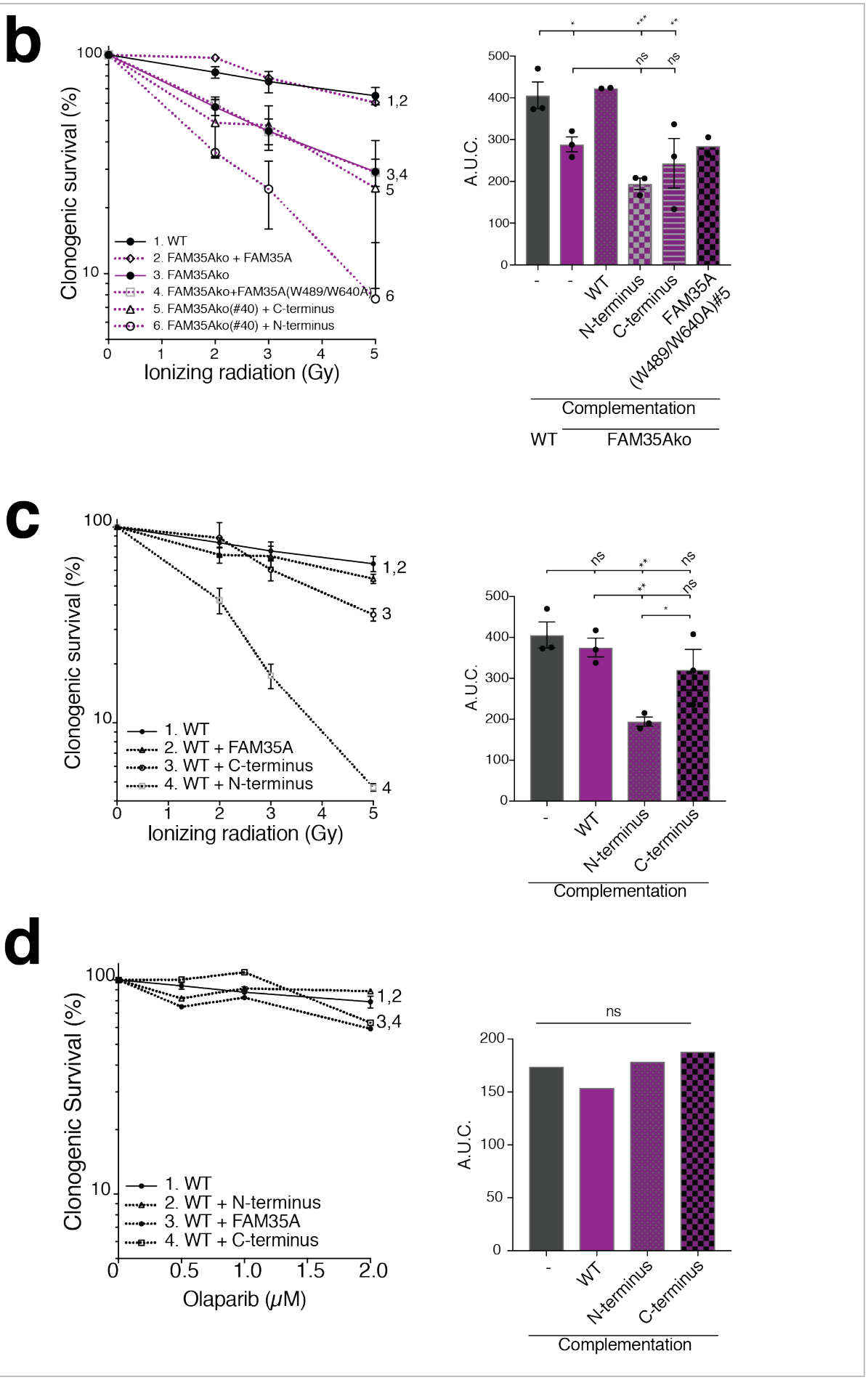
b
Clonogenic survival (%)
Ionizing radiation (Gy)
1. WT
2. FAM35Ako + FAM35A
3. FAM35Ako
4. FAM35Ako+FAM35A(W489/W640A)
5. FAM35Ako(#40) + C-terminus
6. FAM35Ako(#40) + N-terminus
A.U.C.
WT
N-terminus
C-terminus
FAM35A (W489/W640A)#5
Complementation
WT
FAM35Ako
c
Clonogenic survival (%)
Ionizing radiation (Gy)
1. WT
2. WT + FAM35A
3. WT + C-terminus
4. WT + N-terminus
A.U.C.
WT
N-terminus
C-terminus
Complementation
d
Clonogenic Survival (%)
Olaparib (μM)
1. WT
2. WT + N-terminus
3. WT + FAM35A
4. WT + C-terminus
A.U.C.
WT
N-terminus
C-terminus
Complementation

Figure 4.15 FAM35A DNA binding mutant impairs (a) IRIF formation, and (b) fails to suppress IR sensitivity in FAM35A knockout cells. (c) N-terminus over-expression in wildtype cells also has a dominant negative effect on IR sensitivity, but has (d) no effect on response to olaparib. Area under curve shown adjacent to clonogenic survival graphs.

4.2.6. FAM35A or C20orf196 loss restores HR in BRCA1-deficient cells.

Having defined FAM35A/C20orf196 as terminal end-effectors of the 53BP1-RIF1-MAD2L2 axis promoting NHEJ, we next sought to establish any functional relationship with HR factors. It has previously been reported that RIF1 recruitment is inhibited by BRCA1-CtIP in S/G2 (Escribano-Diaz et al., 2013). We also found that FAM35A and C20orf196 IRIF doubled in number when BRCA1 but not BRCA2 was depleted; Figure 4.16a.

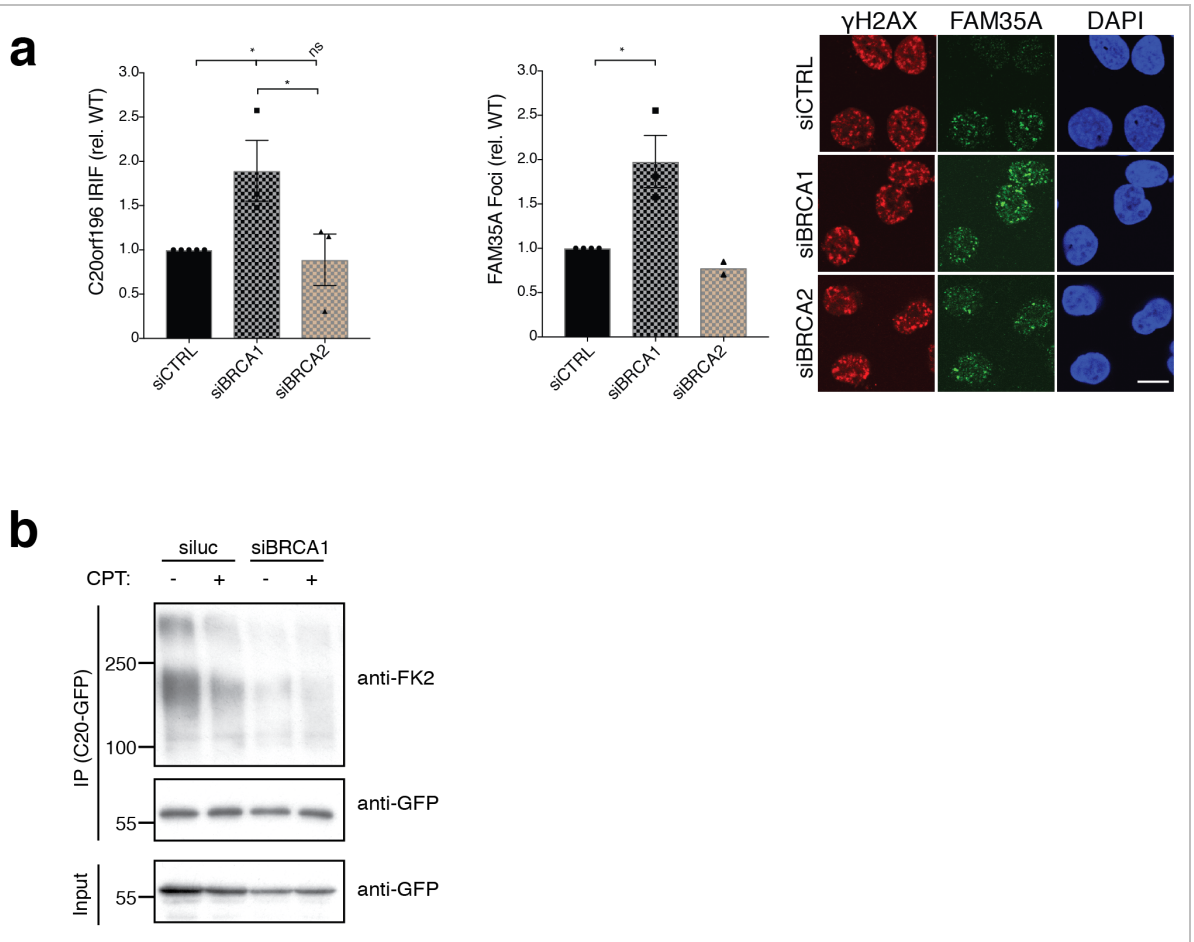

Figure 4.16 (a) C20orf196 and FAM35A IRIF following BRCA1 or BRCA2 depletion (representative micrographs shown for FAM35A). (b) FK2 staining of C20orf196 following BRCA1 depletion.

We exploited the relative ease of quantifying FAM35A foci to study their temporal dynamics. In contrast to 53BP1 IRIF which remained constant, BRCA1 depletion increased baseline formation of FAM35A IRIF, which was maintained throughout the response; Figure 4.17a,b. This suggested

an increased basal occupancy of 53BP1 on chromatin prior to damage, and a capacity to mobilise a similar increase in 53BP1 and FAM35A at the site of a DSB; Figure 4.17a,b. Public datasets suggested potential ubiquitination sites which may regulate its accumulation (phosphosite.org). We performed IP-immunoblotting which appeared to suggest a damage-independent trend in reduced FK2 (conjugated ubiquitin) staining of C20orf196 upon BRCA1 depletion (Figure 4.16b); however this could not be confirmed by SILAC mass spectrometry (data not shown; performed by Petra Beli Group, Mainz, Germany; 2018).

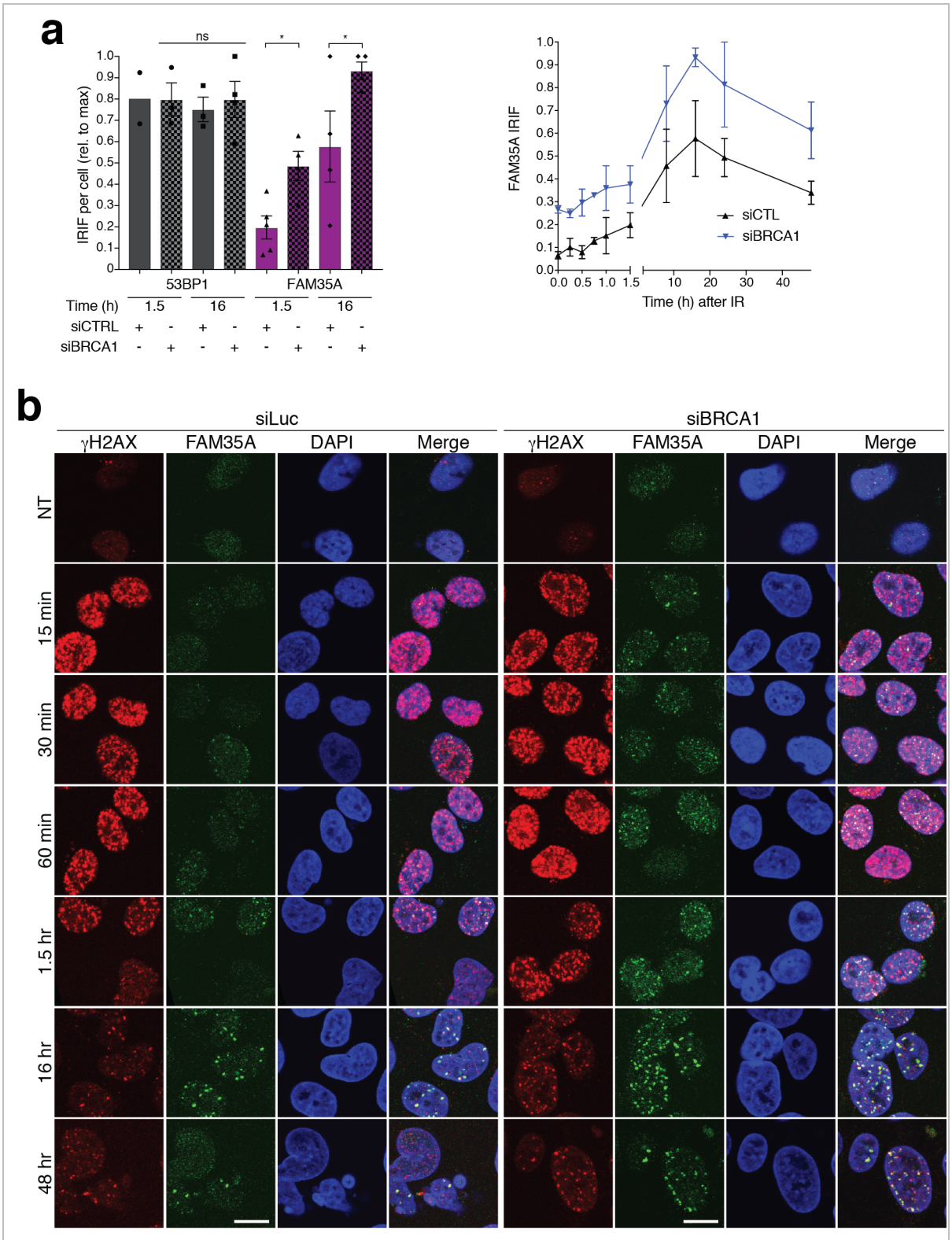

Figure 4.17 Temporal kinetics of FAM35A IRIF formation following BRCA1 depletion. (a) IRIF for 53BP1 and FAM35A, and (b) time-course of FAM35A IRIF, with representative micrographs of time-course.

We next tested whether loss of FAM35A or C20orf196 in the context of BRCA1 deficiency was sufficient to restore the HR defect, as has been described for 53BP1, RIF1 and MAD2L2 (Boersma

et al., 2015, Bothmer et al., 2010, Bouwman et al., 2010, Bunting et al., 2010, Chapman et al., 2013, Di Virgilio et al., 2013, Escribano-Diaz et al., 2013, Feng et al., 2013, Xu et al., 2015, Zimmermann et al., 2013). We described above that FAM35A/C20orf196 protects DNA ends from unscheduled BLM-mediated DNA end-resection, thereby maintaining permissive DNA ends for NHEJ. One potential mechanism for 53BP1-RIF1-MAD2L2 loss restoring HR in the absence of BRCA1 is the disinhibition of DNA end-resection; permitting additional opportunity for effective RAD51 loading. We evaluated nuclear RPA2 intensity in response to camptothecin, which revealed DNA hyper-resection in BRCA1/FAM35A and BRCA1/C20orf196 double knockout cells that phenocopied the effects of depleting the anti-resection factor Abraxas; Figure 4.18. While this may contribute to improved kinetics and efficiency of RAD51 loading and therefore HR, it is important to note that we were unable to identify a DNA end-resection defect under these conditions in RPE-1^{BRCA1ko} cells using this assay (also seen using siRNA depletions in U2OS cells and by BrdU staining; personal communication with Yaron Galanty and Rimma Belotserkovskaya, Postdoctoral scientists, Steve Jackson Group; 2017); see discussion in 4.3 below.

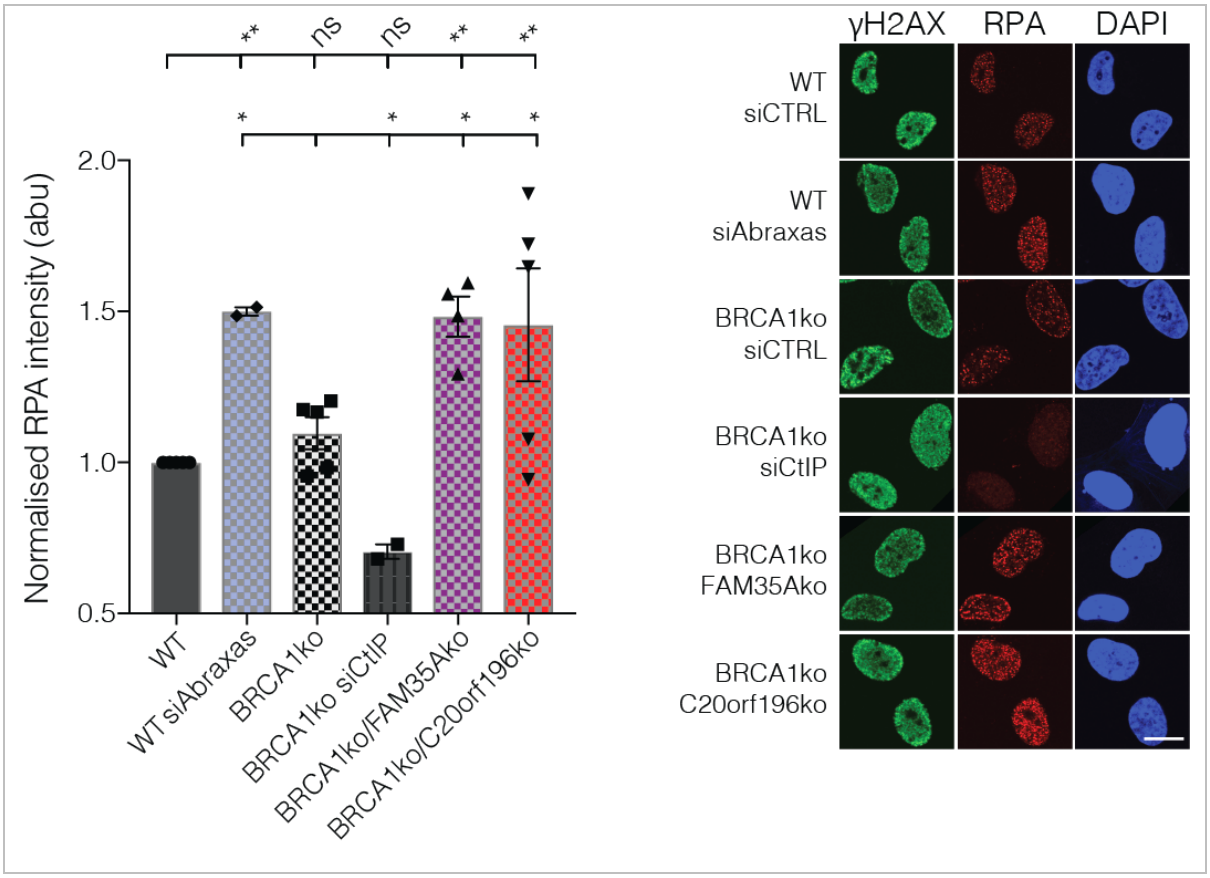

Figure 4.18 FAM35A or C20orf196 loss in BRCA1-deficient cells causes hyper-resection phenotype; quantification (left) and representative micrographs (right).

We verified the ability of FAM35A and C20orf196 knockouts to restore RAD51 loading of BRCA1 knockouts by evaluating S/G2 cells 5.5h after 5Gy irradiation (Figure 4.19a). Both genes phenocopied 53BP1 in terms of number of RAD51 foci per cell. Furthermore, BRCA2 recruitment to laser lines could also be restored to baseline levels (Figure 4.19b), suggesting the restoration of RAD51 loading is occurring at least in part via the canonical BRCA2 (and possibly PALB2) pathways. Finally, the traffic-light-reporter assay was used to confirm functional restoration of HR defect following double depletion of BRCA1 and FAM35A or C20orf196 (Figure 4.19c). See Figure 4.19c (top) for schematic of the traffic-light-reporter assay.

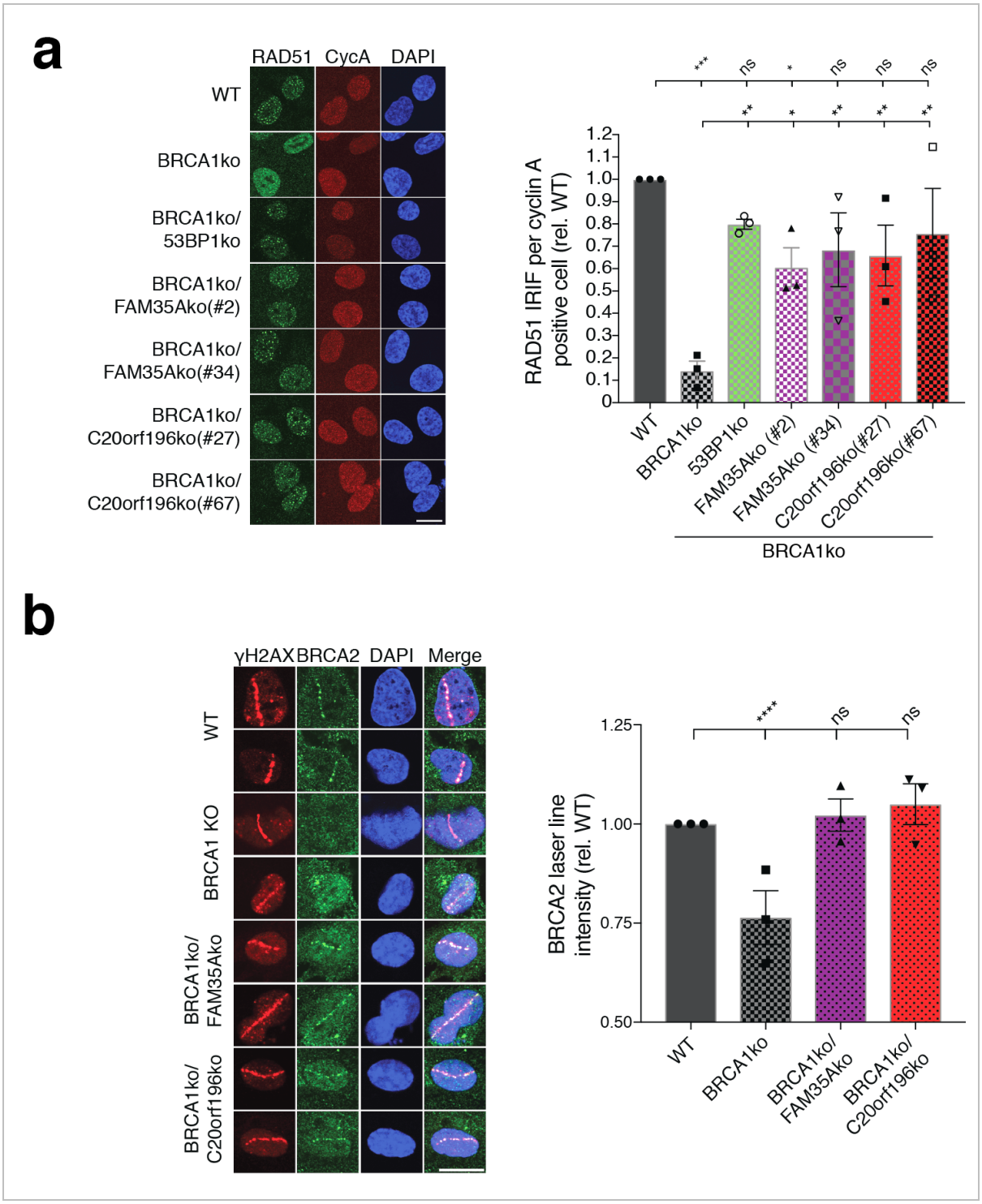
a
RAD51
CycA
DAPI
WT
BRCA1ko
BRCA1ko/ 53BP1ko
BRCA1ko/ FAM35Ako(#2)
BRCA1ko/ FAM35Ako(#34)
BRCA1ko/ C20orf196ko(#27)
BRCA1ko/ C20orf196ko(#67)
RAD51 IRIF per cyclin A positive cell (rel. WT)
***
ns
*
ns
ns
ns
**
*
**
**
**
1.2
1.1
1.0
0.9
0.8
0.7
0.6
0.5
0.4
0.3
0.2
0.1
0
WT
BRCA1ko
53BP1ko
FAM35Ako (#2)
FAM35Ako (#34)
C20orf196ko(#27)
C20orf196ko(#67)
BRCA1ko
b
γH2AX
BRCA2
DAPI
Merge
WT
BRCA1 KO
BRCA1ko/ FAM35Ako
BRCA1ko/ C20orf196ko
BRCA2 laser line intensity (rel. WT)
****
ns
ns
1.25
1.00
0.75
0.50
WT
BRCA1ko
BRCA1ko/ FAM35Ako
BRCA1ko/ C20orf196ko

c

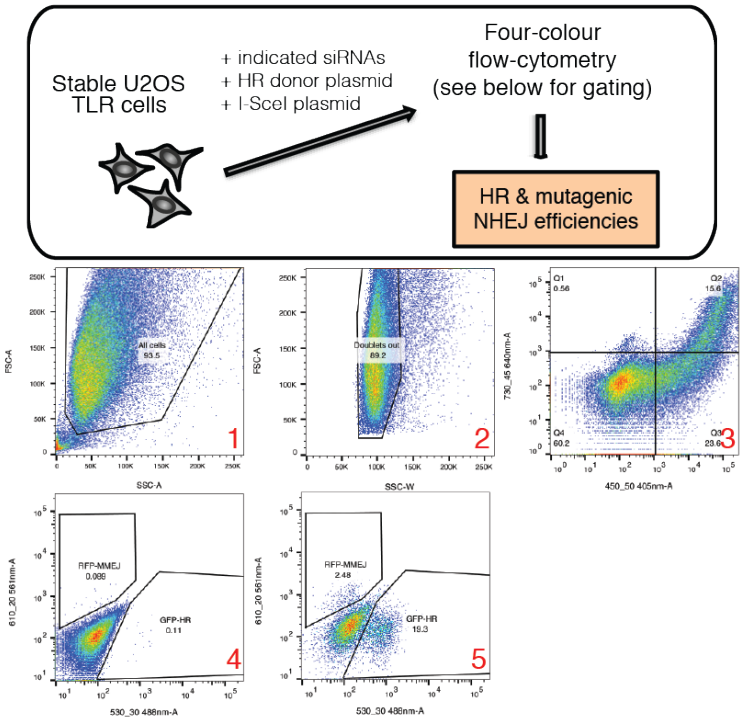

1= All cells

2= Doublets out

3= IFP (I-SceI) vs. BFP (Donor)

4= RFP (HR) vs. GFP (MMEJ) for Q4 (background)

5= RFP (HR) vs. GFP (MMEJ) for Q2 (HR and MMEJ events)

Q1= IFP+ only (I-SceI)

Q2= IFP+ (I-SceI) and BFP+ (Donor)

Q3= BFP+ only (Donor)

Q4= IFP- (I-SceI) and BFP- (Donor)

MMEJ = Erroneous end joining

HR= Homologous recombination

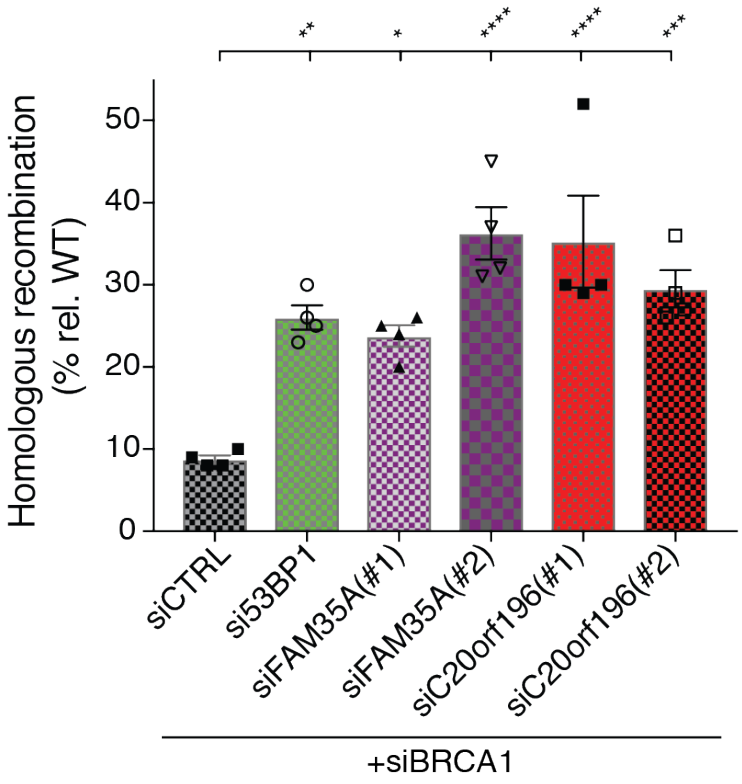

Figure 4.19 FAM35A and C20orf196 loss in BRCA1-deficient cells can restore (a) RAD51, (b) BRCA2 and (c) HR reporter assay (top) and effect of FAM35A/C20orf196 depletion (bottom).

We have described the effect of PARP inhibitor resistance in BRCA1/FAM35A and BRCA1/C20orf196 double knockout cells (Figure 4.2). This effect appears to be epistatic with 53BP1 loss (Figure 4.20a). In the light of FAM35A or C20orf196 loss mediating PARP inhibitor resistance in BRCA1-deficient cells, we next sought to establish the impact of complementing these proteins and derivatives in the double knockout setting; Figure 4.20b. Complementation of full-length FAM35A and C20orf196 was able to re-sensitise cells to olaparib treatment. In the case of FAM35A the N-terminus, but not the C-terminus alone, could suppress PARP inhibitor resistance in the BRCA1/FAM35A double knockout cell (Figure 4.20b). Without the N-terminus to direct the C-terminus to the site of damage, this derivative is unable to partake in damage-dependent recruitment and essentially has no effect. The effect of the N-terminus suggests its chromatinisation as part of the 53BP1-RIF1-MAD2L2/C20orf196 macro-complex is sufficient to provide a barrier which impairs effective RAD51 loading. In other words, the C-terminal DNA-binding domain of FAM35A is necessary for mediating IR sensitivity (and by extension most likely NHEJ), while the N-terminus is sufficient to cause olaparib sensitivity (and hence by implication antagonise RAD51 loading) (cell survival experiments were performed with scientific technician Julia Coates, Steve Jackson Group; 2017).

Collectively these data demonstrate that C20orf196 and FAM35A operate together to 'shield' DSBs from inappropriate activities and promote appropriate modes of DSB repair; we therefore propose the gene names SHLD1 and SHLD2 and that collectively form the 'shieldin complex'.

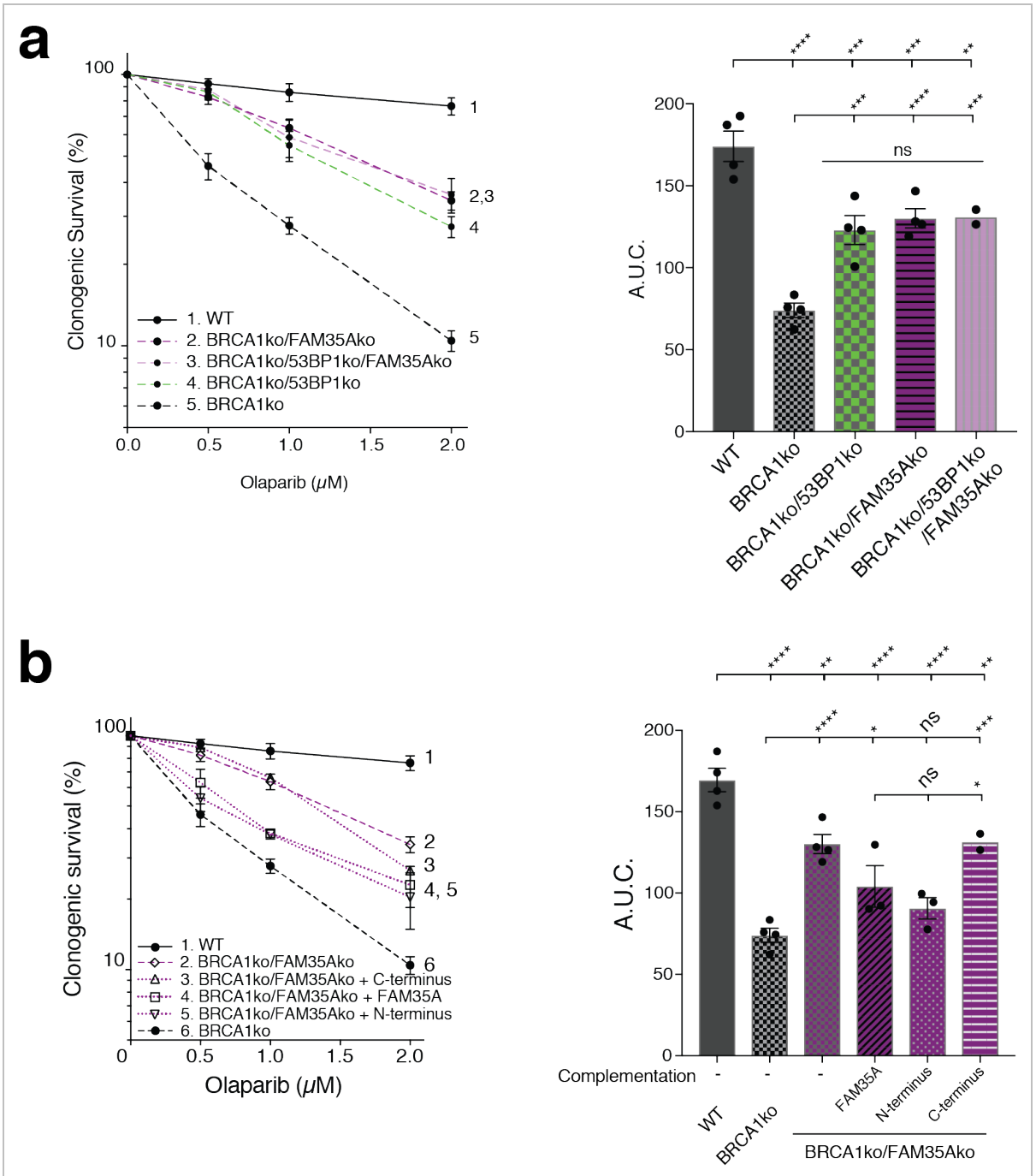

Figure 4.20 Effects of FAM35A and C20orf196 on cell survival due to olaparib. (a) FAM35A loss is epistatic with 53BP1 loss in BRCA1-deficient cells in response to olaparib. (b) The N-terminus alone is capable of resensitising BRCA1ko/FAM35Ako cells to olaparib.

4.2.7. FAM35A or C20orf196 loss correlates with PARP inhibitor resistance in cancers.

Having identified C20orf196/SHLD1 and FAM35A/SHLD2 as mediators of PARP inhibitor resistance in BRCA1-deficient cells, we explored whether there was any pathophysiological relevance to olaparib-resistance in clinical models. We explored the effect of short-term and

sustained PARP inhibitor treatment on BRCA1-deficient patient-derived xenograft models, which were either sensitive or had developed resistance to olaparib (Figure 4.21a). In PDX tumour models which developed treatment resistance (Figure 4.21a), SHLD1 and SHLD2 transcript levels, as well as 53BP1 and PARP1, were found to be downregulated in some tumours; Figure 4.21a (experiments performed by Carlos Caldas Group, CRUK Cambridge Institute; 2018). We also sought to evaluate intrinsic resistance to PARP inhibitor therapy in a series of BRCA1-deficient patient-derived tumour samples from which xenografts were established. In these models, PARP inhibitor sensitivity or resistance correlated with high or low SHLD1 and SHLD2 expression levels respectively, revealing another association between low shieldin expression levels and PARP inhibitor resistance (Figure 4.21b). In two treatment-resistant models with normal shieldin transcript levels, deleterious mutations in 53BP1 were observed. We also observed some models which independently restored BRCA1 nuclear foci (Cruz et al., 2018), while PDX127 demonstrated loss of both FAM35A and C20orf196, suggesting tumours may evolve multiple mechanisms of resistance due to tumour heterogeneity or mechanistic cooperation (experiments performed by Violetta Serra Group, Vall d'Hebron Institute of Oncology, Barcelona; 2018).

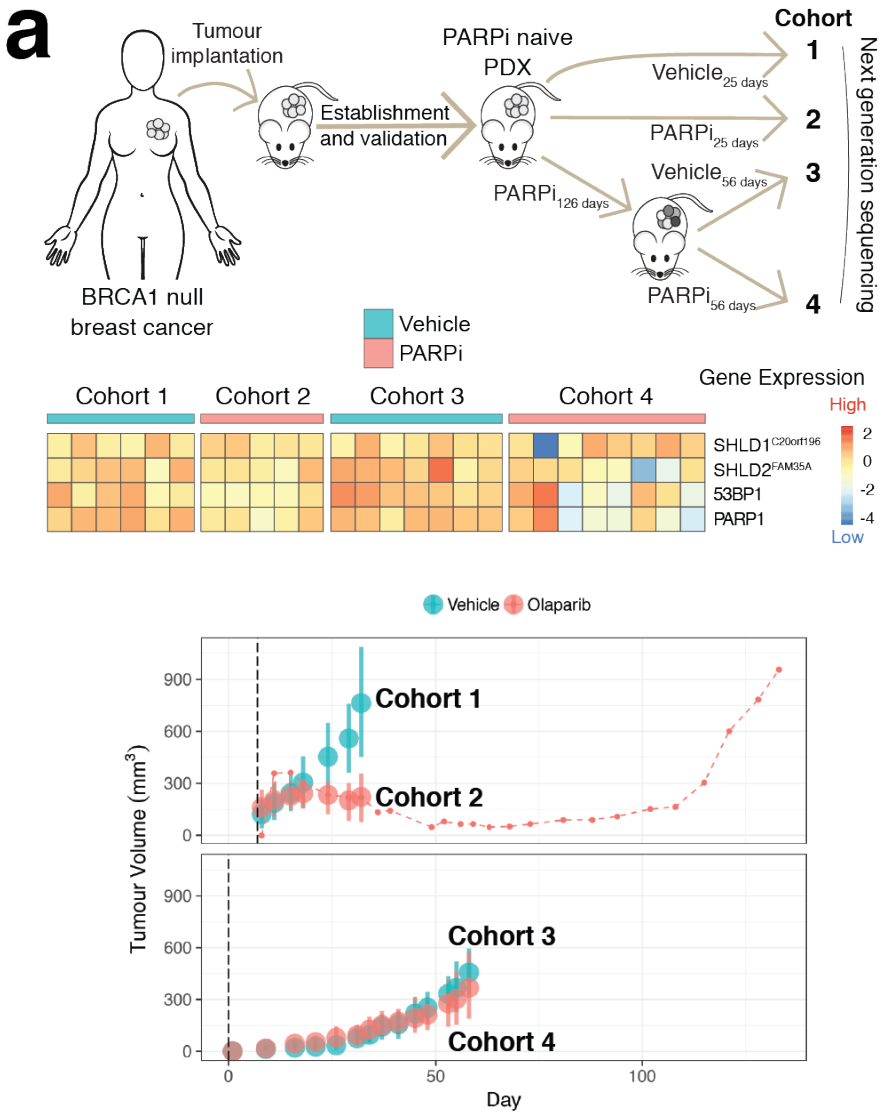
a
Tumour implantation
BRCA1 null breast cancer
Establishment and validation
PARPi naive PDX
Vehicle25 days
PARPi25 days
Vehicle56 days
PARPi126 days
PARPi56 days
Cohort
1
2
3
4
Next generation sequencing
Vehicle
PARPi
Cohort 1
Cohort 2
Cohort 3
Cohort 4
Gene Expression
High
Low
SHLD1C20orf196
SHLD2FAM35A
53BP1
PARP1
Vehicle
Olaparib
Tumour Volume (mm3)
Day

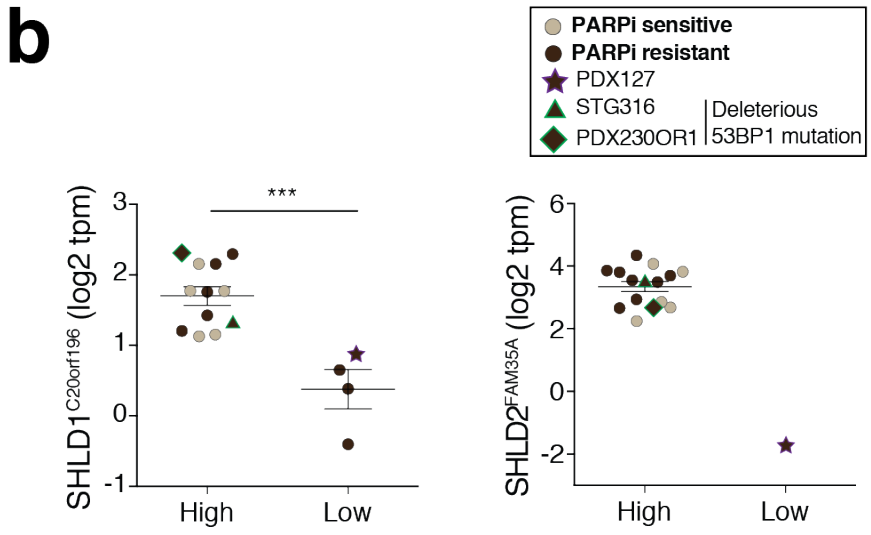
b
PARPi sensitive
PARPi resistant
PDX127
STG316
PDX230OR1
Deleterious 53BP1 mutation
***
SHLD1C20orf196 (log2 tpm)
SHLD2FAM35A (log2 tpm)
High
Low

Figure 4.21 BRCA1-deficient PDX models (a) subject to olaparib treatment generates PARP inhibitor resistance with tumours downregulating shieldin complex components. Schematic of experimental setup (top); relative RNA expression levels of tumour specimens from four cohorts of mice for SHLD1, SHLD2, 53BP1, PARP1 (middle); growth curves of olaparib sensitive and resistant PDX tumours from cohorts 1-4 (bottom). (b) Intrinsic PARP inhibitor resistance correlates with low SHLD1 and SHLD2 expression levels; graphs show SHLD1 and SHLD2 expression levels and their relationship with intrinsic olaparib sensitivity or resistance. Experiments performed by Violeta Serra and Carlos Caldas Groups; 2018.

It is tempting to speculate that the gain of resistance through the loss of a DNA repair factor or complex may generate an alternative therapeutic vulnerability. We tested this hypothesis, by examining the sensitivity of BRCA1/FAM35A and BRCA1/C20orf196 knockouts to irradiation and cisplatin. This revealed an acquired sensitivity in both cases (Figure 4.22a,b).

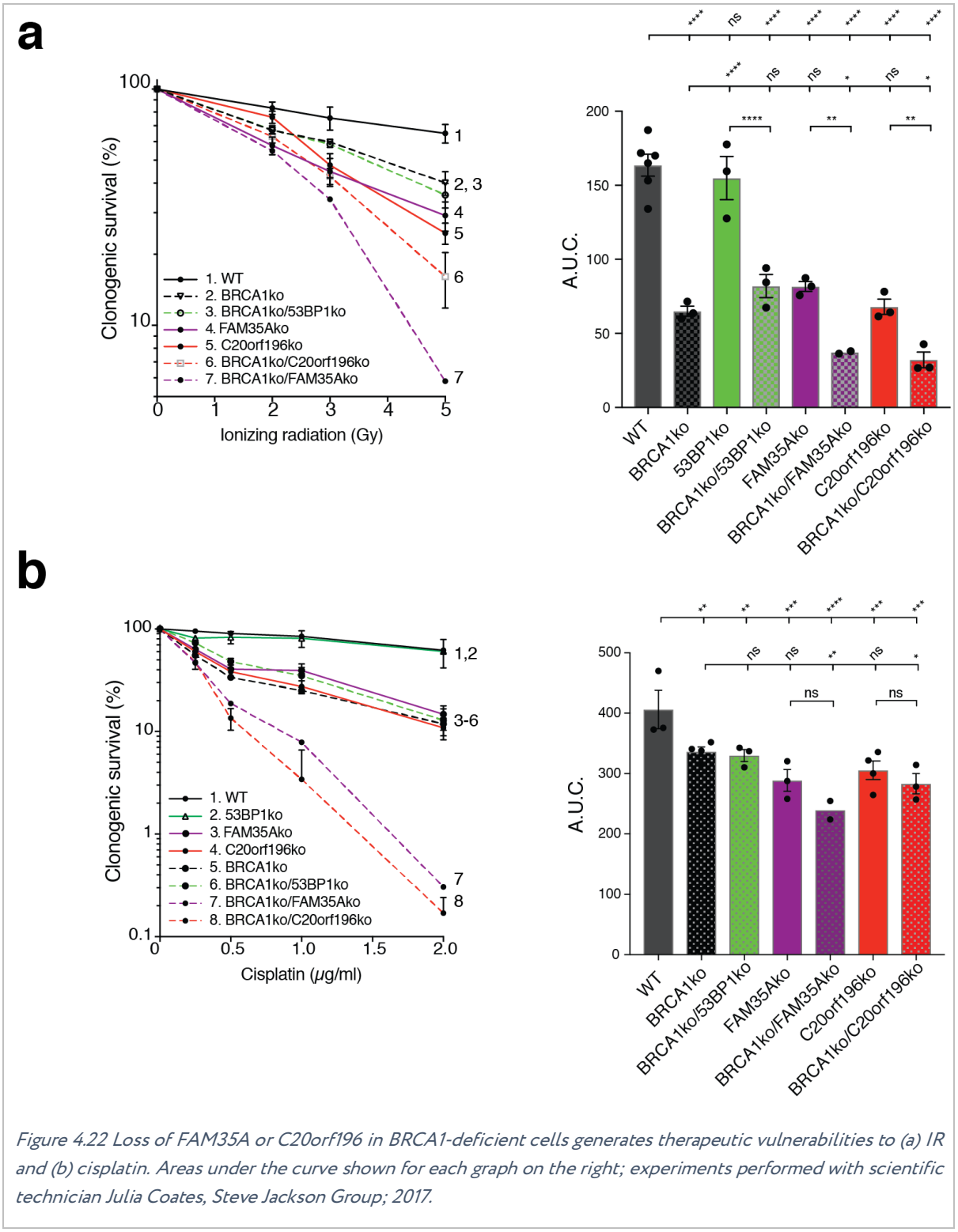

Figure 4.22 Loss of FAM35A or C20orf196 in BRCA1-deficient cells generates therapeutic vulnerabilities to (a) IR and (b) cisplatin. Areas under the curve shown for each graph on the right; experiments performed with scientific technician Julia Coates, Steve Jackson Group; 2017.

The additive effects of BRCA1 and SHLD1/2 loss on IR sensitivity may explain this defect, particularly given the contribution of SHLD1/2 to NHEJ. The additional sensitivity to the cross-linking agent cisplatin was surprising, given the effect of restoring HR which is part of the Fanconi anemia repair pathway. We examined the effect of FAM35A and C20orf196 on the formation of

FANCD2 foci formation in response to cisplatin, and observed an antagonistic relationship which appeared to be enhanced (as measured by FANCD2 foci formation) in our knockout cell lines (Figure 4.23a), and which was not reciprocal on FAM35A/C20orf196 IRIF (Figure 4.23b).

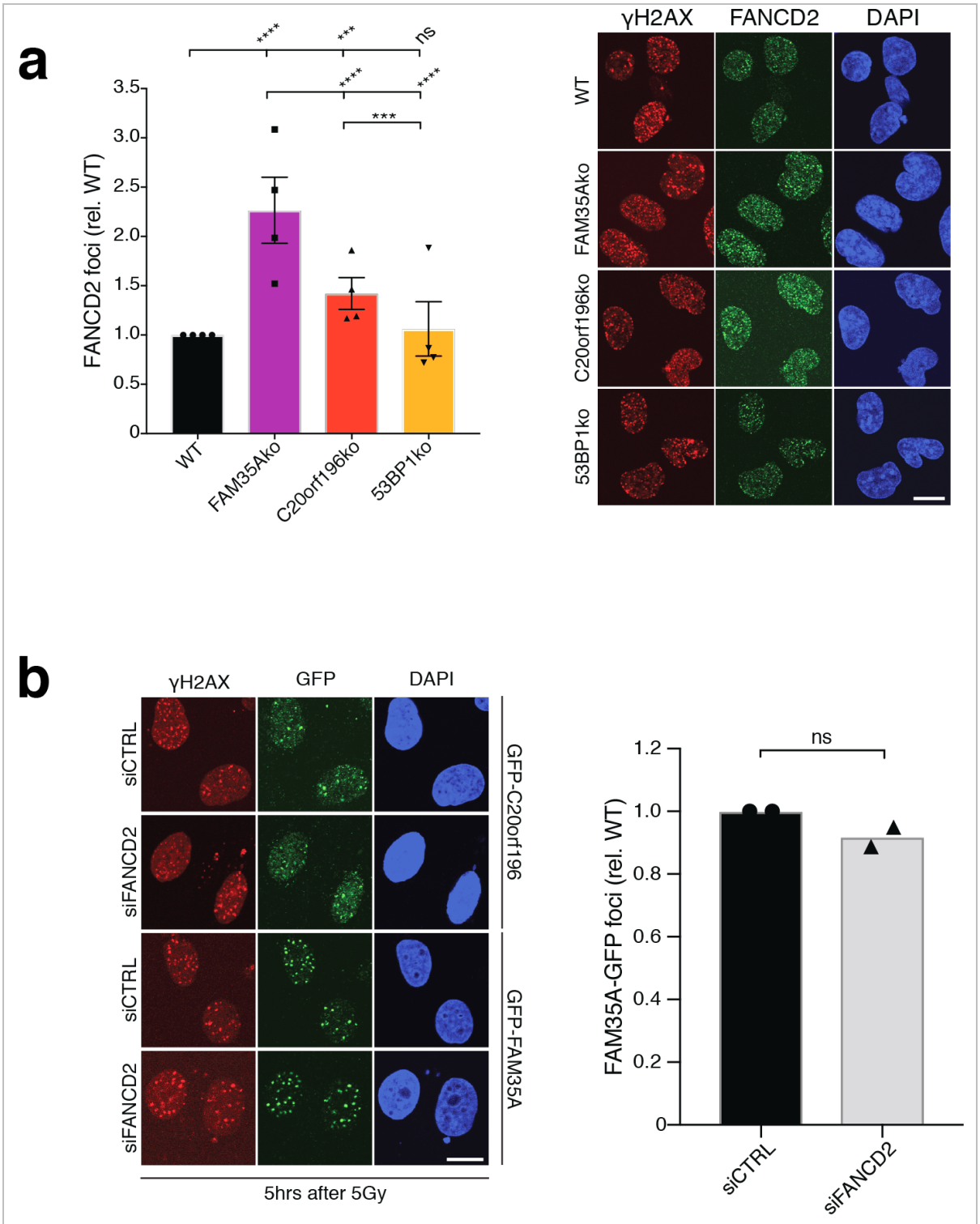

Figure 4.23 FANCD2 foci are de-repressed in the absence of FAM35A or C20orf196. (a) FANCD2 foci following FAM35A, C20orf196 or 53BP1 depletion in response to cisplatin; representative micrograph on right. (b) GFP-C20orf196 and GFP-FAM35A IRIF are unaffected by FANCD2 silencing; quantification for FAM35A on the right.

4.3. Discussion

We have identified a new complex of proteins, termed shieldin, which acts as the distal terminal end-effector of the established 53BP1-RIF1-MAD2L2 axis in promoting NHEJ, and antagonising HR in the absence of BRCA1. Our work suggests a functional equivalence of all members of this axis in terms of their capacity to antagonise HR. Structure-function experiments revealed a requirement for the C-terminal OB-fold containing domains of FAM35A/SHLD2 to bind DNA, and for its role in promoting NHEJ and mediating radioresistance. In contrast, the C-terminus appears dispensable for mediating olaparib sensitivity, as complementation of the N-terminus alone was sufficient to re-sensitise BRCA1ko/FAM35Ako cells to olaparib. The contributions of the various domains of FAM35A to its function that we identified in this study, are summarised in the schematic model in Figure 4.24. We have also attempted to correlate expression levels of components of the shieldin complex with innate and acquired PARP inhibitor resistance in BRCA1-deficient PDX models of breast and ovarian cancer.

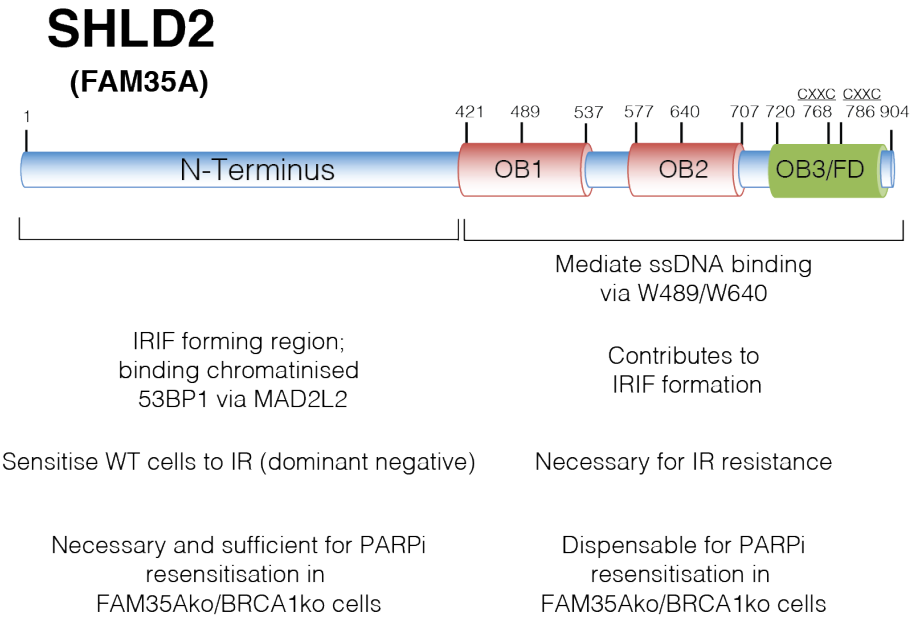

Figure 4.24 Schematic of FAM35A/SHLD2, highlighting results from this work attributable to different domains.

It is tempting to speculate about the two halves of FAM35A and their relevance to its function within the two compartments surrounding a DSB. In the break-proximal compartment the C-terminus may form a stabilising interaction with exposed ssDNA, thereby limiting end-resection. Within the chromatin compartment more distal to a DSB, it is possible that the 53BP1 complex

sits on histones mediating more long-range effects on the break site; this may involve some DNA interaction of FAM35A with e.g. the linker region of DNA, or perhaps simply free exposure of an unbound C-terminus. Our super-resolution experiments suggest that FAM35A does not form long filamentous structures, and we did not establish any evidence of oligomerisation. One possible hypothesis was a role of FAM35A oligomerisation at its C-terminus to stabilise the short length of ssDNA generated by the action of CtIP/MRN. It was possible that the oligomerised C-terminus of FAM35A can cover these short distances, and through a direct interaction with the core end-joining machinery, activate the process of NHEJ. Such a model would necessitate a dynamic equilibrium between short-range resection and its reversal by fill-in synthesis. This model appears to be in part supported by a potential role for the CST (CTC1-STN1-TEN1) complex, that interacts with shieldin and mediates Polα-dependent fill-in synthesis (Mirman et al., 2018). We did observe an interaction between C20orf196 constructs by co-immunoprecipitation, suggesting at the very least that this protein multimerises as a dimer (Figure 4.4f). The smaller size and relatively insignificant domain architecture makes it challenging to predict its precise contribution to this complex. The precise structural interaction of FAM35A with chromatin and DNA, and its relationship with C20orf196 and the rest of the 53BP1 axis members will necessitate further biochemical studies to characterise the structural architecture of this complex, for example by in-vitro reconstitution experiments and cryo-electron microscopy.

We found that loss of shieldin de-represses DNA end-resection driven by BLM, and it is tempting to speculate that the interaction between the OB-folds and ssDNA compete with the recruitment and action of nucleases to achieve long-range resection. Our finding of increased BLM recruitment in the absence of shieldin is also reminiscent of the increased BLM chromatinisation observed with RIF1 silencing (Feng et al., 2013, Xu et al., 2010).

Recent work has suggested a modest but early impact of BRCA1 on damage-induced DNA end-resection which is below the level of detection as evidenced by traditional microscopy methods (Cruz-Garcia et al., 2014). De-repression of end-resection by loss of 53BP1-RIF1-MAD2L2 is well documented, however, evidence for the resection 'defect' in BRCA1^{ko} cells which this it is said to

rescue, is conflicting. Early data relies on immunoblotting of pRPA signalling in mouse cells in response to 30Gy IR, and RPA chip signals at Ig loci during CSR (Chapman et al., 2013, Xu et al., 2015, Bunting et al., 2010, Boersma et al., 2015), in contrast to RPA IRIF which do not reveal any detectible reduction in the absence of BRCA1 (Zhou et al., 2014, Cruz-Garcia et al., 2014).

While the loss of shieldin may indirectly improve the efficiency of RAD51 loading by generating longer lengths of ssDNA than in wildtype cells, the absence of a large detectible DNA end-resection defect by our methods in BRCA1-deficient cells instead supports the predominant role of shieldin in antagonising RAD51 loading directly at the level of competition with PALB2-BRCA2 recruitment on chromatin surrounding a DSB (Zong et al., 2019). In keeping with this theory, the N-terminus of FAM35A could still maintain a complex with C20orf196 and the 53BP1-RIF1-MAD2L2 components upstream; in this case, the persistence of this larger complex would appear to be sufficient to antagonise the loading of RAD51 and hence lead to the olaparib sensitivity we observed.

The contributions of SHLD1/2, both to NHEJ and HR, in the presence and absence of BRCA1, are summarised in the model below; Figure 4.25.

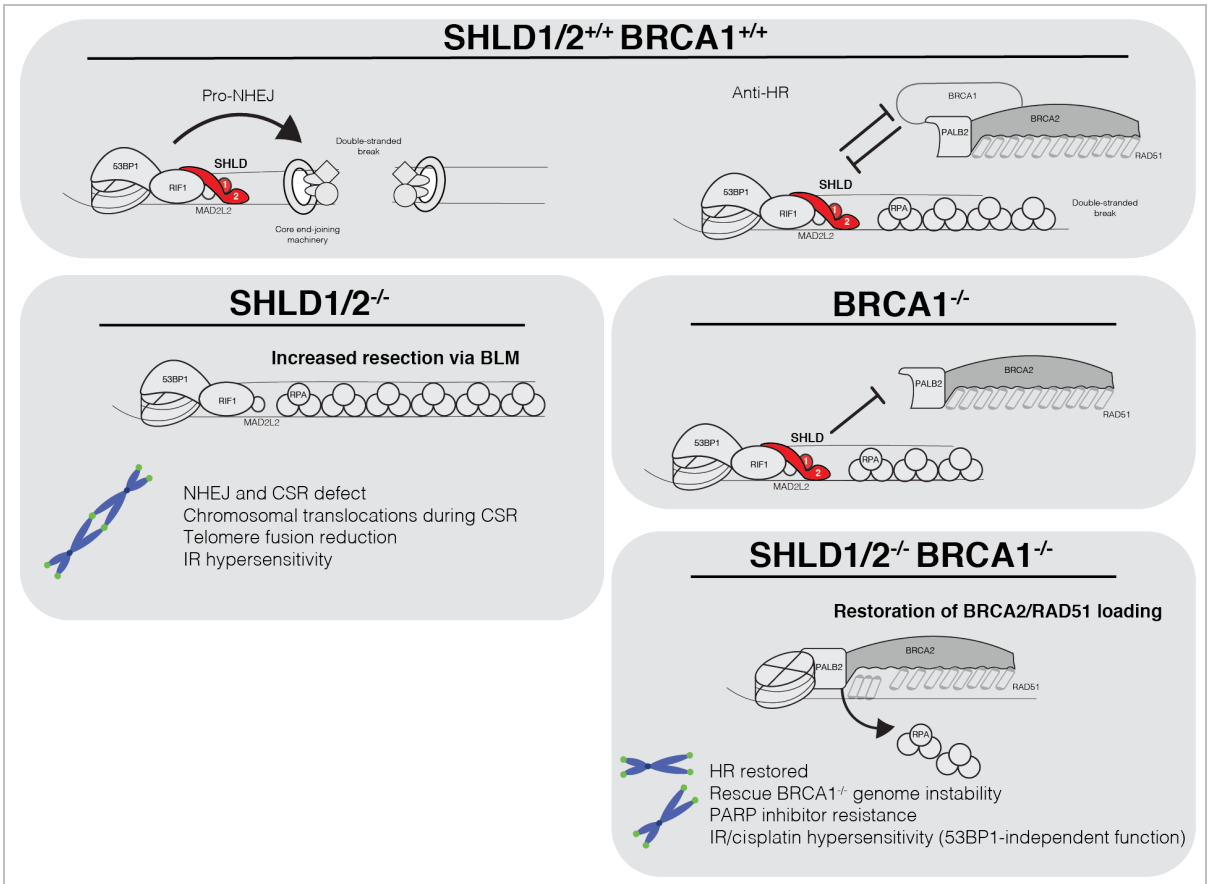

Figure 4.25 Schematic model of SHLD1^{C20orf196}/SHLD2^{FAM35A} function in the presence and absence of BRCA1, as revealed by this work.

We hypothesised that the reciprocal interaction between FAM35A/C20orf196 and BRCA1 may be related to BRCA1's established function as an E3 ubiquitin ligase with its partner BARD1. It has recently been suggested that BRCA1 mediates ubiquitination of H2A, for the purposes of recruiting the chromatin remodeller SMARCAD1 and repositioning 53BP1; in its absence the persistence of 53BP1 maintains the suppression of DNA end-resection (Densham et al., 2016). Pull-downs and mass spectrometry was performed and revealed with high-confidence, ubiquitination of C20orf196 on K128 and K183 residues, and ubiquitination of FAM35A on K468 and K483 residues. However further studies including SILAC which were used to evaluate damage- and BRCA1- dependency failed to reveal any substantial changes in ubiquitination state at these residues. Nevertheless, it is tempting to infer a regulatory role of the K468/K483 ubiquitination sites of FAM35A, given their proximity to the critical DNA binding residue W489, however this modification would have to occur in a camptothecin-independent manner.

The direct antagonistic effect of BRCA1 on FAM35A and C20orf196 IRIF was notable, and reminiscent of previous reports of RIF1 IRIF upon BRCA1 depletion in S/G2 cells (Chapman et al., 2013, Escribano-Diaz et al., 2013, Feng et al., 2013, Zhang et al., 2016); this effect has been shown to require the BRCA1-CtIP interaction, but has only a mild effect on 53BP1 IRIF (Chapman et al., 2012). The reciprocal interaction between BRCA1 and RIF1 suggested that each was responsible for suppressing IRIF in G1 and S/G2 respectively, and suggested that the CDK switch mediating the BRCA1-CtIP interaction may play an important role in pathway choice (see 1.2.3). These findings support our results which show increased occupancy of chromatinised 53BP1 by shieldin in the absence of BRCA1, both in the undamaged state and in response to radiation.

Our characterisations of shieldin using knockout cells appears to phenocopy that of 53BP1, RIF1 and MAD2L2. However we could not demonstrate any dependence of shieldin on PTIP, and these results appear to be in contradiction to one study which defined PTIP in terms of mediating the pathological NHEJ effects (e.g. by telomere fusions) and in opposing BRCA1-dependent HR (Callen et al., 2013). We also could not identify any defect in V(D)J recombination due to shieldin loss (personal communication with Ludovic Deriano Group; 2019), which again contrasts with the role for 53BP1 in 'long-range' V(D)J recombination proposed by the same group (Difilippantonio et al., 2008). It is possible that some of these differences with PTIP are reflected by assay or cell line differences; indeed many of the experiments of the former study were performed in mouse cell lines in contrast to our own bias toward the use of human cell model systems.

We experienced some difficulty with generating knockouts of FAM35A and C20orf196 genes, in part reflecting a degree of essentiality in human cell lines and the relative infrequency with which these genes could be deleted biallelically. We also observed some subtle differences in the phenotypes of the SHLD1 and SHLD2 knockouts, and the character of these IRIF, which may reflect separations of function between the two proteins. We are currently generating C20orf196 knockout mice, however Fam35a itself appears embryonic lethal, again supportive of differences in function, at least in early embryological development (ongoing work with former Postdoctoral scientist G. Balmus; Steve Jackson Group, 2019). It is noteworthy, that while loss of RIF1 is embryonic lethal, 53BP1 deletion can be tolerated, with radiosensitivity and immunodeficiency

phenotypes (Buonomo et al., 2009, Ward et al., 2004, Morales et al., 2003), suggesting that there are various contributions which 53BP1 axis members make outside of their canonical roles in NHEJ and repair pathway choice.

Our screen also revealed several other candidates that have recently been shown to be important in determining repair pathway choice, including TEN1 (part of the CST complex, see above (Mirman et al., 2018)), and DYNLL1 (Becker et al., 2018, He et al., 2018). The ATMIN-DYNLL1 pathway (ATMIN being the transcription factor promoting DYNLL1 expression) has been proposed to work either by its impact on the oligomerisation and therefore DSB recruitment of 53BP1, and/or repressing MRE11 recruitment to directly inhibit DNA end-resection. It is notable that not all components of these complexes demonstrated the same fold change enrichment or significance across the three different PARP inhibitors, and this likely reflects the strength of these suppressors (particularly with respect to the AZD2461 IC70 result), subtle differences in their mechanism of action, and the statistical noise of the screen. There are also differences observed with other similar screens that have been performed, that can often be attributed to differences in screen design, particularly the cell type that has been used.

Since the presentation and publication of our work (Dev et al., 2018), there have been several other studies identifying shieldin as a downstream effector of 53BP1, protecting DNA ends, promoting NHEJ and immunoglobulin class switching, and supporting our findings (Ghezraoui et al., 2018, Gupta et al., 2018, Mirman et al., 2018, Noordermeer et al., 2018, Findlay et al., 2018, Tomida et al., 2018, Gao et al., 2018). Notably, several studies have identified a third component of what is being considered a four-component complex, hence SHLD1, SHLD2 interact with MAD2L2, which itself interacts with the previously unidentified gene CTC-534A2.2 now termed SHLD3. MAD2L2 and SHLD3 are the most proximal elements within the complex localising SHLD1/2 to 53BP1-RIF1, with MAD2L2 interacting with SHLD3 via its C-terminal “seatbelt” (Ghezraoui et al., 2018). Our inability to detect SHLD3 in our whole genome CRISPR-Cas9 screen and mass spectrometry likely reflects the poor annotation of this gene across various datasets. Indeed, only 2/6 guides present within the GeCKO v2.0 library assigned to this gene actually target exons belonging to the SHLD3 protein, as opposed to an alternatively spliced variant that

does not encode for a protein, and these two guides do appear to have some enrichment in the presence of PARP inhibition.

The sequence homology for the OB-folds of SHLD2 to RPA1 and CTC1 held particular relevance, due to one group proposing that the CTC1-STN1-TEN1 (CST) complex is recruited downstream of shieldin to facilitate the recruitment of Polα in a manner reflecting the recruitment of the shelterin complex to a telomeric ends to fill-in excessive overhangs of nascent telomeres (Barazas et al., 2018, Mirman et al., 2018). This finding was supported by the suppression of radial chromosome formation in PARP inhibitor treated BRCA1-deficient cells after Polα inhibition. However, it remains unclear how the DNA binding of SHLD2 cooperates with that of the CST complex to regulate fill-in synthesis and determine DNA end-resection. Shieldin mutants which fail to interact with CST will assist in assigning more precise functions to each of these components (Setiaputra and Durocher, 2019).

The interaction between the N-terminus of FAM35A/SHLD2 and MAD2L2 was further attributed to two prolines (P14, P17) within the highly conserved first 50 residues of SHLD2 (Ghezraoui et al., 2018). To test the contribution of the OB-folds, one study artificially forced the recruitment of SHLD2 to sites of damage through an FHA-fusion protein. In doing so, this led to the inhibition of RAD51 loading in a BRCA1ko/53BP1ko cell line, which required the DNA binding capacity of SHLD2's OB-folds to exhibit this effect. We observed that the DNA binding capacity of SHLD2 was necessary to mediate radioresistance, but that the C-terminus was dispensable for olaparib sensitivity in BRCA1ko cells. The apparent contradiction in conclusions between these two reports remains to be resolved, and could be addressed by a knock-in of W→A in the DNA-binding residues of the endogenous locus of SHLD2, to see whether this would phenocopy SHLD2 loss in a BRCA1-deficient background, and hence how much of the function of SHLD2 can be attributed to its ssDNA binding action. There was an implication in one study of an inability to bind <30nt length region, in contrast to typical tandem OB-fold containing proteins, and is suggestive of binding to longer lengths of ssDNA than say RPA (Gao et al., 2018). This interaction may therefore interfere with RPA binding as a result of the 20-40nt tract length generated by MRN/CtIP, and/or sterically hinder the recruitment of BLM/DNA2 or EXO1

necessary for switching from short to long range resection (Ciccia and Elledge, 2010). In keeping with this theme of negatively antagonising end-resection factors, the 53BP1 interacting protein DYNLL1 has been shown to interfere with the MRE11 nuclease activity at DNA ends (He et al., 2018). It remains to be seen whether this occurs upstream to shieldin activity and whether these two anti-resection functions are connected.

One study explored interacting sites of MAD2L2, and separated residues responsible for its interaction with its TLS polymerase partners REV1 and REV3L, compared with the interactions for SHLD3 binding. The study went on to ascribe this specific function to cross-linker resistance, with mutations abrogating the interaction with REV1/REV3L but preserving the interaction with SHLD3 causing cisplatin and MMC sensitivity (Ghezraoui et al., 2018). We observed a sensitivity to cisplatin and radiation of double BRCA1ko/SHLD1ko or BRCA1ko/SHLD2ko cells. Our results are in keeping with MMC sensitivity observed in HEK293 cells after FAM35A/SHLD2 depletion (Tomida et al., 2018), and the finding that FANCD2 recruitment in response to damage was enhanced in the absence of SHLD1/2 was suggestive of either a direct or indirect effect on the ability to respond to DNA cross-links. One explanation could be that this phenotype reflects an accumulation of damage and an inability to complete downstream resolution of a cross-link after its detection by the Fanconi anaemia core complex and recruitment and ubiquitination of FANCI-D2. The absence of shieldin and the hyper-resection phenotype may interfere with classical HR repair, instead favouring RAD52-mediated SSA and leading to an accumulation of FANCD2 upstream reflecting unresolved cross-links. Whether these experimental results reflect genuine mechanistic differences or else clonal and experimental variation will need to be confirmed.

A broader phenomenon of radiosensitivity conferred by various BRCA1-deficient PARP inhibitor resistance mechanisms has been described from in-vitro and in-vivo model systems (Barazas et al., 2019). In contrast to HR restoration due to restoring BRCA1 expression, 53BP1-RIF1-MAD2L2/shieldin/CST losses appear to further increase radiosensitivity despite the equivalent restoration of HR (Dev et al., 2018, Barazas et al., 2018, Barazas et al., 2019). Both of these results offer a therapeutic opportunity upon the emergence of treatment resistance after PARP

inhibition, that may be clinically exploitable. We observed correlations in shieldin expression levels and PARP inhibitor resistance, that may support the evaluation of the RNA expression of tumour biopsy samples, rather than relying on insights from mutational burden alone. The likelihood of bialleic losses in these genes seems a less likely occurrence than the transcriptional re-wiring that could produce a similar effect. It is also likely that the mechanisms of HR deficiency due to so-called 'BRCAness', as well as the mechanisms which may reverse these effects and cause resistance, are likely to differ depending on the specific HR-gene in question.

A recent CRISPR-Cas9 based suppressor screen in ATM-deficient cells, revealed core end-joining machinery as factors which when individually 'lost' can suppress hypersensitivity to topotecan or olaparib (Balmus et al., 2019). In contrast, 53BP1 loss was unable to reverse the toxicity of topotecan or olaparib in ATM-deficient cells. In the absence of ATM, lethality appears to emerge from the toxic end-joining brought about by core end-joining factors acting upon free seDSBs, and presumably the mitotic catastrophe that results from breakage of aberrantly fused chromosomes. In contrast, core end-joining factors do not appear to be able to rescue the HR defect of BRCA1-deficient cells, suggesting that mechanisms remain intact to prevent toxic end-joining (presumably via ATM activity), and that here cell death arises from accumulation of unrepaired free DNA seDSBs. Previous work did suggest that the absence of LIG4 in BRCA1-deficient cells was sufficient to reduce chromosome rearrangements, but again this was insufficient to restore HR, suggesting that this effect may contribute, but was not sufficient to cause death in BRCA1-deficient cells, or otherwise chromosome fusions simply represent an epiphenomenon (Bunting et al., 2010).

Regardless of the mechanisms of cytotoxicity, it will be important to continue to identify individual factors which contribute to DSB repair pathway choice. In addition, establishing the HR status of patients' tumours, and continuing to define mechanisms of resistance specific to individual genetic defects, will be essential to reliably stratify patients to their optimal therapy. The techniques explored in this thesis and the DDR pathways that we have defined, should support such scientific and translational progress in the future.

5. Future directions

CRISPR-Cas9 pooled genetic screening has emerged as an increasingly important experimental technique for exploring genetic contributions to specific phenotypes. Our work in chapter 4 highlights the use of this technique in identifying genetic suppressors of drug sensitivity, and alternatively, genetic enhancers of drug sensitivity – so-called dropout candidates – are also being explored. The former has the potential to reveal biomarkers of therapeutic resistance (as for shieldin and PARP inhibitor resistance in BRCA1-deficient cells), while the latter can identify new synthetic lethal interactions, which in the context of drug candidates may reveal therapeutic targets for inhibition. It is clear therefore, that the use of whole-genome unbiased cancer cell survival screens may help us to identify new mediators of treatment response, as well as sensitisers of specific genetic backgrounds.

The use of isogenic cell lines for the purposes of exploring genetic interactions between a specific gene and its synthetic *lethal* or *viable* partners, is a useful tool for exploring these relationships. However, many genes exhibit functional interactions that can promote or abrogate important phenotypes without necessarily manifesting in cell survival or death. As a result we necessarily risk missing key players in the DDR by relying upon genetic interactions that cause crude changes in the relative fraction of surviving cells in-vitro. One strategy which overcomes this limitation is a modification of the genotype to phenotype approach, which I have designed and am currently completing. By taking a pooled population of gRNA-infected cells, we can use the single-cell based method of fluorescence activated cell sorting (FACS) to isolate cells which demonstrate significant deviations in detectible signals, thereby identifying genes which when lost, accentuate or attenuate a specific 'cellular response'. This has the potential to allow us to explore a wide variety of signals relevant to the DDR, including changes in the expression level of signalling proteins such as p-p53, pCHK1, pKAP1 and γH2AX. After further optimisation of conditions for cellular pre-extraction, we are now able to detect RPA loading onto ssDNA in response to DNA damage. Our latest series of experiments will explore factors which increase or decrease the amount of RPA loading in cycling cells under control conditions or in response

to the topoisomerase I inhibitor camptothecin. I have optimised a set of conditions, such that at 1h and 10h recovery post-treatment, low and high RPA signals (respectively) can be associated with depletion of CtIP and RAD51 (respectively). In other words, by isolating cells at the 'tail-ends' of each population distribution of RPA intensity, we should be able to identify factors which are involved in DNA end-resection, homologous recombination, and in the absence of camptothecin, mediators of replication stress. This represents an exciting step forward in the ability to explore dynamic cellular responses and identify new genetic determinants of DDR pathways. The establishment of FACS-based screening approaches has other potential advantages which may make it applicable to a translational setting.

While pure isogenic cell lines are well-suited to exploring specific genetic relationships, the relevance of such model systems to the clinic is more limiting. We need faithful models of patient disease in an effort to explore genetic drivers of treatment response in a more representative cellular milieu, and which reflects the heterogeneity observed within a mixed population of cancer cells. Patient-derived xenografts go some way to modelling disease, but performing genetic screens in these systems is costly, time-consuming and not without its own limitations. Primary cultures of patient-derived cells may be an option for performing forward genetic screens, albeit with the practical challenges associated with isolating sufficient epithelial cells from surgical specimens and culturing and expanding them ex-vivo. Fundamentally however, their relatively slow growth indices limit the utility of traditional CRISPR-Cas9 'survival' screens which would rely on high proliferation rates to outcompete slower growing cells. FACS-based CRISPR-Cas9 screening offers an opportunity to explore dynamic cellular signals in response to existing and emerging therapies, using these signals as surrogates of treatment sensitivity or resistance, and hence identifying new drug targets or biomarkers of response.

Using the same methodology may enable us to model the cellular responses of cancer cells taken from individual patients. It is conceivable that a diagnostic biopsy could, alongside its use for routine histopathological assessment, be evaluated by flow cytometry to assess the DDR signalling that results from a specific drug treatment. The ex-vivo cells could be used as a treatment 'avatar' to *phenotype* the patient's tumour, enabling the prediction of responsiveness

prior to the commencement of therapy. Finally, small hyper-focused libraries of druggable targets could be used to predict which drug from a basket of available treatments, would an individual patient stand to gain the most benefit. By feeding this information back to the clinic, such a strategy could conceivably be used to help deliver personalised medicine. We continue to build upon the progress made above, in an effort to help realise this ambition in the coming future.

6. Supplementary information

6.1. List of figures

Figure 3.1 Model of resolving stalled replication intermediates carried over from S-phase during mitosis; taken from Pederson et al. 2015 (Pedersen et al., 2015). Recombination intermediates may interlink sister chromatids, or else post-replicative gaps may persist. TOPBP1 may be recruited to these sites to facilitate the resolution of HJ by SLX4 and if necessary complete replication via MiDAS. The persistence of unresolved interlinked intermediates can lead to the formation of DAPI-stained chromatin bridges or finer PICH-marked ultrafine bridges. Any or all of these, can manifest in the subsequent G1 as 53BP1 nuclear bodies. 47

Figure 3.2 Schematic of 53BP1, demonstrating the major motifs of 53BP1, as well as the focus forming region (FFR) which represents the minimal length of protein necessary for IRIF formation. Importantly, the UDR motif contains T1609 and S1618 which are the sites normally phosphorylated during mitosis to prevent chromatinisation. 48

Figure 3.3 Generation of dox-inducible 53BP1 expressing U2OS cell lines. (a) Immunoblot demonstrating clones with dox-inducible expression of Flag-53BP1 harbouring WT or 'AA' residues at S1609 and T1618. (b) Immunofluorescence demonstrating dox-inducible expression of 53BP1 constructs in U2OS cells. 49

Figure 3.4 $53BP1^{AA}$ promotes replication-stress induced acentromeric micronuclei formation. (a) Workflow for cell treatment prior to fixation, along with representative micrograph demonstrating DAPI-stained micronuclei. (b) Quantification showing (top) significant enrichment in APH-induced micronuclei in $53BP1^{AA}$ (compared to $53BP1^{WT}$) expressing cells; and (bottom) a significant increase in APH-induced centromere negative micronuclei in $53BP1^{AA}$ (compared to $53BP1^{WT}$) expressing cells. 50

Figure 3.5 $53BP1^{AA}$ promotes formation of G1 nuclear bodies in response to replication stress. (a) Workflow for cell treatment prior to fixation, with representative micrograph of 53BP1 nuclear

body formation in response to APH. (b) Quantification of nuclear body formation in response to APH. 51

Figure 3.6 53BP1^{AA} impairs unscheduled DNA synthesis in mitosis. (a) Workflow for cell treatment prior to fixation, with representative micrograph demonstrating FANCD2 co-localisation with EdU signal on condensed chromosomes (DAPI) during mitosis. Quantification of (b) number of FANCD2 foci per cell; (c) % EdU positive FANCD2 foci; (d) mean EdU intensity per EdU focus (as defined by co-localisation with FANCD2). 53

Figure 3.7 53BP1^{AA} impairs unscheduled DNA synthesis after reduced replication origin firing. (a) Immunoblot demonstrating effective MCM5 silencing. Quantification of (b) number of FANCD2 foci per cell; (c) % EdU positive FANCD2 foci; (d) mean EdU intensity per EdU focus (as defined by co-localisation with FANCD2). 54

Figure 3.8 53BP1^{AA} interacts with TOPBP1 in a damage-dependent manner in mitosis. Flag immunoprecipitation in response to (a) IR or (b) APH treatment of U2OS cells. 55

Figure 3.9 Mass spectrometry identifying differential interacting partners of 53BP1^{WT} and 53BP1 ^{AA} recombinants (tandem Flag HA tagged). (a) PAGE and silver staining of nuclear soluble and chromatin fractions was followed by tryptic digestion and mass spectrometry. (b) Unique interacting peptides identified by proteomic analysis of significance $p>0.05$ (experiment performed by Dipanjan Chowdhury Group; 2016). 56

Figure 4.1 (a) Schematic of CRISPR-Cas9 screen for PARP-inhibitor resistance factors in BRCA1-mutant cancer cell line. (b) MAGeCK analysis of guide enrichments following PARP-inhibitor treatment; False Discovery Rate (FDR) of 0.1 shown on each plot. 62

Figure 4.2 (a) siRNA mediated knockdown of FAM35A and C20orf196 rescues BRCA1-null cells, (b) but not BRCA1-proficient cells, from olaparib sensitivity. Area under curve graphs shown below each survival curve. (c) Validation of FAM35A (left) and C20orf196 (right) knockouts rescuing olaparib sensitivity, and complementations. (d) Validation of siRNA efficacy used in (a) by western blot. (e) Validation of CRISPR-Cas9 knockouts by Topo-cloning and sequencing. 64

Figure 4.3 RaptorX modelling (raptorx.uchicago.edu; bottom), schematic (middle) and per-residue analysis of functional changes given a point mutation (predictprotein.org; top) for (a) C20orf196 and (b) FAM35A. 66

Figure 4.4 (a) FAM35A and C20orf196 constructs used in this study, (b) establish an interaction via FAM35A N-terminus and OB3/FAM-domain with C20orf196, quantified in (c). (d) Co-immunoprecipitation demonstrating both FAM35A isoforms interact with C20orf196. (e) Mapping the domains of interaction and (f) non-normalised co-immunoprecipitation assay showing the effects of co-stabilisation. GFP-tagged constructs used as bait for GFP co-immunoprecipitation experiments. 67

Figure 4.5 (a) Protein purification under (a) harsh (2% SDS) and (b) milder (sonication/1% Triton-X) conditions; (c) Recombinant GST-FAM35A and His-C20orf196 interact directly (experiment performed with M. Sczaniecka-Clift, Postdoctoral scientist, Steve Jackson Group, 2017)). 68

Figure 4.6 FAM35A and C20orf196 interact with 53BP1, RIF1 and MAD2L2, by GFP co-immunoprecipitation experiments in BRCA1-proficient HEK293 cells. 69

Figure 4.7 (a) FAM35A and C20orf196 are recruited to localised sites of damage induced by laser micro-irradiation (by live-cell imaging) and (b) camptothecin (immunofluorescence micrographs of fixed cells). (c) Full-length and N-terminus of FAM35A but not its C-terminus form IRIF which can be visualised by IF after pre-extraction. (d) FAM35A and C20orf196 expression levels are not affected by BRCA1/53BP1-axis depletion. (e) FAM35A/C20orf196 do not affect 53BP1 IRIF formation, but 53BP1, RIF1 and MAD2L2 depletions do attenuate (f) FAM35A, and (g) C20orf196 IRIF. (h) PTIP depletion did not affect FAM35A/C20orf196 IRIF. Representative micrographs shown adjacent to quantifications. 72

Figure 4.8 (a) Co-immunoprecipitation showing interaction between N-terminus of FAM35A and MAD2L2, and (b) similar dependencies of FAM35A N-terminus IRIF on 53BP1-RIF1-MAD2L2 axis (with representative micrographs on the right). 72

Figure 4.9 Super-resolution microscopy showing overlap of FAM35A N-terminus and 53BP1 in IRIF. Representative micrographs (top), representative approach of algorithm used to quantify

spatial overlap (middle); histogram showing relative distance of FAM35A pixels from 53BP1 core (bottom). 75

Figure 4.10 FAM35A and C20orf196 contribute to NHEJ as supported by effects of depletion or knockout on (a) random plasmid integration and (b) cellular sensitivity to irradiation; right graph shows area under curve. 75

Figure 4.11 (a) Schematic of class switch recombination assay, demonstrating (b) CSR defect due to Fam35a or C20orf196 knockout in mouse B-cells (experiment performed by Ludovic Deriano Group; 2017). 76

Figure 4.12 (a) Schematic of telomere fusion assay in MEFs, demonstrating (b) Fam35a/C20orf196 mediate telomere fusion upon deprotection by TRF2 depletion (experiment performed by Jacqueline Jacobs Group; 2017). 77

Figure 4.13 FAM35A/C20orf196 knockout promotes (a) ssDNA and (b) RPA2 accumulation, likely resulting in disinhibition of end-resection mediated by (c) BLM accumulation at sites of damage (performed with PhD student D. Pilger, Jackson Group; 2018) (d) FRAP confirms equivalent RPA2 turnover after FAM35A or C20orf196 depletion. 79

Figure 4.14 (a) Schematic structure of FAM35A, and similarity to RPA bound to ssDNA, highlighting two W residues predicted to be relevant for DNA binding; as demonstrated by cell lysate co-incubation and pulldown of biotinylated oligos, which revealed W489/W640 mediated binding to ssDNA (performed with PhD student Jonathan Lam, Steve Jackson Group; 2017). (b) Sequence homology to yRPA2 reveals potential residues critical for DNA binding. (c) EMSA confirms binding to ssDNA mediated via W489 and W640 (EMSA performed by Postdoctoral scientist Qian Wu, Tom Blundell Group; 2017). 80

Figure 4.15 FAM35A DNA binding mutant impairs (a) IRIF formation, and (b) fails to suppress IR sensitivity in FAM35A knockout cells. (c) N-terminus over-expression in wildtype cells also has a dominant negative effect on IR sensitivity, but has (d) no effect on response to olaparib. Area under curve shown adjacent to clonogenic survival graphs. 83

Figure 4.16 (a) C20orf196 and FAM35A IRIF following BRCA1 or BRCA2 depletion (representative micrographs shown for FAM35A). (b) FK2 staining of C20orf196 following BRCA1 depletion. 83

Figure 4.17 Temporal kinetics of FAM35A IRIF formation following BRCA1 depletion. (a) IRIF for 53BP1 and FAM35A, and (b) time-course of FAM35A IRIF, with representative micrographs of time-course. 85

Figure 4.18 FAM35A or C20orf196 loss in BRCA1-deficient cells causes hyper-resection phenotype; quantification (left) and representative micrographs (right). 87

Figure 4.19 FAM35A and C20orf196 loss in BRCA1-deficient cells can restore (a) RAD51, (b) BRCA2 and (c) HR reporter assay (top) and effect of FAM35A/C20orf196 depletion (bottom). 90

Figure 4.20 Effects of FAM35A and C20orf196 on cell survival due to olaparib. (a) FAM35A loss is epistatic with 53BP1 loss in BRCA1-deficient cells in response to olaparib. (b) The N-terminus alone is capable of resensitising BRCA1ko/FAM35Ako cells to olaparib. 91

Figure 4.21 BRCA1-deficient PDX models (a) subject to olaparib treatment generates PARP inhibitor resistance with tumours downregulating shieldin complex components. Schematic of experimental setup (top); relative RNA expression levels of tumour specimens from four cohorts of mice for SHLD1, SHLD2, 53BP1, PARP1 (middle); growth curves of olaparib sensitive and resistant PDX tumours from cohorts 1-4 (bottom). (b) Intrinsic PARP inhibitor resistance correlates with low SHLD1 and SHLD2 expression levels; graphs show SHLD1 and SHLD2 expression levels and their relationship with intrinsic olaparib sensitivity or resistance. Experiments performed by Violeta Serra and Carlos Caldas Groups; 2018. 94

Figure 4.22 Loss of FAM35A or C20orf196 in BRCA1-deficient cells generates therapeutic vulnerabilities to (a) IR and (b) cisplatin. Areas under the curve shown for each graph on the right; experiments performed with scientific technician Julia Coates, Steve Jackson Group; 2017. 95

Figure 4.23 FANCD2 foci are de-repressed in the absence of FAM35A or C20orf196. (a) FANCD2 foci following FAM35A, C20orf196 or 53BP1 depletion in response to cisplatin; representative

micrograph on right. (b) GFP-C20orf196 and GFP-FAM35A IRIF are unaffected by FANCD2 silencing; quantification for FAM35A on the right. 96

Figure 4.24 Schematic of FAM35A/SHLD2, highlighting results from this work attributable to different domains. 97

Figure 4.25 Schematic model of SHLD1^{C20orf196}/SHLD2^{FAM35A} function in the presence and absence of BRCA1, as revealed by this work. 100

6.2. Commonly used abbreviations

53BP1	Tumour Protein P53 Binding Protein 1
Alt-EJ	alternative end-joining
ATM	ataxia-telangiectasia mutated
BLM	BLM RecQ Like Helicase
BRCA1	breast cancer type 1 susceptibility protein
BRCA2	breast cancer type 2 susceptibility protein
CRISPR-Cas9	clustered regularly interspaced short palindromic repeats – CRISPR associated protein 9
DDR	DNA damage response
DSB	double-strand break
FACS	Fluorescence Activated Cell Sorting
FANCD2	Fanconi anaemia complementation group D2
gRNA	guide-RNA
HR	homologous recombination
IR	ionising radiation
MAD2L2	Mitotic Arrest Deficient 2 Like 2
MiDAS	mitotic DNA synthesis
MMEJ	microhomology-mediated end-joining
NHEJ	non-homologous end-joining
PARP	poly(ADP-ribose) polymerase
RIF1	Replication Timing Regulatory Factor 1
RPA	Replication Protein A
seDSB	single ended double-strand break
SHLD1	shieldin 1/C20orf196
SHLD2	shieldin 2/FAM35A
SSA	single-strand annealing
SSB	single-strand break

6.3. Antibodies, plasmids, primers, siRNA, gRNA and knockout sequencing

SPJ number	Antibody	Species	Source	Application (Dilution)
A1480	FAM35A	Rabbit	Abcam ab105521	WB (1:1000)
A1483	C20orf196 (E-15)	Rabbit	Santa-Cruz sc-85394	WB (1:200)
A343	53BP1	Rabbit	Novus NB100-304	WB (1:5000)
A1250	53BP1	Mouse	Millipore MAB3802	IF (1:250)
A648	RIF1	Rabbit	Bethyl A300-569A	WB (1:1000)
A1414	REV7/MAD2L2	Mouse	BD biosciences 612266	IF (1:100)/WB (1:1000)
A1407	BRCA1	Rabbit	Merck 07-434	WB (1:500)
A1016	FANCD2	Mouse	Santa-Cruz sc-20022 (FI17)	IF(1:100)/WB (1:1000)
A571	HA	Mouse	Santa-Cruz sc7392	WB (1:500)
A971	BLM	Rabbit	Bethyl A300-110A	IF(1:100)
A749	CTIP	Mouse	Hybridoma supernatant (Richard Baer)	WB(1:50)
A353	GFP	Mouse	Roche	WB (1:1000)
A1562	Tubulin	Rabbit	Abcam ab52866	WB (1:1000)
A1109	GFP	Rabbit	Roche	IF (1:1000)
A278	PTIP	Rabbit	Abcam ab2614	WB (1:1000)
A1394	Abraxas	Rabbit	Bethyl A302-180A-M	WB (1:1000)
A862	Cyclin A	Mouse	BD Biosciences 611268	IF (1:100)
A557	RAD51	Rabbit	Santa-Cruz sc-8349 (H-92)	IF (1:100)
A140	γH2AX	Mouse	Millipore 05-636	IF (1:100)
A767	RPA2	Mouse	Abcam ab2175	IF (1:200)
A598	γH2AX	Rabbit	Cell Signalling Technology 2577	IF (1:500)
A1417	XRCC4	Goat	Santa Cruz sc-8285 (C-20)	WB (1:1000)
A214	SMC1	Rabbit	Bethyl A300-055A	WB (1:1000)
A705	Total H2AX	Rabbit	Abcam ab11175	WB (1:5000)
A287	GAPDH	Mouse	Abcam ab8245	WB (1:2500)
A622	b-Actin	Mouse	Abcam ab8266	WB (1:5000)
A1109	GFP	Rabbit	Life Technology, A11122	WB (1:1000)
A586	Phospho-RPA32 S4/S8	Rabbit	Bethyl A300-245A	WB (1:1000)
A1483	C20orf196 (E-15)	Rabbit	Santa-Cruz, sc-85394	WB (1:500)
A164	GST	Mouse	Santa-Cruz, sc 138	WB (1:1000)
A331/A332	Alexa Fluor 488 anti mouse/rabbit	Goat	Molecular Probes A11029/A11034	IF (1:500-1:1000)
A330	Alexa Fluor 594 anti mouse/rabbit	Goat	Molecular Probes A11005/A11037	IF (1:500-1:1000)
A764	Alexa Fluor 647 anti mouse	Goat	Molecular Probes A21236	IF (1:500)
A517	HRP anti mouse	Rabbit	Dako Ltd P0260	WB (1:10000)
A519	HRP anti rabbit	Goat	Perbio Science 31462	WB (1:20000)
A518	HRP anti goat	Rabbit	Dako Ltd P0449	WB (1:10000)
	53BP1	Rabbit	Bethyl, A300-272A	WB (1:4000)
	b-Catenin	Mouse	BD, 610154	WB (1:5000)
	MAD2L2	Mouse	Santa Cruz sc135977	IF (1:500)
	V5	Mouse	Invitrogen, R960-25	WB (1:1000)
	Flag-M2	Mouse	Sigma, F1804	IF (1:200)/WB (1:2000)
	TOPBP1	Rabbit	Abcam, ab105109	WB (1:1000)
	FK2	Mouse	Affiniti, 04-263	WB (1:200)
	BrdU	Mouse	GE Healthcare, RPN202	IF (1:1000)

Plasmid	Method	Insert	Protein	Source
pcDNA3.1(-)				Invitrogen
pcDNA3.1(-)HA-FAM35A	PCR from Image Clone	HA-FAM35A	FAM35A (short isoform)	This study
pcDNA3.1(-)GFP-FAM35A	PCR from Image Clone	GFP-FAM35A	FAM35A (short isoform)	This study
pcDNA3.1(-)HA-C20orf196	PCR from Image Clone	HA-C20orf196	C20orf196	This study
pcDNA3.1(-)GFP-C20orf196	PCR from Image Clone	GFP-C20orf196	C20orf196	This study
pcDNA5/FRT-TO/Neomycin	Synthesised from Genscript			Addgene
pcDNA5-GFP-FL/FRT-TO/Neomycin	Synthesised from Genscript	GFP-FL	FAM35A	This study
pcDNA5-GFP-NT/FRT-TO/Neomycin	Synthesised from Genscript	GFP-NT	N-terminus FAM35A (1-420)	This study
pcDNA5-GFP-CT/FRT-TO/Neomycin	Synthesised from Genscript	GFP-CT	C-terminus FAM35A (421-904)	This study
pcDNA5-GFP-OB1/2/FRT-TO/Neomycin	Synthesised from Genscript	GFP-OB1/2	C-terminus FAM35A (421-707)	This study
pcDNA5-GFP-FD(OB3)/FRT-TO/Neomycin	Synthesised from Genscript	GFP-FD(OB3)	C-terminus FAM35A (708-904)	This study
pcDNA5-GFP-FL2WA/FRT-TO/Neomycin	Site Directed Mutagenesis of W489A and W640A	GFP-FL2WA	FAM35A(W489A and W640A)	This study
pcDNA5-GFP-C20/FRT-TO/Neomycin	Synthesised from Genscript	GFP-C20	C20orf196	This study
pcDNA5-GFP-C202KR/FRT-TO/Neomycin	Site Directed Mutagenesis of K128R and K183R	GFP-C202KR	C20orf196 (K128R and K183R)	This study
pDEST-mCherry-LacR				Gift from D. Durocher (Toronto)
pcDNA5-Flag-53BP1(WT)/FRT-TO/Neomycin	PCR from Image Clone		53BP1(WT)	This study
pcDNA5-Flag-53BP1(AA)/FRT-TO/Neomycin	Site Directed Mutagenesis of above		53BP1(AA)	This study
pcDNA5-Flag-53BP1(WT)/FRT-TO/Hygroymcin	PCR from Image Clone		53BP1(WT)	This study
pcDNA5-Flag-53BP1(AA)/FRT-TO/Hygroymcin	Site Directed Mutagenesis of above		53BP1(AA)	This study

Site-directed mutagenesis		
Protein	**SDM**	**SDM oligo sequence**
FAM35A	W489f	GAAGGTTTTTCTGGCGAGGACTGCAGCATTTTG
FAM35A	W489r	CAAAATGCTGCAGTCCTCGCCAGAAAAACCTTC
FAM35A	W640Af	GCGTTAGTATTAGCGGGGTCCTGGAGCAGC
FAM35A	W640Ar	GCTGCTCCAGGACCCGCTAATACTAACGC
53BP1	T1609A	CTTGGCCCCTATGAAGCAGTAGCACCTCTTACAAAGGCAGCAGATATCGCCTTAGACAATTTGGTGGAAGG
53BP1	S1618A	CCTTCCACCAAATTGTCTAAGGCGATATCTGCTGCCTTTGTAAGAGGTGCTACTGCTTCATAGGGGCCAAG

siRNAs	
siRNA	**siRNA sequence**
siCTRL	CGUACGCGGAAUACUUCGA(dTdT)
siC20_1	GCGUGUGACAUAAGAGAUU(dTdT)
SIC20_2	GCUUUCAGUUCUUUGGAAU(dTdT)
siFAM_1	UCAACAUUAUGCGCUUGUA(dTdT)
siFAM_2	GCACCUUCAACCUGAUGUA(dTdT)
siRIF1_1	AGACUUGUCUCAGAUAUAA(dTdT)
siRIF1_2	UCAAGGUGAUGCCUUAGAA(dTdT)
siREV7_1	AGAUCCAGGUCAUCAAGGA(dTdT)
siREV7_2	GGAUGUCCACAUGCAUGAC(dTdT)
siBRCA1	GGAACCUGUCUCCACAAAG(dTdT)
si53BP1	GAAGGACGGAGUACUAAUA(dTdT)
siCtIP	GCUAAAACAGGAACGAAUC(dTdT)
siFANCD2	GGUCAGAGCUGUAUUAUU
siPTIP	ACGUGAUCGGAGUGUGUAUAA
siMCM5	GGAUCUGGCCAGCUUUGAU

Shieldin CRISPR knockouts					Human guide sequences		
Clone reference	**Genotype**	**Allele 1**	**Allele 2**	**Allele 3**	**cas9 strategy**	**Guide_1**	**Guide_2**
27_14_NF	p53- FAM-	+5bp	+362bp/-54bp		Nickase	ACTGCGTGGACTAATACATC	GTTGATTTCACTATACTGAC
27_40_NF	p53- FAM-	-1bp	-5bp		WT	GCGTTAATGACTGCCATTGA	
33FAM_2	p53- BRCA1-FAM-	-10bp	+1bp	-29bp	WT	GCGTTAATGACTGCCATTGA	
33FAM_34	p53- BRCA1-FAM-	+1bp	-20bp	-317bp	WT (exon removal)	CGAACGCAGTAGATAAGTCAAGG	AGTTATATCACTCAGTCTAGAGG
24FAM_46	p53- BRCA1- 53BP1- FAM-	-5bp	-1bp/STOP/+1bp		WT (exon removal)	CGAACGCAGTAGATAAGTCAAGG	AGTTATATCACTCAGTCTAGAGG
27_14NC	p53- c20orf196	+313bp	-25bp	-9bp/+20bp	Nickase	ATCTATCCAGGGATTTCCGA	ATGTTTGGTCATCCACAGCC
33C20_27	p53- BRCA1-c20orf196	+1bp			WT (exon removal)	GTCAAGCCAGAAGTTCTCAGCGG	CGTCCCGGTTGAAGATCACCCGG
33C20_67	p53- BRCA1-c20orf196	+2bp	+1bp		WT (exon removal)	GTCAAGCCAGAAGTTCTCAGCGG	CGTCCCGGTTGAAGATCACCCGG

6.4. Control blots of siRNA used in study

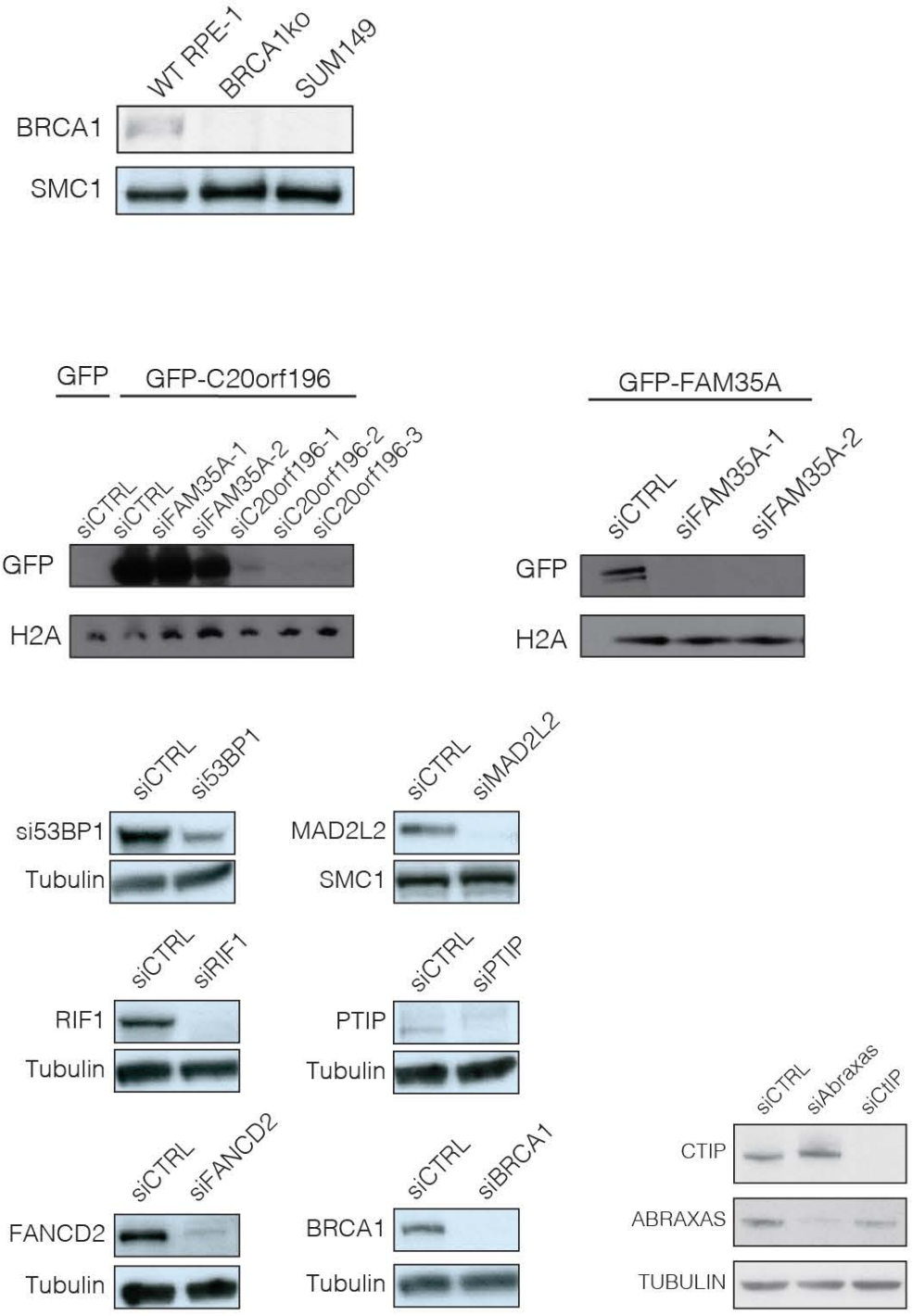

6.5. Top 1000 gene enrichments from CRISPR-Cas9 screen

RANK	Olaparib	Talozoparib	AZD2461
1	FAM35A	C20orf196	C20orf196
2	C20orf196	TP53BP1	SLC44A3
3	TP53BP1	FAM35A	FAM35A
4	RIF1	RIF1	IFT80
5	PAK7	PARP1	FAM122A
6	C15orf48	MATN1	BBS12
7	RHNO1	TEN1	PCMTD1
8	PARG	KCNT1	XKR6
9	MAPK8IP1	MRPS27	ITPKB
10	GNPDA2	DYNLL1	TNFSF15
11	TPM1	OR5M3	NT5DC3
12	RBMY1B	AP5Z1	HRC
13	RBMY1A1	HIF3A	IL1RAPL2
14	hsa-mir-4726	MFF	TSPAN32
15	CCNC	WDR48	C19orf70
16	SLA2	PRR23A	NonTargetingControlGuideForHuman_0495
17	DYNLL1	RAD23A	C11orf24
18	STK35	SLC29A1	PTPN14
19	ABCC3	IRF2BP1	GPNMB
20	ERN1	YIPF1	SPATS2L
21	ZBTB38	ZNF420	ADCY10
22	STK39	NUDT13	TBC1D29
23	BMPR2	TSPAN12	CCL21
24	MIOX	TCTEX1D1	KLHL33
25	ADAM8	CYP11A1	hsa-mir-744
26	SMARCA2	ACER1	FGF2
27	SCD5	hsa-mir-516a-1	LIMS1
28	CRYBB1	ZPLD1	GALR3
29	YBX1	PKP4	TREM2
30	hsa-mir-4469	GP1BB	LPCAT3
31	ACAD9	CLCA2	EIF1
32	SCAF1	ANKDD1A	DEFB105A
34	UQCC1	TERT	DEFB105B
33	UQCC	PATE2	GLO1
35	C1orf94	GNB4	TP53BP1
36	CDK8	GPRIN2	RPL37A
37	SLC38A3	ECSIT	hsa-mir-378h
38	AKT1	MTRR	TROVE2
39	BASP1	RBMY1B	CDCA8
40	PIANP	RBMY1A1	ASB17
41	PLCXD1_Y	TMEM63A	CASP3
42	PLCXD1_X	RTN4IP1	CDK2
43	TSPAN5	ATP10A	DNAJB7
44	FAM180A	MICALL2	TUBD1
45	C9orf170	NPBWR2	CENPO
46	HELT	hsa-mir-4678	SERPINB3
47	CLDN22	DSC1	RPGR
48	OR52E2	ERO1L	hsa-mir-8053
49	FABP4	IQCJ	AHRR
50	VSTM4	IQCJ-SCHIP1	NUP188
51	CXCL11	NCAN	BABAM1
52	SETDB1	hsa-mir-6759	CARS2
53	FRS2	hsa-mir-3920	TNKS1BP1
54	CTNND2	hsa-mir-1265	B3GALNT2
55	F13B	CAMKV	ITPK1
56	C5orf24	ATP13A2	KHDRBS1
57	RTN1	CACYBP	UBE2G2
58	IMPA1	NonTargetingControlGuideForHu	PRR21
59	TPGS1	EGFL7	RNF19B
60	ACER1	PCDH8	REP15
61	hsa-mir-891b	CHST10	KCNH3
62	C13orf45	NonTargetingControlGuideForHu	FAM200A
63	RASGRP1	GRM8	SCAF1
64	RBMY1J	hsa-mir-4695	CXorf57
65	RBMY1F	MEA1	RBP1
66	hsa-mir-3669	RFX3	CCDC74B
67	COX8A	MYL2	OR10G4
68	OR7A5	SMIM17	HIAT1
69	SERPINE2	UBN2	CCL8
70	STAU2	NonTargetingControlGuideForHu	HOXD8
71	PDHA1	PRAMEF13	C16orf54
72	JMJD8	AMER3	SMCO3
73	GCHFR	GRK6	RRP1
74	GSPT1	NPS	MED21
75	CABP1	SHBG	CBX3
76	PSMD13	hsa-mir-3196	ZDHHC22
77	CSDE1	LZTS1	BRE
78	INHBA	ALDH8A1	PDK2
79	hsa-mir-6514	EXTL3	DEFB124
80	ZMYM2	RARRES2	C13orf45
81	OR2A2	TAS2R39	PER2
82	PHOX2B	C6orf58	SMCR7L
83	CAPN12	hsa-mir-3682	GNS
84	SHBG	HIST1H2BC	HSF2BP
85	N4BP1	FBLN2	PCDHA7
86	SPPL2A	FAM72D	PINLYP
87	BCL7C	CCDC117	SCN5A
88	NSFL1C	SLC15A2	MED27
89	PADI3	SERBP1	CSNK1G2
90	REEP4	LOC643037	OPRD1
91	hsa-mir-424	C16orf87	MPI
92	TJP3	ZNF284	WDR24
93	hsa-mir-1248	SPR	TSPY8
94	hsa-mir-6886	HOXA9	GRIK1
95	ANKRD54	hsa-mir-4299	UBC
96	hsa-mir-942	ZMAT1	FUT9
97	RAMP3	ZNF878	EXTL3

Genes of interest		
	OLAPARIB	TALOZAPARIB
DYNLL1	17	10
DYNLL2	20138	18632
ATMIN	316	9261
PARG	8	5194
REV3	17290	6194
REV1	17675	12957
REV7	102	710
TEN1	1387	7
STN1	16261	2568
CTC1	16285	1811

Genes below False Discovery Rate (0.1

98	TFDP1	PDE12	NIN
99	PROCA1	CT47B1	IL13
100	SMPD2	DPRX	PLCG1
101	PGM2L1	CASK	WNT8A
102	MAD2L2	CCNB3	CCSER1
103	KIAA1804	hsa-mir-4770	TGIF2-C20orf24
104	ZMAT4	DLL4	DUSP16
105	CENPBD1	FUBP1	UBE2W
106	HTR1F	OR56A4	C9orf72
107	ZDHHC20	CIAO1	SLMAP
108	hsa-mir-449b	hsa-mir-582	TFPT
109	SPPL2C	ABCG4	IL1R1
110	SLC5A2	CPXM2	CDK5R1
111	LAMB1	SFPQ	RCAN2
112	CWF19L1	TMEM185A	PRRG2
113	REM1	CCNC	PCDH15
114	AGO1	hsa-mir-579	TSPY3
115	ENKUR	TIMM8A	B3GAT1
116	FAM83F	NXPH2	BCMO1
117	CACNA1D	CHRNA7	RPS11
118	BCCIP	POTEE	DCTN4
119	NEK6	POTEM	ANKRD33
120	CCT8L2	SYT11	CLEC2A
121	TMEM81	hsa-mir-551b	OGDHL
122	CCL5	CDK2AP2	NDE1
123	CCDC148	ADRB3	IFNG
124	IMMP1L	hsa-mir-548t	LILRA1
125	hsa-mir-6852	hsa-mir-548ba	hsa-mir-877
126	hsa-mir-7109	CBLN3	PLXNA3
127	URAD	hsa-mir-3140	BATF2
128	PRHOXNB	M6PR	CNPY2
129	NET1	FUK	OR5I1
130	P4HB	MIOS	KLHL28
131	CELSR1	TBC1D8B	CDH9
132	MAST4	ARGLU1	TRIP12
133	PCSK1N	CDKN2A	DPY19L1
134	MN1	ELAVL2	OLR1
135	NonTargetingControlGuideForHu	POPDC2	ATP13A1
136	ABCB10	CAV2	LRP12
137	FAM21C	OR2T10	LOC284385
138	LYPD1	SUMO2	C16orf52
139	DDX10	OR2A25	SDC4
140	ERLEC1	hsa-mir-4455	CAMP
141	SIKE1	MRPL15	TMEM89
142	GRPEL2	SLC15A4	AP1G1
143	PSMC2	hsa-mir-1245a	ZNF839
144	C18orf32	hsa-mir-1245b	HIF3A
145	ELMO3	CCDC171	GPHN
146	NIPA2	OR4Q3	KRT222
147	DHDH	LDLRAD2	CCNC
148	MYBPC1	BOLA3	TMEM165
149	C7orf69	TLR8	SIX1
150	KLRK1	MMP13	METTL7A
151	HLA-E	GFER	OR8K5
152	NonTargetingControlGuideForHu	FBXO34	BNC2
153	MAT1A	FBXO24	SOCS7
154	FBXL19	LDHC	UNCX
155	GSTO1	OR2AE1	SLC7A4
156	HHLA2	MPPED1	CRYGB
157	REEP3	PPFIBP2	SPDYE3
158	ZC3H10	NonTargetingControlGuideForHu	CHST2
159	CCDC88B	NFAT5	NDUFAF2
160	ADPGK	SRPK3	CWH43
161	RSPH1	TEF	APOBEC4
162	TSPAN11	VAC14	NLGN1
163	CDH20	C1orf204	PAM16
164	CUEDC1	AIM2	KATNB1
165	CNTROB	HOXA11	SSBP3
166	FAM169A	hsa-mir-4531	SIM2
167	FAM127B	RAB4A	TNPO1
168	RASSF1	LOC729059	APOL6
169	NonTargetingControlGuideForHu	GUCA1C	CXCR2
170	ASB7	MACF1	CTGF
171	PLA2G12B	NonTargetingControlGuideForHu	EXOSC7
172	CLDN4	SHC1	ZRANB3
173	hsa-mir-3168	ADCY4	DEFA4
174	GNGT2	DSCR4	PLAA
175	KIAA1324	MLEC	PTPRZ1
176	GJA3	ZFP42	KLF14
177	TTC30A	RPS6KA5	ZNF496
178	hsa-mir-4639	STK17B	DNAJC5G
179	PDZD8	MST1R	KRTAP5-10
180	CHST4	MSRB2	ZNF619
181	ZWINT	MCM3AP	PEX16
182	LOC643037	TAOK2	PPP1R3A
183	SERPIND1	PPP1R9B	CXXC1
184	LRRTM3	BDP1	PPIC
185	FAM122A	CXCR3	CRHR1
186	SHCBP1L	SRRM4	ZNF17
187	RRP1	BRD7	DYNLL1
188	MBLAC1	HHATL	CDKN2A
189	THEM6	CADM3	TOMM70A
190	SYT10	UBE4A	ARTN
191	SCRN1	RABL2B	C2orf71
192	ZG16B	ATXN10	SLC4A5
193	OR9A2	MOG	hsa-mir-371a
194	TMEM144	ANGPTL6	CYB5A
195	NTN1	ZNF790	ING3

196	SMPD1	OR6C2	KANSL1L	
197	C1QTNF3	COQ5	RRM2B	
198	MBD6	TRPV6	RAP1GAP	
199	PHF21A	CHD1	CCR4	
200	PUM1	S1PR4	BET1L	
201	MUC6	ZNF580	IRS2	
202	KIAA1551	PLK5	CHST14	
203	CP	DAAM1	ANXA9	
204	AP1S1	TAPBP	ID3	
205	HSD17B14	LIN7A	NBAS	
206	DEFB125	hsa-mir-628	RGS14	
207	FOPNL	CANT1	GSK3A	
208	KIAA0196	GTF2H1	PRODH	
209	BAIAP2	HCLS1	HKR1	
210	MAPK3	HSFY1	ZNF497	
211	RER1	HSFY2	PBK	
212	SKP1	ZHX2	hsa-mir-7849	
213	STK4	KBTBD2	ALDH8A1	
215	hsa-mir-3926-1	MED26	SUGT1	
214	hsa-mir-3926-2	C17orf59	ZBP1	
216	KRTAP5-10	ISG15	TSR3	
217	CCSAP	SUN1	KCNAB3	
218	POLE2	FAM133A	hsa-mir-19b-1	
219	ZBTB21	ZBTB8A	hsa-mir-5197	
220	ANGPTL4	EXTL2	SLC25A11	
221	EDN2	CCDC84	ERGIC2	
222	TMEM39B	LMBRD1	POLG2	
223	YTHDF3	HCAR1	CFHR2	
224	CCDC15	hsa-mir-337	P4HB	
225	PLD4	OR4C13	TNNI1	
226	TRIM44	AP2A1	HNRNPH1	
227	QTRTD1	TMCO1	hsa-mir-6884	
228	ZNF552	CWC27	RAB8B	
229	hsa-mir-4281	NonTargetingControlGuideForHu	CENPQ	
230	SPSB2	VWC2L	TRAPPC13	
231	SCGB2A2	MYOT	YIPF1	
232	PDE7A	BBS10	IRF2BP2	
233	TOR1B	C1orf189	HEBP1	
234	SLC8A1	FAM20B		39508
236	LRP1	CLOCK	RAPSN	
235	NonTargetingControlGuideForHu	RASL10B	SMYD2	
237	ATP2C2	TARBP1	TKTL1	
238	hsa-mir-5707	KCNJ15	PIGV	
239	LYRM9	ZNF93	hsa-mir-940	
240	USP27X	GCNT4	USP17L10	
241	RNF38	C11orf63	GRK7	
242	HAS1	NonTargetingControlGuideForHu	DHX58	
243	hsa-mir-3692	ONECUT1	FSTL1	
244	HERC1	KATNB1	ALS2	
245	IFI27L2	GCG	HS3ST1	
246	HOXC12	GTF3C2	RWDD4	
247	FN3KRP	CDHR3	hsa-mir-4522	
248	AP1S3	JAK2	IFNW1	
249	INO80D	hsa-mir-3914-2	DMGDH	
250	COMMD3	hsa-mir-3914-1	RASGRF2	
251	MS4A6E	PLXDC1	KRTAP10-5	
252	EMC3	CD302	PCDHB9	
253	hsa-mir-129-2	MED29	AQP12B	
254	MOGAT2	RTN1	UPB1	
255	BTN2A1	SNX11	hsa-mir-23b	
256	ABCB9	CECR2	STAU1	
257	NSRP1	STK40	OR5K1	
258	CCDC124	PIANP	TWISTNB	
259	GRM8	IFRD2	ECT2L	
260	CLK4	TMEM8A	SIAH1	
261	PSMD10	NonTargetingControlGuideForHu	CSMD1	
262	TRMT61B	PPP4R4	TVP23A	
263	MPP3	KLK1	TRIM5	
264	NPY4R	VENTX	POU6F1	
265	OR9Q2	KRCC1	CRCT1	
266	hsa-mir-636	CENPQ	RRS1	
267	RHOF	MEOX1	DNASE1L3	
268	STON2	EFNA3	SYNPR	
269	NAV2	FAM216B	RNF130	
270	SPTA1	RRM2	GJB4	
271	IFIT1	CTNNA3	COX8A	
272	RCN1	C1orf95	TTC38	
273	FBXL17	ALAS2	XIAP	
274	FERD3L	EID3	PLCH2	
275	CDK5R1	PCBD2	NCALD	
276	hsa-mir-3118-2	BGLAP	PRR25	
277	hsa-mir-646	SH3RF2	hsa-mir-582	
278	GNPAT	ZNF705A	LYZ	
279	PCYT2	ZNF705D	ESR1	
280	OR51F2	AMY2A	COPS7A	
281	POC1B-GALNT4	SLAMF1	SBSN	
282	DNAJC10	ODF3L2	PLIN3	
283	HTN1	C1orf61	C17orf80	
284	ZC3H4	UBE4B	HJURP	
285	MFF	hsa-mir-520f	NME5	
286	PYCR2	NonTargetingControlGuideForHu	DAPK2	
287	TECPR1	CDC20B	DNAAF1	
288	SENP1	GTF2H2	GRM8	
289	TM7SF3	PRELP	LTB4R	
290	POTED	hsa-mir-1305	GSDMA	
291	39692	PLGRKT	IFNGR1	
292	SCARA5	SLC25A13	RETN	
293	TFAP4	FAM219A	C19orf44	

294	RANBP3L	VASP	NGF
295	KDM3A	BEX2	C15orf26
296	CPNE7	OR8H3	TSPAN4
297	hsa-mir-1293	DEFB114	FBN1
298	CASR	GALNTL5	IL19
299	JRK	POTEG	GLP2R
300	CRISP2	TSSK4	PCOLCE2
301	IL31RA	CSF3R	ZNF800
302	CAPRIN2	RAB24	SMARCA2
303	RAI14	EXOC6	KRTAP9-3
304	IKBIP	FBXO36	TAT
305	ZIK1	TAS2R8	MTMR11
306	PTCH1	CAMK4	C1orf131
307	TET2	MUSTN1	TP53BP2
308	PPP1CA	AHNAK	hsa-mir-196b
309	NARFL	DCAF4	ERLEC1
310	GDF3	SLC25A48	EVC
311	STK38	HDGFRP3	NOX3
312	LHX6	MYEF2	SCAI
313	ZNF641	hsa-mir-4523	TSPAN5
314	JAG2	INTU	CANT1
315	WDR25	CASKIN1	TMEM66
316	ATMIN	SLC6A12	NARFL
317	NOTCH2	LRRC38	CXorf58
318	LEPREL4	KIRREL2	ZNF215
319	UBFD1	JAKMIP1	TM6SF1
320	PIP5KL1	KRBA2	KIAA0226L
321	NonTargetingControlGuideForHu	ZNF735	SLC6A20
322	MARK4	ACSBG2	PLK3
323	NonTargetingControlGuideForHu	PIN4	CUTA
325	USP17L3	PCDHGB6	SLC48A1
324	USP17L1P	PCDHGA8	MFSD11
326	DCAF4L2	GNL2	SDPR
327	IL17REL	SOCS3	KIAA1671
328	NSMAF	PVALB	AFM
329	OR8H3	SOX8	STARD13
330	ARHGAP31	PLD3	CCDC69
331	TMEM156	HDAC8	GALNT11
332	ANKRD6	WNT8A	hsa-mir-519a-1
333	C3orf17	CHRNG	TAZ
334	TRPM2	TMSB10	ALG10
335	LILRB3	CD81	TAF1D
336	C7orf66	MARCKSL1	hsa-mir-514b
337	SLC6A5	LAMTOR4	CCDC15
338	SFTPC	ATP11C	MRPL48
339	TM6SF2	WDR45B	hsa-mir-7108
340	CDAN1	FAM47C	SLC15A4
341	SMIM7	BIRC2	WDR86
342	EZH2	OR2J2	KIAA1328
343	STYX	OR8J3	TRPC4
344	HYAL4	CAMK2D	NOXO1
345	CPT1B	GGA3	MRGPRF
346	IRF2BP1	PLD4	FGFR3
347	MLL	LAG3	CMTR1
348	hsa-mir-219a-2	MAPRE1	TSPAN1
349	PGAM2	ADAMTS2	PHF3
350	FGF6	CYBB	hsa-mir-933
351	SYT17	ERVMER34-1	TCP10L2
352	PDE1B	C11orf16	NXF5
353	OR4D1	ZFYVE28	hsa-mir-509-2
354	CD34	RIPK3	hsa-mir-509-1
355	hsa-mir-3713	ICA1L	CENPJ
356	KIF17	FAM3B	ZNF835
357	IRF7	BTK	TNNI2
358	HDAC2	hsa-mir-4489	PPP1R37
359	TREM1	CDH24	MOCOS
360	ASPM	PLG	DHX33
361	PGM1	LRIG1	SBF2
362	C8orf82	ARRDC4	PARP1
363	PRMT2	CHAC1	SPIRE1
364	NMB	CLDN8	ALG2
365	EEF2K	EFNB2	REG3A
366	MMAB	UCN3	TRIM23
367	FAM76A	NonTargetingControlGuideForHu	MOG
368	MBNL2	hsa-mir-374b	CHCHD3
369	MSX2	hsa-mir-374c	CLSTN3
370	ANKRD39	PRPSAP2	PRMT10
371	PSG2	CNPY4	EIF4A2
372	ZC3H8	BRCC3	COL4A6
373	CDK19	OLR1	ABCG2
374	EEF1D	ZNF341	hsa-mir-6761
375	TOMM40	GJB1	hsa-mir-3065
376	RBP3	NonTargetingControlGuideForHu	hsa-mir-338
377	PRRT1	DRG1	HIST1H2BC
378	PMCH	DYRK1B	CHDH
379	ICAM2	TSPYL5	PIGR
380	FAM117B	TXLNB	BTN3A2
381	NonTargetingControlGuideForHu	LHX6	C1R
382	EFR3B	DCC	hsa-mir-4779
383	C8B	CD163	SFRP4
384	PLS1	NonTargetingControlGuideForHu	PPM1J
385	SLC2A4RG	FAM118B	TGFA
386	GOLT1A	NonTargetingControlGuideForHu	AQPEP
387	CX3CL1	SCRN3	PRKCE
388	PNPO	ANXA2R	CORO7-PAM16
389	UTP11L	GRN	hsa-mir-5090
390	NonTargetingControlGuideForHu	TRIM50	DYRK1B
391	TNIP2	hsa-mir-4253	GPR82

392	KRTAP25-1	UBL7	TMEM194B
393	ADAM7	PROS1	hsa-mir-6130
394	ART4	C8orf34	FBXL19
395	MAN1C1	OR4L1	SLC3A2
396	GP2	KEL	LXN
397	TTLL4	GJC1	ZNF696
399	GCNT7	EREG	PCDHB3
398	FAH	PAM	POP5
400	NonTargetingControlGuideForHu	ZNF668	RPUSD3
401	CUL2	TMEM218	LRRC17
402	hsa-mir-579	PRMT2	HSDL2
403	RNF111	OR6B1	C9orf142
404	CD1C	TBC1D19	ZNF142
405	TEKT1	SAC3D1	PTRF
406	PDE4D	RHOB	TRPC7
407	STAG1	AGPAT1	GRID2
408	GRIK2	ART4	CIR1
409	FAM107A	VAV3	KIAA0754
410	C7orf31	DYNLRB2	SLC25A17
411	STK3	RPS15	ST6GAL1
412	CFHR5	XK	PPP1R10
413	SLAMF1	EVX2	DOCK9
414	C11orf87	RASL12	DAB1
415	KLK5	ERMARD	hsa-mir-6728
416	NonTargetingControlGuideForHu	FOXC2	PRDM16
417	CDK6	PPP2R1B	TEX37
418	C6orf163	DMRTC2	RELT
419	ASB13	CLIP4	CRAMP1L
420	RPL39	FAM170A	ITPRIP
421	TMEM132D	NIPSNAP3B	UPK3A
422	LRRN3	USP21	TRIM62
423	JMJD4	KDELC2	GLDC
424	C3orf36	PCSK7	C15orf32
425	KIAA1143	OR52W1	OR6V1
426	P2RX7	LENG1	L3MBTL2
427	hsa-mir-548aa-1	MCFD2	SLC6A13
428	hsa-mir-548d-1	FAM110D	RALY
429	AK9	hsa-mir-6894	CBR3
430	MRPS18B	RAB19	CXCL11
431	KANSL1L	RPS18	COL17A1
432	KDELC1	NonTargetingControlGuideForHu	CD33
433	ALDH1A2	IGFALS	ARNT
434	MESP2	MLKL	C14orf183
435	LRP6	RBMY1J	ACD
436	COMMD5	RBMY1F	COL5A3
437	C1orf229	MGAT3	TPGS1
438	IL5	HIST1H3D	KIAA1107
439	hsa-mir-5685	ARMC4	KCNK10
440	PSMC5	ATXN3L	KAT6A
441	GRHL1	NXPH3	LIMD1
442	ACSL4	hsa-mir-3148	CACYBP
443	SCNN1D	NonTargetingControlGuideForHu	RPGRIP1
444	PIGW	TCEAL7	ALLC
445	RIC8B	DCTD	HR
446	NARF	TMEM19	UNC50
447	PIGU	hsa-mir-486	PSMD6
448	CCL8	hsa-mir-486-2	VIT
449	PIGS	ANKRD2	CALCOCO1
450	LRRN1	RNF180	ESRRG
451	SMCO3	YWHAH	CWC22
452	PIM2	SCN1B	SKP2
453	ME1	PCDH12	C12orf42
454	TMEM151A	B4GALNT3	SEC61G
455	HECW1	PTX4	SLC26A9
456	HOXD4	hsa-mir-3122	MALT1
457	SCGB1D2	SCARF2	hsa-mir-371b
458	DNAI2	POMT1	ZNF330
459	POLR2H	ASGR1	RNF128
460	MDM1	NonTargetingControlGuideForHu	RIPPLY1
461	ACAP1	hsa-mir-4520b	PDE3A
462	NonTargetingControlGuideForHu	BPGM	PRKAR2B
463	NDUFS1	FAM122A	GABRA2
464	CCNB1	CLC	PPIAL4D
465	PCBD2	ABCC10	hsa-mir-1184-3
466	ASCC1	HDHD2	hsa-mir-1184-2
467	PREPL	CAPN5	hsa-mir-1184-1
468	GAN	hsa-mir-132	FURIN
469	MYCL	EIF3B	FAM169A
470	ZNF286B	B4GALT4	TMEM99
471	SRP19	TMEM69	SMOC2
472	PRPS2	CDH9	GGN
473	ADAM11	PGLYRP4	MS4A14
474	SEC61B	PLA2G4E	PDZRN4
475	GALR2	DENND5B	MMD2
476	NonTargetingControlGuideForHu	BRCA2	LOC100129924
477	STAM	LCA5	SHE
478	CALML4	DNAH5	TCP11L2
479	LZTR1	FATE1	FRMPD4
480	GNG4	C7orf65	EXOSC9
481	TMEM64	CEP290	NYAP2
482	CCDC59	hsa-mir-3909	SPPL2C
483	SERTAD4	SDHA	UMODL1
484	SLC22A18	HIST2H2AC	NIPAL3
485	SORBS2	ADRBK2	COL6A6
486	TEAD4	SLC11A1	RNF186
487	TMTC4	NCSTN	KCNA7
488	ATP5A1	MIOX	CD28
489	HSPB7	hsa-mir-376b	E2F2

490	CMTR1	ZFP64	FUK
491	NT5DC3	WASF2	RARG
492	NHEJ1	MAGEH1	ZNF174
493	RHOB	IHH	ATRIP
494	RHBDF2	TMEM132B	PPP1R35
495	SLC29A1	HERC3	AK8
496	DBP	MAP3K14	C6orf7
497	ASMTL_X	CXCL13	CHRDL1
498	ASMTL_Y	ENKUR	NonTargetingControlGuideForHuman_0916
499	GP5	MMAB	FCGR3B
500	APOL5	NCAPH	DCAF16
501	GRB14	DHX34	RTP3
502	ANAPC7	NonTargetingControlGuideForHu	PNO1
503	OAS2	KRT73	hsa-mir-6129
504	FAM71F1	NonTargetingControlGuideForHu	RANBP1
505	hsa-mir-6837	KTN1	hsa-mir-3679
506	C19orf44	ATG13	CCDC169
507	SLC17A7	CNTLN	TSHZ2
508	GOPC	PLK1S1	PXMP4
509	PKD1L3	SNRNP25	hsa-mir-4271
510	PCDHA4	hsa-mir-3692	THRAP3
511	HADH	AFAP1	MUC16
512	SNX9	hsa-mir-548ag-1	OTX2
513	KLK15	PHLPP2	IL37
514	FHL3	PTN	CPLX4
515	SYNE4	PLA2G4B	HSP90AA1
516	GLYATL1	NRTN	KRTAP6-3
517	APH1A	HAPLN2	ACSS2
518	NLGN1	CASP14	OCA2
519	NonTargetingControlGuideForHu	FSD2	TET1
520	DNAAF1	FAM150A	KRTAP19-6
521	HSPB1	GPR110	FAM63A
522	CTAG1A	COPS4	ACYP1
523	CTAG1B	CELSR2	CPNE9
524	NonTargetingControlGuideForHu	TARS2	KLHL1
525	OR4C46	ARHGAP22	OR4C12
526	POLD4	KRTAP19-8	SATB1
527	KLHL7	MTUS1	ZFP91
528	PPM1E	GPT	EFNA1
529	SPEN	PCDH1	IQSEC2
530	RNASEL	KAT2B	hsa-mir-3168
531	LRRC37A2	ST6GALNAC3	PREP
532	NDNL2	CACNB4	CHPF2
533	RGMA	HBS1L	DNAH3
534	TM4SF19	hsa-mir-361	BPNT1
535	MGA	COL28A1	CHI3L1
536	NonTargetingControlGuideForHu	NonTargetingControlGuideForHu	RNF215
537	CYP21A2	SH2D3A	hsa-mir-6806
538	SLMAP	KCNJ14	WFIKKN2
539	CLPSL2	PSAP	ZNF441
540	NOA1	CACNA1G	HTR6
541	SH3GL1	NonTargetingControlGuideForHu	NPPB
542	WBP5	MSRB1	ANKRD37
543	TEKT3	hsa-mir-4781	FSTL3
544	CMTM2	PAM16	KIAA1217
545	TSHZ1	POFUT2	BRAP
546	MGMT	TMEM161A	GDF1
547	FAM9B	SLITRK3	MTHFS
548	XRCC4	NonTargetingControlGuideForHu	DCLRE1C
549	EMILIN1	BORA	TRIM28
550	MMAA	XRCC4	PGM5
551	NDN	UBQLNL	ATP1A2
552	S100A4	METRNL	BAHCC1
553	NonTargetingControlGuideForHu	GLRA4	hsa-mir-124-1
554	RPGR	NDUFS7	SENP1
555	HORMAD1	NonTargetingControlGuideForHu	ANO5
556	COMMD8	PON1	OVGP1
557	PLEKHB2	C5orf34	TXNDC15
558	KRTAP19-4	C16orf13	CTSE
559	OR4N4	GRM1	hsa-mir-3199-2
564	TSPY8	RAD51AP1	hsa-mir-3199-1
561	TSPY4	C2orf72	SNX18
562	TSPY3	EGFR	NLRC4
563	TSPY1	SRPK1	NBL1
560	TSPY2	ASTN1	FNDC8
566	RBMY1E	hsa-mir-4520a	NonTargetingControlGuideForHuman_0380
565	RBMY1D	SERINC3	KIAA1467
567	TCEB3C	BSG	MAGEA11
568	hsa-mir-4533	PRTG	STON1
569	JAK2	XXYLT1	hsa-mir-4709
570	LYSMD4	KCNC1	CCL17
571	ATP2B2	LARP7	hsa-mir-3942
572	ACTC1	VSNL1	ANKRD65
573	DUS2	ZSCAN1	PRIMA1
574	MAPK6	GPR158	VDAC2
575	CTPS2	DUSP9	HAX1
576	NonTargetingControlGuideForHu	NonTargetingControlGuideForHu	MTCP1
577	ZZEF1	SMPX	SPATC1L
578	RBM39	hsa-mir-4284	VRTN
579	KANK3	GALM	C11orf63
580	KDM2A	KRTAP21-3	PNPLA2
581	CCP110	DDX58	SAYSD1
582	ZNF721	LAMP5	TMEM60
583	CELSR2	KCNK5	SLURP1
584	NDUFB10	DEPDC7	TFF2
585	SNX20	AP1S3	DMRT3
586	RAP2B	STAC2	MOB1A
587	SERPINB13	CNTN1	DECR1

588	LYSMD3	FAM198A	RNF168
589	ZNF75D	OR8K3	GPRIN1
590	hsa-mir-302b	GPR132	HPD
591	NonTargetingControlGuideForHu	NonTargetingControlGuideForHu	ZNF695
592	UNC13D	C1S	SENP6
593	RIMBP3	C10orf107	PRAMEF15
594	hsa-mir-933	C1QC	PRAMEF9
595	SCRG1	ALG14	ELAC1
596	hsa-let-7f-2	MILR1	CENPA
597	NonTargetingControlGuideForHu	ANKRD35	ZMYND8
598	TMEM86A	PTPRZ1	CDH13
599	USP18	CCR4	KLC3
600	CSPG5	CTAGE5	JHDM1D
601	C6orf141	MCCC2	ETFA
602	LRRC1	hsa-mir-4279	AMH
603	C6orf1	FAM19A2	GNAI1
604	FRMD8	hsa-mir-5100	RBKS
605	EHD4	GNG8	TBC1D9
606	PRF1	hsa-mir-411	GTF2A2
607	UBE2U	MAFA	TUBB
608	LONRF3	NonTargetingControlGuideForHu	ANKS4B
609	GTF2H1	CHST4	TAF3
610	TPCN2	MPP6	FBXO7
611	APOM	DUOX1	ZNF7
612	NonTargetingControlGuideForHu	OVOL2	USP3
613	CD46	FAM118A	TRAK2
615	ACOT12	ATP5J2-PTCD1	SGTA
614	NonTargetingControlGuideForHu	hsa-mir-4670	PIK3R1
616	hsa-mir-629	PLCG1	EMC6
617	UTS2R	RGS14	hsa-mir-3652
618	hsa-mir-4418	TRAPPC12	LEPREL2
619	GRB7	RAB11FIP5	P2RY12
620	RASL12	GATSL1	ETV3
621	PTAFR	GATSL2	CACNB4
622	RAB8B	TBRG1	HOXC12
623	KLHDC10	SGOL2	CASP10
624	CHCHD5	CCDC101	ACVR1B
625	CRADD	HBM	CT62
626	CLEC4C	DLX3	TRPV5
627	NDUFA5	NonTargetingControlGuideForHu	RTP2
628	MYLPF	ENO3	NFATC2IP
629	hsa-mir-4740	CLDN15	GNG5
630	ZNF33B	TGIF2LY	BTBD8
631	NCAPD2	FCRL5	PTRH1
632	hsa-mir-4800	CEBPG	ADRBK2
633	CDK17	ZBTB21	KCNN3
634	OTX1	OR52L1	PFKL
635	CEP128	DIEXF	PDE6H
636	MAPK12	CYP11B1	NonTargetingControlGuideForHuman_0792
637	NonTargetingControlGuideForHu	GNPDA2	CDCP1
638	CLASP2	MEAF6	CAT
639	OR2T3	LOXL3	TRA2A
640	RTCA	CNN3	hsa-mir-4666a
641	GPS1	MYOZ3	CDIP1
642	DHX36	GARS	hsa-mir-521-1
643	C8orf86	CEBPZ	DPY19L3
644	GABARAPL1	NonTargetingControlGuideForHu	TRNAU1AP
645	TRPV2	MFAP5	COPS7B
647	hsa-mir-513a-1	YME1L1	S100A7
646	hsa-mir-513a-2	ZNF676	ANKRD6
648	HARS2	hsa-mir-548f-3	MYO1G
649	AKR1E2	hsa-mir-6131	SUV420H1
650	RTN4IP1	SPPL2B	ZNF85
651	NonTargetingControlGuideForHu	CDX4	RDH5
652	DOPEY2	hsa-mir-8086	ABHD14B
653	CLDN20	GNL3L	MAPKBP1
654	OTUB2	CCDC83	ZBTB21
655	CAP2	HIST2H2BF	hsa-mir-199a-1
656	hsa-mir-8082	hsa-mir-6878	C18orf63
657	37226	LCORL	RNF14
658	OR2AK2	TTLL9	PROK2
659	EIF4EBP2	NonTargetingControlGuideForHu	PRPF8
660	FARSB	MIS18BP1	RPN1
661	NonTargetingControlGuideForHu	hsa-mir-301a	BET3L
662	HAX1	RP2	KIAA1755
663	TMEM206	REP15	C1orf141
664	CHRNA1	NKX2-1	RPH3AL
665	NonTargetingControlGuideForHu	NonTargetingControlGuideForHu	UTP23
666	SULT1C3	MGAM	CKLF
667	NonTargetingControlGuideForHu	hsa-mir-3611	hsa-mir-4766
668	SLC10A5	UBALD2	CLEC2D
669	DRD1	UCP1	CD8A
670	TMEM65	C20orf166	PLA2G4E
671	GSDMB	NonTargetingControlGuideForHu	PIANP
672	CASP3	JAGN1	ICK
673	TEX36	hsa-mir-1277	LAMB2
674	TAS2R13	GDF11	HCAR3
675	ARHGAP40	PCDH20	DDX49
676	MFRP	NLGN1	ATE1
677	LYZ	CCDC167	NOS1
678	UPP2	NDUFA7	PITPNA
679	CEP63	ZHX1-C8ORF76	DOPEY2
680	E2F7	C8orf76	ENOX2
681	TUBA8	C16orf54	TRIM8
682	RPUSD1	HLA-DOB	RAP1GDS1
683	FEN1	CCDC71L	hsa-mir-718
684	FLJ45513	FOXC1	hsa-mir-4515
685	C8orf22	hsa-mir-6731	CMTM6

686	RDH8	SPDYE2B	MYT1L
687	hsa-mir-523	SPDYE6	NQO1
688	VGLL4	SPDYE2	NEK11
689	LAMP2	SPDYE2L	OR10A2
690	FAM162B	SPDYE5	hsa-mir-1277
691	hsa-mir-4636	SCAF1	CD22
692	C17orf99	PLEKHJ1	EBLN2
693	MBD4	NonTargetingControlGuideForHu	MAGEB5
694	SCAMP3	ADCK1	ZNF616
695	NonTargetingControlGuideForHu	SLC30A8	ACIN1
696	SEMA4D	CX3CL1	FAM46A
697	PCNXL3	NUDT14	N6AMT1
698	EMCN	SH3BGR	C15orf41
699	LAPTM4B	C11orf31	hsa-mir-3692
700	TCHP	SIRT1	MELK
701	APH1B	CD40	hsa-mir-6124
702	NonTargetingControlGuideForHu	CEP76	GAB3
703	N4BP2L1	NDUFA2	CASP12
704	KDM5A	JDP2	C11orf94
705	C15orf39	RAB27B	ARG1
706	CALM3	FOXL1	hsa-mir-7850
707	FRMPD4	hsa-mir-106b	DPM1
708	C16orf90	TMEM256	RBM42
709	DPY19L3	VSIG4	BLVRB
710	NonTargetingControlGuideForHu	MAD2L2	PHGDH
711	GPR33	hsa-mir-3689d-1	PPP1CB
712	GMFG	GATAD1	ASCL3
713	POLH	PSME2	BLMH
714	IL22RA2	CCDC111	ENPP4
715	KLF2	GRWD1	PON2
716	ELL	hsa-mir-2467	DCAF12L1
717	TSTD3	CHIC1	LIMCH1
718	CD9	FAM9C	SAR1A
719	NFIC	NonTargetingControlGuideForHu	C12orf52
720	C11orf80	RAB6C	RREB1
721	OR10T2	LRRC23	DLGAP3
722	TTYH1	NonTargetingControlGuideForHu	ST3GAL3
723	hsa-mir-5188	hsa-mir-888	hsa-mir-1297
724	IP6K2	KIAA2022	C5orf28
725	RTBDN	SERPING1	OR51B4
726	POMC	ARPC3	QARS
727	PXDN	GCC2	FLT3LG
728	hsa-mir-151b	VMO1	ASF1A
729	HIST1H2BJ	C15orf41	IGSF22
730	hsa-mir-7844	MKRN3	ZNF679
731	MYF5	hsa-mir-1258	SYAP1
733	MAB21L1	NonTargetingControlGuideForHu	GANC
732	RCC1	SFTPC	PCDH10
734	NUP210L	NDUFA9	STK24
735	RAPGEF5	REEP2	hsa-mir-30c-2
736	PARP1	LMO4	UBASH3B
737	SORBS3	PDCD6	ARAP3
738	TOR1AIP1	OR2M3	AWAT1
739	NonTargetingControlGuideForHu	TNFSF15	KRTAP29-1
740	SP2	NonTargetingControlGuideForHu	OR5H1
741	HIPK3	NonTargetingControlGuideForHu	ZG16B
742	GRTP1	PITPNM2	hsa-mir-1471
743	FAM175B	KRTAP19-3	GPR171
745	AGMAT	ANGPT2	hsa-mir-4433b
744	hsa-mir-4499	HS3ST3B1	hsa-mir-4433
746	KIF26B	HS3ST3A1	hsa-mir-3115
747	LEP	MTX1	hsa-mir-4772
748	CTAGE1	ARHGAP40	C7orf43
749	ANO10	ANKRD44	TCTE3
750	PAOX	KSR1	XRCC3
751	hsa-mir-4710	NonTargetingControlGuideForHu	RIC8A
752	hsa-mir-575	DTNBP1	EPPIN
753	PLAG1	LOC100505841	ZNF202
754	GBP3	SSX5	REM1
755	DENND2A	SRPX2	INPP4A
756	F9	MEIS2	TOMM40
757	NonTargetingControlGuideForHu	TMEM18	UGT2A3
758	CD81	CDC42SE2	ICAM1
759	TMEM18	PSD	APOOL
760	SCARF1	hsa-mir-4251	C1orf194
761	DCDC2	TCEB3	DEFB132
762	GTF2A1L	HMX3	TOR3A
763	FTO	ABCA1	CLINT1
764	NonTargetingControlGuideForHu	NonTargetingControlGuideForHu	FCGR1A
765	HIST2H2AB	FOXR2	GP9
766	DNAH9	ADAMTS13	TIGD7
767	ZNF222	COL24A1	ASTL
768	CMPK1	hsa-mir-4319	GPT
769	FAM157A	MESDC1	CTSW
770	VCX3A	PRMT10	RBM4
771	LMF2	C4orf27	CLEC4M
772	TLR2	P4HA3	hsa-mir-3649
773	NonTargetingControlGuideForHu	ECHDC2	SHISA6
777	BAGE4	STX17	GIGYF2
774	BAGE5	GPRC5A	TNIP3
776	BAGE2	PGAP2	STPG2
775	BAGE3	PRRG2	EED
778	ZSCAN2	ZNF598	CCDC88B
779	CERS4	CLRN2	SLC16A3
781	PSPN	NCF1	TSSK2
780	PHB2	SLC5A11	FAM49A
782	AOC1	TACO1	EMD
783	ABP1	MBTPS2	ARAP1

784	CST7	RET	ZSCAN4
785	CEP112	MAP7	VSIG10
786	SWT1	NonTargetingControlGuideForHu	GSTM5
787	MRAP2	MZT2B	RTL1
788	hsa-mir-4486	LAMB3	LMTK2
789	MYH10	EMILIN2	SOCS6
790	NonTargetingControlGuideForHu	RSRC1	ZBTB34
791	POU2AF1	ZZEF1	THBD
792	LGMN	ENTPD2	PTGES2
793	C16orf45	FAM170B	RBL1
794	CX3CR1	CDC42SE1	KIF6
795	HOXC11	hsa-mir-4252	ITGB4
796	TIMD4	GRP	KCNU1
797	TMEM59	NonTargetingControlGuideForHu	NR1H4
798	TCP10L2	hsa-mir-8053	EFCAB4B
799	hsa-mir-519a-1	BEND3	SLC10A5
800	AFF3	TNFRSF10C	WBP2
801	SUFU	CD8A	AAMDC
802	hsa-mir-5692c-2	hsa-mir-4267	hsa-mir-6828
803	MDH2	GABPB1	SERTAD3
804	GLDN	ZNF205	HLA-DMB
805	hsa-mir-8052	SCT	C12orf10
806	TMEM191B	hsa-mir-4462	ADORA2A
807	COMMD6	NRL	ALX1
808	NonTargetingControlGuideForHu	VTI1A	ARL10
809	GINS3	hsa-mir-3164	B3GNTL1
810	FYN	AP1M1	TMEM198
811	PARP8	CBLL1	FRMPD1
812	CABLES1	DRAXIN	CD9
813	GATM	MYH7B	PCDHA9
814	PRSS57	NDFIP1	PCDHA2
815	IQCK	hsa-mir-186	PCDHA11
816	KRT78	hsa-mir-1281	PCDHA1
817	RFPL1	ZNF705B	PCDHA8
818	NonTargetingControlGuideForHu	POLD4	PCDHA13
819	DPEP1	LOC158434	PCDHAC2
821	C1QTNF9B-AS1	hsa-mir-3668	PCDHA5
820	PPP1R12C	NonTargetingControlGuideForHu	PCDHA12
822	STK32C	KLC4	PCDHA6
823	hsa-mir-325	NonTargetingControlGuideForHu	SETMAR
824	TMEM254	ARHGAP28	FKBP11
825	MED18	LAMP3	GLIS2
826	NonTargetingControlGuideForHu	FAM25C	SGK196
827	SMARCA1	FAM25G	GAB1
828	NonTargetingControlGuideForHu	COA1	RBP7
829	SMIM1	NonTargetingControlGuideForHu	ABHD17B
830	SMIM8	ID1	EIF2AK2
831	NonTargetingControlGuideForHu	NonTargetingControlGuideForHu	VPS29
832	ERCC1	PEX7	ZSCAN5A
833	NHLH2	IFI6	AFAP1L2
834	TSTA3	OR4A47	MSH3
835	NCR1	hsa-mir-517c	SREK1IP1
836	MYEOV2	hsa-mir-6767	FOXRED1
837	ORAI1	SLC38A10	ENTPD1
838	TMEM225	EI24	OR8A1
839	TEX38	CTPS2	FAM187B
840	PRDM7	CD2	ACTL9
841	NTMT1	GAS7	KHDC1L
842	UBE2D1	PI15	C6orf222
843	OR2S2	USP33	HLA-DQB2
844	VPS26A	HERC2	SAMD5
845	SLC35C1	MYOM3	PCP2
846	SLC22A14	RNASEL	ELOVL3
847	DEPDC1B	GAGE5	CLRN1
848	hsa-mir-149	GAGE7	RTEL1
849	FAM26F	GAGE6	DNAJA3
851	ATPIF1	GAGE12I	SOST
850	IGSF6	GAGE12B	LAMB1
852	PITPNC1	GAGE12C	NT5C1B-RDH14
853	ABHD17B	GAGE12D	C20orf96
854	EXOSC4	GAGE12E	ERC2
855	TMPRSS15	GAGE12F	HEATR6
856	CD151	GAGE12G	TRIM50
857	NonTargetingControlGuideForHu	GAGE2C	ZNF716
858	HIST1H4F	GAGE2B	ZNF735
859	GRM6	GAGE2A	SPATA33
860	AXIN2	GAGE12H	CSF3R
861	ZNF699	hsa-mir-1301	ZNF223
862	NonTargetingControlGuideForHu	PRRC1	TCTN2
863	FAM175A	PLSCR4	LCORL
864	MRPL24	ZNF322	CHST3
865	ATF1	ZFAND2A	SPTBN4
866	PODXL2	MYL9	ARPC1B
867	LSM6	KIR2DL1	RAPGEF4
868	DCST1	NPEPPS	ANKDD1B
869	GRIN2C	TPK1	TPST1
870	ZFP30	NonTargetingControlGuideForHu	hsa-mir-3689f
871	TRIM16L	DOK1	STAP2
872	SLC2A5	DHX36	SLC26A8
873	NonTargetingControlGuideForHu	C15orf59	ZADH2
874	PHF21B	VKORC1L1	SLC30A2
875	MERTK	STOX1	NBEAL1
876	TMEM11	SLC25A43	AP3B1
877	EVA1B	IRF2BPL	ARMC12
878	SVEP1	ZFYVE27	DOCK8
879	F3	MSGN1	IGFL1
880	HNRNPH2	C5orf15	GIPC3
881	hsa-mir-5693	KRTAP9-1	FLNB

882	TMPRSS6	C9orf64	TSPY2
883	MFI2	hsa-mir-548av	TSPY1
884	NonTargetingControlGuideForHu	PTK6	TSPY4
885	hsa-mir-3942	TNFRSF6B	PDZD4
886	PTPLB	GM2A	VSIG1
887	AHRR	COL4A6	PTPRU
888	DNAJC2	SPATA16	TGFB3
889	UCK2	C1orf186	MIF4GD
890	MRAS	SIM2	ANAPC15
891	hsa-mir-508	BLK	hsa-mir-581
892	LCN1	NonTargetingControlGuideForHu	ITSN1
893	PCSK6	TADA3	LCA5
894	HOXB1	hsa-mir-516a-2	LRRC47
895	hsa-mir-1255a	PDE6A	USP47
898	TRIM49	PRDM5	TMEM204
897	TRIM49B	FRS2	ARRDC5
899	TRIM49C	KRT72	JMJD4
896	TRIM49D1	PRKG1	KDM3A
900	CRELD2	AKAP8L	IQSEC3
901	hsa-mir-30a	HNRNPK	hsa-mir-194-1
902	FOXB2	UCHL3	DENND1A
903	PPP1R2	IDH1	CDKL5
904	MPPED2	hsa-mir-29a	hsa-mir-642a
905	NonTargetingControlGuideForHu	SIPA1L1	PTPN7
906	hsa-mir-1204	ULK4	SPG20
907	POLR2B	PER2	hsa-mir-4295
908	NonTargetingControlGuideForHu	RANBP1	FUCA1
909	RTN3	MUC22	SIK1
910	ARL5A	PIFO	hsa-mir-3169
911	HNRNPA3	THOC2	PDGFA
912	REM2	NAV2	TNFAIP8L3
913	TMPRSS4	MCHR2	C1orf192
914	MYL7	ZBTB46	TP53
915	TTC29	SMC1B	HERC2
916	GRP	PIGW	MNDA
917	PRAM1	HIST1H2BM	LPP
918	LDOC1	SLC25A12	TMEM201
919	CARD9	FARP1	POU2F3
920	KLF13	hsa-mir-518b	FGF9
921	MSLN	ADCYAP1R1	CLCN2
922	TMPRSS7	NonTargetingControlGuideForHu	MUM1L1
923	LHFPL3	ZNF564	GBP3
924	NonTargetingControlGuideForHu	DCAF11	PDCL3
925	CD48	KCNJ2	NFIB
926	PRR16	MPDU1	ARMC9
927	PRR23C	LOC100127983	PREX1
928	WNT11	ITGAV	PNPLA3
929	PRRX2	ZBTB40	PWWP2A
930	PRKCA	PF4V1	NEURL2
931	TLR4	LSG1	DTWD1
932	NonTargetingControlGuideForHu	SPEG	TIAM1
933	DMRTC1	BCAN	hsa-mir-4711
934	DMRTC1B	STON2	DIXDC1
935	CCNB3	HPRT1	ZMYND19
936	AHCTF1	SLC45A4	CCDC134
937	KCNRG	hsa-mir-493	OTOP1
938	ACTN2	POTEJ	MAN2C1
939	RAB40B	POTEI	CYB5B
940	SZRD1	POTEH	SETDB1
941	C16orf13	POTEF	GPR21
942	GCC1	NonTargetingControlGuideForHu	FAM180A
943	hsa-mir-16-1	hsa-mir-421	RFX3
944	GULP1	IFT172	CEACAM7
945	DPP8	TRIM25	BRD7
946	SHMT1	TCP11L1	PLG
947	PLEKHF2	HIST1H2AC	GNG2
948	FKBP9	APLN	EFHC2
949	SIRT1	TRABD2A	GRIN3A
950	RAET1E	TEX9	XRCC4
951	SLITRK1	FAM3A	RAB7L1
952	UQCR11	GLO1	SLIT1
953	GRPR	FAT2	GCA
954	ZC3HAV1L	NonTargetingControlGuideForHu	ECSCR
955	MEIG1	CCL28	CACNA2D4
956	ANKRD17	LOC100129083	C20orf24
957	CNOT2	CCNO	FUCA2
958	ACKR3	SPATA6L	NEURL1B
959	PSMD9	H3F3C	DEFB127
960	LSP1	DNAJC6	TMEFF2
961	ZNF189	MYLPF	LRP2
962	hsa-mir-5698	R3HCC1	COG1
963	EPHX2	SEC23B	FEZ1
964	SAMD3	CEP68	NUP160
965	TPSD1	NUMBL	BPY2B
966	CCL3L1	ADAM33	BPY2C
967	CCL3L3	EFR3A	BPY2
968	LRMP	HOXC12	REEP2
969	GADD45G	IFIH1	HABP2
970	GNB3	KNG1	DNTT
971	WNT2B	hsa-mir-6868	EPPIN-WFDC6
972	NonTargetingControlGuideForHu	EVA1A	GCNT3
973	TNNI2	SEMA4B	SCML4
974	LIPJ	ANXA10	SPSB3
975	ZNF600	OR13C5	PARP3
976	DNAJC28	NSMCE2	hsa-mir-4534
977	DNAJB12	C2orf78	GNB4
978	CCDC3	PIDD	MYEOV
979	C19orf48	NonTargetingControlGuideForHu	RNF11

980	CIDEA	NonTargetingControlGuideForHu	SPSB1
981	HS3ST3B1	BMP8A	METTL10
982	hsa-mir-642a	BMP8B	EIF3M
983	hsa-mir-642b	TLDC1	FBXO36
984	NFKBIA	hsa-mir-7843	PRRC2C
986	IDI2	NonTargetingControlGuideForHu	TSSK3
985	MED25	RBPJL	RSU1
987	KERA	STK35	KIF11
988	hsa-mir-4487	CLNS1A	LAMP3
989	ERP27	GBA	SLC9B2
990	AWAT1	H2AFX	LHX2
991	CUL7	CORO2B	ATAD3B
992	CPSF6	IMPA1	EPG5
993	HIST1H2AG	hsa-mir-378d-2	GLS2
994	HNRNPUL2	CHRFAM7A	HIST2H2BE
995	NonTargetingControlGuideForHu	PPA1	LYST
996	LYZL6	DICER1	HTR1F
997	NonTargetingControlGuideForHu	PFDN4	HMG20A
998	GLRA3	ACOT2	IVL
999	MICAL2	CUZD1	ITSN2
1000	NDRG3	PARK7	ZNF286A

6.6. FAM35A SILAC interactomes

Protein IDs	Majority protein IDs	Protein names	Gene names	Peptides	Unique peptides	Sequence length	Ratio H/L normalized 1	Ratio H/L normalized 2	Intensity
Q86V20-2;Q86V20	Q86V20-2;Q86V20	Protein FAM35A	FAM35A	82	82	904	15.952	0.026482	3.85E+11
P13667	P13667	Protein disulfide-is	PDIA4	12	12	645	7.9634	0.19859	2.52E+08
Q9Y2Z0;Q9Y2Z0-2	Q9Y2Z0;Q9Y2Z0-2	Suppressor of G2 al	SUGT1	32	32	365	6.2976	0.11887	1.27E+10
Q9BTT0-3;Q9BTT0;	Q9BTT0-3;Q9BTT0;	Acidic leucine-rich	ANP32E	5	5	220	5.3043	0.83993	9.06E+08
P30101	P30101	Protein disulfide-is	PDIA3	15	13	505	3.6903	0.83145	1.20E+09
Q15046;Q15046-2	Q15046;Q15046-2	Lysine--tRNA ligase	KARS	37	37	597	3.6655	0.21996	1.95E+10
A0A087X2D5;Q9BI	A0A087X2D5;Q9BI	39S ribosomal prot	MRPL45	4	4	306	3.2063	0.56909	5.04E+08
Q9H089;F8WFC6;H	Q9H089;F8WFC6;H	Large subunit GTPa	LSG1	2	2	658	2.8429	0.49519	3.67E+08
Q9ULX6;Q9ULX6-2	Q9ULX6;Q9ULX6-2	A-kinase anchor pr	AKAP8L	6	6	646	2.7081	0.35218	1.10E+09
F8VYE8;P36873;P3	F8VYE8;P36873;P3	Serine/threonine-p	PPP1CC	18	2	304	2.6681	3.2222	2.74E+08
Q9H9J2	Q9H9J2	39S ribosomal prot	MRPL44	7	7	332	2.5446	0.43297	3.94E+08
H0Y6Y8;B1AL05;Q	H0Y6Y8;B1AL05;Q	39S ribosomal prot	MRPL43	4	4	169	2.5095	NaN	2.91E+08
H7BZJ3	H7BZJ3		PDIA3	3	1	123	2.4947	NaN	4.87E+08
Q13084;A2IDC7;Q	Q13084;A2IDC7;Q	39S ribosomal prot	MRPL28	7	7	256	2.4929	0.43336	2.77E+08
Q8WXX0	Q8WXX0	Dynein heavy chain	DNAH7	1	1	4024	2.4912	0.48863	1.36E+08
X6RJ73;Q96A35;X6	X6RJ73;Q96A35	39S ribosomal prot	MRPL24	4	4	173	2.4115	0.36206	3.24E+08
P46939;P46939-2;	P46939;P46939-2;	Utrophin	UTRN	16	16	3433	2.3994	0.26881	4.87E+08
A0A075B6T1;Q9C0	A0A075B6T1;Q9C0	Activating molecul	AMBRA1	13	13	1179	2.389	0.21254	3.92E+08
C9IY40;Q5T653	C9IY40;Q5T653	39S ribosomal prot	MRPL2	3	3	225	2.3816	0.39441	1.73E+08
Q9P015;E5RIZ4;E5	Q9P015;E5RIZ4;E5	39S ribosomal prot	MRPL15	8	8	296	2.3196	0.45415	3.73E+08
Q9H5H4;H3BS42	Q9H5H4;H3BS42	Zinc finger protein	ZNF768	3	3	540	2.2879	0.075098	7.13E+07
Q13405;H0YDP7;E	Q13405;H0YDP7	39S ribosomal prot	MRPL49	6	6	166	2.2856	0.42215	8.46E+08
Q99575;E5RK39	Q99575;E5RK39	Ribonucleases P/M	POP1	6	6	1024	2.2727	0.5132	2.97E+08
P49406;S4R3W9;A	P49406;S4R3W9;A	39S ribosomal prot	MRPL19	8	8	292	2.2142	0.47026	5.86E+08
A0A0G2JNH5;A0A0	A0A0G2JNH5;A0A0	Cell cycle checkpoi	RAD17	4	4	505	2.2136	0.50627	9.92E+07
P52272-2;P52272;	P52272-2;P52272;	Heterogeneous nuc	HNRNPM	52	52	691	2.2062	0.40004	3.04E+10
E9PKV2;Q9NRX2	E9PKV2;Q9NRX2	39S ribosomal prot	MRPL17	2	2	142	2.2009	0.46277	2.96E+08
B4E1Q4;O14730-2	B4E1Q4;O14730-2	Serine/threonine-p	RIOK3	5	5	503	2.188	0.58278	1.81E+08
B1AK44;Q9UI95;B1	B1AK44;Q9UI95;B1	Mitotic spindle ass	MAD2L2	3	3	224	2.1869	0.99297	8.91E+07
Q8TAE8	Q8TAE8	Growth arrest and I	GADD45GIP1	7	7	222	2.1563	0.40556	1.04E+08
P35251-2;P35251;	P35251-2;P35251	Replication factor (	RFC1	15	15	1147	2.1482	0.37156	7.55E+08
O75446	O75446	Histone deacetylas	SAP30	2	2	220	2.1312	0.71101	2.13E+08
Q96DV4;Q96DV4-2	Q96DV4	39S ribosomal prot	MRPL38	4	4	380	2.1193	0.4113	5.66E+08
G3V170;Q9HA47-2	G3V170;Q9HA47-2	Uridine-cytidine ki	UCK1	2	2	218	2.1086	NaN	1.72E+08
Q7Z2W9;F5H7V8;(	Q7Z2W9;F5H7V8;(	39S ribosomal prot	MRPL21	5	5	205	2.1082	0.38468	1.24E+08
G3V2G1;G3V328;(	G3V2G1;G3V328;(	Ataxin-3	ATXN3	7	7	223	2.1015	0.43946	4.54E+08
H0Y9G6;E7ETU7;P(	H0Y9G6;E7ETU7;P(	39S ribosomal prot	MRPL3	6	6	363	2.0959	0.34331	2.70E+08
Q9P0M9;D6RAN8;I	Q9P0M9;D6RAN8;I	39S ribosomal prot	MRPL27	6	6	148	2.0873	0.46223	1.38E+08
Q9BYD6;H0Y8N7	Q9BYD6;H0Y8N7	39S ribosomal prot	MRPL1	5	5	325	2.0716	0.27676	6.51E+08
P46777;Q5T7N0;R	P46777	60S ribosomal prot	RPL5	22	22	297	2.0616	0.42077	2.00E+09
K7ES61;Q9BYD3;X(	K7ES61;Q9BYD3;X(	39S ribosomal prot	MRPL4	7	7	300	2.0305	0.41806	1.06E+09
Q9HD33-2;Q9HD3	Q9HD33-2;Q9HD3	39S ribosomal prot	MRPL47	10	10	230	2.0253	0.4178	2.20E+08
Q9BYD2;Q5SZR1	Q9BYD2;Q5SZR1	39S ribosomal prot	MRPL9	6	6	267	2.0201	0.47728	1.72E+08
Q9BYD1;E5RJI7;H0	Q9BYD1;E5RJI7	39S ribosomal prot	MRPL13	11	11	178	2.0191	0.53193	5.30E+08
Q8IXM3	Q8IXM3	39S ribosomal prot	MRPL41	4	4	137	2.0158	0.48393	5.16E+08
Q9BVP2-2;Q9BVP2	Q9BVP2-2;Q9BVP2	Guanine nucleotid	GNL3	15	15	537	2.0132	0.51048	2.30E+09
A6NJD9;A8MVT4;A	A6NJD9;A8MVT4;A	39S ribosomal prot	MRPL23	2	2	163	2.0129	0.66492	2.15E+08
Q9H8V3-2;Q9H8V3	Q9H8V3-2;Q9H8V3	Protein ECT2	ECT2	10	10	882	2.0053	0.59793	3.75E+08
O95985-3;O95985	O95985-3;O95985	DNA topoisomeras	TOP3B	9	8	707	1.9975	0.50919	2.54E+08
Q9H0U6	Q9H0U6	39S ribosomal prot	MRPL18	5	5	180	1.9936	0.50141	6.48E+07
Q9NP92;A0A087W	Q9NP92	28S ribosomal prot	MRPS30	9	9	439	1.9929	0.49675	5.71E+08
Q6UWE0-2;Q6UWI	Q6UWE0-2;Q6UWI	E3 ubiquitin-protei	LRSAM1	7	7	696	1.9876	0.36352	4.56E+08
Q5W0B1	Q5W0B1	RING finger protein	RNF219	5	5	726	1.9835	0.39873	3.59E+08
Q08J23-2;Q08J23;	Q08J23-2;Q08J23;	tRNA (cytosine(34)-	NSUN2	38	38	732	1.9769	0.39965	1.24E+10
E9PFK9;Q9UJ41-2;	E9PFK9;Q9UJ41-2;	Rab5 GDP/GTP excl	RABGEF1	4	4	504	1.9675	0.49434	2.26E+08
Q9BZE1;S4R369;A(	Q9BZE1;S4R369	39S ribosomal prot	MRPL37	10	10	423	1.948	0.43364	7.51E+08
Q9BQC6	Q9BQC6	Ribosomal protein	MRPL57	2	2	102	1.9398	0.44894	2.75E+08
Q6ZRV2;J3KPS2	Q6ZRV2;J3KPS2	Protein FAM83H	FAM83H	12	12	1179	1.9288	0.33055	3.12E+08
P41743;E9PBE1;Q(	P41743	Protein kinase C iot	PRKCI	5	5	596	1.9218	0.61895	7.43E+08
P08579	P08579	U2 small nuclear ril	SNRPB2	7	5	225	1.9192	0.71091	5.97E+08
Q9NW82;D6RIW8	Q9NW82;D6RIW8	WD repeat-contain	WDR70	4	4	654	1.9106	0.89759	2.81E+08
Q9Y2I7;E9PDH4;Q(	Q9Y2I7;E9PDH4;Q(	1-phosphatidylinos	PIKFYVE	9	9	2098	1.9076	0.51726	2.73E+08
O15541	O15541	RING finger protein	RNF113A	5	5	343	1.9075	0.35745	2.04E+08
H3BLZ8;Q92841;Q	H3BLZ8;Q92841;Q	Probable ATP-depe	DDX17	41	33	731	1.9059	0.48052	3.01E+10
Q9Y2X9-2;Q9Y2X9	Q9Y2X9-2;Q9Y2X9	Zinc finger protein	ZNF281	11	11	859	1.8999	0.35507	5.59E+08
A0A0D9SF60;Q995	A0A0D9SF60;Q995	Plakophilin-4	PKP4	3	1	1208	1.8984	NaN	2.28E+07
O15381-5;O15381	O15381-5;O15381	Nuclear valosin-cor	NVL	22	22	765	1.8962	0.37308	2.44E+09
Q96D46;C9JA08;C(	Q96D46;C9JA08	60S ribosomal exp	NMD3	15	15	503	1.8919	0.55066	1.48E+09
F5H702;Q96GC5-3	F5H702;Q96GC5-3	39S ribosomal prot	MRPL48	5	5	113	1.8908	0.51976	5.09E+08
Q7Z7F7;Q7Z7F7-2;	Q7Z7F7;Q7Z7F7-2;	39S ribosomal prot	MRPL55	5	5	128	1.8875	0.45571	2.46E+08
O76094;O76094-2	O76094;O76094-2	Signal recognition	SRP72	16	16	671	1.8775	0.51771	2.29E+09
P15924;P15924-2;	P15924;P15924-2;	Desmoplakin	DSP	42	42	2871	1.8746	0.40733	1.82E+09
Q8IY37;F5H3Y4	Q8IY37;F5H3Y4	Probable ATP-depe	DHX37	19	19	1157	1.8654	0.46508	8.70E+08
Q9H2W6;A0A087V	Q9H2W6	39S ribosomal prot	MRPL46	5	5	279	1.8508	0.45408	3.22E+08
P55795;H0YBK1	P55795	Heterogeneous nuc	HNRNPH2	18	8	449	1.8221	0.50409	3.44E+09
P10412;Q02539;P	P10412	Histone H1.4	HIST1H1E	17	5	219	1.8204	0.56378	3.42E+09
Q9UKB1-2;Q9UKB1	Q9UKB1-2;Q9UKB1	F-box/WD repeat-c	FBXW11;BTRC	3	3	508	1.8179	0.53471	2.41E+07
Q9NVN8	Q9NVN8	Guanine nucleotid	GNL3L	4	4	582	1.8152	0.30302	3.72E+08
Q6IQ32	Q6IQ32	ADNP homeobox p	ADNP2	2	2	1131	1.8107	NaN	2.22E+07
Q9NX58	Q9NX58	Cell growth-regulat	LYAR	7	7	379	1.8097	0.54266	2.52E+08
P43487-2;P43487;	P43487-2;P43487;	Ran-specific GTPas	RANBP1	9	9	200	1.8058	0.35542	8.62E+09
O43395;O43395-3	O43395	U4/U6 small nuclea	PRPF3	13	13	683	1.8042	0.62932	5.72E+08
Q96HA7-2;Q96HA7	Q96HA7-2;Q96HA7	Tonsoku-like protei	TONSL	9	9	1378	1.7997	0.51211	3.79E+08
Q5JR08;P08134;E5	Q5JR08;P08134;E5	Rho-related GTP-bi	RHOC	5	2	189	1.7977	2.0207	1.06E+08
Q9NQ50	Q9NQ50	39S ribosomal prot	MRPL40	5	5	206	1.7854	0.42283	4.62E+08
P16403	P16403	Histone H1.2	HIST1H1C	17	5	213	1.7792	0.48771	2.32E+08
E7EVZ1;Q86UP3-2;	E7EVZ1;Q86UP3-2;	Zinc finger homeob	ZFHX4	3	3	3590	1.7784	0.57894	5.06E+07
P18124;A8MUD9;(	P18124;A8MUD9	60S ribosomal prot	RPL7	22	22	248	1.7753	0.53289	1.39E+10
P19338;H7BY16;C(	P19338;H7BY16	Nucleolin	NCL	52	52	710	1.7729	0.46993	4.57E+10
F8WE42;F5H101;C	F8WE42;F5H101;C	Nucleolar protein 8	NOL8	4	4	970	1.772	0.70565	9.54E+07
Q8IWS0;A0A0D9SC	Q8IWS0;A0A0D9SC	PHD finger protein	PHF6	17	17	365	1.7702	0.59399	1.10E+09

Q9HCK8;Q9HCK8-2	Q9HCK8;Q9HCK8-2	Chromodomain-he	CHD8	17	12	2581	1.7682	0.53279	6.36E+08
Q13523;H0YDJ3	Q13523;H0YDJ3	Serine/threonine-p	PRPF4B	7	7	1007	1.7669	0.77007	2.70E+08
Q8WVD3;J3QLQ3;J	Q8WVD3	E3 ubiquitin-protei	RNF138	3	3	245	1.7666	0.44486	1.79E+08
P19525;P19525-2;	P19525;P19525-2	Interferon-induced	EIF2AK2	10	10	551	1.7642	0.59442	1.45E+09
A0A0C4DGT3;A0A0	A0A0C4DGT3;A0A0	IQ motif and SEC7 d	IQSEC1	3	2	814	1.7627	0.77423	1.47E+08
A0A0B4J220;E9PLI	A0A0B4J220			4	4	123	1.7591	0.63531	9.80E+07
Q13823;H0YG10	Q13823	Nucleolar GTP-binc	GNL2	9	9	731	1.7351	0.54163	4.49E+08
O95235-2;O95235	O95235-2;O95235	Kinesin-like proteir	KIF20A	3	3	872	1.7334	0.47964	8.59E+07
K7EJB9;P27797	K7EJB9;P27797	Calreticulin	CALR	4	4	247	1.7318	0.474	1.06E+08
O14979-3;O14979	O14979-3;O14979	Heterogeneous nuc	HNRNPDL	16	14	244	1.7297	0.84168	8.47E+09
J3KTA4;P17844;P1	J3KTA4;P17844;P1	Probable ATP-depe	DDX5	45	37	614	1.7282	0.49236	3.85E+10
P16989-3;P16989;	P16989-3;P16989	Y-box-binding prot	YBX3	9	1	342	1.727	0.46008	6.52E+08
P31483-2;C9JTN7;	P31483-2;C9JTN7;	Nucleolysin TIA-1 is	TIA1	9	0	375	1.7222	0.65341	9.63E+07
Q8N1G0-2;Q8N1G	Q8N1G0-2;Q8N1G	Zinc finger protein	ZNF687	3	3	1103	1.7208	NaN	4.98E+07
Q01831;Q01831-2	Q01831;Q01831-2	DNA repair protein	XPC	3	3	940	1.7207	NaN	3.95E+07
Q6NW34-2;Q6NW	Q6NW34-2;Q6NW	Uncharacterized pr	C3orf17	2	2	497	1.7196	NaN	1.90E+07
Q16778;P33778;P	Q16778;P33778;P	Histone H2B type 2	HIST2H2BE;HIST1H	10	0	126	1.7187	1.3625	1.28E+09
Q9BYC9;I3L2X1;Q9	Q9BYC9	39S ribosomal prot	MRPL20	4	4	149	1.7168	0.39169	1.28E+08
Q7Z6Z7-3;Q7Z6Z7;	Q7Z6Z7-3;Q7Z6Z7;	E3 ubiquitin-protei	HUWE1	107	103	4365	1.7155	0.50342	1.32E+10
Q96GA3;A0A075B6	Q96GA3	Protein LTV1 homc	LTV1	6	6	475	1.7105	0.55668	3.49E+08
P27635;X1WI28;A	P27635;X1WI28;A	60S ribosomal prot	RPL10	15	2	214	1.7027	0.66466	9.22E+09
P62241;Q5JR95	P62241;Q5JR95	40S ribosomal prot	RPS8	14	14	208	1.7022	0.58302	1.64E+10
E7ESL0;A0A0C4DG	E7ESL0;A0A0C4DG	39S ribosomal prot	MRPL22	6	6	212	1.701	0.55323	3.28E+08
B7WPG3;C9IYN3;D	B7WPG3;C9IYN3;D	Heterogeneous nuc	HNRPLL;HNRNPLL	14	14	508	1.6912	0.49883	1.71E+09
Q14684;Q14684-2	Q14684;Q14684-2	Ribosomal RNA pro	RRP1B	8	8	758	1.6831	0.52971	3.00E+08
Q01968;Q01968-2	Q01968;Q01968-2	Inositol polyphosp	OCRL	18	18	901	1.6816	0.42899	1.56E+09
P39019;A0A075B6	P39019;A0A075B6	40S ribosomal prot	RPS19	19	19	145	1.6797	0.59106	1.81E+09
O15226;O15226-2	O15226;O15226-2	NF-kappa-B-repress	NKRF	17	17	690	1.6763	0.61567	5.93E+08
Q96RS0	Q96RS0	Trimethylguanosin	TGS1	2	2	853	1.6746	0.55133	6.12E+07
C9JG87;Q9NYK5;Q	C9JG87;Q9NYK5;Q	39S ribosomal prot	MRPL39	9	9	297	1.6705	0.56825	8.10E+08
A0A075B6F9;Q9Y3	A0A075B6F9;Q9Y3	Nitric oxide syntha	NOSIP	9	9	304	1.6662	0.48972	1.42E+09
P61927;D6R9X9;D	P61927;D6R9X9;D	60S ribosomal prot	RPL37	3	3	97	1.6662	0.71251	4.22E+07
Q9BU61;Q9BU61-2	Q9BU61;Q9BU61-2	NADH dehydrogena	NDUFAF3	4	4	184	1.6543	1.3267	4.09E+07
Q9P0U3-2;Q9P0U3	Q9P0U3-2;Q9P0U3	Sentrin-specific prc	SENP1	4	4	643	1.6536	0.44607	2.39E+08
Q9NV72-2;Q9NV72	Q9NV72-2;Q9NV72	Zinc finger protein	ZNF701;ZSCAN21;Z	2	2	465	1.6496	NaN	1.62E+07
P10398;Q96II5;P1	P10398;Q96II5	Serine/threonine-p	ARAF	8	5	606	1.6483	0.50818	4.74E+08
Q12965;H0YLE5;O	Q12965;H0YLE5;O	Unconventional my	MYO1E;MYO1F	2	2	1108	1.6473	0.5402	1.11E+08
A0A087WYR0;P09	A0A087WYR0;P09	Signal recognition p	SRP19	3	3	120	1.6453	0.68795	3.11E+08
P62081;B5MCP9	P62081;B5MCP9	40S ribosomal prot	RPS7	17	17	194	1.6417	0.53657	3.93E+09
E7ETB7;E7EQ06;A0	E7ETB7;E7EQ06;A0	Caspase-8;Caspase-	CASP8	3	3	198	1.6368	0.59203	2.68E+08
Q5RKV6	Q5RKV6	Exosome complex c	EXOSC6	2	2	272	1.6351	0.81871	4.54E+07
Q9BU76-4;Q9BU76	Q9BU76-4;Q9BU76	Multiple myeloma	MMTAG2	3	3	189	1.6343	0.43024	5.75E+07
Q5SSJ5;X6RGJ2;Q5	Q5SSJ5;X6RGJ2;Q5	Heterochromatin p	HP1BP3	12	12	553	1.6341	0.7902	8.46E+08
K7EQ03;K7EP90;Q	K7EQ03;K7EP90;Q	RNA-binding protei	RBM42	3	3	426	1.6336	0.64405	1.07E+08
Q9BTE1;H3BR94;Q	Q9BTE1;H3BR94;Q	Dynactin subunit 5	DCTN5	6	6	182	1.6332	0.67147	2.05E+08
Q9BSH4	Q9BSH4	Translational activa	TACO1	12	12	297	1.6325	0.50014	4.51E+09
M0R3F6;M0R2Z9;(	M0R3F6;M0R2Z9;(	SURP and G-patch c	SUGP2	6	6	841	1.631	0.53131	2.45E+08
Q02878;F8VZ45;U	Q02878	60S ribosomal prot	RPL6	21	21	288	1.6309	0.59905	1.37E+10
B4DYP1;O94760-2	B4DYP1;O94760-2	N(G),N(G)-dimethyl	DDAH1	3	3	185	1.629	1.0362	2.13E+08
P82914	P82914	28S ribosomal prot	MRPS15	8	8	257	1.6276	0.61459	3.02E+08
Q8NB46	Q8NB46	Serine/threonine-p	ANKRD52	5	5	1076	1.6258	0.802	8.46E+07
Q92793-2;Q92793	Q92793-2;Q92793	CREB-binding prote	CREBBP	8	4	2404	1.6243	0.48402	3.17E+08
P07992-4;P07992	P07992-4;P07992	DNA excision repai	ERCC1	4	4	225	1.619	0.71909	1.68E+08
Q9UBU9;E9PIN3;Q	Q9UBU9;E9PIN3;Q	Nuclear RNA export	NXF1	16	16	619	1.6186	0.60454	2.11E+09
Q16822;B4DW73;I	Q16822;B4DW73;I	Phosphoenolpyruv	PCK2	22	22	640	1.6153	0.6428	4.33E+09
O14530-2;O14530	O14530-2;O14530	Thioredoxin domai	TXNDC9	7	7	188	1.6141	0.53503	8.54E+08
F8W8I6;P31483;E	F8W8I6;P31483;E	Nucleolysin TIA-1 is	TIA1	9	2	385	1.6116	0.8241	1.64E+08
O95071-2;O95071	O95071-2;O95071	E3 ubiquitin-protei	UBR5	46	46	2798	1.61	0.55165	2.78E+09
P61353;K7ELC7;K7	P61353;K7ELC7;K7	60S ribosomal prot	RPL27	12	12	136	1.6091	0.63307	6.39E+09
P11766;H0YAG8;D	P11766;H0YAG8	Alcohol dehydroge	ADH5	4	4	374	1.6078	1.5523	5.62E+08
P62424;Q5T8U3;Q	P62424;Q5T8U3	60S ribosomal prot	RPL7A	19	19	266	1.6057	0.60189	6.52E+09
Q7Z2W4;C9J6P4;C	Q7Z2W4;C9J6P4;C	Zinc finger CCCH-ty	ZC3HAV1	27	27	902	1.6054	0.4884	3.70E+09
Q9NXK8;Q9NXK8-2	Q9NXK8;Q9NXK8-2	F-box/LRR-repeat p	FBXL12	3	3	326	1.6039	0.62093	2.31E+08
A0A0D9SES8;H0YK	A0A0D9SES8;H0YK	Transducin-like enh	LITAF;TLE3	12	6	772	1.6029	0.461	1.06E+09
P30419-2;P30419;	P30419-2;P30419	Glycylpeptide N-tet	NMT1;NMT2	2	2	416	1.6	0.68733	2.95E+08
A0A0A0MRF9;P16	A0A0A0MRF9;P16	1-phosphatidylinos	PLCG2	6	6	1252	1.5981	0.55379	1.89E+08
Q13643	Q13643	Four and a half LIM	FHL3	2	2	280	1.5981	0.76063	1.08E+07
Q8N5N7;Q8N5N7-	Q8N5N7;Q8N5N7-	39S ribosomal prot	MRPL50	4	4	158	1.5977	0.51725	1.09E+08
Q9NRL2;Q9NRL2-2	Q9NRL2;Q9NRL2-2	Bromodomain adja	BAZ1A	23	23	1556	1.596	0.6173	8.00E+08
Q92615;H0Y4V9;H	Q92615	La-related protein 4	LARP4B	13	13	738	1.5899	0.44044	2.08E+09
Q96FZ2;D6R9T3;E7	Q96FZ2;D6R9T3;E7	Embryonic stem ce	HMCES	8	8	354	1.5893	0.46459	5.75E+08
Q08AF3;B4E128;Q	Q08AF3	Schlafen family me	SLFN5	3	3	891	1.5886	0.43549	7.31E+07
Q9Y5T5-2;Q9Y5T5;	Q9Y5T5-2;Q9Y5T5;	Ubiquitin carboxyl	USP16	3	3	822	1.5885	NaN	4.02E+07
H0YKX0;Q96EP0-3;	H0YKX0;Q96EP0-3	E3 ubiquitin-protei	RNF31	4	4	917	1.5882	0.58936	7.92E+07
Q96EB6;B0QZ35;E	Q96EB6;B0QZ35;E	NAD-dependent pr	SIRT1	8	8	747	1.5843	0.48413	4.54E+08
Q9P2D1;A0A087W	Q9P2D1	Chromodomain-he	CHD7	11	7	2997	1.5817	0.51908	1.05E+08
P61247;E9PFI5;H0	P61247;E9PFI5;H0	40S ribosomal prot	RPS3A	28	28	264	1.5757	0.57396	1.29E+10
O75925;O75925-2	O75925;O75925-2	E3 SUMO-protein li	PIAS1	4	3	651	1.5753	0.49141	1.70E+08
P17028;P17028-2;	P17028	Zinc finger protein	ZNF24	8	8	368	1.5745	0.58501	1.23E+08
A0A0D9SFB3;A0A0	A0A0D9SFB3;A0A0	ATP-dependent RN	DDX3X;DDX3Y	39	38	640	1.5713	0.61794	2.05E+10
Q15293;Q15293-2	Q15293;Q15293-2	Reticulocalbin-1	RCN1	7	7	331	1.5713	0.69386	1.13E+09
Q8IZH2-2;Q8IZH2;I	Q8IZH2-2;Q8IZH2;I	5-3 exoribonucleas	XRN1	18	18	1694	1.571	0.61704	1.36E+09
Q9H4L7;Q9H4L7-2	Q9H4L7;Q9H4L7-2	SWI/SNF-related m	SMARCAD1	11	11	1026	1.5706	0.68489	5.89E+08
O75717;O75717-2	O75717;O75717-2	WD repeat and HM	WDHD1	31	31	1129	1.57	0.51452	1.88E+09
F1T0I1;J3KNL6;O1	F1T0I1;J3KNL6;O1	Protein transport p	SEC16A	20	20	2334	1.5696	0.3991	7.16E+08
P07305;P07305-2	P07305;P07305-2	Histone H1.0;Histo	H1F0	5	5	194	1.5683	0.68287	3.48E+08
Q92522	Q92522	Histone H1x	H1FX	6	6	213	1.5658	0.67177	1.40E+09
J3QK89;Q8IWX8	J3QK89;Q8IWX8	Calcium homeosta	CHERP	4	4	927	1.5643	0.58353	1.82E+08
K7EQJ5;P62841;K7	K7EQJ5;P62841;K7	40S ribosomal prot	RPS15	7	7	141	1.5641	0.58148	6.81E+08
P05455;E7ERC4;E9	P05455	Lupus La protein	SSB	11	11	408	1.5634	0.66991	6.47E+08
Q6P158;H7C109;C	Q6P158;H7C109	Putative ATP-deper	DHX57	21	19	1386	1.5622	0.52182	7.80E+08
Q9BVQ7-3;Q9BVQ7	Q9BVQ7-3;Q9BVQ7	Spermatogenesis-a	SPATA5L1	2	2	392	1.5619	0.85712	1.70E+08
O00629;H7C4F6	O00629	Importin subunit a	KPNA4	14	10	521	1.5551	0.43691	1.63E+09

Q00535;Q00535-2	Q00535;Q00535-2	Cyclin-dependent-l	CDK5	13	12	292	1.5545	0.6239	2.64E+09
P62753;A2A3R5;A	P62753;A2A3R5	40S ribosomal prot	RPS6	15	15	249	1.5541	0.59249	5.93E+09
P67809;A0A087X1	P67809;A0A087X1	Nuclease-sensitive	YBX1	14	9	324	1.5528	0.46668	3.76E+09
J3QR09;J3KTE4;P8	J3QR09;J3KTE4;P8	Ribosomal protein	RPL19	11	11	193	1.5524	0.61923	3.62E+09
Q9Y676;A0A0G2JI	Q9Y676;A0A0G2JI	28S ribosomal prot	MRPS18B	5	5	258	1.5504	0.60378	3.54E+08
Q71RC2-5;Q71RC2	Q71RC2-5;Q71RC2	La-related protein	LARP4	9	9	653	1.5481	0.40649	8.75E+08
P55036;P55036-2;	P55036;P55036-2,	26S proteasome nc	PSMD4	12	2	377	1.5474	0.63083	4.25E+09
P18583-2;P18583	P18583-2;P18583	Protein SON	SON	13	13	2140	1.5472	0.296	3.74E+08
Q9UNQ2;A0A0C4D	Q9UNQ2;A0A0C4D	Probable dimethyl	DIMT1	11	11	313	1.5449	0.6227	1.11E+09
P18077;C9K025;F	P18077;C9K025;F	60S ribosomal prot	RPL35A	15	15	110	1.5409	0.69623	2.30E+09
O00411;K7EMH3	O00411	DNA-directed RNA	POLRMT	21	21	1230	1.5397	0.52083	2.47E+09
G5E9A6;P51784	G5E9A6;P51784	Ubiquitin carboxyl	USP11	8	6	920	1.5347	0.66403	3.81E+08
O96017;O96017-9	O96017;O96017-9	Serine/threonine-p	CHEK2	7	7	543	1.5331	0.67182	2.27E+08
Q9BRK5;Q9BRK5-6	Q9BRK5;Q9BRK5-6	45 kDa calcium-bin	SDF4	9	9	362	1.5307	0.53997	3.61E+08
P20585	P20585	DNA mismatch rep	MSH3	12	12	1137	1.53	0.60498	7.80E+08
Q96FC9-4;Q96FC9	Q96FC9-4;Q96FC9	Probable ATP-depe	DDX11	6	1	856	1.5292	0.42881	3.05E+08
V9GYM8;Q92974-3	V9GYM8;Q92974-3	Rho guanine nucle	ARHGEF2	21	21	1031	1.5284	0.55428	1.14E+09
Q9Y3U8;J3QSB5;J3	Q9Y3U8;J3QSB5	60S ribosomal prot	RPL36	8	8	105	1.5258	0.61427	8.53E+08
J3KQN4;P83881;H	J3KQN4;P83881;H	60S ribosomal prot	RPL36A;RPL36A-HI	9	3	142	1.5233	0.63803	9.29E+07
A0A087WYN9;Q7Z	A0A087WYN9;Q7Z	ATP-dependent RN	DHX29	36	35	1370	1.523	0.60233	1.77E+09
Q13472-3;Q13472	Q13472-3;Q13472	DNA topoisomeras	TOP3A	3	2	906	1.5226	NaN	6.10E+07
Q9NY93-2;Q9NY93	Q9NY93-2;Q9NY93	Probable ATP-depe	DDX56	3	3	507	1.5219	0.66161	1.00E+08
Q08211;Q08211-2	Q08211	ATP-dependent RN	DHX9	60	60	1270	1.5212	0.6807	3.55E+10
P39023;G5E9G0;H	P39023;G5E9G0;H	60S ribosomal prot	RPL3	27	27	403	1.5192	0.63909	9.01E+09
J3KQ61;O95696;O	J3KQ61;O95696;O	Bromodomain-con	BRD1	3	3	509	1.5185	0.5966	6.26E+07
Q92917	Q92917	G patch domain an	GPKOW	4	4	476	1.5175	0.81312	2.71E+08
C9J494;Q9H000-2;	C9J494;Q9H000-2,	Probable E3 ubiqui	MKRN2	4	4	414	1.5158	0.52945	4.75E+08
P08621;P08621-2;	P08621;P08621-2,	U1 small nuclear ri	SNRNP70	13	13	437	1.5156	0.72387	6.85E+08
A0A0C4DGA6;Q14	A0A0C4DGA6;Q14	Helicase-like transc	HLTF	15	15	1008	1.5155	0.57667	5.30E+08
Q8N142;G3V5D8;(	Q8N142;G3V5D8;(	Adenylosuccinate s	ADSSL1	6	2	457	1.5135	NaN	3.10E+07
O94817	O94817	Ubiquitin-like prot	ATG12	1	1	140	1.5125	0.23331	2.69E+09
Q9P2P6;Q9P2P6-3	Q9P2P6;Q9P2P6-3	StAR-related lipid t	STARD9	2	2	4700	1.5124	NaN	1.81E+07
Q9H6S0;D6RA70;D	Q9H6S0;D6RA70	Probable ATP-depe	YTHDC2	19	19	1430	1.5123	0.66508	7.03E+08
Q9Y4B4;H0Y760	Q9Y4B4;H0Y760	Helicase ARIP4	RAD54L2	6	6	1467	1.5108	0.72582	1.33E+08
P13489;H0YCR7;E	P13489;H0YCR7	Ribonuclease inhib	RNH1	16	16	461	1.5107	0.70762	6.80E+09
B7Z879;A0A087W	B7Z879;A0A087W	Vacuolar protein sc	VPS11	2	2	931	1.5049	NaN	5.41E+07
H3BSK8;Q7Z6E9-2;	H3BSK8;Q7Z6E9-2;	E3 ubiquitin-protei	RBBP6	2	2	1008	1.5048	0.89154	3.08E+07
Q9BXP5-4;Q9BXP5	Q9BXP5-4;Q9BXP5	Serrate RNA effecto	SRRT	37	37	871	1.5031	0.55242	1.99E+09
O60942-4;O60942	O60942-4;O60942	mRNA-capping enz	RNGTT	6	6	541	1.501	0.47791	3.05E+08
P55265-5;P55265	P55265-5;P55265,	Double-stranded R	ADAR	48	48	931	1.4976	0.53835	1.14E+10
Q96S55-2;Q96S55	Q96S55-2;Q96S55,	ATPase WRNIP1	WRNIP1	10	10	640	1.4955	0.6643	7.79E+08
Q9BQ39;A0A087W	Q9BQ39;A0A087W	ATP-dependent RN	DDX50	8	6	737	1.4952	0.59102	8.66E+08
F8VS10;Q86XZ4	F8VS10;Q86XZ4	Spermatogenesis-a	SPATS2	1	1	295	1.4913	0.84671	7.58E+06
Q9BVJ6-3;Q9BVJ6	Q9BVJ6-3;Q9BVJ6	U3 small nucleolar	UTP14A	10	10	719	1.4896	0.60531	5.14E+08
P28070	P28070	Proteasome subuni	PSMB4	2	2	264	1.4894	NaN	5.18E+07
Q9UG63;Q9UG63-	Q9UG63;Q9UG63-	ATP-binding casset	ABCF2	29	29	623	1.4871	0.51634	7.63E+09
Q5VZL5-4;Q5VZL5	Q5VZL5-4;Q5VZL5	Zinc finger MYM-ty	ZMYM4	17	16	1516	1.4857	0.70512	4.73E+08
Q9H7B4;Q9H7B4-3	Q9H7B4;Q9H7B4-3	Histone-lysine N-m	SMYD3	5	5	428	1.4856	0.59343	3.70E+08
Q9UGR2-2;Q9UGR	Q9UGR2-2;Q9UGR	Zinc finger CCCH dc	ZC3H7B	4	4	977	1.4856	0.78846	1.59E+08
M0QZ28;Q9Y4J8-6	M0QZ28;Q9Y4J8-6	Dystrobrevin alpha	DTNA	3	1	365	1.483	NaN	7.92E+07
Q8N7H5-3;Q8N7H	Q8N7H5-3;Q8N7H	RNA polymerase II-	PAF1	5	5	485	1.4825	0.62506	8.02E+08
Q96PK6;Q96PK6-2	Q96PK6	RNA-binding protei	RBM14	24	18	669	1.4823	0.45796	2.76E+09
Q13425;H0YCS0;Q	Q13425;H0YCS0;Q	Beta-2-syntrophin	SNTB2	5	4	540	1.4816	0.59085	3.30E+08
P62750;H7BY10;K	P62750;H7BY10;K	60S ribosomal prot	RPL23A	15	15	156	1.4811	0.59354	5.39E+09
P42766;F2Z388	P42766;F2Z388	60S ribosomal prot	RPL35	9	9	123	1.4806	0.69633	2.17E+09
Q96PE3-2;Q96PE3	Q96PE3-2;Q96PE3	Type I inositol 3,4-l	INPP4A	5	5	938	1.4802	0.55343	1.02E+08
P26373;P26373-2;	P26373;P26373-2,	60S ribosomal prot	RPL13	13	13	211	1.4799	0.69412	1.01E+10
H0Y2S1;O43824	H0Y2S1;O43824	Putative GTP-bindi	GTPBP6	6	6	516	1.4796	0.62119	1.73E+08
E7EXA6;Q8WVB6;(	E7EXA6;Q8WVB6;(	Chromosome trans	CHTF18	12	12	975	1.4795	0.42861	6.53E+08
P20042	P20042	Eukaryotic translat	EIF2S2	23	23	333	1.4788	0.56179	5.99E+09
P47914;F8WF43;C	P47914	60S ribosomal prot	RPL29	5	5	159	1.4779	0.61448	2.27E+08
P50914;E7EPB3	P50914;E7EPB3	60S ribosomal prot	RPL14	10	10	215	1.4767	0.71483	5.04E+09
Q9Y2L1;Q9Y2L1-2;	Q9Y2L1;Q9Y2L1-2;	Exosome complex e	DIS3	51	51	958	1.4758	0.57745	1.56E+10
P62851	P62851	40S ribosomal prot	RPS25	8	8	125	1.4754	0.71598	4.43E+09
P82933	P82933	28S ribosomal prot	MRPS9	9	9	396	1.4753	0.58347	8.91E+08
Q9NY12-2;Q9NY12	Q9NY12-2;Q9NY12	H/ACA ribonucleop	GAR1	3	3	199	1.4752	NaN	5.41E+07
Q04727-2;Q04727	Q04727-2;Q04727	Transducin-like enh	TLE4;TLE1	10	4	704	1.4742	0.56657	2.01E+08
O43852;O43852-3	O43852;O43852-3	Calumenin	CALU	8	8	315	1.4735	0.7897	3.71E+08
E9PPY3;O43159	E9PPY3;O43159	Ribosomal RNA-pro	RRP8	2	2	306	1.4734	0.75902	1.04E+08
Q5JTH9-2;Q5JTH9	Q5JTH9-2;Q5JTH9	RRP12-like protein	RRP12	24	24	1197	1.4718	0.53388	1.02E+09
Q96EY7;B8ZZQ4;Q	Q96EY7	Pentatricopeptide	PTCD3	8	8	689	1.4715	0.73057	1.07E+09
Q8IWR0;I3L2K5;I3	Q8IWR0;I3L2K5	Zinc finger CCCH dc	ZC3H7A	11	11	971	1.4714	0.55656	6.18E+08
Q9BZE4;Q9BZE4-2;	Q9BZE4;Q9BZE4-2;	Nucleolar GTP-binc	GTPBP4	23	23	634	1.4712	0.66103	2.37E+09
Q96DT7;Q96DT7-2	Q96DT7;Q96DT7-2	Zinc finger and BTB	ZBTB10	4	4	871	1.471	NaN	1.20E+08
P62857	P62857	40S ribosomal prot	RPS28	3	3	69	1.4699	0.7491	1.25E+08
P62854;Q5JNZ5	P62854;Q5JNZ5	40S ribosomal prot	RPS26;RPS26P11	4	4	115	1.468	0.69834	2.84E+09
C9JAG1;A0A087W	C9JAG1;A0A087W	Ethanolaminephos	EPT1	2	2	180	1.4673	1.8561	3.58E+08
Q04864-2;Q04864	Q04864-2;Q04864	Proto-oncogene c-I	REL	3	3	587	1.4635	0.72043	8.60E+07
P62917;E9PKU4;E	P62917;E9PKU4;E	60S ribosomal prot	RPL8	18	18	257	1.4629	0.64086	2.78E+09
Q9H501;A0A087W	Q9H501;A0A087W	ESF1 homolog	ESF1	3	3	851	1.4624	NaN	8.24E+07
B7ZM99;A0A087W	B7ZM99;A0A087W	Monofunctional C1	MTHFD1L	29	28	979	1.4616	0.58629	5.67E+09
J3KNS1;Q9UPW5;(	J3KNS1;Q9UPW5;(	Cytosolic carboxyp	AGTPBP1	6	6	1278	1.4612	0.73418	2.53E+08
P62266;D6RD47;D	P62266;D6RD47;D	40S ribosomal prot	RPS23	6	6	143	1.4608	0.76151	4.18E+09
Q12756;Q12756-3	Q12756;Q12756-3	Kinesin-like protein	KIF1A	31	25	1690	1.4604	0.55234	1.44E+09
P24468-3;P24468	P24468-3;P24468	COUP transcription	NR2F2	6	2	261	1.4591	0.49619	4.16E+08
Q5VYS8-6;Q5VYS8;	Q5VYS8-6;Q5VYS8;	Terminal uridylyltr	ZCCHC6	6	6	1457	1.4579	0.52255	1.64E+08
Q8IY17-5;Q8IY17-2	Q8IY17-5;Q8IY17-2	Neuropathy target	PNPLA6	5	5	1300	1.4566	0.64284	1.83E+08
Q9Y3B9	Q9Y3B9	RRP15-like protein	RRP15	5	5	282	1.4563	0.66309	2.90E+08
Q8WTT2	Q8WTT2	Nucleolar complex	NOC3L	17	17	800	1.4561	0.65487	1.81E+09
P82675;P82675-2	P82675	28S ribosomal prot	MRPS5	7	7	430	1.4531	0.72468	5.83E+08
Q8N1G4	Q8N1G4	Leucine-rich repeat	LRRC47	26	26	583	1.452	0.57629	8.31E+09
P52597	P52597	Heterogeneous nuc	HNRNPF	18	16	415	1.4518	0.60524	1.33E+10
Q9UNX3;E5RIT6;E5	Q9UNX3;E5RIT6	60S ribosomal prot	RPL26L1	16	2	145	1.4501	0.66387	2.27E+07

Q14966-3;Q14966	Q14966-3;Q14966	Zinc finger protein	ZNF638	6	6	1957	1.45	0.7163	1.46E+08
H0Y3N9;Q9UPP1-5	H0Y3N9;Q9UPP1-5	Histone lysine dem	PHF8	3	3	953	1.449	0.64029	1.41E+08
Q9BUF5;K7ESM5;K	Q9BUF5;K7ESM5	Tubulin beta-6 chai	TUBB6	24	11	446	1.449	0.68614	1.64E+10
P49754-2;P49754	P49754-2;P49754	Vacuolar protein sc	VPS41	2	2	802	1.4487	NaN	4.27E+07
B4DJV5;Q13610	B4DJV5;Q13610	Periodic tryptopha	PWP1	5	5	439	1.4475	0.92954	1.83E+08
F8W727;P62910;[	F8W727;P62910;[	60S ribosomal prot	RPL32	16	16	153	1.446	0.57432	6.93E+08
P62899;H7C2W9;(	P62899;H7C2W9;(	60S ribosomal prot	RPL31	12	12	125	1.4458	0.69535	2.91E+09
Q6ZNB6-2;Q6ZNB6	Q6ZNB6-2;Q6ZNB6	NF-X1-type zinc fin	NFXL1	3	3	733	1.4455	0.47885	1.58E+08
Q86V81;E9PB61	Q86V81;E9PB61	THO complex subu	ALYREF	5	5	257	1.4425	0.64593	1.60E+09
Q96J01;Q96J01-2;	Q96J01;Q96J01-2;	THO complex subu	THOC3	12	12	351	1.4412	0.62369	1.98E+09
F5H5R8;P18440	F5H5R8;P18440	Arylamine N-acetyl	NAT1	3	3	352	1.4381	0.58469	3.58E+08
Q5T160;H0Y450	Q5T160	Probable arginine--	RARS2	5	5	578	1.4378	0.80018	3.75E+08
Q9HCE1;Q5JR04;Q	Q9HCE1;Q5JR04;Q	Putative helicase M	MOV10	18	18	1003	1.4371	0.6824	1.43E+09
O00170;E9PMH2;\	O00170;E9PMH2	AH receptor-intera	AIP	7	7	330	1.4329	0.63347	4.38E+08
P83731;C9JXB8;C9	P83731;C9JXB8;C9	60S ribosomal prot	RPL24	14	14	157	1.4321	0.74344	7.36E+09
P36578;H3BM89;H	P36578;H3BM89	60S ribosomal prot	RPL4	33	33	427	1.4297	0.65076	1.90E+10
O95433;O95433-2	O95433;O95433-2	Activator of 90 kDa	AHSA1	14	14	338	1.4281	0.67899	9.76E+09
Q96I24;Q96I24-2	Q96I24;Q96I24-2	Far upstream elem	FUBP3	23	19	572	1.4261	0.76516	3.65E+09
O15371-3;O15371	O15371-3;O15371	Eukaryotic translat	EIF3D	21	21	533	1.4253	0.70216	3.59E+09
P39748;P39748-2;	P39748;P39748-2	Flap endonuclease	FEN1	16	16	380	1.4253	0.67351	4.30E+09
P40429;M0QYS1;C	P40429;M0QYS1;C	60S ribosomal prot	RPL13A;RPL13a	17	17	203	1.4247	0.65208	3.58E+09
C9JJ19;P82930;A0	C9JJ19;P82930;A0	28S ribosomal prot	MRPS34	9	9	225	1.4233	0.67496	1.39E+09
E7ETK0;A0A087WL	E7ETK0;A0A087WL	40S ribosomal prot	RPS24	6	6	131	1.4209	0.71118	2.78E+09
Q9Y3A5;A0A087X0	Q9Y3A5;A0A087X0	Ribosome maturati	SBDS	20	20	250	1.42	0.6762	5.79E+09
O15084;O15084-4	O15084;O15084-4	Serine/threonine-p	ANKRD28	13	12	1053	1.4184	0.60323	6.91E+08
Q15366-6;Q15366	Q15366-6;Q15366	Poly(rC)-binding pr	PCBP2	19	2	361	1.4163	NaN	3.04E+09
X6R700;Q9Y3Y2-4;	X6R700;Q9Y3Y2-4;	Chromatin target o	CHTOP	3	3	223	1.4155	0.76397	4.78E+07
E9PR30;P62861	E9PR30;P62861	40S ribosomal prot	FAU	4	4	98	1.4129	0.65661	2.39E+09
Q96JH7	Q96JH7	Deubiquitinating p	VCPIP1	9	9	1222	1.4122	0.61296	3.25E+08
Q02543;M0R3D6;I	Q02543;M0R3D6;I	60S ribosomal prot	RPL18A	13	13	176	1.4115	0.75879	1.47E+09
C9J7X6;A4D1U4	C9J7X6;A4D1U4	Protein LCHN	KIAA1147;LCHN	3	3	351	1.4107	0.9412	8.30E+07
Q9UG01;Q9UG01-:	Q9UG01;Q9UG01-:	Intraflagellar trans	IFT172	19	19	1749	1.4104	0.52577	5.69E+08
Q9BST8;J3QQH7;J3	Q9BST8;J3QQH7;J3	Hypoxia up-regulat	HYOU1	3	3	147	1.4091	NaN	3.28E+07
F5H6E2;O00159-2;	F5H6E2;O00159-2	Unconventional m	MYO1C	23	23	1039	1.4064	0.70148	2.02E+09
D6RID8;Q6P1K8;Q	D6RID8;Q6P1K8;Q	General transcripti	GTF2H2C;GTF2H2	5	5	253	1.404	0.72865	3.25E+08
J3QQ67;Q07020;G	J3QQ67;Q07020;G	60S ribosomal prot	RPL18	12	12	190	1.4038	0.69306	9.62E+09
Q9NXH9;Q9NXH9-:	Q9NXH9;Q9NXH9-:	tRNA (guanine(26)-	TRMT1;SEMA4B	17	17	659	1.4038	0.56654	1.31E+09
Q8N5C6;Q8N5C6-2	Q8N5C6;Q8N5C6-2	S1 RNA-binding do	SRBD1	14	14	995	1.4031	0.561	6.22E+08
P04350;M0R278;N	P04350	Tubulin beta-4A ch	TUBB4A	31	3	444	1.4003	0.71492	2.40E+09
O76031;H0YM48;H	O76031	ATP-dependent Clp	CLPX	14	14	633	1.4	0.59638	1.61E+09
Q5QPK2;H0Y368;C	Q5QPK2;H0Y368;C	Dolichol-phosphat	DPM1	13	13	287	1.3994	0.68471	5.92E+09
P61513;G5E9R3;Q	P61513;G5E9R3;Q	60S ribosomal prot	RPL37A	6	6	92	1.397	0.73866	1.46E+09
O15047;C9J2Z9	O15047	Histone-lysine N-m	SETD1A	9	9	1707	1.3969	0.41112	3.76E+08
V9GY48;Q8N5A5-3	V9GY48;Q8N5A5-3	Zinc finger CCCH-ty	ZGPAT	3	3	417	1.396	0.41924	9.55E+07
P14618-2;H3BTN5	P14618-2;H3BTN5	Pyruvate kinase PKI	PKM	53	4	531	1.3956	0.62712	1.28E+08
Q6UXN9;C9JBU3	Q6UXN9	WD repeat-contain	WDR82	10	10	313	1.3951	0.61437	1.38E+09
G5E9W7;G5E9V5;F	G5E9W7;G5E9V5;F	28S ribosomal prot	MRPS22	15	15	319	1.3943	0.6445	4.17E+09
Q5VVQ6-2;Q5VVQ6	Q5VVQ6-2;Q5VVQ6	Ubiquitin thioester	YOD1	8	8	304	1.3936	0.53985	1.50E+09
M0R2B7;P28340;N	M0R2B7;P28340;N	DNA polymerase;DI	POLD1	26	26	1133	1.3929	0.60144	2.89E+09
H0Y7P7;Q9UG56;E	H0Y7P7;Q9UG56;E	Phosphatidylserine	PISD	2	2	362	1.3917	NaN	4.19E+07
A0A0A0MQR1;Q9Y	A0A0A0MQR1;Q9Y	Mitogen-activated	MAP4K5	4	4	846	1.3911	0.6729	1.12E+08
E9PDF6;O43795;O	E9PDF6;O43795;O	Unconventional m	MYO1B	16	16	1107	1.388	0.66492	1.47E+09
Q6R327;Q6R327-3	Q6R327;Q6R327-3	Rapamycin-insensit	RICTOR	7	7	1708	1.388	0.6668	2.44E+08
O60506-4;O60506	O60506-4;O60506	Heterogeneous nuc	SYNCRIP	23	18	527	1.3878	0.80557	3.05E+09
Q6N069;Q6N069-4	Q6N069;Q6N069-4	N-alpha-acetyltran	NAA16	10	5	864	1.3876	0.99074	7.65E+07
E7ERS3;Q86VM9;Q	E7ERS3;Q86VM9;Q	Zinc finger CCCH do	ZC3H18	3	3	977	1.3875	0.2708	7.99E+07
P62701;Q8TD47;C	P62701	40S ribosomal prot	RPS4X	24	24	263	1.3861	0.70394	1.93E+10
E7ESC7;Q7L5Y9-3;(	E7ESC7;Q7L5Y9-3;(	Macrophage erythr	MAEA	7	7	434	1.3847	0.53258	2.48E+08
O00311;B1AMW7	O00311	Cell division cycle 7	CDC7	3	3	574	1.3846	0.44167	1.10E+08
G8JLB6;P31943;E9	G8JLB6;P31943;E9	Heterogeneous nuc	HNRNPH1	22	11	472	1.3839	0.63075	4.64E+10
P49643;P49643-2;	P49643	DNA primase large	PRIM2	7	7	509	1.3839	0.71333	7.49E+08
Q9C0J8;B9A053;Q	Q9C0J8	pre-mRNA 3 end pr	WDR33	7	7	1336	1.3792	0.34111	2.63E+08
Q9NZI8;Q9NZI8-2;I	Q9NZI8;Q9NZI8-2	Insulin-like growth	IGF2BP1	31	29	577	1.3766	0.75699	1.38E+10
E9PHA2;Q15003;C	E9PHA2;Q15003;C	Condensin comple	NCAPH	21	21	730	1.3742	0.56424	3.17E+09
Q13509;A0A0B4J2	Q13509;A0A0B4J2	Tubulin beta-3 chai	TUBB3	22	6	450	1.3741	0.68103	7.01E+08
Q9Y3Z3;Q9Y3Z3-3;	Q9Y3Z3;Q9Y3Z3-3;	Deoxynucleoside tr	SAMHD1	20	20	626	1.3731	0.64884	2.86E+09
P43250-2;F8W9W	P43250-2;F8W9W	G protein-coupled	GRK6	3	3	589	1.373	0.57802	1.28E+08
Q15020;Q15020-4	Q15020;Q15020-4	Squamous cell carc	SART3	31	31	963	1.3727	0.70443	2.27E+09
A3KMH1-3;A3KMH	A3KMH1-3;A3KMH	von Willebrand fac	VWA8	15	15	1872	1.3725	0.60217	8.19E+08
F5H562;E7ET55;F5	F5H562;E7ET55;F5	Copper-transportir	ATP7B	2	2	1035	1.3718	0.81494	1.20E+08
Q9Y5Q8;Q9Y5Q8-3	Q9Y5Q8;Q9Y5Q8-3	General transcripti	GTF3C5	10	10	519	1.3686	0.59567	1.49E+09
Q86U86-5;Q86U86	Q86U86-5;Q86U86	Protein polybromo	PBRM1	15	15	1582	1.3679	0.61894	4.95E+08
Q9HBD4;A0A0A0M	Q9HBD4;A0A0A0M	Transcription activ	SMARCA4	39	25	1679	1.367	0.65614	2.66E+09
Q9UGI8-2;Q9UGI8;	Q9UGI8-2;Q9UGI8	Testin	TES	16	16	412	1.3665	0.63467	5.76E+08
B9EGE7;Q8TCN5;Q	B9EGE7;Q8TCN5;Q	Zinc finger protein	ZNF507	4	4	957	1.364	0.50591	4.09E+07
E9PKT9;O96033	E9PKT9;O96033	Molybdopterin syn	MOCS2	2	2	83	1.3639	NaN	4.47E+07
Q9H2P0;E9PQK8	Q9H2P0	Activity-dependent	ADNP	19	19	1102	1.3636	0.56472	1.07E+09
Q9UNY4;Q9UNY4-2	Q9UNY4	Transcription term	TTF2	5	5	1162	1.3625	0.87553	1.10E+08
Q13126-4;Q13126	Q13126-4;Q13126	S-methyl-5-thioade	MTAP	5	5	280	1.3613	1.432	5.53E+08
P28074;P28074-3;	P28074;P28074-3	Proteasome subuni	PSMB5	7	7	263	1.3606	0.6995	1.93E+08
Q9Y6V7;Q9Y6V7-2;	Q9Y6V7;Q9Y6V7-2	Probable ATP-depe	DDX49	7	7	483	1.3601	0.60916	3.81E+08
Q13045;Q13045-3	Q13045;Q13045-3	Protein flightless-1	FLII	25	1	1269	1.3597	0.67551	3.05E+09
Q9Y291;C9JBY7	Q9Y291;C9JBY7	28S ribosomal prot	MRPS33	3	3	106	1.3577	0.74063	1.57E+08
A0A0A0MRI0;P427	A0A0A0MRI0;P427	Cyclin-dependent k	CDKN2A	6	2	170	1.3566	0.34907	2.80E+07
Q09472;I3L0Q1	Q09472	Histone acetyltrans	EP300	8	4	2414	1.356	0.48235	4.65E+07
P46776;E9PJD9;E9	P46776;E9PJD9;E9	60S ribosomal prot	RPL27A	8	8	148	1.3541	0.7847	2.30E+09
H7BXH2;E9PKF6;Q	H7BXH2;E9PKF6;Q	Serine/threonine-p	PPP6R3	20	20	827	1.3536	0.63762	1.68E+09
P46779;H0YKD8;P	P46779;H0YKD8;P	60S ribosomal prot	RPL28	15	15	137	1.3527	0.70496	2.69E+09
M0R0F0;M0R0R2;I	M0R0F0;M0R0R2;I	40S ribosomal prot	RPS5	10	10	200	1.3525	0.66789	1.07E+09
J3QS41;P42694;P4	J3QS41;P42694;P4	Probable helicase v	HELZ	15	15	1943	1.3522	0.67096	5.86E+08
P53621;P53621-2	P53621;P53621-2	Coatomer subunit a	COPA	72	72	1224	1.3521	0.66011	2.50E+10
D6RIC3;A0A0C4DG	D6RIC3;A0A0C4DG	Nucleolar protein 1	NOP16	4	4	150	1.3513	0.75967	2.00E+08
A0A087X0M4;Q9B	A0A087X0M4;Q9B	Kanadaptin	SLC4A1AP	5	5	742	1.3502	0.95007	2.15E+08

O60716-5;O60716	O60716-5;O60716	Catenin delta-1	CTNND1	23	22	933	1.3474	0.60349	1.61E+09
A0A0D9SFM0;Q14	A0A0D9SFM0;Q14	E3 ubiquitin-protei	SHPRH	2	2	1687	1.3473	0.6079	3.79E+07
Q9NZB2;Q9NZB2-6	Q9NZB2;Q9NZB2-6	Constitutive coacti	FAM120A	27	27	1118	1.3466	0.57013	2.65E+09
Q96GD0;B1AHD3	Q96GD0	Pyridoxal phospha	PDXP	13	13	296	1.3447	0.56485	3.04E+09
H3BM14;H3BM74;	H3BM14;H3BM74;	NEDD8 ultimate bu	NUB1	9	9	625	1.344	0.75361	5.61E+08
O75600;O75600-2	O75600;O75600-2	2-amino-3-ketobut	GCAT	6	6	419	1.3435	0.55343	4.82E+08
Q9NVH0-2;Q9NVH	Q9NVH0-2;Q9NVH	Exonuclease 3-5 do	EXD2	8	8	496	1.3425	0.62358	4.56E+08
Q96RP9;C9IZ01;F8	Q96RP9;C9IZ01;F8	Elongation factor G	GFM1	20	1	751	1.3421	0.79366	3.33E+09
P49207	P49207	60S ribosomal prot	RPL34	7	7	117	1.3405	0.85933	7.13E+08
Q96G46;Q96G46-2	Q96G46;Q96G46-2	tRNA-dihydrouridi	DUS3L	13	13	650	1.3404	0.48281	1.06E+09
Q9P2I0;H0YJF4;G3	Q9P2I0	Cleavage and polya	CPSF2	16	16	782	1.3392	0.66326	1.30E+09
A0A075B746;P829	A0A075B746;P829	28S ribosomal prot	MRPS21	2	2	87	1.3386	0.82279	2.98E+08
P31689;P31689-2	P31689;P31689-2	DnaJ homolog subf	DNAJA1	19	19	397	1.3374	0.56648	4.52E+09
Q14257;Q14257-2	Q14257;Q14257-2	Reticulocalbin-2	RCN2	14	14	317	1.3371	0.58802	4.22E+09
P82673;H0YG82;P	P82673;H0YG82;P	28S ribosomal prot	MRPS35	6	6	323	1.3368	0.61889	3.88E+08
O95801	O95801	Tetratricopeptide r	TTC4	2	2	387	1.3367	NaN	1.37E+08
A0A087WXM6;J3C	A0A087WXM6;J3C	60S ribosomal prot	RPL17	14	14	169	1.3366	0.80541	3.14E+09
P41214;P41214-2	P41214;P41214-2	Eukaryotic translat	EIF2D	14	14	584	1.3363	0.57893	1.81E+09
P33981-2;P33981	P33981-2;P33981	Dual specificity pro	TTK	11	11	856	1.336	0.59361	5.92E+08
A0A0A6YYI3;A0A0E	A0A0A6YYI3;A0A0E	Suppressor of SWI4	PPAN	4	4	520	1.3353	0.79868	2.56E+08
P53597;H7C233	P53597	Succinyl-CoA ligase	SUCLG1	11	11	346	1.3351	0.70518	2.14E+09
Q9Y5V3;Q9Y5V3-2	Q9Y5V3;Q9Y5V3-2	Melanoma-associat	MAGED1	4	3	778	1.335	0.44055	1.51E+08
O43719;Q5H918;C	O43719;Q5H918	HIV Tat-specific fac	HTATSF1	16	16	755	1.3331	0.53653	1.15E+09
P54198;P54198-2	P54198;P54198-2	Protein HIRA	HIRA	4	4	1017	1.3316	0.53369	1.08E+08
A0A0A0MSK4;A0A(	A0A0A0MSK4;A0A(	G-protein-signaling	GPSM1	11	11	675	1.3309	0.71665	4.24E+08
P62277;J3KMX5;E	P62277;J3KMX5	40S ribosomal prot	RPS13	13	13	151	1.3309	0.75597	7.11E+09
P61313;E7EQV9;E7	P61313;E7EQV9;E7	60S ribosomal prot	RPL15	13	13	204	1.3303	0.6774	3.37E+09
G3XAG1;Q96ME7-2	G3XAG1;Q96ME7-2	Zinc finger protein	ZNF512	2	2	566	1.3302	0.68681	9.28E+07
Q9BRX2	Q9BRX2	Protein pelota hon	PELO	14	14	385	1.3299	0.75365	1.53E+09
Q14147;H7C504	Q14147	Probable ATP-depe	DHX34	9	9	1143	1.3298	0.51015	4.62E+08
P61254;J3QRI7;J3	P61254;J3QRI7;J3	60S ribosomal prot	RPL26;KRBA2	20	6	145	1.329	0.69324	2.74E+09
A2RTX5-2;A2RTX5;	A2RTX5-2;A2RTX5;	Probable threonine	TARSL2	8	4	707	1.3287	0.84347	1.66E+08
Q9NQW6-2;Q9NQV	Q9NQW6-2;Q9NQV	Actin-binding prot	ANLN	6	6	1087	1.328	0.49559	1.73E+08
P14866;M0QXS5;P	P14866;M0QXS5;P	Heterogeneous nuc	HNRNPL	30	30	589	1.3275	0.65432	2.57E+10
Q05086-2;Q05086	Q05086-2;Q05086	Ubiquitin-protein l	UBE3A	11	11	852	1.3274	0.76953	6.26E+08
Q9BYN8	Q9BYN8	28S ribosomal prot	MRPS26	7	7	205	1.3271	0.71193	1.77E+08
Q9BVA1	Q9BVA1	Tubulin beta-2B ch	TUBB2B	32	2	445	1.327	0.80741	1.49E+10
Q3SY69;Q3SY69-3;	Q3SY69	Mitochondrial 10-f	ALDH1L2	24	20	923	1.3269	0.84702	2.28E+09
Q9BXW6;Q9BXW6	Q9BXW6;Q9BXW6	Oxysterol-binding p	OSBPL1A	4	4	950	1.3269	0.81089	9.93E+07
H3BRU6;F8VZX2	H3BRU6;F8VZX2		PCBP2	18	2	301	1.3266	0.45074	1.02E+09
A0A087WSW7;F6X	A0A087WSW7;F6X	Lymphoid-specific	HELLS	11	11	700	1.3249	0.63385	7.05E+08
B7Z6D5;Q96GQ7;A	B7Z6D5;Q96GQ7	Probable ATP-depe	DDX27	12	12	765	1.3243	0.65186	1.09E+09
Q13123;E7EQZ7;Q	Q13123;E7EQZ7;Q	Protein Red	IK	10	10	557	1.3242	0.63558	8.89E+08
Q9UHB9;Q9UHB9-4	Q9UHB9;Q9UHB9-4	Signal recognition p	SRP68	33	33	627	1.324	0.71893	5.36E+09
Q96CB9-4;Q96CB9	Q96CB9-4;Q96CB9	5-methylcytosine r	NSUN4	3	3	335	1.3235	0.60505	1.49E+08
A0A087WY54;Q15	A0A087WY54;Q15	Zinc finger HIT dom	ZNHIT3	2	2	90	1.3233	NaN	1.50E+07
Q9UDY8;Q9UDY8-2	Q9UDY8;Q9UDY8-2	Mucosa-associated	MALT1	5	5	824	1.323	0.5435	1.39E+08
Q9NYP9	Q9NYP9	Protein Mis18-alph	MIS18A	2	2	233	1.3223	0.87401	1.61E+08
Q12789;Q12789-3	Q12789;Q12789-3	General transcripti	GTF3C1	38	38	2109	1.322	0.78762	1.78E+09
P25786;P25786-2;	P25786;P25786-2;	Proteasome subuni	PSMA1	12	12	263	1.321	0.61862	2.14E+09
Q9NRY4;A2RRE5	Q9NRY4;A2RRE5	Rho GTPase-activat	ARHGAP35;GRLF1	10	10	1499	1.32	0.60745	4.06E+08
C9JP00;A0A0A0M	C9JP00;A0A0A0M	Muscleblind-like pr	MBNL1;MBLL;MBN	8	5	348	1.3197	0.70858	6.62E+08
Q13247-3;Q13247	Q13247-3;Q13247	Serine/arginine-ricl	SRSF6	6	4	335	1.3197	0.67323	1.31E+08
Q96A33;Q96A33-2	Q96A33;Q96A33-2	Coiled-coil domain	CCDC47	8	8	483	1.3178	0.79815	8.02E+08
Q96D53-2;Q96D53	Q96D53-2;Q96D53	AarF domain-conta	ADCK4	2	2	503	1.3176	0.57656	1.06E+08
Q8NEC7;D6R9W2;(	Q8NEC7;D6R9W2;(	Glutathione S-trans	GSTCD	3	3	633	1.3173	0.6237	1.20E+08
Q8TER5-2;Q8TER5-	Q8TER5-2;Q8TER5-	Rho guanine nucle	ARHGEF40	3	3	805	1.3167	NaN	3.97E+07
Q15398-3;Q15398	Q15398-3;Q15398	Disks large-associat	DLGAP5	2	2	842	1.3165	NaN	3.28E+07
O75891;O75891-3	O75891;O75891-3	Cytosolic 10-formy	ALDH1L1	5	2	902	1.3158	0.51931	7.86E+07
Q9BVS4-2;Q9BVS4	Q9BVS4-2;Q9BVS4	Serine/threonine-p	RIOK2	2	2	474	1.3155	0.47398	1.01E+08
Q9Y3B7;Q9Y3B7-2;	Q9Y3B7;Q9Y3B7-2;	39S ribosomal prot	MRPL11	11	11	192	1.3155	0.47995	4.66E+08
Q9H0S4;Q9H0S4-2	Q9H0S4;Q9H0S4-2	Probable ATP-depe	DDX47	12	12	455	1.3147	0.71176	1.86E+09
Q9Y2U8	Q9Y2U8	Inner nuclear mem	LEMD3	3	3	911	1.3143	0.36995	5.38E+07
Q9NYV4-2;Q9NYV4	Q9NYV4-2;Q9NYV4	Cyclin-dependent k	CDK12	5	4	1481	1.3141	0.39798	1.72E+08
O14647-2;O14647	O14647-2;O14647	Chromodomain-he	CHD2	8	4	1739	1.3139	NaN	4.55E+07
Q5T1Z4;Q5T1Z8;Q5	Q5T1Z4;Q5T1Z8;Q5	Pumilio homolog 1	PUM1	12	12	1189	1.3138	0.72529	5.95E+08
A0A0R4J2E8;A8MX	A0A0R4J2E8;A8MX	Matrin-3	MATR3	39	39	847	1.3136	0.70073	1.89E+10
P26358;P26358-2;	P26358;P26358-2;	DNA (cytosine-5)-m	DNMT1	31	31	1616	1.3134	0.65073	1.84E+09
Q06787-6;Q06787	Q06787-6;Q06787	Fragile X mental ret	FMR1	5	4	590	1.3133	0.78713	1.92E+08
Q99766;Q8WXQ4	Q99766	ATP synthase subur	ATP5S	3	3	215	1.3127	0.88039	6.29E+07
Q5VZE5;Q5VZE5-2	Q5VZE5	N-alpha-acetyltran	NAA35	7	7	725	1.3124	0.74943	5.74E+08
E9PMP7;E9PMS6;F	E9PMP7;E9PMS6;F	LIM domain only pr	LMO7	2	2	1046	1.3097	0.78232	4.79E+07
Q86XP3;A0A0A0M	Q86XP3;A0A0A0M	ATP-dependent RN	DDX42	16	16	938	1.3095	0.86754	9.67E+08
M0QY97;Q9UPT8	M0QY97;Q9UPT8	Zinc finger CCCH do	ZC3H4	4	4	910	1.3086	0.50943	6.72E+07
P82663;E7EPW2;P	P82663;E7EPW2;P	28S ribosomal prot	MRPS25	11	11	173	1.3072	0.74849	2.49E+08
Q14999;Q14999-2	Q14999;Q14999-2	Cullin-7	CUL7	7	7	1698	1.3071	0.71273	2.43E+08
Q16543;K7EQA9;K	Q16543;K7EQA9;K	Hsp90 co-chaperon	CDC37	21	21	378	1.3067	0.7107	4.40E+09
Q9UL03-3;Q9UL03	Q9UL03-3;Q9UL03	Integrator complex	INTS6	4	3	874	1.3067	0.5829	1.37E+08
Q6P5Z2	Q6P5Z2	Serine/threonine-p	PKN3	5	4	889	1.3058	0.52095	2.88E+07
Q13885	Q13885	Tubulin beta-2A ch	TUBB2A	32	2	445	1.3051	NaN	1.78E+08
O15305;H3BRM0;I	O15305;H3BRM0;I	Phosphomannomu	PMM2	7	7	246	1.3046	0.83908	6.05E+08
Q9UPY3;Q9UPY3-2	Q9UPY3;Q9UPY3-2	Endoribonuclease I	DICER1	21	21	1922	1.3019	0.67576	9.68E+08
O14646-2;O14646	O14646-2;O14646	Chromodomain-he	CHD1	14	10	1709	1.3005	0.73212	5.52E+08
C9J5N1;Q9BTE6;Q9	C9J5N1;Q9BTE6;Q9	Alanyl-tRNA editing	PTGES3L-AARSD1;A	10	10	495	1.3003	0.82106	9.07E+08
Q9H267;F5H008;C	Q9H267;F5H008;C	Vacuolar protein sc	VPS33B	15	15	617	1.2995	0.56304	1.06E+09
Q03164-2;Q03164	Q03164-2;Q03164	Histone-lysine N-m	KMT2A	3	3	3931	1.2991	0.66686	5.70E+07
Q7L8L6	Q7L8L6	FAST kinase domair	FASTKD5	2	2	764	1.2988	NaN	1.06E+08
P40938;P40938-2;	P40938;P40938-2	Replication factor C	RFC3	10	10	356	1.2985	0.79403	1.48E+09
Q9GZS1-2;Q9GZS1	Q9GZS1-2;Q9GZS1	DNA-directed RNA p	POLR1E	8	8	419	1.2985	0.67551	4.57E+08
P43897;P43897-2;	P43897;P43897-2	Elongation factor T	TSFM	11	11	325	1.2975	0.71037	3.00E+09
P53618;E9PP73;E9	P53618;E9PP73	Coatomer subunit b	COPB1	52	52	953	1.297	0.65471	1.96E+10
G3V5Z7;P60900;G	G3V5Z7;P60900;G	Proteasome subuni	PSMA6	6	6	252	1.2969	0.72565	8.44E+08
Q9Y263;E5RIM3;H	Q9Y263;E5RIM3	Phospholipase A-2-	PLAA	28	28	795	1.2969	0.61552	3.61E+09

Q9Y4K3	Q9Y4K3	TNF receptor-assoc	TRAF6	5	5	522	1.2967	0.62074	3.66E+08
P62191;P62191-2;	P62191;P62191-2	26S protease regul	PSMC1	24	24	440	1.2964	0.72889	6.08E+09
Q6PJI9;Q6PJI9-3;H	Q6PJI9;Q6PJI9-3;H	WD repeat-contain	WDR59	6	6	974	1.2961	0.54164	1.47E+08
Q9C0C9;K7ES11;K	Q9C0C9;K7ES11	E2/E3 hybrid ubiqu	UBE2O	22	22	1292	1.2955	0.87308	1.51E+09
Q14166;V9GY16	Q14166	Tubulin--tyrosine li	TTLL12	15	15	644	1.2945	0.92585	2.67E+09
O60566;O60566-3	O60566;O60566-3	Mitotic checkpoint	BUB1B	6	6	1050	1.2937	0.61309	1.12E+08
Q9UPT9-2;Q9UPT9	Q9UPT9-2;Q9UPT9	Ubiquitin carboxyl	USP22;USP27X	3	3	513	1.2937	0.66036	1.54E+08
O43776;K7EIU7;O	O43776	Asparagine--tRNA li	NARS	29	29	548	1.2928	0.67781	1.04E+10
J3KMX2;B9EGA3;Q	J3KMX2;B9EGA3;Q	SWI/SNF-related m	SMARCD2	5	5	456	1.2921	0.77615	1.91E+08
Q12972;A0A0A0M	Q12972	Nuclear inhibitor o	PPP1R8	15	15	351	1.2914	0.65509	2.50E+09
Q8TDD1;Q8TDD1-2	Q8TDD1;Q8TDD1-2	ATP-dependent RN	DDX54	10	10	881	1.2913	0.7371	3.80E+08
P78344;D3DQV9;P	P78344;D3DQV9;P	Eukaryotic translat	EIF4G2	46	46	907	1.2905	0.59628	8.84E+09
A0A087WY00;G3V	A0A087WY00;G3V	Unconventional m	MYO5A	2	2	1828	1.2901	NaN	2.19E+07
C9JYQ9;H0Y8C2;Q	C9JYQ9;H0Y8C2;Q	60S ribosomal prot	RPL22L1	4	2	121	1.2889	0.77489	1.39E+08
O95983-2;O95983	O95983-2;O95983	Methyl-CpG-bindin	MBD3	4	4	259	1.2884	0.64544	5.08E+08
G3V529;Q9GZR7;C	G3V529;Q9GZR7;C	ATP-dependent RN	DDX24	14	14	816	1.2881	0.58105	4.23E+08
F2Z2W7;Q8IZ69-2;	F2Z2W7;Q8IZ69-2;	tRNA (uracil-5-)-me	TRMT2A	8	8	643	1.288	0.40883	1.98E+08
Q92665	Q92665	28S ribosomal prot	MRPS31	7	7	395	1.2874	0.67647	7.87E+08
Q96EL2;F8VYR5	Q96EL2	28S ribosomal prot	MRPS24	6	6	167	1.2869	0.75644	4.12E+08
P0DN76;Q01081;C	P0DN76;Q01081;C	Splicing factor U2A	U2AF1	9	9	240	1.2868	0.79799	2.58E+09
O43379;O43379-4	O43379;O43379-4	WD repeat-contain	WDR62	3	3	1518	1.2847	0.79404	3.23E+07
A0A087WXC5;E7E	A0A087WXC5;E7E	NADH dehydrogen	NDUFA10	8	8	355	1.2846	0.69761	3.97E+09
Q92995-2;Q92995	Q92995-2;Q92995	Ubiquitin carboxyl	USP13	4	3	798	1.2831	0.7537	1.63E+08
C9JXR7;A8MVM1;F	C9JXR7;A8MVM1;F	Caspase-3;Caspase-	CASP3	3	3	117	1.2826	0.84478	1.01E+08
C9JNE2;Q9Y530;C	C9JNE2;Q9Y530;C	O-acetyl-ADP-ribos	OARD1	5	5	131	1.2812	0.74167	2.44E+08
Q9UBW7;A0A087X	Q9UBW7	Zinc finger MYM-ty	ZMYM2	8	8	1377	1.2812	0.6481	1.18E+08
Q12923-3;Q12923	Q12923-3;Q12923	Tyrosine-protein ph	PTPN13	14	14	2466	1.2809	0.94572	3.57E+08
J3KNN5;Q9UJV9;H	J3KNN5;Q9UJV9	Probable ATP-depe	DDX41	5	5	640	1.2798	0.83659	3.73E+08
A0A087WYU1;Q9Y	A0A087WYU1;Q9Y	Sorting nexin-9	SNX9	7	7	594	1.2784	1.0984	3.38E+08
Q15386;Q15386-2	Q15386	Ubiquitin-protein l	UBE3C	25	25	1083	1.278	0.62615	2.47E+09
Q9Y5Y2;H3BNF0;H	Q9Y5Y2;H3BNF0;H	Cytosolic Fe-S clust	NUBP2	9	9	271	1.2775	0.70226	2.10E+09
Q5QPR4;J3QR29;A	Q5QPR4;J3QR29;A	Cyclin-dependent k	CDK11A;CDK11B;C	2	2	746	1.2767	0.86187	1.63E+08
A0A0C4DFX4;Q6ZF	A0A0C4DFX4;Q6ZF	Helicase SRCAP	SRCAP	11	10	3053	1.2766	0.83417	4.48E+08
Q05655;Q05655-2	Q05655;Q05655-2	Protein kinase C de	PRKCD	6	6	676	1.2756	0.72948	5.91E+08
C9JJN9;Q8N3P4-2;	C9JJN9;Q8N3P4-2;	Vacuolar protein sc	VPS8	4	4	1428	1.2751	0.61811	9.35E+07
Q9P2R3;Q9P2R3-2	Q9P2R3;Q9P2R3-2	Ankyrin repeat and	ANKFY1	22	22	1169	1.2744	0.78294	2.07E+09
B4DZS0;O76075;J3	B4DZS0;O76075;J3	DNA fragmentation	DFFB	4	4	362	1.2736	0.87305	2.14E+08
P37108;H0YLA2	P37108;H0YLA2	Signal recognition p	SRP14	9	9	136	1.2727	0.92125	3.05E+09
P61978;P61978-2;	P61978;P61978-2	Heterogeneous nuc	HNRNPK	34	2	463	1.2715	0.7461	5.11E+10
P62280;M0QZC5;N	P62280;M0QZC5	40S ribosomal prot	RPS11	22	22	158	1.2705	0.86732	3.70E+09
H7C2Q8;Q99848	H7C2Q8;Q99848	Probable rRNA-pro	EBNA1BP2	4	4	361	1.2701	0.48927	2.05E+08
P26368-2;P26368;	P26368-2;P26368;	Splicing factor U2A	U2AF2	15	15	471	1.2695	0.7648	6.29E+09
Q86YP4-2;Q86YP4;	Q86YP4-2;Q86YP4;	Transcriptional rep	GATAD2A	12	11	608	1.268	0.63315	3.49E+08
Q99459	Q99459	Cell division cycle 5	CDC5L	22	22	802	1.2661	0.60975	1.21E+09
H0YF29;Q6P1X6-2;	H0YF29;Q6P1X6-2;	UPF0598 protein C	C8orf82	3	3	261	1.2651	NaN	4.95E+07
P15880;H0YEN5;E	P15880;H0YEN5;E	40S ribosomal prot	RPS2	17	17	293	1.2646	0.73609	2.07E+10
O76021;J3QSV6;I3	O76021;J3QSV6	Ribosomal L1 dom	RSL1D1	20	20	490	1.264	0.81819	3.14E+09
A0A0A0MTH3;Q13	A0A0A0MTH3;Q13	Integrin-linked pro	ILK	10	10	483	1.2639	0.69537	1.04E+09
Q15366-4;Q15366	Q15366-4;Q15366	Poly(rC)-binding pr	PCBP2	20	3	331	1.2637	0.72654	2.00E+10
Q8WUM0	Q8WUM0	Nuclear pore comp	NUP133	29	29	1156	1.2634	0.66192	4.93E+09
Q9UK61-3;Q9UK61	Q9UK61-3;Q9UK61	Protein FAM208A	FAM208A	12	12	1512	1.2634	0.7429	4.20E+08
Q13049;Q5JVY0	Q13049;Q5JVY0	E3 ubiquitin-protei	TRIM32	3	3	653	1.2632	0.56334	1.53E+08
K7EIL6;K7EJ58;K7E	K7EIL6;K7EJ58;K7E	DNA repair protein	RAD51D;hCG_198	2	2	204	1.2626	0.87613	2.73E+07
Q15185-3;Q15185	Q15185-3;Q15185	Prostaglandin E syn	PTGES3	8	8	130	1.2617	0.63257	1.96E+08
Q5HYI8;C9JXM3;F8	Q5HYI8;C9JXM3	Rab-like protein 3	RABL3	7	7	236	1.2615	0.71446	2.70E+08
O43390;O43390-3	O43390;O43390-3	Heterogeneous nuc	HNRNPR	24	3	633	1.2612	0.85843	5.68E+09
H7BXY3;Q7L2E3-3;	H7BXY3;Q7L2E3-3;	Putative ATP-deper	DHX30	43	43	1166	1.2611	0.74056	4.51E+09
P62195;P62195-2;	P62195;P62195-2;	26S protease regul	PSMC5	28	27	406	1.2608	0.80118	1.19E+10
O14733;O14733-4	O14733;O14733-4	Dual specificity mit	MAP2K7	8	8	419	1.2607	0.68689	5.11E+08
P17252;J3KRN5;H	P17252	Protein kinase C alp	PRKCA	7	5	672	1.2607	1.098	5.40E+08
Q96KR1;H0Y8W1	Q96KR1	Zinc finger RNA-bin	ZFR	18	18	1074	1.2607	0.56668	1.19E+09
P09543-2;P09543;	P09543-2;P09543	2,3-cyclic-nucleoti	CNP	17	17	401	1.2606	0.76632	1.48E+09
F6UYG0;F5GWT4;C	F6UYG0;F5GWT4;C	Serine/threonine-p	WNK1	1	1	393	1.2603	NaN	1.06E+07
P50579-3;P50579;	P50579-3;P50579;	Methionine amino	METAP2	5	5	455	1.26	0.65977	8.02E+07
O14964-2;O14964	O14964-2;O14964	Hepatocyte growth	HGS	3	3	690	1.2582	1.2512	3.04E+08
Q01085;E7ETJ9;E7	Q01085;E7ETJ9;E7	Nucleolysin TIAR	TIAL1	12	1	375	1.2581	0.91616	2.13E+09
Q86W42;Q86W42	Q86W42;Q86W42	THO complex subu	THOC6	11	11	341	1.2581	0.68655	3.01E+09
Q9BQG0;Q9BQG0-	Q9BQG0;Q9BQG0-	Myb-binding prote	MYBBP1A	29	29	1328	1.2578	0.69241	3.53E+09
Q9UMY1;H7C2B1;(	Q9UMY1;H7C2B1;(	Nucleolar protein 7	NOL7	5	5	257	1.2577	0.82919	2.15E+08
O00267-2;O00267	O00267-2;O00267	Transcription elong	SUPT5H	18	18	1083	1.2575	0.91643	1.50E+09
Q96P11;Q96P11-2	Q96P11;Q96P11-2	Probable 28S rRNA	NSUN5	12	12	429	1.2573	0.67506	9.40E+08
Q9UBN7;Q9UBN7-	Q9UBN7;Q9UBN7-	Histone deacetylas	HDAC6	4	4	1215	1.2571	0.63089	3.64E+08
G5E933;O95248;O	G5E933;O95248;O	Myotubularin-relat	SBF1	19	18	1868	1.2567	0.58699	5.42E+08
P28072;A0A087X2	P28072;A0A087X2	Proteasome subuni	PSMB6	4	4	239	1.2566	0.73756	5.87E+07
Q9Y399;Q5T8A0	Q9Y399;Q5T8A0	28S ribosomal prot	MRPS2	10	10	296	1.2558	0.78062	9.89E+08
Q8WUA2	Q8WUA2	Peptidyl-prolyl cis-	PPIL4	8	8	492	1.2552	0.79391	2.99E+08
O94832;J3QRN6;K	O94832;J3QRN6;K	Unconventional m	MYO1D	21	21	1006	1.2539	0.68789	1.34E+09
Q9H307;Q9H307-2	Q9H307;Q9H307-2	Pinin	PNN	6	6	717	1.2526	0.94117	3.07E+08
Q8IX18-4;Q8IX18-;	Q8IX18-4;Q8IX18-;	Probable ATP-depe	DHX40	8	8	702	1.252	0.65774	6.74E+08
B1ALB4;E9PD50;Q	B1ALB4;E9PD50;Q	Protein SMG7	SMG7	4	4	757	1.2519	0.78512	3.48E+07
Q5VTR2;C9J0A5;C	Q5VTR2	E3 ubiquitin-protei	RNF20	23	21	975	1.25	0.58678	1.16E+09
Q86U44;H0YFV6;Q	Q86U44;H0YFV6;Q	N6-adenosine-meth	METTL3	6	6	580	1.2497	0.98607	3.33E+08
P84022;H0YMP2;H	P84022;H0YMP2;H	Mothers against de	SMAD3;SMAD2;SM	2	2	425	1.2496	0.51481	1.41E+08
Q13625-2;Q13625	Q13625-2;Q13625	Apoptosis-stimulat	TP53BP2	4	4	1005	1.2492	0.57225	1.57E+08
Q96SI9-2;Q96SI9	Q96SI9-2;Q96SI9	Spermatid perinucl	STRBP	9	5	658	1.2492	0.59875	1.41E+08
P61962;A0A087W	P61962;A0A087W	DDB1- and CUL4-as	DCAF7	8	8	342	1.248	0.66211	1.47E+09
A6NHN7;A6NHB5;(	A6NHN7;A6NHB5;(	Zinc finger MYM-ty	ZMYM3	6	5	1280	1.2479	0.82704	1.85E+08
Q86WX3;F8WFE7	Q86WX3;F8WFE7	Active regulator of	RPS19BP1	2	2	136	1.2475	0.49955	2.70E+08
A0A0A0MR09;P43	A0A0A0MR09;P43	Tyrosine-protein ph	PTPN9	5	5	583	1.2466	0.82777	2.13E+08
P46778;M0R181;C	P46778;M0R181;C	60S ribosomal prot	RPL21	15	15	160	1.2464	0.7505	4.90E+09
Q9H2U1;Q9H2U1-	Q9H2U1;Q9H2U1-	ATP-dependent RN	DHX36	27	26	1008	1.2461	0.7876	3.12E+09
Q9H6T3;Q9H6T3-3	Q9H6T3;Q9H6T3-3	RNA polymerase II-	RPAP3	8	8	665	1.2454	0.67938	7.01E+08
E9PPJ1;Q8NG31-3;	E9PPJ1;Q8NG31-3;	Protein CASC5	CASC5	3	3	1746	1.245	NaN	5.50E+07

O15344;C9J453;O	O15344;C9J453;O	E3 ubiquitin-protei	MID1	10	10	667	1.244	0.96302	6.16E+08
Q8NB90;Q8NB90-2	Q8NB90;Q8NB90-2	Spermatogenesis-a	SPATA5	12	11	893	1.2433	0.55846	4.89E+08
P06748;P06748-3;	P06748;P06748-3;	Nucleophosmin	NPM1	16	16	294	1.2432	0.92843	2.33E+10
P38159;H3BT71;P	P38159;H3BT71;P	RNA-binding motif	RBMX;RBMXL1	13	13	391	1.2426	0.69169	2.49E+09
P43686;P43686-2	P43686;P43686-2	26S protease regul	PSMC4	32	32	418	1.2418	0.74428	1.15E+10
Q9Y3D3;A6ND22;C	Q9Y3D3;A6ND22;C	28S ribosomal prot	MRPS16	2	2	137	1.2417	0.85435	2.85E+08
Q9NWK9-2;Q9NWI	Q9NWK9-2;Q9NW	Box C/D snoRNA pr	ZNHIT6	3	3	431	1.2406	0.51337	8.66E+07
Q86XL3;Q86XL3-2;	Q86XL3;Q86XL3-2	Ankyrin repeat and	ANKLE2	4	4	938	1.2403	0.6394	8.04E+07
O15111	O15111	Inhibitor of nuclea	CHUK	5	5	745	1.2398	0.74055	2.15E+08
A0A087X0R7;Q9H4	A0A087X0R7;Q9H4	Sentrin-specific pro	SENP3	3	3	540	1.2389	0.63232	1.04E+08
O75150;H3BP71;C	O75150;H3BP71;C	E3 ubiquitin-protei	RNF40	17	15	1001	1.2389	0.64596	4.40E+08
Q4G0F5	Q4G0F5	Vacuolar protein so	VPS26B	3	2	336	1.238	NaN	1.04E+08
Q9H1Y0;L7UQJ2;Q	Q9H1Y0;L7UQJ2;Q	Autophagy protein	ATG5	4	4	275	1.2379	0.86604	2.40E+08
A0A024R4M0;P46	A0A024R4M0;P46	40S ribosomal prot	RPS9	20	20	194	1.2375	0.7606	8.62E+09
O14802;Q7Z755;R	O14802	DNA-directed RNA	POLR3A	39	38	1390	1.2369	0.71485	2.37E+09
Q9BY77;F6VRR5;Q	Q9BY77;F6VRR5;Q	Polymerase delta-i	POLDIP3	13	13	421	1.2362	0.72129	2.00E+09
P60891;P60891-2;	P60891;P60891-2	Ribose-phosphate	PRPS1	22	10	318	1.2348	0.83329	1.10E+10
Q8TF05-2;Q8TF05;	Q8TF05-2;Q8TF05;	Serine/threonine-p	PPP4R1	6	6	933	1.2344	0.71298	1.44E+08
C9JE12;C9JCW7;Q	C9JE12;C9JCW7;Q	Transmembrane an	TMUB1	1	1	152	1.2342	1.213	2.38E+07
O94808;E5RJP4	O94808;E5RJP4	Glutamine--fructos	GFPT2	5	3	682	1.2342	0.92441	1.98E+08
P78362;P78362-2;	P78362;P78362-2	SRSF protein kinase	SRPK2;SRPK3	2	1	688	1.2336	NaN	1.63E+07
Q96RY7;Q96RY7-2	Q96RY7;Q96RY7-2	Intraflagellar trans	IFT140	3	3	1462	1.2336	0.69402	1.28E+08
Q8N2K0-3;Q8N2K0	Q8N2K0-3;Q8N2K0	Monoacylglycerol l	ABHD12	4	4	360	1.2335	1.0103	1.91E+08
O43172-2;O43172	O43172-2;O43172	U4/U6 small nuclea	PRPF4	15	15	521	1.2333	0.93803	2.04E+09
A0A087WY71;Q96	A0A087WY71;Q96	AP-2 complex subu	AP2M1	10	10	434	1.233	0.7364	8.07E+08
Q8NI60-3;Q8NI60;	Q8NI60-3;Q8NI60;	Chaperone activity	ADCK3	10	10	595	1.2327	0.64821	1.17E+09
Q9NRF8	Q9NRF8	CTP synthase 2	CTPS2	18	14	586	1.2326	0.75778	1.93E+09
P35250;P35250-2;	P35250;P35250-2	Replication factor C	RFC2	13	13	354	1.2324	0.77704	1.94E+09
Q9H0D6;Q9H0D6-	Q9H0D6;Q9H0D6-	5-3 exoribonucleas	XRN2	21	21	950	1.2324	0.73085	2.37E+09
P49915;P49915-2	P49915;P49915-2	GMP synthase [glut	GMPS	41	41	693	1.2323	0.65738	1.91E+10
P36954;K7EK49;K	P36954;K7EK49;K	DNA-directed RNA	POLR2I	2	2	125	1.232	0.7887	1.93E+08
Q9H9Y6;Q9H9Y6-3	Q9H9Y6;Q9H9Y6-3	DNA-directed RNA	POLR1B	16	16	1135	1.2319	0.82249	1.22E+09
Q6P1J9	Q6P1J9	Parafibromin	CDC73	14	14	531	1.2318	0.75678	1.35E+09
E9PN76;Q8ND24-2	E9PN76;Q8ND24-2	RING finger protein	RNF214	2	2	513	1.231	NaN	1.96E+07
P31327;P31327-3;	P31327;P31327-3	Carbamoyl-phosph	CPS1	22	19	1500	1.2296	0.76878	1.76E+09
P49411;H3BNU3	P49411	Elongation factor T	TUFM	29	29	452	1.2296	0.75076	3.69E+10
P63173;J3KT73;J3	P63173;J3KT73;J3	60S ribosomal prot	RPL38	8	8	70	1.2294	0.76241	7.27E+09
F8W7U8;P49959;F	F8W7U8;P49959;F	Double-strand brea	MRE11A	11	11	707	1.228	0.82777	1.67E+09
Q9BXS5;Q9BXS5-2;	Q9BXS5;Q9BXS5-2	AP-1 complex subu	AP1M1	17	17	423	1.2276	0.71103	1.96E+09
Q16531;F5GY55;Q	Q16531;F5GY55	DNA damage-bindi	DDB1	23	23	1140	1.2272	0.6076	2.20E+09
P05387;H0YDD8	P05387	60S acidic ribosom	RPLP2	11	11	115	1.2271	0.54259	4.88E+09
P23258;Q9NRH3;K	P23258;Q9NRH3	Tubulin gamma-1 c	TUBG1;TUBG2	26	26	451	1.2269	0.62444	4.81E+09
P07900;P07900-2;	P07900;P07900-2	Heat shock protein	HSP90AA1	54	35	732	1.2268	0.91579	3.85E+10
F8W020;F8VY35;F	F8W020;F8VY35;F	Nucleosome assem	NAP1L1	9	7	207	1.2248	1.027	5.44E+09
Q5QPM7;Q92530;I	Q5QPM7;Q92530;I	Proteasome inhibit	PSMF1	4	4	263	1.2231	0.72298	6.06E+08
Q96QG7;E9PR67;C	Q96QG7;E9PR67;C	Myotubularin-relat	MTMR9	2	2	549	1.2217	0.7495	1.85E+08
A0A0D9SEJ5;F5GY(	A0A0D9SEJ5;F5GY(	Constitutive coacti	FAM120B	7	7	922	1.2206	0.72194	3.21E+08
Q6PKG0;Q6PKG0-3	Q6PKG0;Q6PKG0-3	La-related protein 1	LARP1	8	8	1096	1.2206	0.82231	4.85E+08
Q9NW13;Q9NW13	Q9NW13;Q9NW13	RNA-binding protei	RBM28	13	13	759	1.2196	0.71197	8.02E+08
J3QLS3;Q9Y2R9;J3	J3QLS3;Q9Y2R9;J3	28S ribosomal prot	MRPS7	10	10	271	1.2195	0.70598	1.59E+09
A0A087WZZ5;Q13	A0A087WZZ5;Q13	Splicing factor 3B s	SF3B2	13	13	871	1.2184	0.67673	3.85E+08
Q99956	Q99956	Dual specificity pro	DUSP9	5	5	384	1.2183	0.70541	8.38E+08
Q92878;Q92878-2	Q92878;Q92878-2	DNA repair protein	RAD50	42	42	1312	1.2178	0.68094	3.51E+09
R4GNH3;E9PKD5;E	R4GNH3;E9PKD5;E	9PMD8;E9PN50	PSMC3	30	1	423	1.2175	0.87218	9.15E+09
Q7Z6M1;Q7Z6M1-	Q7Z6M1;Q7Z6M1-	Rab9 effector prote	RABEPK	7	7	372	1.2173	1.226	3.87E+08
O60678;A0A0A0M	O60678;A0A0A0M	Protein arginine N-	PRMT3	14	14	531	1.2172	0.76605	1.78E+09
Q9H9A6	Q9H9A6	Leucine-rich repeat	LRRC40	32	32	602	1.217	0.81026	8.20E+09
Q8N3C0;Q8N3C0-4	Q8N3C0	Activating signal co	ASCC3	38	38	2202	1.2155	0.85178	2.50E+09
Q5T9A4;Q5T9A4-3	Q5T9A4;Q5T9A4-3	ATPase family AAA	ATAD3B	26	5	648	1.2151	0.90891	3.75E+08
Q12765;Q12765-2	Q12765;Q12765-2	Secernin-1	SCRN1	4	4	414	1.2148	1.1688	3.44E+08
Q7LBC6;Q7LBC6-2;	Q7LBC6;Q7LBC6-2	Lysine-specific dem	KDM3B	8	8	1761	1.2144	0.65233	1.73E+08
Q07666-2;Q07666	Q07666-2;Q07666	KH domain-contair	KHDRBS1	5	5	418	1.2141	1.0542	2.68E+08
P35249;C9JZI1;P3	P35249;C9JZI1;P3	Replication factor C	RFC4	17	17	363	1.2134	0.70935	2.21E+09
Q96JC1-2;Q96JC1	Q96JC1-2;Q96JC1	Vam6/Vps39-like p	VPS39	4	4	875	1.2127	0.63344	1.87E+08
Q9NZL9-4;Q9NZL9	Q9NZL9-4;Q9NZL9	Methionine adenos	MAT2B	6	6	306	1.2114	1.0614	5.71E+08
O95487-2;O95487	O95487-2;O95487	Protein transport p	SEC24B	16	16	1233	1.2102	0.74197	8.47E+08
A0A0A6YYL4;P577	A0A0A6YYL4;P577	Coronin-7	CORO7	15	15	1048	1.209	0.8499	8.92E+08
P58557;P58557-2;	P58557;P58557-2	Putative ribonucle	YBEY	4	4	167	1.2079	0.68676	9.37E+07
P52701;P52701-3;	P52701;P52701-3	DNA mismatch rep	MSH6	38	38	1360	1.2078	0.79879	5.59E+09
Q9Y2W1	Q9Y2W1	Thyroid hormone r	THRAP3	1	1	955	1.2078	NaN	2.52E+07
J3QLR8	J3QLR8		MRPS23	9	1	152	1.2076	0.6061	6.38E+08
Q92547	Q92547	DNA topoisomeras	TOPBP1	10	10	1522	1.2071	0.51711	1.19E+08
F8W9X7;Q567U6;I	F8W9X7;Q567U6	Coiled-coil domain	CCDC93	6	6	630	1.2069	0.87386	2.48E+08
Q9NW08;Q9NW08	Q9NW08;Q9NW08	DNA-directed RNA	POLR3B	15	15	1133	1.205	0.74894	1.12E+09
P62699	P62699	Protein yippee-like	YPEL5	3	3	121	1.2044	0.80412	5.23E+07
O60884;I3L320;A0	O60884	DnaJ homolog subf	DNAJA2	14	14	412	1.2041	0.7123	3.18E+09
P35658-2;P35658	P35658-2;P35658	Nuclear pore comp	NUP214	18	18	2079	1.2037	0.59807	1.04E+09
E9PC69;Q7KZI7-12	E9PC69;Q7KZI7-12	Serine/threonine-p	MARK2	9	6	778	1.2033	0.58337	1.50E+08
Q7Z5K2;Q7Z5K2-2;	Q7Z5K2;Q7Z5K2-2	Wings apart-like pr	WAPAL	19	19	1190	1.2025	0.60493	1.28E+09
P23378	P23378	Glycine dehydroge	GLDC	2	2	1020	1.2016	NaN	6.88E+07
Q9NX20;E9PI14	Q9NX20	39S ribosomal prot	MRPL16	9	9	251	1.2012	0.79718	2.71E+08
A0A024R4N9;Q9B	A0A024R4N9;Q9B	tRNA-splicing endo	TSEN34	4	4	310	1.2009	0.8036	2.38E+08
Q7L3T8	Q7L3T8	Probable proline--t	PARS2	4	4	475	1.1995	1.2078	2.07E+08
P24666;G5E9R5;P	P24666;G5E9R5;P	Low molecular wei	ACP1	8	8	158	1.1994	0.68467	4.93E+09
Q9Y619;Q5VZD9;F	Q9Y619;Q5VZD9	Mitochondrial orni	SLC25A15	6	6	301	1.1994	0.75601	2.71E+08
P22830;P22830-2;	P22830;P22830-2	Ferrochelatase, mit	FECH	12	12	423	1.1992	0.66309	7.22E+08
P40937;P40937-2;	P40937;P40937-2	Replication factor C	RFC5	15	15	340	1.1991	0.70932	3.70E+09
P21964-2;P21964;	P21964-2;P21964	Catechol O-methyl	COMT	13	13	221	1.1985	0.66854	1.21E+09
Q92620;Q92620-2	Q92620	Pre-mRNA-splicing	DHX38	14	14	1227	1.1984	0.8055	6.63E+08
O75616;J3QSB2;J3	O75616;J3QSB2;J3	GTPase Era, mitoch	ERAL1	7	7	437	1.1983	0.72437	5.25E+08
Q9BU02;G3V5B9;C	Q9BU02;G3V5B9;C	Thiamine-triphospl	THTPA	2	2	230	1.1981	0.96477	1.64E+08
Q9C0D5-2;Q9C0D5	Q9C0D5-2;Q9C0D5	Protein TANC1	TANC1	8	8	1755	1.1978	0.80227	2.50E+08
Q969S9-3;Q969S9;	Q969S9-3;Q969S9	Ribosome-releasing	GFM2	6	6	777	1.1972	0.80651	1.70E+08

A0A087WWP4;Q9I	A0A087WWP4;Q9	Putative RNA-bindi	RBM15	11	11	933	1.1968	0.72648	4.70E+08
P49720;A0A087W	P49720;A0A087W	Proteasome subuni	PSMB3	6	6	205	1.1968	0.80489	3.17E+08
P49914;A0A0A6YY	P49914;A0A0A6YY	5-formyltetrahydrc	MTHFS	4	4	203	1.1968	NaN	8.98E+07
O60783	O60783	28S ribosomal prot	MRPS14	3	3	128	1.1967	0.90129	4.50E+08
H3BPE1;H3BQK9;C	H3BPE1;H3BQK9;C	Microtubule-actin	MACF1	3	2	7555	1.1961	NaN	2.53E+07
Q9NVV4-2;Q9NVV4	Q9NVV4-2;Q9NVV4	Poly(A) RNA polym	MTPAP	8	8	712	1.1949	0.69573	5.22E+08
Q13263;Q13263-2	Q13263;Q13263-2	Transcription inter	TRIM28	32	32	835	1.1936	0.63889	1.43E+10
Q9NX24;D6RC52;[	Q9NX24;D6RC52;[	H/ACA ribonucleop	NHP2	5	5	153	1.1935	0.75664	2.72E+08
Q9NZC9;H7BYI2;H	Q9NZC9;H7BYI2	SWI/SNF-related m	SMARCAL1	4	4	954	1.1935	0.59847	6.60E+07
Q9UNE7;Q9UNE7-2	Q9UNE7;Q9UNE7-2	E3 ubiquitin-protei	STUB1	14	14	303	1.1934	0.92427	1.84E+09
P51398-2;P51398	P51398-2;P51398	28S ribosomal prot	DAP3	10	10	357	1.1932	0.77789	1.51E+09
O15067;H0YGH1;J	O15067	Phosphoribosylfor	PFAS	46	46	1338	1.1931	0.72663	1.39E+10
Q9NYU2-2;Q9NYU2	Q9NYU2-2;Q9NYU2	UDP-glucose:glyco	UGGT1	8	8	1531	1.1928	0.82512	2.22E+08
O14617;O14617-5	O14617;O14617-5	AP-3 complex subu	AP3D1	30	30	1153	1.1923	0.66333	2.72E+09
Q9NUU7;I3L0H8;C	Q9NUU7;I3L0H8;C	ATP-dependent RN	DDX19A;DDX19B	23	3	478	1.1913	0.78525	5.17E+09
Q96MX6-2;Q96MX	Q96MX6-2;Q96MX	WD repeat-contain	WDR92	3	3	288	1.1907	0.9029	1.33E+08
O75419-2;O75419	O75419-2;O75419	Cell division contro	CDC45	14	14	520	1.1898	0.72592	7.91E+08
Q96ST3	Q96ST3	Paired amphipathi	SIN3A	6	6	1273	1.1897	0.94304	1.84E+08
E7EVX8;Q8WWY3;I	E7EVX8;Q8WWY3;I	U4/U6 small nuclea	PRPF31	11	11	493	1.1886	0.7721	1.07E+09
P11908;P11908-2;	P11908;P11908-2	Ribose-phosphate p	PRPS2	19	7	318	1.1886	0.74406	2.26E+09
Q9Y224;G3V4C6;G	Q9Y224;G3V4C6	UPF0568 protein C	C14orf166	4	4	244	1.1879	0.91089	4.49E+08
P31749-2;P31749;	P31749-2;P31749	RAC-alpha serine/th	AKT1	4	4	418	1.1877	0.8113	1.62E+08
O00443;A0A0C4D(	O00443	Phosphatidylinosit	PIK3C2A	24	24	1686	1.1872	0.94118	9.54E+08
E9PC74;Q13144;C	E9PC74;Q13144	Translation initiati	EIF2B5	4	4	705	1.1871	0.69959	4.76E+08
Q9H6R0;I3L1L6;Q	Q9H6R0;I3L1L6;Q	Putative ATP-deper	DHX33	4	4	707	1.1867	0.87973	2.19E+08
O00425;O00425-2	O00425	Insulin-like growth	IGF2BP3	24	20	579	1.1866	0.89545	2.57E+09
P49137;P49137-2	P49137;P49137-2	MAP kinase-activat	MAPKAPK2	4	4	400	1.1866	0.85757	9.33E+07
Q6L8Q7;Q6L8Q7-2	Q6L8Q7;Q6L8Q7-2	2,5-phosphodieste	PDE12	13	13	609	1.1859	0.77675	2.63E+09
Q9BW92;U3KQG0;	Q9BW92;U3KQG0;	Threonine--tRNA lig	TARS2	13	13	718	1.1859	0.76331	9.03E+08
Q99683;Q99683-2	Q99683;Q99683-2	Mitogen-activated	MAP3K5	2	2	1374	1.1858	NaN	4.95E+07
F5GYN4;J3KR44;Q	F5GYN4;J3KR44;Q	Ubiquitin thioester	OTUB1	10	10	241	1.1857	0.92016	1.33E+10
Q9Y4E8-2;Q9Y4E8	Q9Y4E8-2;Q9Y4E8	Ubiquitin carboxyl	USP15	4	3	952	1.1856	0.86631	1.52E+08
Q5SQP8;P56545;P	Q5SQP8;P56545;P	C-terminal-binding	CTBP2	16	11	513	1.1853	0.75269	4.23E+09
Q8WXE1-5;Q8WXE	Q8WXE1-5;Q8WXE	ATR-interacting prc	ATRIP	2	2	664	1.1847	NaN	7.38E+08
Q15424-2;Q15424	Q15424-2;Q15424	Scaffold attachmen	SAFB	2	2	848	1.1843	0.88539	3.88E+07
M0QXB5;O95571;I	M0QXB5;O95571;I	Persulfide dioxyger	ETHE1	2	2	260	1.1842	NaN	1.47E+08
O00273-2;O00273	O00273-2;O00273	DNA fragmentation	DFFA	4	4	268	1.1836	0.84546	4.14E+08
P35998;P35998-2;	P35998;P35998-2	26S protease regul	PSMC2	30	30	433	1.1833	0.76668	1.28E+10
Q8NE71-2;Q8NE71	Q8NE71-2;Q8NE71	ATP-binding casset	ABCF1	18	18	807	1.183	1.0517	1.12E+09
Q14181;E9PIQ6;Q	Q14181;E9PIQ6;Q	DNA polymerase al	POLA2	4	4	598	1.1814	0.81666	2.65E+08
Q99613-2;Q99613	Q99613-2;Q99613	Eukaryotic translat	EIF3C;EIF3CL	34	34	903	1.1813	0.82404	9.33E+09
P12004	P12004	Proliferating cell nu	PCNA	17	17	261	1.1811	0.80929	2.51E+10
Q14315-2;Q14315	Q14315-2;Q14315	Filamin-C	FLNC	59	53	2692	1.1809	0.88798	3.48E+09
Q15365;H3BSP4;C	Q15365	Poly(rC)-binding pr	PCBP1	17	12	356	1.1808	0.74598	7.64E+09
P15104;A0A087W	P15104	Glutamine synthet	GLUL	4	4	373	1.1795	1.2786	6.15E+07
O75592-2;O75592	O75592-2;O75592	E3 ubiquitin-protei	MYCBP2	29	29	4637	1.1793	0.74346	9.05E+08
P68371;M0R2D3;I	P68371	Tubulin beta-4B ch	TUBB4B	34	1	445	1.1789	0.84383	2.61E+11
P29372-5;P29372	P29372-5;P29372	DNA-3-methyladen	MPG	7	7	281	1.1787	0.67654	1.73E+09
F5GX99;H0YGM0;(	F5GX99;H0YGM0;(	Caseinolytic peptid	CLPB	4	4	501	1.1786	0.85017	2.36E+08
Q9BY44-3;Q9BY44	Q9BY44-3;Q9BY44	Eukaryotic translat	EIF2A	17	17	560	1.1786	0.71555	2.87E+09
Q01780;Q01780-2	Q01780;Q01780-2	Exosome compone	EXOSC10	23	23	885	1.1784	0.8036	2.09E+09
Q13217;X6R9L0	Q13217;X6R9L0	DnaJ homolog subf	DNAJC3	6	6	504	1.1782	0.74396	6.68E+08
Q9GZT3-2;Q9GZT3	Q9GZT3-2;Q9GZT3	SRA stem-loop-inte	SLIRP	10	10	107	1.1776	0.75551	8.25E+08
P05198;G3V4T5;H	P05198;G3V4T5;H	Eukaryotic translat	EIF2S1	28	28	315	1.1775	0.7821	1.12E+10
A0A0U1RRM1;Q8V	A0A0U1RRM1;Q8V	Transcriptional rep	GATAD2B	7	6	577	1.1773	0.61387	5.20E+08
B4DHE8;Q96DH6-2	B4DHE8;Q96DH6-2	RNA-binding protei	IGSF9B;MSI2	8	7	324	1.1765	0.80028	1.46E+09
G5E9S8;G3V2E7;F8	G5E9S8;G3V2E7;F8	Kinesin light chain	KLC1	2	2	549	1.1748	0.86704	6.79E+07
P31323	P31323	cAMP-dependent p	PRKAR2B	6	4	418	1.1747	1.0266	1.63E+08
Q8NFW8;Q8NFW8	Q8NFW8;Q8NFW8	N-acylneuraminate	CMAS	11	11	434	1.1744	0.69464	1.37E+09
Q86WA6-2;Q86WA	Q86WA6-2;Q86WA	Valacyclovir hydrol	BPHL	2	2	274	1.1737	0.60001	1.33E+08
O60488-2;O60488	O60488-2;O60488	Long-chain-fatty-ac	ACSL4	16	14	670	1.1736	0.70016	9.52E+08
Q96I25;Q5W011;C	Q96I25;Q5W011;C	Splicing factor 45	RBM17	6	6	401	1.1733	0.53966	1.05E+08
Q2TAL8	Q2TAL8	Glutamine-rich pro	QRICH1	7	7	776	1.173	0.94494	2.85E+08
P13807-2;P13807;	P13807-2;P13807	Glycogen [starch] s	GYS1	12	12	673	1.1728	0.7714	1.91E+09
S4R468;Q8NE86-3;	S4R468;Q8NE86-3	Calcium uniporter	MCU	1	1	167	1.1712	NaN	4.82E+07
Q8TDX7;F5H3U7;F	Q8TDX7	Serine/threonine-p	NEK7	3	3	302	1.1711	0.74115	2.56E+08
A0A087X2I1;P623	A0A087X2I1;P623	26S protease regul	PSMC6	24	24	403	1.1706	0.85199	7.83E+09
Q86VV8-4;Q86VV8	Q86VV8-4;Q86VV8	Rotatin	RTTN	4	4	879	1.1703	1.1811	3.33E+08
Q8IVS2;Q8IVS2-2	Q8IVS2;Q8IVS2-2	Malonyl-CoA-acyl c	MCAT	5	5	390	1.1701	0.63362	2.13E+08
Q9UKG1;C9JAB0;C	Q9UKG1	DCC-interacting pr	APPL1	11	11	709	1.17	0.86033	7.83E+08
Q5SY16	Q5SY16	Polynucleotide 5-h	NOL9	10	10	702	1.1698	0.85185	9.44E+08
Q00577	Q00577	Transcriptional act	PURA	3	3	322	1.1697	0.89773	8.23E+08
Q8IU81	Q8IU81	Interferon regulato	IRF2BP1	3	3	584	1.1694	1.2547	3.05E+08
A0A0G2JIS2;Q96K(	A0A0G2JIS2;Q96K(	Histone-lysine N-m	EHMT2	3	3	1176	1.1691	NaN	1.21E+08
F5GWX5;A0A0C4D	F5GWX5;A0A0C4D	Chromodomain-he	CHD4	47	40	1905	1.1678	0.81295	4.90E+09
P14174	P14174	Macrophage migra	MIF	4	4	115	1.1677	0.54733	3.29E+09
Q8TD30;H3BU54;(	Q8TD30	Alanine aminotran	GPT2	3	3	523	1.1662	NaN	7.90E+07
O95163;F5H2T0;H	O95163;F5H2T0	Elongator complex	IKBKAP	34	34	1332	1.1661	0.91135	4.95E+09
P25205;P25205-2;	P25205;P25205-2	DNA replication lic	MCM3	49	49	808	1.1659	0.77266	1.20E+10
A0A0D9SF63;Q9BZ	A0A0D9SF63;Q9BZ	F-box-like/WD repe	TBL1XR1;TBL1Y;TBI	6	6	474	1.1655	0.81284	2.46E+08
E9PIF2;Q13206	E9PIF2;Q13206	Probable ATP-depe	DDX10	10	10	835	1.165	0.91445	3.66E+08
H7C441;C9JXG5;F8	H7C441;C9JXG5;F8	THO complex subu	THOC5	4	4	176	1.1646	1.0512	9.58E+07
P62269;A0A0G2JC	P62269	40S ribosomal prot	RPS18	22	22	152	1.1645	0.93051	6.91E+09
A8MQ02;F8W9I4;E	A8MQ02		MLLT4	14	1	1781	1.1636	0.57867	4.85E+08
Q969Y2-3;Q969Y2;	Q969Y2-3;Q969Y2	tRNA modification	GTPBP3	2	2	471	1.1635	1.0644	8.99E+07
Q9NQW7-3;Q5T6H	Q9NQW7-3;Q5T6H	Xaa-Pro aminopept	XPNPEP1	4	4	666	1.1631	1.4389	3.83E+08
P60983;G3V4P8;G	P60983;G3V4P8	Glia maturation fac	GMFB	7	7	142	1.1625	1.6763	2.44E+08
O75400-2;O75400	O75400-2;O75400	Pre-mRNA-processi	PRPF40A	5	5	930	1.1624	0.51665	2.77E+08
P56937-3;P56937	P56937-3;P56937	3-keto-steroid redu	HSD17B7	3	3	306	1.1622	0.79093	2.30E+08
A0A0C4DG89;Q7L(	A0A0C4DG89;Q7L(	Probable ATP-depe	DDX46	33	33	1032	1.1621	0.77626	2.60E+09
B1AK87;B1AK88;P	B1AK87;B1AK88;P	F-actin-capping pro	CAPZB	6	6	260	1.162	1.3815	6.18E+08
Q8TD19;G3V459;G	Q8TD19	Serine/threonine-p	NEK9	17	17	979	1.1616	0.81979	1.82E+09
Q14980-2;Q14980	Q14980-2;Q14980	Nuclear mitotic ap	NUMA1	8	8	2101	1.1614	1.2365	1.57E+08

Q7Z4H3-2;Q7Z4H3	Q7Z4H3-2;Q7Z4H3	HD domain-contair	HDDC2	10	10	170	1.1607	0.84884	1.06E+09
Q9Y266;A0A0A0M	Q9Y266	Nuclear migration	NUDC	21	21	331	1.1605	0.94783	2.06E+09
Q5SNT2;H0Y4R5;Q	Q5SNT2;H0Y4R5;Q	Transmembrane pr	TMEM201	3	3	666	1.1604	1.0704	1.05E+08
P36542;P36542-2	P36542;P36542-2	ATP synthase subur	ATP5C1	12	12	298	1.1596	0.81723	4.20E+09
Q9NP77;Q9NP77-2	Q9NP77;Q9NP77-2	RNA polymerase II s	SSU72	7	7	194	1.1587	0.73928	4.26E+08
P58107;A0A075B7	P58107;A0A075B7	Epiplakin	EPPK1	35	29	5090	1.1586	0.86789	1.01E+09
K7EQL6;Q8NFA0;K	K7EQL6;Q8NFA0	Ubiquitin carboxyl	USP32	4	4	1274	1.1585	0.87881	4.22E+07
K7EM18;P41567;C	K7EM18;P41567;C	Eukaryotic translat	EIF1;EIF1B	4	4	121	1.1584	0.80967	9.78E+07
O15235	O15235	28S ribosomal prot	MRPS12	3	3	138	1.1582	0.52995	3.83E+07
Q14103-3;Q14103	Q14103-3;Q14103	Heterogeneous nuc	HNRNPD	21	4	306	1.1564	0.97817	2.48E+10
Q9Y5Q9;Q9Y5Q9-2	Q9Y5Q9	General transcripti	GTF3C3	12	12	886	1.156	0.70412	1.17E+09
P33992;B1AHB1;B	P33992;B1AHB1	DNA replication lic	MCM5	46	46	734	1.155	0.73472	1.44E+10
O00458;O00458-2	O00458;O00458-2	Interferon-related	IFRD1	4	4	451	1.1549	0.84164	2.74E+08
F8W925;Q8NFI3-2	F8W925;Q8NFI3-2	Cytosolic endo-bet	ENGASE	2	2	365	1.1547	0.9139	8.70E+07
P24534;C9JZW3;F	P24534	Elongation factor 1	EEF1B2	13	11	225	1.1545	0.95917	1.10E+10
O94966-4;O94966	O94966-4;O94966	Ubiquitin carboxyl	USP19	10	10	1268	1.1542	0.58238	5.17E+08
P12956;B1AHC9;P	P12956;B1AHC9;P	X-ray repair cross-c	XRCC6	47	47	609	1.154	0.99072	3.44E+10
Q6PD62;H0YCE8	Q6PD62	RNA polymerase-as	CTR9	12	12	1173	1.1536	0.66678	9.60E+08
Q9BVC3	Q9BVC3	Sister chromatid cc	DSCC1	2	2	393	1.1527	0.8211	9.05E+07
P62273;A0A087W	P62273;A0A087W	40S ribosomal prot	RPS29	3	3	56	1.1522	1.1212	1.05E+09
Q9Y4W6;K7EP56	Q9Y4W6	AFG3-like protein 2	AFG3L2	19	18	797	1.1519	0.77218	1.87E+09
Q8IWV8-4;Q8IWV8	Q8IWV8-4;Q8IWV8	E3 ubiquitin-protei	UBR2	16	16	1755	1.1515	0.68761	4.35E+08
Q71U36-2;Q71U36	Q71U36-2;Q71U36	Tubulin alpha-1A cl	TUBA1A;TUBA3C	34	1	416	1.1512	0.8769	8.75E+08
Q5T9B7;P00568;H	Q5T9B7;P00568;H	Adenylate kinase is	AK1	6	6	210	1.1499	0.89545	2.70E+08
P62263;H0YB22;E	P62263;H0YB22;E	40S ribosomal prot	RPS14	11	11	151	1.1494	0.7611	8.72E+09
P47813;O14602;X	P47813;O14602;X	Eukaryotic translat	EIF1AX;EIF1AY	6	6	144	1.1487	0.83885	5.72E+08
Q5TG40;Q9NPF5;C	Q5TG40;Q9NPF5;C	DNA methyltransfe	DMAP1	4	4	302	1.1483	0.81915	1.74E+08
O43347;H0YHB7	O43347	RNA-binding protei	MSI1	9	8	362	1.1482	0.81688	1.59E+09
Q9Y5A9;A0A087W	Q9Y5A9;A0A087W	YTH domain-contai	YTHDF2	13	10	579	1.1475	0.68947	1.76E+09
Q12906;Q12906-7	Q12906;Q12906-7	Interleukin enhanc	ILF3	29	25	894	1.147	0.79997	7.30E+09
O60318;O60318-2	O60318	Germinal-center as	MCM3AP	18	18	1980	1.1464	0.47686	8.49E+08
O75190;A0A0J9YX	O75190;A0A0J9YX	DnaJ homolog subf	DNAJB6	10	9	326	1.1464	0.65855	8.88E+08
P17655;P17655-2	P17655;P17655-2	Calpain-2 catalytic	CAPN2	12	12	700	1.1463	0.92544	6.60E+08
P33993;P33993-3;	P33993;P33993-3	DNA replication lic	MCM7	43	43	719	1.146	0.70821	2.11E+10
Q13242;H0YIB4;S4	Q13242;H0YIB4;S4	Serine/arginine-ricl	SRSF9	5	5	221	1.1456	0.87907	6.20E+08
Q8NHU6-2;Q8NHU	Q8NHU6-2;Q8NHU	Tudor domain-con	TDRD7	4	4	1024	1.1452	NaN	3.11E+07
Q9P253;H0YMC9;I	Q9P253	Vacuolar protein sc	VPS18	4	4	973	1.145	0.68916	1.32E+08
O60231;A0A140T9	O60231;A0A140T9	Putative pre-mRNA	DHX16	18	17	1041	1.1448	1.001	6.87E+08
O15379;O15379-2	O15379;O15379-2	Histone deacetylas	HDAC3	4	3	428	1.1447	0.71763	1.42E+08
O75934	O75934	Pre-mRNA-splicing	BCAS2	3	3	225	1.1443	1.1713	2.88E+08
Q13642-1;Q13642	Q13642-1;Q13642	Four and a half LIM	FHL1	8	8	280	1.144	0.84199	1.06E+09
Q96I59;H0YEL9;E9	Q96I59;H0YEL9;E9	Probable asparagin	NARS2	8	8	477	1.1434	0.81327	1.15E+09
A0A087WV66;P46	A0A087WV66;P46	Antigen KI-67	MKI67	4	4	3255	1.1417	1.0244	9.64E+07
Q9BTY7;E9PIX0	Q9BTY7	Protein HGH1 hom	HGH1	6	6	390	1.1416	0.86214	3.91E+08
Q9NR45;Q5TBR0;C	Q9NR45	Sialic acid synthase	NANS	13	13	359	1.1416	0.9697	3.80E+09
Q14258	Q14258	E3 ubiquitin/ISG15	TRIM25	12	12	630	1.1415	0.7631	1.10E+09
O60684;Q5TFJ7;S4	O60684;Q5TFJ7	Importin subunit a	KPNA6	12	4	536	1.1413	0.75153	9.58E+08
G5E9C8;Q07889;A	G5E9C8;Q07889	Son of sevenless ho	SOS1	3	3	1318	1.1412	0.82991	4.47E+07
Q9Y316-2;Q9Y316	Q9Y316-2;Q9Y316	Protein MEMO1	MEMO1	8	8	274	1.141	0.77156	1.62E+09
P51114-2;P51114	P51114-2;P51114	Fragile X mental ret	FXR1	16	14	539	1.1407	0.87255	1.87E+09
A6NHR9;A6NHR9-2	A6NHR9;A6NHR9-2	Structural mainten	SMCHD1	34	34	2005	1.1403	0.88446	2.17E+09
E9PDQ5;B1ALK7;Q	E9PDQ5;B1ALK7;Q	Rho guanine nucle	ARHGEF7;ARHGEF6	2	2	547	1.1403	0.93215	1.23E+08
P61011;P61011-2;	P61011;P61011-2;	Signal recognition	SRP54	24	24	504	1.1403	0.93996	3.02E+09
P14618;P14618-3;	P14618;P14618-3;	Pyruvate kinase PK	PKM	54	5	531	1.1401	0.84363	1.38E+11
Q9BRA2;I3L2R6;I3	Q9BRA2;I3L2R6	Thioredoxin domai	TXNDC17	6	6	123	1.1383	0.89345	2.04E+09
Q9HBH5	Q9HBH5	Retinol dehydroger	RDH14	4	4	336	1.1374	0.86261	2.29E+08
P17812;P17812-2	P17812;P17812-2	CTP synthase 1	CTPS1	33	29	591	1.1369	0.77619	1.05E+10
Q9HC35;B5MBZ0;(	Q9HC35;B5MBZ0;(	Echinoderm microt	EML4	23	23	981	1.1367	0.78837	9.90E+08
Q9UPR3	Q9UPR3	Protein SMG5	SMG5	3	3	1016	1.1365	NaN	5.94E+07
Q14690;S4R3Q4	Q14690	Protein RRP5 hom	PDCD11	56	56	1871	1.1361	0.90697	6.21E+09
Q02978;I3L1P8;Q(	Q02978;I3L1P8;Q(	Mitochondrial 2-o	SLC25A11	18	18	314	1.1352	0.77131	1.61E+10
A0A140T962;A0A1	A0A140T962;A0A1	HLA class I histocor	HLA-C;HLA-B;HLA-I	4	4	368	1.1345	0.86429	4.23E+08
P46199;H7C213	P46199;H7C213	Translation initiati	MTIF2	4	4	727	1.1341	0.8482	3.08E+08
E7EX90;Q14203-3;	E7EX90;Q14203-3;	Dynactin subunit 1	DCTN1;DKFZp686E	47	47	1256	1.1335	0.76888	4.50E+09
Q9Y4W2-2;Q9Y4W	Q9Y4W2-2;Q9Y4W	Ribosomal biogene	LAS1L	10	10	717	1.1328	0.92928	1.68E+09
H7C1N3;O15155;(	H7C1N3;O15155;(	BET1 homolog	BET1;DKFZp781C0	2	2	133	1.1324	0.9774	2.50E+07
Q9BZX2;Q9BZX2-2	Q9BZX2	Uridine-cytidine ki	UCK2	7	7	261	1.1324	0.79847	1.74E+09
Q9BQC3;E9PLL2;E9	Q9BQC3;E9PLL2;E9	Diphthamide biosy	DPH2	2	2	489	1.1323	0.85452	1.92E+08
Q9Y2X0-2;Q9Y2X0	Q9Y2X0-2;Q9Y2X0	Mediator of RNA pc	MED16	3	3	841	1.1314	0.85249	2.81E+08
Q9Y285;K7ER00;Q	Q9Y285;K7ER00;Q	Phenylalanine--tRN	FARSA	21	21	508	1.1313	0.84587	4.27E+09
P35659;D6R9L5;B	P35659;D6R9L5;B	Protein DEK	DEK	3	3	375	1.1304	1.2923	1.84E+08
Q96C36;A0A087W	Q96C36;A0A087W	Pyrroline-5-carbox	PYCR2	17	16	320	1.1303	0.75089	5.51E+09
P46821;D6RA40;D	P46821	Microtubule-associ	MAP1B	9	9	2468	1.1294	1.0815	8.65E+08
Q9BUK6-3;Q9BUK	Q9BUK6-3;Q9BUK	Protein misato hon	MSTO1	9	8	558	1.1294	0.72418	5.32E+08
Q9UKN8;F2Z356	Q9UKN8	General transcripti	GTF3C4	16	16	822	1.1287	0.77245	1.41E+09
R4GNB1;Q4L235-3	R4GNB1;Q4L235-3	Acyl-CoA synthetas	AASDH	2	2	945	1.1282	0.64311	7.54E+07
P07384;E9PL37;E9	P07384	Calpain-1 catalytic	CAPN1	7	7	714	1.1273	1.0121	4.32E+08
Q13572;G3V4M9;(	Q13572;G3V4M9;(	Inositol-tetrakisph	ITPK1	3	3	414	1.1273	1.0559	1.82E+08
H0YM23;O75179-7	H0YM23;O75179-7	Ankyrin repeat dor	ANKRD17	22	11	2487	1.1266	0.8468	7.74E+08
I3L2Z9;I3L100;I3L	I3L2Z9;I3L100;I3L	Neuralized-like pro	NEURL4	2	2	1017	1.1266	0.59663	4.43E+07
Q9NVP1;H7C452	Q9NVP1	ATP-dependent RN	DDX18	12	12	670	1.1257	0.89523	7.78E+08
D3YTB5;P51617-2;	D3YTB5;P51617-2;	Interleukin-1 recep	IRAK1	10	10	708	1.1253	0.78971	1.34E+09
P50402;Q5HY57;F	P50402;Q5HY57	Emerin	EMD	15	15	254	1.1251	0.71696	2.04E+09
Q9UDY2-5;Q9UDY	Q9UDY2-5;Q9UDY	Tight junction prot	TJP2	2	2	993	1.1248	NaN	4.89E+07
Q14558-2;Q14558	Q14558-2;Q14558	Phosphoribosyl py	PRPSAP1	11	9	385	1.1244	0.92292	4.15E+09
Q5VUJ6-2;Q5VUJ6	Q5VUJ6-2;Q5VUJ6	Leucine-rich repeat	LRCH2	6	6	748	1.1244	0.72925	1.96E+08
E9PGC0;P20936-2;	E9PGC0;P20936-2;	Ras GTPase-activati	RASA1	6	6	881	1.1239	0.87944	1.74E+08
A0A0C4DFR8;Q9UI	A0A0C4DFR8;Q9UI	Protein UXT	UXT	2	2	169	1.1231	1.2429	6.70E+07
Q9NQT5;Q9NQT5-2	Q9NQT5;Q9NQT5-2	Exosome complex	EXOSC3	9	9	275	1.1229	0.87342	2.94E+09
Q9BUQ8;H0YI52;F	Q9BUQ8	Probable ATP-depe	DDX23	18	18	820	1.1226	0.82218	1.26E+09
Q13148;B1AKP7;G	Q13148;B1AKP7;G	TAR DNA-binding p	TARDBP	12	12	414	1.1225	0.82701	4.38E+09
H0Y8R1;F5H5I6;H(	H0Y8R1;F5H5I6;H(	G-rich sequence fac	GRSF1	13	13	417	1.1219	0.82337	9.22E+08
Q5JP53;P07437;Q	Q5JP53;P07437;Q	Tubulin beta chain	TUBB	32	5	426	1.1219	0.91827	1.03E+11

P42166	P42166	Lamina-associated	TMPO	3	3	694	1.1217	0.88374	2.07E+08
P49721;A0A087W	P49721	Proteasome subuni	PSMB2	7	7	201	1.1214	0.82187	2.80E+08
H3BTB7;Q5JPH6;Q	H3BTB7;Q5JPH6;Q	Probable glutamat	EARS2	5	5	506	1.1213	0.47041	5.26E+08
P53350;I3L387;I3I	P53350	Serine/threonine-p	PLK1	10	10	603	1.1212	0.44932	4.70E+08
J3QRV5;Q6P1M3-2	J3QRV5;Q6P1M3-2	Lethal(2) giant larv	SPATS2;LLGL2	2	2	1019	1.1209	NaN	9.60E+06
O75569;O75569-3	O75569;O75569-3	Interferon-inducibl	PRKRA	9	9	313	1.1208	0.9462	9.03E+08
A6NDG6;H3BV17	A6NDG6	Phosphoglycolate p	PGP	10	10	321	1.12	0.75287	2.26E+09
P78417;Q5TA02;P	P78417;Q5TA02;P	Glutathione S-tran	GSTO1	10	10	241	1.1199	0.966	2.54E+09
O76071	O76071	Probable cytosolic	CIAO1	6	6	339	1.1189	0.78588	3.65E+08
P62829;C9JD32;J3	P62829;C9JD32;J3	60S ribosomal prot	RPL23	14	14	140	1.1187	0.87132	1.43E+10
E9PER6;O15530-4;	E9PER6;O15530-4;	3-phosphoinositid	PDPK1;PDPK2	2	2	529	1.1185	0.87377	1.99E+08
O95714;A0A0J9YV	O95714;A0A0J9YV	E3 ubiquitin-protei	HERC2	11	11	4834	1.1183	0.86958	1.54E+08
P78346;P78346-2;	P78346;P78346-2	Ribonuclease P pro	RPP30	11	11	268	1.1176	0.82452	3.25E+09
Q9H9T3-2;Q9H9T3	Q9H9T3-2;Q9H9T3	Elongator complex	ELP3	7	7	533	1.117	1.0559	4.48E+08
M0R300;M0R0P8;I	M0R300;M0R0P8;I	Unconventional m	MYO9B	10	10	2072	1.1169	0.83226	1.85E+08
O60244;H7C3E5;H	O60244	Mediator of RNA pc	MED14	12	12	1454	1.1157	0.78935	3.51E+08
Q8IY81	Q8IY81	pre-rRNA processin	FTSJ3	11	11	847	1.1154	0.72904	1.06E+09
K7EJE8;K7EKE6;P3I	K7EJE8;K7EKE6;P3I	Lon protease homc	LONP1	32	32	829	1.1142	0.8746	6.20E+09
P49792;F8VYC4;PC	P49792	E3 SUMO-protein li	RANBP2	76	55	3224	1.1133	0.79293	7.03E+09
P11940;P11940-2;	P11940;P11940-2	Polyadenylate-binc	PABPC1	22	14	636	1.1131	0.8538	7.50E+09
A0A087WW77;Q1	A0A087WW77;Q1	Lethal(2) giant larv	LLGL1	16	16	1056	1.1122	0.79315	1.28E+09
P15170-2;P15170	P15170-2;P15170	Eukaryotic peptide	GSPT1	18	18	636	1.1121	0.83325	2.35E+09
Q93074-3;Q93074	Q93074-3;Q93074	Mediator of RNA pc	MED12;TNRC11	6	6	2176	1.1121	0.76385	1.33E+08
Q6PHR2-3;Q6PHR2	Q6PHR2-3;Q6PHR2	Serine/threonine-p	ULK3	6	6	470	1.1118	0.56844	2.90E+08
Q8WXX5	Q8WXX5	DnaJ homolog subf	DNAJC9	3	3	260	1.1116	0.58026	2.43E+08
P11498;E9PRE7;P1	P11498;E9PRE7;P1	Pyruvate carboxyla	PC	12	12	1178	1.1113	0.74706	6.06E+08
Q96L92-3;Q96L92;	Q96L92-3;Q96L92	Sorting nexin-27	SNX27	13	13	528	1.1111	0.80433	1.55E+09
P49711;P49711-2;	P49711;P49711-2	Transcriptional rep	CTCF	4	4	727	1.1108	1.0473	2.06E+08
Q99717;Q15797	Q99717;Q15797	Mothers against de	SMAD5;SMAD1	2	2	465	1.1108	0.54798	1.37E+08
B4DP61;E7EQZ4;Q	B4DP61;E7EQZ4;Q	Survival motor neu	SMN1	2	2	227	1.1105	1.0926	4.33E+08
Q01813;Q01813-2	Q01813;Q01813-2	ATP-dependent 6-p	PFKP	30	25	784	1.1104	0.83311	1.42E+10
P62995-3;P62995;	P62995-3;P62995	Transformer-2 prot	TRA2B	5	5	188	1.1096	1.0788	5.60E+08
P78316;E9PFK5;P7	P78316;E9PFK5;P7	Nucleolar protein 1	NOP14	13	13	857	1.1096	0.71025	4.41E+08
Q96DG6	Q96DG6	Carboxymethylene	CMBL	3	3	245	1.1091	0.88142	1.14E+08
P52948-5;P52948;	P52948-5;P52948	Nuclear pore comp	NUP98	18	18	1800	1.109	0.94086	1.41E+09
P68363;P68363-2	P68363;P68363-2	Tubulin alpha-1B cl	TUBA1B	34	0	451	1.1088	0.86795	2.61E+11
Q5JRI1;O75494-5;I	Q5JRI1;O75494-5;I	Serine/arginine-ricl	SRSF10	8	8	172	1.1084	0.83499	7.18E+08
F8WAS3;Q16718;C	F8WAS3;Q16718;C	NADH dehydrogena	NDUFA5	3	3	70	1.1078	NaN	1.69E+08
O95602;B9ZVN9	O95602;B9ZVN9	DNA-directed RNA	POLR1A	52	51	1720	1.1076	0.79364	3.63E+09
P17152	P17152	Transmembrane pr	TMEM11	3	3	192	1.1076	0.63023	3.14E+08
Q9H974-2;Q9H974	Q9H974-2;Q9H974	Queuine tRNA-ribo	QTRTD1	3	3	292	1.1076	1.1684	1.55E+08
P62873-2;P62873;	P62873-2;P62873	Guanine nucleotid	GNB1;GNB2	7	2	332	1.107	0.96826	1.26E+09
E9PK01;P29692;E9	E9PK01;P29692;E9	Elongation factor 1	EEF1D	12	0	261	1.1055	0.9371	1.90E+09
Q15072	Q15072	Zinc finger protein	ZNF146	3	3	292	1.1055	0.62597	3.57E+07
Q9Y2Q9;H0YAT2;H	Q9Y2Q9;H0YAT2;H	28S ribosomal prot	MRPS28	5	5	187	1.1054	0.89158	5.39E+08
Q15233;Q15233-2	Q15233;Q15233-2	Non-POU domain-c	NONO	39	33	471	1.1053	0.9814	1.32E+10
K7ERI7;P35268;K7	K7ERI7;P35268;K7	60S ribosomal prot	RPL22	9	7	95	1.1052	0.84238	5.93E+09
Q9Y5B9;G3V5A4;G	Q9Y5B9	FACT complex subu	SUPT16H	44	44	1047	1.1049	0.97432	1.34E+10
G5EA06;Q92552;Q	G5EA06;Q92552;Q	28S ribosomal prot	MRPS27	14	14	358	1.1048	0.91219	1.29E+09
Q9Y4B6-2;Q9Y4B6;	Q9Y4B6-2;Q9Y4B6	Protein VPRBP	VPRBP	17	17	1506	1.1047	0.94974	6.68E+08
Q5R3I4;H7C089;A9	Q5R3I4;H7C089	Tetratricopeptide r	TTC38	3	3	469	1.1043	0.52939	8.71E+07
Q9BXJ9;A0A0B4J1	Q9BXJ9;A0A0B4J1	N-alpha-acetyltran	NAA15	35	30	866	1.1042	0.91	4.12E+09
Q9NVI7-2;Q9NVI7;	Q9NVI7-2;Q9NVI7;	ATPase family AAA c	ATAD3A	33	11	586	1.1041	0.74732	8.23E+09
O43542;G3V3Q2;C	O43542;G3V3Q2	DNA repair protein	XRCC3	3	3	346	1.1039	0.51474	1.69E+08
O00483	O00483	Cytochrome c oxid	NDUFA4	4	4	81	1.1035	0.90694	4.79E+08
Q15056-2;Q15056	Q15056-2;Q15056	Eukaryotic translat	EIF4H	9	9	228	1.1031	0.99763	1.74E+09
P13674-3;P13674	P13674-3;P13674	Prolyl 4-hydroxylas	P4HA1	1	1	516	1.1029	NaN	4.07E+07
Q92990-2;Q92990	Q92990-2;Q92990	Glomulin	GLMN	2	2	417	1.1028	1.097	7.51E+07
Q9NTX5-6;Q9NTX5	Q9NTX5-6;Q9NTX5	Ethylmalonyl-CoA c	ECHDC1	9	9	284	1.1028	0.88109	1.95E+09
Q8NBM4;X6R5E5;(	Q8NBM4;X6R5E5;(	Ubiquitin-associate	UBAC2	4	4	344	1.1022	0.74111	1.99E+08
Q6NZY4;Q6NZY4-2;	Q6NZY4;Q6NZY4-2	Zinc finger CCHC do	ZCCHC8	6	6	707	1.1021	0.68482	4.80E+08
P46060;B0QYT5;B(	P46060	Ran GTPase-activat	RANGAP1	9	9	587	1.1016	1.0464	9.38E+08
Q8NEN9	Q8NEN9	PDZ domain-contai	PDZD8	5	5	1154	1.1011	0.6068	1.88E+08
Q8N122;Q8N122-3	Q8N122;Q8N122-3	Regulatory-associat	RPTOR	22	22	1335	1.1007	0.80248	1.68E+09
E7EMB1;Q9UH65;E	E7EMB1;Q9UH65	Switch-associated p	SWAP70	4	4	527	1.1004	1.0484	2.15E+08
Q86UV5;Q86UV5-3	Q86UV5;Q86UV5-3	Ubiquitin carboxyl	USP48	12	12	1035	1.1003	0.87908	6.88E+08
Q9BUJ2-2;Q9BUJ2;	Q9BUJ2-2;Q9BUJ2	Heterogeneous nuc	HNRNPUL1	18	18	804	1.0998	0.78572	1.75E+09
Q13310-2;Q13310	Q13310-2;Q13310	Polyadenylate-binc	PABPC4	15	7	631	1.0993	0.78757	6.17E+08
F5H658;Q14562	F5H658;Q14562	ATP-dependent RN	DHX8	6	5	1181	1.0989	1.0274	4.23E+08
P07737;K7EJ44;CC	P07737;K7EJ44	Profilin-1	PFN1	17	17	140	1.098	0.85064	3.86E+10
A2A274;Q99798	A2A274;Q99798	Aconitate hydratas	ACO2	6	6	805	1.0974	1.3117	6.14E+08
O94906;O94906-2	O94906;O94906-2	Pre-mRNA-processi	PRPF6	32	32	941	1.0971	0.86023	1.91E+09
Q8N9T8;H0YFD2;F	Q8N9T8;H0YFD2;F	Protein KRI1 homo	KRI1	4	4	703	1.0971	0.50039	7.74E+07
Q14240;Q14240-2	Q14240;Q14240-2	Eukaryotic initiatic	EIF4A2	19	3	407	1.0963	1.0056	1.27E+08
O60293-2;O60293	O60293-2;O60293	Zinc finger C3H1 do	ZFC3H1	5	5	1910	1.096	0.64198	9.33E+07
Q504Q3-2;Q504Q3	Q504Q3-2;Q504Q3	PAB-dependent pol	PAN2	6	6	1198	1.0958	0.6268	1.83E+08
F5H5N1;A0A087W	F5H5N1;A0A087W	NADH dehydrogena	NDUFS7	2	2	182	1.0953	1.1811	1.78E+08
Q9NV88-3;Q9NV88	Q9NV88-3;Q9NV88	Integrator complex	INTS9	4	4	634	1.0952	0.8611	2.24E+08
Q86W56-3;Q86W5	Q86W56-3;Q86W5	Poly(ADP-ribose) gl	PARG	4	4	868	1.0946	0.96474	1.19E+08
P62244;I3L3P7;I3I	P62244;I3L3P7;I3I	40S ribosomal prot	RPS15A	11	11	130	1.0945	0.86683	6.79E+09
Q6P1N0;Q6P1N0-2	Q6P1N0;Q6P1N0-2	Coiled-coil and C2 c	CC2D1A	11	11	951	1.0939	0.65351	3.73E+08
Q9Y2R4;A0A087X1	Q9Y2R4	Probable ATP-depe	DDX52	8	8	599	1.0938	0.91256	8.55E+08
Q9HBG6-11;Q9HB	Q9HBG6-11;Q9HB	Intraflagellar trans	IFT122	5	5	993	1.0935	0.6355	6.85E+07
Q9NVE7;A0A0G2JR	Q9NVE7;A0A0G2JR	Pantothenate kinas	PANK4	14	14	773	1.0928	0.92308	8.34E+08
P62906	P62906	60S ribosomal prot	RPL10A	16	16	217	1.0925	0.84001	9.00E+09
Q96J02-2;Q96J02;	Q96J02-2;Q96J02	E3 ubiquitin-protei	ITCH	12	12	862	1.0923	0.79036	4.83E+08
Q96ME1-4;Q96ME	Q96ME1-4;Q96ME	F-box/LRR-repeat p	FBXL18	10	10	718	1.0922	0.91112	6.02E+08
Q6NVU6	Q6NVU6	Inactive Ufm1-spec	UFSP1	2	2	142	1.0921	0.79526	2.67E+07
Q93009-3;Q93009	Q93009-3;Q93009	Ubiquitin carboxyl	USP7	26	26	1086	1.092	1.0191	2.34E+09
O95251-2;O95251	O95251-2;O95251	Histone acetyltrans	KAT7	4	4	501	1.0918	0.77905	1.83E+08
P67775-2;P67775;	P67775-2;P67775	Serine/threonine-p	PPP2CA;PPP2CB	7	5	255	1.0915	0.88011	5.08E+08
A0A087WU64;A6N	A0A087WU64;A6N	DNA polymerase;DI	POLA1	23	23	1461	1.0913	0.80934	1.62E+09
P24752;H0YEL7;P2	P24752	Acetyl-CoA acetyltr	ACAT1	22	22	427	1.0913	0.81658	7.59E+09

O60701;O60701-2	O60701;O60701-2	UDP-glucose 6-deh	UGDH	14	14	494	1.0904	0.89309	2.46E+09
Q9UII4;E9PBL0	Q9UII4;E9PBL0	E3 ISG15--protein l	HERC5	4	4	1024	1.0904	0.75753	1.71E+08
A0A0A0MRJ0;Q5V	A0A0A0MRJ0;Q5V	Serine/threonine-p	CDC42BPA	6	5	1699	1.0903	0.67561	1.32E+08
Q8TCD5;J3KRC4;J3	Q8TCD5;J3KRC4;J3	5(3)-deoxyribonucl	NT5C	7	7	201	1.0901	0.80155	1.80E+08
A0A087WUQ6;P07	A0A087WUQ6;P07	Glutathione peroxi	GPX1	2	2	202	1.0898	0.79777	5.30E+07
P43246;P43246-2;	P43246;P43246-2;	DNA mismatch rep	MSH2	32	32	934	1.0893	0.82234	4.08E+09
A0A0A0MQR2;Q9B	A0A0A0MQR2;Q9B	Protein RTF2 homc	RTFDC1	3	3	336	1.0892	0.52267	9.43E+07
Q14697;Q14697-2	Q14697;Q14697-2	Neutral alpha-gluc	GANAB	28	28	944	1.0886	0.96977	2.31E+09
Q00059;H7BYN3;C	Q00059;H7BYN3;C	Transcription facto	TFAM	3	3	246	1.0885	NaN	1.88E+07
P32322;E2QRB3;P	P32322;E2QRB3;P	Pyrroline-5-carbox	PYCR1	20	11	319	1.0884	0.79262	4.26E+09
P06730;P06730-2;	P06730;P06730-2;	Eukaryotic translat	EIF4E	7	7	217	1.0875	0.85689	3.24E+09
Q9BWF3;E9PB51;C	Q9BWF3;E9PB51;C	RNA-binding protei	RBM4	14	0	364	1.0874	1.0138	1.61E+09
Q7Z3K3-5;Q7Z3K3	Q7Z3K3-5;Q7Z3K3	Pogo transposable	POGZ	13	13	1315	1.0871	0.79695	8.15E+08
I6L894;Q01484;A0	I6L894;Q01484;A0	Ankyrin-2	ANK2	5	3	3924	1.0869	1.2173	6.50E+07
P60228;E5RGA2;H	P60228;E5RGA2;H	Eukaryotic translat	EIF3E	18	18	445	1.0868	0.95803	1.99E+09
Q96H79;Q96H79-2	Q96H79	Zinc finger CCCH-ty	ZC3HAV1L	8	8	300	1.0859	0.785	1.50E+09
P08238;Q58FF7	P08238	Heat shock protein	HSP90AB1	56	30	724	1.0858	1.0417	1.77E+11
P49756;P49756-2;	P49756;P49756-2;	RNA-binding protei	RBM25	8	8	843	1.0857	0.80819	4.24E+08
P55809;E9PDW2;F	P55809;E9PDW2;F	Succinyl-CoA:3-ket	OXCT1	10	10	520	1.0856	0.78455	5.57E+08
Q2TAY7;Q2TAY7-2	Q2TAY7;Q2TAY7-2	WD40 repeat-cont	SMU1	17	17	513	1.0856	0.81827	5.56E+09
F8W930;Q9Y6M1-	F8W930;Q9Y6M1-	Insulin-like growth	IGF2BP2	9	6	605	1.0852	1.1933	2.90E+08
Q9P2R7-2;Q9P2R7	Q9P2R7-2;Q9P2R7	Succinyl-CoA ligase	SUCLA2	15	15	441	1.0848	0.83602	1.76E+09
P49368;P49368-2;	P49368;P49368-2;	T-complex protein	CCT3	43	43	545	1.0847	0.84586	5.10E+10
P19174;P19174-2;	P19174;P19174-2	1-phosphatidylino	PLCG1	18	18	1290	1.0839	0.89605	9.40E+08
H3BLV9;Q5R363;C	H3BLV9;Q5R363;C	SRSF protein kinase	SRPK1	8	7	671	1.0833	0.85835	6.77E+08
O43865;O43865-2	O43865;O43865-2	Putative adenosylh	AHCYL1	7	5	530	1.083	0.95717	5.01E+08
O94806;H0Y5M6;F	O94806;H0Y5M6;F	Serine/threonine-p	PRKD3;PRKD1	2	2	890	1.083	NaN	6.38E+07
A0A096LNJ4;A0A0	A0A096LNJ4;A0A0	Putative bifunctior	ALG13	2	2	132	1.0828	NaN	2.41E+08
F5GYT8;E9PHF7;Q9	F5GYT8;E9PHF7;Q9	Methylcrotonoyl-C	MCCC1	5	5	575	1.0823	0.60947	2.75E+08
Q96EE3;Q96EE3-1;	Q96EE3;Q96EE3-1;	Nucleoporin SEH1	SEH1L	10	10	360	1.0814	0.83097	2.24E+09
P46783;F6U211;S4	P46783;F6U211;S4	40S ribosomal prot	RPS10;RPS10-NUD	9	9	165	1.0813	0.89513	3.38E+09
A0A087WW06;Q9	A0A087WW06;Q9	Tetratricopeptide r	TTC28	22	22	2354	1.0805	0.88504	7.22E+08
O43396;K7ER96;K	O43396;K7ER96	Thioredoxin-like pr	TXNL1	13	13	289	1.0802	0.87468	2.48E+09
E9PS17;E9PK59;Q9	E9PS17;E9PK59;Q9	N-terminal kinase-l	SCYL1	13	13	775	1.0801	0.86066	4.62E+08
Q15126	Q15126	Phosphomevalonat	PMVK	5	5	192	1.0801	1.2495	1.23E+08
Q96AC1-2;Q96AC1	Q96AC1-2;Q96AC1	Fermitin family hor	FERMT2	9	9	633	1.0799	1.0439	7.33E+08
Q13601;Q13601-2	Q13601;Q13601-2	KRR1 small subunit	KRR1	8	8	381	1.0793	0.90722	4.51E+08
Q9BQ67;M0QX71	Q9BQ67;M0QX71	Glutamate-rich WD	GRWD1	12	12	446	1.0793	1.0094	5.36E+09
Q8NFH4;F8VTY2	Q8NFH4;F8VTY2	Nucleoporin Nup37	NUP37	8	8	326	1.0786	0.90766	1.25E+09
Q9NUD5;Q9NUD5-	Q9NUD5;Q9NUD5-	Zinc finger CCHC do	ZCCHC3	5	5	404	1.0784	1.1774	3.93E+08
Q86WJ1;Q86WJ1-	Q86WJ1;Q86WJ1-	Chromodomain-he	CHD1L	21	2	897	1.0782	0.83151	1.04E+09
P61081;M0QX69;M	P61081	NEDD8-conjugatin	UBE2M	13	13	183	1.0772	0.83355	3.61E+09
Q9Y613;J3KTH7	Q9Y613	FH1/FH2 domain-c	FHOD1	4	4	1164	1.0771	0.87564	6.68E+07
P51553;P51553-2;	P51553;P51553-2;	Isocitrate dehydro	IDH3G	11	11	393	1.0767	1.0035	1.65E+09
P82664	P82664	28S ribosomal prot	MRPS10	6	6	201	1.0767	0.75927	2.62E+08
P27694;I3L4R8;I3I	P27694	Replication protein	RPA1	26	26	616	1.0766	0.90379	8.78E+09
Q7Z392;D6RHE5;Q	Q7Z392;D6RHE5;Q	Trafficking protein	TRAPPC11	5	5	1133	1.076	1.2475	1.39E+08
E9PD68;Q14194;Q	E9PD68;Q14194;Q	Dihydropyrimidina	CRMP1	5	3	570	1.0758	1.4544	2.04E+08
O43143	O43143	Putative pre-mRNA	DHX15	27	26	795	1.0757	1.135	6.55E+09
Q9NRG9;Q9NRG9-	Q9NRG9;Q9NRG9-	Aladin	AAAS	11	11	546	1.0757	0.86137	1.35E+09
Q9BTZ2;Q9BTZ2-8;	Q9BTZ2;Q9BTZ2-8;	Dehydrogenase/rec	DHRS4	8	8	278	1.0752	0.87005	4.03E+08
H9KV28;A0A140T8	H9KV28;A0A140T8	Protein diaphanou	DIAPH1	25	25	1228	1.0742	0.68358	1.12E+09
J3KMZ8;Q92785-2	J3KMZ8;Q92785-2	Zinc finger protein	DPF2	4	4	405	1.0741	0.85036	4.07E+08
P61764;P61764-2;	P61764;P61764-2	Syntaxin-binding p	STXBP1	9	9	594	1.074	0.94439	3.44E+08
Q13363-2;Q13363	Q13363-2;Q13363	C-terminal-binding	CTBP1	14	9	429	1.074	1.0483	3.13E+09
Q8WXF1-2;Q8WXF	Q8WXF1-2;Q8WXF	Paraspeckle compc	PSPC1	14	10	393	1.074	0.9889	1.55E+09
O14531;Q5T0Q6	O14531;Q5T0Q6	Dihydropyrimidina	DPYSL4	3	3	572	1.0737	1.2784	8.18E+07
P62136;P62136-2;	P62136;P62136-2;	Serine/threonine-p	PPP1CA	21	5	330	1.0735	0.77692	1.40E+10
P62140;E7ETD8;C9	P62140;E7ETD8;C9	Serine/threonine-p	PPP1CB	18	6	327	1.0735	1.0184	1.27E+09
P41227;P41227-2;	P41227;P41227-2;	N-alpha-acetyltran	NAA10	9	9	235	1.0731	0.93443	7.95E+08
Q9NPD3;E9PI41;E9	Q9NPD3;E9PI41	Exosome complex c	EXOSC4	3	3	245	1.0729	0.98093	1.92E+08
I3L397;I3L504;P63	I3L397;I3L504;P63	Eukaryotic translat	EIF5A;EIF5AL1;EIF5	13	13	147	1.0725	1.0225	5.43E+09
Q96F86;H3BSQ0;H	Q96F86	Enhancer of mRNA-	EDC3	13	13	508	1.0721	0.79509	8.65E+08
O75828	O75828	Carbonyl reductase	CBR3	6	4	277	1.072	0.78638	2.28E+08
K7ESN3;Q8N2G8-2	K7ESN3;Q8N2G8-2	GH3 domain-conta	GHDC	3	3	479	1.0716	NaN	7.41E+07
Q9UET6-2;Q9UET6;	Q9UET6-2;Q9UET6;	Putative tRNA (cyti	FTSJ1	2	2	327	1.0713	1.0775	1.51E+08
P42696;A2A2V2;P4	P42696;A2A2V2;P4	RNA-binding protei	RBM34	7	7	430	1.07	0.88953	6.53E+08
A0A087WUB9;Q8V	A0A087WUB9;Q8V	Beta-catenin-like p	CTNNBL1	9	9	568	1.0693	0.99223	5.90E+08
O43251-6;O43251	O43251-6;O43251	RNA binding protei	RBFOX2;RBFOX1	7	7	450	1.0693	0.73579	4.17E+08
A0A0C4DFL7;Q168	A0A0C4DFL7;Q168	Lanosterol 14-alph	CYP51A1	4	4	509	1.0691	0.97727	2.75E+08
Q5VY60;Q7Z4H7-3	Q5VY60;Q7Z4H7-3	HAUS augmin-like c	HAUS6	7	7	802	1.0673	0.80145	3.59E+08
Q96JM3;S4R3K0	Q96JM3	Chromosome align	CHAMP1	5	5	812	1.0671	0.68474	2.58E+08
O15354	O15354	Prosaposin recepto	GPR37	1	1	613	1.0668	NaN	1.47E+07
Q02790;F5H1U3;F	Q02790	Peptidyl-prolyl cis-	FKBP4	24	24	459	1.0663	1.2138	4.47E+09
E7ENQ1;G3XAA2;H	E7ENQ1;G3XAA2;H	Mitogen-activated	MAP4K4;TNIK;MIN	8	8	1154	1.066	0.88723	3.98E+08
Q3B7T1-5;Q3B7T1;	Q3B7T1-5;Q3B7T1	Erythroid differenti	EDRF1	6	6	1204	1.066	0.94012	8.39E+07
Q7Z406-6;Q7Z406	Q7Z406-6;Q7Z406	Myosin-14	MYH14	22	14	2003	1.0659	1.2077	1.37E+09
O00139-2;O00139	O00139-2;O00139	Kinesin-like protein	KIF2A	13	12	660	1.0658	0.89219	9.12E+08
P11021	P11021	78 kDa glucose-reg	HSPA5	42	40	654	1.0654	0.76857	2.37E+10
Q13155;A8MU58;I	Q13155;A8MU58;I	Aminoacyl tRNA sy	AIMP2	11	11	320	1.0654	0.99735	4.04E+09
Q15149-7;Q15149	Q15149-7;Q15149	Plectin	PLEC	58	51	4515	1.0654	0.80505	3.18E+09
Q8WVM0	Q8WVM0	Dimethyladenosine	TFB1M	5	5	346	1.0654	0.74599	3.18E+08
Q9P2J5;Q9P2J5-2;	Q9P2J5;Q9P2J5-2	Leucine--tRNA ligas	LARS	50	50	1176	1.0652	0.97017	2.03E+10
O95376;C9JZ71;C9	O95376	E3 ubiquitin-protei	ARIH2	9	9	493	1.0651	0.79192	7.42E+08
Q9BXB4;H7C487;C	Q9BXB4	Oxysterol-binding p	OSBPL11	5	5	747	1.0647	1.3492	3.09E+08
Q7Z2T5;X6RK96;Q	Q7Z2T5;X6RK96	TRMT1-like protein	TRMT1L	8	8	733	1.0643	0.83462	6.21E+08
Q9BYB4;Q9BYB4-2;	Q9BYB4	Guanine nucleotid	GNB1L	6	6	327	1.0643	0.62282	5.13E+08
Q96QK1;I3L4S0;I3I	Q96QK1	Vacuolar protein sc	VPS35	31	31	796	1.064	0.94374	6.46E+09
Q9ULX3;H3BUR4	Q9ULX3;H3BUR4	RNA-binding protei	NOB1	10	10	412	1.0638	0.77286	1.58E+09
Q96S44;Q5JZ02	Q96S44;Q5JZ02	TP53-regulating kir	TP53RK	4	4	253	1.0634	0.95717	9.54E+08
P49916-3;P49916;	P49916-3;P49916;	DNA ligase 3	LIG3	28	28	922	1.0631	0.77227	2.25E+09
Q6IN85-2;Q6IN85;	Q6IN85-2;Q6IN85;	Serine/threonine-p	SMEK1	14	12	820	1.0625	0.88108	7.40E+08
Q8IWV7;A0A087W	Q8IWV7	E3 ubiquitin-protei	UBR1	8	8	1749	1.0621	0.96828	4.33E+08

Q9HAD4;H0YAA3;C	Q9HAD4;H0YAA3;C	WD repeat-contain	WDR41	6	6	459	1.062	0.95972	6.74E+08
A0A087WZN1;O43	A0A087WZN1;O43	Isocitrate dehydrog	IDH3B	15	15	387	1.0618	0.91674	2.26E+09
O60343-2;O60343	O60343-2;O60343	TBC1 domain famil	TBC1D4	23	21	1235	1.0617	0.98086	2.61E+09
P49761-1;P49761;	P49761-1;P49761	Dual specificity pro	CLK3	2	2	490	1.0613	NaN	1.07E+08
Q16513;Q16513-3	Q16513;Q16513-3	Serine/threonine-p	PKN2	37	36	984	1.0608	0.76002	4.14E+09
O94874-2;O94874	O94874-2;O94874	E3 UFM1-protein li	UFL1	18	18	729	1.0607	1.0364	1.02E+09
F8W8R3;P49005;A	F8W8R3;P49005;A	DNA polymerase de	POLD2	9	9	455	1.0594	0.75702	1.53E+09
O14545;F8VNX8;F	O14545;F8VNX8	TRAF-type zinc fing	TRAFD1	3	3	582	1.0586	0.67488	8.97E+07
C9JKF1;Q5K651	C9JKF1;Q5K651	Sterile alpha motif	SAMD9	3	3	1283	1.0585	1.1389	4.98E+07
Q13043-2;Q13043	Q13043-2;Q13043	Serine/threonine-p	STK4;STK3	2	2	462	1.0584	NaN	7.49E+07
Q52LJ0;Q52LJ0-2;I	Q52LJ0;Q52LJ0-2	Protein FAM98B	FAM98B	5	4	330	1.0584	1.0109	4.67E+08
Q9NSD9;Q9NSD9-2	Q9NSD9;Q9NSD9-2	Phenylalanine--tRN	FARSB	20	20	589	1.0583	0.96061	3.56E+09
A0A087WX08;Q9U	A0A087WX08;Q9U	Gamma-adducin	ADD3	5	5	672	1.0579	0.98737	5.10E+08
Q15050	Q15050	Ribosome biogenes	RRS1	2	2	365	1.0578	NaN	1.16E+08
Q5TDH0;Q5TDH0-3	Q5TDH0;Q5TDH0-3	Protein DDI1 homc	DDI2	9	9	399	1.0575	0.82104	2.17E+09
E9PF10;O75694;O	E9PF10;O75694;O	Nuclear pore comp	NUP155	40	40	1327	1.0573	0.93972	5.74E+09
O75131;A0A087W	O75131;A0A087W	Copine-3	CPNE3	21	21	537	1.0573	1.0401	5.64E+09
Q92889;Q92889-2	Q92889	DNA repair endonu	ERCC4	5	5	916	1.0572	0.89618	8.96E+07
Q96TA2-3;Q96TA2	Q96TA2-3;Q96TA2	ATP-dependent zin	YME1L1	7	7	683	1.057	0.88268	6.40E+08
Q8TEM1;Q8TEM1-2	Q8TEM1;Q8TEM1-2	Nuclear pore memb	NUP210	30	30	1887	1.0569	1.0229	2.60E+09
Q9Y4X5;H3BNB9;A	Q9Y4X5;H3BNB9	E3 ubiquitin-protei	ARIH1	6	6	557	1.0566	0.71533	4.27E+08
Q07864;F5H1D6;F	Q07864;F5H1D6	DNA polymerase ep	POLE	33	33	2286	1.0564	0.80587	1.69E+09
Q9BZE9;Q9BZE9-2;	Q9BZE9;Q9BZE9-2;	Tether containing U	ASPSCR1	6	6	553	1.0564	0.78465	4.87E+08
Q7RTV0	Q7RTV0	PHD finger-like don	PHF5A	5	5	110	1.0562	0.93813	1.08E+08
F5H5D3;Q9BQE3;F	F5H5D3;Q9BQE3	Tubulin alpha-1C cl	TUBA1C	34	4	519	1.0558	NaN	4.11E+08
Q8N1G2;H0YCQ1	Q8N1G2	Cap-specific mRNA	CMTR1	4	4	835	1.0556	1.123	1.68E+08
Q9UQE7	Q9UQE7	Structural mainten	SMC3	66	66	1217	1.0549	0.90073	9.31E+09
Q96BY7	Q96BY7	Autophagy-related	ATG2B	2	2	2078	1.0547	1.5189	4.34E+07
Q8WYQ5-3;Q8WYC	Q8WYQ5-3;Q8WYC	Microprocessor co	DGCR8	2	2	740	1.0545	NaN	1.38E+07
O94822;O94822-3	O94822;O94822-3	E3 ubiquitin-protei	LTN1	11	7	1766	1.0539	1.0168	4.57E+08
Q8IWZ3;Q8IWZ3-4	Q8IWZ3;Q8IWZ3-4	Ankyrin repeat and	ANKHD1	25	14	2542	1.0536	0.73442	1.98E+09
O76003	O76003	Glutaredoxin-3	GLRX3	11	11	335	1.0531	1.0358	3.31E+09
G3V4K3;Q9H9C1-2	G3V4K3;Q9H9C1-2	Spermatogenesis-d	VIPAS39	7	7	519	1.0528	0.57497	1.99E+08
O14654	O14654	Insulin receptor sul	IRS4	47	47	1257	1.0525	0.69061	6.92E+09
F5H5P2;P12694;P	F5H5P2;P12694;P	2-oxoisovalerate de	BCKDHA	4	4	479	1.0519	0.56334	2.09E+08
Q02880-2;Q02880	Q02880-2;Q02880	DNA topoisomeras	TOP2B	23	13	1621	1.0513	1.2102	8.55E+08
Q12955-7;Q12955	Q12955-7;Q12955	Ankyrin-3	ANK3	9	8	1465	1.0513	0.9772	2.07E+08
O95782-2;O95782	O95782-2;O95782	AP-2 complex subu	AP2A1	26	17	955	1.0511	0.71583	1.19E+09
Q9BY32;Q9BY32-3;	Q9BY32;Q9BY32-3	Inosine triphospha	ITPA	5	5	194	1.0508	1.0219	5.58E+08
P18031;B4DSN5	P18031;B4DSN5	Tyrosine-protein ph	PTPN1	9	9	435	1.0506	1.1181	8.75E+08
Q8NCN5;A8MT40;I	Q8NCN5;A8MT40;I	Pyruvate dehydrog	PDPR	6	6	879	1.0506	0.6686	2.29E+08
Q3ZCQ8;Q3ZCQ8-2	Q3ZCQ8;Q3ZCQ8-2	Mitochondrial imp	TIMM50	11	11	353	1.0504	0.76266	2.57E+09
Q9NPF4;G3V445;G	Q9NPF4	Probable tRNA N6-a	OSGEP	8	8	335	1.0503	0.90505	1.07E+09
Q8TED1;E7ETY7;J3I	Q8TED1;E7ETY7;J3I	Probable glutathio	GPX8	4	4	209	1.0502	0.77601	1.61E+08
O15294;O15294-3	O15294;O15294-3	UDP-N-acetylgluco	OGT	10	10	1046	1.0494	0.90158	6.02E+08
Q6PL18;Q6PL18-2;	Q6PL18;Q6PL18-2	ATPase family AAA d	ATAD2	4	4	1390	1.0491	0.74758	1.13E+08
E9PJH7;Q9H936;AI	E9PJH7;Q9H936;AI	Mitochondrial glut	SLC25A22	9	9	313	1.0489	0.9254	2.52E+09
O75436;S4R3Q6;O	O75436;S4R3Q6;O	Vacuolar protein sc	VPS26A	11	10	327	1.0487	0.8202	1.97E+09
Q7L0Y3;C9JVB6	Q7L0Y3;C9JVB6	Mitochondrial ribo	TRMT10C	8	8	403	1.0483	0.81531	2.67E+08
Q96EK4	Q96EK4	THAP domain-cont	THAP11	3	3	314	1.0481	0.84166	1.89E+08
M0QXB4;O14579;A	M0QXB4;O14579;A	Coatomer subunit e	COPE	16	16	331	1.048	0.87978	6.15E+09
P78347-2;P78347	P78347-2;P78347	General transcripti	GTF2I	39	39	957	1.0479	0.81094	6.07E+09
C9JVN9;Q9H9P8-2	C9JVN9;Q9H9P8-2	L-2-hydroxyglutara	L2HGDH	9	9	441	1.0473	0.77973	1.31E+09
P62879;C9JZN1;C9	P62879;C9JZN1;C9	Guanine nucleotide	GNB2;GNB4	7	2	340	1.0468	0.9548	1.38E+09
Q8WWM7-6;Q8W\	Q8WWM7-6;Q8W\	Ataxin-2-like protei	ATXN2L	8	8	968	1.0468	0.69617	2.83E+08
Q9H5Q4	Q9H5Q4	Dimethyladenosine	TFB2M	7	7	396	1.0468	0.73483	3.46E+08
Q9Y4P1-6;Q9Y4P1;	Q9Y4P1-6;Q9Y4P1	Cysteine protease A	ATG4B	9	9	380	1.0463	1.0367	1.03E+09
P62913	P62913	60S ribosomal prot	RPL11	12	2	178	1.0453	1.0677	1.32E+10
Q8TAT6;Q8TAT6-2;	Q8TAT6;Q8TAT6-2	Nuclear protein loc	NPLOC4	12	12	608	1.0453	1.1609	9.71E+08
Q9UHD2	Q9UHD2	Serine/threonine-p	TBK1	5	5	729	1.0446	0.94737	3.19E+08
Q8WWH5	Q8WWH5	Probable tRNA pse	TRUB1	8	8	349	1.0443	0.8796	6.41E+08
P46063;F8WA66;F	P46063	ATP-dependent DN	RECQL	22	22	649	1.0442	0.88161	4.39E+09
M0QZR4;Q92888;(	M0QZR4;Q92888;(	Rho guanine nucle	ARHGEF1	11	11	968	1.0441	0.85372	3.37E+08
P50995-2;P50995;	P50995-2;P50995	Annexin A11	ANXA11	16	16	472	1.044	1.0672	1.66E+09
P57740;P57740-2;	P57740;P57740-2	Nuclear pore comp	NUP107	28	28	925	1.0438	0.72406	3.28E+09
Q9Y450-4;Q9Y450	Q9Y450-4;Q9Y450	HBS1-like protein	HBS1L	17	17	642	1.0435	0.87155	1.99E+09
O75191-2;O75191	O75191-2;O75191	Xylulose kinase	XYLB	2	2	399	1.0433	NaN	5.83E+07
Q08945;E9PMD4;A	Q08945	FACT complex subu	SSRP1	27	27	709	1.0433	0.94402	1.09E+10
P32929-2;P32929	P32929-2;P32929	Cystathionine gam	CTH	4	4	361	1.0431	NaN	1.27E+08
Q9NWT1	Q9NWT1	p21-activated prot	PAK1IP1	3	3	392	1.0431	1.0732	1.51E+08
P25685;P25685-2;	P25685;P25685-2	DnaJ homolog subf	DNAJB1	9	9	340	1.043	1.2393	4.03E+08
Q8TC12;Q8TC12-2;	Q8TC12;Q8TC12-2	Retinol dehydroger	RDH11	8	8	318	1.0423	0.90935	1.79E+09
Q99426;Q99426-2	Q99426;Q99426-2	Tubulin-folding cof	TBCB	12	12	244	1.042	1.0412	1.06E+09
J3QRS3;P19105;O	J3QRS3;P19105;O	Myosin regulatory l	MYL12A;MYL12B;M	8	8	177	1.0411	1.1509	1.11E+09
Q9UER7-3;Q9UER7	Q9UER7-3;Q9UER7	Death domain-asso	DAXX	1	1	665	1.0411	NaN	7.72E+07
P35573;P35573-2;	P35573;P35573-2	Glycogen debranch	AGL	63	63	1532	1.0407	0.8649	8.28E+09
P63010;P63010-2;	P63010;P63010-2	AP-2 complex subu	AP2B1	27	14	937	1.0407	0.8404	1.76E+09
Q9NXC5;Q9NXC5-2	Q9NXC5;Q9NXC5-2	WD repeat-contain	MIOS	7	7	875	1.0407	0.72433	3.06E+08
Q9BZH6;S4R3Z0;S4	Q9BZH6	WD repeat-contain	WDR11	15	15	1224	1.0405	0.73163	1.08E+09
Q9UQR0;H0Y6S1;C	Q9UQR0	Sex comb on midle	SCML2	5	5	700	1.0403	0.85748	3.98E+08
A0A087X1N2;Q03	A0A087X1N2;Q03	CCAAT/enhancer-bi	CEBPZ	13	13	998	1.0392	0.91842	4.78E+08
A2RRP1-2;A2RRP1;	A2RRP1-2;A2RRP1	Neuroblastoma-am	NBAS	17	17	2251	1.039	0.88952	8.29E+08
Q99623;J3KPX7;F9	Q99623;J3KPX7;F9	Prohibitin-2	PHB2	23	23	299	1.0388	1.1757	1.87E+10
P68366-2;P68366;	P68366-2;P68366	Tubulin alpha-4A cl	TUBA4A	27	3	433	1.0386	0.81794	5.40E+08
Q7KZ85;Q7KZ85-2;	Q7KZ85	Transcription elong	SUPT6H	33	33	1726	1.0386	1.0378	2.20E+09
H0YNU5;P54132;H	H0YNU5;P54132	Bloom syndrome p	BLM	5	5	1286	1.0382	0.56047	1.25E+08
Q9NSV4-7;Q9NSV4	Q9NSV4-7;Q9NSV4	Protein diaphanou	DIAPH3	7	7	1112	1.038	0.8661	6.09E+07
Q8TF46-2;Q8TF46-	Q8TF46-2;Q8TF46-	DIS3-like exonuclea	DIS3L	3	3	920	1.0379	0.50523	9.59E+07
A8K968;A0A0A0MI	A8K968;A0A0A0MI	Band 4.1-like prote	EPB41L3	17	17	756	1.0377	0.76753	1.01E+09
D6RH30;P19838;P	D6RH30;P19838;P	Nuclear factor NF-k	NFKB1	2	2	198	1.0376	1.029	1.25E+08
Q13547;Q5TEE2;E9	Q13547;Q5TEE2	Histone deacetylas	HDAC1	11	7	482	1.0375	1.0541	2.93E+09
Q15054;Q15054-3	Q15054;Q15054-3	DNA polymerase de	POLD3	5	5	466	1.0375	0.72871	2.70E+08
O75116;Q14DU5;E	O75116;Q14DU5;E	Rho-associated pro	ROCK2	4	4	1388	1.0373	1.161	6.26E+07

Q86UK7-2;Q86UK7	Q86UK7-2;Q86UK7	Zinc finger protein	ZNF598	7	7	896	1.0368	0.52414	4.15E+08
O00165;O00165-2	O00165;O00165-2	HCLS1-associated p	HAX1	9	9	279	1.0356	0.78289	1.48E+09
A0A087WZ13;E9P/	A0A087WZ13;E9P/	Ribonucleoprotein	RAVER1	13	13	739	1.0348	0.88991	8.24E+08
Q5QJE6;J3KP30	Q5QJE6	Deoxynucleotidylt	DNTTIP2	4	4	756	1.0348	1.2481	6.26E+07
Q9H3P7	Q9H3P7	Golgi resident prot	ACBD3	11	11	528	1.0348	0.99351	4.62E+08
A0A087WWS7;Q1!	A0A087WWS7;Q1!	Syntaxin-binding p	STXBP2;ZNF14	4	4	579	1.0347	0.88571	1.01E+08
P49327;A0A0U1R(	P49327;A0A0U1R(	Fatty acid synthase	FASN	130	130	2511	1.0339	0.82683	1.33E+11
Q9Y4G6;H0YMT1;H	Q9Y4G6;H0YMT1	Talin-2	TLN2	3	2	2542	1.0339	0.82936	1.13E+08
E9PF19;Q9Y4P3;Q!	E9PF19;Q9Y4P3;Q!	Transducin beta-lik	TBL2	9	9	411	1.0338	1.0799	3.64E+08
E9PKP7;P17480-2;	E9PKP7;P17480-2;	Nucleolar transcrip	UBTF	8	8	745	1.0337	0.79397	6.50E+08
Q96EY1;Q96EY1-2;	Q96EY1;Q96EY1-2	DnaJ homolog subf	DNAJA3	8	8	480	1.0337	0.98662	1.64E+09
F5H8D7;P18887;N	F5H8D7;P18887	DNA repair protein	FOXH1;XRCC1	5	5	602	1.0326	0.78912	1.31E+08
Q6ZN17;Q6ZN17-2	Q6ZN17	Protein lin-28 hom	LIN28B	5	5	250	1.0326	1.1613	2.89E+08
P52564;P52564-2;	P52564;P52564-2	Dual specificity mit	MAP2K6	5	3	334	1.0325	0.96932	3.22E+08
D6RF48;Q9P2W9;I	D6RF48;Q9P2W9	Syntaxin-18	STX18	7	7	308	1.0318	1.2631	3.25E+08
Q9BV44;H7C3J3;H	Q9BV44;H7C3J3;H	THUMP domain-co	THUMPD3	8	8	507	1.0306	0.99012	5.92E+08
A0A0A0MTL5;Q13:	A0A0A0MTL5;Q13:	S-phase kinase-asso	SKP2	7	7	435	1.0294	0.53315	4.18E+08
P38117;P38117-2;	P38117;P38117-2;	Electron transfer fl	ETFB	6	6	255	1.0294	1.1031	4.35E+08
Q9NVM9;Q9NVM9	Q9NVM9;Q9NVM9	Protein asunder ho	ASUN	3	3	706	1.0294	1.2535	2.24E+08
O43929;O43929-2	O43929;O43929-2	Origin recognition	ORC4	7	7	436	1.029	0.93171	3.39E+08
O14976-2;O14976	O14976-2;O14976	Cyclin-G-associatec	GAK	6	6	1232	1.0288	0.8633	5.20E+08
P08243-2;P08243;	P08243-2;P08243;	Asparagine synthet	ASNS	24	24	540	1.0283	1.2634	9.14E+09
Q9Y265;Q9Y265-2;	Q9Y265;Q9Y265-2	RuvB-like 1	RUVBL1	28	28	456	1.0271	0.9426	1.08E+10
P11586;F5H2F4;V!	P11586;F5H2F4	C-1-tetrahydrofola	MTHFD1	61	60	935	1.0264	0.90422	2.78E+10
Q9NSE4	Q9NSE4	Isoleucine--tRNA lig	IARS2	27	27	1012	1.0261	0.96102	2.55E+09
C4B7M2;Q96JI7-2;	C4B7M2;Q96JI7-2;	Spatacsin	SPG11	2	2	2265	1.026	1.1873	1.31E+07
P06132;H0Y5R6;Q	P06132;H0Y5R6;Q	Uroporphyrinogen	UROD	8	8	367	1.0259	0.908	1.43E+09
K7EQ02;K7EQ55;K	K7EQ02;K7EQ55;K	DAZ-associated pro	DAZAP1	8	8	327	1.0247	0.8792	5.87E+08
P53992;G5EA31;P!	P53992;G5EA31	Protein transport p	SEC24C	22	22	1094	1.0247	0.74204	3.20E+09
A0A087X295;Q9NI	A0A087X295;Q9NI	WD repeat-contain	WDR6	16	16	1151	1.0246	0.8043	1.14E+09
Q9Y283-2;Q9Y283	Q9Y283-2;Q9Y283	Inversin	INVS	1	1	895	1.0246	1.2668	1.93E+07
P08708;H0YN88;A	P08708;H0YN88;A	40S ribosomal prot	RPS17	13	13	135	1.0244	0.94747	2.35E+09
Q13951-2;J3KTD8	Q13951-2	Core-binding factor	CBFB	8	2	187	1.024	1.1572	5.77E+08
J3QRD1;P51648;P!	J3QRD1;P51648;P!	Fatty aldehyde deh	ALDH3A2	3	3	393	1.0232	1.1786	2.59E+08
Q16512;Q16512-2	Q16512;Q16512-2	Serine/threonine-p	PKN1	15	14	942	1.0231	0.74304	8.44E+08
Q15751;H0YNB1	Q15751;H0YNB1	Probable E3 ubiqui	HERC1	4	4	4861	1.023	NaN	2.16E+07
O43175;Q5SZU1	O43175;Q5SZU1	D-3-phosphoglycer	PHGDH	24	24	533	1.0226	1.1985	3.03E+10
F5H269;Q9Y485	F5H269;Q9Y485	DmX-like protein 1	DMXL1	2	2	3048	1.0222	NaN	1.64E+07
Q9UIM3	Q9UIM3	FK506-binding pro	FKBPL	3	3	349	1.0222	NaN	1.36E+08
A0A087WVQ6;Q0(	A0A087WVQ6;Q0(	Clathrin heavy chai	CLTC	94	73	1679	1.0219	1.0234	9.15E+10
O75746;O75746-2	O75746;O75746-2	Calcium-binding m	SLC25A12	16	11	678	1.0213	0.9196	1.93E+09
E7EU96;Q5U5J2;P(	E7EU96;Q5U5J2;P(	Casein kinase II sub	CSNK2A1;CSNK2A3	14	14	385	1.021	1.0258	4.39E+09
Q96HW7;Q96HW7	Q96HW7;Q96HW7	Integrator complex	INTS4	11	11	963	1.0195	0.84889	4.85E+08
Q96K76-4;Q96K76	Q96K76-4;Q96K76	Ubiquitin carboxyl	USP47	11	11	1355	1.0195	1.0551	4.65E+08
P78527;P78527-2;	P78527;P78527-2	DNA-dependent pr	PRKDC	206	206	4128	1.0192	1.0843	4.81E+10
Q15717;Q15717-2	Q15717;Q15717-2	ELAV-like protein 1	ELAVL1	20	20	326	1.019	1.0562	1.24E+10
A0A0A0MTH9;O14	A0A0A0MTH9;O14	TATA-binding prote	BTAF1	28	28	1849	1.0186	0.8773	1.93E+09
S4R3H4;E7EQT4;Q!	S4R3H4;E7EQT4;Q!	Apoptotic chromat	ACIN1	2	2	1283	1.0186	1.2116	7.51E+07
Q58FF8	Q58FF8	Putative heat shocl	HSP90AB2P	13	2	381	1.0186	1.0807	4.39E+09
P84090;G3V279	P84090;G3V279	Enhancer of rudime	ERH	4	4	104	1.0185	1.2569	3.99E+08
A8MYT4;Q8NEB9;K	A8MYT4;Q8NEB9	Phosphatidylinosit	PIK3C3	3	3	824	1.0183	NaN	8.41E+07
Q9Y383;A0A0A6YY	Q9Y383;A0A0A6YY	Putative RNA-bindi	LUC7L2	6	6	392	1.0183	1.2141	2.52E+08
Q9Y3A4	Q9Y3A4	Ribosomal RNA-prc	RRP7A	2	2	280	1.0182	NaN	3.42E+07
P23246;P23246-2;	P23246;P23246-2	Splicing factor, pro	SFPQ	21	18	707	1.018	1.224	5.86E+09
O00505;H0Y4S9	O00505	Importin subunit a	KPNA3	14	10	521	1.0176	0.92458	1.28E+09
P11172;P11172-3;	P11172;P11172-3	Uridine 5-monoph	UMPS	22	22	480	1.0175	1.1428	3.36E+09
A0PJW6	A0PJW6	Transmembrane pr	TMEM223	2	2	202	1.0173	NaN	8.17E+07
Q9NXG2;H3BNW0	Q9NXG2	THUMP domain-co	THUMPD1	9	9	353	1.0173	0.84764	4.90E+08
Q8N163-2;Q8N16:	Q8N163-2;Q8N16:	Cell cycle and apop	CCAR2	23	23	923	1.0172	0.96063	2.95E+09
Q66K14-2;Q66K14	Q66K14-2;Q66K14	TBC1 domain famil	TBC1D9B	10	10	1233	1.0169	0.69145	4.63E+08
Q8ND04;Q8ND04-:	Q8ND04;Q8ND04-:	Protein SMG8	SMG8	8	8	991	1.0167	0.69169	2.03E+08
P08559-3;P08559;	P08559-3;P08559;	Pyruvate dehydrog	PDHA1	22	22	359	1.0165	0.87667	9.99E+09
P40939;H0YFD6;P(	P40939	Trifunctional enzyn	HADHA	33	33	763	1.0163	0.97636	1.33E+10
A6PW57;Q99755-:	A6PW57;Q99755-:	Phosphatidylinosit	PIP5K1A	5	4	550	1.0162	0.75435	5.71E+08
P52294;C9JYI4;C9.	P52294;C9JYI4	Importin subunit a	KPNA1	13	6	538	1.0162	0.89304	1.83E+09
Q9Y4E6-2;Q9Y4E6;	Q9Y4E6-2;Q9Y4E6;	WD repeat-contain	WDR7	6	6	1457	1.0158	0.68778	2.04E+08
P40227;P40227-2	P40227;P40227-2	T-complex protein	CCT6A	34	29	531	1.0156	0.94945	3.78E+10
Q5T5C7;P49591	Q5T5C7;P49591	Serine--tRNA ligase,	SARS	12	12	536	1.0155	1.393	2.38E+09
P23381;P23381-2;	P23381;P23381-2	Tryptophan--tRNA l	WARS	29	29	471	1.0143	0.97123	1.33E+10
Q15120;Q15120-2	Q15120;Q15120-2	[Pyruvate dehydrog	PDK3	4	4	406	1.0143	0.87137	1.65E+08
P51570;P51570-2;	P51570;P51570-2	Galactokinase	GALK1	22	22	392	1.014	0.77815	5.78E+09
Q9Y223;Q9Y223-2;	Q9Y223;Q9Y223-2	Bifunctional UDP-N	GNE	12	12	722	1.0139	0.95608	1.37E+09
Q69YN4-3;Q69YN4	Q69YN4-3;Q69YN4	Protein virilizer hoi	KIAA1429	10	10	1797	1.0133	0.98004	3.98E+08
Q05048;A0A0A0M	Q05048;A0A0A0M	Cleavage stimulatic	CSTF1	14	14	431	1.0131	0.97137	1.13E+09
Q5SRQ6;P67870;Q	Q5SRQ6;P67870;Q	Casein kinase II sub	CSNK2B;CSNK2B-L'	6	6	234	1.013	0.81289	3.88E+08
Q9UIG0-2;Q9UIG0	Q9UIG0-2;Q9UIG0	Tyrosine-protein ki	BAZ1B	17	17	1479	1.0129	0.93557	8.91E+08
O43318-2;O43318	O43318-2;O43318	Mitogen-activated	MAP3K7;DKFZp58(	3	3	579	1.0117	0.93592	1.18E+08
E9PRF4;Q15047-3;	E9PRF4;Q15047-3;	Histone-lysine N-m	SETDB1	6	6	1259	1.0114	0.77783	2.02E+08
Q15048;E9PP40;E!	Q15048;E9PP40	Leucine-rich repeat	LRRC14	6	6	493	1.0114	0.75814	2.43E+08
Q5JTZ9	Q5JTZ9	Alanine--tRNA ligas	AARS2	20	20	985	1.0112	0.78177	1.60E+09
Q9UI43;E9PGN6	Q9UI43;E9PGN6	Putative ribosomal	FTSJ2	2	2	246	1.0111	NaN	3.47E+06
H0Y4Z8;Q3YEC7;Q:	H0Y4Z8;Q3YEC7;Q:	Rab-like protein 6	RABL6	3	3	730	1.011	0.94171	6.90E+07
O60563;O60563-2	O60563	Cyclin-T1	CCNT1	6	6	726	1.0108	0.76558	1.09E+08
P62380;Q7Z6T9;Q	P62380;Q7Z6T9;Q	TATA box-binding p	TBPL1	3	3	186	1.0108	0.84778	2.59E+08
A0A087WV73;P46	A0A087WV73;P46	Probable 28S rRNA	NOP2	20	20	855	1.0104	1.0587	2.97E+09
H7C5A7;E9PJN0;O	H7C5A7;E9PJN0;O	Acyl-coenzyme A th	ACOT8	3	3	209	1.0104	0.86457	3.62E+08
P43490;A0A0C4DF	P43490;A0A0C4DF	Nicotinamide phos	NAMPT	25	25	491	1.0104	0.90811	1.06E+10
I3L0N3;P46459;P4	I3L0N3;P46459;P4	Vesicle-fusing ATPa	NSF	36	36	739	1.0103	0.9249	4.94E+09
P48643;E7ENZ3;B7	P48643;E7ENZ3;B7	T-complex protein	CCT5	42	42	541	1.0102	0.95101	2.32E+10
Q96CW5;Q96CW5	Q96CW5;Q96CW5	Gamma-tubulin co	TUBGCP3	13	13	907	1.0097	0.93126	8.80E+08
Q9Y2L5;J3QQJ5;Q!	Q9Y2L5;J3QQJ5;Q!	Trafficking protein	TRAPPC8	27	27	1435	1.0097	0.88408	1.56E+09
P43034;I3L3N5;I3I	P43034	Platelet-activating	PAFAH1B1	14	14	410	1.0096	1.0019	1.40E+09
Q9NSI2-2;Q9NSI2;(	Q9NSI2-2;Q9NSI2	Protein FAM207A	FAM207A	3	3	215	1.0094	1.0807	2.06E+08

Q8N335;C9K0P5;C	Q8N335	Glycerol-3-phosph	GPD1L	4	4	351	1.009	1.2093	1.13E+08
Q6P4A7;Q6P4A7-2	Q6P4A7;Q6P4A7-2	Sideroflexin-4	SFXN4	9	9	337	1.0089	0.68529	1.78E+09
Q99666;J3KQ37;O	Q99666;J3KQ37;O	RANBP2-like and G	RGPD5;RGPD8	21	4	1765	1.0081	0.7954	9.19E+07
Q9Y230;Q9Y230-2;	Q9Y230;Q9Y230-2	RuvB-like 2	RUVBL2	31	31	463	1.0081	0.9458	1.63E+10
Q8TDN6	Q8TDN6	Ribosome biogenes	BRIX1	9	9	353	1.0076	1.0131	8.53E+08
E9PM35;P49407-2	E9PM35;P49407-2	Beta-arrestin-1	ARRB1	3	2	258	1.0075	0.89747	1.77E+08
O75643;O75643-2	O75643	U5 small nuclear ril	SNRNP200	91	91	2136	1.0075	1.0089	1.63E+10
O00178;F5H716	O00178	GTP-binding protei	GTPBP1	3	3	669	1.0071	1.3951	4.78E+08
E7EN20;Q9UPN9;H	E7EN20;Q9UPN9;H	E3 ubiquitin-protei	TRIM33	8	8	1119	1.0069	0.93602	4.54E+08
Q9UJW0;Q9UJW0-	Q9UJW0;Q9UJW0-	Dynactin subunit 4	DCTN4	9	9	460	1.0069	0.7752	1.04E+09
P41252;A0A0A0M	P41252;A0A0A0M	Isoleucine--tRNA lig	IARS	69	69	1262	1.0066	1.0628	3.08E+10
O60832;O60832-2	O60832;O60832-2	H/ACA ribonucleop	DKC1	16	16	514	1.0057	0.99192	1.52E+09
A1L0T0;E9PJS0;M0	A1L0T0;E9PJS0;M0	Acetolactate synth	ILVBL	4	4	632	1.0053	1.0133	2.66E+08
Q9GZT9-2;Q9GZT9;	Q9GZT9-2;Q9GZT9	Egl nine homolog 1	EGLN1	3	3	404	1.0052	0.68971	1.01E+08
F8WA39;Q13613;H	F8WA39;Q13613;H	Myotubularin-relat	MTMR1	3	3	673	1.0051	0.73991	2.14E+08
K7ERG2;Q9NYR9-2	K7ERG2;Q9NYR9-2	NF-kappa-B inhibit	NKIRAS2	4	4	141	1.0051	0.65302	2.59E+08
H7BZ14;Q9H2H8;E	H7BZ14;Q9H2H8;E	Peptidyl-prolyl cis-	PPIL3	3	3	180	1.005	NaN	3.15E+07
P50213;H0YL72;P	P50213;H0YL72;P	Isocitrate dehydro	IDH3A	10	10	366	1.0046	1.0046	4.48E+09
P55039;A8MZF9;J	P55039;A8MZF9	Developmentally-r	DRG2	9	9	364	1.0044	1.2913	1.39E+09
Q01469	Q01469	Fatty acid-binding	FABP5	7	7	135	1.0041	0.89274	5.56E+08
O95486;O95486-2	O95486	Protein transport p	SEC24A	5	5	1093	1.004	0.97914	3.81E+08
P62249;M0R210;A	P62249;M0R210;A	40S ribosomal prot	RPS16	20	20	146	1.0039	1.0185	1.61E+10
P35244;B5MC59	P35244;B5MC59	Replication proteir	RPA3	4	4	121	1.0038	1.1138	3.07E+08
Q9UJS0;Q9UJS0-2;	Q9UJS0;Q9UJS0-2	Calcium-binding m	SLC25A13	29	24	675	1.0034	0.9335	1.29E+10
Q9Y697-2;Q9Y697	Q9Y697-2;Q9Y697	Cysteine desulfuras	NFS1	4	4	397	1.003	0.97179	2.25E+08
Q9BS26	Q9BS26	Endoplasmic reticu	ERP44	4	4	406	1.0029	1.2658	4.40E+08
C9J9K3;A0A0C4DG	C9J9K3;A0A0C4DG	40S ribosomal prot	RPSA	13	13	264	1.0028	1.3343	3.71E+09
Q7Z4S6-6;Q7Z4S6-	Q7Z4S6-6;Q7Z4S6-	Kinesin-like proteir	KIF21A	7	6	1621	1.0019	0.90278	2.51E+08
Q9UHI6;E9PJ60;Q	Q9UHI6	Probable ATP-depe	DDX20	21	21	824	1.0019	0.78007	1.65E+09
P62888;E5RI99;A0	P62888;E5RI99;A0	60S ribosomal prot	RPL30	8	8	115	1.0014	0.97971	3.01E+09
Q9UN37;I3L4J1	Q9UN37;I3L4J1	Vacuolar protein sc	VPS4A	10	7	437	1.0014	0.97401	1.61E+09
Q709C8-4;Q709C8	Q709C8-4;Q709C8	Vacuolar protein sc	VPS13C	10	10	3585	1.0003	1.3978	3.18E+08
P22307-4;P22307	P22307-4;P22307	Non-specific lipid-t	SCP2	4	4	466	1	0.99774	2.81E+08
Q969Z3;X1WI34;Q	Q969Z3;X1WI34;Q	Mitochondrial ami	02-Mar	2	2	335	0.99982	1.2463	1.08E+08
P10586-2;P10586;	P10586-2;P10586	Receptor-type tyro	PTPRF	7	7	1898	0.99981	1.0419	1.90E+08
H7C2Z6;H7BXD5;P	H7C2Z6;H7BXD5;P	Grancalcin	GCA	2	2	146	0.99905	NaN	3.91E+07
P20618	P20618	Proteasome subuni	PSMB1	7	7	241	0.99868	0.7979	4.32E+08
O60256;O60256-3	O60256;O60256-3	Phosphoribosyl py	PRPSAP2	16	14	369	0.99842	0.94287	5.33E+09
Q14318;Q14318-2	Q14318;Q14318-2	Peptidyl-prolyl cis-	FKBP8	10	10	412	0.99841	1.1175	9.44E+08
P53004;C9J1E1	P53004	Biliverdin reductas	BLVRA	19	19	296	0.99833	0.8863	6.21E+09
F8W6I7;P09651-3;	F8W6I7;P09651-3	Heterogeneous nuc	HNRNPA1;HNRNPA	23	21	307	0.99828	0.97832	2.10E+10
Q5TA45-2;Q5TA45	Q5TA45-2;Q5TA45	Integrator complex	CPSF3L	8	8	499	0.99787	0.85507	3.01E+08
J3KTL2;Q07955;Q	J3KTL2;Q07955;Q	Serine/arginine-ric	SRSF1	3	3	253	0.99776	0.70444	1.93E+08
H7BYN4;Q02241-3	H7BYN4;Q02241-3	Kinesin-like proteir	KIF23	6	6	952	0.99774	0.91507	3.63E+08
Q9NYY8-2;Q9NYY8	Q9NYY8-2;Q9NYY8	FAST kinase domair	FASTKD2	9	9	648	0.99773	0.90773	5.52E+08
P23396;P23396-2;	P23396;P23396-2	40S ribosomal prot	RPS3	28	27	243	0.99759	0.9414	5.37E+10
B7ZAX5;Q01415-2;	B7ZAX5;Q01415-2	N-acetylgalactosam	GALK2	3	3	434	0.99755	0.84758	1.88E+08
Q13451;Q13451-2	Q13451	Peptidyl-prolyl cis-	FKBP5	13	13	457	0.99742	1.0294	8.87E+08
P50750;P50750-2;	P50750;P50750-2	Cyclin-dependent k	CDK9	10	9	372	0.99712	0.91682	7.55E+08
O00743;O00743-2	O00743;O00743-2	Serine/threonine-p	PPP6C	10	10	305	0.99705	0.8484	1.29E+09
O60934;A0A0C4D	O60934;A0A0C4D	Nibrin	NBN	5	5	754	0.99683	NaN	1.16E+08
K7EIG1;I3L4B5;I3L	K7EIG1		CLUH	41	0	1251	0.99676	0.94666	4.13E+09
Q6P3X3;F8WCH1	Q6P3X3	Tetratricopeptide r	TTC27	8	8	843	0.99675	1.0491	3.91E+09
C9J2P0;P51965;H	C9J2P0;P51965;H	Ubiquitin-conjugat	UBE2E1;UBE2E3;UI	4	4	147	0.99654	0.87147	1.78E+08
Q06124-3;Q06124	Q06124-3;Q06124	Tyrosine-protein ph	PTPN11	2	2	460	0.99588	1.3704	2.43E+08
P12236;Q9H0C2	P12236	ADP/ATP transloca	SLC25A6	29	10	298	0.99535	1.0598	5.42E+10
Q9BR61	Q9BR61	Acyl-CoA-binding d	ACBD6	2	2	282	0.99515	0.8308	1.03E+08
A0A0A0MRI2;Q9UI	A0A0A0MRI2;Q9UI	Sorting nexin-6;Sor	SNX6	2	2	418	0.99513	0.98045	5.08E+07
P32121;P32121-3;	P32121;P32121-3	Beta-arrestin-2	ARRB2;DKFZp686L	6	5	409	0.99497	0.64738	3.40E+08
O00186	O00186	Syntaxin-binding p	STXBP3	10	10	592	0.99467	1.1538	8.44E+08
Q12800-2;Q12800	Q12800-2;Q12800	Alpha-globin transc	TFCP2;UBP1	2	2	450	0.9943	NaN	2.08E+08
Q9BQ52;G5E9D5;C	Q9BQ52;G5E9D5;C	Zinc phosphodiest	ELAC2	18	18	826	0.99374	0.88583	2.95E+09
Q96L91-4;Q96L91	Q96L91-4;Q96L91	E1A-binding protei	EP400	12	12	3042	0.9936	0.69373	1.88E+08
Q13257;Q13257-2	Q13257	Mitotic spindle ass	MAD2L1	7	7	205	0.99306	0.91024	1.37E+09
O95336;M0R261;M	O95336;M0R261;M	6-phosphoglucono	PGLS	11	11	258	0.993	1.1103	4.13E+09
P55884;P55884-2;	P55884;P55884-2	Eukaryotic translat	EIF3B	26	26	814	0.99284	1.0946	5.60E+09
Q7KZJ0;J3QKK3;O4	Q7KZJ0;J3QKK3;O4	DNA repair protein	RAD51C	3	3	134	0.99213	0.8709	2.52E+08
Q96A65;Q96A65-2	Q96A65;Q96A65-2	Exocyst complex co	EXOC4	15	15	974	0.99192	0.89359	8.76E+08
Q9GZS3;H0YL19;H	Q9GZS3;H0YL19;H	WD repeat-contain	WDR61	9	9	305	0.99191	1.0128	2.21E+09
O75792	O75792	Ribonuclease H2 su	RNASEH2A	9	9	299	0.99171	1.0039	1.19E+09
H7BXI1;A0FGR8-2;	H7BXI1;A0FGR8-2;	Extended synaptot	ESYT2	8	8	884	0.99131	0.85175	8.14E+08
Q9BZF1-3;Q9BZF1-	Q9BZF1-3;Q9BZF1-	Oxysterol-binding p	OSBPL8	9	9	847	0.99123	1.0327	3.21E+08
Q9BQS8;Q9BQS8-4	Q9BQS8;Q9BQS8-4	FYVE and coiled-coi	FYCO1	2	2	1478	0.99115	0.92963	8.66E+07
O00442;O00442-2	O00442;O00442-2	RNA 3-terminal phc	RTCA	12	12	366	0.99081	0.91046	2.97E+09
P28288;P28288-2;	P28288;P28288-2	ATP-binding cassett	ABCD3	24	24	659	0.99038	0.91234	4.20E+09
I3L0E3;Q9Y2R5;E9	I3L0E3;Q9Y2R5;E9	28S ribosomal prot	MRPS17	5	5	225	0.99026	0.93315	6.13E+08
P06400	P06400	Retinoblastoma-as	RB1	7	7	928	0.99	0.8447	7.50E+08
Q86UA1;Q86UA1-2	Q86UA1;Q86UA1-2	Pre-mRNA-processi	PRPF39	4	4	669	0.98968	1.1999	2.85E+08
F8VYY9;P54619-2;I	F8VYY9;P54619-2;	5-AMP-activated pr	PRKAG1	8	8	280	0.98863	1.3388	5.37E+08
Q15650;H0YL91	Q15650	Activating signal co	TRIP4	3	3	581	0.98843	NaN	3.72E+07
Q9H2C0	Q9H2C0	Gigaxonin	GAN	4	4	597	0.98833	0.95615	2.35E+08
P19623;K7ESL0;K7	P19623	Spermidine synthas	SRM	17	17	302	0.98818	1.1397	6.90E+09
P14923;C9JTX4;C9	P14923;C9JTX4;C9	Junction plakoglob	JUP	7	5	745	0.98812	1.1524	4.63E+08
P63167;F8VXL2;F8	P63167;F8VXL2;F8	Dynein light chain	DYNLL1	5	4	89	0.98761	0.85249	1.52E+08
Q7Z3B4-2;Q7Z3B4	Q7Z3B4-2;Q7Z3B4	Nucleoporin p54	NUP54	2	2	291	0.98761	1.2388	1.94E+08
A0A0G2JNZ2;A0A0	A0A0G2JNZ2;A0A0	Protein scribble ho	SCRIB	7	6	1630	0.98726	0.79768	4.88E+08
A0A0A0MRM8;Q9U	A0A0A0MRM8;Q9U	Unconventional m	MYO6	35	35	1253	0.98721	0.96832	2.15E+09
Q14677;Q14677-3	Q14677;Q14677-3	Clathrin interactor	CLINT1	5	5	625	0.98668	1.1289	2.58E+08
Q86TP1;Q86TP1-2;	Q86TP1;Q86TP1-2	Protein prune hom	PRUNE	7	7	453	0.98625	1.0063	4.84E+08
B4DJ81;P28331-3;	B4DJ81;P28331-3;	NADH-ubiquinone	NDUFS1	7	7	611	0.98602	1.2	9.67E+08
Q15118;C9JKT3;Q	Q15118;C9JKT3;Q	[Pyruvate dehydro	PDK1	4	4	436	0.98556	1.0175	1.86E+08
P78345;Q5VUC9;C	P78345	Ribonuclease P pro	RPP38	3	3	283	0.98554	0.93616	1.23E+08
Q5JRX3;Q5JRX3-2;	Q5JRX3;Q5JRX3-2	Presequence prote	PITRM1	34	34	1037	0.9852	0.88856	4.57E+09

Q66K74-2;Q66K74	Q66K74-2;Q66K74	Microtubule-associ	MAP1S	8	8	1033	0.98504	0.82961	6.20E+08
Q9Y2S0;A0A0R4J2	Q9Y2S0;A0A0R4J2	DNA-directed RNA	POLR1D	6	6	133	0.98477	0.95432	3.00E+08
P48651-3;P48651	P48651-3;P48651	Phosphatidylserine	PTDSS1	2	2	301	0.98459	0.92205	4.81E+08
O43684-2;O43684	O43684-2;O43684	Mitotic checkpoint	BUB3	15	15	326	0.98307	0.97419	4.76E+09
Q5H928;Q99714-2	Q5H928;Q99714-2	3-hydroxyacyl-CoA	HSD17B10	2	2	169	0.98273	NaN	6.24E+07
Q15477;H7C5N0;H	Q15477	Helicase SKI2W	SKIV2L	28	28	1246	0.98268	1.0099	1.44E+09
Q8N684-2;Q8N684	Q8N684-2;Q8N684	Cleavage and polya	CPSF7	8	8	462	0.98261	1.2119	1.03E+09
P55735;A0A0C4DF	P55735;A0A0C4DF	Protein SEC13 hom	SEC13	8	8	322	0.98256	1.181	2.78E+09
P42677;Q5T4L4;C	P42677;Q5T4L4	40S ribosomal prot	RPS27	7	3	84	0.98173	0.84438	3.21E+09
P55010;H0YK29;H	P55010	Eukaryotic translat	EIF5	5	5	431	0.98173	1.1018	3.23E+08
O60341;O60341-2	O60341;O60341-2	Lysine-specific hist	KDM1A	10	10	852	0.98165	1.2354	8.00E+08
Q9UBB9;F6SQZ1;F	Q9UBB9	Tuftelin-interacting	TFIP11	7	7	837	0.98097	0.73338	2.08E+08
Q6P1L8	Q6P1L8	39S ribosomal prot	MRPL14	4	4	145	0.98048	1.0951	1.54E+08
Q5JVF3-3;Q5JVF3	Q5JVF3-3;Q5JVF3	PCI domain-contai	PCID2	13	13	376	0.98016	0.80238	5.94E+08
Q8TB36-2;Q8TB36	Q8TB36-2;Q8TB36	Ganglioside-induce	GDAP1	3	3	290	0.98003	0.78235	7.41E+07
Q9UKF6;G5E9W3;(	Q9UKF6;G5E9W3	Cleavage and polya	CPSF3	13	13	684	0.9798	0.94824	1.45E+09
M0R0N4;M0QYZ2;I	M0R0N4;M0QYZ2;	AP-2 complex subu	AP2S1	6	6	144	0.97937	0.86883	2.38E+08
Q9Y2H6-2;Q9Y2H6	Q9Y2H6-2;Q9Y2H6	Fibronectin type-III	FNDC3A	3	3	1142	0.97917	1.8365	1.17E+08
Q96HS1;Q96HS1-2	Q96HS1;Q96HS1-2	Serine/threonine-p	PGAM5	16	16	289	0.97899	0.90897	1.26E+09
Q06203;D6RE15;D	Q06203	Amidophosphoribo	PPAT	3	3	517	0.97852	1.7085	2.63E+08
O60502-4;O60502	O60502-4;O60502	Bifunctional protei	MGEA5	14	14	863	0.97815	0.87325	1.39E+09
Q6P1X5;H0YB55	Q6P1X5;H0YB55	Transcription initia	TAF2	2	2	1199	0.97802	1.049	7.97E+07
H3BSB3;H3BNT4;(	H3BSB3;H3BNT4;(	M-phase phosphop	MPHOSPH6	5	5	131	0.97759	0.63123	8.51E+07
P05141	P05141	ADP/ATP transloca	SLC25A5	28	12	298	0.97754	1.0827	2.77E+10
Q86UT6-2;Q86UT6	Q86UT6-2;Q86UT6	NLR family membe	NLRX1	7	7	921	0.97751	0.92085	2.30E+08
O60826	O60826	Coiled-coil domain	CCDC22	6	6	627	0.97722	1.0865	1.14E+08
P61201;P61201-2;	P61201;P61201-2	COP9 signalosome	COPS2	12	12	443	0.97711	1.2559	1.65E+09
Q7Z4Q2;Q7Z4Q2-2	Q7Z4Q2;Q7Z4Q2-2	HEAT repeat-contai	HEATR3	10	10	680	0.97693	0.89338	7.76E+08
Q8WVM8;Q8WVM	Q8WVM8;Q8WVM	Sec1 family domair	SCFD1	17	17	642	0.97668	1.0045	2.08E+09
K7EMQ8;J3QKS7;B	K7EMQ8;J3QKS7;B	SWI/SNF-related m	SMARCE1	3	3	177	0.97546	1.0537	1.09E+08
O15269;O15269-2	O15269	Serine palmitoyltra	SPTLC1	7	7	473	0.97523	0.94955	1.45E+09
B1AHD1;P55769	B1AHD1;P55769	NHP2-like protein 1	NHP2L1	4	4	132	0.9752	1.0214	1.10E+08
A0A087WTP3;Q92	A0A087WTP3;Q92	Far upstream elem	KHSRP	6	4	711	0.97494	1.0461	2.63E+08
Q92696;H0YLH3;H	Q92696;H0YLH3;H	Geranylgeranyl trar	RABGGTA	4	4	567	0.97456	1.1773	6.32E+08
P50991;P50991-2	P50991;P50991-2	T-complex protein	CCT4	36	36	539	0.97454	0.95324	5.48E+10
P35606-2;P35606;	P35606-2;P35606	Coatomer subunit	COPB2	33	33	877	0.97441	1.0503	5.77E+09
Q14571	Q14571	Inositol 1,4,5-trisp	ITPR2	10	7	2701	0.97404	1.0766	1.70E+08
P19784;H3BSA1;H	P19784;H3BSA1;H	Casein kinase II sub	CSNK2A2	7	7	350	0.97268	0.94895	4.10E+08
O94925-3;B8ZZA8;	O94925-3	Glutaminase kidne	GLS	13	2	598	0.97252	1.1738	1.91E+09
O15160;O15160-2	O15160;O15160-2	DNA-directed RNA	POLR1C	13	13	346	0.9723	0.98886	3.07E+09
P27348;E9PG15	P27348	14-3-3 protein thet	YWHAQ	8	3	245	0.97214	1.0989	2.49E+08
Q9Y333	Q9Y333	U6 snRNA-associate	LSM2	1	1	95	0.97145	1.2419	7.48E+07
H0YDU8;P53041;A	H0YDU8;P53041;A	Serine/threonine-p	PPP5C	4	4	485	0.97134	1.3127	9.83E+07
P13010;C9JZ81;H7	P13010	X-ray repair cross-c	XRCC5	46	46	732	0.97069	1.1983	3.12E+10
Q9HC21-2;Q9HC21	Q9HC21-2;Q9HC21	Mitochondrial thia	SLC25A19	6	6	263	0.97038	1.081	4.03E+08
Q2TAM5;E9PKH5;A	Q2TAM5;E9PKH5;A	Transcription facto	RELA	7	7	377	0.97002	0.86696	3.97E+08
Q8N8A6	Q8N8A6	ATP-dependent RN	DDX51	5	5	666	0.96997	0.81866	3.29E+08
Q8WUK0;Q8WUK0	Q8WUK0;Q8WUK0	Phosphatidylglycer	PTPMT1	6	6	201	0.9699	0.81699	4.88E+08
P13639	P13639	Elongation factor 2	EEF2	56	55	858	0.96989	1.1564	2.99E+10
Q99832;Q99832-3	Q99832;Q99832-3	T-complex protein	CCT7	41	41	543	0.96942	0.99349	2.86E+10
Q16555-2;Q16555	Q16555-2;Q16555	Dihydropyrimidina	DPYSL2	6	4	536	0.96921	1.2868	4.50E+08
Q8N6R0-3;Q8N6R0	Q8N6R0-3;Q8N6R0	Methyltransferase-l	METTL13	13	13	613	0.96898	0.99868	6.58E+08
P22033	P22033	Methylmalonyl-Co	MUT	6	6	750	0.96872	0.73904	2.10E+08
P31146;H3BTU6;H	P31146;H3BTU6;H	Coronin-1A;Coroni	CORO1A	2	2	461	0.96865	1.0326	7.01E+07
O75489;E9PS48;O	O75489	NADH dehydrogena	NDUFS3	12	12	264	0.96856	1.2545	1.68E+09
F5H365;Q15436;Q	F5H365;Q15436;Q	Protein transport p	SEC23A	14	12	736	0.96847	1.0368	1.98E+09
P15927;P15927-2;	P15927;P15927-2	Replication protein	RPA2	8	8	270	0.96833	0.94141	1.57E+09
P41240;H3BUM9;I	P41240	Tyrosine-protein ki	CSK	14	14	450	0.96819	1.1839	1.77E+09
A0A0B4J1S8;Q9UB	A0A0B4J1S8;Q9UB	Phosphatidylinosit	PI4KB	6	6	828	0.96802	1.0019	2.57E+08
Q13085;Q13085-4	Q13085;Q13085-4	Acetyl-CoA carboxy	ACACA	48	48	2346	0.96788	1.1415	3.69E+09
P49189;P49189-2	P49189;P49189-2	4-trimethylaminob	ALDH9A1	19	19	494	0.96774	1.0497	7.56E+09
D6RAN4;P32969;E	D6RAN4;P32969;E	60S ribosomal prot	RPL9	11	11	182	0.9677	1.159	6.66E+09
Q86U42-2;Q86U42	Q86U42-2;Q86U42	Polyadenylate-binc	PABPN1	2	2	296	0.96689	1.139	3.91E+08
Q1KMD3;H3BQZ7	Q1KMD3;H3BQZ7	Heterogeneous nuc	HNRNPUL2;HNRNF	7	7	747	0.96673	0.92057	4.24E+08
A0A0U1RQC9;P04(	A0A0U1RQC9;P04(	Cellular tumor anti	TP53	15	15	410	0.96636	0.93811	1.52E+09
P05388;F8VWS0;P	P05388;F8VWS0;P	60S acidic ribosom	RPLP0;RPLP0P6	21	21	317	0.96594	1.015	4.53E+10
Q9UN86-2;Q9UN8	Q9UN86-2;Q9UN8	Ras GTPase-activati	G3BP2	9	8	449	0.96577	1.0181	1.44E+09
Q9NVH2-3;Q9NVH	Q9NVH2-3;Q9NVH	Integrator complex	INTS7	16	16	942	0.96554	0.84227	7.02E+08
P09110;H7C131;C	P09110;H7C131;C	3-ketoacyl-CoA thi	ACAA1	5	5	424	0.96541	1.0097	5.69E+08
Q12797-10;Q1279	Q12797-10;Q1279	Aspartyl/asparagin	ASPH	5	5	729	0.96498	0.72386	5.56E+08
H0Y7A7;P62158;E	H0Y7A7;P62158;E	Calmodulin	CALM2;CALM1;CAL	6	6	187	0.9648	0.66445	3.88E+08
Q3MHD2;Q3MHD2	Q3MHD2;Q3MHD2	Protein LSM12 hon	LSM12	8	8	195	0.96477	0.84531	1.75E+09
E9PIR7;F8W809;A(	E9PIR7;F8W809;A(	Thioredoxin reduct	GML;TXNRD1	5	5	482	0.9643	1.4904	4.80E+08
O94973;O94973-2	O94973;O94973-2	AP-2 complex subu	AP2A2	27	18	939	0.96407	0.883	3.17E+09
O95831-3;O95831	O95831-3;O95831	Apoptosis-inducing	AIFM1	27	27	609	0.96362	1.0244	7.17E+09
H7C0Q6;Q9C037-3	H7C0Q6;Q9C037-3	Tripartite motif-co	TRIM4	2	2	202	0.96341	2.0449	3.08E+09
P33176	P33176	Kinesin-1 heavy cha	KIF5B	33	24	963	0.96309	0.92068	2.56E+09
Q9Y3B2;R4GMQ7;I	Q9Y3B2;R4GMQ7;I	Exosome complex c	EXOSC1	8	8	195	0.96262	0.88967	4.10E+08
O95340;O95340-2	O95340;O95340-2	Bifunctional 3-pho	PAPSS2	6	6	614	0.96249	0.88553	2.83E+08
Q9H0C8;F8SNU7;H	Q9H0C8;F8SNU7;H	Integrin-linked kina	ILKAP;ILKAP3	15	15	392	0.96239	0.87566	1.26E+09
B4DTS2;Q9BZL6;Q	B4DTS2;Q9BZL6;Q	Serine/threonine-p	PRKD2	4	4	888	0.96176	0.91441	2.99E+08
G3V5T9;P24941-2;	G3V5T9;P24941-2	Cyclin-dependent k	CDK2	7	5	346	0.9614	0.91718	1.11E+09
O15143;C9JBJ7;C9	O15143	Actin-related prote	ARPC1B	5	5	372	0.96138	1.2518	4.22E+08
A0A024RA52;P257	A0A024RA52;P257	Proteasome subuni	PSMA2	6	6	234	0.96129	0.94866	3.86E+08
U3KQC1;A0A0A0M	U3KQC1;A0A0A0M	WD repeat-contain	WDR18	10	10	394	0.96113	1.0311	6.50E+08
Q5TH30;Q9UGV2-2	Q5TH30;Q9UGV2-2	Protein NDRG3	NDRG3	3	3	388	0.96084	1.2525	2.80E+08
Q9UKX7-2;Q9UKX7	Q9UKX7-2;Q9UKX7	Nuclear pore comp	NUP50	3	3	440	0.96071	0.74677	1.16E+08
P22059;H0YCV6	P22059;H0YCV6	Oxysterol-binding p	OSBP	2	2	807	0.95992	NaN	1.19E+08
O43491;E9PHY5;O	O43491;E9PHY5;O	Band 4.1-like prote	EPB41L2	30	30	1005	0.95969	0.93819	3.26E+09
A0A0X1KG71;Q8W	A0A0X1KG71;Q8W	Negative elongatio	NELFB	7	7	628	0.95944	1.1159	4.76E+08
Q9UNS2;Q9UNS2-2	Q9UNS2;Q9UNS2-2	COP9 signalosome	COPS3	4	4	423	0.95867	1.2745	1.49E+08
H0YH69;Q9HBU6;I	H0YH69;Q9HBU6;I	Ethanolamine kina	ETNK1	2	2	425	0.95859	0.79258	5.50E+07
O14874-2;O14874	O14874-2;O14874	[3-methyl-2-oxobu	BCKDK	2	2	335	0.95816	0.76157	2.24E+08

A3KFL1;A3KFL5;A3	A3KFL1;A3KFL5;A3	Exosome complex (	EXOSC2	2	2	200	0.95691	1.1498	1.22E+08
Q13546;Q13546-2	Q13546;Q13546-2	Receptor-interacti	RIPK1	7	7	671	0.95677	1.2647	1.77E+08
Q15042;Q15042-3	Q15042;Q15042-3	Rab3 GTPase-activa	RAB3GAP1	16	16	981	0.95642	1.0709	7.64E+08
C9JOI9;Q86WB0;Q	C9JOI9;Q86WB0;Q	Nuclear-interacting	ZC3HC1	3	3	459	0.9559	0.99262	4.40E+08
O15357;O15357-2	O15357;O15357-2	Phosphatidylinosit	INPPL1	3	3	1258	0.95556	0.76967	1.40E+08
Q9Y678;H0Y8X7;D	Q9Y678	Coatomer subunit (	COPG1	40	36	874	0.955	0.91432	9.12E+09
Q9UID3-2;Q9UID3	Q9UID3-2;Q9UID3	Vacuolar protein sc	VPS51	7	7	658	0.95494	0.88483	3.90E+08
Q9H7B2;Q5VXN0	Q9H7B2;Q5VXN0	Ribosome producti	RPF2	4	4	306	0.95436	1.1682	2.11E+08
B4DGU4;P35222	B4DGU4;P35222	Catenin beta-1	CTNNB1	6	4	774	0.95434	1.0089	2.10E+08
Q92597;Q92597-3	Q92597;Q92597-3	Protein NDRG1	NDRG1	8	8	394	0.95402	0.8806	7.87E+08
Q147X3;Q147X3-2	Q147X3;Q147X3-2	N-alpha-acetyltran	NAA30	7	7	362	0.95389	0.91702	5.60E+08
Q92900-2;Q92900	Q92900-2;Q92900	Regulator of nonse	UPF1	47	47	1118	0.95388	1.1442	9.40E+09
P25788-2;P25788	P25788-2;P25788	Proteasome subuni	PSMA3	9	9	248	0.95379	0.94585	1.19E+09
Q06587;Q06587-2	Q06587;Q06587-2	E3 ubiquitin-protei	RING1	4	3	406	0.95377	1.1408	5.91E+08
Q99615;Q99615-2	Q99615;Q99615-2	DnaJ homolog subf	DNAJC7	18	18	494	0.95343	1.1256	5.68E+08
O43660;O43660-2	O43660;O43660-2	Pleiotropic regulat	PLRG1	8	8	514	0.95306	1.1893	5.72E+08
P49841;P49841-2	P49841;P49841-2	Glycogen synthase	GSK3B	3	2	420	0.95303	0.90579	2.52E+08
C9JP03;Q5T6P2;C	C9JP03;Q5T6P2;C	SLAIN motif-contai	SLAIN1	3	3	99	0.95285	NaN	8.31E+07
Q86YS7;Q86YS7-2;	Q86YS7;Q86YS7-2;	C2 domain-contain	C2CD5	2	2	1000	0.95238	1.1395	1.34E+08
Q5RIB5;Q5JTY2;A0	Q5RIB5;Q5JTY2;A0	COBW domain-con	CBWD5;CBWD3;CE	2	2	113	0.95207	1.1347	1.71E+08
A2ABE9;H7C2J4;AC	A2ABE9;H7C2J4;AC	MutS protein homc	MSH5	2	2	333	0.95205	0.95809	1.43E+08
Q96GK7;C9JGM0;(	Q96GK7;C9JGM0;(	Fumarylacetoaceta	FAHD2A;FAHD2B	4	4	314	0.95144	1.0237	2.31E+08
Q13526;K7EN45;K	Q13526;K7EN45;K	Peptidyl-prolyl cis-	PIN1	8	8	163	0.95141	1.2501	1.56E+09
P30050;P30050-2	P30050;P30050-2	60S ribosomal prot	RPL12	10	10	165	0.95122	1.1514	4.35E+09
A0A087WUZ3;Q01	A0A087WUZ3;Q01	Spectrin beta chain	SPTBN1	9	9	2366	0.95049	1.3516	3.76E+08
C9JP16;O75718	C9JP16;O75718	Cartilage-associate	CRTAP	3	3	358	0.94944	1.416	1.34E+08
Q02252-2;Q02252	Q02252-2;Q02252	Methylmalonate-se	ALDH6A1	7	7	522	0.94936	0.8187	3.64E+08
Q96KP1	Q96KP1	Exocyst complex cc	EXOC2	9	9	924	0.94903	0.91267	4.75E+08
P62495;B7Z7P8;P(	P62495;B7Z7P8;P(	Eukaryotic peptide	ETF1	5	5	437	0.9481	1.6214	4.72E+08
Q9HCS7	Q9HCS7	Pre-mRNA-splicing	XAB2	11	11	855	0.94795	0.89631	3.34E+08
A0A087WVD7;Q9Y	A0A087WVD7;Q9Y	Adenylate kinase is	AK6;TAF9	4	4	109	0.94779	1.0372	6.66E+08
P27707;D6RFG8;D	P27707;D6RFG8	Deoxycytidine kina	DCK	5	5	260	0.94744	1.1901	4.70E+08
Q13158	Q13158	FAS-associated deal	FADD	1	1	208	0.94728	0.98328	6.73E+07
Q9NTJ3;E9PD53;Q	Q9NTJ3;E9PD53;Q	Structural mainten	SMC4	63	63	1288	0.94707	1.0428	5.28E+09
Q5HYK3;F8VVX6;B	Q5HYK3;F8VVX6;B	2-methoxy-6-polyp	COQ5	6	6	327	0.947	1.0594	2.03E+08
Q86T03;Q86T03-2;	Q86T03;Q86T03-2;	Type 1 phosphatidy	TMEM55B	2	2	277	0.94694	0.74947	3.29E+08
P60604;F8WCB9;F	P60604;F8WCB9;F	Ubiquitin-conjugat	UBE2G2	2	2	165	0.94651	0.97927	1.44E+08
Q86X55-1;Q86X55	Q86X55-1;Q86X55	Histone-arginine m	CARM1	14	14	585	0.94642	1.06	2.19E+09
Q16658;C9JFC0;AC	Q16658	Fascin	FSCN1	14	14	493	0.94614	1.0664	2.64E+09
P55210;P55210-3;	P55210;P55210-3;	Caspase-7;Caspase-	CASP7	6	4	303	0.94599	1.006	5.58E+08
A0A0U1RR46;A0AC	A0A0U1RR46;A0AC	InaD-like protein	INADL	1	1	683	0.94561	NaN	9.91E+06
P42704;A0A0C4DC	P42704	Leucine-rich PPR m	LRPPRC	77	77	1394	0.94539	1.0889	2.12E+10
P19367;P19367-4;	P19367;P19367-4;	Hexokinase-1	HK1	43	39	917	0.94534	0.97991	7.76E+09
E9PEB5;Q96AE4;Q	E9PEB5;Q96AE4;Q	Far upstream elem	FUBP1	9	5	655	0.94533	0.89679	3.00E+08
P48444;B0YIW6;P	P48444;B0YIW6;P	Coatomer subunit (	ARCN1	27	27	511	0.94502	0.97507	7.17E+09
Q6P1M0;Q6P1M0-	Q6P1M0	Long-chain fatty ac	SLC27A4	8	8	643	0.94491	1.0553	6.62E+08
Q96P48-3;Q96P48	Q96P48-3;Q96P48	Arf-GAP with Rho-(	ARAP1	9	9	1439	0.94474	0.85649	3.20E+08
Q5JY65;Q9BZJ0-2;(	Q5JY65;Q9BZJ0-2;(	Crooked neck-like p	CRNKL1	8	8	836	0.94468	1.0322	5.80E+08
Q70CQ2-3;Q70CQ2	Q70CQ2-3;Q70CQ2	Ubiquitin carboxyl	USP34	7	7	3312	0.94424	1.1548	1.55E+08
O75534-2;O75534	O75534-2;O75534	Cold shock domain	CSDE1	28	28	767	0.94405	1.1527	3.78E+09
Q9H7Z7;A6NHH0;Q	Q9H7Z7	Prostaglandin E syn	PTGES2	7	7	377	0.94388	1.2409	6.14E+08
Q3B726	Q3B726	DNA-directed RNA	TWISTNB	3	3	338	0.94382	NaN	1.14E+08
Q9Y3I0	Q9Y3I0	tRNA-splicing ligase	RTCB	24	24	505	0.94345	1.1693	1.05E+10
C9JG97;C9JEH3;Q1	C9JG97;C9JEH3;Q1	Angio-associated m	AAMP	5	5	415	0.94237	1.0511	9.56E+08
Q9P265	Q9P265	Disco-interacting p	DIP2B	2	2	1576	0.94172	1.0365	1.80E+07
Q9HD47-4;Q9HD4	Q9HD47-4;Q9HD4	Ran guanine nuclec	RANGRF	2	2	118	0.94156	NaN	3.96E+07
O95202;O95202-2	O95202	LETM1 and EF-hand	LETM1	7	7	739	0.94149	0.97872	3.68E+08
Q9NYJ8;Q9NYJ8-2;	Q9NYJ8;Q9NYJ8-2	TGF-beta-activated	TAB2	5	5	693	0.94088	0.8716	1.78E+08
O14925;Q5SRD1;B	O14925;Q5SRD1;B	Mitochondrial imp	TIMM23;TIMM23B	4	4	209	0.94068	0.99595	1.01E+09
P31040;D6RFM5;P	P31040;D6RFM5;P	Succinate dehydro	SDHA	13	13	664	0.94052	1.3927	6.42E+08
P42285;H0YAC4;H	P42285	Superkiller viralicic	SKIV2L2	35	35	1042	0.94007	0.97944	5.22E+09
P11388;P11388-2;	P11388;P11388-2;	DNA topoisomeras	TOP2A	51	41	1531	0.93985	1.1234	6.61E+09
F8VPD4;P27708;H	F8VPD4;P27708	CAD protein;Glutar	CAD	85	82	2162	0.93971	0.96669	3.50E+10
P10768;X6RA14;H	P10768;X6RA14;H	S-formylglutathion	ESD	8	8	282	0.93941	1.2307	3.40E+09
Q9Y679-2;Q9Y679;	Q9Y679-2;Q9Y679;	Ancient ubiquitous	AUP1	9	9	410	0.93939	0.91899	6.29E+08
Q8IVD9	Q8IVD9	NudC domain-cont	NUDCD3	4	4	361	0.93932	1.1281	1.23E+08
Q15058	Q15058	Kinesin-like protein	KIF14	4	4	1648	0.93915	NaN	5.28E+07
Q9UBE0;B3KNJ4;Q	Q9UBE0;B3KNJ4;Q	SUMO-activating en	SAE1	27	27	346	0.93875	0.92526	6.57E+09
P13804-2;P13804;	P13804-2;P13804;	Electron transfer fla	ETFA	12	12	284	0.93838	1.1851	5.26E+09
Q5TDF0;Q9BSD7	Q5TDF0;Q9BSD7	Cancer-related nuc	NTPCR	7	7	228	0.93828	0.94929	1.98E+09
P14625;Q96GW1;I	P14625	Endoplasmin	HSP90B1	33	31	803	0.93728	1.3513	7.44E+09
B2R4S9;U3KQK0;Q	B2R4S9;U3KQK0;Q	Histone H2B;Histor	HIST1H2BC;HIST1H	11	0	126	0.93662	1.3767	1.04E+08
A0A087X1A5;O957	A0A087X1A5;O957	Double-stranded RI	STAU1	12	11	493	0.9366	0.85522	1.25E+09
O43252	O43252	Bifunctional 3-pho	PAPSS1	11	11	624	0.93653	1.0517	1.65E+09
Q9Y2Z4;H0YHS6	Q9Y2Z4;H0YHS6	Tyrosine--tRNA liga	YARS2	8	8	477	0.9365	1.1694	9.55E+08
O95573;F5GWH2;I	O95573	Long-chain-fatty-ac	ACSL3	21	19	720	0.93638	0.95259	2.83E+09
Q9BTE7;E9PM04;H	Q9BTE7;E9PM04;H	DCN1-like protein 5	DCUN1D5	4	4	237	0.936	0.99137	7.90E+07
P22626;P22626-2;	P22626;P22626-2;	Heterogeneous nuc	HNRNPA2B1	25	24	353	0.93564	1.0194	1.54E+10
E9PEX6;P09622;P(	E9PEX6;P09622;P(	Dihydrolipoyl dehy	DLD	12	12	486	0.93552	0.89604	1.66E+09
P07814;V9GYZ6;V	P07814;V9GYZ6	Bifunctional glutan	EPRS	70	70	1512	0.93548	1.0741	1.93E+10
O15144;H7C3F9	O15144;H7C3F9	Actin-related prote	ARPC2	6	6	300	0.93525	1.5635	3.43E+08
F8VZJ2;F8W0W4;H	F8VZJ2;F8W0W4;H	Nascent polypeptic	NACA	5	5	136	0.93449	1.2181	4.34E+09
O95394;O95394-3	O95394;O95394-3	Phosphoacetylgluc	PGM3	14	14	542	0.93442	1.1527	7.60E+08
Q8WUM4;Q8WUM	Q8WUM4;Q8WUM	Programmed cell d	PDCD6IP	43	43	868	0.9341	1.0085	5.97E+09
G3V5T0;A0A0C4DF	G3V5T0;A0A0C4DF	Maleylacetoacetate	GSTZ1	6	6	202	0.93378	1.0461	5.40E+08
Q9P035;H3BS72;H	Q9P035;H3BS72;H	Very-long-chain (3F	PTPLAD1	14	14	362	0.93364	1.0824	4.34E+09
Q14683;G8JLG1;H	Q14683;G8JLG1	Structural mainten	SMC1A	69	69	1233	0.93335	0.94949	7.44E+09
A8MX75;P18074;E	A8MX75;P18074;E	TFIIH basal transcri	ERCC2	5	5	706	0.93333	0.96854	3.90E+08
P57053	P57053	Histone H2B type F	H2BFS	11	1	126	0.93309	1.2814	1.65E+10
P52732	P52732	Kinesin-like protein	KIF11	18	18	1056	0.9324	0.77763	6.70E+08
Q6PJ69;H0YGS7;H	Q6PJ69;H0YGS7;H	Tripartite motif-cor	TRIM65	3	3	517	0.93228	0.93572	1.51E+08
P33991;E5RG31;E	P33991	DNA replication lic	MCM4	41	41	863	0.93197	0.8552	1.30E+10
Q6P6C2;Q6P6C2-1	Q6P6C2;Q6P6C2-1	RNA demethylase A	ALKBH5	2	2	394	0.93196	NaN	1.61E+08

O00148;O00148-2	O00148;O00148-2	ATP-dependent RN	DDX39A	25	10	427	0.93157	1.0724	1.59E+10
P50416-2;P50416	P50416-2;P50416	Carnitine O-palmit	CPT1A	7	7	756	0.93088	1.3853	5.31E+08
Q13409-3;Q13409	Q13409-3;Q13409	Cytoplasmic dynei	DYNC1I2	11	11	612	0.93064	1.0781	4.78E+08
Q7Z3C6;Q7Z3C6-2	Q7Z3C6;Q7Z3C6-2	Autophagy-related	ATG9A	10	10	839	0.93058	0.85551	4.22E+08
J3KN36;Q5JPE7-2;	J3KN36;Q5JPE7-2;	Nodal modulator 2	NOMO3;NOMO2	9	1	1267	0.93016	1.013	4.50E+08
Q13616;A0A0C4D	Q13616;A0A0C4D	Cullin-1	CUL1	15	15	776	0.92998	1.1654	1.48E+09
Q9Y5S2;H0YLY0	Q9Y5S2;H0YLY0	Serine/threonine-p	CDC42BPB	7	6	1711	0.92971	0.8416	1.79E+08
A0A0A0MTR7;A0A	A0A0A0MTR7;A0A	E3 ubiquitin-protei	RNF213	38	38	5207	0.92962	1.0732	1.20E+09
Q9UBT2;K7EPL2;Q	Q9UBT2;K7EPL2;Q	SUMO-activating e	UBA2	7	7	640	0.92939	1.4687	2.71E+08
B1AJY5;B1AJY7;O7	B1AJY5;B1AJY7;O7	26S proteasome no	PSMD10	14	14	185	0.92925	1.0164	2.12E+09
P55072;C9JUP7;C	P55072	Transitional endop	VCP	47	47	806	0.92898	0.79715	1.62E+10
Q93077;Q7L7L0;P	Q93077;Q7L7L0;P	Histone H2A type 1	HIST1H2AC;HIST3H	6	1	130	0.92874	1.3999	8.76E+08
Q16763;K7EPJ1	Q16763;K7EPJ1	Ubiquitin-conjugat	UBE2S	4	4	222	0.92852	1.0079	1.69E+08
Q9BTE3-2;Q9BTE3;	Q9BTE3-2;Q9BTE3;	Mini-chromosome	MCMBP	8	8	640	0.92829	1.0348	2.78E+08
H0Y645;B0QY35;B	H0Y645;B0QY35;B	Casein kinase I isofc	CSNK1E;CSNK1D	3	3	270	0.92824	1.1656	1.23E+08
P50502;H7C3I1;F6	P50502;H7C3I1;F6	Hsc70-interacting p	ST13;ST13P4;ST13	6	6	369	0.92819	1.148	1.28E+09
P09960-4;P09960	P09960-4;P09960	Leukotriene A-4 hy	LTA4H	11	11	587	0.92818	1.2776	8.08E+08
O94776;O94776-2	O94776;O94776-2	Metastasis-associat	MTA2	16	11	668	0.92803	1.2009	1.21E+09
O75306-2;O75306	O75306-2;O75306	NADH dehydrogen	NDUFS2	12	12	457	0.92797	1.0301	1.27E+09
F8VQX6;H0YI09;Q	F8VQX6;H0YI09;Q	Methyltransferase-l	METTL7A	2	2	180	0.92773	1.5027	8.62E+07
P45974-2;P45974	P45974-2;P45974	Ubiquitin carboxyl	USP5	23	22	835	0.92747	1.0653	1.81E+09
Q9BUP3-3;Q9BUP	Q9BUP3-3;Q9BUP	Oxidoreductase HT	HTATIP2	7	7	276	0.92617	0.73112	3.44E+08
Q9NVX2;A0A0A0M	Q9NVX2;A0A0A0M	Notchless protein h	NLE1	9	9	485	0.92617	0.91348	1.26E+09
O43913;O43913-2	O43913;O43913-2	Origin recognition	ORC5	9	9	435	0.92612	1.2184	7.40E+08
P56537;A0A0U1R(	P56537;A0A0U1R(	Eukaryotic translat	EIF6	3	3	245	0.9261	1.2671	2.87E+08
Q92572;F5H459	Q92572;F5H459	AP-3 complex subu	AP3S1	7	7	193	0.92608	1.0425	2.52E+08
Q99733;Q99733-2	Q99733;Q99733-2	Nucleosome assem	NAP1L4	9	7	375	0.9258	1.2856	2.45E+08
G3V4F2;A0A087X(	G3V4F2;A0A087X(	Acyl-coenzyme A th	ACOT1;ACOT2	11	11	395	0.92539	0.85463	1.12E+09
E9PH64;E7EWZ0;E	E9PH64;E7EWZ0;E	NADH dehydrogen	NDUFB9	2	2	168	0.92509	NaN	7.52E+07
H0YBS1;Q75QN2-2	H0YBS1;Q75QN2-2	Integrator complex	INTS8	6	6	800	0.92506	0.87451	2.31E+08
Q6P2Q9;I3L0J9;I3I	Q6P2Q9	Pre-mRNA-processi	PRPF8	92	92	2335	0.92493	1.0796	1.41E+10
Q96I99;E9PDQ8;Q	Q96I99;E9PDQ8;Q	Succinyl-CoA ligase	SUCLG2	12	12	432	0.92493	1.0917	1.78E+09
P30153;B3KQV6;C	P30153;B3KQV6;C	Serine/threonine-p	PPP2R1A	16	16	589	0.92459	0.98502	1.92E+09
O95400	O95400	CD2 antigen cytopl	CD2BP2	5	5	341	0.92435	1.1686	4.52E+08
Q6GMV2;E2QRN5;I	Q6GMV2;E2QRN5;	SET and MYND dom	SMYD5	2	2	418	0.92394	1.5931	2.00E+08
J3KRR7;Q9NQC7-2	J3KRR7;Q9NQC7-2	Ubiquitin carboxyl	FAM134C;CYLD	1	1	910	0.92389	NaN	5.55E+07
P13984	P13984	General transcripti	GTF2F2	3	3	249	0.92372	1.1426	9.95E+07
P36404;V9GYD0;P	P36404;V9GYD0;P	ADP-ribosylation fa	ARL2;ARL2-SNX15	10	10	184	0.92355	1.0829	1.18E+09
D6REX3;O94979-6	D6REX3;O94979-6	Protein transport p	SEC31A	25	25	1251	0.92326	1.1526	2.98E+09
O75155-2;O75155	O75155-2;O75155	Cullin-associated N	CAND2	13	10	1119	0.92279	0.89572	6.47E+08
D6R9P3;D6RD18;D	D6R9P3;D6RD18;D	Heterogeneous nuc	HNRNPAB	12	12	280	0.92257	1.1807	4.78E+09
P17987;E7EQR6;E7	P17987;E7EQR6;E7	T-complex protein	TCP1	35	35	556	0.92242	1.0278	4.39E+10
Q969X5-2;Q969X5	Q969X5-2;Q969X5	Endoplasmic reticu	ERGIC1	3	3	198	0.92241	1.1206	1.74E+08
D6RIY6;Q06265;Q	D6RIY6;Q06265;Q	Exosome complex c	EXOSC9	4	4	423	0.92235	1.3797	7.18E+08
Q01518;Q01518-2	Q01518;Q01518-2	Adenylyl cyclase-as	CAP1	13	13	475	0.92205	1.4511	1.38E+09
Q9NXE4-2;Q9NXE4	Q9NXE4-2;Q9NXE4	Sphingomyelin pho	SMPD4	8	8	798	0.92191	0.92868	6.35E+08
Q13200;Q13200-3	Q13200;Q13200-3	26S proteasome no	PSMD2	41	41	908	0.92171	0.95999	8.41E+09
Q14152-2;Q14152	Q14152-2;Q14152	Eukaryotic translat	EIF3A	32	32	1348	0.92151	1.1318	5.16E+09
Q9UJU6;Q9UJU6-2	Q9UJU6;Q9UJU6-2	Drebrin-like protei	DBNL	8	8	430	0.92127	1.2642	3.50E+08
Q5VWZ2-2;Q5VWZ	Q5VWZ2-2;Q5VWZ	Lysophospholipase	LYPLAL1	6	6	221	0.92078	1.4849	4.59E+08
Q92890;Q92890-1	Q92890;Q92890-1	Ubiquitin fusion de	UFD1L	4	4	307	0.92073	1.2857	8.89E+08
Q9BXW9-3;Q9BXW	Q9BXW9-3;Q9BXW	Fanconi anemia gro	FANCD2	8	8	1249	0.92063	1.0309	2.62E+08
E9PF18;A0A0A0M	E9PF18;A0A0A0M	Hydroxyacyl-coenz	HADH	4	4	318	0.92011	NaN	2.46E+08
O75153	O75153	Clustered mitocho	CLUH	41	2	1309	0.92002	0.68664	5.28E+07
Q9UHR6	Q9UHR6	Zinc finger HIT dom	ZNHIT2	3	3	403	0.91947	0.93591	1.50E+08
H3BND4;Q6P996-3	H3BND4;Q6P996-3	Pyridoxal-depende	PDXDC1	11	11	806	0.91937	1.1782	6.61E+08
A0A088AWN3;A0A	A0A088AWN3;A0A	Dedicator of cytoki	DOCK9	2	2	2079	0.91929	1.181	5.71E+07
A0A0C4DFM7;Q5T	A0A0C4DFM7;Q5T	Terminal uridylyltr	ZCCHC11	3	3	1645	0.91867	0.77757	9.40E+07
Q96EK6;G3V5E4;G	Q96EK6;G3V5E4;G	Glucosamine 6-phc	GNPNAT1	7	7	184	0.91866	1.2111	8.40E+08
Q00325-2;Q00325	Q00325-2;Q00325	Phosphate carrier p	SLC25A3	18	18	361	0.91863	0.90878	1.21E+10
Q13112	Q13112	Chromatin assembl	CHAF1B	3	3	559	0.91816	1.022	3.09E+08
Q96HR8-2;Q96HR8	Q96HR8-2;Q96HR8	H/ACA ribonucleop	NAF1	1	1	389	0.91787	0.90776	1.01E+08
Q96EY5-2;Q96EY5;	Q96EY5-2;Q96EY5;	Multivesicular bod	MVB12A	2	2	233	0.91783	NaN	1.58E+08
D6RAX7;D6RFN0;C	D6RAX7;D6RFN0;C	COP9 signalosome	COPS4	9	9	420	0.91775	1.1913	5.20E+08
Q9BQA1;Q9BQA1-2	Q9BQA1;Q9BQA1-2	Methylosome prot	WDR77	7	7	342	0.91748	1.4588	1.02E+09
O95239;O95239-2	O95239;O95239-2	Chromosome-asso	KIF4A	9	8	1232	0.91718	0.93823	2.67E+08
Q15084-3;Q15084	Q15084-3;Q15084	Protein disulfide-is	PDIA6	14	14	437	0.91693	0.99681	5.73E+09
Q15648-3;Q15648	Q15648-3;Q15648	Mediator of RNA pc	MED1	1	1	556	0.91627	1.1362	6.03E+07
Q8WUA4;H0Y4Q6;	Q8WUA4;H0Y4Q6;	General transcripti	GTF3C2	6	6	911	0.91611	0.71799	1.41E+08
Q9H3U1-2;Q9H3U	Q9H3U1-2;Q9H3U	Protein unc-45 hor	UNC45A	33	33	929	0.916	1.033	3.71E+09
P15374;A0A087W	P15374;A0A087W	Ubiquitin carboxyl	UCHL3	4	4	230	0.91577	1.4523	1.37E+08
A0A087X1F4;Q9H9	A0A087X1F4;Q9H9	Mediator of RNA pc	MED20	2	2	211	0.9157	1.1434	1.34E+08
P53007;B4DP62	P53007;B4DP62	Tricarboxylate tran	SLC25A1	11	11	311	0.91454	0.82511	2.81E+09
A0A0U1RR32;A0A	A0A0U1RR32;A0A	Histone H2A type 1	HIST1H2AJ;HIST1H	6	1	169	0.91425	1.2117	1.64E+10
P49588;P49588-2;	P49588;P49588-2	Alanine--tRNA ligas	AARS	37	37	968	0.91414	1.2464	4.28E+09
G5E975;Q12824-2	G5E975;Q12824-2	SWI/SNF-related m	SMARCB1	6	1	394	0.914	1.0441	9.38E+08
Q99570;D6RJ98;D	Q99570	Phosphoinositide 3	PIK3R4	16	16	1358	0.91379	0.96865	2.81E+09
Q5SWX3;A0A0A0M	Q5SWX3;A0A0A0M	Calcium/calmoduli	CAMK2G	8	3	516	0.91361	1.0155	5.90E+08
O75083;O75083-3	O75083;O75083-3	WD repeat-contain	WDR1	21	21	606	0.91356	1.2696	6.68E+09
Q92769-3;Q92769	Q92769-3;Q92769	Histone deacetylas	HDAC2	8	4	458	0.913	0.90967	5.05E+08
Q9UMS4;F5GY56;F	Q9UMS4;F5GY56	Pre-mRNA-processi	PRPF19	13	13	504	0.91226	1.2214	3.90E+09
Q9BW27;J3KT10;C	Q9BW27;J3KT10;C	Nuclear pore comp	NUP85	12	12	656	0.91223	1.1831	1.47E+09
F8VSA6;E9PS38;S4	F8VSA6;E9PS38;S4	NEDD8	NEDD8;NEDD8-MD	2	2	50	0.91208	0.91358	7.93E+08
Q9C0B7	Q9C0B7	Transport and Golg	TANGO6	8	8	1094	0.91202	0.79889	2.64E+08
Q96EK5;A0A0D9SF	Q96EK5	KIF1-binding prote	KIAA1279	10	10	621	0.91156	1.1707	1.51E+09
A8MTY9;O14972-2	A8MTY9;O14972-2	Down syndrome cr	DSCR3	4	4	249	0.91087	0.94278	4.09E+08
P52789;E9PB90;P5	P52789;E9PB90	Hexokinase-2	HK2	29	25	917	0.9104	1.0747	2.17E+09
O00399;E5RK00	O00399	Dynactin subunit 6	DCTN6	4	4	190	0.90996	0.90333	1.05E+08
Q8WYP5;Q8WYP5-	Q8WYP5;Q8WYP5-	Protein ELYS	AHCTF1	11	11	2266	0.90965	1.381	3.71E+08
P05165-3;P05165	P05165-3;P05165	Propionyl-CoA carb	PCCA	1	1	681	0.90939	1.2929	3.60E+07
B7Z9I1;Q5T4U5;P1	B7Z9I1;Q5T4U5;P1	Medium-chain spec	ACADM	10	10	385	0.90925	1.0865	1.64E+09
Q9H2M9;F8WDJ2;	Q9H2M9	Rab3 GTPase-activa	RAB3GAP2	21	21	1393	0.90878	1.198	2.14E+09
Q7Z417	Q7Z417	Nuclear fragile X m	NUFIP2	2	2	695	0.90871	0.96427	8.52E+07

J3KMX1;Q99567	J3KMX1;Q99567	Nuclear pore comp	NUP88	5	5	696	0.90868	1.1593	3.72E+08
Q96FX7;H0Y2Q1	Q96FX7;H0Y2Q1	tRNA (adenine(58)-	TRMT61A	5	5	289	0.90826	1.2243	4.66E+08
F5H7K1;E7EWW0;I	F5H7K1;E7EWW0;I	UPF0505 protein C	C16orf62	7	7	959	0.9079	1.1919	2.45E+08
P54886-2;P54886	P54886-2;P54886	Delta-1-pyrroline-5	ALDH18A1	32	32	793	0.90767	1.2331	8.09E+09
Q13907;Q13907-2	Q13907;Q13907-2	Isopentenyl-diphos	IDI1	8	8	227	0.90757	0.96475	1.45E+09
Q9Y2T2;E5RJ52;P5	Q9Y2T2	AP-3 complex subu	AP3M1	8	8	418	0.9075	0.98646	7.02E+08
P46736-2;P46736	P46736-2;P46736	Lys-63-specific deu	BRCC3	9	9	291	0.90734	1.1263	9.58E+08
Q5T760;Q05519-2	Q5T760;Q05519-2	Serine/arginine-ricl	SRSF11	3	3	389	0.9067	1.3598	4.06E+08
P02545-2;P02545	P02545-2;P02545	Prelamin-A/C;Lami	LMNA	11	10	572	0.90634	1.2278	2.12E+08
P18754;P18754-2;	P18754;P18754-2;	Regulator of chrom	RCC1	12	12	421	0.90632	1.4388	4.40E+09
G3V582;F5H039;Q	G3V582;F5H039;Q	Gephyrin;Molybdo	GPHN	3	3	380	0.90622	1.1344	1.79E+08
P31153;P31153-2;	P31153;P31153-2	S-adenosylmethion	MAT2A	12	12	395	0.9062	1.2618	2.60E+09
A3KN83-4;A3KN83	A3KN83-4;A3KN83	Protein strawberry	SBNO1	3	3	732	0.90618	1.2927	3.93E+07
K7EMT0;Q15428	K7EMT0;Q15428	Splicing factor 3A s	SF3A2	2	2	135	0.90601	1.0992	1.07E+08
P35579;P35579-2;	P35579;P35579-2	Myosin-9	MYH9	107	89	1960	0.906	1.1298	2.46E+10
A0A087WTA5;E7EF	A0A087WTA5;E7EF	Translation initiati	EIF2B4	9	9	520	0.90597	0.86137	8.63E+08
O75340-2;O75340	O75340-2;O75340	Programmed cell d	PDCD6;hCG_1985	5	5	189	0.90591	1.2719	3.20E+08
P42765;A0A0B4J2	P42765;A0A0B4J2	3-ketoacyl-CoA thi	ACAA2	19	19	397	0.9057	0.90945	2.68E+09
Q12769;G3V198;E	Q12769;G3V198;E	Nuclear pore comp	NUP160	31	31	1436	0.90552	1.1248	3.44E+09
P13995;B9A062;P	P13995;B9A062;P	Bifunctional methy	MTHFD2	6	6	350	0.90542	1.3117	7.26E+08
Q13151	Q13151	Heterogeneous nuc	HNRNPA0	18	18	305	0.90516	1.2027	4.84E+09
P23919-2;P23919;	P23919-2;P23919	Thymidylate kinase	DTYMK	10	10	188	0.90478	0.98157	5.60E+08
O95347;O95347-2	O95347;O95347-2	Structural mainten	SMC2	34	34	1197	0.90452	1.0439	3.47E+09
Q96NB2;R4GMW0	Q96NB2	Sideroflexin-2	SFXN2	6	6	322	0.90424	0.72763	2.60E+08
Q99707;Q99707-2	Q99707;Q99707-2	Methionine syntha	MTR	15	15	1265	0.90412	1.2276	7.72E+08
Q13356;Q13356-2	Q13356;Q13356-2	Peptidyl-prolyl cis-	PPIL2	5	5	520	0.90402	0.84815	1.75E+08
P11274-2;P11274;	P11274-2;P11274	Breakpoint cluster	BCR	7	6	1227	0.90389	1.0188	4.02E+08
O60573;C9JEL3;B9	O60573;C9JEL3;B9	Eukaryotic translat	EIF4E2	4	4	245	0.90384	1.3559	2.06E+08
Q96EK9	Q96EK9	Protein KTI12 hom	KTI12	3	3	354	0.90376	0.95197	8.80E+07
D6RFI1;Q16643;Q	D6RFI1;Q16643;Q	Drebrin	DBN1	2	2	124	0.90343	1.4162	2.32E+08
K7EMM8;Q49A26-1	K7EMM8;Q49A26-1	Putative oxidoredu	GLYR1	1	1	524	0.90318	0.85783	1.22E+08
P26639;P26639-2;	P26639;P26639-2	Threonine--tRNA lig	TARS	41	37	723	0.90316	1.1797	1.11E+10
A6NIW2;Q5JSL3;A(	A6NIW2;Q5JSL3;A(	Dedicator of cytoki	DOCK11	21	21	2077	0.90307	1.2213	9.45E+08
Q6YP21-3;Q6YP21	Q6YP21-3;Q6YP21	Kynurenine--oxogl	CCBL2	7	7	420	0.90306	1.2773	6.57E+08
Q8N1F7;H3BVG0;C	Q8N1F7;H3BVG0;C	Nuclear pore comp	NUP93	45	45	819	0.90258	1.0417	6.90E+09
F5GZ28;P18858-3;	F5GZ28;P18858-3;	DNA ligase;DNA liga	LIG1	10	10	851	0.90256	0.98653	4.57E+08
P62314;J3QLI9;J3(	P62314;J3QLI9	Small nuclear ribor	SNRPD1	4	4	119	0.90176	1.1728	2.65E+09
Q9NZ32;V9GYX7;G	Q9NZ32;V9GYX7;G	Actin-related prote	ACTR10	6	6	417	0.90166	0.90972	2.56E+08
Q9H0A0;Q9H0A0-2	Q9H0A0;Q9H0A0-2	N-acetyltransferase	NAT10	30	30	1025	0.90136	1.0125	2.04E+09
P55084;P55084-2;	P55084;P55084-2	Trifunctional enzyn	HADHB	24	24	474	0.90075	1.1305	4.73E+09
Q5VWN6;Q5VWN6	Q5VWN6;Q5VWN6	Protein FAM208B	FAM208B	2	2	2430	0.90072	NaN	2.35E+07
P00558;P00558-2;	P00558;P00558-2	Phosphoglycerate k	PGK1	35	35	417	0.9004	1.11	2.42E+10
O00116;B8ZZ81	O00116	Alkyldihydroxyacet	AGPS	17	17	658	0.90011	1.1078	2.92E+09
Q9UI30-2;Q9UI30;	Q9UI30-2;Q9UI30;	Multifunctional me	TRMT112	6	6	120	0.90007	1.0459	6.37E+08
C9J2Y9;P30876;C9	C9J2Y9;P30876;C9	DNA-directed RNA	POLR2B	36	36	1167	0.8997	0.9731	6.48E+09
Q96SK2-3;Q96SK2	Q96SK2-3;Q96SK2	Transmembrane pr	TMEM209	3	3	519	0.89953	0.8049	1.92E+08
H0YCM7;Q5JVZ5;Q	H0YCM7;Q5JVZ5;Q	Engulfment and cel	ELMO2	3	3	441	0.89927	1.1666	2.29E+08
O95104-3;O95104	O95104-3;O95104	Splicing factor, argi	SCAF4;SCAF8	2	2	1132	0.89915	NaN	5.15E+07
P16152;E9PQ63;A(	P16152;E9PQ63;A(	Carbonyl reductase	CBR1	17	15	277	0.89898	1.2581	1.66E+10
Q9NW64-2;Q9NW	Q9NW64-2;Q9NW	Pre-mRNA-splicing	RBM22	9	9	371	0.89885	1.0385	6.63E+08
A0A087WU65;Q9N	A0A087WU65;Q9N	Vacuolar protein sc	VPS45	2	2	447	0.8988	0.95511	3.10E+07
P08237;P08237-3;	P08237;P08237-3	ATP-dependent 6-p	PFKM	23	19	780	0.89823	1.0827	4.79E+09
Q9H7Z3;G3V338	Q9H7Z3	Protein NRDE2 hon	NRDE2	3	3	1164	0.8982	NaN	1.99E+07
F5H8F7;Q9UBL3-3;	F5H8F7;Q9UBL3-3	Set1/Ash2 histone	ASH2L	4	4	489	0.89711	1.2381	3.02E+08
Q9NPQ8-4;Q9NPQ	Q9NPQ8-4;Q9NPQ	Synembryn-A	RIC8A	11	11	530	0.89681	1.0497	1.39E+09
Q709F0;F8WEV0;D	Q709F0;F8WEV0;D	Acyl-CoA dehydrog	ACAD11	6	6	780	0.8966	0.98485	7.10E+08
Q15031;E9PHM2;(	Q15031;E9PHM2	Probable leucine--t	LARS2	4	4	903	0.89634	1.2414	4.39E+07
Q9NXR7-4;Q9NXR7	Q9NXR7-4;Q9NXR7	BRCA1-A complex s	BRE	6	6	376	0.896	1.0326	1.35E+09
P60842;J3KT12;P6	P60842;J3KT12;P6	Eukaryotic initiatic	EIF4A1	33	17	406	0.89571	1.1088	6.02E+10
A0A0C4DGQ8;Q6IA	A0A0C4DGQ8;Q6IA	Dehydrogenase/rec	DHRS7B	10	10	310	0.89561	1.1665	1.20E+09
Q29RF7;Q29RF7-3;	Q29RF7	Sister chromatid cc	PDS5A	15	14	1337	0.89524	1.2326	7.77E+08
P27144;D3DQ64	P27144;D3DQ64	Adenylate kinase 4,	AK4	5	5	223	0.89523	1.011	7.60E+08
Q15654;A0A0D9SF	Q15654;A0A0D9SF	Thyroid receptor-ir	TRIP6	4	4	476	0.89481	0.77277	3.02E+08
R4GN43;A0A0C4D	R4GN43;A0A0C4D	NADH dehydrogena	NDUFA6	3	3	71	0.89454	1.1611	1.69E+08
Q92922;F8WE13;F	Q92922	SWI/SNF complex s	SMARCC1	6	6	1105	0.89434	0.69436	1.65E+08
O15355	O15355	Protein phosphata	PPM1G	9	9	546	0.89363	1.1449	9.29E+08
H0YN26;P39687;H	H0YN26;P39687;H	Acidic leucine-rich	ANP32A;ANP32B;A	2	2	177	0.89293	1.3523	7.59E+07
Q9P260-2;A0A075	Q9P260-2;A0A075	LisH domain and HI	KIAA1468	3	3	1250	0.8925	0.59969	8.56E+07
H0YCY8;P53634;P	H0YCY8;P53634;P	Dipeptidyl peptida	CTSC	2	2	245	0.89185	1.2609	5.57E+07
Q7Z2Z2-2;Q7Z2Z2	Q7Z2Z2-2;Q7Z2Z2	Elongation factor T	EFTUD1	10	10	1069	0.89153	1.0337	2.76E+08
O43615;M0QXU7;I	O43615;M0QXU7	Mitochondrial imp	TIMM44	21	21	452	0.89139	1.312	3.75E+09
Q6PI48	Q6PI48	Aspartate--tRNA lig	DARS2	22	22	645	0.89137	1.2444	5.28E+09
B4DLN1;F6QW41	B4DLN1		MRPL12	12	0	442	0.89096	1.1126	4.05E+09
Q6IA86-4;Q6IA86-2	Q6IA86-4;Q6IA86-2	Elongator complex	ELP2	4	4	705	0.89094	0.88027	1.05E+08
I3L2B0	I3L2B0		CLUH	36	2	1236	0.89071	0.84018	1.47E+07
O75152;E9PQ61;E	O75152;E9PQ61;E	Zinc finger CCCH do	ZC3H11A	15	15	810	0.89069	0.89583	7.60E+08
O15164-2;O15164	O15164-2;O15164	Transcription inter	TRIM24	3	3	1016	0.89014	0.71302	9.47E+07
Q5VZU9;P29144	Q5VZU9;P29144	Tripeptidyl-peptida	TPP2	22	22	1262	0.89012	1.0261	1.36E+09
Q9NR50;Q9NR50-3	Q9NR50;Q9NR50-3	Translation initiati	EIF2B3	7	7	452	0.88987	1.2679	5.87E+08
Q8NAV1	Q8NAV1	Pre-mRNA-splicing	PRPF38A	4	4	312	0.88962	1.5511	2.28E+08
A0A0J9YXM6;Q562	A0A0J9YXM6;Q562	WD repeat-contain	WDR81	4	4	1940	0.88909	0.87488	6.99E+07
Q00796;H0YLA4;H	Q00796;H0YLA4	Sorbitol dehydroge	SORD	9	9	357	0.88902	1.1798	2.08E+09
Q9H2G2-2;Q9H2G	Q9H2G2-2;Q9H2G	STE20-like serine/th	SLK	18	18	1204	0.88889	0.93361	4.02E+08
Q9Y490	Q9Y490	Talin-1	TLN1	21	20	2541	0.88845	0.91266	1.66E+09
Q9H832-2;Q9H832	Q9H832-2;Q9H832	Ubiquitin-conjugat	UBE2Z	4	4	246	0.88839	1.1893	1.91E+08
Q9UI12-2;Q9UI12;	Q9UI12-2;Q9UI12;	V-type proton ATPa	ATP6V1H	8	8	465	0.8882	1.1184	6.15E+08
A0A0A0MTN0;Q13	A0A0A0MTN0;Q13	Cullin-2	CUL2	8	8	758	0.88794	1.3815	4.43E+08
Q13136-2;Q13136	Q13136-2;Q13136	Liprin-alpha-1	PPFIA1	7	7	1185	0.88729	0.96213	3.17E+08
Q16186;A0A087W	Q16186;A0A087W	Proteasomal ubiqu	ADRM1	3	3	407	0.88728	1.2252	3.17E+08
B3KS98;O15372;A(	B3KS98;O15372;A(	Eukaryotic translat	EIF3S3;EIF3H	6	6	366	0.88724	1.4434	1.64E+08
P14868;P14868-2;	P14868;P14868-2	Aspartate--tRNA lig	DARS	24	24	501	0.88718	1.1269	3.94E+09
A0A0D9SFR6;Q86X	A0A0D9SFR6;Q86X	Diacylglycerol kina	DGKH	5	5	1028	0.88675	1.2868	1.11E+08
Q96GA7;F8VYZ3;F8	Q96GA7;F8VYZ3	Serine dehydratase	SDSL	4	4	329	0.88669	1.3182	1.67E+08

G8JLB3;Q9Y606-2;	G8JLB3;Q9Y606-2;	tRNA pseudouridin	PUS1	8	8	384	0.88613	1.1727	9.17E+08
P62318-2;P62318;	P62318-2;P62318	Small nuclear ribor	SNRPD3	3	3	120	0.88611	1.2959	7.42E+09
H3BMZ9;H3BPP3;H	H3BMZ9;H3BPP3;H	Mannose-6-phosph	MPI	4	4	264	0.88607	1.3546	2.96E+08
Q53H96-2;Q53H9(	Q53H96-2;Q53H9(	Pyrroline-5-carbox	PYCRL	8	8	254	0.88601	0.78351	2.73E+08
Q9UQ80;Q9UQ80-;	Q9UQ80;Q9UQ80-;	Proliferation-assoc	PA2G4	29	29	394	0.88598	1.1234	1.87E+10
F8W1R7;G3V1V0;F	F8W1R7;G3V1V0;F	Myosin light polype	PDE6H;MYL6	8	8	145	0.88588	1.2975	1.03E+09
P30044-2;P30044;	P30044-2;P30044	Peroxiredoxin-5, m	PRDX5	4	4	162	0.88588	0.96544	1.44E+08
C9JFE4;A0A096LP(	C9JFE4;A0A096LP(	COP9 signalosome	GPS1	4	4	471	0.88558	1.0266	3.60E+08
A8MT37;P49840;N	A8MT37;P49840;N	Glycogen synthase	GSK3A	5	4	401	0.885	0.97	3.87E+08
F2Z2U4;Q9Y4A5-2;	F2Z2U4;Q9Y4A5-2;	Transformation/tra	TRRAP	28	28	3848	0.88492	1.0537	1.45E+09
A0A087WXI1;Q6N'	A0A087WXI1;Q6N'	3-hydroxyisobutyr	HIBCH	10	10	380	0.88475	1.0001	7.51E+08
P23528;E9PP50;E9	P23528;E9PP50;E9	Cofilin-1	CFL1	17	13	166	0.88472	1.1873	1.28E+10
Q15018	Q15018	BRISC complex sub	FAM175B	9	9	415	0.88456	0.93608	6.92E+08
Q9NU22;Q5T795;F	Q9NU22	Midasin	MDN1	76	76	5596	0.88425	1.1738	4.64E+09
O14744;O14744-5	O14744;O14744-5	Protein arginine N-	PRMT5	12	12	637	0.88404	1.321	1.21E+09
A6NIT2;A6NMN0;P	A6NIT2;A6NMN0;P	Phosphorylase b kii	PHKA1	4	3	1181	0.88375	1.2538	2.35E+08
P10155;P10155-3;	P10155;P10155-3	60 kDa SS-A/Ro ribo	TROVE2	16	16	538	0.88375	1.2793	2.34E+09
Q96CS3;D6RBG6	Q96CS3	FAS-associated fact	FAF2	19	19	445	0.88368	0.99466	4.79E+09
P78371;F5GWF6;P	P78371;F5GWF6;P	T-complex protein	CCT2	35	35	535	0.88335	1.1368	1.65E+10
Q96CU9-3;Q96CU9	Q96CU9-3;Q96CU9	FAD-dependent oxi	FOXRED1	2	2	472	0.88297	NaN	1.40E+08
P20700;E9PBF6;A(	P20700;E9PBF6;A(	Lamin-B1	LMNB1	32	28	586	0.88285	1.3002	3.21E+09
Q5T6V5;Q5T6V7;Q	Q5T6V5	UPF0553 protein C	C9orf64	14	14	341	0.88259	1.0487	1.56E+10
D6RE77;B7Z7Y1;A(	D6RE77;B7Z7Y1;A(	Rap guanine nucleo	RAPGEF6	6	6	1114	0.88214	1.1711	3.35E+08
H0YBP1;E7ESA6;Q(	H0YBP1;E7ESA6;Q(	Focal adhesion kina	PTK2	7	7	1017	0.8821	0.70735	2.75E+08
F6RFD5;P60981;P(	F6RFD5;P60981;P(	Destrin	DSTN	5	4	135	0.88209	1.1457	9.88E+08
Q93008-1;Q93008	Q93008-1;Q93008	Probable ubiquitin	USP9X	44	44	2554	0.88198	1.1613	4.12E+09
Q92499;Q92499-2	Q92499;Q92499-2	ATP-dependent RN/	DDX1	24	24	740	0.88169	1.3517	3.24E+09
Q96P47;Q96P47-2	Q96P47;Q96P47-2	Arf-GAP with GTPas	AGAP3	5	5	875	0.88167	0.94491	3.38E+08
Q0VDF9;H7C2A1;B	Q0VDF9	Heat shock 70 kDa p	HSPA14	10	10	509	0.8814	1.1853	1.43E+09
Q00839;Q00839-2	Q00839;Q00839-2	Heterogeneous nuc	HNRNPU	36	36	825	0.88089	1.0431	3.81E+10
Q15773;F5H0Y3;F!	Q15773	Myeloid leukemia f	MLF2	7	7	248	0.88056	0.92346	3.67E+08
Q9HCN8	Q9HCN8	Stromal cell-derive	SDF2L1	3	3	221	0.87902	0.93293	2.80E+08
Q9H553;Q9H553-2	Q9H553;Q9H553-2	Alpha-1,3/1,6-man	ALG2	6	6	416	0.87899	1.0057	3.13E+08
Q8NI27;A0A0C4D(	Q8NI27;A0A0C4D(	THO complex subu	THOC2	23	23	1593	0.87844	1.168	2.07E+09
J3KN10;P42356;P/	J3KN10;P42356	Phosphatidylinosit	PI4KA	24	24	2102	0.87801	1.0393	9.79E+08
A0A0G2JQK5;Q6DI	A0A0G2JQK5;Q6DI	Nucleoredoxin	NXN	3	3	120	0.87785	1.2686	9.44E+07
A0A087WVR3;A0A	A0A087WVR3;A0A	E3 ubiquitin-protei	UHRF1	4	4	806	0.87756	0.90771	1.66E+08
Q9UJZ1;A0A087W'	Q9UJZ1;A0A087W'	Stomatin-like prote	STOML2	19	19	356	0.87741	1.1901	8.16E+09
V9GZ56;Q9Y4Z0;M	V9GZ56;Q9Y4Z0;M	U6 snRNA-associate	LSM4	3	3	238	0.87712	0.95691	2.25E+08
Q7LGA3-3;Q7LGA3	Q7LGA3-3;Q7LGA3	Heparan sulfate 2-(	HS2ST1	2	2	229	0.87697	1.289	1.76E+08
Q13838;Q13838-2	Q13838;Q13838-2	Spliceosome RNA h	DDX39B	24	9	428	0.87687	1.351	5.33E+09
Q9Y696;A6PVS0;Q!	Q9Y696	Chloride intracellu	CLIC4	12	12	253	0.87632	1.0913	1.81E+09
Q969U7-2;Q969U7	Q969U7-2;Q969U7	Proteasome assemb	PSMG2	7	7	233	0.87631	1.2022	2.63E+08
Q12931-2;Q12931	Q12931-2;Q12931	Heat shock protein	TRAP1	19	19	651	0.87624	1.447	3.76E+09
P35270	P35270	Sepiapterin reducta	SPR	7	7	261	0.87619	1.3228	2.73E+09
Q9NQE9	Q9NQE9	Histidine triad nucl	HINT3	3	3	182	0.87609	1.1264	1.29E+08
P26641;P26641-2	P26641;P26641-2	Elongation factor 1	EEF1G	27	27	437	0.87575	1.3643	3.41E+10
Q13595-4;Q13595	Q13595-4;Q13595	Transformer-2 prot	TRA2A	5	5	180	0.87572	1.0483	2.26E+08
Q99797	Q99797	Mitochondrial inte	MIPEP	2	2	713	0.87561	1.0444	4.59E+07
P00966;Q5T6L6;Q!	P00966;Q5T6L6	Argininosuccinate s	ASS1	16	16	412	0.87551	1.2151	1.70E+09
Q8NF37;A0A0G2JC	Q8NF37;A0A0G2JC	Lysophosphatidylc	LPCAT1	7	7	534	0.87537	1.0812	4.23E+08
Q8IYB8;B1AR60	Q8IYB8	ATP-dependent RN/	SUPV3L1	14	14	786	0.87531	1.0491	1.59E+09
P30084	P30084	Enoyl-CoA hydratas	ECHS1	11	11	290	0.87521	1.2406	1.80E+09
Q9Y6Y8;Q9Y6Y8-2;	Q9Y6Y8;Q9Y6Y8-2	SEC23-interacting p	SEC23IP	22	22	1000	0.87515	1.0956	1.33E+09
Q7KZF4;H7C597	Q7KZF4	Staphylococcal nuc	SND1	46	46	910	0.87475	1.2544	1.23E+10
H7BYC8;Q8TCX1-3;	H7BYC8;Q8TCX1-3;	Cytoplasmic dynein	DYNC2LI1	3	3	318	0.87422	1.1596	1.36E+08
Q9UKD2	Q9UKD2	mRNA turnover pro	MRTO4	11	11	239	0.87415	0.93758	1.56E+09
Q96GM8;Q96GM8	Q96GM8;Q96GM8	Target of EGR1 prot	TOE1	6	6	510	0.87414	1.0621	7.02E+08
P48047;H7C0C1;H	P48047;H7C0C1	ATP synthase subur	ATP5O	9	9	213	0.87405	1.2495	1.99E+09
Q9BST9;Q9BST9-3;	Q9BST9;Q9BST9-3;	Rhotekin	RTKN	2	2	563	0.87385	NaN	1.00E+08
O75439;G3V0E4;F	O75439;G3V0E4	Mitochondrial-pro	PMPCB	13	12	489	0.87355	1.1507	2.75E+09
P49736;H0Y8E6;F8	P49736;H0Y8E6	DNA replication lic	MCM2	31	31	904	0.87351	1.1745	4.82E+09
Q9HB71;Q9HB71-3	Q9HB71;Q9HB71-3	Calcyclin-binding p	CACYBP	16	16	228	0.87346	1.491	7.60E+09
P35232;C9JW96;C	P35232;C9JW96;C	Prohibitin	PHB	15	15	272	0.87335	1.4822	1.47E+10
Q96BW9-3;Q96BW	Q96BW9-3;Q96BW	Phosphatidate cyti	TAMM41	8	8	337	0.87331	1.0676	1.14E+09
P56962;E9PJW1;E!	P56962;E9PJW1;E!	Syntaxin-17	STX17	2	2	302	0.87263	1.0614	1.13E+08
D6R938;E9PBG7;E!	D6R938;E9PBG7;E!	Calcium/calmoduli	CAMK2D	13	9	498	0.87227	1.1237	1.51E+09
Q8WVI0	Q8WVI0	Small integral mem	SMIM4	2	2	70	0.87164	NaN	4.31E+07
Q16795;F5H0J3;H(	Q16795	NADH dehydrogena	NDUFA9	9	9	377	0.87159	1.3712	1.48E+09
A0A0D9SF54;A0A0	A0A0D9SF54;A0A0	Spectrin alpha chai	SPTAN1	6	6	2457	0.87143	1.2796	1.74E+08
O75170-6;O75170	O75170-6;O75170	Serine/threonine-p	PPP6R2	3	3	905	0.87135	1.5156	9.22E+07
P50748;E7ES84;P5	P50748;E7ES84	Kinetochore-associ	KNTC1	25	25	2209	0.87108	1.1861	1.19E+09
Q9H5X1;H0YKV4;C	Q9H5X1;H0YKV4;C	MIP18 family prote	FAM96A	4	4	160	0.87053	1.1261	7.54E+07
Q04656-5;Q04656	Q04656-5;Q04656	Copper-transportir	ATP7A	2	2	1422	0.87001	NaN	4.62E+07
A0A024RCR6;A0A(	A0A024RCR6;A0A(	Large proline-rich p	BAT3;BAG6	22	22	1126	0.8697	0.69301	2.82E+09
Q9NRX4;Q9NRX4-2	Q9NRX4	14 kDa phosphohis	PHPT1	3	3	125	0.86926	1.2143	1.32E+08
J3KN66;Q5JTV8-3;,	J3KN66;Q5JTV8-3;,	Torsin-1A-interacti	TOR1AIP1	3	3	599	0.86894	1.0862	3.40E+08
Q9Y5S9-2;Q9Y5S9;	Q9Y5S9-2;Q9Y5S9	RNA-binding protei	RBM8A	3	3	173	0.86859	1.095	1.65E+08
O43324;D6RBD7;C	O43324;D6RBD7;C	Eukaryotic translat	EEF1E1;EEF1E1-BLC	5	5	174	0.86858	1.5746	5.85E+08
P11171-2;P11171;	P11171-2;P11171	Protein 4.1	EPB41	15	15	831	0.86812	0.99663	8.21E+08
Q9P287-2;Q9P287	Q9P287-2;Q9P287	BRCA2 and CDKN1/	BCCIP	4	1	322	0.86796	1.2408	1.61E+09
H0YH87;V9GY86;C	H0YH87;V9GY86;C	Ataxin-2	ATXN2	9	9	916	0.86775	0.69619	2.66E+08
Q9UFC0;H7C5S6;F	Q9UFC0;H7C5S6	Leucine-rich repeat	LRWD1	5	5	647	0.86772	1.0719	4.00E+08
P84095;F8WET9;B	P84095	Rho-related GTP-bi	RHOG	8	7	191	0.86761	1.1028	1.99E+08
O43149;I3L141;O4	O43149	Zinc finger ZZ-type	ZZEF1	7	7	2961	0.86757	1.0313	2.92E+08
Q9UBS4;H7C2Y5	Q9UBS4	DnaJ homolog subf	DNAJB11	9	9	358	0.86732	1.1772	1.45E+09
A0A087X256;Q2M	A0A087X256;Q2M	WASH complex sub	KIAA1033	11	11	1174	0.86704	1.2928	5.13E+08
Q04837;A0A0G2JL	Q04837;A0A0G2JL	Single-stranded DN	SSBP1	8	8	148	0.86694	1.0518	7.06E+08
Q9BSJ2;Q9BSJ2-4;I	Q9BSJ2;Q9BSJ2-4;I	Gamma-tubulin co	TUBGCP2	20	20	902	0.86668	1.0609	1.90E+09
Q9BT22;Q9BT22-2;	Q9BT22;Q9BT22-2	Chitobiosyldiphosp	ALG1	6	6	464	0.86648	1.3001	1.26E+09
E9PH82;Q8NCA5-2	E9PH82;Q8NCA5-2	Protein FAM98A	FAM98A	4	3	312	0.86647	1.2499	4.72E+08
P16435;H0Y4R2;E'	P16435;H0Y4R2;E'	NADPH--cytochrom	POR	6	6	677	0.86639	1.8181	2.29E+08
Q8IY18	Q8IY18	Structural mainten	SMC5	10	10	1101	0.86628	1.0739	2.62E+08

Q9NUQ9;E5RI16;E5	Q9NUQ9;E5RI16	Protein FAM49B	FAM49B	3	3	324	0.86618	1.4009	2.16E+08
F5H345;P08397-2;	F5H345;P08397-2	Porphobilinogen d	HMBS	5	5	330	0.86546	0.959	5.12E+08
Q8IUF8-4;Q8IUF8;(	Q8IUF8-4;Q8IUF8;(	Bifunctional lysine-	MINA	6	6	464	0.86546	1.1229	6.02E+08
Q96GW9	Q96GW9	Methionine--tRNA l	MARS2	6	6	593	0.86497	0.71018	2.36E+08
P35580;P35580-5;	P35580;P35580-5	Myosin-10	MYH10	66	47	1976	0.86489	1.3927	6.75E+09
Q9P0J7;C9J3I2	Q9P0J7	E3 ubiquitin-protei	KCMF1	3	3	381	0.86459	1.1542	2.52E+08
Q16527;F8VQR7;F(	Q16527;F8VQR7;F(	Cysteine and glycin	CSRP2	8	8	193	0.86448	0.81259	3.96E+07
P63104;E7EX29;B(	P63104;E7EX29;B(	14-3-3 protein zeta	YWHAZ	15	9	245	0.86444	1.1961	2.02E+09
Q9UBD5-3;Q9UBD!	Q9UBD5-3;Q9UBD	Origin recognition	ORC3	4	4	568	0.86432	1.4917	2.71E+08
Q9H6K4;Q9H6K4-2	Q9H6K4;Q9H6K4-2	Optic atrophy 3 pro	OPA3	2	2	179	0.86425	0.99774	8.88E+07
Q8NEZ5;Q8NEZ5-3;	Q8NEZ5;Q8NEZ5-3	F-box only protein	FBXO22	6	6	403	0.86412	1.2748	6.96E+08
G8JLP4;Q9Y4F3-3;(	G8JLP4;Q9Y4F3-3;(	Meiosis arrest fema	KIAA0430;KTN1	2	2	1577	0.86377	NaN	6.68E+07
Q8WWC4;H7C0V0	Q8WWC4	Uncharacterized pr	C2orf47	5	5	291	0.86334	0.94207	1.57E+08
Q14498-3;Q14498	Q14498-3;Q14498	RNA-binding protei	RBM39	18	16	508	0.86295	1.2616	5.15E+09
P62316;P62316-2;	P62316;P62316-2	Small nuclear ribor	SNRPD2	12	12	118	0.86273	1.1649	1.31E+09
Q99661-2;Q99661	Q99661-2;Q99661	Kinesin-like protein	KIF2C	5	4	671	0.86262	1.2528	9.29E+07
Q9HAU5;Q9HAU5-:	Q9HAU5	Regulator of nonse	UPF2	11	11	1272	0.86262	1.0577	5.87E+08
Q15437;Q5QPE2;C	Q15437;Q5QPE2	Protein transport p	SEC23B	12	10	767	0.86229	1.0354	8.48E+08
Q9GZT4;I3L3N0;V9	Q9GZT4;I3L3N0;V9	Serine racemase	SRR	4	4	340	0.86217	1.1595	4.52E+08
P49458;E9PE20;P4	P49458;E9PE20;P4	Signal recognition	SRP9	5	5	86	0.86138	1.2185	1.40E+08
Q15370;Q15370-2	Q15370;Q15370-2	Transcription elong	TCEB2	4	4	118	0.86057	0.91878	1.21E+08
P61978-3;Q5T6W2	P61978-3;Q5T6W2	Heterogeneous nuc	HNRNPK	33	1	440	0.8602	1.3393	1.01E+09
J3QRU1;P06241-3;	J3QRU1;P06241-3	Tyrosine-protein ki	YES1;FYN;SRC;LCK;I	2	2	548	0.86019	1.3278	9.47E+07
E5RJR5;P63208;E7	E5RJR5;P63208;E7	S-phase kinase-asso	SKP1	4	2	163	0.85988	0.50683	3.78E+07
Q15029-2;Q15029	Q15029-2;Q15029	116 kDa U5 small n	EFTUD2	39	38	937	0.85965	1.0161	6.79E+09
Q14566	Q14566	DNA replication lic	MCM6	39	39	821	0.85904	1.0453	1.15E+10
A0A087X0B7;H7C3	A0A087X0B7;H7C3	Synaptosomal-asso	SNAP47	2	2	419	0.85875	NaN	7.92E+07
Q9NXF1-2;Q9NXF1	Q9NXF1-2;Q9NXF1	Testis-expressed se	TEX10	9	9	913	0.85872	1.0448	4.03E+08
G5EA36;P30260;P:	G5EA36;P30260;P:	Cell division cycle p	CDC27	11	11	823	0.85869	1.028	9.35E+08
P30837;A0A0U1R(	P30837	Aldehyde dehydrog	ALDH1B1	20	20	517	0.85779	1.228	3.50E+09
P14324-2;P14324;	P14324-2;P14324	Farnesyl pyrophosp	FDPS	8	8	353	0.85768	1.0353	5.91E+09
P21359-2;P21359-	P21359-2;P21359-	Neurofibromin;Ne	NF1	18	18	2818	0.85654	1.0661	9.21E+08
P57772;P57772-2;	P57772;P57772-2	Selenocysteine-spe	EEFSEC	6	6	596	0.85603	0.92454	3.01E+08
E9PHH9;Q9BUI4	E9PHH9;Q9BUI4	DNA-directed RNA	POLR3C	3	3	411	0.85574	1.3958	2.55E+08
Q5SRN1;O60508	Q5SRN1;O60508	Pre-mRNA-processi	CDC40	3	3	539	0.85565	1.4187	2.76E+08
O95140;Q5JXC5	O95140	Mitofusin-2	MFN2	5	5	757	0.85564	1.0603	2.26E+08
P30520;G3V232	P30520	Adenylosuccinate s	ADSS	21	17	456	0.85557	1.0455	8.83E+09
C9JYM0;O75817	C9JYM0;O75817	Ribonuclease P pro	POP7	2	2	137	0.85554	0.95866	1.10E+08
Q13895;H7BY94;F(	Q13895	Bystin	BYSL	4	4	437	0.85553	NaN	7.03E+07
H0Y9R3;Q9H7D7-2	H0Y9R3;Q9H7D7-2	WD repeat-contain	WDR26	5	5	295	0.85546	1.1346	2.25E+08
B3KT28;Q9UNN5;E	B3KT28;Q9UNN5;E	FAS-associated fact	FAF1	3	3	464	0.85533	1.3874	1.16E+08
P62330	P62330	ADP-ribosylation fa	ARF6	4	4	175	0.85456	1.4202	5.52E+08
Q00005-6;Q00005	Q00005-6;Q00005	Serine/threonine-p	PPP2R2B;PPP2R2A	2	2	432	0.8544	NaN	1.09E+08
P48735;P48735-2;	P48735;P48735-2	Isocitrate dehydrog	IDH2	19	18	452	0.85391	1.1558	4.33E+09
H7C3X5;E9PNU4;C	H7C3X5;E9PNU4;C	Syntaxin-5	STX5	1	1	158	0.85335	NaN	1.24E+07
O43264;O43264-2	O43264;O43264-2	Centromere/kinetc	ZW10	4	4	779	0.85295	1.3849	3.79E+08
Q96IU4;B4DQI4;F8	Q96IU4;B4DQI4;F8	Alpha/beta hydrola	ABHD14B	9	9	210	0.8525	1.1388	1.17E+09
P25098;E9PRV7;P:	P25098;E9PRV7;P:	Beta-adrenergic rec	ADRBK1;ADRBK2	3	3	689	0.85232	1.133	8.62E+07
Q14573;B7ZMI3	Q14573	Inositol 1,4,5-trisp	ITPR3	9	6	2671	0.8523	1.1156	1.89E+08
Q08752;H0Y8J0	Q08752	Peptidyl-prolyl cis-	PPID	7	7	370	0.85121	1.635	2.86E+08
O75475	O75475	PC4 and SFRS1-inte	PSIP1	1	1	530	0.85077	1.3187	4.93E+07
P50990;P50990-2;	P50990;P50990-2	T-complex protein	CCT8	44	44	548	0.85041	1.1863	3.43E+10
Q99961-3;Q99961	Q99961-3;Q99961	Endophilin-A2	SH3GL1	2	2	304	0.84988	NaN	6.77E+07
P62487;E9PIU7;H(	P62487	DNA-directed RNA	POLR2G	3	3	172	0.84978	1.0017	7.59E+07
O00303;H0YDT6;E	O00303	Eukaryotic translat	EIF3F	14	14	357	0.8495	1.4837	1.09E+10
B1AHR1;Q9UH03-2	B1AHR1;Q9UH03-2	Neuronal-specific s	03-Sep	3	3	294	0.84947	1.2521	1.19E+08
Q04917;A2IDB2;F8	Q04917;A2IDB2	14-3-3 protein eta	YWHAH	9	5	246	0.84929	0.9794	8.24E+07
Q00587-2;Q00587	Q00587-2;Q00587	Cdc42 effector pro	CDC42EP1	2	2	384	0.8491	NaN	9.38E+07
Q6KC79-2;Q6KC79	Q6KC79-2;Q6KC79	Nipped-B-like prote	NIPBL	6	6	2697	0.84885	0.98052	2.13E+08
Q13347;Q5TFK1	Q13347	Eukaryotic translat	EIF3I	15	15	325	0.8488	1.273	3.82E+09
O75369-2;O75369	O75369-2;O75369	Filamin-B	FLNB	60	54	2578	0.84849	1.1957	5.10E+09
Q7L576;Q7L576-2;	Q7L576;Q7L576-2	Cytoplasmic FMR1-	CYFIP1	32	19	1253	0.84806	1.1738	3.40E+09
Q9H3N1;G3V448	Q9H3N1	Thioredoxin-relate	TMX1	6	6	280	0.8476	1.0134	1.40E+08
Q93100-4;Q93100	Q93100-4;Q93100	Phosphorylase b kii	PHKB	5	5	1086	0.84706	1.0737	2.56E+08
P51116;I3L1Z2	P51116	Fragile X mental ret	FXR2	6	4	673	0.84689	1.6507	1.24E+08
Q8TEQ6	Q8TEQ6	Gem-associated pro	GEMIN5	33	33	1508	0.84688	1.1408	3.10E+09
P52298-3;P52298;	P52298-3;P52298	Nuclear cap-bindin	NCBP2	4	4	103	0.84662	1.2646	2.77E+08
H0YME5;Q9P2K8-2	H0YME5;Q9P2K8-2	Eukaryotic translat	EIF2AK4	8	8	1427	0.84627	1.3298	4.55E+08
Q8IYQ7	Q8IYQ7	Threonine synthase	THNSL1	4	4	743	0.84558	0.85538	1.26E+08
Q14019;H3BT58	Q14019;H3BT58	Coactosin-like prot	COTL1	7	7	142	0.84557	1.1095	2.49E+08
P34896-2;P34896;	P34896-2;P34896	Serine hydroxymet	SHMT1	8	7	444	0.8453	1.0647	7.96E+08
Q9UBF2;Q9UBF2-2	Q9UBF2;Q9UBF2-2	Coatomer subunit	COPG2	18	14	871	0.84478	1.1587	1.47E+09
O95352-3;O95352	O95352-3;O95352	Ubiquitin-like mod	ATG7	3	3	623	0.8444	1.2929	3.43E+08
A0A087X0S7;A0A0	A0A087X0S7;A0A0	Leucine-rich repeat	LRRC41	2	2	521	0.84433	NaN	1.41E+08
O75165;H0Y8Q2;H	O75165	DnaJ homolog subf	DNAJC13	32	32	2243	0.84396	1.2132	1.50E+09
P51665;H3BNT7;H	P51665;H3BNT7;H	26S proteasome nc	PSMD7	7	7	324	0.84385	1.2516	4.14E+08
Q12904;Q12904-2	Q12904;Q12904-2	Aminoacyl tRNA syı	AIMP1	12	12	312	0.8436	1.1526	5.95E+09
O60547-2;O60547	O60547-2;O60547	GDP-mannose 4,6 (	GMDS	6	6	342	0.84354	1.4044	2.65E+08
P11413;P11413-3;	P11413;P11413-3	Glucose-6-phospha	G6PD	9	9	515	0.84346	1.4121	9.18E+08
O60306;H0YH15;H	O60306	Intron-binding pro	AQR	22	22	1485	0.84331	1.3508	9.12E+08
P20290-2;P20290;	P20290-2;P20290	Transcription facto	BTF3	3	3	162	0.84327	1.2734	2.37E+08
Q9NZ01;M0R3C3;(	Q9NZ01	Very-long-chain en	TECR	12	12	308	0.84317	0.97278	1.70E+09
O75794;X6RKY7;X(	O75794;X6RKY7;X(	Cell division cycle p	CDC123	4	4	336	0.84314	1.1492	3.08E+08
P07237;H7BZ94;I3	P07237;H7BZ94;I3	Protein disulfide-is	P4HB	16	16	508	0.84256	1.5029	1.95E+09
M0QXN5;P37198	M0QXN5;P37198	Nuclear pore glyco	NUP62	3	3	446	0.84235	NaN	1.04E+08
P31939-2;P31939;	P31939-2;P31939	Bifunctional purine	ATIC	9	9	591	0.84226	0.97441	5.76E+08
B0QY89;Q9Y262-2;	B0QY89;Q9Y262-2	Eukaryotic translat	EIF3L	12	12	607	0.84145	1.418	1.24E+09
Q9NXX6;Q9NXX6-2	Q9NXX6	Non-structural mai	NSMCE4A	3	3	385	0.84135	0.98245	1.37E+08
J3KMZ7;Q9H0H0	J3KMZ7;Q9H0H0	Integrator complex	INTS2	6	6	1196	0.84106	1.3001	2.38E+08
Q9NWH9;H0YLW7	Q9NWH9;H0YLW7	SAFB-like transcript	SLTM	3	3	1034	0.84097	1.2559	2.82E+07
E7ET15;O15042-3;	E7ET15;O15042-3;	U2 snRNP-associate	U2SURP	4	4	1028	0.84096	1.0382	1.09E+08
P41091;Q2VIR3;F8	P41091;Q2VIR3;F8	Eukaryotic translat	EIF2S3;EIF2S3L	17	17	472	0.8408	1.0803	6.69E+09
Q5T0A6;Q86SQ9-3	Q5T0A6;Q86SQ9-3	Dehydrodolichyl di	DHDDS	3	3	169	0.84034	1.034	5.96E+07

F8W9T3;O95219;C	F8W9T3;O95219	Sorting nexin-4	SNX4	3	3	155	0.84029	NaN	1.65E+07
H7BXZ6;Q8IXI2-4;(	H7BXZ6;Q8IXI2-4;(	Mitochondrial Rho	TMEM91;RHOT1	3	2	597	0.83994	1.2141	1.77E+08
P26374;P24386	P26374;P24386	Rab proteins geran	CHML;CHM	2	2	656	0.8398	NaN	3.26E+07
Q6P587;Q6P587-2	Q6P587;Q6P587-2	Acylpyruvase FAHD	FAHD1	3	3	224	0.83914	0.87254	4.55E+08
G5EA30;Q92879-2	G5EA30;Q92879-2	CUGBP Elav-like fan	CELF1	7	7	514	0.83901	1.1977	8.71E+07
Q8NBU5;Q8NBU5-:	Q8NBU5	ATPase family AAA (	ATAD1	3	3	361	0.83863	0.90143	1.65E+08
Q9NRX1;F8WBJ6	Q9NRX1;F8WBJ6	RNA-binding protei	PNO1	5	5	252	0.83852	1.0823	5.07E+08
O95470;H0Y3V8;H	O95470;H0Y3V8;H	Sphingosine-1-pho	SGPL1	6	6	568	0.83849	1.1707	1.43E+08
Q7L523;Q5VZM2-2	Q7L523;Q5VZM2-2	Ras-related GTP-bir	RRAGA;RRAGB	4	4	313	0.83763	1.2036	2.75E+08
A0A087WVZ9;P19	A0A087WVZ9;P19	DNA-directed RNA	POLR2E	5	5	184	0.83759	0.87213	1.69E+08
H0YDT0;Q96D71-2	H0YDT0;Q96D71-2	RalBP1-associated I	REPS1	3	3	754	0.83723	0.78944	1.01E+08
Q9HCN4;Q9HCN4-:	Q9HCN4;Q9HCN4-:	GPN-loop GTPase 1	GPN1	3	3	374	0.837	NaN	1.42E+08
Q8N201	Q8N201	Integrator complex	INTS1	16	16	2190	0.83687	1.736	7.00E+08
P57088;D6RAA6;H	P57088;D6RAA6	Transmembrane pr	TMEM33	8	8	247	0.83685	1.1192	3.24E+09
Q96HC4;Q96HC4-7	Q96HC4;Q96HC4-7	PDZ and LIM domai	PDLIM5	6	6	596	0.83669	1.1898	3.03E+08
P09936;D6RE83;D	P09936;D6RE83;D	Ubiquitin carboxyl	UCHL1	12	12	223	0.8364	1.4304	9.12E+08
Q96RG2;Q96RG2-2	Q96RG2;Q96RG2-2	PAS domain-contai	PASK	4	4	1323	0.83631	0.99476	1.53E+08
F5H4B6;Q8IZ83-3;(	F5H4B6;Q8IZ83-3;(	Aldehyde dehydrog	ALDH16A1	6	6	639	0.83623	0.98689	4.31E+08
P56134-3;P56134	P56134-3;P56134	ATP synthase subur	ATP5J2	4	2	55	0.83606	1.5272	5.77E+08
P61586;C9JNR4;C9	P61586;C9JNR4;C9	Transforming prote	RHOA	6	3	193	0.83567	1.5501	3.71E+08
Q14694;Q14694-3	Q14694;Q14694-3	Ubiquitin carboxyl	USP10	8	8	798	0.83566	1.0681	5.79E+08
B7Z7F3;Q9H6Z4-3;	B7Z7F3;Q9H6Z4-3;	Ran-binding protei	ZNF8;RANBP3	3	3	494	0.83522	NaN	5.74E+07
A0A0A0MQU1;Q27	A0A0A0MQU1;Q27	Inverted formin-2	INF2	6	6	717	0.83512	0.9522	1.09E+08
P48507;P48507-2	P48507;P48507-2	Glutamate--cystein	GCLM	6	6	274	0.83489	1.2472	9.85E+08
A0A0C4DGY8;D6R/	A0A0C4DGY8;D6R/	Enolase-phosphata	ENOPH1	2	2	149	0.83469	1.3467	3.61E+08
Q9Y241;Q9Y241-2;	Q9Y241;Q9Y241-2;	HIG1 domain famil	HIGD1A	4	4	93	0.83463	1.2461	7.61E+08
P61981	P61981	14-3-3 protein gam	YWHAG	11	6	247	0.83457	1.3019	1.48E+08
Q68EM7-2;Q68EM	Q68EM7-2;Q68EM	Rho GTPase-activat	ARHGAP17	9	9	803	0.8345	0.76044	3.49E+08
P54136;P54136-2;	P54136;P54136-2	Arginine--tRNA liga	RARS	32	32	660	0.83423	1.2326	9.66E+09
E7ESY4;Q13330-3;(	E7ESY4;Q13330-3;(	Metastasis-associat	MTA1	9	4	703	0.83415	1.4323	4.70E+08
A6NJA2;P54578-2;	A6NJA2;P54578-2;	Ubiquitin carboxyl	USP14	13	13	448	0.83411	1.1558	2.23E+09
P11717;S4R328	P11717	Cation-independen	IGF2R	5	5	2491	0.834	3.1924	7.31E+08
F5H442;Q99816;Q	F5H442;Q99816	Tumor susceptibili	TSG101	5	5	365	0.83364	1.5372	4.92E+08
P35813-2;P35813;	P35813-2;P35813	Protein phosphata	PPM1A	3	3	324	0.83351	1.3824	4.22E+07
P17858;P17858-2	P17858;P17858-2	ATP-dependent 6-p	PFKL	22	17	780	0.83332	1.2032	4.12E+09
A0A0C4DG33;O43!	A0A0C4DG33;O43!	Peroxisome biogen	PEX1	9	9	1226	0.83309	0.9617	2.75E+08
J9JIC5;Q9HAS0;J3K	J9JIC5;Q9HAS0;J3K	Protein Njmu-R1	C17orf75	4	4	396	0.83296	1.2162	2.48E+08
C9J2I0;B8ZZY2;P5	C9J2I0;B8ZZY2;P5	Arf-GAP domain an	AGFG1	2	2	238	0.8327	0.95626	1.03E+08
P45954-2;P45954	P45954-2;P45954	Short/branched ch	ACADSB	7	7	330	0.8326	1.2329	6.08E+08
Q9BV20;Q9BV20-2	Q9BV20;Q9BV20-2	Methylthioribose-1	MRI1	13	13	369	0.83207	1.0291	4.59E+09
Q9Y6A9;C9JBL1;X6	Q9Y6A9;C9JBL1;X6	Signal peptidase co	SPCS1	2	2	102	0.83188	1.0705	6.51E+07
Q14669-4;Q14669	Q14669-4;Q14669	E3 ubiquitin-protei	TRIP12	20	20	1722	0.83181	0.825	9.82E+08
Q7Z4L5;Q7Z4L5-2;	Q7Z4L5	Tetratricopeptide r	TTC21B	6	6	1316	0.83148	1.0301	2.38E+08
O43447;C9JQD4;O	O43447;C9JQD4;O	Peptidyl-prolyl cis-	PPIH	12	12	177	0.83127	1.1363	2.09E+09
E9PFN5;Q9Y2Q3-4;	E9PFN5;Q9Y2Q3-4;	Glutathione S-tran	GSTK1	3	3	190	0.83097	1.2309	1.96E+08
P05976-2;P05976;	P05976-2;P05976;	Myosin light chain	MYL1;MYL3	1	1	150	0.83082	1.39	7.70E+07
P82912-2;P82912;	P82912-2;P82912;	28S ribosomal prot	MRPS11	4	4	193	0.83081	1.1851	1.68E+08
Q969F9-2;Q969F9;	Q969F9-2;Q969F9;	Hermansky-Pudlak	HPS3	3	3	890	0.83049	1.3118	1.02E+08
O00154-4;O00154	O00154-4;O00154	Cytosolic acyl coen	ACOT7	17	17	338	0.82988	1.3514	7.00E+09
Q13395	Q13395	Probable methyltra	TARBP1	11	11	1621	0.8297	1.2219	5.15E+08
C9J3L8;C9J5W0;E9	C9J3L8;C9J5W0;E9	Translocon-associa	SSR1	2	2	265	0.8292	1.3586	1.35E+09
P62805	P62805	Histone H4	HIST1H4A	15	15	103	0.8292	1.541	3.38E+10
Q8N1B4-2;Q8N1B4	Q8N1B4-2;Q8N1B4	Vacuolar protein so	VPS52	4	4	598	0.82916	0.96434	2.60E+08
Q15555-4;Q15555	Q15555-4;Q15555	Microtubule-associ	MAPRE2	7	7	274	0.82909	1.112	1.70E+09
O00487;C9JW37	O00487	26S proteasome no	PSMD14	9	9	310	0.82862	1.3974	1.77E+09
Q5VYK3;J3KN16;R4	Q5VYK3;J3KN16	Proteasome-associa	ECM29;KIAA0368	35	35	1845	0.82843	1.1332	2.55E+09
Q8WU90;F8WB26;	Q8WU90;F8WB26	Zinc finger CCCH do	ZC3H15	3	3	426	0.82807	1.102	2.40E+08
Q9BYG3;C9J808;C9	Q9BYG3;C9J808;C9	MKI67 FHA domain	NIFK	7	7	293	0.82807	1.1211	6.78E+08
O94925;C9JIJ6;B7Z	O94925	Glutaminase kidne	GLS	13	2	669	0.82787	1.3774	5.05E+07
A0A087WUC6;Q15	A0A087WUC6;Q15	Signal peptidase co	SPCS2	16	16	227	0.82702	1.1933	7.57E+08
O43242;O43242-2	O43242;O43242-2	26S proteasome no	PSMD3	32	32	534	0.82692	1.3281	9.02E+09
O75607	O75607	Nucleoplasmin-3	NPM3	4	4	178	0.8268	1.1064	6.89E+09
P06737-2;P06737;	P06737-2;P06737	Glycogen phospho	PYGL	37	32	813	0.8267	1.1606	6.91E+09
A0A0B4J1Z1;C9JAE	A0A0B4J1Z1;C9JAE	Serine/arginine-ricl	SRSF7	2	2	137	0.82655	1.1966	2.23E+08
P11142;E9PKE3;E9	P11142;E9PKE3;E9	Heat shock cognate	HSPA8	46	19	646	0.82654	1.1627	1.03E+11
Q2NKX8;B5MDQ0	Q2NKX8;B5MDQ0	DNA excision repai	ERCC6L	11	11	1250	0.82533	1.1813	3.53E+08
P49441;C9J128;C9	P49441	Inositol polyphosp	INPP1	3	3	399	0.82505	1.2572	3.15E+08
Q8N3U4;Q8N3U4-:	Q8N3U4;Q8N3U4-:	Cohesin subunit SA	STAG2	3	3	1231	0.8249	1.4622	4.79E+07
P84103-2;P84103;	P84103-2;P84103	Serine/arginine-ricl	SRSF3	5	5	124	0.82481	0.97329	9.96E+08
P42224;J3KPM9;P	P42224;J3KPM9;P	Signal transducer a	STAT1	16	16	750	0.82467	1.4739	1.41E+09
P09874;Q5VX84;Q	P09874	Poly [ADP-ribose] p	PARP1	53	53	1014	0.82449	1.375	3.36E+10
Q9UIC8-3;Q9UIC8;	Q9UIC8-3;Q9UIC8;	Leucine carboxyl m	LCMT1	4	4	279	0.8242	1.074	3.45E+08
J3KRA9;Q96Q15-2;	J3KRA9;Q96Q15-2	Serine/threonine-p	SMG1	3	3	3551	0.82406	1.0948	7.07E+07
Q13283;E5RIZ6;E5	Q13283	Ras GTPase-activati	G3BP1	11	10	466	0.824	1.2329	2.32E+09
F8VYN9;P40616-2;	F8VYN9;P40616-2;	ADP-ribosylation fa	ARL1	5	5	194	0.8236	1.2039	1.23E+09
P06493;A0A024Q2	P06493;A0A024Q2	Cyclin-dependent k	CDK1;CDC2	18	16	297	0.82344	1.0767	5.58E+09
E7ESP9;P07197;E7	E7ESP9;P07197;E7	Neurofilament mec	NEFM	9	7	877	0.82313	1.7049	7.01E+08
Q9NVH1-3;Q9NVH	Q9NVH1-3;Q9NVH	DnaJ homolog subf	DNAJC11	7	7	507	0.82313	1.1737	5.22E+08
Q14126;J3KSI6	Q14126	Desmoglein-2	DSG2	4	4	1118	0.82308	0.94301	1.30E+08
Q96E14;I3L2E0	Q96E14	RecQ-mediated gen	RMI2	3	3	147	0.82281	1.1936	1.09E+08
P62875	P62875	DNA-directed RNA	POLR2L	2	2	67	0.8218	1.2131	4.86E+08
O14776-2;O14776	O14776-2;O14776	Transcription elong	TCERG1	5	5	1077	0.82159	0.69998	1.30E+08
Q9Y277;Q9Y277-2;	Q9Y277;Q9Y277-2	Voltage-dependent	VDAC3	8	8	283	0.82149	1.4916	5.05E+09
O43809;H3BND3;H	O43809;H3BND3	Cleavage and polya	NUDT21	4	4	227	0.82116	1.3831	7.72E+07
B1AHQ7;B1AHQ6;(	B1AHQ7;B1AHQ6;(	Centromere protei	CENPM	2	2	73	0.82086	1.7516	1.02E+08
Q8N584-2;Q8N584	Q8N584-2;Q8N584	Tetratricopeptide r	TTC39C	3	3	522	0.82073	0.8524	1.47E+08
P11177-2;P11177;	P11177-2;P11177	Pyruvate dehydrog	PDHB	14	14	341	0.82037	1.1583	7.29E+09
H0YNG3;P67812-4	H0YNG3;P67812-4	Signal peptidase co	SEC11A	7	7	163	0.8202	1.2979	8.13E+08
Q9H845;H0Y8Z9;D	Q9H845;H0Y8Z9	Acyl-CoA dehydrog	ACAD9	6	6	621	0.81962	1.5408	4.39E+08
O95456-2;O95456	O95456-2;O95456	Proteasome assem	PSMG1	6	6	267	0.81933	1.0317	1.87E+09
Q9NVI1;Q9NVI1-1;	Q9NVI1;Q9NVI1-1;	Fanconi anemia grc	FANCI	40	40	1328	0.81926	1.1961	3.21E+09
R4GNB2;R4GN35;(	R4GNB2;R4GN35;(	DENN domain-cont	DENND4C	6	6	1909	0.81914	1.4974	1.91E+08
H7C0C7;Q9UKZ1	H7C0C7;Q9UKZ1	CCR4-NOT transcri	CNOT11	2	2	127	0.81865	NaN	1.35E+08

P22102;P22102-2;	P22102	Trifunctional purin	GART	46	46	1010	0.81766	1.19	1.30E+10
Q60FE5;P21333-2;	Q60FE5;P21333-2;	Filamin-A	FLNA	67	62	2620	0.81727	1.2522	6.74E+09
O00203-3;O00203	O00203-3;O00203	AP-3 complex subu	AP3B1	11	8	1045	0.81693	1.6322	4.90E+08
Q6YN16;Q6YN16-2	Q6YN16;Q6YN16-2	Hydroxysteroid del	HSDL2	9	9	418	0.81691	0.86075	1.06E+09
A0A0A0MRK6;Q13	A0A0A0MRK6;Q13	Metaxin-1	MTX1	3	3	466	0.81671	1.3289	2.90E+08
E9PKG1;H7C2I1;Q	E9PKG1;H7C2I1;Q	Protein arginine N-	PRMT1	14	14	325	0.81655	1.511	3.18E+09
A0A087X2H1;Q9U	A0A087X2H1;Q9U	E3 ubiquitin-protei	HECTD1	33	33	2614	0.81626	0.97721	2.01E+09
B4DXW1;P61158;I	B4DXW1;P61158	Actin-related prote	ACTR3	18	18	367	0.81626	1.333	3.51E+09
P12814;P12814-3;	P12814;P12814-3;	Alpha-actinin-1	ACTN1	28	15	892	0.81596	1.2639	9.31E+08
Q9H1A4;H0Y564;F	Q9H1A4;H0Y564	Anaphase-promoti	ANAPC1	19	19	1944	0.81549	1.1673	1.01E+09
Q71DI3;Q16695;P	Q71DI3;Q16695;P	Histone H3.2;Histo	HIST2H3A;HIST3H3	6	2	136	0.81532	1.5729	2.87E+09
Q96SB8;Q96SB8-2;	Q96SB8;Q96SB8-2;	Structural mainten	SMC6	9	9	1091	0.81466	1.1748	3.91E+08
Q9HB90;Q9NQL2;(	Q9HB90;Q9NQL2	Ras-related GTP-bir	RRAGC;RRAGD	7	7	399	0.81427	1.123	3.10E+08
Q14232;Q14232-2	Q14232;Q14232-2	Translation initiati	EIF2B1	12	12	305	0.81424	1.1239	1.81E+09
O15270	O15270	Serine palmitoyltra	SPTLC2	2	2	562	0.81387	0.94233	1.85E+08
Q6ZW49;Q6ZW49-	Q6ZW49;Q6ZW49-	PAX-interacting pr	PAXIP1	5	5	1069	0.81386	0.8834	2.79E+08
P30566;A0A0A6YY	P30566;A0A0A6YY	Adenylosuccinate l	ADSL	16	16	484	0.81375	1.1751	5.03E+09
P62258;P62258-2;	P62258;P62258-2;	14-3-3 protein epsi	YWHAE	15	12	255	0.81301	1.0041	9.26E+08
P31946-2;P31946;	P31946-2;P31946	14-3-3 protein beta	YWHAB	10	4	244	0.81292	1.0874	1.73E+08
P31942-2;P31942;	P31942-2;P31942	Heterogeneous nuc	HNRNPH3	7	6	331	0.81278	1.4263	1.37E+09
Q9NXV6;J3KNE1;D	Q9NXV6	CDKN2A-interactin	CDKN2AIP	3	3	580	0.81275	1.3036	6.71E+07
P00367;P49448;P	P00367;P49448;P	Glutamate dehydro	GLUD1;GLUD2	9	9	558	0.81261	0.94078	5.54E+08
P21912;A0A087W	P21912;A0A087W	Succinate dehydro	SDHB	3	3	280	0.8126	1.2365	4.03E+08
P53582;H0Y955;H	P53582;H0Y955	Methionine amino	METAP1	4	4	386	0.81245	1.1895	1.80E+08
F8W6G1;Q9UHY1;I	F8W6G1;Q9UHY1	Nuclear receptor-b	NRBP1	3	3	543	0.81233	1.7013	3.28E+08
P62913-2;Q5VVC8	P62913-2;Q5VVC8	60S ribosomal prot	RPL11	11	1	177	0.81229	NaN	4.28E+06
J3QL14;R4GN72;F	J3QL14;R4GN72;F	V-type proton ATPa	ATP6V0D1	2	2	232	0.81214	NaN	1.20E+08
Q5JWT2;Q9ULK4-4	Q5JWT2;Q9ULK4-4	Mediator of RNA pc	MED23	19	19	1374	0.81212	1.1625	1.18E+09
P49593;P49593-2;	P49593;P49593-2;	Protein phosphata	PPM1F	11	11	454	0.8118	0.98413	1.71E+09
P51812;B1AXG1;E	P51812;B1AXG1	Ribosomal protein	RPS6KA3	3	3	740	0.81154	2.0048	1.80E+08
Q9Y2A7;Q9Y2A7-2	Q9Y2A7;Q9Y2A7-2	Nck-associated pro	NCKAP1	23	23	1128	0.81102	1.2599	2.23E+09
Q6P2E9;Q6P2E9-2;	Q6P2E9;Q6P2E9-2	Enhancer of mRNA-	EDC4	17	17	1401	0.81098	1.005	7.97E+08
P22087;M0R299;N	P22087;M0R299;N	rRNA 2-O-methyltr	FBL	12	11	321	0.8109	1.1849	5.59E+09
Q8NB37;Q8NB37-2	Q8NB37;Q8NB37-2	Parkinson disease 7	PDDC1	3	3	220	0.81045	0.88639	1.15E+08
Q9HA77;H0YFV1;F	Q9HA77;H0YFV1;F	Probable cysteine--	CARS2	2	2	564	0.80997	0.93566	1.44E+08
O95168;O95168-2	O95168;O95168-2	NADH dehydrogena	NDUFB4	6	6	129	0.80993	1.3247	3.75E+08
Q9P258	Q9P258	Protein RCC2	RCC2	4	4	522	0.80927	1.4843	1.33E+08
Q9UM13;D6R9Q5;	Q9UM13;D6R9Q5;	Anaphase-promoti	ANAPC10	2	2	185	0.80924	0.89733	6.79E+07
A0A0A0MRP6;B7ZI	A0A0A0MRP6;B7ZI	Probable global tra	SMARCA1	20	7	1058	0.80911	1.5165	1.83E+08
Q71UI9;P0C0S5;C	Q71UI9;P0C0S5;C	Histone H2A.V;Hist	H2AFV;H2AFZ	5	3	128	0.80861	1.4134	5.32E+08
Q9Y315;E9PPM8;G	Q9Y315;E9PPM8;G	Putative deoxyribo	DERA	7	7	318	0.80857	1.2939	3.83E+08
Q9NTJ5;F8WCQ2;E	Q9NTJ5;F8WCQ2;E	Phosphatidylinosit	SACM1L	4	4	587	0.80845	1.4593	1.13E+08
Q9UEW8-2;Q9UEW	Q9UEW8-2;Q9UEW	STE20/SPS1-relatec	STK39	11	8	526	0.80826	1.0003	3.94E+08
P04843;B7Z4L4;F8	P04843;B7Z4L4	Dolichyl-diphosphi	RPN1	29	29	607	0.80731	1.7769	7.28E+09
Q9Y4C2;Q9Y4C2-2;	Q9Y4C2;Q9Y4C2-2	Protein FAM115A	FAM115A	13	13	921	0.80661	0.7864	6.80E+08
O15397;O15397-2	O15397;O15397-2	Importin-8	IPO8	11	10	1037	0.80631	1.2456	4.83E+08
A0A0C4DGS9;Q9Y6	A0A0C4DGS9;Q9Y6	Choline/ethanolam	CEPT1	1	1	280	0.80598	NaN	2.13E+08
A0A0C4DGZ0;P24S	A0A0C4DGZ0;P24S	DNA-directed RNA	POLR2A	47	47	1970	0.80577	1.0969	3.08E+09
Q9NUQ8-2;Q9NUQ	Q9NUQ8-2;Q9NUQ	ATP-binding cassett	ABCF3	6	6	703	0.80569	1.106	3.19E+08
A0A087WY12;Q9B	A0A087WY12;Q9B	Mitochondrial 2-o	SLC25A21	2	2	234	0.80565	0.9496	8.31E+07
P11441;Q5HY81	P11441;Q5HY81	Ubiquitin-like prot	UBL4A	3	3	157	0.80543	0.56833	3.91E+07
O75821;K7EL20;K	O75821;K7EL20;K	Eukaryotic translat	EIF3G	12	12	320	0.80534	1.2954	2.24E+09
P23921;E9PL69;E9	P23921;E9PL69	Ribonucleoside-dip	RRM1	20	20	792	0.80528	1.0304	1.80E+09
Q5LJA5;Q5LJA9;Q9	Q5LJA5;Q5LJA9;Q9	Ubiquitin carboxyl	UCHL5	12	12	355	0.80516	1.4108	3.94E+09
E7EM64;Q7L5N1;H	E7EM64;Q7L5N1	COP9 signalosome	COPS6	4	4	326	0.80441	1.2783	3.98E+08
J3KPT4;Q9H4I3-2;(	J3KPT4;Q9H4I3-2;(	TraB domain-conta	TRABD	4	4	379	0.80438	1.0782	2.68E+08
P61163;R4GMT0	P61163;R4GMT0	Alpha-centractin	ACTR1A	14	9	376	0.80407	1.3377	5.58E+09
Q969V3-2;Q969V3	Q969V3-2;Q969V3	Nicalin	NCLN	16	16	562	0.80406	1.3898	1.07E+09
Q9UBX3;Q9UBX3-2	Q9UBX3;Q9UBX3-2	Mitochondrial dica	SLC25A10	8	1	287	0.80395	1.2272	1.04E+08
P53396;P53396-2;	P53396;P53396-2;	ATP-citrate synthas	ACLY	60	60	1101	0.80387	1.1536	3.16E+10
Q53GQ0;E9PI21;Q	Q53GQ0	Estradiol 17-beta-d	HSD17B12	14	14	312	0.80382	1.3475	5.53E+09
Q10469	Q10469	Alpha-1,6-mannos	MGAT2	2	2	447	0.80366	0.81482	7.97E+07
O43592;F8WDU6;I	O43592	Exportin-T	XPOT	23	23	962	0.80338	1.2356	3.99E+09
Q8N4Q0;Q8N4Q0-;	Q8N4Q0;Q8N4Q0-;	Zinc-binding alcoh	ZADH2	2	2	377	0.80306	1.0024	3.77E+08
Q9UBB6-2;Q9UBB6	Q9UBB6-2;Q9UBB6	Neurochondrin	NCDN	3	3	712	0.80246	2.1405	5.66E+07
A0A087X0Q1;Q7Z7	A0A087X0Q1;Q7Z7	YTH domain-contai	YTHDF3	6	2	583	0.80195	1.4488	2.36E+08
Q86X76-2;Q86X76	Q86X76-2;Q86X76	Nitrilase homolog 1	NIT1	3	3	291	0.8019	1.3433	2.17E+08
P62308;A8MWD9;	P62308;A8MWD9;	Small nuclear ribor	SNRPG;SNRPGP15	4	4	76	0.8015	1.3238	8.04E+08
O94855;O94855-2	O94855;O94855-2	Protein transport p	SEC24D	5	5	1032	0.80146	1.6684	3.68E+08
Q8NBY1;B4E0Y9;Q	Q8NBY1;B4E0Y9;Q	Serine/threonine-p	RBM4B;MST4;STK2	7	3	392	0.80112	1.3352	6.32E+08
E9PN81;Q8TDP1-2	E9PN81;Q8TDP1-2	Ribonuclease H2 su	RNASEH2C	5	5	247	0.80001	0.88641	1.05E+08
Q13185;C9JMM0;I	Q13185	Chromobox protei	CBX3	5	4	183	0.7999	1.2982	6.38E+08
P55263-3;P55263-	P55263-3;P55263-	Adenosine kinase	ADK	2	2	305	0.79987	1.5632	4.06E+07
P36405	P36405	ADP-ribosylation fa	ARL3	3	3	182	0.79986	1.6157	6.63E+07
K7ERF1;Q9UBQ5;K	K7ERF1;Q9UBQ5;K	Eukaryotic translat	EIF3K	6	6	192	0.79982	1.1964	1.86E+08
H0YJV7;P25490;H(	H0YJV7;P25490	Transcriptional rep	YY1	6	6	190	0.7996	1.1187	9.89E+07
Q9P0J0;Q9P0J0-2;	Q9P0J0;Q9P0J0-2;	NADH dehydrogena	NDUFA13	7	7	144	0.7993	1.2263	5.72E+08
P0CG13;J3KSJ7;H3	P0CG13;J3KSJ7;H3	Chromosome trans	CHTF8	3	3	121	0.79908	1.1174	2.79E+07
Q14676-3;Q14676	Q14676-3;Q14676	Mediator of DNA da	MDC1	9	9	1802	0.79871	1.4532	2.75E+08
O14929;O14929-2	O14929;O14929-2	Histone acetyltrans	HAT1	9	9	419	0.79816	1.4413	1.31E+09
Q86XI2;Q86XI2-2;I	Q86XI2;Q86XI2-2;I	Condensin-2 comp	NCAPG2	17	17	1143	0.79809	0.98549	9.46E+08
Q8IX12-2;Q8IX12;A	Q8IX12-2;Q8IX12;A	Cell division cycle a	CCAR1	17	17	1135	0.79768	1.3033	1.42E+09
B4E1G1;Q9BUN8-2	B4E1G1;Q9BUN8-2	Derlin-1	DERL1	3	3	151	0.79728	1.4745	2.26E+08
Q9NP97;B1AKR6;C	Q9NP97;B1AKR6;C	Dynein light chain	DYNLRB1;DYNLRB2	4	4	96	0.79687	1.1879	3.65E+08
A0A087WUA5;Q9H	A0A087WUA5;Q9H	EH domain-contain	EHD4	8	7	540	0.79661	1.5321	8.26E+08
E7EQR4;P26038;P3	E7EQR4;P26038;P3	Moesin;Radixin;Ezr	EZR;MSN;RDX	3	3	586	0.79658	1.5617	9.17E+07
P10809;E7ESH4;E7	P10809	60 kDa heat shock p	HSPD1	40	40	573	0.79613	1.2451	1.49E+10
Q9H900-2;Q9H90(	Q9H900-2;Q9H90(	Protein zwilch hon	ZWILCH	2	2	477	0.79606	1.3291	3.59E+08
Q12792;F8VS81;Q	Q12792;F8VS81;Q	Twinfilin-1	TWF1	3	3	350	0.79589	1.6715	1.04E+08
Q8IZ07;H0YIN8;F8	Q8IZ07;H0YIN8	Ankyrin repeat don	ANKRD13A	4	3	590	0.79451	0.81921	5.32E+07
P19387;H3BRR2	P19387	DNA-directed RNA	POLR2C	5	5	275	0.79449	1.3449	7.61E+08
P55060-3;P55060;	P55060-3;P55060	Exportin-2	CSE1L	34	34	945	0.79387	1.176	2.08E+10
Q96DI7;Q96DI7-2;	Q96DI7;Q96DI7-2;	U5 small nuclear ril	SNRNP40;DKFZp43	7	7	357	0.79384	1.3487	1.53E+09

P51571;A6NLM8	P51571;A6NLM8	Translocon-associa	SSR4	7	7	173	0.79366	1.3531	1.58E+09
Q9NWX5;F6TX30	Q9NWX5;F6TX30	Ankyrin repeat and	ASB6	3	3	421	0.7936	0.82675	1.70E+08
O75874	O75874	Isocitrate dehydrog	IDH1	4	3	414	0.79356	NaN	4.12E+07
Q9BSF4;K7ENF5	Q9BSF4	Uncharacterized pr	C19orf52	4	4	260	0.79305	1.283	4.75E+08
C9JRZ6;F8WAR4;Q	C9JRZ6;F8WAR4;Q	MICOS complex sut	CHCHD3	4	4	232	0.79298	0.97274	8.80E+07
Q9BX68	Q9BX68	Histidine triad nucl	HINT2	3	3	163	0.79286	1.403	1.59E+08
Q01167-3;Q01167	Q01167-3;Q01167	Forkhead box prote	FOXK2	1	1	328	0.79275	NaN	2.08E+07
P08047-3;P08047	P08047-3;P08047	Transcription facto	SP1	2	2	737	0.79243	0.96543	1.91E+08
E9PS41;Q6RFH5-2;	E9PS41;Q6RFH5-2;	WD repeat-contain	WDR74	2	2	328	0.79211	0.98843	4.85E+07
P47897;P47897-2;	P47897;P47897-2;	Glutamine--tRNA li	QARS	33	33	775	0.79151	1.2443	5.72E+09
P23526;P23526-2	P23526;P23526-2	Adenosylhomocyst	AHCY	25	25	432	0.7913	1.1872	1.46E+10
Q7L2H7;Q7L2H7-2	Q7L2H7;Q7L2H7-2	Eukaryotic translat	EIF3M	17	17	374	0.79118	1.5464	4.50E+09
Q8TCE6-2;Q8TCE6;	Q8TCE6-2;Q8TCE6;	Protein FAM45A;Pr	FAM45A;FAM45B	6	6	349	0.79106	0.99555	4.21E+08
Q16576;E9PC52;Q	Q16576;E9PC52;Q	Histone-binding pr	RBBP7	13	6	425	0.79099	1.215	3.27E+09
Q9NTI5-2;Q9NTI5;(	Q9NTI5-2;Q9NTI5	Sister chromatid cc	PDS5B	17	16	1391	0.7909	1.1397	1.39E+09
Q6PML9;D6R9M6	Q6PML9	Zinc transporter 9	SLC30A9	5	5	568	0.79054	1.2632	1.65E+08
Q5T4S7-3;Q5T4S7-	Q5T4S7-3;Q5T4S7-	E3 ubiquitin-protei	UBR4	77	77	5159	0.79047	1.2727	5.61E+09
Q9NR12;D6RH06;(	Q9NR12;D6RH06;(	PDZ and LIM domai	PDLIM7	6	6	457	0.78956	1.0026	6.26E+08
P61009	P61009	Signal peptidase co	SPCS3	6	6	180	0.78951	1.3508	1.89E+08
P68104;Q5VTE0;A(	P68104;Q5VTE0;A(	Elongation factor 1	EEF1A1;EEF1A1P5	25	13	462	0.78927	1.6357	6.80E+10
Q9Y3F4;Q9Y3F4-2;	Q9Y3F4;Q9Y3F4-2	Serine-threonine ki	STRAP	12	12	350	0.78914	1.3888	1.96E+09
O14818;O14818-2	O14818;O14818-2	Proteasome subuni	PSMA7	12	12	248	0.78899	1.2135	2.99E+09
Q02809;Q02809-2	Q02809;Q02809-2	Procollagen-lysine,	PLOD1	7	7	727	0.78873	1.4139	4.57E+08
Q9H6R4-4;Q9H6R4	Q9H6R4-4;Q9H6R4	Nucleolar protein 6	NOL6	18	18	1143	0.78847	1.3151	8.76E+08
O95372;Q5QPQ1;(	O95372;Q5QPQ1;(	Acyl-protein thioes	LYPLA2	5	5	231	0.78813	1.0152	6.86E+07
P42345;B1AKP8;B	P42345	Serine/threonine-p	MTOR	13	13	2549	0.78783	1.0526	7.53E+08
G8JLD5;O00429-4;	G8JLD5;O00429-4	Dynamin-1-like pro	DNM1L	3	3	712	0.78772	1.7465	1.76E+08
Q07021;I3L3Q7;I3	Q07021;I3L3Q7;I3	Complement comp	C1QBP	8	8	282	0.7877	1.3972	6.33E+09
E7ESC6;Q9UIA9;E5	E7ESC6;Q9UIA9;E5	Exportin-7	XPO7	2	2	1088	0.78757	1.4087	4.02E+07
H0YLI7;P59780;Q7	H0YLI7;P59780;Q7	AP-3 complex subu	AP3S2	5	5	205	0.78742	0.99963	6.17E+07
A0A0A0MRN4;Q5B	A0A0A0MRN4;Q5B	DBIRD complex sut	ZNF326	2	2	493	0.78739	0.9725	2.73E+08
Q9BTV4	Q9BTV4	Transmembrane pr	TMEM43	2	2	400	0.78726	NaN	6.51E+07
O00299	O00299	Chloride intracellu	CLIC1	11	11	241	0.78722	1.2927	4.20E+09
Q96GJ1-3;Q96GJ1·	Q96GJ1-3;Q96GJ1·	tRNA (uracil(54)-C(!	TRMT2B	2	2	459	0.78695	NaN	2.81E+07
F8WDV0;Q9UI26;(	F8WDV0;Q9UI26;(	Importin-11	IPO11	4	4	863	0.78688	1.6323	1.81E+08
P36957;P36957-2;	P36957;P36957-2;	Dihydrolipoyllysin	DLST	5	5	453	0.78682	1.7288	5.90E+08
P16615-5;P16615·	P16615-5;P16615·	Sarcoplasmic/endo	ATP2A2	37	37	997	0.78653	1.1411	1.21E+10
B3KQ25;K7ESG5;P	B3KQ25;K7ESG5;P	Proteasome activat	PSME3	4	4	193	0.7857	0.83027	2.47E+08
P25398	P25398	40S ribosomal prot	RPS12	8	8	132	0.78526	1.3641	2.34E+09
Q15397;S4R3K8	Q15397;S4R3K8	Pumilio domain-co	KIAA0020	2	2	648	0.78497	NaN	9.48E+07
Q04323;E9PRQ7;E	Q04323;E9PRQ7;E	UBX domain-conta	UBXN1	14	14	297	0.78479	1.0288	2.50E+09
Q13162;H7C3T4;A	Q13162;H7C3T4	Peroxiredoxin-4	PRDX4	7	4	271	0.78465	1.523	8.58E+08
P52907	P52907	F-actin-capping pro	CAPZA1	8	6	286	0.78413	1.284	2.31E+09
Q8NCM8;Q8NCM8	Q8NCM8;Q8NCM8	Cytoplasmic dynei	DYNC2H1	23	23	4307	0.78366	1.4653	9.03E+08
Q8NAT1	Q8NAT1	Protein O-linked-m	POMGNT2	2	2	580	0.78355	1.3015	8.55E+07
P86791;P86790	P86791;P86790	Vacuolar fusion pro	CCZ1;CCZ1B	3	3	482	0.78334	0.90381	1.50E+08
P50851	P50851	Lipopolysaccharide	LRBA	22	0	2863	0.78309	1.1299	1.17E+09
Q9NVA1-2;Q9NVA1	Q9NVA1-2;Q9NVA1	Ubiquinol-cytochr	UQCC1	3	3	273	0.78299	2.0789	7.67E+07
Q8IYB7;H7C440;Q8	Q8IYB7;H7C440;Q8	DIS3-like exonucle	DIS3L2	8	8	885	0.78283	0.97908	2.52E+08
Q8TED0-3;Q8TED0;	Q8TED0-3;Q8TED0;	U3 small nucleolar	UTP15	7	7	499	0.78265	1.1179	6.86E+08
E9PN51;F8W9K7;E	E9PN51;F8W9K7;E	NADH dehydrogena	NDUFS8	4	4	110	0.78197	1.1401	9.39E+07
Q9HCJ3-2;Q9HCJ3;	Q9HCJ3-2;Q9HCJ3	Ribonucleoprotein	RAVER2	3	3	678	0.78167	NaN	9.95E+07
P63244;H0YAF8;J3	P63244;H0YAF8;J3	Guanine nucleotid	GNB2L1	11	11	317	0.78166	1.3544	2.81E+09
H0Y6T7;Q92542-2;	H0Y6T7;Q92542-2;	Nicastrin	NCSTN	3	3	275	0.78153	1.5125	9.93E+07
Q6PGP7;D6RCE2;H	Q6PGP7	Tetratricopeptide r	TTC37	22	22	1564	0.78123	1.1842	1.40E+09
Q9UBI1;R4GMW6;	Q9UBI1;R4GMW6;	COMM domain-cor	COMMD3;COMMD	7	7	195	0.7812	1.3552	1.77E+08
O00258;B7Z1T1;O	O00258;B7Z1T1;O	Tail-anchored prot	WRB	3	3	174	0.78094	1.4975	9.46E+07
Q92621;U3KPX2;U	Q92621	Nuclear pore comp	NUP205	56	56	2012	0.78028	1.1636	7.58E+09
Q9UI09;F8VXI1;F8	Q9UI09;F8VXI1;F8	NADH dehydrogena	NDUFA12	4	4	145	0.77997	1.8853	1.46E+08
B9A018;Q53GS9;A	B9A018;Q53GS9;A	U4/U6.U5 tri-snRN	USP39	8	8	536	0.77981	1.4466	1.05E+09
Q6PD74;Q6PD74-2	Q6PD74;Q6PD74-2	Alpha- and gamma-	AAGAB	3	3	315	0.77951	0.98278	2.12E+08
E7EWC2;F5H7S7;Q	E7EWC2;F5H7S7;Q	Ras GTPase-activati	IQGAP2	7	5	1402	0.77909	1.3636	1.47E+08
Q5VIR6-4;F6VX93;(	Q5VIR6-4;F6VX93;(	Vacuolar protein sc	VPS53	5	5	832	0.77906	1.0505	1.87E+08
P38919;I3L3H2	P38919	Eukaryotic initiatic	EIF4A3	26	21	411	0.7784	1.2292	8.86E+09
P11387;Q969P6-2	P11387	DNA topoisomeras	TOP1	25	25	765	0.77836	1.2144	3.26E+09
M0QYT9;Q14653;N	M0QYT9;Q14653;N	Interferon regulato	IRF3	2	2	281	0.77799	NaN	1.31E+08
I3L2C7;P57678;I3I	I3L2C7;P57678	Gem-associated pro	GEMIN4	22	22	1047	0.77782	1.1915	1.97E+09
E9PC15;Q53H12;E	E9PC15;Q53H12;E	Acylglycerol kinase	AGK	10	10	394	0.77764	1.2756	1.38E+09
O60287	O60287	Nucleolar pre-ribos	URB1	22	22	2271	0.77756	1.2524	1.18E+09
Q15813;Q15813-2	Q15813;Q15813-2	Tubulin-specific ch	TBCE	8	8	527	0.77756	1.3485	1.26E+09
Q9Y295;H0YI06;F8	Q9Y295	Developmentally-r	DRG1	7	7	367	0.77741	1.3168	1.06E+09
Q5SRE5;Q5SRE5-2;	Q5SRE5;Q5SRE5-2	Nucleoporin NUP1	NUP188	34	34	1749	0.77727	1.1274	2.32E+09
Q9BPX3;D6RA93;H	Q9BPX3	Condensin comple	NCAPG	25	25	1015	0.77723	1.2223	1.56E+09
A0A087X1K9;O75(	A0A087X1K9;O75(	Acyl-protein thioes	LYPLA1	4	4	166	0.77629	1.0942	7.80E+08
O75351	O75351	Vacuolar protein sc	VPS4B	8	5	444	0.77625	1.1568	7.04E+08
Q14692	Q14692	Ribosome biogenes	BMS1	19	19	1282	0.77617	1.1449	1.21E+09
P51970	P51970	NADH dehydrogena	NDUFA8	3	3	172	0.77573	0.77786	5.10E+07
Q9HCU5;H7C2N7;I	Q9HCU5;H7C2N7;I	Prolactin regulator	PREB	4	4	417	0.77515	NaN	1.97E+08
J3QLE5;A8MT02;P:	J3QLE5;A8MT02;P:	Small nuclear ribor	SNRPN;SNRPB	7	7	169	0.77503	1.1835	3.61E+09
P13861-2;P13861;	P13861-2;P13861;	cAMP-dependent p	PRKAR2A	8	6	382	0.77423	1.4112	6.67E+08
Q14739;C9JXK0;C	Q14739;C9JXK0	Lamin-B receptor	LBR	12	12	615	0.77421	1.4247	2.90E+09
A2A2Q9;Q9Y312	A2A2Q9;Q9Y312	Protein AAR2 hom	AAR2	9	9	398	0.77417	0.90214	5.90E+08
E7EV99;E7ENY0;P3	E7EV99;E7ENY0;P3	Alpha-adducin	ADD1	8	7	632	0.77315	1.123	1.06E+09
P00403	P00403	Cytochrome c oxid	MT-CO2	6	6	227	0.77266	1.4578	7.60E+08
P62304;A6NHK2	P62304;A6NHK2	Small nuclear ribor	SNRPE	4	4	92	0.77201	1.3802	1.94E+09
Q9C0D3;A8DPD7;(	Q9C0D3;A8DPD7	Protein zyg-11 hon	ZYG11B	3	3	744	0.7719	1.409	1.45E+08
P50453;H7BXK7;C	P50453	Serpin B9	SERPINB9	4	4	376	0.77188	1.5033	1.48E+08
O95298;E9PM14;A	O95298;E9PM14;A	NADH dehydrogena	NDUFC2;NDUFC2-I	3	3	119	0.77146	1.246	1.30E+07
Q15750-2;Q15750	Q15750-2;Q15750	TGF-beta-activated	TAB1	5	5	462	0.77126	1.0653	5.96E+08
K7EP06;O43148;O	K7EP06;O43148;O	mRNA cap guanine·	RNMT	2	2	298	0.77119	1.66	1.50E+08
Q6VY07;Q6VY07-2;	Q6VY07;Q6VY07-2	Phosphofurin acidi	PACS1	2	2	963	0.77084	NaN	2.10E+07
Q6P9B6;H3BM75;I	Q6P9B6;H3BM75	TLD domain-contai	TLDC1	3	3	456	0.77065	1.8354	5.09E+08
P30085;Q5T0D2;P	P30085;Q5T0D2	UMP-CMP kinase	CMPK1	7	7	196	0.77049	1.1514	1.28E+08

P45880-2;P45880;	P45880-2;P45880	Voltage-dependent	VDAC2	9	9	283	0.77045	1.5994	6.90E+09
P56192;P56192-2;	P56192;P56192-2	Methionine--tRNA l	MARS	38	38	900	0.77041	1.179	1.26E+10
A0A0U1RQQ9;Q6P	A0A0U1RQQ9;Q6P	SCY1-like protein 2	SCYL2	12	12	933	0.76981	1.0194	6.20E+08
Q9UPU5;A0A0U1R	Q9UPU5	Ubiquitin carboxyl	USP24	26	26	2620	0.76966	1.2693	1.54E+09
F8VVA7;P61923;F8	F8VVA7;P61923;F8	Coatomer subunit z	COPZ1	6	6	198	0.76944	1.4594	1.48E+09
P04844-2;P04844;	P04844-2;P04844	Dolichyl-diphosphı	RPN2	14	14	615	0.76942	1.7524	2.91E+09
Q9H061;E9PI90;Q9	Q9H061;E9PI90;Q9	Transmembrane pr	TMEM126A	4	4	195	0.76905	1.1877	2.12E+08
P04406;P04406-2;	P04406;P04406-2	Glyceraldehyde-3-p	GAPDH	21	21	335	0.76885	1.3819	1.25E+10
P56589;Q7Z6V3	P56589;Q7Z6V3	Peroxisomal bioger	PEX3	3	3	373	0.7685	0.95395	3.81E+07
Q9BR76;A0A087W	Q9BR76	Coronin-1B	CORO1B	5	5	489	0.76824	1.155	3.01E+08
Q9Y320-2;Q9Y320;	Q9Y320-2;Q9Y320	Thioredoxin-relate	TMX2	3	3	258	0.76815	1.0784	5.58E+08
A0A096LPI6;A0A0I	A0A096LPI6;A0A0I	ES1 protein homol	C21orf33	11	8	279	0.76795	1.0398	8.13E+08
Q15036;Q15036-2	Q15036;Q15036-2	Sorting nexin-17	SNX17	5	5	470	0.76768	1.0954	2.32E+08
Q5TFE4;Q5TFE4-2;(	Q5TFE4;Q5TFE4-2;(	5-nucleotidase dor	NT5DC1	11	11	455	0.76755	1.2894	1.42E+09
P20073-2;P20073	P20073-2;P20073	Annexin A7	ANXA7	6	6	466	0.76733	1.6907	3.65E+08
Q3SXM5;Q3SXM5-;	Q3SXM5;Q3SXM5-;	Inactive hydroxyste	HSDL1	9	9	330	0.76665	1.4914	8.05E+08
E5RHG8;Q15369;R	E5RHG8;Q15369;R	Transcription elong	TCEB1	7	7	89	0.76636	1.2339	8.08E+08
Q96KP4-2;Q96KP4	Q96KP4-2;Q96KP4	Cytosolic non-spec	CNDP2	3	3	391	0.76635	1.5339	2.68E+08
Q86VP6;Q86VP6-2	Q86VP6;Q86VP6-2	Cullin-associated N	CAND1	37	34	1230	0.76604	1.1045	7.56E+09
F6SS63;Q8N5C8-2;	F6SS63;Q8N5C8-2;	TGF-beta-activated	TAB3	1	1	608	0.76601	1.1445	8.31E+07
Q9UHV9	Q9UHV9	Prefoldin subunit 2	PFDN2	3	3	154	0.76591	1.0228	1.26E+08
P10606	P10606	Cytochrome c oxid	COX5B	6	6	129	0.76576	1.0219	2.22E+08
Q05639	Q05639	Elongation factor 1	EEF1A2	14	2	463	0.76576	1.5732	2.12E+08
P62979;J3QS39;J3	P62979;J3QS39;J3	Ubiquitin-40S ribo	RPS27A;UBB;UBC;U	14	6	156	0.76569	1.3286	1.46E+11
E3W994;J3KR49;A	E3W994;J3KR49;A	CLIP-associating pr	CLASP2	5	5	1273	0.76568	0.98964	1.39E+08
P15121;E9PEF9;E9	P15121;E9PEF9;E9	Aldose reductase	AKR1B1	3	3	316	0.76552	1.5183	9.33E+07
J9JID7;Q03252	J9JID7;Q03252	Lamin-B2	LMNB2	8	4	620	0.76547	1.388	1.28E+08
Q9NZJ7-2;Q9NZJ7;	Q9NZJ7-2;Q9NZJ7;	Mitochondrial carr	MTCH1	9	9	372	0.76479	1.5254	3.17E+08
Q14008-2;Q14008	Q14008-2;Q14008	Cytoskeleton-assoc	CKAP5	7	7	1972	0.76444	0.80003	2.91E+08
Q14964;C9JB90	Q14964	Ras-related protein	RAB39A	6	5	217	0.7639	0.98872	3.41E+08
Q9BWH6;Q9BWH6	Q9BWH6;Q9BWH6	RNA polymerase II-i	RPAP1	15	15	1393	0.76359	1.1738	7.12E+08
Q9Y5M8;H7C4H2;(	Q9Y5M8	Signal recognition p	SRPRB	7	7	271	0.76302	1.4732	6.83E+08
P49257	P49257	Protein ERGIC-53	LMAN1	5	5	510	0.76273	1.5612	2.58E+08
P05091;P05091-2;	P05091;P05091-2	Aldehyde dehydrog	ALDH2	7	7	517	0.76262	1.573	4.71E+08
O95396	O95396	Adenylyltransferas	MOCS3	8	8	460	0.76255	0.99462	4.26E+08
Q96I51-3;Q96I51;A	Q96I51-3;Q96I51;A	Williams-Beuren sy	WBSCR16	4	4	454	0.76235	0.87067	1.76E+08
O15145;F8VR50;C!	O15145;F8VR50;C!	Actin-related prote	ARPC3	5	5	178	0.76227	1.5706	5.56E+08
P35914;P35914-3;	P35914	Hydroxymethylglut	HMGCL	3	3	325	0.76215	1.2873	9.22E+07
P52788-2;P52788;	P52788-2;P52788	Spermine synthase	SMS	5	5	313	0.76208	1.2576	7.53E+08
P51649;P51649-2;	P51649;P51649-2	Succinate-semialde	ALDH5A1	11	11	535	0.76206	1.0509	5.73E+08
B5MCF9;O00541-2	B5MCF9;O00541-2	Pescadillo homolo	PES1	15	15	571	0.76184	1.3936	6.66E+08
Q86Y56;Q86Y56-2;	Q86Y56;Q86Y56-2	HEAT repeat-contai	HEATR2	10	10	855	0.76156	1.3436	7.96E+08
Q14204;H0YJ21	Q14204	Cytoplasmic dynei	DYNC1H1	201	200	4646	0.76143	1.4503	3.02E+10
F5H619;Q86XA9-2	F5H619;Q86XA9-2	HEAT repeat-contai	HEATR5A	5	5	2046	0.76048	1.8886	2.36E+08
C9JA28;Q9UNL2;Q	C9JA28;Q9UNL2;Q	Translocon-associa	SSR3	2	2	174	0.76018	1.6126	6.12E+08
A0A087X0Q9;Q9B\	A0A087X0Q9;Q9B\	Selenoprotein O	SELO	1	1	668	0.75999	NaN	1.36E+08
Q9Y5J1;J3KSR7;J3(	Q9Y5J1	U3 small nucleolar	UTP18	7	7	556	0.75896	1.1853	3.63E+08
P41250;H7C443;F!	P41250	Glycine--tRNA ligas	GARS	33	33	739	0.75894	1.1996	1.03E+10
A0A087WXP7;Q9H	A0A087WXP7;Q9H	Diphthine synthase	DPH5	7	7	243	0.75887	1.1875	9.47E+08
O43747;O43747-2	O43747;O43747-2	AP-1 complex subu	AP1G1	14	14	822	0.75852	1.6254	1.60E+09
H7C1E4;P61966;P!	H7C1E4;P61966;P!	AP-1 complex subu	AP1S1	3	3	191	0.75817	1.8069	1.60E+08
A6NF51;O95861-4	A6NF51;O95861-4	3(2),5-bisphosphat	BPNT1	5	5	291	0.75797	1.6766	2.45E+08
B4DKY1;P49589-2;	B4DKY1;P49589-2	Cysteine--tRNA liga	CARS	5	5	739	0.75783	1.6657	1.19E+08
P46019	P46019	Phosphorylase b ki	PHKA2	3	2	1235	0.75762	1.0521	6.06E+07
Q16698-2;Q16698	Q16698-2;Q16698	2,4-dienoyl-CoA re	DECR1	4	4	326	0.75739	1.5617	2.97E+08
P27824;P27824-2;	P27824;P27824-2	Calnexin	CANX	14	14	592	0.757	1.3208	2.97E+09
P62310	P62310	U6 snRNA-associate	LSM3	3	3	102	0.75688	0.99923	6.94E+07
O00231;O00231-2	O00231;O00231-2	26S proteasome no	PSMD11	22	22	422	0.75667	1.7272	3.37E+09
O75396;A0A087X1	O75396	Vesicle-trafficking p	SEC22B	5	5	215	0.75646	1.2244	5.75E+08
P50570-3;P50570	P50570-3;P50570	Dynamin-2	DNM2	21	15	866	0.75611	1.2481	1.57E+09
Q96TC7;H0YNE5;H	Q96TC7;H0YNE5;H	Regulator of microt	RMDN3	3	3	470	0.7559	1.2846	3.76E+08
Q9UNM6;A0A087V	Q9UNM6;A0A087V	26S proteasome no	PSMD13	12	12	376	0.75543	1.6168	7.95E+08
P26196;Q8IV96	P26196	Probable ATP-depe	DDX6	15	15	483	0.75517	1.3714	5.50E+09
P09382	P09382	Galectin-1	LGALS1	3	3	135	0.75516	1.9146	3.62E+08
P22314-2;P22314;	P22314-2;P22314	Ubiquitin-like mod	UBA1	23	23	1018	0.75479	1.5545	3.96E+09
Q9UDR5;F8WAH1;	Q9UDR5;F8WAH1	Alpha-aminoadipic	AASS	4	4	926	0.75471	1.2111	7.71E+07
P26640;A0A140T9	P26640;A0A140T9	Valine--tRNA ligase	VARS	42	42	1264	0.75423	1.1463	9.54E+09
Q9Y6G9;E9PHI6	Q9Y6G9;E9PHI6	Cytoplasmic dynei	DYNC1LI1	5	5	523	0.75305	1.7409	4.12E+08
H3BMQ0;P49815-(	H3BMQ0;P49815-(	Tuberin	TSC2	14	14	1751	0.75279	1.1963	8.86E+08
P51991;H7C1J8	P51991	Heterogeneous nuc	HNRNPA3	21	4	378	0.7527	1.2066	6.52E+09
P08574	P08574	Cytochrome c1, he	CYC1	6	6	325	0.75223	1.2875	1.34E+09
Q15291-2;Q15291	Q15291-2;Q15291	Retinoblastoma-bi	RBBP5	4	4	500	0.75205	1.1865	3.32E+08
Q96T76;Q96T76-8;	Q96T76;Q96T76-8;	MMS19 nucleotide	MMS19	24	24	1030	0.75197	1.2307	3.21E+09
O00567;H0YDU4;H	O00567	Nucleolar protein 5	NOP56	26	26	594	0.75192	1.4301	5.38E+09
Q15645;H0YAL2;Q	Q15645	Pachytene checkpo	TRIP13	12	12	432	0.75176	1.2837	2.54E+09
A0A0C4DG54;Q5R	A0A0C4DG54;Q5R	Rab GTPase-activat	RABGAP1L	2	2	582	0.75158	1.6886	8.26E+07
Q06210-2;Q06210	Q06210-2;Q06210	Glutamine--fructos	GFPT1	24	22	681	0.75156	1.3725	4.89E+09
P21796;C9JI87	P21796;C9JI87	Voltage-dependent	VDAC1	15	15	283	0.75071	1.5595	5.42E+09
Q9Y3D0;J3KS95;H:	Q9Y3D0;J3KS95	Mitotic spindle-ass	FAM96B	7	7	163	0.75005	1.3748	7.62E+08
Q15459;Q15459-2	Q15459;Q15459-2	Splicing factor 3A s	SF3A1	4	4	793	0.74998	1.1369	1.26E+08
P36871;P36871-2;	P36871;P36871-2	Phosphoglucomut	PGM1	13	13	562	0.74944	1.3991	9.76E+08
Q9Y281;Q9Y281-3;	Q9Y281;Q9Y281-3	Cofilin-2	CFL2	6	2	166	0.74941	1.3159	1.48E+08
O14735;B3KY94;O	O14735;B3KY94;O	CDP-diacylglycerol	CDIPT	6	6	213	0.74916	1.2401	1.13E+09
Q9UDW1;Q9NZY4;	Q9UDW1;Q9NZY4;	Cytochrome b-c1 c	UQCR10	3	3	63	0.74811	1.4246	2.93E+08
I3L3S0;Q9Y5R8;I3L	I3L3S0;Q9Y5R8;I3L	Trafficking protein	TRAPPC1	3	3	95	0.74746	1.4313	1.11E+08
P42025	P42025	Beta-centractin	ACTR1B	6	1	376	0.74721	1.1866	1.27E+09
Q8WTW3;A0A087\	Q8WTW3;A0A087\	Conserved oligome	COG1;ADCK1	18	18	980	0.74711	0.93595	9.62E+08
Q9NUQ7;D6RGX2;I	Q9NUQ7;D6RGX2;I	Ufm1-specific prot	UFSP2	11	11	469	0.74669	1.0301	1.05E+09
Q32MN6;P20226-;	Q32MN6;P20226-;	TATA-box-binding p	TBP;TBPL2	2	2	288	0.74666	NaN	1.74E+08
P25705;P25705-2;	P25705;P25705-2	ATP synthase subur	ATP5A1	37	37	553	0.74654	1.5618	1.93E+10
E9PMY3;E9PML8;E	E9PMY3;E9PML8;E	Protein tyrosine ph	PTP4A2;PTP4A1	2	2	63	0.74651	1.2167	4.49E+07
C9J5D1;E7EQ69;Q9	C9J5D1;E7EQ69;Q9	N-alpha-acetyltran	NAA50	12	12	129	0.74649	1.3848	8.55E+08
Q86YV9	Q86YV9	Hermansky-Pudlak	HPS6	3	3	775	0.74599	1.0617	1.38E+08

Q9Y2S7;B4DEM9	Q9Y2S7;B4DEM9	Polymerase delta-i	POLDIP2		3	3	368	0.74553	1.3501	2.57E+08
Q658Y4;E7ER68	Q658Y4;E7ER68	Protein FAM91A1	FAM91A1		4	4	838	0.74527	NaN	9.51E+07
Q9NR30;Q9NR30-2	Q9NR30;Q9NR30-2	Nucleolar RNA heli	DDX21		49	47	783	0.74513	1.1757	2.02E+10
A0A0A0MSK6;Q13	A0A0A0MSK6;Q13	Rho GTPase-activat	ARHGAP5		2	2	1498	0.74509	NaN	2.26E+07
O95630;C9JK83;O	O95630;C9JK83;O	STAM-binding prot	STAMBP		2	2	424	0.74454	NaN	8.81E+07
Q96SI1-2;Q96SI1;K	Q96SI1-2;Q96SI1;K	BTB/POZ domain-c	KCTD15		3	3	234	0.74409	1.1651	1.38E+08
O95155-2;O95155	O95155-2;O95155	Ubiquitin conjugat	UBE4B		9	9	1173	0.74311	1.1068	2.77E+08
F5H0C4;Q9BRP4-2	F5H0C4;Q9BRP4-2	Proteasomal ATPas	PAAF1		2	2	393	0.743	NaN	7.46E+07
Q9UL25	Q9UL25	Ras-related protein	RAB21		8	8	225	0.74274	1.4381	1.11E+09
O14949	O14949	Cytochrome b-c1 c	UQCRQ		5	5	82	0.74225	1.2805	5.66E+08
P62306;A0A0B4J2	P62306	Small nuclear ribor	SNRPF		3	3	86	0.74225	1.2377	2.18E+08
P34932;A0A087W	P34932;A0A087W	Heat shock 70 kDa	HSPA4		21	19	840	0.74182	1.2529	2.77E+09
E5RIF2;Q9Y6D6;E5	E5RIF2;Q9Y6D6;E5	Brefeldin A-inhibite	ARFGEF1		3	3	1279	0.74129	1.434	7.24E+07
Q96P70	Q96P70	Importin-9	IPO9		16	16	1041	0.74117	1.2551	2.34E+09
H0Y8C6;O00410;O	H0Y8C6;O00410;O	Importin-5	IPO5		12	12	1099	0.74087	0.99118	5.87E+08
Q8N0U8	Q8N0U8	Vitamin K epoxide	VKORC1L1		2	2	176	0.74076	NaN	2.79E+07
P34897-3;P34897	P34897-3;P34897	Serine hydroxymet	SHMT2		10	9	483	0.74059	1.3649	1.03E+09
O00330-3;O00330	O00330-3;O00330	Pyruvate dehydrog	PDHX		7	7	486	0.73982	1.2185	2.84E+08
O60271-4;A0A087	O60271-4;A0A087	C-Jun-amino-termi	SPAG9		26	26	1307	0.73932	1.274	7.87E+08
Q6NUK1;Q6NUK1-	Q6NUK1;Q6NUK1-	Calcium-binding m	SLC25A24		9	9	477	0.73841	1.3227	8.18E+08
Q9BWJ5	Q9BWJ5	Splicing factor 3B s	SF3B5		3	3	86	0.73828	1.5474	1.45E+08
Q8IUI8-2;Q8IUI8	Q8IUI8-2;Q8IUI8	Cytokine receptor-l	CRLF3		1	1	438	0.73825	1.1188	1.73E+08
O75955;A0A140T9	O75955;A0A140T9	Flotillin-1	FLOT1		8	8	427	0.73824	1.3144	3.58E+08
P08240;P08240-2	P08240;P08240-2	Signal recognition	SRPR		9	9	638	0.73807	1.362	7.53E+08
Q9BSJ8;Q9BSJ8-2;I	Q9BSJ8;Q9BSJ8-2	Extended synaptot	ESYT1		16	16	1104	0.73791	1.5402	1.30E+09
P0DMV9;P0DMV8;	P0DMV9;P0DMV8;	A0A0G2JIW1;P0DM	HSPA1A		49	26	641	0.73742	1.2021	1.65E+11
A0A096LP25;Q6ZS	A0A096LP25;Q6ZS	Uncharacterized protein	FLJ45252		2	2	511	0.73697	NaN	4.32E+07
A0AVF1-2;A0AVF1-	A0AVF1-2;A0AVF1-	Tetratricopeptide r	TTC26		3	3	487	0.73623	1.326	3.09E+07
Q5TEC6	Q5TEC6	Histone H3	HIST2H3PS2		5	1	136	0.73602	1.6181	7.99E+08
F5H895;A0A0B4J2	F5H895;A0A0B4J2	Dolichyl-diphosphi	DAD1		2	2	65	0.73596	1.7492	1.99E+08
Q9UHD8-5;Q9UHD	Q9UHD8-5;Q9UHD	Septin-9		09-Sep	27	27	579	0.73577	1.2167	3.00E+09
Q9BXW7-2;Q9BXW	Q9BXW7-2;Q9BXW	Cat eye syndrome c	CECR5		11	11	393	0.73574	1.1938	2.43E+09
Q13561;Q13561-3	Q13561;Q13561-3	Dynactin subunit 2	DCTN2		7	7	401	0.73508	0.59225	3.79E+08
Q6UWP7-3;Q6UWI	Q6UWP7-3;Q6UW	Lysocardiolipin acy	LCLAT1		4	4	376	0.73474	1.8804	1.68E+08
Q9UBQ7;U3KQ56;(	Q9UBQ7;U3KQ56	Glyoxylate reducta	GRHPR		13	13	328	0.73448	1.2315	4.80E+09
Q9UNX4;Q6PDA5	Q9UNX4	WD repeat-contain	WDR3		29	29	943	0.73433	1.1892	1.94E+09
O43301;K7ELE6	O43301	Heat shock 70 kDa	HSPA12A		4	4	675	0.73408	1.307	2.05E+08
Q15393;Q15393-2	Q15393	Splicing factor 3B s	SF3B3		38	38	1217	0.734	1.268	9.27E+09
P10620;F5GX73;F5	P10620;F5GX73;F5	Microsomal glutath	MGST1		2	2	155	0.73331	1.2952	5.46E+07
A0A087X0Z7;H0YJ	A0A087X0Z7;H0YJ	Dehydrogenase/rec	DHRS7		5	5	376	0.73326	1.9328	1.38E+08
Q8WVC2;P63220;(	Q8WVC2;P63220;(	40S ribosomal prot	RPS21		6	6	81	0.73276	1.3394	4.18E+08
P29218;P29218-3;	P29218;P29218-3;	Inositol monophos	IMPA1		4	4	277	0.73232	1.8185	3.68E+08
J3KPS0;Q9NXW2;(	J3KPS0;Q9NXW2;(	DnaJ homolog subf	DNAJB12		3	3	409	0.73222	0.71213	3.39E+08
K7EM02;K7EIJ8;Q8	K7EM02;K7EIJ8;Q8	Katanin p60 ATPas	KATNAL2		1	1	128	0.73217	NaN	1.29E+09
A0A0C4DGU2;Q9Y	A0A0C4DGU2;Q9Y	Methylmalonic aci	MMACHC		2	2	225	0.73208	0.84419	1.10E+08
Q10567-3;Q10567	Q10567-3;Q10567	AP-1 complex subu	AP1B1		21	8	939	0.7319	1.3211	3.42E+08
P30040;F8VY02;P3	P30040;F8VY02;P3	Endoplasmic reticu	ERP29		2	2	261	0.73159	1.1815	8.80E+07
P09661;H0YKK0;H	P09661;H0YKK0	U2 small nuclear ri	SNRPA1		24	24	255	0.73142	1.2813	3.02E+10
Q68DK2-2;Q68DK2	Q68DK2-2;Q68DK2	Zinc finger FYVE do	ZFYVE26		2	2	2518	0.73101	NaN	7.00E+06
F8W726;Q14157-4	F8W726;Q14157-4	Ubiquitin-associate	UBAP2L		4	4	1079	0.7309	1.3566	2.06E+08
K7EMY7;K7ER15;Q	K7EMY7;K7ER15;Q	Haloacid dehalogen	HDHD2		3	3	146	0.73084	1.2385	1.43E+08
C9J0J7;G5E9Q6;P3	C9J0J7;G5E9Q6;P3	Profilin;Profilin-2	PFN2		6	3	91	0.73077	1.3243	1.19E+08
Q15021;E7EN77;F5	Q15021;E7EN77	Condensin comple	NCAPD2		27	27	1401	0.73061	1.3966	2.57E+09
P38646;D6RJI2;H0	P38646	Stress-70 protein, r	HSPA9		40	39	679	0.73004	1.5507	1.43E+10
P00338;P00338-3;	P00338;P00338-3;	L-lactate dehydrog	LDHA		15	15	332	0.73003	1.3879	2.76E+09
P49903;P49903-2;	P49903;P49903-2;	Selenide, water dik	SEPHS1		4	4	392	0.72973	1.6062	2.93E+08
Q14674;Q14674-2	Q14674;Q14674-2	Separin	ESPL1		4	4	2120	0.72968	1.2921	9.63E+07
P56377;H7BZG6;H	P56377;H7BZG6;H	AP-1 complex subu	AP1S2		2	2	157	0.72936	1.3808	2.80E+08
Q9ULC4-2;Q9ULC4	Q9ULC4-2;Q9ULC4	Malignant T-cell-an	MCTS1		6	6	169	0.72934	1.4169	7.37E+08
Q99497;K7ELW0;K	Q99497;K7ELW0	Protein DJ-1	PARK7		7	7	189	0.72928	1.432	7.29E+08
P30041	P30041	Peroxiredoxin-6	PRDX6		13	13	224	0.72902	1.4963	6.45E+08
P08133-2;P08133;	P08133-2;P08133;	Annexin A6;Annexi	ANXA6		5	5	641	0.72899	1.6662	2.40E+08
Q14657	Q14657	EKC/KEOPS comple	LAGE3		2	2	143	0.72881	NaN	2.56E+07
Q9NPE3;H0YM60	Q9NPE3	H/ACA ribonucleop	NOP10		5	5	64	0.72851	1.209	1.62E+08
A0A0C4DGS1;P39(	A0A0C4DGS1;P39(	Dolichyl-diphosphi	DDOST		13	13	439	0.72762	1.818	3.11E+09
Q9Y5P6;Q9Y5P6-2	Q9Y5P6;Q9Y5P6-2	Mannose-1-phosph	GMPPB		6	6	360	0.72696	1.1238	5.43E+08
Q6NXE6-2;Q6NXE6	Q6NXE6-2;Q6NXE6	Armadillo repeat-c	ARMC6		11	11	476	0.72679	1.3999	1.49E+09
H0Y7L2;Q96N67-4	H0Y7L2;Q96N67-4	Dedicator of cytoki	DOCK7		52	47	2129	0.72659	1.429	2.48E+09
J9JIE6;Q9UM00-2;I	J9JIE6;Q9UM00-2;I	Transmembrane an	TMCO1		4	4	239	0.72654	1.1791	1.61E+08
B8ZZN6;P63165;B8	B8ZZN6;P63165;B8	Small ubiquitin-rel	SUMO1		2	2	146	0.72605	1.428	8.09E+07
Q9ULE6	Q9ULE6	Paladin	PALD1		7	7	856	0.72603	0.94232	2.72E+08
O60725	O60725	Protein-S-isoprenyl	ICMT		3	3	284	0.72596	1.0977	3.50E+08
F2Z2V0;B0QZ18;Q9	F2Z2V0;B0QZ18;Q9	Copine-1	CPNE1		9	9	533	0.72527	1.2896	1.19E+09
J3KTF4;J3QRG5;J3	J3KTF4;J3QRG5;J3	Uncharacterized pr	C17orf62		2	2	88	0.72488	NaN	2.67E+07
A0A0A0MRJ6;H7B	A0A0A0MRJ6;H7B	Protein-L-isoaspart	PCMT1		12	12	285	0.7248	1.4107	7.86E+08
Q9Y512	Q9Y512	Sorting and assemb	SAMM50		5	5	469	0.72461	NaN	3.41E+08
Q9Y276;C9J8G3;C9	Q9Y276;C9J8G3;C9	Mitochondrial cha	BCS1L		6	6	419	0.72399	1.4627	1.38E+08
Q96IX5	Q96IX5	Up-regulated durin	USMG5		4	4	58	0.72302	1.0519	3.91E+08
Q09028-3;Q09028	Q09028-3;Q09028	Histone-binding pr	RBBP4		11	4	410	0.72301	1.5631	2.89E+09
P60174-1;P60174;	P60174-1;P60174	Triosephosphate is	TPI1		11	11	249	0.72279	1.5828	1.69E+09
P0DN79;P35520;P	P0DN79;P35520;P	Cystathionine beta	CBS		18	18	551	0.72277	1.0599	1.95E+09
Q68CQ4	Q68CQ4	Digestive organ exp	DIEXF		2	2	756	0.72182	1.0118	7.23E+07
P63096;P63096-2;	P63096;P63096-2;	Guanine nucleotid	GNAI1		6	2	354	0.7212	1.6284	3.50E+08
V9GY93;Q9HC07-2	V9GY93;Q9HC07-2	Transmembrane pr	TMEM165		3	3	158	0.72055	1.8216	1.49E+08
Q8NFF5-3;Q8NFF5	Q8NFF5-3;Q8NFF5	FAD synthase;Moly	FLAD1		7	7	446	0.72044	1.2965	6.59E+08
H3BSW3;H3BQF1;I	H3BSW3;H3BQF1;I	Adenine phosphori	APRT		4	4	63	0.72024	1.605	2.23E+08
Q7L5D6;Q7L5D6-2	Q7L5D6;Q7L5D6-2	Golgi to ER traffic p	GET4		6	6	327	0.71933	1.3308	9.21E+08
P04792;F8WE04;C	P04792	Heat shock protein	HSPB1		16	16	205	0.71918	1.0985	3.15E+09
Q13535-2;Q13535	Q13535-2;Q13535	Serine/threonine-p	ATR		4	4	2580	0.71863	1.4207	1.75E+08
Q8NFH3;Q8NFH3-2	Q8NFH3	Nucleoporin Nup4	NUP43		3	3	380	0.71801	1.565	3.55E+08
Q5QNZ2;P24539	Q5QNZ2;P24539	ATP synthase F(0) c	ATP5F1		10	10	195	0.71794	1.8826	3.08E+08
F8VZY9;P05783;CC	F8VZY9;P05783	Keratin, type I cyto	KRT18		13	7	391	0.71734	1.2573	8.97E+08
P12532;P12532-2;	P12532;P12532-2;	Creatine kinase U-t	CKMT1A;CKMT1B		6	6	417	0.71667	1.4648	5.02E+08

Q9NWV8;M0R3F4;	Q9NWV8;M0R3F4;	BRISC and BRCA1-A	BABAM1		5	5	329	0.71633	0.9253	1.28E+08
P08754;P04899;P(	P08754;P04899;P(	Guanine nucleotid	GNAI3;GNAI2		8	4	354	0.71613	1.4853	1.63E+09
Q96G61;Q8NFP7	Q96G61;Q8NFP7	Diphosphoinositol	NUDT11;NUDT10		3	3	164	0.71598	0.80334	9.04E+07
Q96RL7-4;Q96RL7-	Q96RL7-4;Q96RL7-	Vacuolar protein sc	VPS13A		4	4	3069	0.71588	1.1379	9.54E+07
Q9H9A5-4;Q9H9A5	Q9H9A5-4;Q9H9A5	CCR4-NOT transcrip	CNOT10		2	2	695	0.71524	1.3755	2.22E+08
P62877	P62877	E3 ubiquitin-protei	RBX1		2	2	108	0.7151	NaN	1.49E+07
Q9UBM7;E9PM00;	Q9UBM7;E9PM00	7-dehydrocholeste	DHCR7		6	6	475	0.71486	1.2694	1.22E+09
P18085;C9JPM4;C	P18085;C9JPM4;C	ADP-ribosylation fa	ARF4		8	5	180	0.71473	1.124	3.51E+08
Q99653;H0YKE7;F!	Q99653;H0YKE7;F!	Calcineurin B hom	CHP1		8	8	195	0.71466	1.3251	3.29E+08
P51149;C9J592;C!	P51149;C9J592;C!	Ras-related protein	RAB7A		5	5	207	0.7145	1.6227	3.15E+08
X6RJP6;P37802;P3	X6RJP6;P37802;P3	Transgelin-2	TAGLN2		3	3	187	0.71399	1.599	1.63E+08
P22695;H3BRG4;H	P22695;H3BRG4;H	Cytochrome b-c1 c	UQCRC2		20	20	453	0.71393	1.5103	1.08E+10
E9PGT6;Q99627-2;	E9PGT6;Q99627-2;	COP9 signalosome	COPS8		4	4	173	0.71378	1.0122	2.11E+08
C9JQV3;Q8N1F8;Q	C9JQV3;Q8N1F8;Q	Serine/threonine-p	STK11IP		5	5	1088	0.7134	1.2368	1.87E+08
P60866;P60866-2;	P60866;P60866-2;	40S ribosomal prot	RPS20		9	9	119	0.71301	1.3654	1.06E+10
Q9UNZ2;Q9UNZ2-5	Q9UNZ2;Q9UNZ2-5	NSFL1 cofactor p47	NSFL1C		7	7	370	0.71243	1.0407	3.10E+08
Q8IXI1;H3BST5;I3L	Q8IXI1;H3BST5;I3L	Mitochondrial Rho	RHOT2		6	5	618	0.71192	1.1489	1.21E+09
Q14139;Q14139-2	Q14139;Q14139-2	Ubiquitin conjugat	UBE4A		3	3	1066	0.7119	1.2301	1.08E+08
Q15019;Q15019-3	Q15019;Q15019-3	Septin-2		02-Sep	14	14	361	0.71185	1.9749	1.52E+09
Q9NY61;A0A087W	Q9NY61;A0A087W	Protein AATF	AATF		3	3	560	0.71169	NaN	2.71E+08
P49773;D6RC06;D	P49773	Histidine triad nucl	HINT1		3	3	126	0.71121	1.9964	1.62E+08
P42695;G3V1A9;E!	P42695;G3V1A9;E!	Condensin-2 comp	NCAPD3		17	17	1498	0.71109	1.1565	9.28E+08
P09496-2;P09496-	P09496-2;P09496-	Clathrin light chain	CLTA		3	3	218	0.71073	1.0869	2.75E+07
Q8N766-4;Q8N766	Q8N766-4;Q8N766	ER membrane prot	EMC1		6	6	971	0.71056	1.3549	2.21E+08
Q6NSI4;Q6NSI4-2;(	Q6NSI4;Q6NSI4-2;(	Uncharacterized pr	CXorf57		4	4	855	0.71053	0.9121	7.41E+07
Q9NRK6;A0A0G2JL	Q9NRK6;A0A0G2JL	ATP-binding casset	ABCB10;TAP2;ABCI		2	2	738	0.70962	1.3037	4.68E+07
P14735;P14735-2;	P14735	Insulin-degrading e	IDE		13	13	1019	0.70883	1.4	7.95E+08
A0A0U1RRM4;P26	A0A0U1RRM4;P26	Polypyrimidine tra	PTBP1		12	12	588	0.70815	1.7383	3.64E+09
Q9NRZ5;H0Y5R3;Q	Q9NRZ5;H0Y5R3;Q	1-acyl-sn-glycerol-3	AGPAT4		2	2	378	0.70712	NaN	4.04E+06
Q16891-2;Q16891	Q16891-2;Q16891	MICOS complex sul	IMMT		25	25	747	0.70647	1.2172	2.46E+09
P36507;G5E9C7;N	P36507	Dual specificity mit	MAP2K2		14	9	400	0.70644	1.322	1.11E+09
Q8N4V1;Q8N4V1-2	Q8N4V1;Q8N4V1-2	Membrane magnes	MMGT1		2	2	131	0.70631	1.3754	1.13E+08
F5H6I7;Q6DD88;F!	F5H6I7;Q6DD88;F!	Atlastin-3	ATL3		2	2	523	0.7063	1.3912	1.59E+08
G3V1A0;G5EA23;E!	G3V1A0;G5EA23;E!	Trafficking protein	TRAPPC4		2	2	117	0.70614	1.155	3.18E+07
Q9NZ45	Q9NZ45	CDGSH iron-sulfur	CISD1		3	3	108	0.70589	1.2805	1.12E+08
P51659;E7ER27;E7	P51659;E7ER27;E7	Peroxisomal multif	HSD17B4		15	15	736	0.70552	1.5463	2.54E+09
J3QQW9;Q15022	J3QQW9;Q15022	Polycomb protein !	SUZ12		2	2	716	0.70525	1.4826	1.69E+08
Q14C86-3;Q14C86	Q14C86-3;Q14C86	GTPase-activating p	GAPVD1		24	24	1433	0.70524	0.98475	1.83E+09
Q10570;A0A087X1	Q10570	Cleavage and polya	CPSF1		32	32	1443	0.70516	1.3415	3.47E+09
F8VQE1;Q9UHB6-2	F8VQE1;Q9UHB6-2	LIM domain and ac	TRMT1;LIMA1		8	8	598	0.70481	1.6271	3.45E+08
P61077;P61077-2;	P61077;P61077-2;	Ubiquitin-conjugat	UBE2D3;UBE2D2		2	2	147	0.70477	1.4208	2.40E+08
P51809-3;P51809;	P51809-3;P51809;	Vesicle-associated r	VAMP7		4	4	179	0.70464	1.5854	1.75E+08
Q9Y3P9;Q9Y3P9-3;	Q9Y3P9	Rab GTPase-activat	RABGAP1		5	3	1069	0.70434	1.5624	1.55E+08
A0A140T9L0;A0A0	A0A140T9L0;A0A0G2JJL1				4	1	322	0.70427	1.1928	2.48E+08
H7C1S7;C9JNL5;H7	H7C1S7;C9JNL5;H7	Selenocysteine lyas	SCLY		2	2	168	0.70358	1.0667	9.59E+07
Q9BT73	Q9BT73	Proteasome assembl	PSMG3		1	1	122	0.70283	NaN	2.95E+07
Q9BT25-2;Q9BT25-	Q9BT25-2;Q9BT25-	HAUS augmin-like c	HAUS8		1	1	349	0.70183	NaN	8.61E+07
P04181-2;P04181	P04181-2;P04181	Ornithine aminotra	OAT		3	3	301	0.70157	1.4086	8.20E+07
E7EVJ5;Q96F07-2;(	E7EVJ5;Q96F07-2;(	Cytoplasmic FMR1-	CYFIP2		21	8	1227	0.70134	0.9427	1.88E+08
E7ES33;E7EPK1;Q1	E7ES33;E7EPK1;Q1	Septin-7		07-Sep	8	8	417	0.7012	1.7931	7.52E+08
A0A087WY55;Q9N	A0A087WY55;Q9N	Vacuolar protein sc	VTA1		7	7	280	0.70096	1.2127	1.24E+09
Q9ULV4;Q9ULV4-2	Q9ULV4;Q9ULV4-2	Coronin-1C;Coroni	CORO1C		12	12	474	0.70078	1.356	1.58E+09
O00232;O00232-2	O00232;O00232-2	26S proteasome no	PSMD12		17	17	456	0.70036	1.8214	1.78E+09
H0Y2Y8;Q15942;H	H0Y2Y8;Q15942;H	Zyxin	ZYX		7	7	540	0.69953	1.2805	1.26E+08
A0A140TA86;Q5XK	A0A140TA86;Q5XK	Protein QIL1	QIL1;C19orf70		2	2	140	0.69876	NaN	7.03E+07
P61026	P61026	Ras-related protein	RAB10		5	3	200	0.69661	1.7659	1.02E+08
P62937;P62937-2;	P62937;P62937-2;	Peptidyl-prolyl cis-	PPIA		13	13	165	0.6952	1.5848	5.63E+09
H0YMV8;Q71UM5;	H0YMV8;Q71UM5;	40S ribosomal prot	RPS27L		6	2	100	0.69504	0.63454	1.69E+08
Q96A72;F5H6N1;F	Q96A72;F5H6N1	Protein mago nashi	MAGOHB		6	1	148	0.6937	1.3401	2.77E+08
Q8WVX9;E9PNW8;	Q8WVX9;E9PNW8	Fatty acyl-CoA redu	FAR1		8	8	515	0.69362	1.0838	8.57E+08
Q9HD20-2;Q9HD2(	Q9HD20-2;Q9HD2(	Manganese-transpo	ATP13A1		7	7	1086	0.69205	1.0368	2.02E+08
Q9NRP0;A0A087W	Q9NRP0;A0A087W	Oligosaccharyltran	OSTC		2	2	149	0.69196	1.4255	1.01E+08
P20020-6;P20020-	P20020-6;P20020-	Plasma membrane	ATP2B1;ATP2B4		8	8	1184	0.69156	1.1136	4.66E+08
O95816;O95816-2	O95816;O95816-2	BAG family molecu	BAG2		4	4	211	0.6902	1.559	1.28E+08
Q9GZL7	Q9GZL7	Ribosome biogenes	WDR12		9	9	423	0.6899	1.4064	9.11E+08
Q9BVG4;A6NDF3	Q9BVG4	Protein PBDC1	PBDC1		5	5	233	0.68986	1.8139	2.78E+08
A0A096LNH6;Q14:	A0A096LNH6;Q14:	Dedicator of cytoki	DOCK1		3	3	1886	0.68965	1.2856	5.70E+07
D6RGE2;Q96CN7	D6RGE2;Q96CN7	Isochorismatase do	ISOC1		2	2	188	0.68895	1.0639	2.49E+08
Q9Y3B4	Q9Y3B4	Splicing factor 3B s	SF3B6		3	3	125	0.68852	1.5299	2.57E+08
Q9Y3T9	Q9Y3T9	Nucleolar complex	NOC2L		16	16	749	0.68703	1.4124	1.91E+09
A0A0J9YWJ4;K7EJI	A0A0J9YWJ4;K7EJI	RNA polymerase II s	CTDP1		4	4	737	0.68677	1.046	9.73E+07
A0A0C4DGP2;A0A(	A0A0C4DGP2;A0A(	Kinesin-like protein	KIF18B		3	3	833	0.68641	NaN	2.47E+07
Q13315;E9PIN0	Q13315;E9PIN0	Serine-protein kina	ATM		9	9	3056	0.68617	1.3609	1.29E+08
Q14146;Q5VYD0	Q14146	Unhealthy ribosom	URB2		21	21	1524	0.68594	1.3787	1.31E+09
P31930	P31930	Cytochrome b-c1 c	UQCRC1		20	19	480	0.68586	1.6263	6.56E+09
B1AMS2;Q14141-2	B1AMS2;Q14141-2	Septin-6		06-Sep	3	2	431	0.68575	1.9478	2.37E+08
O60264	O60264	SWI/SNF-related m	SMARCA5		36	23	1052	0.68434	1.3631	3.68E+09
P61221;D6R9I9;D(	P61221;D6R9I9	ATP-binding casset	ABCE1		16	16	599	0.68319	1.6903	1.73E+09
C9JLU1;P52434-3;	C9JLU1;P52434-3;	DNA-directed RNA	POLR2H		5	5	149	0.68283	1.576	2.91E+08
G3V0I5;P49821-2;	G3V0I5;P49821-2;	NADH dehydrogena	NDUFV1		2	2	457	0.68188	1.2148	6.31E+07
P52292;J3QLL0;J3	P52292;J3QLL0;J3	Importin subunit a	KPNA2;POU2F2		17	17	529	0.68167	1.3997	4.03E+09
J3KPS3;P04075;P0	J3KPS3;P04075;P0	Fructose-bisphosp	ALDOA		22	21	368	0.68129	2.1453	4.26E+09
K4DI93;Q13620-3;	K4DI93;Q13620-3;	Cullin-4B	CUL4B		11	6	900	0.68072	1.4863	6.79E+08
E9PHG5;Q6UW02-	E9PHG5;Q6UW02-	Cytochrome P450	CYP20A1		2	2	470	0.6798	NaN	9.04E+07
A0A087X207;A0A(	A0A087X207;A0A(	Breast carcinoma-a	BCAS3		2	2	650	0.67935	1.2959	1.82E+08
O95373;E9PLB2;E!	O95373	Importin-7	IPO7		20	19	1038	0.67906	1.3159	1.89E+09
P31948;P31948-3;	P31948;P31948-3;	Stress-induced-pho	STIP1		10	10	543	0.67848	1.2652	6.37E+08
P47985;P0C7P4	P47985;P0C7P4	Cytochrome b-c1 c	UQCRFS1;UQCRFS1		5	5	274	0.67809	1.4646	5.36E+08
Q9BTX1-6;Q9BTX1-	Q9BTX1-6;Q9BTX1-	Nucleoporin NDC1	NDC1		5	5	559	0.6772	1.4381	2.19E+08
P40926;P40926-2;	P40926;P40926-2;	Malate dehydrogen	MDH2		5	5	338	0.67629	1.6244	7.36E+08
O14980;C9JKM9;C	O14980	Exportin-1	XPO1		27	27	1071	0.67602	1.4464	6.15E+09
Q6DKI1;R4GMU7;(	Q6DKI1;R4GMU7;(	60S ribosomal prot	RPL7L1		6	6	246	0.67582	1.4415	1.15E+09
J3KNE0;A6NKT7	J3KNE0;A6NKT7	RanBP2-like and GF	RGPD3		23	0	1760	0.6757	0.7399	1.58E+08

P22234;E9PBS1;P2	P22234;E9PBS1;P2	Multifunctional pr	PAICS	21	21	425	0.67556	2.1108	5.96E+09
A0A0J9YYL3;A0A0J	A0A0J9YYL3;A0A0J	Poly(U)-binding-spl	PUF60	10	10	505	0.67542	1.7611	1.18E+09
B1AH87;P30536	B1AH87;P30536	Translocator protei	TSPO	1	1	107	0.67441	1.3315	3.81E+07
Q96CX2;Q68DU8	Q96CX2	BTB/POZ domain-c	KCTD12	9	9	325	0.67371	1.3865	1.31E+09
Q9H8Y8-2;Q9H8Y8	Q9H8Y8-2;Q9H8Y8	Golgi reassembly-st	GORASP2	2	2	384	0.67334	NaN	3.62E+07
Q9HAV4;H0Y9I3;E2	Q9HAV4	Exportin-5	XPO5	12	12	1204	0.67312	1.5142	9.22E+08
Q9H9B4;D6RFI0;S4	Q9H9B4;D6RFI0;S4	Sideroflexin-1	SFXN1	16	15	322	0.67232	1.4372	1.10E+10
G3XAN4;Q15629-2	G3XAN4;Q15629-2	Translocating chair	TRAM1	2	2	288	0.67219	NaN	1.57E+08
P10515;H0YDD4;E	P10515;H0YDD4;E	Dihydrolipoyllysin	DLAT	10	10	647	0.67198	1.6987	1.82E+09
C9JTK6;J3KQ32;Q9	C9JTK6;J3KQ32;Q9	Obg-like ATPase 1	OLA1	1	1	116	0.6714	NaN	6.59E+07
P12235;V9GYG0	P12235;V9GYG0	ADP/ATP transloca	SLC25A4	21	5	298	0.67111	0.8012	1.39E+09
Q96JG6;Q96JG6-3;	Q96JG6;Q96JG6-3;	Coiled-coil domain	CCDC132	6	6	964	0.67077	1.1748	1.47E+08
P32119;A6NIW5;P	P32119;A6NIW5	Peroxiredoxin-2	PRDX2	15	14	198	0.67052	2.007	5.97E+09
O43818	O43818	U3 small nucleolar	RRP9	2	2	475	0.66999	1.0459	6.07E+07
H3BUV4;Q9NWW5	H3BUV4;Q9NWW5	Ceroid-lipofuscino	CLN6	3	3	213	0.66989	NaN	2.57E+08
P07195;C9J7H8;A	P07195;C9J7H8;A	L-lactate dehydrog	LDHB	10	10	334	0.66871	1.6525	3.40E+09
O60763;O60763-2	O60763;O60763-2	General vesicular tr	USO1	24	24	962	0.66866	1.3489	2.02E+09
G3XAH6;P51003;P	G3XAH6;P51003;P	Poly(A) polymerase	PAPOLA;PAPOLB	8	8	724	0.66672	1.2858	5.79E+08
P51153;A0A087W	P51153;A0A087W	Ras-related protein	RAB13	5	2	203	0.66572	1.3218	1.21E+08
Q15008;Q15008-4	Q15008;Q15008-4	26S proteasome no	PSMD6	14	14	389	0.66479	1.1436	1.84E+09
Q9UBB4-2;Q9UBB4	Q9UBB4-2;Q9UBB4	Ataxin-10	ATXN10	10	10	411	0.66343	1.3143	1.01E+09
Q68E01-2;Q68E01;	Q68E01-2;Q68E01;	Integrator complex	INTS3	12	12	1042	0.66337	1.0585	3.73E+08
E9PLK3;P55786;P5	E9PLK3;P55786;P5	Puromycin-sensitiv	NPEPPS	28	28	915	0.66313	1.4432	3.23E+09
P61160;P61160-2;	P61160;P61160-2;	Actin-related prote	ACTR2	6	6	394	0.66305	1.4323	8.71E+08
Q9UBQ0;F8VXU5;C	Q9UBQ0;F8VXU5;C	Vacuolar protein sc	VPS29	4	4	182	0.66287	1.3646	3.67E+08
Q9NVQ4;Q9NVQ4-2	Q9NVQ4;Q9NVQ4-	Fas apoptotic inhib	FAIM	6	6	179	0.66255	1.7027	3.62E+08
P00505;P00505-2	P00505;P00505-2	Aspartate aminotra	GOT2	5	5	430	0.66221	1.7554	4.17E+08
Q8N138-4;Q8N138	Q8N138-4;Q8N138	ORM1-like protein	ORMDL3	2	2	137	0.66068	1.0965	4.90E+06
P21266;A0A0A0M	P21266;A0A0A0M	Glutathione S-tran	GSTM3	9	9	225	0.65928	1.5685	9.76E+08
Q9NZJ4;Q9NZJ4-2;	Q9NZJ4;Q9NZJ4-2	Sacsin	SACS	3	3	4579	0.65878	NaN	1.84E+07
Q9Y221;Q9Y221-2;	Q9Y221;Q9Y221-2;	60S ribosome subu	NIP7	4	4	180	0.65856	1.3277	1.86E+08
P06576;H0YH81;F	P06576;H0YH81	ATP synthase subur	ATP5B	22	22	529	0.65763	1.6798	7.07E+09
Q9H3K6-2;Q9H3K6	Q9H3K6-2;Q9H3K6	BolA-like protein 2	BOLA2;BOLA2B	3	3	58	0.65756	1.3067	3.22E+08
Q8N0X7	Q8N0X7	Spartin	SPG20	9	9	666	0.65739	1.3648	7.93E+08
P12277;H0YJG0;G	P12277;H0YJG0	Creatine kinase B-ty	CKB	11	11	381	0.65634	1.6624	1.10E+09
E9PFH4;Q9Y5L0-3;	E9PFH4;Q9Y5L0-3;	Transportin-3	TNPO3	7	7	857	0.65409	1.5779	5.83E+08
A6NEM2;P51610-2	A6NEM2;P51610-2	Host cell factor 1;H	HCFC1	10	10	2080	0.65318	1.4457	1.07E+09
P61956-2;P61956;	P61956-2;P61956	Small ubiquitin-rel	SUMO2	3	3	71	0.65257	1.3964	2.35E+08
Q8IWA0	Q8IWA0	WD repeat-contain	WDR75	9	9	830	0.65248	1.3767	1.02E+09
Q9Y570;Q9Y570-4;	Q9Y570;Q9Y570-4;	Protein phosphata	PPME1	8	8	386	0.65209	1.3625	8.99E+08
G8JLH9;P40763-3;	G8JLH9;P40763-3;	Signal transducer a	STAT3	2	2	672	0.65186	1.8651	1.21E+08
A0A0A0MSI0;Q068	A0A0A0MSI0;Q068	Peroxiredoxin-1	PRDX1	13	9	171	0.65109	1.6958	2.51E+09
A0A0A0MRB5;Q8W	A0A0A0MRB5;Q8W	MAP kinase-activat	MADD	2	2	1588	0.65059	2.3232	1.68E+07
Q9HCC0-2;Q9HCC	Q9HCC0-2;Q9HCC	Methylcrotonoyl-C	MCCC2	2	2	525	0.64976	1.0225	1.07E+08
Q09161;X6R941	Q09161	Nuclear cap-bindin	NCBP1	11	11	790	0.64975	1.6546	1.15E+09
Q92616	Q92616	Translational activa	GCN1L1	84	84	2671	0.64954	1.6932	7.03E+09
P11216;H0Y4Z6	P11216	Glycogen phospho	PYGB	11	6	843	0.64895	1.4799	3.40E+08
J3KTF8;J3QQX2;P5	J3KTF8;J3QQX2;P5	Rho GDP-dissociati	ARHGDIA	6	6	194	0.64716	2.0454	1.53E+09
B5MDF5;P62826;F	B5MDF5;P62826;F	GTP-binding nucle	RAN	10	10	233	0.64673	1.9402	2.91E+09
Q96IJ6;Q96IJ6-2;A	Q96IJ6;Q96IJ6-2;A	Mannose-1-phosph	GMPPA	5	5	420	0.64553	1.2973	5.15E+08
Q9BWD1;Q9BWD1	Q9BWD1;Q9BWD1	Acetyl-CoA acetyltr	ACAT2	12	12	397	0.64509	1.2942	2.38E+09
P49755;G3V2K7	P49755;G3V2K7	Transmembrane em	TMED10	6	6	219	0.64489	2.0031	4.84E+08
Q86V85	Q86V85	Integral membrane	GPR180	2	2	440	0.64423	1.5922	7.81E+06
P25789;H0YN18;P	P25789;H0YN18;P	Proteasome subuni	PSMA4	10	10	261	0.64397	1.184	1.02E+09
P09972;K7EKH5;C	P09972;K7EKH5;C	Fructose-bisphosph	ALDOC	3	2	364	0.64369	2.1853	1.28E+09
V9GYG2;V9GYP9;C	V9GYG2;V9GYP9;C	Alcohol dehydroge	AKR1A1	1	1	119	0.64347	NaN	7.62E+07
Q6RW13;Q6RW13	Q6RW13;Q6RW13	Type-1 angiotensin	AGTRAP	2	2	159	0.64263	NaN	5.50E+07
P28066;P28066-2	P28066;P28066-2	Proteasome subuni	PSMA5	6	6	241	0.64161	1.2416	6.08E+08
Q5SWX8-4;Q5SWX	Q5SWX8-4;Q5SWX	Protein odr-4 hom	ODR4	4	4	422	0.64069	1.2018	3.11E+08
A6NFX8;Q9UKK9;A	A6NFX8;Q9UKK9	ADP-sugar pyropho	NUDT5	5	5	232	0.64066	1.0143	2.81E+08
O75947;O75947-2	O75947;O75947-2	ATP synthase subur	ATP5H	3	3	161	0.63982	1.1453	6.51E+07
P49642;F8VNY2	P49642;F8VNY2	DNA primase small	PRIM1	3	3	420	0.63928	1.2152	1.80E+08
Q5VW36	Q5VW36	Focadhesin	FOCAD	12	4	1801	0.63913	1.3396	4.73E+08
A0A067XG54;Q8NI	A0A067XG54;Q8N	Phospholipid-trans	ATP11C	2	2	1113	0.63896	1.0599	8.11E+07
E7EQ61;Q9GZZ9;E7	E7EQ61;Q9GZZ9;E7	Ubiquitin-like mod	UBA5	2	2	377	0.63597	NaN	1.22E+08
E2QRD4;Q6ZRQ5	E2QRD4;Q6ZRQ5	Protein MMS22-lik	MMS22L	2	2	1203	0.63562	NaN	5.73E+07
A0A0B4J1R6;P294	A0A0B4J1R6;P294	Transketolase	TKT	7	7	457	0.63554	1.2438	5.03E+08
Q9Y2V2;H3BTK3;I3	Q9Y2V2;H3BTK3;I3	Calcium-regulated	CARHSP1	2	2	147	0.63548	1.511	7.08E+07
B8ZZ47;H0Y714;Q9	B8ZZ47;H0Y714;Q9	U3 small nucleolar	IMP4	2	2	248	0.63535	1.2056	3.32E+08
O60216;E5RFZ5;E5	O60216;E5RFZ5	Double-strand-brea	RAD21	8	8	631	0.6349	1.2146	3.81E+08
Q5QJ74;E9PP54	Q5QJ74;E9PP54	Tubulin-specific ch	TBCEL	2	2	424	0.63434	0.9218	1.36E+08
P56385	P56385	ATP synthase subur	ATP5I	2	2	69	0.63356	1.6979	1.40E+08
Q9H773;H3BSA6	Q9H773;H3BSA6	dCTP pyrophospha	DCTPP1	4	4	170	0.63341	1.0915	6.31E+07
O43808;B0QYW5;I	O43808;B0QYW5;I	Peroxisomal memb	SLC25A17	3	3	307	0.63285	1.5569	2.22E+08
E9PN17;O75964;O	E9PN17;O75964	ATP synthase subur	ATP5L	6	6	76	0.63227	1.8322	6.30E+08
B4DR61;P61619;F	B4DR61;P61619;F	Protein transport p	SEC61A1;SEC61A2	8	8	482	0.63184	1.3566	2.15E+08
Q8TB61-5;Q8TB61	Q8TB61-5;Q8TB61	Adenosine 3-phosp	SLC35B2	2	2	299	0.6312	1.6432	1.34E+08
P31350;P31350-2;	P31350;P31350-2;	Ribonucleoside-dip	RRM2	6	6	389	0.63045	1.6862	4.23E+08
C9JS59;C9J266;Q5	C9JS59;C9J266;Q5	E3 ubiquitin-protei	RNF123	3	3	721	0.63033	0.84487	9.09E+07
Q92973-2;Q92973	Q92973-2;Q92973	Transportin-1;Tran	TNPO1;TNPO2	7	7	890	0.62929	1.2744	3.24E+08
Q14974;Q14974-2	Q14974;Q14974-2	Importin subunit b	KPNB1	29	29	876	0.62893	1.5822	1.09E+10
P50395-2;P50395;	P50395-2;P50395;	Rab GDP dissociati	GDI2	4	4	400	0.62787	1.9369	3.54E+08
P84077;P61204;F	P84077;P61204;F	ADP-ribosylation fa	ARF1;ARF3	10	6	181	0.62745	1.7094	2.74E+09
P20674;H3BRM5;H	P20674;H3BRM5;H	Cytochrome c oxid	COX5A	3	3	150	0.62743	1.3265	4.43E+07
P52209-2;P52209;	P52209-2;P52209	6-phosphoglucona	PGD	23	23	470	0.62688	1.9836	6.63E+09
P30048-2;P30048	P30048-2;P30048	Thioredoxin-depen	PRDX3	5	5	238	0.6262	1.943	3.80E+08
P62942;Q1JUQ3;C	P62942;Q1JUQ3;C	Peptidyl-prolyl cis-	FKBP1A;FKBP12-Ex	2	2	108	0.62491	1.501	4.63E+07
Q96GD4-4;Q96GD	Q96GD4-4;Q96GD	Aurora kinase B	AURKB	5	5	303	0.62482	1.1354	3.02E+08
P49419-2;P49419;	P49419-2;P49419;	Alpha-aminoadipic	ALDH7A1	12	12	511	0.62439	1.8937	1.75E+09
D6RG15;Q6IBS0;H	D6RG15;Q6IBS0	Twinfilin-2	TWF2	3	3	254	0.62419	2.0336	2.29E+08
P00492	P00492	Hypoxanthine-guar	HPRT1	7	6	218	0.62398	1.844	1.39E+09
Q6Y1H2	Q6Y1H2	Very-long-chain (3F	PTPLB	2	2	254	0.62296	1.4981	1.21E+07
Q9UIV1-2;Q9UIV1;	Q9UIV1-2;Q9UIV1;	CCR4-NOT transcri	CNOT7	3	3	244	0.62197	1.6232	1.55E+08

Q6SZW1;Q6SZW1-:	Q6SZW1;Q6SZW1-:	Sterile alpha and TI	SARM1	5	5	724	0.61981	1.4996	2.70E+08
F8WCF6;P59998;F	F8WCF6;P59998;F	Actin-related prote	ARPC4-TTLL3;ARPC	5	5	181	0.61929	1.7531	1.59E+09
E9PNN3;Q03393	E9PNN3;Q03393	6-pyruvoyl tetrahy	PTS	2	2	77	0.61921	0.96098	2.17E+07
Q9BPU6;E7EWB4;E	Q9BPU6	Dihydropyrimidina	DPYSL5	10	10	564	0.61878	1.7026	1.05E+09
Q969X6;H3BSH7;C	Q969X6;H3BSH7;C	Cirhin	CIRH1A	8	8	686	0.61754	1.5124	1.34E+09
P03886	P03886	NADH-ubiquinone	MT-ND1	4	4	318	0.61739	1.564	8.81E+07
P46940;H0YLE8;A(	P46940;H0YLE8;A(	Ras GTPase-activati	IQGAP1	40	38	1657	0.61677	1.6084	4.82E+09
Q9H7E9;Q9H7E9-2	Q9H7E9;Q9H7E9-2	UPF0488 protein C	C8orf33	2	2	229	0.61521	NaN	1.26E+07
P38432	P38432	Coilin	COIL	2	2	576	0.61464	1.7663	3.29E+08
P05023-4;P05023;	P05023-4;P05023	Sodium/potassium	ATP1A1	45	27	1023	0.61408	1.6054	1.08E+10
Q5BJF2;Q86XC5;J3	Q5BJF2;Q86XC5;J3	Transmembrane pr	TMEM97	2	2	176	0.6137	1.3054	1.99E+08
Q9UNF1;Q5H909;(	Q9UNF1;Q5H909;(	Melanoma-associat	MAGED2	17	16	606	0.61113	1.4569	1.47E+09
C9J1Z8;P84085;F5	C9J1Z8;P84085	ADP-ribosylation fa	ARF5	7	3	150	0.61092	1.1992	2.79E+07
Q9UJA5;Q9UJA5-4;	Q9UJA5;Q9UJA5-4	tRNA (adenine(58)-	TRMT6	3	3	497	0.61054	1.1801	7.43E+07
O00264;O00264-2	O00264;O00264-2	Membrane-associat	PGRMC1	7	7	195	0.61045	1.2315	2.29E+08
K7ES52;K7ERJ1;K7	K7ES52;K7ERJ1;K7	Thymidine kinase;T	TK1	3	3	180	0.61009	NaN	1.36E+08
Q5VTU3;P63172	Q5VTU3;P63172	Dynein light chain '	DYNLT1	3	3	92	0.60964	1.4198	1.09E+08
H0YNW5;H0YKC5;I	H0YNW5;H0YKC5;I	Deoxyuridine 5-trip	DUT	3	3	167	0.60947	1.2927	3.31E+07
A6NLH6;Q9P003	A6NLH6;Q9P003	Protein cornichon	CNIH4	1	1	137	0.60817	1.6674	1.71E+09
P51148;P51148-2;	P51148;P51148-2	Ras-related protein	RAB5C	6	6	216	0.60799	1.5888	2.48E+08
P46977;P46977-2;	P46977;P46977-2	Dolichyl-diphosph	STT3A	10	10	705	0.60771	2.2213	1.21E+09
Q7LC14;A0A087W	Q7LC14;A0A087W	NF-kappa-B inhibit	NFKBIE	2	2	361	0.60699	NaN	5.82E+07
Q7Z3U7-2;Q7Z3U7	Q7Z3U7-2;Q7Z3U7	Protein MON2 hon	MON2	9	9	1675	0.60685	1.5671	3.85E+08
Q6P9B9	Q6P9B9	Integrator complex	INTS5	4	4	1019	0.60614	1.4847	2.32E+08
Q9H8M7;X6R9S5;)	Q9H8M7;X6R9S5;)	Protein FAM188A	FAM188A	2	2	445	0.60572	NaN	6.25E+07
Q8TEX9;Q8TEX9-2;	Q8TEX9;Q8TEX9-2;	Importin-4	IPO4	19	19	1081	0.60452	1.4238	1.95E+09
Q15738;C9JDR0	Q15738;C9JDR0	Sterol-4-alpha-carb	NSDHL	4	4	373	0.60441	1.412	2.73E+08
Q9H583;Q5T3Q7;C	Q9H583;Q5T3Q7	HEAT repeat-contai	HEATR1	43	43	2144	0.60401	1.4422	4.99E+09
G3V4W0;B4DY08;I	G3V4W0;B4DY08;I	Heterogeneous nuc	HNRNPC;LOC6493	22	3	262	0.60318	1.5075	2.18E+10
A0A0A0MSQ0;P13	A0A0A0MSQ0;P13	Plastin-3	PLS3	10	8	617	0.60274	2.382	6.98E+08
P28838-2;P28838	P28838-2;P28838	Cytosol aminopept	LAP3	2	2	488	0.60235	NaN	3.92E+07
D6RCD0;Q8NBQ5	D6RCD0;Q8NBQ5	Estradiol 17-beta-d	HSD17B11	3	3	256	0.6023	1.1561	2.88E+08
P54709;H7C547;F	P54709;H7C547;F	Sodium/potassium	ATP1B3	4	4	279	0.60152	2.1359	4.61E+08
H3BMH2;H3BSC1;I	H3BMH2;H3BSC1;I	Ras-related protein	RAB11A;RAB11B	5	5	155	0.60076	2.0192	1.73E+08
P23284	P23284	Peptidyl-prolyl cis-	PPIB	5	5	216	0.59931	1.4143	1.68E+08
Q86Y39;K7EQ77;K	Q86Y39;K7EQ77;K	NADH dehydrogena	NDUFA11	3	3	141	0.59894	1.3252	6.61E+07
Q92538-3;Q92538	Q92538-3;Q92538	Golgi-specific brefe	GBF1	21	21	1855	0.5971	1.581	9.85E+08
O75533;B4DGZ4;H	O75533	Splicing factor 3B s	SF3B1	36	36	1304	0.59692	1.2783	2.80E+09
Q8NC51-4;Q8NC51	Q8NC51-4;Q8NC51	Plasminogen activa	SERBP1	5	5	387	0.59657	1.5169	3.49E+08
Q96B26;H7C581	Q96B26	Exosome complex (	EXOSC8	4	4	276	0.59555	1.8027	8.46E+08
A0A024QZX5;A0A0	A0A024QZX5;A0A0	Serpin B6	SERPINB6	4	4	380	0.59479	1.5834	3.64E+08
A5YKK6-2;A5YKK6;	A5YKK6-2;A5YKK6;	CCR4-NOT transcrip	CNOT1	32	32	2371	0.59466	1.5551	1.79E+09
G3V2I3;A6NED2	G3V2I3;A6NED2	RCC1 domain-cont	RCCD1	3	3	374	0.59303	1.191	1.22E+08
O96008;O96008-2	O96008;O96008-2	Mitochondrial imp	TOMM40	8	8	361	0.59299	1.9665	1.50E+09
Q15417-3;Q15417	Q15417-3;Q15417	Calponin-3	CNN3	3	3	283	0.5922	NaN	4.60E+07
O95757;E9PDE8;D	O95757;E9PDE8;D	Heat shock 70 kDa	HSPA4L	15	13	839	0.59048	1.1589	7.41E+08
B8ZZG1;Q9NZW5	B8ZZG1;Q9NZW5	MAGUK p55 subfan	MPP6	2	1	428	0.58936	NaN	7.74E+07
P09211;A8MX94;A	P09211;A8MX94	Glutathione S-trans	GSTP1	6	6	210	0.58908	1.8473	9.77E+08
O43707;O43707-2	O43707;O43707-2	Alpha-actinin-4	ACTN4	47	34	911	0.58891	1.6374	8.70E+09
H0YGS2;H0YG62;J:	H0YGS2;H0YG62;J:	Transcriptional enh	TEAD4;TEAD1;TEAD	2	2	175	0.58758	NaN	5.02E+06
A0A087X2B5;P356	A0A087X2B5;P356	Basigin	BSG	4	4	221	0.58683	1.851	3.15E+08
Q9P0M6;Q5SQT3	Q9P0M6	Core histone macro	H2AFY2	8	7	372	0.58312	1.5206	1.05E+09
O75844	O75844	CAAX prenyl protea	ZMPSTE24	10	10	475	0.58245	1.9268	6.14E+08
Q5T092;A0A0A0MI	Q5T092;A0A0A0MI	Protein RER1	RER1	3	3	158	0.58088	1.455	9.45E+07
Q12788;J3KNP2;A(	Q12788;J3KNP2	Transducin beta-lik	TBL3	15	15	808	0.57877	1.3674	1.46E+09
K7EJR3;R4GMR5;P	K7EJR3;R4GMR5;P	26S proteasome no	PSMD8	3	3	251	0.57876	1.6714	2.66E+08
B3KPJ4;A0A0A0MS	B3KPJ4;A0A0A0MS	Polyhomeotic-like	PHC2;PHC3	2	2	464	0.57825	NaN	7.73E+07
C9J315;P48449-2;	C9J315;P48449-2;	Lanosterol synthas	LSS	2	2	262	0.57708	1.3196	1.17E+08
O75691	O75691	Small subunit proc	UTP20	23	23	2785	0.57639	1.6096	1.13E+09
P52306-6;P52306	P52306-6;P52306	Rap1 GTPase-GDP d	RAP1GDS1	3	3	516	0.5758	1.4536	1.31E+08
O75367-2;O75367	O75367-2;O75367	Core histone macro	H2AFY	7	6	369	0.57494	1.4633	2.13E+09
P00491;G3V393;G	P00491	Purine nucleoside p	PNP	3	3	289	0.57454	1.6847	1.34E+08
Q9Y2X3;H7BZ72;F	Q9Y2X3	Nucleolar protein 5	NOP58	21	21	529	0.57348	1.739	6.84E+09
A0A087WUT6;O60	A0A087WUT6;O60	Eukaryotic translat	EIF5B	10	10	1220	0.57326	1.6687	7.91E+08
O96007	O96007	Molybdopterin syn	MOCS2	3	3	188	0.57295	1.489	8.24E+07
Q96BM9	Q96BM9	ADP-ribosylation fa	ARL8A	1	1	186	0.57158	1.4685	1.04E+08
Q9NUQ2;H0YC22	Q9NUQ2;H0YC22	1-acyl-sn-glycerol-3	AGPAT5	2	2	364	0.57112	1.7355	4.25E+07
Q3LIE7;Q15392-2;(	Q3LIE7;Q15392-2;(	Delta(24)-sterol rec	Nbla03646;DHCR2	6	6	427	0.57053	0.87658	1.05E+08
Q7KZN9-2;Q7KZN9	Q7KZN9-2;Q7KZN9	Cytochrome c oxid	COX15	8	8	388	0.57022	1.4944	7.31E+08
B4DY09;Q12905;X	B4DY09;Q12905	Interleukin enhanc	ILF2	16	16	352	0.5694	1.9111	1.09E+10
Q15125;C9J719;C(	Q15125;C9J719;C(	3-beta-hydroxyster	EBP	3	3	230	0.5687	1.6209	6.78E+07
Q9NS69	Q9NS69	Mitochondrial imp	TOMM22	6	6	142	0.56843	1.7543	1.39E+09
E7EN32;O00255-2;	E7EN32;O00255-2	Menin	MEN1	3	3	555	0.56828	0.91282	6.06E+07
P42858;H0YA07	P42858	Huntingtin	HTT	26	26	3142	0.56619	1.8313	1.38E+09
Q9NV31	Q9NV31	U3 small nucleolar	IMP3	5	5	184	0.56567	1.3173	3.71E+08
P06733;K7EM90;P	P06733;K7EM90;P	Alpha-enolase;Enol	ENO1	19	19	434	0.56342	1.513	2.98E+09
P17066;P48741	P17066	Heat shock 70 kDa	HSPA6	23	11	643	0.56257	1.3041	1.91E+09
K7EM73;K7ELJ7;A(	K7EM73;K7ELJ7;A(	Calpain small subu	CAPNS1	2	2	163	0.56225	1.3855	1.15E+08
P52435;A0A0B4J2	P52435;A0A0B4J2	DNA-directed RNA	POLR2J;POLR2J3;P	4	4	117	0.56205	1.4456	7.17E+07
H0Y4R1;P12268;E:	H0Y4R1;P12268;E:	Inosine-5-monoph	IMPDH2	10	10	470	0.56087	1.3245	4.37E+08
P61019-2;P61019;	P61019-2;P61019	Ras-related protein	RAB2A;DKFZp313C	3	3	188	0.55987	1.7582	1.09E+08
A0A087WT20;Q9N	A0A087WT20;Q9N	DDB1- and CUL4-as	DCAF13	5	5	597	0.55784	1.4761	2.63E+08
E7EPM6;P33121-2	E7EPM6;P33121-2	Long-chain-fatty-ac	ACSL1	3	3	664	0.55752	1.0783	2.10E+08
P50454;E9PR70;E:	P50454;E9PR70;E:	Serpin H1	SERPINH1	15	15	418	0.55542	1.9479	5.53E+09
Q15181;Q5SQT6	Q15181;Q5SQT6	Inorganic pyropho	PPA1	12	12	289	0.55358	2.0602	3.71E+09
Q9P2D3-3;Q9P2D3	Q9P2D3-3;Q9P2D3	HEAT repeat-contai	HEATR5B	7	7	1982	0.55289	1.5567	1.43E+08
P30086	P30086	Phosphatidylethan	PEBP1	2	2	187	0.54959	1.3529	5.03E+07
Q5T7C4;P09429;B(	Q5T7C4;P09429;B(	High mobility grou	HMGB1;HMGB1P1	2	2	158	0.54838	NaN	3.41E+07
Q32Q12;P22392-2	Q32Q12;P22392-2	Nucleoside diphos	NME1-NME2;NME2	11	3	292	0.54669	1.6151	1.07E+09
P54577;A0A0C4D(	P54577	Tyrosine--tRNA liga	YARS	3	3	528	0.54497	2.3855	1.80E+08
Q9H8H0;J3QR28;J:	Q9H8H0;J3QR28	Nucleolar protein 1	NOL11	11	11	719	0.54496	1.7243	1.24E+09
Q14137-2;Q14137	Q14137-2;Q14137	Ribosome biogenes	BOP1	10	10	634	0.53941	1.1836	8.88E+08
O95747;C9JIG9;F8	O95747;C9JIG9	Serine/threonine-p	OXSR1	12	9	527	0.53867	1.6954	1.64E+09

Q9Y6C9;E9PIE4	Q9Y6C9;E9PIE4	Mitochondrial carr	MTCH2	8	8	303	0.53845	1.9913	2.81E+09
Q9BPX5	Q9BPX5	Actin-related prote	ARPC5L	2	2	153	0.53813	1.3955	5.05E+07
Q5VV89;O14880;C	Q5VV89;O14880	Microsomal glutatl	MGST3	4	4	166	0.53812	2.0039	3.13E+08
Q86X10;Q86X10-3	Q86X10;Q86X10-3	Ral GTPase-activati	RALGAPB	9	9	1494	0.5367	1.1911	8.90E+08
Q8N6L1;Q8N6L1-2	Q8N6L1;Q8N6L1-2	Keratinocyte-assoc	KRTCAP2	1	1	136	0.5366	1.7247	1.15E+08
Q9HD45;Q5TB53	Q9HD45;Q5TB53	Transmembrane 9 s	TM9SF3	7	7	589	0.53571	1.759	4.27E+08
B5MC22;Q9UDX5;I	B5MC22;Q9UDX5;I	Mitochondrial fissi	MTFP1	3	3	143	0.53491	2.5712	1.34E+08
P00918;E5RID5;E5	P00918;E5RID5;E5	Carbonic anhydras	CA2	3	3	260	0.53449	NaN	3.86E+08
Q04760-2;Q04760	Q04760-2;Q04760	Lactoylglutathione	GLO1	4	4	169	0.53382	1.922	1.38E+08
G3V144;A1X283	G3V144;A1X283	SH3 and PX domair	SH3PXD2B	2	2	430	0.53297	0.9046	2.33E+07
S4R350;A2A2G4;Q	S4R350;A2A2G4;Q	Dolichyl pyrophosp	ALG6	1	1	281	0.52993	NaN	1.42E+08
Q562R1	Q562R1	Beta-actin-like prot	ACTBL2	7	1	376	0.52981	NaN	8.26E+07
Q9Y3C6	Q9Y3C6	Peptidyl-prolyl cis-	PPIL1	2	2	166	0.529	1.7746	4.80E+07
Q6AI08;K7EIX2;A0	Q6AI08;K7EIX2;A0	HEAT repeat-contai	HEATR6	7	7	1181	0.52892	1.4855	3.95E+08
O60493-2;O60493	O60493-2;O60493	Sorting nexin-3	SNX3	3	3	130	0.52887	3.0872	2.15E+07
P27105-2;P27105	P27105-2;P27105	Erythrocyte band 7	STOM	1	1	123	0.52789	1.5941	2.38E+07
Q9Y3D6	Q9Y3D6	Mitochondrial fissi	FIS1	2	2	152	0.52789	1.9306	4.68E+07
K7ESP4;Q8WVC6;C	K7ESP4;Q8WVC6;C	Dephospho-CoA kir	DCAKD	7	7	209	0.52627	1.6716	2.14E+08
E9PJ42;Q5BJD5-3;I	E9PJ42;Q5BJD5-3;I	Transmembrane pr	TMEM41B	1	1	196	0.52619	1.3837	9.47E+06
F5GZS6;J3KPF3;P0	F5GZS6;J3KPF3;P0	4F2 cell-surface ant	SLC3A2	22	22	599	0.52613	2.0154	7.67E+09
Q8TDZ2;Q8TDZ2-4;	Q8TDZ2;Q8TDZ2-4;	Protein-methionin	MICAL1	4	4	1067	0.52472	1.7262	9.44E+07
P45985;P45985-2;	P45985;P45985-2	Dual specificity mit	MAP2K4	4	4	399	0.52438	1.2998	1.55E+08
E9PHS0;O43813;F	E9PHS0;O43813;F	LanC-like protein 1	LANCL1	3	3	196	0.52435	0.63042	3.47E+09
A0A024R4E5;Q003	A0A024R4E5;Q003	Vigilin	HDLBP	29	29	1268	0.52383	1.9729	2.16E+09
Q9NPI6-2;Q9NPI6;	Q9NPI6-2;Q9NPI6	mRNA-decapping e	DCP1A	6	6	544	0.52119	1.6237	5.13E+08
Q9NR09;H7C094;H	Q9NR09	Baculoviral IAP rep	BIRC6	38	38	4857	0.52025	1.7166	1.68E+09
P00387-2;P00387;	P00387-2;P00387;	NADH-cytochrome	CYB5R3	10	10	278	0.51866	1.2063	2.06E+09
P61006;P61006-2	P61006;P61006-2	Ras-related protein	RAB8A	4	2	207	0.51855	1.5769	2.33E+07
Q12768;E7EQI7;E5	Q12768;E7EQI7	WASH complex sub	KIAA0196	9	9	1159	0.51683	1.7772	3.99E+08
S4R329;H0YK61;HI	S4R329;H0YK61;HI	ER membrane prot	EMC4	2	2	72	0.51601	NaN	5.62E+07
Q96K37;H7C1I0;Q	Q96K37;H7C1I0	Solute carrier famil	SLC35E1	3	3	410	0.51499	1.1781	1.61E+08
E7ES96;P49768-2;I	E7ES96;P49768-2;I	Presenilin;Presenili	PSEN1	2	2	375	0.51347	1.4359	6.36E+07
Q969Z0;C9J7P5;C9	Q969Z0;C9J7P5;C9	Protein TBRG4	TBRG4	8	8	631	0.5132	2.1556	2.10E+08
P32189-1;P32189	P32189-1;P32189	Glycerol kinase;Put	GK;GK3P	2	2	524	0.5125	NaN	1.94E+07
P18669;P15259	P18669;P15259	Phosphoglycerate r	PGAM1;PGAM2	2	2	254	0.51169	NaN	6.42E+07
Q69YN2;Q69YN2-3	Q69YN2;Q69YN2-3	CWF19-like proteir	CWF19L1	9	9	538	0.51112	2.0935	6.46E+08
E9PLD0;Q9H0U4;A	E9PLD0;Q9H0U4;A	Ras-related protein	RAB1B;RAB1C	6	3	169	0.51108	1.6677	4.30E+08
Q5R3B4;O95563	Q5R3B4;O95563	Mitochondrial pyru	MPC2	3	3	105	0.50899	1.9872	5.52E+07
B0QZ43;O75477	B0QZ43;O75477	Erlin-1	ERLIN1	6	2	275	0.50738	NaN	1.72E+08
Q96DA2	Q96DA2	Ras-related protein	RAB39B	3	3	213	0.50562	NaN	2.65E+07
E9PF16;Q96CM8-4	E9PF16;Q96CM8-4	Acyl-CoA synthetas	ACSF2	2	2	572	0.49788	1.0849	2.02E+08
O94905;E5RHW4;I	O94905;E5RHW4	Erlin-2	ERLIN2	17	13	339	0.49579	1.7554	3.09E+09
Q8IYI0;A0A0A0MS(	Q8IYI0	Uncharacterized pr	C20orf196	5	5	205	0.4921	0.9693	2.28E+09
Q8TCT9-5;Q8TCT9;	Q8TCT9-5;Q8TCT9;	Minor histocompat	HM13	3	3	335	0.49063	1.9174	4.61E+08
Q04637-5;Q04637	Q04637-5;Q04637	Eukaryotic translat	EIF4G1	23	23	1435	0.48629	1.5224	1.41E+09
A0A0B4J2E5;Q152	A0A0B4J2E5;Q152	Periodic tryptopha	PWP2	20	17	919	0.48622	1.5704	3.01E+09
P51572;P51572-2;	P51572;P51572-2	B-cell receptor-assc	BCAP31	4	4	246	0.4842	2.1243	1.13E+08
Q92598-2;Q92598	Q92598-2;Q92598	Heat shock protein	HSPH1	32	30	814	0.48373	1.6975	5.33E+09
Q7Z494;Q7Z494-2;	Q7Z494;Q7Z494-2	Nephrocystin-3	NPHP3	7	7	1330	0.48186	1.7056	1.96E+08
P63261;I3L3I0;I3L	P63261;I3L3I0;I3L	Actin, cytoplasmic	ACTG1	21	1	375	0.4814	1.9435	3.92E+10
Q8IZD4;F5GZK9;Q8	Q8IZD4;F5GZK9;Q8	mRNA-decapping e	DCP1B	3	3	617	0.48056	NaN	8.03E+07
Q5QPL9;Q9UKM9-;	Q5QPL9;Q9UKM9-;	RNA-binding protei	RALY	9	9	237	0.4759	1.9664	1.02E+09
P62820;E7END7;P	P62820;E7END7;P	Ras-related protein	RAB1A	5	2	205	0.4751	1.5403	9.68E+07
Q9GZN8;Q9GZN8-2	Q9GZN8;Q9GZN8-2	UPF0687 protein C	C20orf27	3	3	174	0.47423	1.838	1.57E+08
Q9H3G5;H7C0X5;A	Q9H3G5;H7C0X5;A	Probable serine car	CPVL	5	5	476	0.47348	2.2955	3.27E+08
P33527-5;P33527-	P33527-5;P33527-	Multidrug resistanc	ABCC1	13	13	1416	0.47323	1.8133	4.11E+08
O15511;O15511-2	O15511;O15511-2	Actin-related prote	ARPC5	3	3	151	0.46938	2.4997	1.21E+08
Q9NZJ9-2;Q9NZJ9-	Q9NZJ9-2;Q9NZJ9-	Diphosphoinositol	NUDT4	2	2	181	0.46748	3.4367	1.59E+10
Q13232;H3BPR2;H	Q13232;H3BPR2	Nucleoside diphosp	NME3	9	9	169	0.46247	1.7131	4.04E+08
Q01650;A0A0C4D(	Q01650	Large neutral amin	SLC7A5	6	6	507	0.46124	2.2516	4.12E+08
Q6YHU6;Q6YHU6-3	Q6YHU6;Q6YHU6-3	Thyroid adenoma-a	THADA	11	11	1953	0.46122	1.4853	4.29E+08
P07196;A0A087X0	P07196	Neurofilament ligh	NEFL	5	3	543	0.45369	1.9041	2.49E+08
J3QLD9;E7EMK3;Q	J3QLD9;E7EMK3;Q	Flotillin-2	FLOT2	7	7	428	0.4533	1.3113	2.82E+08
P68133;P68032;P	P68133;P68032;P	Actin, alpha skeleta	ACTA1;ACTC1;ACTC	14	1	377	0.45088	2.1851	1.34E+09
A0A087WVD4;Q9H	A0A087WVD4;Q9H	Arsenite methyltra	AS3MT	4	4	338	0.44338	2.6605	5.72E+08
P08670;B0YJC4;B0	P08670;B0YJC4	Vimentin	VIM	47	43	466	0.44287	2.2218	2.49E+10
C9JC03;A0A024R5	C9JC03;A0A024R5	EH domain-contair	EHD1	7	6	374	0.44249	2.7177	2.50E+08
Q5T8U5;O15260-2	Q5T8U5;O15260-2	Surfeit locus protei	SURF4	3	3	186	0.44218	1.8736	3.92E+07
A6NEM5;Q92643;E	A6NEM5;Q92643;E	GPI-anchor transan	PIGK	2	2	332	0.44162	0.66374	7.86E+07
P04080	P04080	Cystatin-B	CSTB	2	2	98	0.43902	1.5144	1.09E+08
V9GYR2;P05026-2;	V9GYR2;P05026-2;	Sodium/potassium	ATP1B1	2	2	130	0.43506	2.145	1.80E+08
Q02750;Q02750-2	Q02750;Q02750-2	Dual specificity mit	MAP2K1	8	3	393	0.42916	NaN	7.00E+07
P63000;P63000-2	P63000;P63000-2	Ras-related C3 bot	RAC1	3	1	192	0.42839	1.2766	6.74E+07
Q9NRW1;P20340-;	Q9NRW1;P20340-;	Ras-related protein	RAB6B;RAB6A	3	2	208	0.42592	1.1993	1.31E+08
Q9UHD1-2;Q9UHD	Q9UHD1-2;Q9UHD	Cysteine and histid	CHORDC1	6	6	313	0.42317	2.3312	5.06E+08
P10599-2;P10599	P10599-2;P10599	Thioredoxin	TXN	4	4	85	0.42312	NaN	4.92E+07
P63092-3;P63092	P63092-3;P63092	Guanine nucleotid	GNAS	7	6	379	0.42151	1.8829	9.26E+08
C9J880;Q68CQ7-2;	C9J880;Q68CQ7-2;	Glycosyltransferase	GLT8D1	2	2	174	0.42116	NaN	6.43E+07
Q13423;E9PCX7;D	Q13423;E9PCX7	NAD(P) transhydro	NNT	11	11	1086	0.4211	2.3287	3.71E+08
J3KR97;Q9BTW9;C	J3KR97;Q9BTW9;C	Tubulin-specific ch	TBCD	17	17	1230	0.4193	2.3193	1.27E+09
O43924;B8ZZK5;C	O43924;B8ZZK5;C	Retinal rod rhodop	PDE6D	3	3	150	0.41435	0.6219	9.00E+07
O14828-2;O14828	O14828-2;O14828	Secretory carrier-as	SCAMP3	4	4	321	0.41409	2.1623	1.04E+08
P60953;Q5JYX0;P6	P60953;Q5JYX0;P6	Cell division contro	CDC42	3	2	191	0.41197	1.9722	1.79E+08
Q99460-2;Q99460	Q99460-2;Q99460	26S proteasome no	PSMD1	40	40	922	0.41063	2.337	6.59E+09
P53985;Q5T8R3;Q	P53985;Q5T8R3;Q	Monocarboxylate t	SLC16A1	8	8	500	0.40746	2.145	5.59E+08
B4DWR3;P61758	B4DWR3;P61758	Prefoldin subunit 3	VBP1	4	4	192	0.4051	2.1883	6.46E+07
A0A0B4J2A0;Q9UH	A0A0B4J2A0;Q9UH	Sedoheptulokinase	SHPK	3	3	478	0.40103	2.1532	1.92E+08
Q7Z7K6-3;Q7Z7K6;	Q7Z7K6-3;Q7Z7K6;	Centromere protei	CENPV	3	3	272	0.39937	2.2163	4.34E+08
Q9NYH9;J3KRR8	Q9NYH9	U3 small nucleolar	UTP6	7	7	597	0.3967	1.6227	2.72E+08
K7ELQ9;Q6UW68;I	K7ELQ9;Q6UW68;I	Transmembrane pr	TMEM205	3	3	170	0.39321	2.4352	5.10E+07
K7ENI6;K7ERE1;Q8	K7ENI6;K7ERE1;Q8	Transmembrane pr	TMEM256	3	3	41	0.38916	2.0002	6.79E+07
P02786;G3V0E5;H	P02786;G3V0E5	Transferrin recepto	TFRC	15	15	760	0.38238	3.3026	1.40E+09
Q9Y2P8;Q5VZU3;Q	Q9Y2P8	RNA 3-terminal phc	RCL1	7	7	373	0.37975	2.5764	1.07E+09

Q9NR31;X1WI22;[	Q9NR31;X1WI22;[	GTP-binding protei	SAR1A;SAR1B	3	3	198	0.37183	2.8518	5.83E+08
A0A0A0MTB8;Q8N	A0A0A0MTB8;Q8N	WD repeat-contain	WDR36	6	6	895	0.36887	1.5737	3.29E+08
J3QS48;I3L295;J3I	J3QS48;I3L295;J3I	Mannose-P-dolichc	MPDU1;HBEBP2BP	3	3	101	0.36672	2.3419	7.34E+07
Q15061;C9JEE7;C9	Q15061	WD repeat-contain	WDR43	10	10	677	0.33831	2.0942	6.09E+08
P00374-2;P00374;	P00374-2;P00374	Dihydrofolate redu	DHFR	3	3	135	0.33516	4.1108	1.04E+08
Q9Y289	Q9Y289	Sodium-dependent	SLC5A6	2	2	635	0.32059	2.0846	1.00E+08
X6RCC3;A0A087W	X6RCC3;A0A087W	Stromal membrane	SMAP2	2	2	174	0.31628	NaN	1.70E+08
P11166	P11166	Solute carrier famil	SLC2A1	2	2	492	0.31546	NaN	3.68E+07
Q99536;K7ESA3;Q	Q99536;K7ESA3;Q	Synaptic vesicle me	VAT1	3	3	393	0.30754	NaN	1.46E+08
Q15758;M0QXM4;	Q15758;M0QXM4;	Neutral amino acid	SLC1A5	10	10	541	0.2956	3.0599	1.99E+09
P42771;J3QRG6;P	P42771;J3QRG6;P	Cyclin-dependent k	CDKN2A	7	3	156	0.24369	3.7259	7.53E+08
P07355;H0YKS4;H	P07355;H0YKS4;H	Annexin A2;Annexi	ANXA2;ANXA2P2	10	10	339	0.242	3.4018	9.41E+08
F6R5I9;B4DZ60;P1	F6R5I9;B4DZ60;P1	S-adenosylmethion	AMD1	1	1	48	0.22681	NaN	3.22E+07
X6RFL8;P61106	X6RFL8;P61106	Ras-related protein	RAB14	3	3	181	0.22551	1.6937	7.07E+07
J3KR58;Q99611	J3KR58;Q99611	Selenide, water dik	SEPHS2	1	1	448	0.19453	NaN	5.36E+07
A0A087WTM7;P04	A0A087WTM7;P04	Apolipoprotein B-1	APOB	6	3	4344	0.062725	NaN	1.17E+08
K7ELU5;Q7Z3V5	K7ELU5;Q7Z3V5	Zinc finger protein	ZNF571	1	1	84	0.039252	NaN	1.85E+10

6.7. C20orf196 SILAC interactomes

Protein IDs	Majority protein	Protein names	Gene names	Peptides	Unique peptides	Sequence length	Q-value	Score	Ratio H/L normal	Ratio H/L normal	Intensity
Q8TDX7;F8WAG2	Q8TDX7	Serine/threonine-	NEK7	5	4	302	0	18.891	9.8112	0.17384	7.99E+08
A0A087WVC4;A0	A0A087WVC4;A0	cAMP-dependent	PRKACB	4	4	338	0	51.985	7.8972	0.2157	4.76E+08
P11766;H0YAG8;	P11766;H0YAG8	Alcohol dehydrog	ADH5	4	4	374	0	55.901	6.594	0.13017	7.07E+08
H3BPB8;P34949;	H3BPB8;P34949;	Mannose-6-phosp	MPI	5	5	403	0	31.786	6.5408	0.60263	4.37E+08
F5H7K1;E7EWW(	F5H7K1;E7EWW(	UPF0505 protein	C16orf62	13	13	959	0	68.34	6.1668	0.7711	1.50E+09
Q8IYI0;Q5TGB0;C	Q8IYI0;Q5TGB0	Uncharacterized p	C20orf196	21	16	205	0	323.31	6.0396	0.013471	4.27E+11
Q9H8Y8;Q9H8Y8·	Q9H8Y8;Q9H8Y8·	Golgi reassembly-	GORASP2	11	11	452	0	111.3	5.4436	0.18291	1.60E+09
Q9Y535-2;Q9Y53	Q9Y535-2;Q9Y53	DNA-directed RN/	POLR3H	3	3	175	0	55.178	4.8326	0.18942	3.42E+08
O95983-2;O9598	O95983-2;O9598	Methyl-CpG-bind	MBD3	5	5	259	0	38.158	4.732	0.4654	7.64E+08
B1AK45;B1AK43;	B1AK45;B1AK43;	Mitotic spindle as	MAD2L2	2	2	167	0	9.038	4.6463	0.20681	4.10E+08
Q9H7Z6;Q9H7Z6·	Q9H7Z6;Q9H7Z6·	Histone acetyltra	KAT8	3	3	458	0	8.8365	4.5107	NaN	4.72E+07
H0YH87;V9GY86;	H0YH87;V9GY86;	Ataxin-2	ATXN2	10	10	916	0	63.022	4.4873	0.62468	4.56E+08
Q9NVJ2;Q9NVJ2·	Q9NVJ2;Q9NVJ2·	ADP-ribosylation	ARL8B	4	3	186	0	10.522	4.229	0.69566	9.22E+07
Q96FK6;G3V4B8	Q96FK6;G3V4B8	WD repeat-contai	WDR89	5	5	387	0	52.646	3.9262	1.1788	3.48E+08
Q7L273;K7ENB5;	Q7L273;K7ENB5;	BTB/POZ domain-	KCTD9	2	2	389	0	6.6722	3.8941	NaN	8.44E+07
Q8TCT9-5;Q8TCT9	Q8TCT9-5;Q8TCT9	Minor histocomp	HM13	3	3	335	0	21.284	3.7788	NaN	5.96E+08
O94760;B4DYP1;	O94760;B4DYP1;	N(G),N(G)-dimeth	DDAH1	7	7	285	0	30.106	3.7151	0.58237	2.96E+08
M0QY97;Q9UPT8	M0QY97;Q9UPT8	Zinc finger CCCH	ZC3H4	4	4	910	0	38.764	3.614	0.20506	1.56E+08
Q8WWH5	Q8WWH5	Probable tRNA ps	TRUB1	13	13	349	0	60.421	3.3743	0.52817	1.30E+09
Q3B726	Q3B726	DNA-directed RN/	TWISTNB	3	3	338	0	30.471	3.2574	0.85254	7.15E+07
P0C7P0	P0C7P0	CDGSH iron-sulfu	CISD3	1	1	127	0	4.6985	3.0902	NaN	1.16E+08
Q96BM9	Q96BM9	ADP-ribosylation	ARL8A	2	1	186	0	4.3574	2.972	0.15729	2.86E+08
Q6P1R4;H0YGW8	Q6P1R4;H0YGW8	tRNA-dihydrouric	DUS1L	4	4	473	0	14.277	2.8904	NaN	9.58E+07
Q92905;E5RHH5;	Q92905;E5RHH5	COP9 signalosom	COPS5	3	3	334	0	12.707	2.8807	1.0056	2.42E+08
Q70Z53-2;Q70Z5	Q70Z53-2;Q70Z5	Protein FRA10AC	FRA10AC1	2	2	276	0	11.44	2.8576	0.083071	2.90E+08
P47813;X6RAC9;	P47813;X6RAC9;	Eukaryotic transl	EIF1AX;EIF1AY	7	7	144	0	102.88	2.8432	0.29041	2.47E+09
Q9NQT5;Q9NQT5	Q9NQT5;Q9NQT5	Exosome comple	EXOSC3	11	11	275	0	120.06	2.7359	0.36167	2.89E+09
A0A0A0MRB5;Q8	A0A0A0MRB5;Q8	MAP kinase-activ	MADD	4	4	1588	0	14.729	2.7195	1.5158	6.91E+07
Q7KZJ0;J3QKK3;(	Q7KZJ0;J3QKK3;(	DNA repair protei	RAD51C	3	3	134	0	31.856	2.7194	0.89126	3.72E+08
G3V1N5;B4E3L3;	G3V1N5;B4E3L3;	Ubiquitin carbox	USP28	2	2	753	0.0047524	2.4381	2.654	NaN	2.93E+07
Q8N6Q8;H0YIN2;	Q8N6Q8;H0YIN2;	Methyltransferas	METTL25	2	2	603	0	3.8923	2.6374	NaN	3.06E+07
F8W9B8;A0A0A0	F8W9B8;A0A0A0	Exocyst complex	EXOC5	3	3	643	0	7.0314	2.5969	NaN	6.94E+07
A0A087X2D5;Q9I	A0A087X2D5;Q9I	39S ribosomal pr	MRPL45	3	3	306	0	15.5	2.5616	0.1163	3.97E+08
H0Y7A7;P62158;	H0Y7A7;P62158;	Calmodulin	CALM2;CALM1;C/	6	6	187	0	152	2.5085	0.52873	9.57E+08
P12236	P12236	ADP/ATP transloc	SLC25A6	32	11	298	0	270.47	2.477	0.33654	3.35E+10
A6NHG8;Q13114	A6NHG8;Q13114	TNF receptor-ass	TRAF3	2	2	543	0.0020688	2.962	2.4536	NaN	9.08E+07
O60645-2;O6064	O60645-2;O6064	Exocyst complex	EXOC3	7	7	641	0	23.893	2.4526	0.88073	4.51E+08
Q15785	Q15785	Mitochondrial im	TOMM34	5	5	309	0	92.838	2.4434	0.90012	3.54E+08
P11182;Q5VVL7	P11182;Q5VVL7	Lipoamide acyltra	DBT	4	4	482	0	22.041	2.4356	0.79635	1.22E+08
Q96SI1-2;Q96SI1	Q96SI1-2;Q96SI1	BTB/POZ domain-	KCTD15	4	4	234	0	23.732	2.4181	0.92958	2.50E+08
Q2NKJ3;Q2NKJ3-	Q2NKJ3;Q2NKJ3-	CST complex subu	CTC1	3	3	1217	0	17.311	2.3908	NaN	1.50E+08
Q9UBW7;A0A087	Q9UBW7	Zinc finger MYM-t	ZMYM2	7	6	1377	0	21.612	2.3873	0.85472	1.46E+08
Q9BTV4	Q9BTV4	Transmembrane p	TMEM43	4	4	400	0	17.964	2.3771	0.41173	1.73E+08
Q9BR61	Q9BR61	Acyl-CoA-binding	ACBD6	5	5	282	0	27.274	2.3748	0.279	1.60E+08
K7ERV3;P04183;I	K7ERV3;P04183;I	Thymidine kinase	TK1	4	4	267	0	21.566	2.3712	0.24466	4.82E+08
Q16778;P33778;	Q16778;P33778;	Histone H2B type	HIST2H2BE;HIST1	9	0	126	0	13.58	2.3574	0.31781	3.58E+09
Q96GD4-4;Q96GI	Q96GD4-4;Q96GI	Aurora kinase B	AURKB	5	5	303	0	31.922	2.3242	0.23341	6.33E+08
P63167;F8VXL2;I	P63167;F8VXL2;I	Dynein light chai	DYNLL1	7	5	89	0	36.971	2.3226	0.37144	6.25E+08
P82664	P82664	28S ribosomal pr	MRPS10	6	6	201	0	50.713	2.3223	0.66378	1.03E+09
A0A087WT67;O1	A0A087WT67;O1	Zinc finger protei	ZNF195	4	3	633	0	10.649	2.3143	NaN	4.90E+07
O75190;A0A0J9Y	O75190;A0A0J9Y	DnaJ homolog sul	DNAJB6	14	2	326	0	122.28	2.3006	0.37276	5.42E+09
Q96FJ2	Q96FJ2	Dynein light chai	DYNLL2	5	3	89	0	14.104	2.266	0.19323	1.30E+08
A0A075B6F9;Q9\	A0A075B6F9;Q9\	Nitric oxide synth	NOSIP	9	9	304	0	82.776	2.2523	0.4305	1.34E+09
Q15366-2;Q1536	Q15366-2;Q1536	Poly(rC)-binding p	PCBP2	19	0	366	0	10.808	2.1826	0.12461	4.09E+09
Q9C037-2;Q9C03	Q9C037-2;Q9C03	Tripartite motif-c	TRIM4	3	3	474	0	7.9096	2.1751	1.1298	6.16E+09
K7EQH1;A0A087\	K7EQH1;A0A087\	Uncharacterized p	C18orf25;ARKL1	1	1	146	0	18.909	2.1621	NaN	1.17E+07
K7ELA4;B5MD17;	K7ELA4;B5MD17;	Chromobox prote	CBX1	3	2	138	0	40.847	2.1582	0.52991	2.32E+08
Q9NR45;Q5TBR0;	Q9NR45	Sialic acid syntha	NANS	16	16	359	0	199.54	2.1342	0.4655	7.28E+09
Q15554;J3KSZ6;L	Q15554;J3KSZ6;L	Telomeric repeat-	TERF2	3	3	542	0	6.5662	2.1107	NaN	3.55E+07
Q9Y697-2;Q9Y69	Q9Y697-2;Q9Y69	Cysteine desulfur	NFS1	7	7	397	0	25.26	2.1061	0.83717	1.91E+08
Q96NW4;K7ELM:	Q96NW4;K7ELM:	Ankyrin repeat do	ANKRD27	2	2	1050	0	6.7286	2.0849	NaN	6.26E+07
H7BY83;Q5JSH3-:	H7BY83;Q5JSH3-:	WD repeat-contai	WDR44	5	5	806	0	16.786	2.0737	0.89028	6.36E+07
Q86XZ4;F8VS10	Q86XZ4;F8VS10	Spermatogenesis-	SPATS2	6	6	545	0	29.965	2.0649	NaN	6.46E+07
Q9BPZ7-5;Q9BPZ	Q9BPZ7-5;Q9BPZ	Target of rapamyc	MAPKAP1	2	2	323	0	16.258	2.0487	NaN	1.86E+08
Q8NAV1	Q8NAV1	Pre-mRNA-splicin	PRPF38A	6	6	312	0	31.665	2.0465	0.42664	1.63E+08
Q13642-1;Q1364	Q13642-1;Q1364	Four and a half LI	FHL1	13	13	280	0	93.83	2.0196	0.10659	3.28E+09
O15541	O15541	RING finger prote	RNF113A	3	3	343	0	8.3916	2.0161	NaN	6.52E+06
A0A0A0MQR8;A0	A0A0A0MQR8;A0	MAP/microtubul	MARK3	11	3	713	0	17.047	2.0081	0.58561	1.15E+08
F5H562;E7ET55;F	F5H562;E7ET55;F	Copper-transport	ATP7B	5	5	1035	0	22.607	1.9834	0.70432	2.98E+08
Q6ZRV2;J3KPS2	Q6ZRV2;J3KPS2	Protein FAM83H	FAM83H	16	16	1179	0	154.88	1.9697	0.59051	7.81E+08
P52435;A0A0B4J	P52435;A0A0B4J	DNA-directed RN/	POLR2J;POLR2J3;	4	4	117	0	13.279	1.9688	0.27943	2.50E+08
Q9UJY1;H0YG30	Q9UJY1	Heat shock protei	HSPB8	4	4	196	0	7.4407	1.9651	0.82032	1.95E+08
Q9H3N1;G3V448	Q9H3N1	Thioredoxin-relat	TMX1	5	5	280	0	22.717	1.9528	1.2118	1.10E+08
F6QDS0	F6QDS0			24	0	479	0	64.507	1.9441	NaN	3.63E+08
O95219;O95219·	O95219;O95219·	Sorting nexin-4	SNX4	6	6	450	0	58.047	1.9354	0.84938	2.41E+08
O43852;O43852·	O43852;O43852·	Calumenin	CALU	10	10	315	0	164.14	1.9302	0.23335	9.74E+08
Q9ULX6;Q9ULX6·	Q9ULX6;Q9ULX6·	A-kinase anchor p	AKAP8L	9	9	646	0	105.45	1.9203	0.57224	2.23E+09
H7C5F9;B4E2D5;	H7C5F9;B4E2D5;	Transcription fact	SUPT20H	1	1	378	0	32.623	1.9085	NaN	1.27E+08
Q14687-2;Q1468	Q14687-2;Q1468	Genetic suppress	GSE1	6	6	1113	0	34.066	1.899	0.64689	1.36E+08
Q9UGR2-2;Q9UG	Q9UGR2-2;Q9UG	Zinc finger CCCH	ZC3H7B	8	8	977	0	54.039	1.8946	1.1298	7.17E+08
O00443;A0A0C4I	O00443	Phosphatidylinos	PIK3C2A	27	27	1686	0	235.74	1.8942	0.66923	1.25E+09
Q9UGP4;C9JRJ5	Q9UGP4;C9JRJ5	LIM domain-cont	LIMD1	5	5	676	0	20.905	1.8924	1.2032	1.67E+08
Q9HB71;Q9HB71	Q9HB71;Q9HB71	Calcyclin-binding	CACYBP	20	20	228	0	307.88	1.8859	0.60158	1.13E+10
Q7L8W6;H0YND7	Q7L8W6;H0YND7	Diphthine--ammo	DPH6	4	4	267	0	38.415	1.8808	4.0816	2.78E+08
Q13136-2;Q1313	Q13136-2;Q1313	Liprin-alpha-1	PPFIA1	6	6	1185	0	46.365	1.8805	0.25433	3.18E+08
H3BNT4;Q99547;	H3BNT4;Q99547;	M-phase phospho	MPHOSPH6	9	9	142	0	36.253	1.8762	0.52481	4.99E+08
Q92540-2;Q9254	Q92540-2;Q9254	Protein SMG7	SMG7	10	10	1091	0	30.263	1.8762	0.76246	2.14E+08
A0A0G2JH68;O6(	A0A0G2JH68;O6(	Protein diaphano	DIAPH1	41	41	1272	0	323.31	1.8685	0.44794	4.32E+09
Q9BXY0	Q9BXY0	Protein MAK16 h	MAK16	2	2	300	0	15.857	1.8678	0.50965	2.19E+08
Q09666;E9PQE3;	Q09666;E9PQE3;	Neuroblast differ	AHNAK	2	2	5890	0	5.8365	1.8644	NaN	2.13E+08
O75446	O75446	Histone deacetyla	SAP30	4	4	220	0	20.198	1.8626	0.23987	4.33E+08
Q6ZW49;Q6ZW4!	Q6ZW49;Q6ZW4!	PAX-interacting p	PAXIP1	6	6	1069	0	24.231	1.8612	1.3341	4.19E+08
K7ENL4;J3QL63;J	K7ENL4;J3QL63;J	Golgi apparatus n	TVP23B;TVP23C	2	2	132	0	12.669	1.8515	NaN	4.51E+07
P49914;A0A0A6\	P49914;A0A0A6\	5-formyltetrahyd	MTHFS	7	7	203	0	51.449	1.85	0.62285	4.84E+08
Q9NVX0-3;Q9NV	Q9NVX0-3;Q9NV	HAUS augmin-like	HAUS2	4	4	204	0	6.581	1.8442	NaN	7.02E+07
Q9NWH9;H7BXE:	Q9NWH9;H7BXE:	SAFB-like transcri	SLTM	4	4	1034	0	47.386	1.8365	0.88745	9.27E+07
Q5T7C4;P09429;	Q5T7C4;P09429	High mobility gro	HMGB1	3	3	158	0	9.1165	1.8295	NaN	1.80E+08
Q9Y6D5	Q9Y6D5	Brefeldin A-inhibi	ARFGEF2	10	8	1785	0	44.792	1.8189	0.70601	1.87E+08
Q6P6B7;Q6P6B7·	Q6P6B7;Q6P6B7·	Ankyrin repeat do	ANKRD16	3	3	361	0	13.255	1.814	1.0292	8.94E+07
Q14289-2;Q1428	Q14289-2;Q1428	Protein-tyrosine k	PTK2B	2	2	967	0.0063882	2.1936	1.8077	0.44513	1.11E+07
A0A087WTX2;Q9	A0A087WTX2;Q9	Zinc transporter S	SLC39A7	1	1	429	0	4.9764	1.8072	NaN	9.72E+06
Q09472;I3L0Q1	Q09472	Histone acetyltra	EP300	13	5	2414	0	25.08	1.8069	0.81878	1.62E+08
A6NML8;K4DI95;	A6NML8;K4DI95;	Protein diaphano	DIAPH2	7	7	1096	0	30.85	1.8035	0.77487	2.24E+08

Q12765;Q12765-	Q12765;Q12765-	Secernin-1	SCRN1	7	7	414	0	35.999	1.8035	0.90208	5.61E+08
Q7Z7H8;Q7Z7H8-	Q7Z7H8;Q7Z7H8-	39S ribosomal pr	MRPL10	4	4	261	0	27.585	1.7978	0.60536	4.62E+08
Q15020;Q15020-	Q15020;Q15020-	Squamous cell ca	SART3	33	7	963	0	323.31	1.7922	0.53142	4.48E+09
Q96JM3;S4R3K0	Q96JM3	Chromosome alig	CHAMP1	14	14	812	0	164.85	1.7921	0.40329	9.17E+08
A0A0U1RR32;A0/	A0A0U1RR32;A0/	Histone H2A type	HIST1H2AJ;HIST1	7	2	169	0	61.065	1.7918	0.42253	5.85E+09
Q9Y673-2;Q9Y67	Q9Y673-2;Q9Y67	Dolichyl-phospha	ALG5	2	2	294	0	8.1759	1.7898	NaN	5.63E+07
Q9BTE1;H3BR94;	Q9BTE1;H3BR94;	Dynactin subunit	DCTN5	6	6	182	0	47.367	1.7815	0.48545	5.30E+08
Q9Y383;A0A0A6\	Q9Y383;A0A0A6\	Putative RNA-bin	LUC7L2	9	7	392	0	60.83	1.7793	0.73242	8.41E+08
H3BPE1;H3BQK9;	H3BPE1;H3BQK9;	Microtubule-acti	MACF1	13	12	7555	0	43.353	1.7766	0.60833	3.51E+08
H0YMV8;Q71UM!	H0YMV8;Q71UM!	40S ribosomal pr	RPS27L	6	2	100	0	22.586	1.7748	NaN	4.91E+08
H7BYN4;Q02241-	H7BYN4;Q02241-	Kinesin-like prote	KIF23	16	16	952	0	125.13	1.771	0.63539	1.25E+09
Q5SZR1;Q9BYD2	Q5SZR1;Q9BYD2	39S ribosomal pr	MRPL9	3	3	233	0	30.794	1.7689	NaN	8.14E+07
P15880;H0YEN5;	P15880;H0YEN5;	40S ribosomal pr	RPS2	19	19	293	0	214.1	1.764	0.6309	2.39E+10
Q9NQW6-2;Q9N(	Q9NQW6-2;Q9N(	Actin-binding pro	ANLN	6	6	1087	0	82.235	1.7567	2.0077	2.16E+08
Q9UBI9	Q9UBI9	Headcase protein	HECA	3	3	543	0	9.7163	1.7543	NaN	5.88E+07
Q12824-2;G5E97	Q12824-2;G5E97	SWI/SNF-related r	SMARCB1	9	9	376	0	171.41	1.754	0.83057	2.19E+09
Q16527;F8VQR7;	Q16527;F8VQR7;	Cysteine and glyci	CSRP2	10	10	193	0	85.194	1.7465	0.56288	3.29E+08
Q16720-8;Q1672	Q16720-8;Q1672	Plasma membran	ATP2B3	11	2	1115	0.00026638	3.4969	1.7417	NaN	4.24E+06
Q9Y283-2;Q9Y28	Q9Y283-2;Q9Y28	Inversin	INVS	1	1	895	0.0013082	3.1286	1.7404	0.47671	4.65E+07
Q86TJ2-3;Q86TJ2	Q86TJ2-3;Q86TJ2	Transcriptional ac	TADA2B	5	5	328	0	20.292	1.7325	0.73152	1.70E+08
Q6R327;Q6R327-	Q6R327;Q6R327-	Rapamycin-insen	RICTOR	14	14	1708	0	79.801	1.7293	0.76288	5.78E+08
C9JP00;A0A0A0M	C9JP00;A0A0A0M	Muscleblind-like	MBNL1	9	2	348	0	71.646	1.7263	0.48953	1.62E+09
P24534;C9JZW3;	P24534	Elongation factor	EEF1B2	14	12	225	0	164.82	1.7256	0.3244	1.90E+10
Q9HD26-2;Q9HD	Q9HD26-2;Q9HD	Golgi-associated I	GOPC	11	11	454	0	110.41	1.7206	0.89681	4.16E+08
Q6Y1H2;C9JWG1	Q6Y1H2	Very-long-chain (3	PTPLB	5	5	254	0	11.942	1.717	0.86575	1.28E+08
P35249;C9JZI1;P	P35249;C9JZI1;P	Replication factor	RFC4	19	19	363	0	311.23	1.7133	0.5929	3.52E+09
Q9BT25-2;Q9BT2	Q9BT25-2;Q9BT2	HAUS augmin-like	HAUS8	7	7	349	0	183.73	1.7122	0.46742	1.40E+09
Q9BTT0-3;Q9BTT(	Q9BTT0-3;Q9BTT(	Acidic leucine-ric	ANP32E	5	5	220	0	109.18	1.7121	0.38943	1.35E+09
Q5T280;R4GNG4	Q5T280	Uncharacterized p	C9orf114	3	3	376	0	13.798	1.7077	0.6212	1.03E+08
A0A0C4DFM7;Q5	A0A0C4DFM7;Q5	Terminal uridylyl	ZCCHC11	5	5	1645	0	59.325	1.7049	0.69429	1.58E+08
Q9Y5V3;Q9Y5V3-	Q9Y5V3;Q9Y5V3-	Melanoma-associ	MAGED1	13	12	778	0	256.2	1.6982	0.39423	1.02E+09
P42166;P42167-	P42166	Lamina-associate	TMPO	15	11	694	0	158.15	1.6947	0.51763	1.51E+09
Q6IQ49-2;Q6IQ4!	Q6IQ49-2;Q6IQ4!	Protein SDE2 hon	SDE2	1	1	439	0.0087634	2.0635	1.6882	NaN	9.66E+06
E9PQG4;A0A0A0I	E9PQG4;A0A0A0I	Myomegalin	PDE4DIP	3	3	740	0	16.128	1.6856	NaN	4.11E+07
P82914	P82914	28S ribosomal pr	MRPS15	7	7	257	0	14.749	1.6855	0.48324	1.19E+09
Q3MHD2;Q3MHE	Q3MHD2;Q3MHE	Protein LSM12 ho	LSM12	8	8	195	0	57.201	1.6829	0.56269	3.51E+09
E9PH99;Q9Y4E5-:	E9PH99;Q9Y4E5-:	Zinc finger protei	ZNF451	6	6	1041	0	21.352	1.6742	0.89122	7.03E+07
P53621;P53621-	P53621;P53621-	Coatomer subuni	COPA	87	87	1224	0	323.31	1.6738	0.54565	5.52E+10
P53350;I3L2H5;I	P53350	Serine/threonine	PLK1	8	8	603	0	56.668	1.6693	NaN	4.25E+08
P53985;Q5T8R5;	P53985;Q5T8R5;	Monocarboxylate	SLC16A1	9	9	500	0	97.127	1.6685	0.96056	1.15E+09
P39748;P39748-	P39748;P39748-	Flap endonucleas	FEN1	22	22	380	0	323.31	1.6611	0.56668	1.10E+10
K7EP32;Q9BZV1;I	K7EP32;Q9BZV1;I	UBX domain-cont	UBXN6	5	5	371	0	15.799	1.6606	0.75819	2.55E+08
Q9UKX7-2;Q9UK)	Q9UKX7-2;Q9UK)	Nuclear pore com	NUP50	2	2	440	0	6.1075	1.6579	NaN	3.41E+07
F8VR31;P51530-:	F8VR31;P51530-:	DNA replication A	DNA2	4	4	867	0	8.0722	1.6563	0.6016	1.00E+08
Q9UI43;E9PGN6	Q9UI43;E9PGN6	Putative ribosom	FTSJ2	3	3	246	0	6.289	1.6503	NaN	5.09E+07
E7EN20;Q9UPN9;	E7EN20;Q9UPN9;	E3 ubiquitin-prot	TRIM33	12	2	1119	0	114.67	1.6471	0.51758	1.55E+09
E7EPP6;J3KN87;(	E7EPP6;J3KN87;(	Serine/threonine	CHEK1	5	5	492	0	27.944	1.6464	1.0474	3.65E+08
Q96KP1;Q2MDF5	Q96KP1	Exocyst complex	EXOC2	17	17	924	0	106.57	1.6424	0.5155	1.65E+09
Q9H2P0;E9PQK8	Q9H2P0	Activity-depende	ADNP	25	25	1102	0	176.85	1.6393	0.60649	2.60E+09
Q9NQE9	Q9NQE9	Histidine triad nu	HINT3	3	3	182	0	16.423	1.6375	5.3158	4.39E+08
A0A0A0MRN5;Q9	A0A0A0MRN5;Q9	Opioid growth fac	OGFR	4	4	625	0	29.893	1.6357	0.74122	2.27E+08
A0A075B6T1;Q9(	A0A075B6T1;Q9(	Activating molecu	AMBRA1	9	9	1179	0	67.728	1.6335	0.70103	4.19E+08
Q7Z4H7-3;Q7Z4H	Q7Z4H7-3;Q7Z4H	HAUS augmin-like	HAUS6	16	16	920	0	68.246	1.6321	0.42936	1.26E+09
Q8TER5-2;Q8TER!	Q8TER5-2;Q8TER!	Rho guanine nucl	ARHGEF40	2	2	805	0	4.7199	1.6312	NaN	4.46E+07
Q8N5C6;Q8N5C6	Q8N5C6;Q8N5C6	S1 RNA-binding d	SRBD1	20	20	995	0	168.09	1.6302	0.70671	2.22E+09
P13804;P13804-	P13804;P13804-	Electron transfer	ETFA	17	8	333	0	266.33	1.6284	0.57361	1.13E+10
Q9UHR4	Q9UHR4	Brain-specific ang	BAIAP2L1	4	4	511	0	15.565	1.6234	NaN	1.11E+08
P35251-2;P3525	P35251-2;P3525	Replication factor	RFC1	9	9	1147	0	58.565	1.6228	0.59615	8.64E+08
O15164-2;O1516	O15164-2;O1516	Transcription inte	TRIM24	11	11	1016	0	35.363	1.6159	0.67124	4.98E+08
D6W601;Q96EY9	D6W601;Q96EY9	Probable inactive	hCG_22695;ADA1	2	2	367	0.0023018	2.7901	1.6106	NaN	1.88E+07
O15371-3;O1537	O15371-3;O1537	Eukaryotic transl	EIF3D	22	22	533	0	309.02	1.6096	0.83668	4.48E+09
Q9H0H5;F8VRD2	Q9H0H5;F8VRD2	Rac GTPase-activa	RACGAP1	5	5	632	0	11.849	1.6035	NaN	6.40E+07
A0A0A0MRM8;Q!	A0A0A0MRM8;Q!	Unconventional r	MYO6	48	48	1253	0	323.31	1.5916	0.67775	6.51E+09
M0QZR4;Q92888	M0QZR4;Q92888	Rho guanine nucl	ARHGEF1	21	21	968	0	232.71	1.5913	0.60962	1.30E+09
A0A087X1F4;Q9I	A0A087X1F4;Q9I	Mediator of RNA p	MED20	3	3	211	0	9.5897	1.5887	NaN	1.10E+08
P37108;H0YLA2;I	P37108;H0YLA2	Signal recognitior	SRP14	10	10	136	0	75.295	1.5887	0.5867	6.43E+09
J3KNB8;F5H538;I	J3KNB8;F5H538;I	Mitogen-activate	MAP3K4	6	6	1554	0	22.858	1.5821	0.75042	2.50E+08
O43719;Q5H918	O43719	HIV Tat-specific fa	HTATSF1	27	27	755	0	323.31	1.5806	0.60411	2.61E+09
V9GYM8;Q92974	V9GYM8;Q92974	Rho guanine nucl	ARHGEF2	31	31	1031	0	323.31	1.5804	0.60652	3.75E+09
Q9UGN5-2;Q9UG	Q9UGN5-2;Q9UG	Poly [ADP-ribose]	PARP2	4	4	570	0	10.17	1.5801	NaN	2.02E+07
P43034;I3L3N5;I	P43034	Platelet-activatin	PAFAH1B1	20	20	410	0	186.91	1.5787	0.53467	5.17E+09
Q13409-3;Q1340	Q13409-3;Q1340	Cytoplasmic dyne	DYNC1I2	7	7	612	0	56.639	1.5764	0.86979	8.65E+08
Q8NFW8;Q8NFW	Q8NFW8;Q8NFW	N-acylneuramina	CMAS	19	19	434	0	98.956	1.5763	0.54575	5.74E+09
Q8IWS0-5;Q8IWS	Q8IWS0-5;Q8IWS	PHD finger protei	PHF6	13	13	331	0	98.176	1.5744	0.72394	2.40E+09
Q86YP4-2;Q86YP	Q86YP4-2;Q86YP	Transcriptional re	GATAD2A	16	15	608	0	97.688	1.5739	0.76588	6.82E+08
I3VM54;Q9Y2K7-	I3VM54;Q9Y2K7-	Lysine-specific de	KDM2A	6	6	1145	0	15.625	1.5716	0.79155	2.40E+08
H0Y3N9;Q9UPP1	H0Y3N9;Q9UPP1	Histone lysine der	PHF8	6	5	953	0	32.188	1.5671	0.60446	3.00E+08
Q9NSV4;Q9NSV4-	Q9NSV4;Q9NSV4-	Protein diaphano	DIAPH3	24	24	1193	0	180.46	1.5668	0.76986	7.51E+08
P52732	P52732	Kinesin-like prote	KIF11	33	33	1056	0	262.99	1.5658	0.56616	3.42E+09
Q9UNI6;V9GYV5;	Q9UNI6	Dual specificity p	DUSP12	4	4	340	0	13.051	1.5644	0.69765	2.70E+08
M0QXA7;O95785	M0QXA7;O95785	Protein Wiz	WIZ	4	4	968	0	79.117	1.5643	NaN	7.56E+07
Q9NP77;Q9NP77	Q9NP77;Q9NP77	RNA polymerase I	SSU72	7	7	194	0	34.406	1.5639	0.59556	1.05E+09
A6NKD9;G3V5D5	A6NKD9	Coiled-coil domai	CCDC85C	3	3	419	0	20.795	1.5576	0.70474	3.31E+07
Q14149	Q14149	MORC family CW-	MORC3	4	4	939	0	21.086	1.5541	0.95962	9.73E+07
P35658-2;P3565	P35658-2;P3565	Nuclear pore com	NUP214	22	22	2079	0	323.31	1.5528	0.58982	1.93E+09
Q9ULV4;Q9ULV4-	Q9ULV4;Q9ULV4-	Coronin-1C;Coro	CORO1C	19	19	474	0	205.19	1.5509	0.86896	3.40E+09
Q15293;Q15293-	Q15293;Q15293-	Reticulocalbin-1	RCN1	11	11	331	0	145.49	1.55	0.65809	2.03E+09
E9PDR5;E7EPI0;C	E9PDR5;E7EPI0;C	Inhibitor of Bruto	IBTK	3	3	1152	0	5.4257	1.5498	0.98936	7.72E+07
O94927;U3KQJ5;	O94927;U3KQJ5;	HAUS augmin-like	HAUS5	2	2	633	0.0023077	2.817	1.5492	NaN	6.02E+06
G5E9A6;P51784	G5E9A6;P51784	Ubiquitin carbox	USP11	8	6	920	0	21.987	1.5479	0.80164	4.70E+08
P52272-2;P5227	P52272-2;P5227	Heterogeneous nu	HNRNPM	51	51	691	0	323.31	1.5461	0.70408	3.80E+10
P53803	P53803	DNA-directed RNA	POLR2K	2	2	58	0.0070818	2.1267	1.546	0.54193	6.49E+08
P49841-2;P4984	P49841-2;P4984	Glycogen synthas	GSK3B	4	3	433	0	22.838	1.5451	0.81898	3.82E+08
B4DZS0;O76075;	B4DZS0;O76075	DNA fragmentatic	DFFB	5	5	362	0	39.012	1.543	0.67019	6.40E+08
O75146-2;O7514	O75146-2;O7514	Huntingtin-intera	HIP1R	2	2	615	0	24.411	1.5425	NaN	2.17E+07
P15924;P15924-	P15924;P15924-	Desmoplakin	DSP	45	45	2871	0	323.31	1.5409	0.50328	1.92E+09
F5H5V4;F5GX23;	F5H5V4;F5GX23;	26S proteasome r	PSMD9	5	5	153	0	18.956	1.5396	NaN	9.95E+07
Q14258	Q14258	E3 ubiquitin/ISG1	TRIM25	20	20	630	0	108.22	1.5395	NaN	2.30E+09
Q96A65;Q96A65-	Q96A65	Exocyst complex	EXOC4	32	32	974	0	197.34	1.5376	0.55734	3.70E+09
O43683-2;O4368	O43683-2;O4368	Mitotic checkpoi	BUB1	9	9	1028	0	46.761	1.5346	0.40607	3.71E+08
I6L9J0;F8W8M9;	I6L9J0;F8W8M9;	Protein unc-13 ho	UNC13B;UNC13A	2	2	1197	0	10.098	1.5322	NaN	2.88E+07
A0A0A0MQR2;Q9	A0A0A0MQR2;Q9	Protein RTF2 hon	RTFDC1	7	7	336	0	30.349	1.5312	0.50829	1.97E+08
Q8N3F8;B0QY91;	Q8N3F8;B0QY91;	MICAL-like protei	MICALL1	3	3	863	0	4.4802	1.5304	NaN	7.60E+07
A0A087WTZ0;Q8	A0A087WTZ0;Q8	Myotubularin-rel	MTMR14	2	2	520	0	3.8221	1.5303	NaN	3.84E+07

Q93034;H0YCA0	Q93034	Cullin-5	CUL5	17	17	780	0	158.23	1.5294		0.69971	1.43E+09
Q9P0U4;Q9P0U4	Q9P0U4;Q9P0U4	CXXC-type zinc fir	CXXC1	4	4	656	0	25.374	1.5293		0.41679	5.13E+07
P33981-2;P3398	P33981-2;P3398	Dual specificity pı	TTK	16	16	856	0	143.08	1.5282		0.82929	1.67E+09
A0A087WXM6;J3	A0A087WXM6;J3	60S ribosomal pr	RPL17	15	15	169	0	137.61	1.5273		0.28844	1.03E+10
C9JRD2;C9JXB9;F	C9JRD2;C9JXB9;F	DnaJ homolog sul	DNAJB2	4	3	228	0	6.9573	1.5263	NaN		6.91E+07
Q96BT7;Q96BT7-	Q96BT7;Q96BT7-	Alkylated DNA rep	ALKBH8	3	3	664	0	9.091	1.5261	NaN		7.66E+07
Q15773;F5H0Y3;	Q15773	Myeloid leukemia	MLF2	10	10	248	0	120.75	1.5246		0.45449	2.11E+09
O14530;O14530-	O14530;O14530-	Thioredoxin dom	TXNDC9	9	9	226	0	70.935	1.5243		0.61319	1.87E+09
Q6P1N0;Q6P1N0	Q6P1N0;Q6P1N0	Coiled-coil and C2	CC2D1A	14	14	951	0	66.52	1.5234		0.53084	9.87E+08
P41223;P41223-	P41223;P41223-	Protein BUD31 ho	BUD31	3	3	144	0	8.9576	1.5219		0.71204	1.68E+08
Q96HS1;Q96HS1	Q96HS1;Q96HS1-	Serine/threonine-	PGAM5	21	21	289	0	105.02	1.5217		0.75478	2.61E+09
Q9H089;H7C2X7	Q9H089	Large subunit GTF	LSG1	5	5	658	0	22.744	1.5206		0.81826	4.74E+08
Q96JC1-2;Q96JC1	Q96JC1-2;Q96JC1	Vam6/Vps39-like	VPS39	6	6	875	0	19.967	1.5201		0.60725	3.99E+08
O00165;O00165	O00165;O00165-	HCLS1-associated	HAX1	14	14	279	0	147.91	1.518		0.57667	3.05E+09
P61247;E9PFI5;D	P61247;E9PFI5;D	40S ribosomal pr	RPS3A	27	27	264	0	323.31	1.518		0.68046	1.47E+10
Q9C0J8;C9J8B4	Q9C0J8	pre-mRNA 3 end p	WDR33	4	4	1336	0	27.863	1.5175		0.90258	2.40E+08
P62877	P62877	E3 ubiquitin-prot	RBX1	3	3	108	0	20.762	1.5173		0.22496	5.97E+07
Q6PHR2-3;Q6PHI	Q6PHR2-3;Q6PHI	Serine/threonine-	ULK3	14	14	470	0	54.277	1.5169		0.62633	1.03E+09
E9PFK9;Q9UJ41-;	E9PFK9;Q9UJ41-;	Rab5 GDP/GTP ex	RABGEF1	5	5	504	0	14.042	1.5159	NaN		2.12E+08
O76041-2	O76041-2			2	2	270	0	5.4112	1.5146	NaN		3.18E+07
Q9BUH6	Q9BUH6	Uncharacterized p	C9orf142	6	6	204	0	21.983	1.5112		0.47218	1.96E+08
O76031;H0YM48	O76031	ATP-dependent Cl	CLPX	24	24	633	0	283.17	1.5068	NaN		2.37E+09
Q96QF0-8;Q96QF	Q96QF0-8;Q96QF	Rab-3A-interactin	RAB3IP	2	2	254	0	3.8302	1.504	NaN		3.22E+07
P46939-4;P4693	P46939-4;P4693	Utrophin	UTRN	10	10	1347	0	55.923	1.5027		0.70067	3.62E+08
P20585	P20585	DNA mismatch re	MSH3	21	21	1137	0	278.01	1.4986		0.56253	2.16E+09
O14733;O14733	O14733;O14733-	Dual specificity m	MAP2K7	8	8	419	0	27.443	1.4971		0.6288	1.12E+09
P17028;P17028-	P17028;P17028-	Zinc finger protei	ZNF24	8	8	368	0	31.609	1.4965		0.57749	3.91E+08
Q15185-4;Q1518	Q15185-4;Q1518	Prostaglandin E sy	PTGES3	9	9	139	0	182.45	1.4942		0.59716	6.52E+08
O00411;K7EMH3	O00411	DNA-directed RN	POLRMT	34	34	1230	0	284.9	1.4903		0.63451	5.81E+09
O60870-2;O6087	O60870-2;O6087	DNA/RNA-binding	KIN	2	2	374	0	4.5718	1.4894	NaN		3.35E+07
O15305;H3BV55;	O15305;H3BV55;	Phosphomannom	PMM2	14	14	246	0	65.687	1.4885		0.45691	1.96E+09
Q5THJ4-2;Q5THJ4	Q5THJ4-2;Q5THJ4	Vacuolar protein	VPS13D	7	7	4363	0	35.266	1.4877		1.366	1.94E+08
Q9NVV4-2;Q9NV	Q9NVV4-2;Q9NV	Poly(A) RNA polyr	MTPAP	9	9	712	0	56.376	1.4857	NaN		6.91E+08
Q9H8V3-2;Q9H8	Q9H8V3-2;Q9H8	Protein ECT2	ECT2	5	5	882	0	19.798	1.4845		0.59608	2.04E+08
Q9BTE7;H0YCN4;	Q9BTE7;H0YCN4;	DCN1-like protein	DCUN1D5	6	6	237	0	22.438	1.48		0.6848	4.62E+08
Q6UWE0;Q6UWE	Q6UWE0;Q6UWE	E3 ubiquitin-prot	LRSAM1	12	12	723	0	93.265	1.4798		0.96575	1.07E+09
Q9H3S7	Q9H3S7	Tyrosine-protein p	PTPN23	4	4	1636	0	8.329	1.4749		0.78398	1.01E+08
P20042	P20042	Eukaryotic transla	EIF2S2	22	22	333	0	258.88	1.4734		0.5746	8.40E+09
K7ERD7;O95707;	K7ERD7;O95707	Ribonuclease P pr	POP4	3	3	181	0	8.5684	1.4731	NaN		1.41E+08
A0A087WV66;P4	A0A087WV66;P4	Antigen KI-67	MKI67	10	10	3255	0	65.028	1.4726		0.98144	2.10E+08
Q8WVM0	Q8WVM0	Dimethyladenosin	TFB1M	9	9	346	0	32.576	1.4711		0.64272	1.65E+09
O94817	O94817	Ubiquitin-like pro	ATG12	2	2	140	0	3.7102	1.4707		1.2225	4.26E+09
Q6IQ32	Q6IQ32	ADNP homeobox	ADNP2	2	2	1131	0	10.535	1.4703		0.59168	8.95E+07
Q96G61;Q8NFP7	Q96G61;Q8NFP7	Diphosphoinositc	NUDT11;NUDT10	7	6	164	0	24.066	1.47		0.53491	6.26E+08
G3V5T9;P24941;	G3V5T9;P24941;	Cyclin-dependent	CDK2	15	13	346	0	89.871	1.4654		0.30548	3.31E+09
P62269;A0A0G2J	P62269	40S ribosomal pr	RPS18	23	23	152	0	91.464	1.4639		0.55371	2.70E+10
P24468-3;P2446	P24468-3;P2446	COUP transcriptic	NR2F2	9	4	261	0	88.642	1.4629		0.67886	1.46E+09
Q7L2H7;Q7L2H7	Q7L2H7;Q7L2H7	Eukaryotic transla	EIF3M	22	22	374	0	300.31	1.4613		0.75614	1.37E+10
Q96BW9-3;Q96B	Q96BW9-3;Q96B	Phosphatidate cy	TAMM41	9	9	337	0	82.782	1.4608		0.60754	1.15E+09
O95235-2;O9523	O95235-2;O9523	Kinesin-like prote	KIF20A	3	3	872	0	37.884	1.46		0.93022	1.84E+08
Q68EM7-5;Q68EM	Q68EM7-5;Q68EM	Rho GTPase-activa	ARHGAP17	13	13	867	0	50.86	1.4581		0.71397	9.79E+08
Q9P2R7-2;Q9P2R	Q9P2R7-2;Q9P2R	Succinyl-CoA liga	SUCLA2	19	19	441	0	87.607	1.4569		0.66104	3.11E+09
Q96FC9-4;Q96FC	Q96FC9-4;Q96FC	Probable ATP-dep	DDX11;DDX11L8	10	10	856	0	50.816	1.4563		0.749	8.54E+08
O94826	O94826	Mitochondrial im	TOMM70A	5	5	608	0	16.987	1.4562	NaN		3.59E+08
O43663-3;O4366	O43663-3;O4366	Protein regulator	PRC1	3	3	525	0	10.924	1.4547	NaN		2.76E+08
H0Y360;Q01433-	H0Y360;Q01433-	AMP deaminase 2	AMPD2	14	14	861	0	59.249	1.4543		0.62215	7.04E+08
Q9BY77;F6VRR5;I	Q9BY77;F6VRR5;I	Polymerase delta-	POLDIP3	17	3	421	0	97.779	1.4539		0.66049	3.82E+09
P08708;H0YN88;	P08708;H0YN88;	40S ribosomal pr	RPS17	14	14	135	0	314.41	1.4518		0.47724	8.19E+09
Q15047-3;Q1504	Q15047-3;Q1504	Histone-lysine N-	SETDB1	8	8	1290	0	48.726	1.4517		0.75893	2.90E+08
Q9BVC3	Q9BVC3	Sister chromatid	DSCC1	2	2	393	0	9.2087	1.4516		0.6573	2.09E+08
P40939;H0YFD6;	P40939	Trifunctional enz	HADHA	46	46	763	0	323.31	1.4509		0.6709	4.18E+10
P04792;F8WE04;	P04792	Heat shock protei	HSPB1	20	20	205	0	256.68	1.4504		0.39273	1.84E+10
A0A0G2JNH5;A0/	A0A0G2JNH5;A0/	Cell cycle checkp	RAD17	4	4	505	0	22.032	1.4499		2.318	2.68E+08
D4Q8H0;Q9NYL2	D4Q8H0;Q9NYL2	Mitogen-activate	pk;ZAK	7	3	455	0	50.76	1.4499		0.80914	3.91E+08
Q16543;K7EKQ2;	Q16543;K7EKQ2;	Hsp90 co-chaper	CDC37	28	28	378	0	188.43	1.4497		0.66564	8.81E+09
Q9H4L7;Q9H4L7	Q9H4L7;Q9H4L7	SWI/SNF-related r	SMARCAD1	14	14	1026	0	52.465	1.4491		0.70252	7.14E+08
P33992;B1AHB1;	P33992;B1AHB1	DNA replication li	MCM5	56	56	734	0	323.31	1.4473		0.68464	3.92E+10
O00487;C9JW37	O00487	26S proteasome r	PSMD14	8	8	310	0	164.04	1.4465		0.6838	3.66E+09
O95059	O95059	Ribonuclease P pr	RPP14	6	6	124	0	36.91	1.4464		1.024	6.41E+08
E9PHI4;O94901-(	E9PHI4;O94901-(	SUN domain-cont	SUN1	2	2	822	0	6.9944	1.4455		0.82485	1.23E+08
Q5T1C6;F6XC58;I	Q5T1C6;F6XC58;I	Acyl-coenzyme A	THEM4	4	4	240	0	24.506	1.4434		0.73028	3.93E+08
P38117;P38117-	P38117;P38117-	Electron transfer	ETFB	15	15	255	0	60.216	1.4407		0.4159	1.56E+09
P62306;A0A0B4J	P62306;A0A0B4J	Small nuclear ribo	SNRPF	4	4	86	0	39.726	1.4406		1.0013	6.07E+08
Q01780;Q01780	Q01780;Q01780	Exosome compon	EXOSC10	39	39	885	0	264.37	1.4393		0.74862	6.50E+09
Q6ZT12;Q6ZT12-4	Q6ZT12;Q6ZT12-4	E3 ubiquitin-prot	UBR3	3	3	1888	0	9.6061	1.4391	NaN		3.91E+07
E7ESC7;Q7L5Y9;(	E7ESC7;Q7L5Y9;(	Macrophage eryth	MAEA	9	9	434	0	33.348	1.4388		0.77233	4.11E+08
P51970	P51970	NADH dehydroge	NDUFA8	2	2	172	0	9.0935	1.4385	NaN		2.71E+07
Q8IY17-5;Q8IY17	Q8IY17-5;Q8IY17	Neuropathy targe	PNPLA6	4	4	1300	0	18.085	1.4356		0.4261	8.56E+07
P49407-2;P4940	P49407-2;P4940	Beta-arrestin-1	ARRB1	7	7	410	0	30.212	1.4342		0.85418	3.58E+08
E9PHA2;Q15003;	E9PHA2;Q15003;	Condensin compl	NCAPH	28	28	730	0	279.6	1.4337		0.59457	7.09E+09
B8ZZY2;P52594-2	B8ZZY2;P52594-2	Arf-GAP domain a	AGFG1	8	7	541	0	78.495	1.4336		0.24087	3.58E+08
Q8TC07-2;Q8TC0	Q8TC07-2;Q8TC0	TBC1 domain fam	TBC1D15	9	9	674	0	22.314	1.4315	NaN		6.16E+08
Q01469;I6L8B7;A	Q01469	Fatty acid-bindin	FABP5	9	9	135	0	84.572	1.4308		0.50437	2.32E+09
O15145;F8VR50;	O15145	Actin-related pro	ARPC3	7	7	178	0	96.766	1.4307		0.9386	2.76E+09
A0A087X1X7;E9P	A0A087X1X7;E9P	Elongation factor	EEF1D	18	3	631	0	193.61	1.4297		0.62168	6.39E+09
Q01518;Q5T0R5;	Q01518	Adenylyl cyclase-a	CAP1	28	1	475	0	320.8	1.4277		0.55136	1.29E+10
A0A0A0MTN0;Q1	A0A0A0MTN0;Q1	Cullin-2	CUL2	24	24	758	0	157.12	1.4271		0.64206	3.63E+09
O15091-4;O1509	O15091-4;O1509	Mitochondrial rib	KIAA0391	4	4	488	0	14.143	1.427	NaN		1.67E+08
Q96CB9-4;Q96CB	Q96CB9-4;Q96CB	5-methylcytosine	NSUN4	3	3	335	0	13.814	1.4266		0.86547	1.82E+08
F8W727;P62910	F8W727;P62910	60S ribosomal pr	RPL32	14	14	153	0	50.845	1.4244		0.6805	9.02E+08
P22695;H3BRG4;	P22695;H3BRG4;	Cytochrome b-c1	UQCRC2	24	24	453	0	323.31	1.4243		0.63128	3.10E+10
Q9NXV6	Q9NXV6	CDKN2A-interacti	CDKN2AIP	6	6	580	0	57.537	1.424	NaN		1.33E+08
Q96JH7	Q96JH7	Deubiquitinating	VCPIP1	10	10	1222	0	55.55	1.4235		0.80646	3.41E+08
Q8NEW0	Q8NEW0	Zinc transporter 7	SLC30A7	2	2	376	0	5.7707	1.4202		1.2681	2.51E+08
B3KPJ4;A0A0A0M	B3KPJ4;A0A0A0M	Polyhomeotic-lik	PHC2	3	3	464	0	7.9566	1.4201		1.0581	1.38E+08
P62280;M0QZC5	P62280;M0QZC5	40S ribosomal pr	RPS11	23	23	158	0	119.42	1.4198		0.23149	1.43E+10
Q8N7H5-3;Q8N7H	Q8N7H5-3;Q8N7H	RNA polymerase I	PAF1	10	10	485	0	91.537	1.4197	NaN		8.08E+08
O43572;E7EMD6	O43572;E7EMD6	A-kinase anchor p	AKAP10	5	5	662	0	24.44	1.4171	NaN		1.45E+08
Q9H078-2;Q9H07	Q9H078-2;Q9H07	Caseinolytic pept	CLPB	12	12	677	0	78.937	1.4165	NaN		5.77E+08
Q9BSH4	Q9BSH4	Translational acti	TACO1	14	14	297	0	158.69	1.4162		0.34228	6.35E+09
C9JNK6;O75431-	C9JNK6;O75431-	Metaxin-2	MTX2	3	3	207	0	26.201	1.4157		0.30945	1.38E+08
E7EVJ5;Q96F07-2	E7EVJ5;Q96F07-2	Cytoplasmic FMR	CYFIP2	35	14	1227	0	60.475	1.4156		0.5697	9.33E+08
A6NHB5;Q14202	A6NHB5;Q14202	Zinc finger MYM-t	ZMYM3	10	8	1372	0	54.073	1.4143		0.41162	3.96E+08
Q5W0B1	Q5W0B1	RING finger prote	RNF219	8	8	726	0	109.67	1.4142		1.0493	6.18E+08

Q9Y266;A0A0A0I	Q9Y266	Nuclear migratio	NUDC	27	27	331	0	178.92	1.4136	0.59776	4.03E+09
A0A087WZN1;O4	A0A087WZN1;O4	Isocitrate dehydr	IDH3B	24	24	387	0	193.69	1.4135	0.54351	9.53E+09
A0A075B746;P82	A0A075B746;P82	28S ribosomal pr	MRPS21	4	4	87	0	32.243	1.4131	0.67803	1.00E+09
Q99567;J3KMX1;	Q99567;J3KMX1	Nuclear pore com	NUP88	11	11	741	0	76.073	1.4127	1.1032	6.27E+08
Q9NUP7	Q9NUP7	tRNA:m(4)X modi	TRMT13	2	2	481	0	7.6775	1.4123	NaN	1.46E+08
Q9UNY4;Q9UNY4	Q9UNY4;Q9UNY4	Transcription ter	TTF2	17	17	1162	0	127.08	1.4119	0.74271	7.17E+08
Q96G46;Q96G46	Q96G46;Q96G46	tRNA-dihydrouric	DUS3L	22	22	650	0	311.07	1.4104	0.57355	4.43E+09
C9JEL3;B9A044;E	C9JEL3;B9A044;E	Eukaryotic transl	EIF4E2	6	6	213	0	24.557	1.41	0.5031	2.29E+08
Q8IXW5-2;Q8IXW	Q8IXW5-2;Q8IXW	Putative RNA pol	RPAP2	3	3	584	0	8.8754	1.4081	0.38216	1.82E+08
A0A0D9SFB3;A0A	A0A0D9SFB3;A0A	ATP-dependent R	DDX3X;DDX3Y	41	40	640	0	323.31	1.407	0.86593	2.17E+10
P36542;P36542-	P36542;P36542-	ATP synthase sub	ATP5C1	15	15	298	0	89.025	1.4067	0.70952	8.03E+09
A0A0A0MSK4;A0	A0A0A0MSK4;A0	G-protein-signali	GPSM1	12	12	675	0	62.757	1.4051	0.7376	8.38E+08
Q9P253	Q9P253	Vacuolar protein	VPS18	8	8	973	0	34.349	1.403	0.88425	7.32E+08
Q8IVD9	Q8IVD9	NudC domain-co	NUDCD3	5	5	361	0	21.192	1.4025	0.61913	3.89E+08
O15020-2;O1502	O15020-2;O1502	Spectrin beta cha	SPTBN2	8	7	2365	0	29.218	1.4022	0.7284	1.32E+08
P05198;G3V4T5;	P05198;G3V4T5;	Eukaryotic transl	EIF2S1	28	28	315	0	323.31	1.3997	0.7258	1.52E+10
Q8IWR0;I3L2K5;I	Q8IWR0;I3L2K5	Zinc finger CCCH	ZC3H7A	17	17	971	0	71.814	1.3987	0.33291	9.19E+08
O15460-2;O1546	O15460-2;O1546	Prolyl 4-hydroxyl	P4HA2	3	3	533	0	10.784	1.3984	3.3856	1.27E+08
Q99797	Q99797	Mitochondrial int	MIPEP	7	7	713	0	14.81	1.3974	NaN	1.78E+08
P27540-2;P2754	P27540-2;P2754	Aryl hydrocarbon	ARNT	4	4	774	0	25.67	1.3968	1.2609	1.39E+08
Q13625-2;Q1362	Q13625-2;Q1362	Apoptosis-stimul	TP53BP2	8	8	1005	0	79.429	1.3952	0.68624	3.15E+08
Q86UK7-2;Q86UI	Q86UK7-2;Q86UI	Zinc finger protei	ZNF598	10	10	896	0	47.988	1.3943	0.5833	2.10E+08
Q7RTV0	Q7RTV0	PHD finger-like dc	PHF5A	7	7	110	0	25.493	1.394	0.5892	8.93E+08
P18583-6;P1858	P18583-6;P1858	Protein SON	SON	12	12	2108	0	50.951	1.3932	0.69792	3.65E+08
Q9Y2X9-2;Q9Y2X	Q9Y2X9-2;Q9Y2X	Zinc finger protei	ZNF281	13	13	859	0	206.95	1.3931	0.56444	1.12E+09
C9JGR9;E7EQ49;/	C9JGR9;E7EQ49;/	WD repeat-contai	WDR37	3	3	209	0	24.238	1.3928	NaN	1.93E+08
Q9UBX3;Q9UBX3	Q9UBX3;Q9UBX3	Mitochondrial di	SLC25A10	15	1	287	0	10.751	1.3923	0.81005	7.44E+07
P62136;P62136-	P62136;P62136-	Serine/threonine	PPP1CA	24	6	330	0	320.86	1.3921	0.6755	2.36E+10
Q9UGJ1-2;Q9UGJ	Q9UGJ1-2;Q9UGJ	Gamma-tubulin c	TUBGCP4	3	3	666	0	6.4184	1.3899	NaN	4.63E+07
Q9P0U3-2;Q9P0(	Q9P0U3-2;Q9P0(	Sentrin-specific p	SENP1	7	7	643	0	56.719	1.3886	NaN	2.81E+08
P05771-2;P0577	P05771-2;P0577	Protein kinase C b	PRKCB	5	2	673	0	26.407	1.3866	0.7741	3.57E+08
P62140;E7ETD8;(	P62140;E7ETD8;(	Serine/threonine	PPP1CB	20	6	327	0	35.086	1.3863	0.7475	2.76E+09
C9JJN9;Q8N3P4-	C9JJN9;Q8N3P4-	Vacuolar protein	VPS8	6	6	1428	0	29.232	1.3854	0.61391	3.17E+08
Q3SY69;Q3SY69-	Q3SY69	Mitochondrial 10	ALDH1L2	32	28	923	0	248.06	1.3854	0.68776	4.39E+09
A0A0G2JKR7;P28	A0A0G2JKR7;P28	Retinoic acid rece	RXRB	7	4	347	0	30.949	1.3852	NaN	4.08E+08
Q9H1Z4-2;Q9H12	Q9H1Z4-2;Q9H12	WD repeat-contai	WDR13	3	3	393	0	10.932	1.3838	0.9606	7.62E+07
Q7Z5K2;Q7Z5K2-	Q7Z5K2;Q7Z5K2-	Wings apart-like p	WAPAL	28	28	1190	0	246.28	1.3837	0.56345	2.33E+09
H3BM14;H3BM7	H3BM14;H3BM7	NEDD8 ultimate b	NUB1	10	10	625	0	61.273	1.3836	0.71841	7.18E+08
Q8NBT2;Q8NBT2	Q8NBT2;Q8NBT2	Kinetochore prot	SPC24	8	1	197	0	99.164	1.3832	0.65331	6.07E+08
Q15072	Q15072	Zinc finger protei	ZNF146	4	4	292	0	10.029	1.3827	0.67167	1.43E+08
Q9UBE0;B3KNJ4;	Q9UBE0;B3KNJ4;	SUMO-activating	SAE1	29	29	346	0	323.31	1.3819	0.67516	2.04E+10
P05783;F8VZY9;(	P05783;F8VZY9	Keratin, type I cyt	KRT18	18	12	430	0	114.6	1.3818	0.88225	1.90E+09
Q15650;H0YLN7;	Q15650	Activating signal	TRIP4	6	6	581	0	53.913	1.3814	NaN	2.02E+08
J3QRS3;P19105;(	J3QRS3;P19105;(	Myosin regulator	MYL12A;MYL12B;	9	9	177	0	176.05	1.3797	0.73751	3.34E+09
Q6ZNB6-2;Q6ZNB	Q6ZNB6-2;Q6ZNB	NF-X1-type zinc fi	NFXL1	5	5	733	0	123.76	1.3762	0.67411	6.09E+08
Q9Y3A5;A0A087)	Q9Y3A5;A0A087)	Ribosome matura	SBDS	24	24	250	0	323.31	1.376	0.52916	1.39E+10
Q9BRZ2;C9JI91;C	Q9BRZ2	E3 ubiquitin-prot	TRIM56	4	4	755	0	27.081	1.3754	0.76714	7.94E+07
Q12972;Q12972-	Q12972	Nuclear inhibitor	PPP1R8	16	16	351	0	244.68	1.3727	0.66776	4.34E+09
E9PJN5;G3V2G1;	E9PJN5;G3V2G1;	Ataxin-3	ATXN3	3	3	205	0	7.4872	1.3724	0.87296	2.13E+08
P61201;P61201-	P61201;P61201-	COP9 signalosom	COPS2	21	21	443	0	246.07	1.3724	0.6916	5.13E+09
P53597;H7C233	P53597	Succinyl-CoA liga	SUCLG1	14	14	346	0	288.59	1.3722	0.71118	3.34E+09
B7ZAX5;Q01415-	B7ZAX5;Q01415-	N-acetylgalactosa	GALK2	6	6	434	0	29.107	1.3717	0.76116	4.42E+08
E7EQ01;E7EVN1;I	E7EQ01;E7EVN1;I	Caspase-8;Caspas	CASP8	3	3	116	0	38.924	1.3716	2.7411	2.46E+08
P41091;Q2VIR3;I	P41091;Q2VIR3;I	Eukaryotic transl	EIF2S3;EIF2S3L	26	26	472	0	323.31	1.3713	0.639	2.41E+10
Q7LBC6;Q7LBC6-	Q7LBC6;Q7LBC6-	Lysine-specific de	KDM3B	10	10	1761	0	150.78	1.3713	0.59294	3.68E+08
Q8NDV3-2;Q8ND	Q8NDV3-2;Q8ND	Structural mainte	SMC1B	3	3	1161	0	4.5391	1.3708	0.78791	2.29E+07
A0A087X0R7;Q9I	A0A087X0R7;Q9I	Sentrin-specific p	SENP3	6	6	540	0	29.119	1.3699	NaN	2.75E+08
Q86UA1;Q86UA1	Q86UA1	Pre-mRNA-proces	PRPF39	12	12	669	0	48.611	1.3697	0.75048	1.01E+09
Q96HP0;K7ESB7	Q96HP0;K7ESB7	Dedicator of cyto	DOCK6	7	3	2047	0	9.7591	1.3697	NaN	6.61E+07
C9JG87;Q9NYK5;	C9JG87;Q9NYK5;	39S ribosomal pr	MRPL39	5	5	297	0	30.705	1.369	1.0722	5.17E+08
Q8IXQ5-5;Q8IXQ5	Q8IXQ5-5;Q8IXQ5	Kelch-like protein	KLHL7	2	2	538	0.0065966	2.1392	1.369	NaN	5.29E+07
P40937;P40937-	P40937;P40937-	Replication factor	RFC5	17	17	340	0	304.03	1.368	0.68131	8.52E+09
Q9BXP5-4;Q9BXP	Q9BXP5-4;Q9BXP	Serrate RNA effect	SRRT	37	37	871	0	219.43	1.3678	0.70308	3.99E+09
A0A0D9SFK2;Q92	A0A0D9SFK2;Q92	Unconventional r	MYO18A	9	9	2038	0	57.185	1.3675	2.6989	2.26E+08
Q6P587;Q6P587-	Q6P587;Q6P587-	Acylpyruvase FAH	FAHD1	8	8	224	0	101.12	1.3674	0.80348	2.09E+09
O95817;C9JFK9	O95817;C9JFK9	BAG family molec	BAG3	4	4	575	0	14.581	1.367	1.8317	1.18E+08
O14964;O14964-	O14964;O14964-	Hepatocyte growt	HGS	13	13	777	0	32.628	1.3668	0.56511	4.31E+08
P56377;F6SFB5;/	P56377;F6SFB5;/	AP-1 complex sub	AP1S2	3	3	157	0	56.059	1.3666	0.98518	4.62E+08
E7ERS3;Q86VM9-	E7ERS3;Q86VM9-	Zinc finger CCCH	ZC3H18	7	7	977	0	16.488	1.3664	2.045	7.54E+07
Q86U86-5;Q86UI	Q86U86-5;Q86UI	Protein polybrom	PBRM1	14	14	1582	0	140.61	1.3657	1.1158	5.98E+08
B4E1Q4;O14730-	B4E1Q4;O14730-	Serine/threonine	RIOK3	5	5	503	0	20.988	1.3653	NaN	2.59E+08
P41227;P41227-	P41227;P41227-	N-alpha-acetyltra	NAA10	12	12	235	0	188.1	1.3646	0.67754	1.19E+09
J3KNL6;O15027;I	J3KNL6;O15027;I	Protein transport	SEC16A	15	15	2357	0	106.84	1.3644	0.75442	1.03E+09
Q9HB21;Q5RGS4	Q9HB21;Q5RGS4	Pleckstrin homol	PLEKHA1	3	3	404	0	9.3434	1.3644	0.49427	5.72E+07
P50402;Q5HY57;	P50402;Q5HY57	Emerin	EMD	17	17	254	0	144.01	1.3639	0.637	4.06E+09
Q8WUH6	Q8WUH6	Transmembrane p	TMEM263	2	2	116	0	9.9273	1.3632	0.7242	2.39E+08
Q9NV70-2;Q9NV	Q9NV70-2;Q9NV	Exocyst complex	EXOC1	4	4	879	0	9.1863	1.3624	0.85467	8.55E+07
P40938;P40938-	P40938;P40938-	Replication factor	RFC3	14	14	356	0	145.79	1.3621	0.4821	2.28E+09
Q15056-2;Q1505	Q15056-2;Q1505	Eukaryotic transl	EIF4H	10	10	228	0	197.31	1.3591	0.53263	4.50E+09
Q96IZ6;F8WAS9;/	Q96IZ6	Methyltransferas	METTL2A	6	1	378	0	45.433	1.3587	1.0131	3.37E+08
Q92783-2;Q9278	Q92783-2;Q9278	Signal transducin	STAM	5	4	403	0	32.814	1.3584	NaN	1.34E+08
Q13616;A0A0C4I	Q13616;A0A0C4I	Cullin-1	CUL1	41	41	776	0	323.31	1.3577	0.59821	7.35E+09
Q08J23;Q08J23-;	Q08J23;Q08J23-;	tRNA (cytosine(34	NSUN2	44	44	767	0	323.31	1.3573	0.73763	1.97E+10
Q96I99;Q96I99-2	Q96I99;Q96I99-2	Succinyl-CoA liga	SUCLG2	16	16	432	0	126.06	1.357	0.75202	3.01E+09
P19525;P19525-	P19525;P19525-	Interferon-induce	EIF2AK2	18	18	551	0	108.62	1.3551	NaN	1.71E+09
Q9NPL8;C9JU35;	Q9NPL8;C9JU35;	Complex I assemb	TIMMDC1	8	8	285	0	46.829	1.3548	1.1188	4.71E+08
Q92917	Q92917	G patch domain a	GPKOW	7	7	476	0	31.909	1.3541	0.24031	3.11E+08
A0A0A0MR05;Q9	A0A0A0MR05;Q9	Target of rapamyc	MLST8	5	5	327	0	35.72	1.354	0.55318	2.39E+08
H3BLZ8;Q92841;	H3BLZ8;Q92841;	Probable ATP-dep	DDX17	41	33	731	0	323.31	1.3535	0.70289	3.57E+10
Q32P41	Q32P41	tRNA (guanine(37	TRMT5	7	7	509	0	56.991	1.3522	1.8566	2.34E+08
Q9NW08;Q9NWC	Q9NW08;Q9NWC	DNA-directed RN	POLR3B	24	24	1133	0	99.987	1.3512	0.82959	1.98E+09
P46779;H0YKD8;	P46779;H0YKD8;	60S ribosomal pr	RPL28	15	15	137	0	45.712	1.3502	0.60895	3.57E+09
Q8NG08;F5H1I4;	Q8NG08;F5H1I4	DNA helicase B	HELB	3	3	1087	0	6.9167	1.3489	NaN	7.03E+07
A6NFX8;Q9UKK9;	A6NFX8;Q9UKK9;	ADP-sugar pyroph	NUDT5	11	11	232	0	49.944	1.3487	0.53877	1.80E+09
Q9UHD1;Q9UHD	Q9UHD1;Q9UHD	Cysteine and histi	CHORDC1	12	12	332	0	80.474	1.3485	0.16602	1.56E+09
Q9Y2S0;A0A0R4J	Q9Y2S0;A0A0R4J	DNA-directed RN	POLR1D	5	5	133	0	55.293	1.3483	0.69463	1.18E+09
P22059;H0YCV6;	P22059	Oxysterol-binding	OSBP	14	14	807	0	111.85	1.3474	0.92621	1.10E+09
P78344;D3DQV9	P78344;D3DQV9	Eukaryotic transl	EIF4G2	45	45	907	0	323.31	1.3471	0.64377	1.93E+10
S4R3N1;Q9Y3A3-	S4R3N1;Q9Y3A3-	MOB-like protein	HSPE1-MOB4;MO	4	4	261	0	21.717	1.3471	NaN	7.52E+07
A0A087WY55;Q9	A0A087WY55;Q9	Vacuolar protein	VTA1	8	8	280	0	203.06	1.347	0.69491	2.63E+09
P62841;K7EM56;	P62841;K7EM56;	40S ribosomal pr	RPS15	7	7	145	0	60.13	1.3463	0.55263	7.09E+08
Q9NX20;E9PI14	Q9NX20	39S ribosomal pr	MRPL16	9	9	251	0	74.227	1.3463	0.34512	1.28E+09
Q6NUQ1;C9J5S3	Q6NUQ1	RAD50-interactin	RINT1	6	6	792	0	31.189	1.346	0.74842	3.48E+08
O00139-2;O0013	O00139-2;O0013	Kinesin-like prote	KIF2A	23	22	660	0	115.12	1.345	0.65706	3.40E+09

G3V4S6;G3V433;	G3V4S6;G3V433;	Protein numb ho	NUMB	1	1	67	0	4.0785	1.3447	NaN	1.20E+07
Q9H7Z3;H0YJT0;(	Q9H7Z3	Protein NRDE2 hc	NRDE2	10	10	1164	0	50.259	1.3443	0.8217	2.19E+08
H0YM23;O75179	H0YM23;O75179	Ankyrin repeat dc	ANKRD17	25	14	2487	0	143.44	1.3437	0.76194	1.23E+09
P84095	P84095	Rho-related GTP-l	RHOG	5	4	191	0	39.684	1.3434	0.91812	8.52E+08
O75436;S4R3Q6;	O75436;S4R3Q6;	Vacuolar protein	VPS26A	14	13	327	0	140.71	1.3433	0.77576	5.31E+09
Q96S44;Q5JZ02	Q96S44	TP53-regulating k	TP53RK	7	7	253	0	78.724	1.3433	0.5819	2.49E+09
Q86V81;E9PB61	Q86V81;E9PB61	THO complex sub	ALYREF	6	6	257	0	162.63	1.3427	0.29044	1.80E+09
Q9H5Q4	Q9H5Q4	Dimethyladenosi	TFB2M	8	8	396	0	23.026	1.3422	0.75328	3.45E+08
O00267-2;O0026	O00267-2;O0026	Transcription elo	SUPT5H	36	36	1083	0	298.26	1.3421	0.82591	5.34E+09
Q8TBE9	Q8TBE9	N-acylneuramina	NANP	5	5	248	0	55.712	1.3421	0.76326	4.40E+08
Q9NVN8	Q9NVN8	Guanine nucleoti	GNL3L	8	8	582	0	57.77	1.3394	NaN	4.56E+08
P51553;P51553-	P51553;P51553-	Isocitrate dehydr	IDH3G	18	18	393	0	307.48	1.3388	0.77921	4.40E+09
O75190-2	O75190-2	DnaJ homolog sul	DNAJB6	13	1	241	0	4.4815	1.3387	NaN	7.65E+07
Q5BKZ1;A0A0A0I	Q5BKZ1;A0A0A0I	DBIRD complex s	ZNF326	7	7	582	0	30.38	1.3381	NaN	2.33E+08
Q9H832-2;Q9H8	Q9H832-2;Q9H8	Ubiquitin-conjug	UBE2Z	7	7	246	0	22.103	1.3378	0.99658	5.90E+08
Q5VZL5-4;Q5VZL	Q5VZL5-4;Q5VZL	Zinc finger MYM-t	ZMYM4	18	16	1516	0	150.72	1.3376	0.75883	8.73E+08
P55809;E9PDW2	P55809;E9PDW2	Succinyl-CoA:3-k	OXCT1	17	17	520	0	211.69	1.3375	0.64706	3.56E+09
P30039-2;P3003	P30039-2;P3003	Phenazine biosyn	PBLD	5	5	280	0	44.313	1.337	0.62732	2.95E+08
P17987;E7EQR6;I	P17987;E7EQR6;I	T-complex protei	TCP1	44	44	556	0	323.31	1.3365	0.67172	5.74E+10
E9PGT1;Q15631;	E9PGT1;Q15631;	Translin	TSN	4	4	223	0	20.615	1.3364	0.77466	2.32E+08
Q5BJF2;Q86XC5;.	Q5BJF2;Q86XC5;.	Transmembrane p	TMEM97	2	2	176	0	8.3912	1.3356	NaN	3.54E+07
A0A0B4J1W3;Q9	A0A0B4J1W3;Q9	N-alpha-acetyltra	NAA15	48	41	865	0	251.37	1.3347	0.67145	1.14E+10
Q12756;Q12756-	Q12756;Q12756-	Kinesin-like prote	KIF1A	31	25	1690	0	221.38	1.3343	0.66747	1.93E+09
Q9BY32;Q9BY32-	Q9BY32;Q9BY32-	Inosine triphosph	ITPA	8	8	194	0	80.118	1.3342	0.20616	2.17E+09
Q9UG63;Q9UG6	Q9UG63;Q9UG6	ATP-binding casse	ABCF2	32	32	623	0	150.7	1.3338	0.7407	6.22E+09
Q8WXI9;A0A0U1	Q8WXI9;A0A0U1	Transcriptional re	GATAD2B	16	15	593	0	94.147	1.3335	NaN	1.10E+09
P32121;P32121-	P32121;P32121-	Beta-arrestin-2	ARRB2	7	7	409	0	23.213	1.3334	1.027	3.89E+08
V9GY48;Q8N5A5·	V9GY48;Q8N5A5·	Zinc finger CCCH-t	ZGPAT	6	6	417	0	53.03	1.333	NaN	1.04E+08
O60678;A0A0A0I	O60678;A0A0A0I	Protein arginine N	PRMT3	17	17	531	0	77.485	1.3329	NaN	2.37E+09
Q9NXH9-2;Q9NXI	Q9NXH9-2;Q9NXI	tRNA (guanine(26	TRMT1;SEMA4B	18	18	630	0	138.18	1.3325	1.6879	1.11E+09
Q9UNM6;Q9UNV	Q9UNM6;Q9UNV	26S proteasome r	PSMD13	19	19	376	0	135.23	1.3323	0.81089	3.70E+09
Q13045;Q13045·	Q13045;Q13045·	Protein flightless-	FLII	37	2	1269	0	323.31	1.3321	0.72454	5.06E+09
Q7Z4L5;Q7Z4L5-;	Q7Z4L5	Tetratricopeptide	TTC21B	12	11	1316	0	146.19	1.3318	0.77174	6.93E+08
A0A0R4J2E8;A8M	A0A0R4J2E8;A8M	Matrin-3	MATR3	43	43	847	0	323.31	1.331	0.69992	4.71E+10
P67775;P62714;	P67775;P62714;	Serine/threonine·	PPP2CA;PPP2CB	12	11	309	0	110.29	1.3308	0.88689	2.09E+09
Q14257;Q14257·	Q14257;Q14257·	Reticulocalbin-2	RCN2	13	13	317	0	280.3	1.3308	0.62246	3.21E+09
A0A0C4DFZ9;Q5E	A0A0C4DFZ9;Q5E	PAB-dependent p	PAN3	7	7	687	0	27.637	1.3299	NaN	1.74E+08
Q96GX5-2;Q96G)	Q96GX5-2;Q96G)	Serine/threonine·	MASTL	4	4	840	0	13.804	1.3286	0.50122	3.97E+08
E7ESL0;A0A0C4D	E7ESL0;A0A0C4D	39S ribosomal pr	MRPL22	6	6	212	0	30.278	1.3282	0.75217	3.07E+08
Q16186;A0A087\	Q16186;A0A087\	Proteasomal ubiq	ADRM1	9	9	407	0	38.548	1.3282	0.62678	5.12E+08
P15056;H7C5K3;	P15056	Serine/threonine·	BRAF	3	3	766	0	10.725	1.328	0.9613	1.06E+08
Q96RS0	Q96RS0	Trimethylguanosi	TGS1	3	3	853	0	7.5902	1.3277	0.64608	8.13E+07
Q15233;Q15233·	Q15233;Q15233·	Non-POU domain	NONO	37	33	471	0	323.31	1.3274	0.73625	2.15E+10
Q14677;Q14677·	Q14677;Q14677·	Clathrin interacto	CLINT1	11	11	625	0	125.68	1.3264	NaN	9.16E+08
Q96IX5	Q96IX5	Up-regulated duri	USMG5	4	4	58	0	71.892	1.3252	1.0522	1.23E+09
Q9Y224;G3V4C6;	Q9Y224;G3V4C6;	UPF0568 protein	C14orf166	8	8	244	0	36.043	1.325	0.63205	4.59E+08
J3KRA9;Q96Q15·	J3KRA9;Q96Q15·	Serine/threonine·	SMG1	14	14	3551	0	89.72	1.3245	1.1428	3.32E+08
Q8IVS2;Q8IVS2-2	Q8IVS2	Malonyl-CoA-acyl	MCAT	9	9	390	0	44.104	1.3245	0.85125	8.03E+08
Q01968-2;Q0196	Q01968-2;Q0196	Inositol polyphos	OCRL	21	21	893	0	126.78	1.3237	0.63839	3.08E+09
Q9NRY4;A2RRE5	Q9NRY4;A2RRE5	Rho GTPase-activ	ARHGAP35;GRLF1	14	14	1499	0	52.625	1.3231	0.67517	5.53E+08
Q96JG6-3;Q96JG	Q96JG6-3;Q96JG	Coiled-coil domai	CCDC132	10	10	934	0	35.769	1.3224	0.82838	3.00E+08
Q9NV35	Q9NV35	Probable 8-oxo-d	NUDT15	3	3	164	0	8.6961	1.3216	0.72232	2.15E+08
P43250-2;D6RHX	P43250-2;D6RHX	G protein-couple	GRK6	7	7	589	0	49.57	1.3214	NaN	3.20E+08
P43405-2;P4340	P43405-2;P4340	Tyrosine-protein	SYK	6	6	612	0	41.331	1.3209	NaN	2.48E+08
P82933;H7BZC4	P82933	28S ribosomal pr	MRPS9	16	16	396	0	98.029	1.3207	0.8507	1.69E+09
P45973;F8VNY3	P45973	Chromobox prote	CBX5	13	13	191	0	88.021	1.3194	0.2031	8.21E+08
F5H345;P08397-	F5H345;P08397-	Porphobilinogen	HMBS	8	8	330	0	137.33	1.3191	0.80513	1.18E+09
Q9UL03-3;Q9UL0	Q9UL03-3;Q9UL0	Integrator compl	INTS6	3	1	874	0	7.4391	1.3191	0.84009	1.67E+08
E7EWM3;A0A087	E7EWM3;A0A087	Zinc finger MIZ do	ZMIZ2;ZMIZ1	2	2	888	0	29.629	1.3185	NaN	1.76E+08
P09936;D6RE83;	P09936;D6RE83;	Ubiquitin carbox	UCHL1	12	12	223	0	151.85	1.3182	0.46032	2.79E+09
P62913	P62913	60S ribosomal pr	RPL11	13	2	178	0	80.568	1.3179	0.66051	1.88E+10
Q7Z4H3;Q7Z4H3·	Q7Z4H3;Q7Z4H3·	HD domain-conta	HDDC2	14	14	204	0	179.17	1.3173	0.54749	4.51E+09
Q9H269;Q9H269	Q9H269;Q9H269	Vacuolar protein	VPS16	9	9	839	0	45.88	1.317	1.2031	8.32E+08
P17252;J3KRN5;I	P17252;J3KRN5	Protein kinase C a	PRKCA	10	7	672	0	50.288	1.3169	0.83516	1.47E+09
Q9UPU7-2;Q9UPI	Q9UPU7-2;Q9UPI	TBC1 domain fam	TBC1D2B	8	8	914	0	61.455	1.3152	1.0921	2.84E+08
P61981	P61981	14-3-3 protein ga	YWHAG	13	8	247	0	42.848	1.3144	0.57778	9.24E+08
Q9UNQ2;A0A0C4	Q9UNQ2;A0A0C4	Probable dimeth	DIMT1	14	14	313	0	76.428	1.3144	0.73764	2.07E+09
C9J494;Q9H000·	C9J494;Q9H000·	Probable E3 ubiq	MKRN2	7	7	414	0	26.671	1.314	0.55333	1.22E+09
D3DTZ5;J3QSB9;I	D3DTZ5;J3QSB9;I	Transcription elo	SUPT4H1	2	2	76	0	9.8856	1.314	0.71237	5.11E+08
O75569-3;O7556	O75569-3;O7556	Interferon-induci	PRKRA	7	7	288	0	58.382	1.3139	0.87771	2.08E+09
O75828	O75828	Carbonyl reducta	CBR3	12	8	277	0	35.17	1.3138	0.67537	7.31E+08
Q9UEY8-2;A0A08	Q9UEY8-2;A0A08	Gamma-adducin	ADD3	13	12	674	0	106.21	1.3138	0.7798	1.50E+09
E9PGE5;Q9NUY8·	E9PGE5;Q9NUY8·	TBC1 domain fam	TBC1D23	2	2	562	0	5.6229	1.3132	NaN	4.76E+07
Q9NVE7;A0A0G2.	Q9NVE7;A0A0G2.	Pantothenate kin	PANK4	23	23	773	0	131.74	1.3124	0.78376	1.92E+09
Q5VUJ6-2;Q5VUJ	Q5VUJ6-2;Q5VUJ	Leucine-rich repe	LRCH2	10	10	748	0	57.914	1.3123	0.85522	8.11E+08
Q9BVA0;H3BPK1;	Q9BVA0	Katanin p80 WD4	KATNB1	7	7	655	0	41.859	1.3116	NaN	1.41E+08
O43823;M0QYL4	O43823	A-kinase anchor p	AKAP8	7	7	692	0	42.074	1.3104	1.0996	3.02E+08
Q99661;Q99661·	Q99661;Q99661·	Kinesin-like prote	KIF2C	12	11	725	0	131.82	1.3102	0.78635	8.58E+08
E9PK01;P29692;I	E9PK01;P29692;I	Elongation factor	EEF1D	16	0	261	0.0018172	3.0255	1.3093	NaN	5.75E+08
Q96H79;Q96H79	Q96H79	Zinc finger CCCH-t	ZC3HAV1L	11	11	300	0	201.13	1.3083	0.68575	3.52E+09
Q9Y6D9-3;Q9Y6D	Q9Y6D9-3;Q9Y6D	Mitotic spindle as	MAD1L1	4	4	626	0	10.168	1.308	0.75103	1.35E+08
Q6P5Z2	Q6P5Z2	Serine/threonine·	PKN3	9	8	889	0	32.896	1.3079	0.77162	3.43E+08
Q14019;H3BT58	Q14019;H3BT58	Coactosin-like pr	COTL1	12	12	142	0	47.484	1.3078	0.66572	4.32E+08
O95155-2;O9515	O95155-2;O9515	Ubiquitin conjug	UBE4B	17	17	1173	0	89.579	1.3076	0.63336	1.07E+09
Q9BUP3-3;Q9BUI	Q9BUP3-3;Q9BUI	Oxidoreductase H	HTATIP2	10	10	276	0	62.721	1.3072	0.61477	2.19E+09
J3QK89;Q8IWX8	J3QK89;Q8IWX8	Calcium homeost	CHERP	6	6	927	0	21.478	1.3069	0.92396	3.89E+08
G3V4K3;Q9H9C1	G3V4K3;Q9H9C1	Spermatogenesis·	VIPAS39	15	15	519	0	57.515	1.3058	0.80757	3.65E+08
A0A087WZZ5;Q1	A0A087WZZ5;Q1	Splicing factor 3B	SF3B2	7	7	871	0	25.705	1.3053	0.94476	2.65E+08
P48735;P48735-	P48735;P48735-	Isocitrate dehydr	IDH2	26	24	452	0	306.11	1.305	0.6082	1.22E+10
O95071-2;O9507	O95071-2;O9507	E3 ubiquitin-prot	UBR5	44	44	2798	0	242.74	1.3031	0.7894	3.21E+09
A0A0A0MRF3;Q5	A0A0A0MRF3;Q5	Transcriptional e	TEAD4;TEAD1;TEA	4	4	391	0	11.123	1.3028	1.2055	7.93E+07
Q8NBU5;Q8NBU5	Q8NBU5;Q8NBU5	ATPase family AA	ATAD1	8	8	361	0	38.175	1.3027	0.9544	6.20E+08
E3W994;J3KR49;	E3W994;J3KR49;	CLIP-associating p	CLASP2	10	10	1273	0	38.003	1.3026	2.1783	3.88E+08
Q86US8	Q86US8	Telomerase-bindi	SMG6	2	2	1419	0	8.2325	1.3026	NaN	3.63E+07
C9J0I9;Q86WB0;	C9J0I9;Q86WB0;	Nuclear-interacti	ZC3HC1	5	5	459	0	22.049	1.302	NaN	7.01E+08
O94874-2;O9487	O94874-2;O9487	E3 UFM1-protein	UFL1	21	20	729	0	215.72	1.3014	0.76667	3.79E+09
Q5T6V5;Q5T6V7;	Q5T6V5;Q5T6V7	UPF0553 protein	C9orf64	17	17	341	0	85.215	1.3013	0.89282	6.92E+09
Q9NX74;E7EUN9	Q9NX74;E7EUN9	tRNA-dihydrouric	DUS2	11	11	493	0	34.923	1.3013	0.97581	4.29E+08
Q7Z2W4;C9J6P4;	Q7Z2W4;C9J6P4;	Zinc finger CCCH-t	ZC3HAV1	34	34	902	0	297.89	1.3009	0.78511	5.73E+09
O00231;O00231·	O00231;O00231·	26S proteasome r	PSMD11	26	26	422	0	242.82	1.3008	0.71747	1.00E+10
Q9UKU7;Q9UKU7	Q9UKU7;Q9UKU7	Isobutyryl-CoA de	ACAD8	4	4	415	0	13.593	1.3007	1.0092	1.06E+08
Q5T5C7;P49591	Q5T5C7;P49591	Serine--tRNA ligas	SARS	19	19	536	0	183.46	1.3006	0.83982	3.54E+09
Q9Y6D6;E5RIF2;E	Q9Y6D6;E5RIF2	Brefeldin A-inhibi	ARFGEF1	7	5	1849	0	42.563	1.3002	0.83889	1.99E+08
Q9Y285;K7ER00;I	Q9Y285;K7ER00;I	Phenylalanine--tR	FARSA	22	22	508	0	277.51	1.2996	NaN	4.84E+09

O75170-6;O7517	O75170-6;O7517	Serine/threonine-	PPP6R2	1	1	905	0	7.7846	1.2991	0.85333	2.73E+08
P61927;D6R9X9;	P61927;D6R9X9;	60S ribosomal pr	RPL37	2	2	97	0	3.8026	1.2991	0.86977	2.23E+07
P62750;H7BY10;	P62750;H7BY10;	60S ribosomal pr	RPL23A	13	13	156	0	45.891	1.2978	0.54714	5.55E+09
Q96EE3;Q96EE3-:	Q96EE3;Q96EE3-:	Nucleoporin SEH:	SEH1L	18	18	360	0	171.41	1.2977	0.78793	5.55E+09
Q96RE7;K7ENW4	Q96RE7	Nucleus accumbe	NACC1	3	3	527	0	13.472	1.2953	NaN	2.15E+08
H0Y6H0;Q8NB78	H0Y6H0;Q8NB78	Lysine-specific his	KDM1B	2	2	640	0	9.0564	1.295	0.59173	1.41E+08
P42285;H0YAC4;	P42285	Superkiller viralic	SKIV2L2	53	53	1042	0	323.31	1.2948	0.67184	1.44E+10
H0YN26;P39687;	H0YN26;P39687;	Acidic leucine-ric	ANP32A;ANP32B;	2	2	177	0	5.9188	1.2941	0.85227	1.14E+08
Q92665	Q92665	28S ribosomal pr	MRPS31	10	10	395	0	121.91	1.2941	0.84416	1.47E+09
Q8NCN5;A8MT40	Q8NCN5;A8MT40	Pyruvate dehydro	PDPR	12	12	879	0	42.522	1.2939	0.79857	1.09E+09
Q14571;Q14571·	Q14571	Inositol 1,4,5-tris	ITPR2	8	6	2701	0	17.622	1.2921	1.1714	1.66E+08
Q13523;H0YDJ3	Q13523;H0YDJ3	Serine/threonine-	PRPF4B	9	9	1007	0	38.032	1.2903	1.0934	3.96E+08
Q14573	Q14573	Inositol 1,4,5-tris	ITPR3	15	13	2671	0	74.002	1.2902	0.34842	4.23E+08
O00429-3;O0042	O00429-3;O0042	Dynamin-1-like pi	DNM1L	16	16	710	0	289.11	1.2897	0.84327	9.98E+08
Q13217;X6R9L0	Q13217;X6R9L0	DnaJ homolog sul	DNAJC3	16	16	504	0	133.14	1.2895	0.82662	2.48E+09
P78347-2;P7834	P78347-2;P7834	General transcrip	GTF2I	48	48	957	0	323.31	1.2889	0.65034	1.57E+10
Q9NXG2;H3BNW	Q9NXG2	THUMP domain-c	THUMPD1	17	17	353	0	70.096	1.2879	0.80052	1.87E+09
P55084;P55084-	P55084;P55084-	Trifunctional enz	HADHB	28	28	474	0	323.31	1.2878	0.72066	2.68E+10
O00170;E9PMH2	O00170;E9PMH2	AH receptor-inter	AIP	4	4	330	0	46.193	1.2875	0.69893	1.19E+09
P52735-3;P5273	P52735-3;P5273	Guanine nucleoti	VAV2	8	8	839	0	39.121	1.2874	0.77795	4.53E+08
F5H6E2;O00159-	F5H6E2;O00159-	Unconventional r	MYO1C	31	31	1039	0	203.89	1.2871	0.79327	4.46E+09
Q52LJ0;Q52LJ0-2	Q52LJ0;Q52LJ0-2	Protein FAM98B	FAM98B	5	5	330	0	65.416	1.2869	0.80045	8.52E+08
Q13263;Q13263·	Q13263;Q13263·	Transcription inte	TRIM28	38	38	835	0	323.31	1.2866	0.64335	2.62E+10
P02545;P02545-	P02545;P02545-	Prelamin-A/C;Lan	LMNA	20	2	664	0	159.18	1.2863	1.0009	8.42E+08
Q9H0R6;X6R772;	Q9H0R6;X6R772;	Glutamyl-tRNA(G	QRSL1	4	4	528	0	23.878	1.2855	NaN	9.64E+07
A6NDG6;H3BV17	A6NDG6	Phosphoglycolate	PGP	11	11	321	0	102.9	1.2851	0.63327	3.98E+09
Q9UKN8;F2Z356	Q9UKN8	General transcrip	GTF3C4	32	32	822	0	323.31	1.2851	0.66199	4.08E+09
Q9UKG1;C9JAB0;	Q9UKG1	DCC-interacting p	APPL1	17	17	709	0	180.79	1.285	0.7723	1.94E+09
Q9P287;Q9P287·	Q9P287;Q9P287·	BRCA2 and CDKN	BCCIP	9	2	314	0	123.05	1.2848	0.9306	5.44E+09
O15269;O15269·	O15269	Serine palmitoylt	SPTLC1	16	16	473	0	143.68	1.2847	0.74349	2.82E+09
Q9UQE7	Q9UQE7	Structural mainte	SMC3	76	76	1217	0	323.31	1.2847	0.80635	1.41E+10
A0A087WYU1;Q9	A0A087WYU1;Q9	Sorting nexin-9	SNX9	13	13	594	0	167.76	1.2845	NaN	7.77E+08
A6NMQ1;P09884	A6NMQ1;P09884	DNA polymerase;I	POLA1	25	25	1468	0	237.04	1.2844	0.71547	3.34E+09
Q5T9B7;P00568;	Q5T9B7;P00568;	Adenylate kinase i	AK1	7	7	210	0	22.81	1.2841	0.5703	8.11E+08
A0A087WYN9;Q7	A0A087WYN9;Q7	ATP-dependent RI	DHX29	41	41	1370	0	323.31	1.2826	0.75786	3.04E+09
E7EMB1;Q9UH65	E7EMB1;Q9UH65	Switch-associatec	SWAP70	5	5	527	0	16.484	1.2824	NaN	1.53E+08
A0A087WUB9;Q8	A0A087WUB9;Q8	Beta-catenin-like	CTNNBL1	13	13	568	0	42.558	1.2818	NaN	7.10E+08
Q9NTI5-2;Q9NTI5	Q9NTI5-2;Q9NTI5	Sister chromatid	PDS5B	33	31	1391	0	279.83	1.2815	0.76624	3.91E+09
P27707;D6RFG8;	P27707;D6RFG8;	Deoxycytidine kir	DCK	8	8	260	0	49.595	1.2812	0.61008	9.36E+08
P06400	P06400	Retinoblastoma-a	RB1	14	14	928	0	117.65	1.2808	0.8892	1.84E+09
E9PKG1;H7C2I1;(	E9PKG1;H7C2I1;(	Protein arginine M	PRMT1	15	15	325	0	114.27	1.2805	0.70086	5.86E+09
P49321-4;P4932	P49321-4;P4932	Nuclear autoantig	NASP	4	4	724	0	26.628	1.2795	NaN	1.06E+08
O00399;E5RK00	O00399	Dynactin subunit	DCTN6	5	5	190	0	29.536	1.2786	0.47028	7.33E+08
P30084	P30084	Enoyl-CoA hydrat	ECHS1	19	19	290	0	209.17	1.2784	0.5552	6.43E+09
P55039;A8MZF9;	P55039;A8MZF9;	Developmentally·	DRG2	15	14	364	0	121.25	1.278	0.87833	3.34E+09
Q8IYB8;B1AR60	Q8IYB8	ATP-dependent RI	SUPV3L1	24	24	786	0	186.12	1.2776	0.7602	6.31E+09
Q9HAU5;Q9HAU5	Q9HAU5	Regulator of nons	UPF2	21	21	1272	0	104.29	1.2775	0.67588	1.52E+09
Q9BRX2	Q9BRX2	Protein pelota ho	PELO	15	15	385	0	175.95	1.277	0.82332	2.67E+09
O60716-5;O6071	O60716-5;O6071	Catenin delta-1	CTNND1	30	30	933	0	251.67	1.2768	0.75316	3.82E+09
Q9UK58-4;Q9UK5	Q9UK58-4;Q9UK5	Cyclin-L1	CCNL1	2	2	232	0	30.631	1.2766	NaN	8.65E+07
Q8N1G2;H0YCQ1	Q8N1G2	Cap-specific mRN	CMTR1	8	8	835	0	27.548	1.276	0.95542	6.94E+08
Q9NTX5-6;Q9NTX	Q9NTX5-6;Q9NTX	Ethylmalonyl-CoA	ECHDC1	12	12	284	0	164.28	1.2758	0.79601	2.18E+09
Q96D71-3;Q96D7	Q96D71-3;Q96D7	RalBP1-associate	REPS1	5	5	795	0	71.29	1.2751	0.69755	4.21E+08
A0A024RAC6;Q1	A0A024RAC6;Q1	Transcription elo	TCEB3	4	4	772	0	41.604	1.2749	0.99746	2.00E+08
P78527;P78527-	P78527;P78527-	DNA-dependent p	PRKDC	233	233	4128	0	323.31	1.2729	0.8353	1.02E+11
Q00535;Q00535·	Q00535;Q00535·	Cyclin-dependent	CDK5	16	15	292	0	81.432	1.2727	0.73099	4.32E+09
P45985;P45985-	P45985;P45985-	Dual specificity m	MAP2K4	3	3	399	0	9.015	1.2726	0.8212	4.56E+08
H0YCE7;O43427-	H0YCE7;O43427-	Acidic fibroblast g	FIBP	4	4	137	0	8.9649	1.2722	0.63182	4.19E+08
H3BPJ9;O96000;	H3BPJ9;O96000;	NADH dehydroge	NDUFB10	2	2	161	0	7.4692	1.2722	NaN	1.22E+08
Q9UJF2;Q9UJF2-:	Q9UJF2;Q9UJF2-:	Ras GTPase-activa	RASAL2	4	4	1139	0	19.145	1.2713	3.8943	1.30E+08
Q96G03;Q96G03	Q96G03;Q96G03	Phosphoglucomu	PGM2	3	3	612	0	33.462	1.2711	NaN	1.51E+08
Q14562;F5H658;	Q14562;F5H658	ATP-dependent RI	DHX8	11	10	1220	0	74.753	1.2703	0.77657	6.64E+08
Q6IN85;Q6IN85-:	Q6IN85;Q6IN85-:	Serine/threonine-	SMEK1	16	16	833	0	90.388	1.2703	0.77426	1.95E+09
P20020-6;P2002	P20020-6;P2002	Plasma membran	ATP2B1	25	14	1184	0	129.75	1.2691	0.79549	1.59E+09
Q9BUI4;E9PHH9	Q9BUI4;E9PHH9	DNA-directed RN	POLR3C	10	10	534	0	129.8	1.2687	NaN	4.32E+08
Q3B7T1;Q3B7T1-	Q3B7T1;Q3B7T1-	Erythroid differen	EDRF1	11	11	1238	0	52.839	1.2686	0.61978	4.34E+08
A0A0A0MQV2;O7	A0A0A0MQV2;O7	Ribosomal protei	RPS6KA5	8	6	807	0	31.604	1.2684	0.71224	3.41E+08
Q7L1Q6-2;Q7L1C	Q7L1Q6-2;Q7L1C	Basic leucine zipp	BZW1	9	8	353	0	17.896	1.268	1.1209	3.65E+08
P30837;A0A0U1I	P30837	Aldehyde dehydr	ALDH1B1	24	22	517	0	306.51	1.2677	0.77274	1.03E+10
A0A087WW58;Q	A0A087WW58;Q	Ethanolaminepho	EPT1	2	2	396	0	38.867	1.2673	0.5312	4.37E+08
Q9HB90;Q9NQL2	Q9HB90	Ras-related GTP-b	RRAGC	9	9	399	0	28.668	1.2673	0.93936	7.02E+08
Q14315;Q14315·	Q14315;Q14315·	Filamin-C	FLNC	67	60	2725	0	323.31	1.267	0.95114	7.09E+09
A0A096LNV3;A0/	A0A096LNV3;A0/	E3 ubiquitin-prot	RNF114	4	4	188	0	10.134	1.2662	0.39001	1.31E+08
P42677;Q5T4L4;I	P42677;Q5T4L4	40S ribosomal pr	RPS27	7	3	84	0	56.313	1.266	0.65838	1.73E+10
P13674-3;P1367	P13674-3;P1367	Prolyl 4-hydroxyl	P4HA1	2	2	516	0	16.194	1.2648	NaN	1.20E+08
P55263-3;P5526	P55263-3;P5526	Adenosine kinase	ADK	3	3	305	0	18.928	1.2639	0.65094	1.48E+08
Q15120;Q15120·	Q15120;Q15120·	[Pyruvate dehydr	PDK3	7	7	406	0	18.902	1.2637	0.91479	5.24E+08
P78417;Q5TA02;	P78417;Q5TA02;	Glutathione S-tra	GSTO1	18	18	241	0	89.435	1.2632	0.48777	8.52E+09
R4GN43;A0A0C4I	R4GN43;A0A0C4I	NADH dehydroge	NDUFA6	4	4	71	0	12.436	1.2627	0.33362	3.65E+08
Q58EX7-2;Q58EX	Q58EX7-2;Q58EX	Puratrophin-1	PLEKHG4	2	2	1110	0	9.6349	1.2626	2.5328	8.29E+07
Q7Z4S6-6;Q7Z4S(	Q7Z4S6-6;Q7Z4S(	Kinesin-like prote	KIF21A	8	7	1621	0	128.94	1.2613	0.64084	4.42E+08
Q9NR12;Q9NR12	Q9NR12;Q9NR12	PDZ and LIM dom	PDLIM7	10	10	457	0	118.95	1.2608	0.87806	1.08E+09
Q12830-4;Q1283	Q12830-4;Q1283	Nucleosome-rem	BPTF	19	19	2903	0	98.334	1.2603	0.61876	5.05E+08
C9J9W2;Q14847	C9J9W2;Q14847	LIM and SH3 dom	LASP1	3	3	166	0	18.102	1.2591	0.58357	8.40E+07
Q9Y619;Q5VZD9;	Q9Y619	Mitochondrial or	SLC25A15	8	8	301	0	22.952	1.2591	0.62056	4.75E+08
H7BXH2;E9PKF6;	H7BXH2;E9PKF6;	Serine/threonine-	PPP6R3	21	21	827	0	225.64	1.2589	0.58966	4.05E+09
H3BSM7;Q96GQ5	H3BSM7;Q96GQ5	UPF0420 protein	C16orf58	4	4	466	0	13.176	1.2581	0.68061	1.73E+08
Q93009;Q93009·	Q93009;Q93009·	Ubiquitin carbox	USP7	43	43	1102	0	312.82	1.2579	0.70364	5.15E+09
B4DFG0;P35659-	B4DFG0;P35659-	Protein DEK	DEK	4	4	347	0	17.437	1.2576	0.89795	5.39E+08
O60547-2;O6054	O60547-2;O6054	GDP-mannose 4,6	GMDS	8	8	342	0	50.045	1.2574	0.80595	1.14E+09
Q8NEN9	Q8NEN9	PDZ domain-cont	PDZD8	7	7	1154	0	45.616	1.2565	0.95607	4.15E+08
P49792;F8WBP7	P49792	E3 SUMO-protein	RANBP2	95	65	3224	0	323.31	1.2561	0.74393	1.23E+10
Q9Y315;E9PPM8;	Q9Y315;E9PPM8;	Putative deoxyrib	DERA	12	12	318	0	124.16	1.256	0.83612	7.41E+08
R4GMQ5;P07858	R4GMQ5;P07858	Cathepsin B;Cath	CTSB	1	1	76	0	7.6677	1.2559	NaN	1.38E+07
Q8NCA5-2;Q8NC/	Q8NCA5-2;Q8NC/	Protein FAM98A	FAM98A	5	5	518	0	106.26	1.2543	NaN	4.86E+08
P42224;J3KPM9;	P42224;J3KPM9;	Signal transducer	STAT1	27	27	750	0	236.72	1.2542	0.8724	4.89E+09
Q8IWZ3;Q8IWZ3·	Q8IWZ3;Q8IWZ3·	Ankyrin repeat an	ANKHD1	27	16	2542	0	265.74	1.254	0.6637	2.81E+09
A0A087X0M4;Q9	A0A087X0M4;Q9	Kanadaptin	SLC4A1AP	6	6	742	0	65.271	1.2537	0.58012	4.31E+08
Q9HC21-2;Q9HC/	Q9HC21-2;Q9HC/	Mitochondrial th	SLC25A19	6	5	263	0	24.398	1.2536	0.79401	6.30E+08
Q02252-2;Q0225	Q02252-2;Q0225	Methylmalonate-	ALDH6A1	8	8	522	0	83.235	1.253	0.79767	1.14E+09
P50750;P50750-	P50750;P50750-	Cyclin-dependent	CDK9	11	10	372	0	51.138	1.2528	0.73886	9.75E+08
P00966;Q5T6L6;I	P00966;Q5T6L6	Argininosuccinat	ASS1	24	24	412	0	234.55	1.2526	0.73653	5.30E+09
P67809;A0A087>	P67809;A0A087>	Nuclease-sensitiv	YBX1	11	6	324	0	274.77	1.2525	0.64838	2.32E+09
Q9Y2Z0-2;Q9Y2Z(	Q9Y2Z0-2;Q9Y2Z(	Suppressor of G2	SUGT1	23	23	333	0	266.72	1.2525	0.79672	4.05E+09

Q96EK6;G3V5E4;	Q96EK6;G3V5E4;	Glucosamine 6-ph	GNPNAT1	8	8	184	0	75.348	1.252	0.67007	2.41E+09
C9J384;Q9BQ75-	C9J384;Q9BQ75-	Protein CMSS1	CMSS1	3	3	225	0	13.227	1.2518	1.0589	2.25E+08
O43929;O43929-	O43929;O43929-	Origin recognitio	ORC4	9	9	436	0	75	1.2518	0.64752	8.99E+08
P07737;K7EJ44;(	P07737;K7EJ44	Profilin-1	PFN1	20	20	140	0	285.87	1.2518	0.74413	9.18E+10
P63104;E7EX29;I	P63104;E7EX29;I	14-3-3 protein ze	YWHAZ	16	11	245	0	280.89	1.2518	0.20507	3.43E+09
Q9NZJ7-2;Q9NZJ7	Q9NZJ7-2;Q9NZJ7	Mitochondrial ca	MTCH1	13	13	372	0	51.766	1.2512	0.55746	8.90E+08
B4DHE8;Q96DH6	B4DHE8;Q96DH6	RNA-binding prot	IGSF9B;MSI2	9	8	324	0	85.71	1.2501	0.88692	2.00E+09
A0A0J9YWJ4;K7E	A0A0J9YWJ4;K7E	RNA polymerase I	CTDP1	3	3	737	0	7.4779	1.2495	1.1079	1.17E+08
O60488-2;O6048	O60488-2;O6048	Long-chain-fatty-a	ACSL4	20	18	670	0	124.08	1.2491	1.0057	1.84E+09
E9PP76;J3KNF4;(	E9PP76;J3KNF4;(	Superoxide dismu	CCS	2	2	68	0	5.9071	1.2489	NaN	9.86E+07
Q14103-3;Q1410	Q14103-3;Q1410	Heterogeneous nu	HNRNPD	23	20	306	0	323.31	1.2487	0.71201	3.49E+10
Q8WUK0;Q8WUK	Q8WUK0;Q8WUK	Phosphatidylglyc	PTPMT1	6	6	201	0	42.787	1.2483	0.49435	1.05E+09
Q04727-4;Q0472	Q04727-4;Q0472	Transducin-like en	TLE4	11	3	748	0	29.143	1.2481	0.90476	6.83E+08
Q9Y2Z2-2;Q9Y2Z	Q9Y2Z2-2;Q9Y2Z	Protein MTO1 ho	MTO1	1	1	595	0	4.7376	1.248	NaN	9.46E+07
Q13526;K7EMU7	Q13526;K7EMU7	Peptidyl-prolyl ci	PIN1	10	10	163	0	153	1.2479	0.80044	3.43E+09
P50995-2;P5099	P50995-2;P5099	Annexin A11	ANXA11	20	20	472	0	166.72	1.2474	0.65002	5.85E+09
Q8TAV0;Q8TAV0-	Q8TAV0;Q8TAV0-	Protein FAM76A	FAM76A	5	5	307	0	24.367	1.2474	0.30357	8.22E+07
Q14194;E9PD68;	Q14194;E9PD68;	Dihydropyrimidir	CRMP1	10	9	572	0	90.555	1.2469	NaN	7.95E+08
A0A087X256;Q2I	A0A087X256;Q2I	WASH complex su	KIAA1033	25	25	1174	0	211.82	1.2466	0.85445	2.10E+09
Q9NZC9;H7BYI2;I	Q9NZC9;H7BYI2	SWI/SNF-related r	SMARCAL1	7	7	954	0	20.944	1.2466	1.2095	3.65E+08
H0Y2S1;O43824	H0Y2S1;O43824	Putative GTP-bin	GTPBP6	5	5	516	0	15.909	1.2461	0.9966	1.15E+08
Q71U36-2;Q71U3	Q71U36-2;Q71U3	Tubulin alpha-1A	TUBA1A;TUBA3C	41	1	416	0	31.996	1.2458	0.84965	2.54E+09
O43491;Q6R5J7;	O43491	Band 4.1-like pro	EPB41L2	42	1	1005	0	323.31	1.2455	0.71457	5.54E+09
P32322;E2QRB3;	P32322;E2QRB3;	Pyrroline-5-carbo	PYCR1	20	19	319	0	317.77	1.2453	0.72367	6.57E+09
F8W9X7;Q567U6	F8W9X7;Q567U6	Coiled-coil domai	CCDC93	6	6	630	0	47.391	1.2452	NaN	1.67E+08
O60934;A0A0C4I	O60934;A0A0C4I	Nibrin	NBN	19	19	754	0	133.59	1.2448	0.62191	1.33E+09
X6RLT1;H0UI80;(	X6RLT1;H0UI80;(	Negative elongati	NELFCD;TH1L	2	2	593	0	4.2964	1.2446	NaN	3.73E+07
P41214;P41214-	P41214;P41214-	Eukaryotic transl	EIF2D	21	21	584	0	148.87	1.2446	NaN	2.32E+09
M0R300;M0R0P8	M0R300;M0R0P8	Unconventional r	MYO9B	14	12	2072	0	51.052	1.2444	1.0067	4.62E+08
Q96D09;Q5JY77	Q96D09	G-protein couple	GPRASP2	8	8	838	0	153.39	1.2442	0.60632	2.82E+08
Q9Y399;Q5T8A0	Q9Y399;Q5T8A0	28S ribosomal pr	MRPS2	14	14	296	0	58.096	1.2438	0.85659	2.42E+09
C9J5N1;Q9BTE6;(	C9J5N1;Q9BTE6;(	Alanyl-tRNA editi	PTGES3L-AARSD1	14	14	495	0	139.24	1.2435	0.61667	2.23E+09
Q93074-3;Q9307	Q93074-3;Q9307	Mediator of RNA p	MED12;TNRC11	8	8	2176	0	26.983	1.2431	0.88072	3.30E+08
Q9Y2J2-2;A8K96	Q9Y2J2-2;A8K96	Band 4.1-like pro	EPB41L3	33	28	865	0	323.31	1.2431	0.6998	3.69E+09
P31153;P31153-	P31153;P31153-	S-adenosylmethic	MAT2A	13	13	395	0	137.62	1.243	1.1268	4.07E+09
O00458;O00458-	O00458;O00458-	Interferon-relatec	IFRD1	6	6	451	0	48.808	1.2429	0.84406	5.85E+08
P62081;B5MCP9	P62081;B5MCP9	40S ribosomal pr	RPS7	18	18	194	0	273.06	1.2422	0.72843	6.75E+09
H7C0E5;H7BZM7	H7C0E5;H7BZM7	Zinc finger protei	ZPR1	2	2	386	0	10.869	1.2418	NaN	8.33E+07
F5H101;Q76FK4-	F5H101;Q76FK4-	Nucleolar protein	NOL8	6	6	1085	0	150.73	1.2415	1.1124	1.73E+08
Q92878;Q92878-	Q92878;Q92878-	DNA repair protei	RAD50	58	58	1312	0	323.31	1.2414	0.77253	3.74E+09
E7EXA6;Q8WVB6	E7EXA6;Q8WVB6	Chromosome trar	CHTF18	11	10	975	0	34.322	1.2411	0.7769	4.91E+08
Q13572;G3V4M9	Q13572;G3V4M9	Inositol-tetrakisp	ITPK1	3	3	414	0	26.106	1.2407	0.80032	5.11E+08
Q15149;Q15149-	Q15149;Q15149-	Plectin	PLEC	67	57	4684	0	323.31	1.2405	0.88944	4.49E+09
P62829;J3KT29;(	P62829;J3KT29;(	60S ribosomal pr	RPL23	18	18	140	0	116.98	1.2401	0.76748	3.04E+10
Q96HC4;Q96HC4	Q96HC4;Q96HC4	PDZ and LIM dom	PDLIM5	18	18	596	0	90.15	1.2401	0.76463	1.04E+09
Q15126	Q15126	Phosphomevalon	PMVK	11	11	192	0	53.642	1.2397	0.70588	7.33E+08
Q96B26;H7C581	Q96B26	Exosome comple	EXOSC8	6	6	276	0	49.755	1.2396	1.0874	1.04E+09
Q96D46;C9JA08;	Q96D46;C9JA08;	60S ribosomal ex	NMD3	18	18	503	0	183.12	1.2393	NaN	1.51E+09
A2A2Q9;Q9Y312	A2A2Q9;Q9Y312	Protein AAR2 hon	AAR2	8	8	398	0	52.8	1.2391	0.94142	7.88E+08
Q5T1Z4;Q5T1Z8;(	Q5T1Z4;Q5T1Z8;(	Pumilio homolog	PUM1	14	1	1189	0	86.31	1.2391	0.93776	9.16E+08
Q9Y490	Q9Y490	Talin-1	TLN1	45	41	2541	0	323.31	1.2391	0.70625	5.23E+09
J3QLS3;Q9Y2R9;J	J3QLS3;Q9Y2R9;J	28S ribosomal pr	MRPS7	10	10	271	0	49.392	1.238	0.89277	1.73E+09
K4DI93;Q13620-	K4DI93;Q13620-	Cullin-4B	CUL4B	34	22	900	0	280.22	1.2379	0.77215	4.99E+09
O76071	O76071	Probable cytosoli	CIAO1	9	9	339	0	153.3	1.2371	0.749	1.81E+09
Q8NHV4;Q8NHV4	Q8NHV4;Q8NHV4	Protein NEDD1	NEDD1	4	4	660	0	75.287	1.2371	NaN	7.67E+07
P13010;C9JZ81;I	P13010	X-ray repair cross	XRCC5	55	55	732	0	323.31	1.236	0.71207	9.50E+10
P22033	P22033	Methylmalonyl-C	MUT	13	13	750	0	60.655	1.2355	0.72632	1.05E+09
Q96RL7-4;Q96RL	Q96RL7-4;Q96RL	Vacuolar protein	VPS13A	11	11	3069	0	35.796	1.2342	1.1046	2.58E+08
Q8NI27;A0A0C4I	Q8NI27;A0A0C4I	THO complex sub	THOC2	38	38	1593	0	199.29	1.2339	0.81819	5.61E+09
Q9BRK5-6;Q9BRK	Q9BRK5-6;Q9BRK	45 kDa calcium-b	SDF4	7	7	348	0	47.245	1.2339	0.62051	7.14E+08
Q9NZB2;Q9NZB2-	Q9NZB2;Q9NZB2-	Constitutive coac	FAM120A	31	31	1118	0	188.6	1.2332	0.78982	3.23E+09
P14618-2;H3BTN	P14618-2;H3BTN	Pyruvate kinase P	PKM	56	5	531	0	29.931	1.2328	NaN	2.22E+08
Q9Y2R4;A0A087	Q9Y2R4	Probable ATP-dep	DDX52	13	13	599	0	95.547	1.2328	NaN	9.21E+08
Q6UXN9;C9JBU3	Q6UXN9	WD repeat-contai	WDR82	13	13	313	0	127.36	1.2323	0.83163	2.09E+09
P62888;E5RI99;A	P62888;E5RI99;A	60S ribosomal pr	RPL30	8	8	115	0	65.784	1.2321	0.68462	6.09E+09
P60228;E5RGA2;	P60228;E5RGA2	Eukaryotic transl	EIF3E	21	21	445	0	105.81	1.2317	0.75586	3.96E+09
O43592;F8WDU6	O43592	Exportin-T	XPOT	37	37	962	0	323.31	1.2308	0.82341	1.11E+10
Q5T4U5;P11310;	Q5T4U5;P11310;	Medium-chain sp	ACADM	13	13	454	0	111.68	1.2307	0.75391	3.98E+09
E9PC74;Q13144;	E9PC74;Q13144	Translation initia	EIF2B5	15	15	705	0	78.203	1.2305	0.88035	1.67E+09
Q92733	Q92733	Proline-rich prote	PRCC	2	2	491	0	11.396	1.2305	NaN	4.86E+07
Q96C36;A0A087	Q96C36;A0A087	Pyrroline-5-carbo	PYCR2	20	19	320	0	141.88	1.2305	0.70039	1.05E+10
O15111;Q9UPZ9	O15111	Inhibitor of nucle	CHUK	19	18	745	0	215.51	1.2293	0.64765	1.60E+09
O60749-2;O6074	O60749-2;O6074	Sorting nexin-2	SNX2	8	8	402	0	51.066	1.2288	NaN	3.91E+08
P43246;E9PHA6;	P43246;E9PHA6;	DNA mismatch re	MSH2	40	40	934	0	323.31	1.2284	0.78987	1.05E+10
Q96RY7;Q96RY7-	Q96RY7;Q96RY7-	Intraflagellar tran	IFT140	7	7	1462	0	33.554	1.2272	0.84686	2.44E+08
P08559-3;P0855	P08559-3;P0855	Pyruvate dehydro	PDHA1	25	25	359	0	312.13	1.2259	0.72729	1.59E+10
Q9H6Q4-3;Q9H6	Q9H6Q4-3;Q9H6	Cytosolic Fe-S clu	NARFL	3	3	374	0	16.293	1.2256	0.83763	5.37E+07
Q6P1K8;Q13888;	Q6P1K8;Q13888;	General transcrip	GTF2H2C;GTF2H2	6	6	395	0	19.592	1.2255	0.7672	5.40E+08
Q7L8L6	Q7L8L6	FAST kinase doma	FASTKD5	9	9	764	0	97.106	1.225	NaN	3.87E+08
O14979-3;O1497	O14979-3;O1497	Heterogeneous nu	HNRNPDL	14	1	244	0	263.32	1.2248	0.41218	1.09E+10
Q96AC1;Q96AC1	Q96AC1;Q96AC1	Fermitin family ho	FERMT2	23	22	680	0	264.96	1.2248	0.69674	4.24E+09
P50570-4;P5057	P50570-4;P5057	Dynamin-2	DNM2	33	2	870	0	301.63	1.2242	0.78447	5.97E+09
O15344;O15344	O15344;O15344	E3 ubiquitin-prot	MID1	16	16	667	0	52.467	1.2239	NaN	4.44E+08
Q9NYV4-2;Q9NYV	Q9NYV4-2;Q9NYV	Cyclin-dependent	CDK12	5	3	1481	0	12.742	1.2237	0.82765	3.83E+08
M0QXB5;O95571	M0QXB5;O95571	Persulfide dioxyg	ETHE1	3	3	260	0	30.02	1.2234	0.70426	6.06E+08
Q9UI09;F8VXI1;F	Q9UI09;F8VXI1;F	NADH dehydroge	NDUFA12	5	5	145	0	26.818	1.2233	1.012	3.07E+08
O60566;O60566	O60566;O60566	Mitotic checkpoi	BUB1B	5	5	1050	0	29.811	1.2232	0.99255	1.69E+08
P21266;A0A0A0	P21266;A0A0A0	Glutathione S-tra	GSTM3	12	12	225	0	66.223	1.2231	0.76575	5.17E+09
P50336;H0YFP3;I	P50336;H0YFP3	Protoporphyrino	PPOX	3	3	477	0	7.7912	1.223	NaN	6.63E+07
P62273;P62273-	P62273;P62273-	40S ribosomal pr	RPS29	5	5	56	0	25.355	1.223	0.86847	3.85E+09
Q9UBU9;E9PIN3;	Q9UBU9;E9PIN3;	Nuclear RNA expo	NXF1	24	24	619	0	162.95	1.2229	NaN	2.45E+09
P49368;P49368-	P49368;P49368-	T-complex protei	CCT3	43	43	545	0	323.31	1.2227	0.67906	5.38E+10
P20700;E9PBF6;/	P20700;E9PBF6;/	Lamin-B1	LMNB1	46	42	586	0	323.31	1.2225	0.98847	6.12E+09
Q15637-4;Q1563	Q15637-4;Q1563	Splicing factor 1	SF1	5	5	548	0	17.274	1.2222	NaN	1.35E+08
Q5SVZ6	Q5SVZ6	Zinc finger MYM-t	ZMYM1	7	6	1142	0	22.328	1.2217	0.91455	2.88E+08
Q8NI60-3;Q8NI6(	Q8NI60-3;Q8NI6(	Chaperone activit	ADCK3	8	8	595	0	112.38	1.2217	0.77824	1.89E+09
J3QKS7;B4DGM3	J3QKS7;B4DGM3	SWI/SNF-related r	SMARCE1	4	4	288	0	20.073	1.2213	1.0044	2.91E+08
V9GZ56;Q9Y4Z0;I	V9GZ56;Q9Y4Z0;I	U6 snRNA-associa	LSM4	4	4	238	0	21.178	1.2211	0.13263	9.63E+08
J3KTA4;P17844;F	J3KTA4;P17844;F	Probable ATP-dep	DDX5	44	36	614	0	323.31	1.2209	0.74791	3.79E+10
Q9NPF4;G3V445;	Q9NPF4	Probable tRNA N6	OSGEP	12	12	335	0	104.25	1.2209	0.77992	3.26E+09
Q9P0K7-4;Q9P0K	Q9P0K7-4;Q9P0K	Ankycorbin	RAI14	5	5	951	0	32.378	1.2209	0.9038	7.38E+08
P00558;P00558-	P00558;P00558-	Phosphoglycerate	PGK1	40	40	417	0	323.31	1.2208	0.47212	5.00E+10
O95985-3;O9598	O95985-3;O9598	DNA topoisomera	TOP3B	7	7	707	0	15.087	1.2203	1.0131	3.59E+08
Q8TCD5;J3KRC4;.	Q8TCD5;J3KRC4;.	5(3)-deoxyribonu	NT5C	8	8	201	0	87.908	1.2199	0.84214	1.68E+09

B5MBZ8;C9JD73;	B5MBZ8;C9JD73;	Protein phosphat	PPP1R7	2	2	274	0	3.9932	1.2193	NaN	4.16E+07
P52298;P52298-	P52298;P52298-	Nuclear cap-bindi	NCBP2	5	5	156	0	20.733	1.2193	0.61696	1.04E+09
Q8WYQ5-3;Q8W\	Q8WYQ5-3;Q8W\	Microprocessor c	DGCR8	3	3	740	0	8.873	1.2186	0.67482	3.07E+08
J3QRN6;O94832;	J3QRN6;O94832;	Unconventional r	MYO1D	22	22	961	0	182.69	1.2183	0.77702	2.90E+09
P46063;F8WA66	P46063	ATP-dependent D	RECQL	30	30	649	0	323.31	1.2176	NaN	5.08E+09
Q7Z406;Q7Z406-	Q7Z406;Q7Z406-	Myosin-14	MYH14	27	18	1995	0	123.74	1.2176	0.88841	2.56E+09
A0A0A0MTH9;O1	A0A0A0MTH9;O1	TATA-binding pro	BTAF1	36	36	1849	0	196.34	1.2171	0.83819	3.19E+09
Q12923-3;Q1292	Q12923-3;Q1292	Tyrosine-protein	PTPN13	9	9	2466	0	50.161	1.2165	1.0536	3.82E+08
Q96GD0;B1AHD3	Q96GD0	Pyridoxal phosph	PDXP	15	15	296	0	77.89	1.2165	0.79577	3.88E+09
Q9Y5P6;Q9Y5P6-	Q9Y5P6;Q9Y5P6-	Mannose-1-phosp	GMPPB	8	8	360	0	53.815	1.2165	0.8857	1.29E+09
E7EX90;Q14203-	E7EX90;Q14203-	Dynactin subunit	DCTN1;DKFZp68	43	43	1256	0	323.31	1.2154	0.77991	6.89E+09
P52701;P52701-	P52701;P52701-	DNA mismatch re	MSH6	47	47	1360	0	323.31	1.2149	0.7771	1.01E+10
Q16555-2;Q1655	Q16555-2;Q1655	Dihydropyrimidir	DPYSL2	9	8	536	0	57.367	1.2149	NaN	4.45E+08
O75340-2;O7534	O75340-2;O7534	Programmed cell	PDCD6;hCG_198	7	7	189	0	25.196	1.2147	0.88004	8.66E+08
Q16878	Q16878	Cysteine dioxyger	CDO1	1	1	200	0.0090024	2.0627	1.2143	NaN	3.74E+08
J3QLR8;Q9Y3D9	J3QLR8;Q9Y3D9	28S ribosomal pr	MRPS23	8	8	152	0	39.568	1.2138	0.85695	2.09E+09
O15067;H0YGH1	O15067	Phosphoribosylfc	PFAS	57	57	1338	0	323.31	1.2135	0.7884	2.40E+10
P23381;P23381-	P23381;P23381-	Tryptophan--tRN/	WARS	34	34	471	0	323.31	1.2134	0.75402	3.43E+10
J3KMX2;B9EGA3;	J3KMX2;B9EGA3;	SWI/SNF-related r	SMARCD2	10	8	456	0	66.94	1.2133	NaN	4.31E+08
J3KNN5;Q9UJV9;	J3KNN5;Q9UJV9	Probable ATP-dep	DDX41	12	12	640	0	35.534	1.2132	NaN	6.29E+08
O15226;O15226-	O15226;O15226-	NF-kappa-B repre	NKRF	20	20	690	0	86.036	1.2128	0.92709	1.33E+09
P47756-2;B1AK8	P47756-2;B1AK8	F-actin-capping p	CAPZB	11	11	272	0	90.988	1.2128	0.89173	3.34E+09
D6REA0;O75879;	D6REA0;O75879	Glutamyl-tRNA(G	PET112	7	7	516	0	20.149	1.2127	0.76084	2.70E+08
P60660-2;F8W1F	P60660-2;F8W1F	Myosin light poly	MYL6;PDE6H	9	9	151	0	153.76	1.2117	0.87671	4.82E+09
D6RAX7;Q9BT78;	D6RAX7;Q9BT78;	COP9 signalosom	COPS4	11	11	420	0	66.268	1.2115	0.78228	1.22E+09
P13489;H0YCR7;	P13489;H0YCR7	Ribonuclease inhi	RNH1	20	20	461	0	241.85	1.2107	0.81719	1.30E+10
Q99832;Q99832-	Q99832;Q99832-	T-complex protei	CCT7	46	46	543	0	323.31	1.2104	0.58546	3.38E+10
M0R2Z9;Q8IX01-	M0R2Z9;Q8IX01-	SURP and G-patch	SUGP2	19	19	1096	0	251.68	1.2102	0.92714	1.46E+09
Q08211;Q08211-	Q08211	ATP-dependent RI	DHX9	69	69	1270	0	323.31	1.2092	1.0215	4.80E+10
Q9NR50-3;Q9NR!	Q9NR50-3;Q9NR!	Translation initia	EIF2B3	11	11	401	0	77.419	1.2088	1.0329	1.65E+09
Q96PE3-2;Q96PE	Q96PE3-2;Q96PE	Type I inositol 3,4	INPP4A	8	8	938	0	29.611	1.2087	0.77801	5.15E+08
Q3KQV9;Q3KQV9	Q3KQV9;Q3KQV9	UDP-N-acetylhex	UAP1L1	2	1	507	0.00053036	3.4117	1.2081	NaN	9.40E+07
P43897;P43897-	P43897;P43897-	Elongation factor	TSFM	10	10	325	0	256.07	1.2079	0.61664	7.24E+09
O96011-2;O9601	O96011-2;O9601	Peroxisomal mer	PEX11B	4	4	245	0	8.5391	1.2077	0.49243	1.54E+08
P27635;X1WI28;	P27635;X1WI28;	60S ribosomal pr	RPL10	16	16	214	0	217.92	1.2072	0.94757	1.65E+10
Q96DT7-2;Q96D1	Q96DT7-2;Q96D1	Zinc finger and BT	ZBTB10	7	7	847	0	63.777	1.2071	1.1429	3.17E+08
O00154-6;O0015	O00154-6;O0015	Cytosolic acyl coe	ACOT7	19	19	329	0	159.24	1.2068	0.81728	1.23E+10
G3V5T0;A0A0C4I	G3V5T0;A0A0C4I	Maleylacetoaceta	GSTZ1	7	7	202	0	82.389	1.2066	0.55193	1.82E+09
Q9NZI8;Q9NZI8-2	Q9NZI8;Q9NZI8-2	Insulin-like growt	IGF2BP1	29	27	577	0	282.61	1.2063	0.9239	1.59E+10
P62701;Q8TD47	P62701	40S ribosomal pr	RPS4X	32	19	263	0	305.3	1.2059	0.80967	3.49E+10
Q9NWT6;E9PNR8	Q9NWT6	Hypoxia-inducibl	HIF1AN	3	3	349	0	19.387	1.2059	0.50624	2.57E+08
Q9NW82;D6RIW!	Q9NW82;D6RIW!	WD repeat-contai	WDR70	12	12	654	0	120.59	1.2055	0.96747	7.17E+08
Q15042;Q15042-	Q15042;Q15042-	Rab3 GTPase-acti	RAB3GAP1	22	22	981	0	205.58	1.2054	0.82394	3.06E+09
G5E933;O95248;	G5E933;O95248;	Myotubularin-rel	SBF1	19	19	1868	0	89.31	1.2042	0.73563	6.53E+08
Q969U7-2;Q969U	Q969U7-2;Q969U	Proteasome assen	PSMG2	9	9	233	0	34.212	1.2042	0.77985	8.64E+08
P23396;P23396-	P23396;P23396-	40S ribosomal pr	RPS3	34	33	243	0	299.93	1.2039	0.82258	9.63E+10
Q96HA7-2;Q96H/	Q96HA7-2;Q96H/	Tonsoku-like prot	TONSL	11	11	1378	0	91.903	1.2038	0.90273	3.04E+08
Q92615;A0A087)	Q92615	La-related protei	LARP4B	13	9	738	0	100.8	1.2033	0.82122	2.46E+09
B4DK25;H0Y5C2;	B4DK25;H0Y5C2;	Arginyl-tRNA--prc	ATE1	3	3	403	0	22.341	1.2027	NaN	6.19E+07
Q9NVI1;Q9NVI1-:	Q9NVI1;Q9NVI1-:	Fanconi anemia g	FANCI	50	50	1328	0	323.31	1.2027	0.74028	7.24E+09
Q6N069;Q6N069	Q6N069;Q6N069	N-alpha-acetyltra	NAA16	12	5	864	0	16.818	1.2024	0.53258	2.39E+08
J3KNS1;Q9UPW5	J3KNS1;Q9UPW5	Cytosolic carboxy	AGTPBP1	8	8	1278	0	71.859	1.202	0.80619	5.10E+08
Q9HBD4;A0A0A0	Q9HBD4;A0A0A0	Transcription acti	SMARCA4	37	22	1679	0	323.31	1.2018	0.78455	3.58E+09
H7C1A0;Q9HC62	H7C1A0;Q9HC62	Sentrin-specific p	SENP2	1	1	203	0	10.627	1.2016	NaN	5.04E+07
Q13769;F8WCP5	Q13769;F8WCP5	THO complex sub	THOC5	19	19	683	0	136.22	1.2016	0.87	1.51E+09
P62263;H0YB22;	P62263;H0YB22;	40S ribosomal pr	RPS14	11	11	151	0	169.39	1.2009	0.57744	2.80E+10
A8MT37;P49840;	A8MT37;P49840;	Glycogen synthas	GSK3A	8	7	401	0	30.138	1.2008	0.72043	8.25E+08
Q9Y5S2;H0YLY0;/	Q9Y5S2;H0YLY0	Serine/threonine-	CDC42BPB	10	7	1711	0	43.974	1.2007	0.83321	1.92E+08
P85037;P85037-	P85037;P85037-	Forkhead box pro	FOXK1	4	4	733	0	41.069	1.2006	0.93286	6.80E+08
O95487-2;O9548	O95487-2;O9548	Protein transport	SEC24B	20	20	1233	0	147.88	1.2004	0.80635	2.04E+09
Q8WUY1;H0YAR9	Q8WUY1;H0YAR9	Protein THEM6	THEM6	2	2	208	0	5.6237	1.2	NaN	5.37E+07
P61978;P61978-	P61978;P61978-	Heterogeneous nu	HNRNPK	34	2	463	0	323.31	1.1996	0.89435	5.43E+10
Q16795;F5H0J3;I	Q16795	NADH dehydroge	NDUFA9	9	9	377	0	40.921	1.1995	0.92852	2.55E+09
P35250;P35250-	P35250;P35250-	Replication factor	RFC2	17	17	354	0	233.04	1.1994	0.76385	3.39E+09
P41743	P41743	Protein kinase C i	PRKCI	11	9	596	0	112.91	1.1993	NaN	4.42E+08
A0A0D9SES8;H0Y	A0A0D9SES8;H0Y	Transducin-like en	LITAF;TLE3	14	9	772	0	94.81	1.199	0.88372	2.64E+09
Q99613;Q99613-	Q99613;Q99613-	Eukaryotic transl	EIF3C;EIF3CL	41	41	913	0	323.31	1.1984	0.83362	1.85E+10
K7ERI7;P35268;K	K7ERI7;P35268;K	60S ribosomal pr	RPL22	9	7	95	0	104.12	1.1983	0.60319	1.33E+10
Q9Y6Y8;Q9Y6Y8-:	Q9Y6Y8;Q9Y6Y8-:	SEC23-interacting	SEC23IP	27	27	1000	0	190.61	1.1979	0.95341	3.92E+09
B1AJY7;O75832;I	B1AJY7;O75832;I	26S proteasome r	PSMD10	15	15	193	0	258.16	1.1972	0.50269	1.13E+10
G3V0G5;Q8IV38	G3V0G5;Q8IV38	Ankyrin repeat an	ANKMY2	2	2	341	0	20.765	1.1971	0.95347	1.34E+08
Q9Y3A2-2;Q9Y3A	Q9Y3A2-2;Q9Y3A	Probable U3 smal	UTP11L	2	2	148	0.0049517	2.3198	1.197	NaN	3.65E+06
Q96QK1;I3L4S0;I	Q96QK1	Vacuolar protein	VPS35	45	45	796	0	323.31	1.196	0.85061	1.66E+10
O75891;O75891-	O75891;O75891-	Cytosolic 10-form	ALDH1L1	6	2	902	0	20.955	1.1959	0.67364	3.06E+08
Q99623;J3KPX7;I	Q99623;J3KPX7;I	Prohibitin-2	PHB2	26	26	299	0	269.51	1.195	0.8146	4.28E+10
P47755;C9JUG7;	P47755;C9JUG7;	F-actin-capping p	CAPZA2	6	4	286	0	68.764	1.1949	0.96331	1.36E+09
Q2TAY7;Q2TAY7-:	Q2TAY7;Q2TAY7-:	WD40 repeat-con	SMU1	22	22	513	0	323.31	1.1949	0.86095	1.22E+10
Q9C0B7	Q9C0B7	Transport and Go	TANGO6	6	6	1094	0	67.446	1.1949	0.65647	4.15E+08
P61764;P61764-	P61764;P61764-	Syntaxin-binding	STXBP1	10	10	594	0	63.422	1.1944	NaN	4.16E+08
Q9NZ45	Q9NZ45	CDGSH iron-sulfu	CISD1	2	2	108	0	16.242	1.1941	0.85513	3.58E+08
A0A087X1H5;Q1!	A0A087X1H5;Q1!	Arf-GAP with coil	ACAP2	10	10	777	0	71.874	1.1934	1.3303	6.20E+08
Q96ST3;H3BNZ3;	Q96ST3	Paired amphipath	SIN3A	15	15	1273	0	137.92	1.1931	0.78135	9.28E+08
O60942;O60942-	O60942;O60942-	mRNA-capping en	RNGTT	8	8	597	0	43.763	1.1929	NaN	4.03E+08
Q6P3W7;F8VSC5	Q6P3W7;F8VSC5	SCY1-like protein	SCYL2	14	14	929	0	119.34	1.1924	0.81404	1.54E+09
Q504Q3-2;Q504(	Q504Q3-2;Q504(	PAB-dependent p	PAN2	11	11	1198	0	56.91	1.1908	0.48051	4.91E+08
A6NJ78;A0A0U1I	A6NJ78	Probable methylt	METTL15	5	5	407	0	18.482	1.1906	1.0456	3.29E+08
K7EQ02;K7EQ55;	K7EQ02;K7EQ55;	DAZ-associated pr	DAZAP1	7	7	327	0	110.3	1.1906	0.85683	2.72E+09
P30154-4;P3015	P30154-4;P3015	Serine/threonine-	PPP2R1B	7	2	556	0	9.6035	1.1906	NaN	1.15E+08
A0A0D9SFR6;Q8(	A0A0D9SFR6;Q8(	Diacylglycerol kin	DGKH	3	3	1028	0	11.191	1.1903	1.4132	1.09E+08
O15357;O15357-	O15357;O15357-	Phosphatidylinos	INPPL1	6	6	1258	0	19.477	1.1903	0.68833	2.02E+08
J3KNQ4;Q9NVD7	J3KNQ4;Q9NVD7	Alpha-parvin;Beta	PARVA;PARVB	2	2	412	0	33.582	1.1902	NaN	1.07E+08
P55795	P55795	Heterogeneous nu	HNRNPH2	17	8	449	0	143.77	1.19	0.85432	5.08E+09
A0A087WX71;Q9	A0A087WX71;Q9	ESF1 homolog	ESF1	2	2	456	0	10.195	1.1895	0.30625	1.73E+08
A6NHR9;A6NHR9	A6NHR9;A6NHR9	Structural mainte	SMCHD1	50	50	2005	0	323.31	1.1892	0.78657	4.09E+09
Q99598;Q5VVQ1	Q99598;Q5VVQ1	Translin-associate	TSNAX;DISC1	2	2	290	0	23.413	1.1886	0.97193	4.69E+08
D6RAN4;P32969;	D6RAN4;P32969;	60S ribosomal pr	RPL9	16	16	182	0	173.14	1.1884	0.95908	2.33E+10
Q2NKX8;B5MDQ(	Q2NKX8;B5MDQ(	DNA excision rep	ERCC6L	20	20	1250	0	219.96	1.1883	0.96344	1.16E+09
Q13151	Q13151	Heterogeneous nu	HNRNPA0	18	18	305	0	323.31	1.188	1.1209	7.87E+09
Q9Y277;Q9Y277-	Q9Y277;Q9Y277-	Voltage-depender	VDAC3	9	9	283	0	190.49	1.1878	0.85882	8.33E+09
Q27J81-2;Q27J8:	Q27J81-2;Q27J8:	Inverted formin-2	INF2	10	10	1240	0	78.757	1.1875	0.84224	2.39E+08
E9PF18;A0A0A0M	E9PF18;A0A0A0M	Hydroxyacyl-coer	HADH	7	7	318	0	75.273	1.1871	1.1762	1.83E+09
Q9NTJ5;F8WCQ2	Q9NTJ5;F8WCQ2	Phosphatidylinos	SACM1L	6	6	587	0	12.963	1.1871	NaN	8.71E+07
J3KR44;Q96FW1;	J3KR44;Q96FW1;	Ubiquitin thioest	OTUB1	13	13	272	0	180.99	1.1869	0.92573	1.56E+10
P63096;P63096-	P63096;P63096-	Guanine nucleoti	GNAI1	8	3	354	0	22.158	1.1869	0.8371	7.85E+08

D6RBD7;C9J1V9;	D6RBD7;C9J1V9;	Eukaryotic transl	EEF1E1;EEF1E1-Bl	6	6	150	0	75.989	1.1865	1.1216	1.32E+09
Q9Y450-4;Q9Y45	Q9Y450-4;Q9Y45	HBS1-like protein	HBS1L	27	27	642	0	181.05	1.1864	0.8498	3.61E+09
E9PEX6;P09622;I	E9PEX6;P09622;I	Dihydrolipoyl del	DLD	15	15	486	0	98.151	1.1863	0.72755	3.64E+09
O14617;O14617·	O14617;O14617·	AP-3 complex sub	AP3D1	38	38	1153	0	323.31	1.1863	0.77233	5.91E+09
A0A087X0B7;Q5	A0A087X0B7;Q5	Synaptosomal-ass	SNAP47	7	7	419	0	43.64	1.1859	0.86905	5.90E+08
Q9GZL7	Q9GZL7	Ribosome biogen	WDR12	15	15	423	0	134.94	1.1846	0.95104	4.75E+09
P49916-3;P4991	P49916-3;P4991	DNA ligase 3	LIG3	33	33	922	0	323.31	1.1845	0.81502	5.59E+09
Q96SB8;Q96SB8·	Q96SB8;Q96SB8·	Structural mainte	SMC6	15	15	1091	0	128.75	1.1845	0.86238	7.91E+08
Q8N5M1;C9J2Q2	Q8N5M1	ATP synthase mit	ATPAF2	3	3	289	0	15.672	1.1843	0.50662	1.98E+08
Q05086-2;Q0508	Q05086-2;Q0508	Ubiquitin-protein	UBE3A	16	16	852	0	176.81	1.1841	0.81843	1.20E+09
P11171-2;P1117	P11171-2;P1117	Protein 4.1	EPB41	23	20	831	0	121.88	1.1834	0.73098	2.17E+09
O60826	O60826	Coiled-coil domai	CCDC22	12	12	627	0	121.53	1.1833	NaN	5.52E+08
P78316;E9PFK5;I	P78316;E9PFK5;I	Nucleolar protein	NOP14	9	9	857	0	57.245	1.1833	1.0887	6.39E+08
Q9NTJ3;E9PD53;(	Q9NTJ3;E9PD53;(	Structural mainte	SMC4	69	69	1288	0	323.31	1.1833	0.81489	9.87E+09
P08047-3;P0804	P08047-3;P0804	Transcription fact	SP1	2	2	737	0	94.611	1.1822	0.83304	3.81E+08
A0A087WU53;Q5	A0A087WU53;Q5	Magnesium trans	MAGT1	4	4	367	0	33.575	1.1821	1.3445	1.70E+08
P61254;J3KTJ8;J	P61254;J3KTJ8;J	60S ribosomal pr	RPL26;KRBA2	16	5	145	0	44.027	1.1821	1.5824	3.95E+09
P11498;P11498·	P11498	Pyruvate carboxy	PC	27	27	1178	0	206.75	1.1815	0.86015	1.74E+09
P23526;P23526·	P23526;P23526·	Adenosylhomocy	AHCY	31	31	432	0	323.31	1.1811	0.70548	4.33E+10
E9PKP7;P17480-:	E9PKP7;P17480-:	Nucleolar transcr	UBTF	11	11	745	0	46.444	1.181	0.98193	1.60E+09
G3V325;O75127;	G3V325;O75127	Pentatricopeptid	ATP5J2-PTCD1;P1	10	8	749	0	33.111	1.1807	0.93624	1.66E+09
Q13395	Q13395	Probable methylt	TARBP1	23	23	1621	0	142.78	1.1806	0.80954	1.49E+09
Q70CQ2-3;Q70C(	Q70CQ2-3;Q70C(	Ubiquitin carbox	USP34	10	10	3312	0	66.112	1.1805	0.95065	2.99E+08
Q9GZS1-2;Q9GZS	Q9GZS1-2;Q9GZS	DNA-directed RN/	POLR1E	14	14	419	0	67.51	1.1803	0.72076	1.17E+09
Q9NSI2-2;Q9NSI2	Q9NSI2-2;Q9NSI2	Protein FAM207A	FAM207A	8	8	215	0	36.225	1.1801	0.80396	5.94E+08
P50851;H0YA17	P50851	Lipopolysacchari	LRBA	35	0	2863	0	182.54	1.1799	0.88894	2.40E+09
O75306-2;O7530	O75306-2;O7530	NADH dehydroge	NDUFS2	13	13	457	0	106.17	1.1797	0.83019	3.39E+09
P41252;A0A0A0I	P41252;A0A0A0I	Isoleucine--tRNA	IARS	79	79	1262	0	323.31	1.1796	0.88716	5.54E+10
P11274-2;P1127	P11274-2;P1127	Breakpoint cluste	BCR	9	8	1227	0	32.431	1.1794	0.88282	6.20E+08
C9JPE1;O43772;I	C9JPE1;O43772	Mitochondrial ca	SLC25A20	6	6	228	0	15.951	1.1788	0.7375	2.99E+08
Q6NVY1;A0A087\	Q6NVY1;A0A087\	3-hydroxyisobuty	HIBCH	16	16	386	0	128.7	1.1788	0.67614	2.23E+09
H0YFS7;E7EW59;	H0YFS7;E7EW59;	Sal-like protein 2	SALL2	3	3	902	0	15.335	1.1786	0.83598	1.46E+08
P11177-2;P1117	P11177-2;P1117	Pyruvate dehydro	PDHB	16	16	341	0	199.73	1.1785	0.85341	1.76E+10
P24666;G5E9R5;	P24666;G5E9R5;	Low molecular we	ACP1	9	4	158	0	122.25	1.1785	0.66782	9.26E+09
H3BRM5;H3BV69	H3BRM5;H3BV69	Cytochrome c oxi	COX5A	2	2	69	0.0015633	3.0676	1.1784	1.3153	3.90E+07
P40227;P40227·	P40227;P40227·	T-complex protei	CCT6A	36	29	531	0	323.31	1.178	0.70252	4.10E+10
O43252	O43252	Bifunctional 3'-ph	PAPSS1	15	15	624	0	165.95	1.1777	NaN	2.44E+09
Q7Z6Z7-2;Q7Z6Z7	Q7Z6Z7-2;Q7Z6Z7	E3 ubiquitin-prot	HUWE1	107	107	4358	0	323.31	1.1776	0.84913	1.90E+10
J3KN16;Q5VYK3;I	J3KN16;Q5VYK3	Proteasome-asso	KIAA0368;ECM29	46	46	2017	0	323.31	1.1768	0.83296	4.86E+09
Q99459	Q99459	Cell division cycle	CDC5L	20	20	802	0	228.82	1.1761	0.647	2.12E+09
P61224-2;P6122	P61224-2;P6122	Ras-related protei	RAP1B;RAP1A	3	3	137	0	8.7938	1.176	NaN	7.02E+07
M0R2B7;P28340	M0R2B7;P28340	DNA polymerase;	POLD1	43	43	1133	0	323.31	1.1755	0.69587	5.86E+09
P25398	P25398	40S ribosomal pr	RPS12	10	10	132	0	93.415	1.1745	0.63778	5.21E+09
Q16513;Q16513·	Q16513;Q16513·	Serine/threonine	PKN2	38	37	984	0	323.31	1.1744	0.76317	7.55E+09
P23528;G3V1A4;	P23528;G3V1A4;	Cofilin-1	CFL1	23	19	166	0	323.31	1.1742	0.37148	3.76E+10
A0A0X1KG71;Q8'	A0A0X1KG71;Q8'	Negative elongati	NELFB	13	13	628	0	45.329	1.1735	NaN	8.20E+08
O95470;H0Y3V8;	O95470	Sphingosine-1-ph	SGPL1	9	9	568	0	35.251	1.1735	NaN	2.82E+08
Q9NVM9;Q9NVM	Q9NVM9;Q9NVM	Protein asunder h	ASUN	11	11	706	0	50.174	1.173	0.68721	9.77E+08
P15927;P15927·	P15927;P15927·	Replication prote	RPA2	10	10	270	0	126.89	1.1721	0.97308	1.47E+09
Q13425;H7BY41;	Q13425;H7BY41;	Beta-2-syntrophi	SNTB2	2	2	540	0	4.9822	1.1721	NaN	8.98E+07
Q9UGI8-2;Q9UGI	Q9UGI8-2;Q9UGI	Testin	TES	20	20	412	0	120.07	1.172	0.75445	1.45E+09
Q86VP6;Q86VP6·	Q86VP6;Q86VP6·	Cullin-associated	CAND1	52	46	1230	0	323.31	1.1717	0.8352	1.90E+10
E7EWP2;E7EPJ7;(	E7EWP2;E7EPJ7;(	Triple functional	TRIO	3	3	2309	0	11.437	1.1715	1.209	6.64E+07
Q9NW64-2;Q9NV	Q9NW64-2;Q9NV	Pre-mRNA-splicin	RBM22	10	10	371	0	89.62	1.1714	0.97869	1.28E+09
C9J9K3;A0A0C4D	C9J9K3;A0A0C4D	40S ribosomal pr	RPSA	15	15	264	0	216.08	1.1713	1.1391	6.98E+09
P36954;K7EKS1;I	P36954;K7EKS1	DNA-directed RN/	POLR2I	4	4	125	0	36.248	1.1713	0.7308	1.08E+09
J3KQ48;Q9Y3E5	J3KQ48;Q9Y3E5	Peptidyl-tRNA hy	PTRH2	4	4	180	0	102.28	1.1711	0.34988	4.88E+08
B4DJ81;P28331-:	B4DJ81;P28331-:	NADH-ubiquinon	NDUFS1	15	15	611	0	99.614	1.171	0.74031	1.21E+09
A3KN83-3;A3KN8	A3KN83-3;A3KN8	Protein strawberr	SBNO1	8	8	1391	0	45.634	1.1704	0.90895	3.13E+08
Q9NXC5;Q9NXC5	Q9NXC5;Q9NXC5	WD repeat-contai	MIOS	9	9	875	0	47.303	1.1701	1.1388	5.43E+08
Q9Y4E8-2;Q9Y4E8	Q9Y4E8-2;Q9Y4E8	Ubiquitin carbox	USP15	10	9	952	0	200.94	1.1701	0.93951	8.84E+08
Q96I51-2;Q96I51	Q96I51-2;Q96I51	Williams-Beuren	WBSCR16	5	5	358	0	20.23	1.17	1.3019	5.53E+07
Q96P11-2;Q96P1	Q96P11-2;Q96P1	Probable 28S rRN	NSUN5	16	16	466	0	63.148	1.1698	0.83402	1.17E+09
Q9Y5M8;H7C4H2	Q9Y5M8;H7C4H2	Signal recognitio	SRPRB	12	12	271	0	148.93	1.1696	0.7379	3.00E+09
O95202;O95202·	O95202	LETM1 and EF-har	LETM1	11	11	739	0	64.345	1.1691	0.86379	7.61E+08
P49643;A0A096I	P49643	DNA primase larg	PRIM2	7	7	509	0	35.059	1.169	NaN	6.34E+08
Q8ND04;Q8ND04	Q8ND04;Q8ND04	Protein SMG8	SMG8	14	14	991	0	249.23	1.1689	0.73745	1.17E+09
P21964-2;P2196	P21964-2;P2196	Catechol O-meth	COMT	19	19	221	0	203.7	1.1688	0.53465	2.66E+09
Q6P1J9	Q6P1J9	Parafibromin	CDC73	21	21	531	0	64.512	1.1686	NaN	1.35E+09
Q9Y3Z3;Q9Y3Z3-4	Q9Y3Z3;Q9Y3Z3-4	Deoxynucleoside	SAMHD1	25	25	626	0	165.58	1.1686	1.7579	3.83E+09
E9PC66;P17029;I	E9PC66;P17029;I	Zinc finger protei	ZKSCAN1	2	2	527	0	37.08	1.1684	NaN	6.33E+07
O43865;O43865·	O43865;O43865·	Putative adenosyl	AHCYL1	11	7	530	0	42.55	1.1674	NaN	9.27E+08
Q13045-2;J3KS3!	Q13045-2	Protein flightless-	FLII	36	0	1214	0	12.662	1.1673	NaN	1.10E+08
Q14008-2;Q1400	Q14008-2;Q1400	Cytoskeleton-ass	CKAP5	16	16	1972	0	71.282	1.1673	0.58292	1.03E+09
Q9Y316;Q9Y316·	Q9Y316;Q9Y316·	Protein MEMO1	MEMO1	10	10	297	0	161.17	1.1673	0.8524	1.56E+09
Q96QG7;Q96QG7	Q96QG7;Q96QG7	Myotubularin-rel	MTMR9	8	8	549	0	17.189	1.1668	0.81265	6.42E+08
Q5VYS8-6;Q5VYS(	Q5VYS8-6;Q5VYS(	Terminal uridylyl	ZCCHC6	6	6	1457	0	16.425	1.1667	0.41013	1.97E+08
Q6P3X3;F8WCH1	Q6P3X3	Tetratricopeptide	TTC27	15	15	843	0	125.14	1.1666	0.87148	3.88E+09
P31946-2;A0A0J!	P31946-2	14-3-3 protein be	YWHAB	14	1	244	0	240.76	1.1661	0.75376	8.13E+08
O60563;O60563·	O60563	Cyclin-T1	CCNT1	13	13	726	0	145.73	1.1659	0.69522	1.72E+09
P53004;C9J1E1	P53004	Biliverdin reduct	BLVRA	21	21	296	0	255.84	1.1658	0.77421	9.17E+09
B0QZ35;E9PC49;I	B0QZ35;E9PC49;I	NAD-dependent p	SIRT1	7	7	444	0	182.68	1.1654	1.0167	5.47E+08
P08754;P11488;	P08754	Guanine nucleoti	GNAI3	12	8	354	0	159.06	1.1652	1.0752	3.16E+09
P55196-1;J3KN0:	P55196-1;J3KN0:	Afadin	MLLT4	19	2	1816	0	129.84	1.1652	0.90783	1.06E+09
Q02790;F5H1U3;	Q02790	Peptidyl-prolyl ci	FKBP4	29	29	459	0	323.31	1.1652	0.77231	2.05E+10
Q8TEU7;B7Z7Y1;I	Q8TEU7;B7Z7Y1;I	Rap guanine nucl	RAPGEF6	11	10	1601	0	101.94	1.1644	0.58739	6.28E+08
F5GWX5;A0A0C4	F5GWX5;A0A0C4	Chromodomain-h	CHD4	58	58	1905	0	323.31	1.1636	0.84123	7.73E+09
X6RCC3;A0A087\	X6RCC3;A0A087\	Stromal membra	SMAP2	3	2	174	0	7.6907	1.1634	0.88561	2.73E+08
P14625;Q96GW1	P14625	Endoplasmin	HSP90B1	45	43	803	0	323.31	1.1629	0.84678	1.60E+10
Q8IWV7;A0A087'	Q8IWV7;A0A087'	E3 ubiquitin-prot	UBR1	19	19	1749	0	87.337	1.1628	0.76536	1.08E+09
P48729-3;P4872	P48729-3;P4872	Casein kinase I iso	CSNK1A1;CSNK1/	6	6	325	0	14.841	1.1626	0.85627	1.69E+08
Q7L576;A0A0G2J	Q7L576;A0A0G2J	Cytoplasmic FMR	CYFIP1	53	32	1253	0	286.01	1.1623	0.80876	9.26E+09
Q96RP9;C9IZ01;F	Q96RP9;C9IZ01;F	Elongation factor	GFM1	30	1	751	0	149.13	1.1621	0.86894	7.53E+09
P55265-5;P5526	P55265-5;P5526	Double-stranded	ADAR	52	3	931	0	316.68	1.1618	0.75619	1.50E+10
Q9Y6V7;Q9Y6V7·	Q9Y6V7	Probable ATP-dep	DDX49	7	7	483	0	22.698	1.1618	0.7442	6.82E+08
Q9Y547;A6NIR2;I	Q9Y547;A6NIR2;I	Intraflagellar tran	HSPB11	2	2	144	0	72.463	1.1615	1.2883	7.51E+08
J3KMZ8;Q92785;	J3KMZ8;Q92785;	Zinc finger protei	DPF2	8	8	405	0	53.561	1.1614	0.63867	1.07E+09
P36404;V9GYD0;	P36404;V9GYD0;	ADP-ribosylation	ARL2;ARL2-SNX1!	11	11	184	0	129.7	1.1611	0.77725	2.35E+09
O43747;O43747·	O43747;O43747·	AP-1 complex sub	AP1G1	29	29	822	0	323.31	1.1609	0.8122	7.78E+09
Q8N1G4	Q8N1G4	Leucine-rich repe	LRRC47	25	25	583	0	201.38	1.1602	1.1373	6.40E+09
E9PDF6;O43795;	E9PDF6;O43795;	Unconventional r	MYO1B	23	23	1107	0	185.24	1.1601	0.73008	2.87E+09
P68363;P68363·	P68363;P68363·	Tubulin alpha-1B	TUBA1B	41	0	451	0	323.31	1.1601	0.90292	4.61E+11
A0A087WY12;Q9	A0A087WY12;Q9	Mitochondrial 2-(	SLC25A21	3	3	234	0	15.294	1.1598	0.57643	7.06E+07
O75934	O75934	Pre-mRNA-splicin	BCAS2	9	9	225	0	84.368	1.1595	0.647	1.13E+09

A3KMH1-3;A3KM	A3KMH1-3;A3KM	von Willebrand fa	VWA8	21	21	1872	0	112.44	1.1593	0.68449	8.92E+08
E7EU96;Q5U5J2;I	E7EU96;Q5U5J2;I	Casein kinase II su	CSNK2A1;CSNK2A	16	16	385	0	323.31	1.1591	0.80607	8.86E+09
Q9H2G2-2;Q9H2(	Q9H2G2-2;Q9H2(	STE20-like serine/	SLK	20	20	1204	0	151.56	1.1587	0.832	5.39E+08
Q9NVV0;H7C3B3	Q9NVV0;H7C3B3	Trimeric intracell	TMEM38B	3	3	291	0	31.134	1.1586	0.40328	1.20E+08
P25786;P25786-	P25786;P25786-	Proteasome subu	PSMA1	16	16	263	0	95.639	1.1581	0.71591	3.45E+09
P26374	P26374	Rab proteins gera	CHML	4	4	656	0	11.649	1.1581	1.0793	7.35E+08
Q13315;E9PIN0;I	Q13315	Serine-protein kir	ATM	21	21	3056	0	117.54	1.1578	0.82164	6.68E+08
Q8N3C0;Q8N3C0	Q8N3C0	Activating signal (	ASCC3	55	55	2202	0	323.31	1.1568	0.83251	3.96E+09
P43490;A0A0C4I	P43490;A0A0C4I	Nicotinamide phc	NAMPT	30	30	491	0	323.31	1.1562	0.7229	3.10E+10
Q96KR1;H0Y8W1	Q96KR1	Zinc finger RNA-bi	ZFR	29	29	1074	0	323.31	1.1557	0.70227	2.19E+09
E9PKT9;O96033	E9PKT9;O96033	Molybdopterin sy	MOCS2	2	2	83	0.0030449	2.6564	1.1553	NaN	2.99E+08
Q9BXW9;Q9BXW	Q9BXW9;Q9BXW	Fanconi anemia g	FANCD2	18	18	1451	0	110.56	1.1546	0.89831	8.60E+08
Q13123;E7EQZ7;I	Q13123;E7EQZ7	Protein Red	IK	10	10	557	0	76.217	1.1544	NaN	6.45E+08
O95347;O95347·	O95347;O95347·	Structural mainte	SMC2	53	53	1197	0	323.31	1.1539	0.88634	7.76E+09
Q9Y2I7;E9PDH4;(	Q9Y2I7;E9PDH4	1-phosphatidylin	PIKFYVE	12	12	2098	0	36.008	1.1537	0.71416	3.82E+08
P62249;M0R210	P62249;M0R210	40S ribosomal pr	RPS16	23	23	146	0	83.554	1.1536	0.9049	3.58E+10
Q7L0Y3;C9JVB6	Q7L0Y3;C9JVB6	Mitochondrial rit	TRMT10C	13	13	403	0	140.29	1.1535	0.91256	1.93E+09
A0A087WTU3;Q9	A0A087WTU3;Q9	Testis-expressed s	TEX264	2	2	239	0	4.8707	1.1532	0.76052	8.37E+07
Q8N1G0-2;Q8N1(	Q8N1G0-2;Q8N1(	Zinc finger protei	ZNF687	4	4	1103	0	10.965	1.153	1.1965	1.39E+08
Q0PNE2;C9IYN7;(	Q0PNE2;C9IYN7;(	Elongator comple	ELP6	7	7	266	0	50.403	1.1529	0.84318	3.98E+08
Q92499;F1T0B3;,	Q92499;F1T0B3;,	ATP-dependent RI	DDX1	37	37	740	0	323.31	1.1526	0.93866	1.17E+10
Q92541;H0YKX1	Q92541	RNA polymerase-s	RTF1	11	11	710	0	61.965	1.1519	0.82259	7.85E+08
Q2TAM5;E9PKH5	Q2TAM5;E9PKH5	Transcription fact	RELA	8	8	377	0	28.457	1.1518	NaN	7.72E+08
Q9BSJ2;Q9BSJ2-4	Q9BSJ2;Q9BSJ2-4	Gamma-tubulin c	TUBGCP2	32	32	902	0	323.31	1.1517	0.79808	5.36E+09
F2Z2U4;Q9Y4A5-;	F2Z2U4;Q9Y4A5-;	Transformation/t	TRRAP	48	48	3848	0	176.1	1.1514	0.7615	1.80E+09
Q5JVZ5;Q96JJ3;C	Q5JVZ5;Q96JJ3;C	Engulfment and c	ELMO2	9	7	718	0	45.373	1.1512	0.79673	4.34E+08
P42766;F2Z388	P42766;F2Z388	60S ribosomal pr	RPL35	8	8	123	0	57.376	1.1508	0.69406	2.56E+09
A0A0A0MTH3;Q1	A0A0A0MTH3;Q1	Integrin-linked pr	ILK	16	16	483	0	76.87	1.1507	0.80133	2.44E+09
E9PGT6;Q99627·	E9PGT6;Q99627·	COP9 signalosom	COPS8	3	3	173	0	48.505	1.1506	0.9071	3.83E+08
Q86U44;F5H6D8	Q86U44;F5H6D8	N6-adenosine-me	METTL3	7	7	580	0	31.304	1.1504	NaN	4.46E+08
P45880;A0A0A0I	P45880;A0A0A0I	Voltage-depender	VDAC2	13	13	294	0	323.31	1.1503	1.0763	1.15E+10
E7ESY4;Q13330-;	E7ESY4;Q13330-;	Metastasis-associ	MTA1	13	8	703	0	82.875	1.1502	1.1242	1.31E+09
Q7Z3B4-3;Q7Z3B	Q7Z3B4-3;Q7Z3B	Nucleoporin p54	NUP54	10	10	459	0	103.86	1.1498	NaN	3.68E+08
Q9HBH5;C9J2C7	Q9HBH5	Retinol dehydrog	RDH14	5	5	336	0	35.776	1.1497	1.0478	4.96E+08
P26639;P26639-	P26639;P26639-	Threonine--tRNA l	TARS	50	46	723	0	323.31	1.1496	0.7993	2.95E+10
P62873;P62873-	P62873;P62873-	Guanine nucleoti	GNB1	10	4	340	0	129.79	1.1496	0.7225	2.25E+09
Q9NUQ8-2;Q9NU	Q9NUQ8-2;Q9NU	ATP-binding casse	ABCF3	14	14	703	0	87.796	1.1495	0.90992	1.10E+09
Q5TFE4;Q5TFE4-2	Q5TFE4;Q5TFE4-2	5-nucleotidase dc	NT5DC1	19	19	455	0	187.57	1.1489	0.66672	4.34E+09
P21359-2;P2135	P21359-2;P2135	Neurofibromin;N	NF1	36	36	2818	0	189.95	1.1486	0.86806	2.52E+09
P49411;H3BNU3	P49411	Elongation factor	TUFM	32	32	452	0	323.31	1.1486	0.6881	5.04E+10
P02545-2;Q3BDL	P02545-2;Q3BDL	Prelamin-A/C;Lan	LMNA	19	1	572	0	28.075	1.1485	NaN	4.93E+07
O43615;M0QXU7	O43615;M0QXU7	Mitochondrial im	TIMM44	23	23	452	0	148.67	1.1484	0.84441	5.34E+09
O95456-2;O9545	O95456-2;O9545	Proteasome assen	PSMG1	8	8	267	0	33.78	1.1482	0.81024	2.99E+09
P62195;P62195-	P62195;P62195-	26S protease regu	PSMC5	29	28	406	0	323.31	1.1481	0.78921	1.79E+10
Q9Y2L1;Q9Y2L1-;	Q9Y2L1;Q9Y2L1-;	Exosome comple	DIS3	58	58	958	0	323.31	1.1481	0.78147	2.99E+10
Q02978;I3L1P8;(	Q02978;I3L1P8;(	Mitochondrial 2-(	SLC25A11	21	21	314	0	312.26	1.1476	0.81288	2.36E+10
Q96DG6	Q96DG6	Carboxymethylen	CMBL	8	8	245	0	17.735	1.1474	0.63826	3.20E+08
P23919;P23919-	P23919;P23919-	Thymidylate kina	DTYMK	15	15	212	0	47.668	1.1471	0.59714	2.20E+09
Q16822;B4DW7;	Q16822;B4DW7;	Phosphoenolpyru	PCK2	26	26	640	0	150.17	1.1469	1.2215	5.25E+09
E5KLK1;E5KLJ6;E	E5KLK1;E5KLJ6;E	Dynamin-like 120	OPA1	13	13	961	0	48.882	1.1467	0.67062	7.43E+08
O15160;O15160·	O15160;O15160·	DNA-directed RN/	POLR1C	9	9	346	0	64.569	1.1467	1.0219	3.50E+09
Q9Y2U8	Q9Y2U8	Inner nuclear mer	LEMD3	3	3	911	0	13.995	1.1467	0.94867	1.30E+08
P14923;C9JTX4;(	P14923	Junction plakogl	JUP	21	19	745	0	156.35	1.1465	0.86971	2.33E+09
Q05655;Q05655·	Q05655;Q05655·	Protein kinase C d	PRKCD	9	9	676	0	46.335	1.1462	0.78701	7.19E+08
Q9Y4U1;A0A0C4I	Q9Y4U1;A0A0C4I	Methylmalonic ac	MMACHC	3	3	282	0	14.168	1.1462	0.4135	8.61E+07
P41250;H7C443;	P41250	Glycine--tRNA lig	GARS	40	40	739	0	323.31	1.1461	0.79187	2.64E+10
Q7Z2T5;Q7Z2T5-;	Q7Z2T5;Q7Z2T5-;	TRMT1-like protei	TRMT1L	23	23	733	0	318.25	1.1453	0.84762	3.23E+09
P53618;E9PP73;I	P53618;E9PP73	Coatomer subuni	COPB1	54	54	953	0	323.31	1.145	0.85521	3.86E+10
A0A0B4J1V9;Q9N	A0A0B4J1V9;Q9N	Lymphoid-specifi	HELLS	18	18	884	0	51.287	1.1446	0.79323	1.05E+09
P35579;P35579-	P35579;P35579-	Myosin-9	MYH9	123	100	1960	0	323.31	1.1444	0.89427	5.68E+10
A0A0C4DGT3;A0/	A0A0C4DGT3;A0/	IQ motif and SEC7	IQSEC1	3	3	814	0	34.018	1.1443	NaN	8.51E+07
P62316;P62316-	P62316;P62316-	Small nuclear ribo	SNRPD2	14	14	118	0	159.96	1.1442	0.80387	4.58E+09
Q9HBD1-6;Q9HB	Q9HBD1-6;Q9HB	Roquin-2;Roquin	RC3H2;RC3H1	3	3	869	0	11.979	1.1439	NaN	7.94E+07
Q96PK6;Q96PK6·	Q96PK6	RNA-binding prot	RBM14	27	21	669	0	160.69	1.1437	0.72858	3.12E+09
Q13618-2;Q1361	Q13618-2;Q1361	Cullin-3	CUL3	16	16	744	0	140.54	1.1435	1.0507	9.16E+08
Q8WUM4;Q8WU	Q8WUM4;Q8WU	Programmed cell	PDCD6IP	56	56	868	0	323.31	1.1435	0.76722	1.87E+10
P30153;B3KQV6;	P30153;B3KQV6	Serine/threonine·	PPP2R1A	23	18	589	0	185.54	1.1431	0.51146	2.07E+09
Q12955-5;Q1295	Q12955-5;Q1295	Ankyrin-3	ANK3	15	14	1861	0	132.45	1.1431	0.72906	1.14E+09
O95340;O95340·	O95340;O95340·	Bifunctional 3-ph	PAPSS2	8	8	614	0	45.371	1.143	NaN	8.98E+08
K7ENF0	K7ENF0	NARS		2	2	47	0	8.1512	1.1429	NaN	2.08E+08
O60684;Q5TFJ7;S	O60684;Q5TFJ7	Importin subunit	KPNA6	16	8	536	0	156.08	1.1429	NaN	2.33E+09
Q9UKB1-2;Q9UKI	Q9UKB1-2;Q9UKI	F-box/WD repeat·	FBXW11	4	1	508	0	10.686	1.1428	0.55371	9.07E+07
O14920-4;O1492	O14920-4;O1492	Inhibitor of nucle	IKBKB	6	5	697	0	14.681	1.1414	0.78614	2.75E+08
P53582;H0Y955;	P53582;H0Y955	Methionine amin	METAP1	7	7	386	0	49.167	1.141	0.71648	5.77E+08
Q9Y3D8;A0A087\	Q9Y3D8;A0A087\	Adenylate kinase i	AK6;TAF9	5	5	172	0	20.934	1.1409	1.0656	1.65E+09
P28288;P28288-	P28288;P28288-	ATP-binding casse	ABCD3	31	31	659	0	211.81	1.1408	NaN	6.26E+09
P35244;B5MC59	P35244;B5MC59	Replication prote	RPA3	5	5	121	0	216.03	1.1408	0.8221	8.42E+08
Q9H1D9	Q9H1D9	DNA-directed RN/	POLR3F	6	6	316	0	22.599	1.1407	0.78856	7.14E+08
F5GWT4;Q9H4A3	F5GWT4;Q9H4A3	Serine/threonine·	WNK1	7	7	2134	0	17.207	1.1404	0.7936	1.98E+08
Q6YN16;Q6YN16·	Q6YN16;Q6YN16·	Hydroxysteroid d	HSDL2	15	15	418	0	88.34	1.14	0.66983	2.41E+09
G5E9X5;E9PG35;	G5E9X5;E9PG35;	Methylcrotonoyl·	MCCC1	8	8	434	0	82.604	1.1396	0.67199	6.68E+08
Q5SNT2-2;Q5SNT	Q5SNT2-2;Q5SNT	Transmembrane p	TMEM201	3	3	392	0	19.534	1.1396	1.2176	2.40E+08
Q9Y3B2;R4GMQ7	Q9Y3B2;R4GMQ7	Exosome comple	EXOSC1	7	7	195	0	48.146	1.1391	0.84333	1.54E+09
Q86TP1;Q86TP1-	Q86TP1;Q86TP1-	Protein prune hor	PRUNE	13	13	453	0	87.937	1.1389	0.70083	1.16E+09
P46783;F6U211;	P46783;F6U211;	40S ribosomal pr	RPS10;RPS10-NU	13	12	165	0	92.838	1.1387	0.73519	6.38E+09
P07992-2;P0799	P07992-2;P0799	DNA excision repa	ERCC1	5	5	273	0	18.229	1.1385	0.97107	2.46E+08
Q92597;Q92597·	Q92597;Q92597·	Protein NDRG1	NDRG1	7	7	394	0	66.801	1.1381	0.78057	8.79E+08
Q9BTY7;E9PIX0	Q9BTY7	Protein HGH1 hor	HGH1	5	5	390	0	25.948	1.1381	0.88688	6.52E+08
P51157-3;P5115	P51157-3;P5115	Ras-related protei	RAB28	2	2	204	0	25.311	1.138	NaN	4.63E+07
Q9Y6J9;E9PP94	Q9Y6J9	TAF6-like RNA pol	TAF6L	4	4	622	0	23.596	1.1379	NaN	1.78E+08
O00311;B1AMW	O00311	Cell division cycle	CDC7	9	9	574	0	20.875	1.1378	NaN	1.96E+08
Q9H9A6	Q9H9A6	Leucine-rich repe	LRRC40	31	31	602	0	323.31	1.1378	0.54137	8.92E+09
E7EQR4;P15311;I	E7EQR4;P15311;I	Ezrin;Moesin;Rad	EZR;MSN;RDX	4	4	586	0	12.187	1.1375	NaN	2.36E+08
Q9C0D5-2;Q9C0I	Q9C0D5-2;Q9C0I	Protein TANC1	TANC1	5	5	1755	0	11.423	1.1372	0.676	2.09E+08
A0A087X2I1;P62	A0A087X2I1;P62	26S protease regu	PSMC6	22	22	403	0	224.7	1.137	0.88245	1.51E+10
Q9UPT9-2;Q9UPT	Q9UPT9-2;Q9UPT	Ubiquitin carbox	USP22;USP27X	10	10	513	0	117	1.137	NaN	9.29E+08
A0A087WY00;G3	A0A087WY00;G3	Unconventional r	MYO5A	7	5	1828	0	49.24	1.1369	1.1256	1.33E+08
C9JK83;O95630-;	C9JK83;O95630-;	STAM-binding pro	STAMBP	5	5	318	0	11.038	1.1369	0.84586	2.13E+08
Q92616	Q92616	Translational acti	GCN1L1	122	122	2671	0	323.31	1.1369	0.88109	2.08E+10
Q99575;E5RK39	Q99575	Ribonucleases P/I	POP1	5	5	1024	0	14.344	1.1369	0.8689	2.38E+08
Q9NUD5;Q9NUD!	Q9NUD5;Q9NUD!	Zinc finger CCHC (	ZCCHC3	8	8	404	0	53.233	1.1367	0.78873	7.27E+08
K7ERG2;Q9NYR9·	K7ERG2;Q9NYR9·	NF-kappa-B inhibi	NKIRAS2	4	4	141	0	11.663	1.1365	0.60564	3.99E+08
Q8WY54-2;Q8W\	Q8WY54-2;Q8W\	Protein phosphat	PPM1E	5	5	755	0	35.83	1.1362	0.87534	3.16E+08
Q9UQR0;H0Y6S1;	Q9UQR0	Sex comb on midl	SCML2	9	9	700	0	40.649	1.1362	0.67046	8.40E+08

Q96FZ2;D6R9T3;I	Q96FZ2;D6R9T3;I	Embryonic stem c	HMCES	7	7	354	0	31.806	1.136	0.61103	4.39E+08
G5EA30;Q92879-	G5EA30;Q92879-	CUGBP Elav-like f	CELF1	13	13	514	0	69.389	1.1358	0.82808	8.16E+08
O14531;Q5T0Q6	O14531;Q5T0Q6	Dihydropyrimidir	DPYSL4	9	9	572	0	42.603	1.1348	NaN	2.81E+08
Q13356;Q13356-	Q13356;Q13356-	Peptidyl-prolyl ci	PPIL2	6	6	520	0	75.843	1.1348	NaN	3.48E+08
Q96HW7;Q96HW	Q96HW7	Integrator compl	INTS4	15	15	963	0	84.84	1.1347	0.6504	9.69E+08
Q9UID3-2;Q9UID	Q9UID3-2;Q9UID	Vacuolar protein	VPS51	19	19	658	0	102.38	1.1347	0.73496	1.81E+09
Q9NVH1-3;Q9NV	Q9NVH1-3;Q9NV	DnaJ homolog sul	DNAJC11	9	9	507	0	127.61	1.1343	NaN	7.41E+08
Q04917;A2IDB2;I	Q04917;A2IDB2	14-3-3 protein et	YWHAH	16	13	246	0	184.67	1.134	0.65337	1.80E+09
Q8TD19;G3V459;	Q8TD19	Serine/threonine	NEK9	21	21	979	0	190.11	1.1337	0.82392	3.75E+09
Q7Z4Q2;Q7Z4Q2	Q7Z4Q2;Q7Z4Q2	HEAT repeat-cont	HEATR3	10	10	680	0	46.424	1.1334	NaN	7.09E+08
Q8NG31-2;Q8NG	Q8NG31-2;Q8NG	Protein CASC5	CASC5	6	6	2316	0	22.008	1.1329	0.71616	1.08E+08
Q2TAL8;C9JAL2;C	Q2TAL8	Glutamine-rich p	QRICH1	13	13	776	0	180.78	1.1328	0.85144	1.23E+09
P62424;Q5T8U3;	P62424;Q5T8U3	60S ribosomal pr	RPL7A	16	16	266	0	70.867	1.1326	1.6626	3.63E+09
P46734-2;P4673	P46734-2;P4673	Dual specificity m	MAP2K3	9	6	318	0	45.855	1.1322	0.71404	6.31E+08
Q8WTW3;A0A08	Q8WTW3;A0A08	Conserved oligon	COG1;ADCK1	22	22	980	0	323.31	1.1321	0.773	2.24E+09
Q9BW83-2;Q9BW	Q9BW83-2;Q9BW	Intraflagellar tran	IFT27	3	3	185	0	7.706	1.132	0.67556	1.32E+08
P23378	P23378	Glycine dehydrog	GLDC	2	2	1020	0	10.717	1.1317	NaN	1.01E+08
E9PLA9;G3V153;	E9PLA9;G3V153;	Caprin-1	CAPRIN1	2	2	186	0	4.4281	1.1315	NaN	1.08E+08
Q06124-2;Q0612	Q06124-2;Q0612	Tyrosine-protein	PTPN11	18	18	593	0	96.27	1.1313	NaN	6.33E+08
Q9BZK7;A0A0D9	Q9BZK7;A0A0D9	F-box-like/WD re	TBL1XR1	7	7	514	0	98.044	1.1302	0.98814	5.45E+08
P05423;E5RHT4;I	P05423	DNA-directed RN	POLR3D	5	5	398	0	28.774	1.13	0.81255	3.57E+08
Q15019;Q15019	Q15019;Q15019	Septin-2	02-Sep	11	11	361	0	111.07	1.1296	1.1444	1.98E+09
Q00325-2;Q0032	Q00325-2;Q0032	Phosphate carrie	SLC25A3	18	18	361	0	143.77	1.1295	0.74948	2.07E+10
Q86Y39;K7EQ77;	Q86Y39;K7EQ77;	NADH dehydroge	NDUFA11	3	3	141	0	12.51	1.1286	0.27701	1.75E+08
P53992;G5EA31;	P53992;G5EA31	Protein transport	SEC24C	26	25	1094	0	205.63	1.1284	0.78109	7.27E+09
P27348;E9PG15	P27348;E9PG15	14-3-3 protein th	YWHAQ	16	11	245	0	213.66	1.1278	0.4471	7.84E+08
Q9Y2A7;Q9Y2A7-	Q9Y2A7;Q9Y2A7-	Nck-associated pr	NCKAP1	35	35	1128	0	192.68	1.1275	1.0134	5.14E+09
Q66K14-2;Q66K1	Q66K14-2;Q66K1	TBC1 domain fam	TBC1D9B	14	14	1233	0	83.365	1.1273	0.86604	8.77E+08
P38935	P38935	DNA-binding prot	IGHMBP2	3	3	993	0	22.298	1.127	0.9549	2.03E+08
Q9Y263;E5RIM3;I	Q9Y263;E5RIM3	Phospholipase A-	PLAA	33	33	795	0	323.31	1.127	0.92662	6.80E+09
F5H452;Q5JSB6;(	F5H452;Q5JSB6;(	Transcription fact	TFDP1	1	1	119	0	18.008	1.1269	NaN	2.28E+08
P58107	P58107	Epiplakin	EPPK1	38	2	5090	0	323.31	1.1269	0.79171	1.48E+09
P31323	P31323	cAMP-dependent	PRKAR2B	6	3	418	0	20.603	1.1266	0.83316	3.28E+08
Q5SRQ6;P67870;	Q5SRQ6;P67870;	Casein kinase II su	CSNK2B;CSNK2B-	7	7	234	0	45.25	1.1263	0.62915	1.09E+09
Q8N684-2;Q8N68	Q8N684-2;Q8N6	Cleavage and poly	CPSF7	15	15	462	0	137.33	1.1263	0.903	4.05E+09
Q709C8-4;Q709C	Q709C8-4;Q709C	Vacuolar protein	VPS13C	18	18	3585	0	111.92	1.126	0.92634	9.71E+08
H0Y7L2;Q96N67-	H0Y7L2;Q96N67-	Dedicator of cyto	DOCK7	68	62	2129	0	323.31	1.1257	0.95103	4.46E+09
O96017;O96017	O96017;O96017	Serine/threonine	CHEK2	10	10	543	0	48.672	1.1257	NaN	4.01E+08
Q9GZT3-2;Q9GZT	Q9GZT3-2;Q9GZT	SRA stem-loop-int	SLIRP	10	10	107	0	58.573	1.1248	0.9183	3.06E+09
Q9NXR7-4;Q9NX	Q9NXR7-4;Q9NX	BRCA1-A complex	BRE	6	6	376	0	48.203	1.1246	0.90529	2.39E+09
Q15843;F8VSA6;I	Q15843;F8VSA6;I	NEDD8	NEDD8;NEDD8-M	3	3	81	0	44.66	1.1242	0.63858	2.41E+09
P06730;P06730-	P06730;P06730-	Eukaryotic transl	EIF4E	9	9	217	0	71.73	1.1241	0.75933	4.74E+09
Q9H0C8;F8SNU7;	Q9H0C8;F8SNU7;	Integrin-linked ki	ILKAP;ILKAP3	14	14	392	0	71.191	1.1239	0.91079	2.56E+09
Q6PJG6;Q6PJG6-	Q6PJG6	BRCA1-associated	BRAT1	5	5	821	0	64.48	1.1238	1.15	3.40E+08
Q9H6T3;Q9H6T3	Q9H6T3;Q9H6T3	RNA polymerase I	RPAP3	12	12	665	0	99.226	1.1238	0.79505	1.03E+09
P61586;C9JNR4;I	P61586;C9JNR4;I	Transforming pro	RHOA	10	5	193	0	115.27	1.1237	1.0169	1.71E+09
O95905-2;O9590	O95905-2;O9590	Protein SGT1	ECD	3	3	601	0	18.119	1.1236	NaN	4.05E+07
Q86XP3;A0A0A0I	Q86XP3;A0A0A0I	ATP-dependent RI	DDX42	25	25	938	0	140.28	1.1235	0.78948	3.26E+09
Q9UBD5;Q9UBD5	Q9UBD5;Q9UBD5	Origin recognitio	ORC3	9	9	711	0	61.964	1.1235	0.99223	6.35E+08
Q8WUM0	Q8WUM0	Nuclear pore com	NUP133	43	43	1156	0	323.31	1.123	0.80506	8.75E+09
Q5HYI8;C9JXM3;I	Q5HYI8;C9JXM3;I	Rab-like protein 3	RABL3	8	8	236	0	105.4	1.1229	0.72913	6.18E+08
Q9H267;F5H008;	Q9H267;F5H008;	Vacuolar protein	VPS33B	14	14	617	0	56.696	1.1229	NaN	1.14E+09
Q9P2D1;Q9P2D1	Q9P2D1	Chromodomain-h	CHD7	9	5	2997	0	14.332	1.1229	0.82196	1.60E+08
Q658Y4;E7ER68;(	Q658Y4;E7ER68	Protein FAM91A1	FAM91A1	9	9	838	0	39.389	1.1228	0.84332	6.47E+08
Q14166;V9GY16	Q14166	Tubulin--tyrosine	TTLL12	20	20	644	0	153.27	1.1224	0.66492	2.29E+09
Q05048;A0A0A0I	Q05048;A0A0A0I	Cleavage stimulat	CSTF1	14	14	431	0	323.31	1.1222	0.71899	5.58E+09
Q13049;Q5JVY0	Q13049;Q5JVY0	E3 ubiquitin-prot	TRIM32	2	2	653	0	10.945	1.122	NaN	6.13E+07
Q9H1P3-2;Q9H1I	Q9H1P3-2;Q9H1I	Oxysterol-binding	OSBPL2	6	6	468	0	13.303	1.1213	4.4752	3.50E+08
P0DN76;Q01081	P0DN76;Q01081	Splicing factor U2	U2AF1	9	9	240	0	101.24	1.1206	0.72232	3.17E+09
P26641;P26641-	P26641;P26641-	Elongation factor	EEF1G	34	34	437	0	323.31	1.1198	0.84475	1.06E+11
Q5QPK2;H0Y368;	Q5QPK2;H0Y368;	Dolichol-phospha	DPM1	13	13	287	0	122.45	1.119	0.89987	4.95E+09
P40616-2;P4061	P40616-2;P4061	ADP-ribosylation	ARL1	9	9	164	0	83.711	1.1189	0.84573	2.81E+09
Q9Y4W6;K7EP56	Q9Y4W6	AFG3-like protein	AFG3L2	28	27	797	0	273.98	1.1187	0.72911	3.87E+09
Q9Y5Y2;H3BNF0;	Q9Y5Y2;H3BNF0;	Cytosolic Fe-S clu	NUBP2	9	9	271	0	82.349	1.1184	0.8722	2.50E+09
P49207	P49207	60S ribosomal pr	RPL34	5	5	117	0	14.861	1.1181	0.82416	2.03E+09
P62318-2;P6231	P62318-2;P6231	Small nuclear ribo	SNRPD3	5	5	120	0	161.15	1.118	0.9455	1.41E+10
Q13451;Q13451	Q13451	Peptidyl-prolyl ci	FKBP5	23	23	457	0	289.29	1.1179	0.63055	3.38E+09
F5H5P2;P12694;	F5H5P2;P12694;	2-oxoisovalerate	BCKDHA	4	4	479	0	41.55	1.1176	0.81144	3.44E+08
Q86WA6;Q86WA	Q86WA6;Q86WA	Valacyclovir hydr	BPHL	6	6	291	0	17.63	1.1172	0.69224	5.31E+08
P19784;H3BSA1;	P19784;H3BSA1	Casein kinase II su	CSNK2A2	10	10	350	0	80.933	1.1171	0.84849	1.60E+09
P46821;D6RA32;	P46821	Microtubule-asso	MAP1B	18	17	2468	0	177.18	1.1169	0.83171	1.60E+09
Q8WWY3;E7EVX8	Q8WWY3;E7EVX8	U4/U6 small nucl	PRPF31	13	13	499	0	102.82	1.1167	NaN	1.50E+09
B4DXW1;P61158	B4DXW1;P61158	Actin-related pro	ACTR3	17	17	367	0	151.97	1.1165	0.80466	6.78E+09
H7C147;H7C3W1	H7C147;H7C3W1	Non-syndromic h	DFNA5	1	1	192	0	4.7876	1.1162	NaN	1.50E+07
Q9UBN7;Q9UBN7	Q9UBN7;Q9UBN7	Histone deacetyla	HDAC6	5	5	1215	0	47.414	1.1162	0.70276	3.28E+08
Q6ZN17	Q6ZN17	Protein lin-28 ho	LIN28B	3	3	250	0	17.116	1.1161	1.1748	4.72E+08
Q13185;S4R2Y4;	Q13185;S4R2Y4	Chromobox prote	CBX3	5	4	183	0	42.814	1.116	0.82108	2.01E+09
O43264;O43264	O43264;O43264	Centromere/kine	ZW10	9	9	779	0	97.594	1.1154	0.90923	8.10E+08
A0A0D9SF70;G5E	A0A0D9SF70;G5E	ADP-ribosylation	ARFGAP2	6	5	385	0	30.071	1.1153	NaN	3.01E+08
P23921;E9PL69;I	P23921;E9PL69	Ribonucleoside-d	RRM1	26	26	792	0	275.28	1.1151	0.8449	6.73E+09
E9PGC0;P20936-	E9PGC0;P20936-	Ras GTPase-activa	RASA1	7	7	881	0	35.782	1.115	0.71637	3.50E+08
P35573;P35573-	P35573;P35573-	Glycogen debranc	AGL	68	68	1532	0	323.31	1.115	0.83849	1.14E+10
A0A0R4J2F6;Q12	A0A0R4J2F6;Q12	Interferon-relate	IFRD2	6	6	442	0	20.928	1.1144	0.84952	4.09E+08
A0A024QZX5;A0/	A0A024QZX5;A0/	Serpin B6	SERPINB6	8	8	380	0	39.819	1.1142	0.93044	7.69E+08
C9JRZ6;F8WAR4;	C9JRZ6;F8WAR4;	MICOS complex s	CHCHD3	8	8	232	0	39.995	1.1141	0.38642	2.95E+08
Q9NX08	Q9NX08	COMM domain-co	COMMD8	3	3	183	0	29.618	1.114	0.66606	1.09E+09
P18031;B4DSN5	P18031;B4DSN5	Tyrosine-protein	PTPN1	13	13	435	0	56.476	1.1139	1.2984	2.47E+09
H0Y4Z8;Q3YEC7;(	H0Y4Z8;Q3YEC7;(	Rab-like protein 6	RABL6	3	3	730	0	19.997	1.1137	0.96804	2.65E+08
O15047;C9J2Z9	O15047	Histone-lysine N-	SETD1A	12	11	1707	0	51.97	1.1137	0.73537	5.05E+08
Q9P2J5;Q9P2J5-;	Q9P2J5;Q9P2J5-;	Leucine--tRNA lig	LARS	62	62	1176	0	323.31	1.1131	0.94137	3.58E+10
P21796;C9JI87	P21796;C9JI87	Voltage-depender	VDAC1	18	18	283	0	323.31	1.113	0.95191	1.25E+10
P49915;P49915-	P49915;P49915-	GMP synthase [gl	GMPS	46	46	693	0	323.31	1.1126	0.60898	1.51E+10
Q8WWM7-6;Q8V	Q8WWM7-6;Q8V	Ataxin-2-like prot	ATXN2L	13	13	968	0	81.915	1.1122	1.5503	5.10E+08
P52948-5;P5294	P52948-5;P5294	Nuclear pore com	NUP98	29	29	1800	0	287.9	1.1121	0.86924	4.16E+09
P31749-2;P3174	P31749-2;P3174	RAC-alpha serine/	AKT1	5	5	418	0	20.893	1.1112	NaN	1.80E+08
Q5VTR2;C9JWJ4;	Q5VTR2	E3 ubiquitin-prot	RNF20	19	16	975	0	181.05	1.111	0.80254	9.48E+08
Q9BTZ2-8;Q9BTZ	Q9BTZ2-8;Q9BTZ	Dehydrogenase/r	DHRS4	7	7	226	0	21.531	1.1109	0.76086	1.21E+09
Q9H2U1;Q9H2U1	Q9H2U1;Q9H2U1	ATP-dependent RI	DHX36	29	28	1008	0	215.14	1.1109	0.98592	4.23E+09
Q9C0C9;K7ES11;I	Q9C0C9;K7ES11	E2/E3 hybrid ubic	UBE2O	23	23	1292	0	167.97	1.1107	0.90397	2.47E+09
Q12933-4;Q1293	Q12933-4;Q1293	TNF receptor-asso	TRAF2	5	5	476	0	21.572	1.1106	NaN	2.30E+08
Q15555-5;Q1555	Q15555-5;Q1555	Microtubule-asso	MAPRE2	14	14	284	0	283.39	1.1106	0.74931	4.37E+09
P09543-2;P0954	P09543-2;P0954	2,3-cyclic-nucleo	CNP	20	20	401	0	118.86	1.1104	0.95569	1.99E+09
A6PW57;Q99755	A6PW57;Q99755	Phosphatidylinos	PIP5K1A	7	3	550	0	20.658	1.1102	NaN	1.99E+08
Q4G0F5;H0YCI7	Q4G0F5	Vacuolar protein	VPS26B	5	4	336	0	13.425	1.1096	1.2969	3.00E+08

Q8NEC7;D6R9W2	Q8NEC7;D6R9W2	Glutathione S-tra	GSTCD	7	7	633	0	17.503	1.1096	NaN	1.52E+08
Q9H553;Q9H553	Q9H553;Q9H553	Alpha-1,3/1,6-ma	ALG2	7	7	416	0	22.286	1.1091	0.97289	3.21E+08
Q9NSD9;Q9NSD9	Q9NSD9;Q9NSD9	Phenylalanine--tR	FARSB	19	19	589	0	202.17	1.1091	0.61221	3.97E+09
Q6KCM7;Q6KCM	Q6KCM7;Q6KCM	Calcium-binding	SLC25A25	3	3	469	0	9.041	1.109	0.76956	5.66E+07
P19174;P19174-	P19174;P19174-	1-phosphatidylin	PLCG1	22	22	1290	0	229.36	1.1088	0.78864	1.21E+09
O75717;O75717-	O75717;O75717-	WD repeat and HI	WDHD1	28	28	1129	0	323.31	1.1087	0.88306	1.73E+09
Q08752	Q08752	Peptidyl-prolyl ci	PPID	3	3	370	0	8.3734	1.1085	0.59996	1.41E+08
Q99959-2;Q9995	Q99959-2;Q9995	Plakophilin-2	PKP2	4	4	837	0	7.7318	1.1078	1.665	3.59E+07
A0A087WXC5;E7	A0A087WXC5;E7	NADH dehydroge	NDUFA10	12	12	355	0	112.08	1.1077	0.83522	6.55E+09
Q14232;F5H0D0;	Q14232;F5H0D0;	Translation initia	EIF2B1	15	15	305	0	118.4	1.1069	0.73135	4.70E+09
Q8N584-2;Q8N5	Q8N584-2;Q8N5	Tetratricopeptide	TTC39C	7	7	522	0	35.448	1.1069	NaN	1.91E+08
Q96L91-3;Q96L9	Q96L91-3;Q96L9	E1A-binding prot	EP400	14	14	3086	0	59.434	1.1067	0.74827	7.56E+08
P62380;Q7Z6U2;	P62380;Q7Z6U2	TATA box-binding	TBPL1	3	3	186	0	51.751	1.1065	0.7882	4.60E+08
P47985;P0C7P4	P47985;P0C7P4	Cytochrome b-c1	UQCRFS1;UQCRF	11	11	274	0	166.81	1.1064	0.69216	3.48E+09
Q9NXW2;J3KPS0	Q9NXW2;J3KPS0	DnaJ homolog sul	DNAJB12	8	8	375	0	27.062	1.1063	0.57434	2.71E+08
G3V0I5;P49821-;	G3V0I5;P49821-;	NADH dehydroge	NDUFV1	6	6	457	0	16.566	1.1062	NaN	1.78E+08
A2RTX5;A2RTX5-;	A2RTX5;A2RTX5-;	Probable threoni	TARSL2	13	9	802	0	30.16	1.1061	1.0291	4.36E+08
O95376;C9JZ71;(	O95376	E3 ubiquitin-prot	ARIH2	11	11	493	0	165.29	1.1057	NaN	9.38E+08
Q13363;Q13363-	Q13363;Q13363-	C-terminal-bindir	CTBP1	16	11	440	0	142.83	1.1056	0.91589	4.61E+09
P52597	P52597	Heterogeneous nu	HNRNPF	16	14	415	0	323.31	1.1049	0.91734	1.93E+10
B3KS98;O15372;	B3KS98;O15372;	Eukaryotic transl	EIF3S3;EIF3H	12	12	366	0	110.84	1.1047	0.84824	3.11E+09
Q5JVF3-3;Q5JVF3	Q5JVF3-3;Q5JVF3	PCI domain-cont	PCID2	15	15	376	0	180.76	1.1039	0.80382	1.57E+09
Q5VVQ6-2;Q5VV	Q5VVQ6-2;Q5VV	Ubiquitin thioest	YOD1	9	9	304	0	57.946	1.1037	0.83657	9.19E+08
P26373;P26373-	P26373;P26373-	60S ribosomal pr	RPL13	19	19	211	0	114.51	1.1036	1.0058	1.12E+10
Q01813;Q01813-	Q01813;Q01813-	ATP-dependent 6-	PFKP	37	32	784	0	323.31	1.1034	0.86713	2.88E+10
Q8IZH2-2;Q8IZH2	Q8IZH2-2;Q8IZH2	5-3 exoribonucle	XRN1	23	23	1694	0	105.66	1.1032	0.77621	1.77E+09
O75925;O75925-	O75925;O75925-	E3 SUMO-protein	PIAS1	4	3	651	0	69.49	1.103	NaN	2.19E+08
Q8N5X7-2;Q8N5	Q8N5X7-2;Q8N5	Eukaryotic transl	EIF4E3	2	2	118	0	6.7361	1.1028	NaN	1.66E+07
Q14690;S4R3Q4	Q14690	Protein RRP5 hon	PDCD11	67	67	1871	0	323.31	1.1027	0.97928	9.65E+09
F5H702;Q96GC5-	F5H702;Q96GC5-	39S ribosomal pr	MRPL48	5	5	113	0	32.718	1.1023	0.36086	3.05E+08
Q9UPU5	Q9UPU5	Ubiquitin carbox	USP24	35	35	2620	0	323.31	1.1023	0.8234	3.47E+09
Q9UQ80;Q9UQ8(	Q9UQ80;Q9UQ8(	Proliferation-assc	PA2G4	31	31	394	0	323.31	1.1023	0.86033	3.01E+10
Q5VV42-2;Q5VV4	Q5VV42-2;Q5VV4	Threonylcarbamc	CDKAL1	3	3	488	0	18.197	1.1021	NaN	1.36E+08
Q9UBB9;Q9UBB9	Q9UBB9	Tuftelin-interacti	TFIP11	16	16	837	0	86.748	1.1008	0.87693	1.28E+09
H0YBR0;Q96Q05-	H0YBR0;Q96Q05-	Trafficking protei	TRAPPC9	3	3	992	0	6.4994	1.1007	5.7822	1.88E+08
Q9BZE2;E9PNY6;I	Q9BZE2	tRNA pseudouridi	PUS3	3	3	481	0	6.6982	1.0999	0.86085	1.37E+08
H7C1E4;P61966;	H7C1E4;P61966;	AP-1 complex sub	AP1S1	2	2	191	0	52.586	1.0998	0.84615	4.78E+08
O75150;H3BP71;	O75150;H3BP71;	E3 ubiquitin-prot	RNF40	25	22	1001	0	166.63	1.0996	0.78992	1.02E+09
Q9GZT9-2;Q9GZT	Q9GZT9-2;Q9GZT	Egl nine homolog	EGLN1	7	7	404	0	39	1.0995	0.69495	3.77E+08
Q5SY16	Q5SY16	Polynucleotide 5-	NOL9	15	15	702	0	133.45	1.0993	1.0531	2.31E+09
Q9Y5A9;A0A087\	Q9Y5A9;A0A087\	YTH domain-cont	YTHDF2	15	11	579	0	183.97	1.0992	0.96554	1.86E+09
Q14156-2;Q1415	Q14156-2;Q1415	Protein EFR3 hon	EFR3A	5	5	785	0	60.103	1.0987	1.0898	3.16E+08
Q14689-6;Q1468	Q14689-6;Q1468	Disco-interacting	DIP2A	3	2	1567	0	7.8892	1.0985	1.2429	7.69E+07
J9JIC5;Q9HAS0;J	J9JIC5;Q9HAS0;J	Protein Njmu-R1	C17orf75	5	5	396	0	12.584	1.0984	1.093	4.37E+08
P25205;P25205-	P25205;P25205-	DNA replication li	MCM3	52	52	808	0	323.31	1.098	0.91541	2.36E+10
Q8NAF0	Q8NAF0	Zinc finger protei	ZNF579	3	3	562	0	35.395	1.0975	NaN	2.46E+07
Q14CX7-2;Q14CX	Q14CX7-2;Q14CX	N-alpha-acetyltra	NAA25	3	3	859	0	9.019	1.0973	NaN	1.22E+08
Q9NVQ4;Q9NVQ4	Q9NVQ4;Q9NVQ4	Fas apoptotic inh	FAIM	9	9	179	0	52.424	1.0971	0.80777	1.04E+09
Q5VIR6-4;Q5VIR6	Q5VIR6-4;Q5VIR6	Vacuolar protein	VPS53	11	11	832	0	38	1.097	0.93359	7.26E+08
Q9UI12-2;Q9UI1:	Q9UI12-2;Q9UI1:	V-type proton ATI	ATP6V1H	12	12	465	0	114.85	1.0969	0.91737	1.78E+09
I3L397;I3L504;P(	I3L397;I3L504;P(	Eukaryotic transl	EIF5A;EIF5AL1;EIF	15	7	147	0	323.31	1.0967	0.76415	1.81E+10
C9JP03;Q5T6P2;(	C9JP03;Q5T6P2;(	SLAIN motif-cont	SLAIN1	2	2	99	0	9.063	1.0963	NaN	9.86E+06
Q13325-2;Q1332	Q13325-2;Q1332	Interferon-induce	IFIT5	3	3	434	0	20.402	1.0956	0.82935	3.07E+08
Q9H7Z7;X6RJ95;,	Q9H7Z7	Prostaglandin E s	PTGES2	7	7	377	0	72.999	1.0955	0.87653	7.24E+08
A0A096LNH6;Q1	A0A096LNH6;Q1	Dedicator of cyto	DOCK1	5	5	1886	0	23.521	1.095	1.2765	1.46E+08
Q96I24;Q96I24-2	Q96I24	Far upstream elen	FUBP3	25	21	572	0	300.11	1.0949	1.0502	3.11E+09
Q9Y3F4;Q9Y3F4-;	Q9Y3F4;Q9Y3F4-;	Serine-threonine	STRAP	17	17	350	0	121.45	1.0946	1.1082	3.31E+09
Q6GMV2;E2QRN9	Q6GMV2	SET and MYND do	SMYD5	4	4	418	0	44.08	1.094	0.83454	6.93E+08
Q59GN2;P62891	Q59GN2;P62891	Putative 60S ribo	RPL39P5;RPL39	2	2	51	0	5.4106	1.0939	NaN	3.12E+08
Q9H6S0;D6RA70;	Q9H6S0;D6RA70	Probable ATP-dep	YTHDC2	18	18	1430	0	93.498	1.0939	1.1909	9.45E+08
P29144;Q5VZU9	P29144;Q5VZU9	Tripeptidyl-peptic	TPP2	31	31	1249	0	323.31	1.0938	0.85239	3.22E+09
O75694-2;O7569	O75694-2;O7569	Nuclear pore com	NUP155	44	44	1332	0	323.31	1.0937	0.86957	1.03E+10
Q9HCE5;A0A0D9	Q9HCE5	N6-adenosine-me	METTL14	5	5	456	0	47.856	1.0934	NaN	2.49E+08
Q92845-2;Q9284	Q92845-2;Q9284	Kinesin-associate	KIFAP3	5	4	748	0	153.47	1.0933	0.57407	4.00E+08
Q9NUU7;I3L0H8;	Q9NUU7;I3L0H8;	ATP-dependent RI	DDX19A	26	4	478	0	275.45	1.0932	0.83782	8.24E+09
Q86Y56;Q86Y56-	Q86Y56;Q86Y56-	HEAT repeat-cont	HEATR2	19	19	855	0	262.36	1.0928	1.0414	2.89E+09
O95714;A0A0J9Y	O95714;A0A0J9Y	E3 ubiquitin-prot	HERC2	11	11	4834	0	35.362	1.0927	2.1181	2.73E+08
P49790-2;P4979	P49790-2;P4979	Nuclear pore com	NUP153	4	4	1433	0	8.5446	1.0921	0.68987	1.07E+08
O00273;O00273-	O00273;O00273-	DNA fragmentatic	DFFA	7	7	331	0	45.046	1.0919	0.65738	9.28E+08
Q8NC60	Q8NC60	Nitric oxide-assoc	NOA1	2	2	698	0	16.988	1.0917	NaN	6.91E+07
P61081;M0QX69	P61081	NEDD8-conjugati	UBE2M	12	12	183	0	73.213	1.0916	0.71985	6.71E+09
Q9UJW0;Q9UJW	Q9UJW0;Q9UJW	Dynactin subunit	DCTN4	13	13	460	0	85.725	1.0912	NaN	1.38E+09
P42574;C9JXR7;/	P42574;C9JXR7;/	Caspase-3;Caspas	CASP3	7	7	277	0	28.837	1.0909	1.8737	4.84E+08
P48444;B0YIW6;	P48444;B0YIW6;	Coatomer subuni	ARCN1	33	33	511	0	229.22	1.0907	0.66823	7.96E+09
P22830;P22830-	P22830;P22830-	Ferrochelatase, m	FECH	13	13	423	0	66.029	1.0905	0.84641	1.71E+09
Q86W56-3;Q86W	Q86W56-3;Q86W	Poly(ADP-ribose)	PARG	5	5	868	0	24.301	1.0899	1.0344	4.00E+08
Q13158	Q13158	FAS-associated de	FADD	3	3	208	0	10.428	1.0897	0.98026	2.19E+08
B0QYK0;Q01844-	B0QYK0;Q01844-	RNA-binding prot	EWSR1	2	2	618	0	37.32	1.0892	1.0534	1.55E+08
P48047;H7C0C1;	P48047;H7C0C1	ATP synthase sub	ATP5O	12	12	213	0	132.81	1.0889	0.7087	6.33E+09
O00186	O00186	Syntaxin-binding	STXBP3	12	12	592	0	102.05	1.0887	NaN	9.34E+08
Q9BXS5;Q9BXS5-	Q9BXS5;Q9BXS5-	AP-1 complex sub	AP1M1	14	14	423	0	100.12	1.0885	0.80517	3.63E+09
I3L112;P52429	I3L112;P52429	Diacylglycerol kin	DGKE	3	3	456	0	7.9998	1.0883	NaN	9.46E+07
E7ESP9;P07197;E	E7ESP9;P07197;E	Neurofilament m	NEFM	23	21	877	0	228.09	1.0879	1.1815	2.36E+09
K7EM73;K7ELJ7;/	K7EM73;K7ELJ7;/	Calpain small sub	CAPNS1	3	3	163	0	23.21	1.0876	0.6146	2.06E+08
Q9H974-2;Q9H9	Q9H974-2;Q9H9	Queuine tRNA-rib	QTRTD1	6	6	292	0	39.035	1.0876	1.1143	9.95E+08
Q6IBS0;D6RG15;I	Q6IBS0;D6RG15	Twinfilin-2	TWF2	7	6	349	0	85.832	1.0873	0.40249	1.02E+09
O15084;O15084-	O15084;O15084-	Serine/threonine-	ANKRD28	10	10	1053	0	41.967	1.0872	0.95558	4.91E+08
M0QXB4;O14579	M0QXB4;O14579	Coatomer subuni	COPE	17	17	331	0	323.31	1.0866	0.77879	1.34E+10
Q9Y2Q9;H0YAT2;	Q9Y2Q9;H0YAT2;	28S ribosomal pr	MRPS28	4	4	187	0	12.414	1.0864	1.044	1.20E+09
Q9Y4K3	Q9Y4K3	TNF receptor-assc	TRAF6	7	7	522	0	30.918	1.0862	NaN	4.27E+08
Q7L2E3-2;H7BXY	Q7L2E3-2;H7BXY	Putative ATP-dep	DHX30	54	54	1222	0	323.31	1.0858	1.0008	8.62E+09
Q01085-2	Q01085-2	Nucleolysin TIAR	TIAL1	13	3	392	0	93.687	1.0851	1.3944	2.29E+09
Q96EK5;A0A0D9	Q96EK5	KIF1-binding prot	KIAA1279	16	16	621	0	168.91	1.085	1.9668	2.26E+09
P54098;A0A0D9	P54098	DNA polymerase s	POLG	6	6	1239	0	51.719	1.0847	1.0487	1.53E+08
Q8TF05-2;Q8TF0	Q8TF05-2;Q8TF0	Serine/threonine-	PPP4R1	7	7	933	0	19.553	1.0845	0.60176	3.46E+08
H3BPK3;H3BPQ4	H3BPK3;H3BPQ4	Hydroxyacylgluta	HAGH	2	2	239	0	9.9643	1.0839	0.88782	8.33E+07
Q9NPF5;Q5TG40;	Q9NPF5;Q5TG40	DNA methyltransf	DMAP1	5	5	467	0	60.124	1.0839	NaN	1.82E+08
E7EPM6;P33121-	E7EPM6;P33121-	Long-chain-fatty-	ACSL1	6	6	664	0	14.016	1.0837	NaN	3.04E+08
Q969S9-3;Q969S	Q969S9-3;Q969S	Ribosome-releasi	GFM2	15	15	777	0	84.475	1.0833	0.69161	9.47E+08
Q8N1F7;H3BVG0	Q8N1F7;H3BVG0	Nuclear pore com	NUP93	52	52	819	0	323.31	1.0831	0.86049	1.48E+10
B8ZZG1;Q9NZW5	B8ZZG1;Q9NZW5	MAGUK p55 subfa	MPP6	3	2	428	0	11.094	1.0828	NaN	1.55E+08
P57740;P57740-	P57740;P57740-	Nuclear pore com	NUP107	32	32	925	0	299.5	1.0828	0.86331	6.36E+09
Q9Y5L0-3;Q9Y5L(	Q9Y5L0-3;Q9Y5L(	Transportin-3	TNPO3	13	13	909	0	169.44	1.0824	0.85656	1.75E+09
E9PF19;Q9Y4P3;(	E9PF19;Q9Y4P3;(	Transducin beta-l	TBL2	11	11	411	0	81.933	1.0821	0.82837	8.20E+08

A8MX75;P18074	A8MX75;P18074	TFIIH basal transc	ERCC2	9	9	706	0	55.262	1.0819	0.81805	9.78E+08
P06132;Q5T446;	P06132;Q5T446;	Uroporphyrinoge	UROD	13	13	367	0	195.09	1.0819	0.76635	4.70E+09
Q9BVG4;A6NDF3	Q9BVG4;A6NDF3	Protein PBDC1	PBDC1	6	6	233	0	20.086	1.0819	1.084	6.48E+08
A6NIW2;Q5JSL3;/	A6NIW2;Q5JSL3;/	Dedicator of cyto	DOCK11	32	31	2077	0	214.98	1.0815	0.83919	1.81E+09
A2ABE9;H7C2J4;/	A2ABE9;H7C2J4;/	MutS protein hon	MSH5	2	2	333	0.0047405	2.4123	1.0814	0.74998	3.96E+08
P06493;A0A024(	P06493;A0A024(	Cyclin-dependent	CDK1;CDC2	20	18	297	0	205.41	1.0809	0.71204	9.03E+09
Q9Y4W2-2;Q9Y4\	Q9Y4W2-2;Q9Y4\	Ribosomal bioger	LAS1L	17	17	717	0	133.32	1.0808	1.055	3.95E+09
Q9NV31	Q9NV31	U3 small nucleola	IMP3	7	7	184	0	56.617	1.0803	1.3187	1.14E+09
A0A0D9SF60;Q9	A0A0D9SF60;Q9	Plakophilin-4	PKP4	2	2	1208	0	7.1673	1.0801	NaN	3.61E+07
P14618;P14618-	P14618;P14618-	Pyruvate kinase P	PKM	56	5	531	0	323.31	1.08	0.83229	1.17E+11
Q6PD62;H0YCE8	Q6PD62	RNA polymerase-a	CTR9	17	17	1173	0	159.29	1.079	1.0499	1.65E+09
Q9Y613;J3KTH7	Q9Y613	FH1/FH2 domain-	FHOD1	9	9	1164	0	40.004	1.0789	1.1111	3.35E+08
A0A087WWP4;Q	A0A087WWP4;Q	Putative RNA-bin	RBM15	16	15	933	0	92.743	1.0783	0.60495	1.45E+09
Q9BWF3;E9PB51	Q9BWF3;E9PB51	RNA-binding prot	RBM4	12	0	364	0	147.7	1.0782	0.8713	3.57E+09
Q12931-2;Q1293	Q12931-2;Q1293	Heat shock protei	TRAP1	25	25	651	0	267.54	1.0775	2.4093	4.94E+09
Q9NRL2-2;Q9NRL	Q9NRL2-2;Q9NRL	Bromodomain ad	BAZ1A	24	24	1524	0	187.88	1.0775	0.84782	9.65E+08
A0A067XG54;Q8I	A0A067XG54;Q8I	Phospholipid-tra	ATP11C	6	6	1113	0	30.622	1.0772	0.76738	2.96E+08
Q15366-5;Q1536	Q15366-5;Q1536	Poly(rC)-binding p	PCBP2	20	0	335	0	323.31	1.0772	0.90877	3.06E+10
O75792	O75792	Ribonuclease H2 s	RNASEH2A	10	10	299	0	67.828	1.0771	0.98422	1.67E+09
P31327;P31327-	P31327;P31327-	Carbamoyl-phosp	CPS1	30	26	1500	0	208.3	1.0763	0.76301	2.60E+09
P04150-13;P041	P04150-13;P041	Glucocorticoid re	NR3C1	2	2	680	0.0028047	2.741	1.0754	NaN	8.17E+07
J3KTF8;J3QQX2;P	J3KTF8;J3QQX2;P	Rho GDP-dissocia	ARHGDIA	9	9	194	0	120.15	1.0749	0.91975	3.51E+09
O00743;O00743-	O00743;O00743-	Serine/threonine-	PPP6C	11	11	305	0	85.866	1.0749	0.85457	2.93E+09
Q6NZY4;Q6NZY4-	Q6NZY4;Q6NZY4-	Zinc finger CCHC	ZCCHC8	8	8	707	0	74.45	1.0744	0.62726	1.08E+09
P11908;P11908-	P11908;P11908-	Ribose-phosphate	PRPS2	21	9	318	0	103.38	1.0739	0.97226	2.54E+09
P49137;P49137-	P49137;P49137-	MAP kinase-activa	MAPKAPK2	4	3	400	0	9.6068	1.0737	1.0101	2.23E+08
C9J6A7;Q96AT9-5	C9J6A7;Q96AT9-5	Ribulose-phospha	RPE;RPEL1	3	3	159	0	13.921	1.0736	0.75397	5.96E+08
Q9BQ52;Q9BQ52	Q9BQ52;Q9BQ52	Zinc phosphodies	ELAC2	35	35	826	0	323.31	1.0725	0.76365	7.28E+09
Q9UL25	Q9UL25	Ras-related protei	RAB21	11	11	225	0	99.716	1.0717	0.8584	3.68E+09
H3BTB7;Q5JPH6;	H3BTB7;Q5JPH6;	Probable glutama	EARS2	14	14	506	0	41.249	1.0709	0.7007	1.78E+09
O00232;O00232-	O00232;O00232-	26S proteasome r	PSMD12	23	23	456	0	209.38	1.0709	0.96149	7.11E+09
Q5JTZ9;A0A087W	Q5JTZ9	Alanine--tRNA liga	AARS2	29	29	985	0	229.69	1.0706	0.80085	2.84E+09
Q9UHB6;Q9UHB6	Q9UHB6;Q9UHB6	LIM domain and a	LIMA1;TRMT1	23	23	759	0	215.78	1.0706	0.79149	1.59E+09
Q8IY18	Q8IY18	Structural mainte	SMC5	10	10	1101	0	47.355	1.0705	0.89538	6.07E+08
A0A0B4J1W0;O7	A0A0B4J1W0;O7	Mediator of RNA p	MED24	4	4	1014	0	17.08	1.0704	1.2299	1.72E+08
E9PMP7;E9PMS6	E9PMP7;E9PMS6	LIM domain only	LMO7	5	5	1046	0	22.991	1.0702	0.62818	1.54E+08
P82912-2;P8291	P82912-2;P8291	28S ribosomal pr	MRPS11	4	4	193	0	18.648	1.0702	0.76914	4.18E+08
Q8ND24;Q8ND24	Q8ND24;Q8ND24	RING finger prote	RNF214	5	5	703	0	15.234	1.0701	NaN	2.16E+08
Q9UI26;F8WDV0	Q9UI26;F8WDV0	Importin-11	IPO11	14	14	975	0	223.86	1.0701	0.92683	1.73E+09
P49458;E9PE20;I	P49458	Signal recognitio	SRP9	6	6	86	0	13.978	1.07	0.88891	1.04E+08
P19623;K7EKM4;	P19623	Spermidine synth	SRM	14	14	302	0	260.46	1.0699	0.83547	1.23E+10
P04350;M0R278	P04350	Tubulin beta-4A c	TUBB4A	34	4	444	0	222.42	1.0691	0.97182	6.43E+09
Q9BSD7;Q5TDF0	Q9BSD7;Q5TDF0	Cancer-related nu	NTPCR	7	7	190	0	34.969	1.0691	0.90354	3.65E+09
D6REX3;O94979-	D6REX3;O94979-	Protein transport	SEC31A	36	36	1251	0	283.86	1.069	0.88831	5.69E+09
O75600;O75600-	O75600;O75600-	2-amino-3-ketobu	GCAT	7	7	419	0	55.214	1.0687	1.1817	1.09E+09
Q13619;A0A0A0I	Q13619;A0A0A0I	Cullin-4A	CUL4A	16	4	759	0	18.952	1.0684	4.9467	2.00E+08
O95298;O95298-	O95298;O95298-	NADH dehydroge	NDUFC2;NDUFC2	6	6	119	0	21.93	1.0683	0.48155	1.41E+08
Q9BXW6;Q9BXW	Q9BXW6	Oxysterol-binding	OSBPL1A	6	6	950	0	19.461	1.0683	0.71218	1.44E+08
O14925;Q5SRD1;	O14925;Q5SRD1	Mitochondrial im	TIMM23;TIMM23	7	7	209	0	69.59	1.0677	0.91341	2.05E+09
Q9BRA2;I3L2R6;I	Q9BRA2;I3L2R6;I	Thioredoxin dom	TXNDC17	6	6	123	0	41.623	1.0676	0.79478	5.48E+09
Q14683;G8JLG1;	Q14683;G8JLG1	Structural mainte	SMC1A	71	71	1233	0	323.31	1.0674	0.91587	9.22E+09
Q9P260-2;Q9P26	Q9P260-2;Q9P26	LisH domain and	KIAA1468	5	5	1250	0	17.338	1.0674	0.93347	4.22E+08
P46060;B0QYT5;I	P46060	Ran GTPase-activa	RANGAP1	15	15	587	0	105.75	1.0673	0.87321	2.09E+09
A0A087WW06;Q	A0A087WW06;Q	Tetratricopeptide	TTC28	24	24	2354	0	128.04	1.0672	1.054	9.38E+08
P11216;H0Y4Z6	P11216	Glycogen phosph	PYGB	16	9	843	0	59.556	1.067	1.3815	1.13E+09
Q29RF7;Q29RF7-	Q29RF7	Sister chromatid	PDS5A	28	26	1337	0	323.31	1.067	0.90929	2.09E+09
Q9UHY1;F8W6G1	Q9UHY1;F8W6G1	Nuclear receptor-	NRBP1	6	6	535	0	55.667	1.0667	NaN	9.88E+08
Q8N4Q0;Q8N4Q0	Q8N4Q0	Zinc-binding alco	ZADH2	7	7	377	0	47.43	1.0664	0.81486	1.22E+09
A0A0C4DG02;F8\	A0A0C4DG02;F8\	DNA (cytosine-5)-	DNMT3A	2	2	689	0	6.4915	1.0663	NaN	2.75E+07
E5RHG8;Q15369;	E5RHG8;Q15369;	Transcription elo	TCEB1	6	6	89	0	99.623	1.0659	1.0151	1.59E+09
D3YTB5;P51617-	D3YTB5;P51617-	Interleukin-1 rece	IRAK1	10	10	708	0	148.94	1.0658	0.84475	2.91E+09
P31930	P31930	Cytochrome b-c1	UQCRC1	24	23	480	0	323.31	1.0655	0.92721	1.92E+10
Q96EK9	Q96EK9	Protein KTI12 hor	KTI12	5	5	354	0	11.532	1.0647	0.85733	2.49E+08
Q9H3U1;Q9H3U1	Q9H3U1	Protein unc-45 ho	UNC45A	41	2	944	0	323.31	1.0647	0.85637	8.02E+09
B3KQ25;K7ESG5;	B3KQ25;K7ESG5;	Proteasome activ	PSME3	4	4	193	0	32.77	1.0644	1.4899	3.94E+08
Q9P2R3;Q9P2R3-	Q9P2R3;Q9P2R3-	Ankyrin repeat an	ANKFY1	27	27	1169	0	323.31	1.0641	0.96117	3.12E+09
Q9H0D6;Q9H0D6	Q9H0D6;Q9H0D6	5-3 exoribonucle	XRN2	26	26	950	0	195.9	1.064	0.95404	3.52E+09
O14802;Q7Z755;	O14802	DNA-directed RN	POLR3A	42	41	1390	0	257.87	1.0635	0.77725	3.86E+09
B4E3T4;Q93062-2	B4E3T4;Q93062-2	RNA-binding prot	RBPMS	3	2	224	0	26.81	1.0633	NaN	1.00E+08
E9PC69;Q7KZI7-1	E9PC69;Q7KZI7-1	Serine/threonine-	MARK2	21	15	778	0	104.8	1.0623	0.64008	9.07E+08
O60524-4;O6052	O60524-4;O6052	Nuclear export m	NEMF	9	9	1034	0	20.5	1.0623	0.63524	3.33E+08
O75821;K7EL20;I	O75821;K7EL20;I	Eukaryotic transla	EIF3G	15	15	320	0	140.61	1.0621	0.21599	4.20E+09
Q9BXB4;H7C487;	Q9BXB4	Oxysterol-binding	OSBPL11	10	10	747	0	122.22	1.0618	0.79738	1.22E+09
Q86XL3;Q86XL3-	Q86XL3	Ankyrin repeat an	ANKLE2	5	5	938	0	58.157	1.0616	0.73759	9.77E+07
Q9Y5Q9;Q9Y5Q9-	Q9Y5Q9	General transcrip	GTF3C3	19	19	886	0	144.78	1.0616	1.0438	2.52E+09
P05165-3;P0516	P05165-3;P0516	Propionyl-CoA ca	PCCA	8	8	681	0	36.938	1.0615	NaN	2.73E+08
A0A087X1K9;O7!	A0A087X1K9;O7!	Acyl-protein thio	LYPLA1	6	6	166	0	21.385	1.0614	0.69854	1.97E+09
Q7Z3C6;Q7Z3C6-	Q7Z3C6;Q7Z3C6-	Autophagy-relate	ATG9A	13	13	839	0	66.235	1.061	0.97874	1.09E+09
Q9Y5K5-2;Q9Y5K	Q9Y5K5-2;Q9Y5K	Ubiquitin carboxy	UCHL5	19	19	316	0	147.05	1.0608	0.96166	5.50E+09
Q15365;H3BSP4;	Q15365	Poly(rC)-binding p	PCBP1	17	12	356	0	323.31	1.0607	0.87374	1.65E+10
Q6PJI9;Q6PJI9-2;	Q6PJI9;Q6PJI9-2;	WD repeat-contai	WDR59	8	8	974	0	45.323	1.0607	1.526	3.78E+08
P61006;P61006-	P61006;P61006-	Ras-related protei	RAB8A;RAB8B	4	2	207	0	13.452	1.0605	1.0473	8.24E+07
P23258;Q9NRH3	P23258;Q9NRH3	Tubulin gamma-1	TUBG1;TUBG2	25	25	451	0	323.31	1.0594	0.83216	1.34E+10
P51531-2;P5153	P51531-2;P5153	Probable global tr	SMARCA2	18	3	1572	0	14.318	1.0589	NaN	9.67E+07
Q15386;Q15386-	Q15386	Ubiquitin-protein	UBE3C	27	27	1083	0	166.17	1.0589	0.98406	4.04E+09
E7EN19;E7ESS2;E	E7EN19;E7ESS2;E	Mitogen-activate	MAP4K4	11	4	1272	0	30.827	1.0588	0.87129	3.86E+08
O15381;O15381-	O15381;O15381-	Nuclear valosin-c	NVL	17	17	856	0	91.561	1.0588	0.73675	2.01E+09
C9JYQ9;H0Y8C2;(	C9JYQ9;H0Y8C2;(	60S ribosomal pr	RPL22L1	5	3	121	0	19.623	1.0587	0.58084	9.24E+08
O00203-3;O0020	O00203-3;O0020	AP-3 complex sub	AP3B1	17	17	1045	0	113.45	1.0584	0.94473	1.56E+09
F8WA39;Q13613	F8WA39;Q13613	Myotubularin-rel	MTMR1	8	8	673	0	42.543	1.0582	NaN	3.64E+08
C9JLV4;O14727-5	C9JLV4;O14727-5	Apoptotic protea	APAF1	5	5	1163	0	31.504	1.0579	1.1467	1.97E+08
O75439;G3V0E4;	O75439;G3V0E4	Mitochondrial-pr	PMPCB	17	16	489	0	243.81	1.0576	0.88714	6.05E+09
P36507;G5E9C7;	P36507;G5E9C7	Dual specificity m	MAP2K2	16	10	400	0	119.31	1.0569	0.75503	2.59E+09
O60231;A0A140T	O60231;A0A140T	Putative pre-mRN	DHX16	18	17	1041	0	85.256	1.0567	1.1381	8.96E+08
Q7Z6M1;Q5T1S5;	Q7Z6M1;Q5T1S5;	Rab9 effector pro	RABEPK	4	4	372	0	26.422	1.0567	0.85229	4.09E+08
Q5VZE5;Q5VZE5-2	Q5VZE5	N-alpha-acetyltra	NAA35	12	12	725	0	56.193	1.0566	0.75275	1.40E+09
Q96CW5;Q96CW	Q96CW5;Q96CW	Gamma-tubulin c	TUBGCP3	20	20	907	0	280.66	1.0566	1.0247	2.37E+09
Q9BV20;Q9BV20	Q9BV20;Q9BV20	Methylthioribose	MRI1	18	18	369	0	131.95	1.0564	0.91046	7.85E+09
B4DGU4;P35222	B4DGU4;P35222	Catenin beta-1	CTNNB1	18	16	774	0	110.61	1.0561	0.83277	1.09E+09
Q9H2M9;Q9H2M	Q9H2M9	Rab3 GTPase-acti	RAB3GAP2	33	33	1393	0	281.43	1.0561	0.82579	3.92E+09
O95628-8;O9562	O95628-8;O9562	CCR4-NOT transc	CNOT4	2	2	639	0	37.879	1.0559	NaN	1.05E+08
Q92747;E9PF58;I	Q92747;E9PF58;I	Actin-related prot	ARPC1A	10	9	370	0	50.688	1.0551	0.80919	5.89E+08
Q9BS26	Q9BS26	Endoplasmic retic	ERP44	4	4	406	0	10.656	1.055	0.85579	6.13E+08
O94822;O94822-	O94822;O94822-	E3 ubiquitin-prot	LTN1	18	18	1766	0	124.26	1.0549	0.92969	1.52E+09

P12004	P12004	Proliferating cell ı	PCNA	16	16	261	0	312.05	1.0549	0.91019	3.08E+10
Q9BUJ2-2;Q9BUJ	Q9BUJ2-2;Q9BUJ	Heterogeneous nı	HNRNPUL1	23	23	804	0	170.84	1.0547	0.96301	2.55E+09
Q15370;Q15370·	Q15370;Q15370·	Transcription elo	TCEB2	9	9	118	0	27.85	1.0545	0.6364	1.92E+09
O75165;H0Y8Q2;	O75165	DnaJ homolog sul	DNAJC13	41	41	2243	0	192.59	1.0544	0.89105	3.04E+09
Q96J01;Q96J01-;	Q96J01;Q96J01-;	THO complex sub	THOC3	13	13	351	0	123.26	1.0543	0.90974	2.42E+09
P58557;P58557-	P58557;P58557-	Putative ribonucl	YBEY	4	4	167	0	12.433	1.0542	0.53424	3.86E+08
G5EA06;Q92552;	G5EA06;Q92552;	28S ribosomal pr	MRPS27	14	14	358	0	90.629	1.0539	1.0833	2.40E+09
O14646-2;O1464	O14646-2;O1464	Chromodomain-h	CHD1	11	8	1709	0	35.672	1.0535	0.83349	5.06E+08
O15143;C9J4Z7;I	O15143	Actin-related pro	ARPC1B	10	9	372	0	79.089	1.0533	1.0844	5.58E+08
P48643;E7ENZ3;I	P48643;E7ENZ3;I	T-complex protei	CCT5	44	44	541	0	323.31	1.0532	0.75934	2.32E+10
Q8IY37;F5H3Y4	Q8IY37;F5H3Y4	Probable ATP-dep	DHX37	12	12	1157	0	50.183	1.0532	0.73736	6.43E+08
Q14147;H7C504	Q14147	Probable ATP-dep	DHX34	12	12	1143	0	127.07	1.0529	0.83139	9.88E+08
A0A087WVS8;Q7	A0A087WVS8;Q7	MOB kinase activ	MOB2	2	2	236	0	4.0426	1.0528	NaN	1.49E+08
Q9NXF1-2;Q9NXF	Q9NXF1-2;Q9NXF	Testis-expressed s	TEX10	12	12	913	0	85.679	1.0528	1.0963	9.69E+08
Q9UHB9;Q9UHB9	Q9UHB9;Q9UHB9	Signal recognitior	SRP68	39	39	627	0	285.26	1.0528	0.98911	5.19E+09
A2A2G4;Q9Y672;	A2A2G4;Q9Y672;	Dolichyl pyropho	ALG6	2	2	509	0	5.5501	1.0527	4.7786	2.14E+08
Q12789;Q12789·	Q12789;Q12789·	General transcrip	GTF3C1	48	48	2109	0	286.18	1.0525	0.83398	3.11E+09
A0A0B4J1S8;Q9U	A0A0B4J1S8;Q9U	Phosphatidylinos	PI4KB	9	9	828	0	46.693	1.0523	0.82183	9.11E+08
B4DY09;Q12905;	B4DY09;Q12905	Interleukin enhan	ILF2	24	24	352	0	323.31	1.0523	0.78129	2.47E+10
P54886;P54886·	P54886;P54886·	Delta-1-pyrroline	ALDH18A1	43	43	795	0	323.31	1.0522	0.92142	2.00E+10
Q8WUA2	Q8WUA2	Peptidyl-prolyl ci	PPIL4	7	7	492	0	45.715	1.0517	NaN	4.88E+08
A0A087X140;A0/	A0A087X140;A0/	COBW domain-co	CBWD5;CBWD7;(	4	4	347	0	28.417	1.0511	0.73155	4.29E+08
Q9HCK8;Q9HCK8	Q9HCK8;Q9HCK8	Chromodomain-h	CHD8	14	10	2581	0	96.596	1.0511	1.0293	7.89E+08
Q9Y320-2;Q9Y32	Q9Y320-2;Q9Y32	Thioredoxin-relat	TMX2	5	5	258	0	18.732	1.0511	0.75875	1.09E+09
O95394;O95394·	O95394;O95394·	Phosphoacetylglu	PGM3	17	17	542	0	91.797	1.051	NaN	9.67E+08
E7EQZ4;Q16637-	E7EQZ4;Q16637-	Survival motor ne	SMN1	6	6	294	0	78.179	1.0506	0.88192	8.37E+08
P20073-2;P2007	P20073-2;P2007	Annexin A7	ANXA7	12	12	466	0	60.134	1.0502	0.76457	1.38E+09
G8JLB3;Q9Y606-;	G8JLB3;Q9Y606-;	tRNA pseudouridi	PUS1	14	14	384	0	72.025	1.0501	0.81292	1.60E+09
P07384;E9PL37;I	P07384	Calpain-1 catalyti	CAPN1	23	23	714	0	106.02	1.0501	0.61613	3.23E+09
P34932;A0A087\	P34932;A0A087\	Heat shock 70 kD	HSPA4	29	27	840	0	276.84	1.05	1.1315	4.78E+09
B9EGE7;Q8TCN5;	B9EGE7;Q8TCN5;	Zinc finger protei	ZNF507	2	2	957	0	3.8165	1.0498	0.7769	1.13E+07
P55060-3;P5506	P55060-3;P5506	Exportin-2	CSE1L	39	39	945	0	323.31	1.0496	0.93974	3.18E+10
O60306;H0YH15;	O60306	Intron-binding pr	AQR	30	30	1485	0	323.31	1.0495	0.85408	2.14E+09
P31350;P31350-	P31350;P31350-	Ribonucleoside-d	RRM2	8	8	389	0	40.493	1.0495	1.0725	1.13E+09
Q53GQ0;E9PI21;I	Q53GQ0	Estradiol 17-beta	HSD17B12	16	16	312	0	199.65	1.0489	1.0009	7.38E+09
Q13148;B1AKP7;	Q13148;B1AKP7;	TAR DNA-binding	TARDBP	10	10	414	0	289.34	1.0485	0.97813	1.33E+10
Q9BQA9-2;Q9BQ/	Q9BQA9-2;Q9BQ/	Uncharacterized p	C17orf62	2	2	173	0	5.2781	1.0485	NaN	1.25E+08
O95602;B9ZVN9	O95602;B9ZVN9	DNA-directed RN/	POLR1A	55	54	1720	0	323.31	1.0481	0.91632	5.10E+09
G3XAH6;P51003;	G3XAH6;P51003;	Poly(A) polymera	PAPOLA	20	18	724	0	157.86	1.0477	0.80588	2.72E+09
C9JFE4;Q13098-5	C9JFE4;Q13098-5	COP9 signalosom	GPS1	14	14	471	0	53.764	1.0474	0.7932	1.20E+09
Q86UV5;Q86UV5	Q86UV5;Q86UV5	Ubiquitin carbox	USP48	13	13	1035	0	152.94	1.0474	0.70197	1.34E+09
Q8TAT6;Q8TAT6-;	Q8TAT6;Q8TAT6-;	Nuclear protein lo	NPLOC4	14	14	608	0	218.94	1.0467	NaN	1.26E+09
Q9H1Y0;Q9H1Y0·	Q9H1Y0;Q9H1Y0·	Autophagy protei	ATG5	6	6	275	0	32.757	1.0461	0.81875	8.85E+08
Q9ULC3	Q9ULC3	Ras-related protei	RAB23	4	4	237	0	36.216	1.0459	0.84919	2.99E+08
A0A0A0MRF9;P1(	A0A0A0MRF9;P1(	1-phosphatidylin	PLCG2	4	4	1252	0	38.068	1.0458	1.2114	2.16E+08
P42704;A0A0C4[	P42704	Leucine-rich PPR	LRPPRC	96	96	1394	0	323.31	1.0458	0.99342	4.08E+10
O75884;A0A087\	O75884;A0A087\	Putative hydrolas	RBBP9	4	4	186	0	18.091	1.0455	0.73525	4.02E+08
Q969H6;Q969H6	Q969H6;Q969H6	Ribonuclease P/M	POP5	4	4	163	0	14.226	1.0451	0.79802	1.23E+08
Q9Y4X5;A0A087\	Q9Y4X5	E3 ubiquitin-prot	ARIH1	10	10	557	0	54.202	1.0451	NaN	1.18E+09
A2RRP1-2;A2RRP	A2RRP1-2;A2RRP	Neuroblastoma-a	NBAS	23	23	2251	0	168.74	1.0448	0.98754	1.27E+09
P30044-2;P3004	P30044-2;P3004	Peroxiredoxin-5,	PRDX5	5	5	162	0	28.628	1.0448	1.2243	5.35E+08
F5H4V9;Q16342-	F5H4V9;Q16342-	Programmed cell	PDCD2	3	3	298	0	22.282	1.0447	0.57532	2.71E+08
Q96K76-4;Q96K7	Q96K76-4;Q96K7	Ubiquitin carbox	USP47	14	14	1355	0	86.755	1.0447	0.80454	6.87E+08
O43776;K7EIU7;I	O43776	Asparagine--tRNA	NARS	26	26	548	0	323.31	1.0446	0.84469	9.81E+09
Q9Y2T2;E5RJ52;I	Q9Y2T2	AP-3 complex sub	AP3M1	13	13	418	0	151.05	1.0443	0.83218	1.75E+09
P26358;P26358-	P26358;P26358-	DNA (cytosine-5)-	DNMT1	32	32	1616	0	203.45	1.0428	0.78426	2.33E+09
Q9Y241;Q9Y241-	Q9Y241;Q9Y241-	HIG1 domain fam	HIGD1A	4	4	93	0	46.086	1.0428	0.8578	9.92E+08
F2Z2I2;Q5W015;	F2Z2I2;Q5W015;	6-phosphofructo	PFKFB3;PFKFB2	4	4	455	0	6.0419	1.0427	NaN	5.19E+07
C9J5D1;E7EQ69;(	C9J5D1;E7EQ69;(	N-alpha-acetyltra	NAA50	14	14	129	0	73.838	1.0426	0.50105	3.18E+09
O60671-2;O6067	O60671-2;O6067	Cell cycle checkp	RAD1	2	2	246	0	7.1835	1.0426	NaN	1.58E+08
P50213;H0YL72;I	P50213;H0YL72;I	Isocitrate dehydr	IDH3A	14	14	366	0	209.71	1.0424	0.77422	9.36E+09
P49756;P49756-	P49756;P49756-	RNA-binding prot	RBM25	8	8	843	0	24.75	1.042	0.78984	6.75E+08
A2A274;Q99798	A2A274;Q99798	Aconitate hydrat	ACO2	14	14	805	0	90.685	1.0419	0.99258	1.73E+09
Q9GZS3;H0YN81;	Q9GZS3;H0YN81;	WD repeat-contai	WDR61	11	11	305	0	160.28	1.0417	0.97578	2.55E+09
F5GZ28;P18858;I	F5GZ28;P18858;I	DNA ligase;DNA li	LIG1	14	14	851	0	93.943	1.0414	0.80533	1.95E+09
A0A087WUC6;Q1	A0A087WUC6;Q1	Signal peptidase c	SPCS2	18	18	227	0	245.55	1.0413	0.7756	5.75E+09
Q07864;F5H1D6;	Q07864;F5H1D6	DNA polymerase e	POLE	33	33	2286	0	239.79	1.0413	0.79908	2.35E+09
A0A0A0MR09;P4	A0A0A0MR09;P4	Tyrosine-protein	PTPN9	9	9	583	0	41.434	1.0411	NaN	3.83E+08
P25098;E9PRV7;I	P25098;E9PRV7	Beta-adrenergic r	ADRBK1	8	8	689	0	26.82	1.0411	0.92133	3.78E+08
Q9Y570;Q9Y570-	Q9Y570;Q9Y570-	Protein phosphat	PPME1	9	9	386	0	32.836	1.041	1.4253	9.17E+08
O94973;O94973·	O94973;O94973·	AP-2 complex sub	AP2A2	36	24	939	0	316.65	1.0406	0.8527	9.35E+09
D6RCD0;Q8NBQ5	D6RCD0;Q8NBQ5	Estradiol 17-beta	HSD17B11	5	5	256	0	53.273	1.0405	1.0459	3.63E+08
Q66K74-2;Q66K7	Q66K74-2;Q66K7	Microtubule-asso	MAP1S	9	9	1033	0	47.826	1.0405	0.99435	9.34E+08
Q96EL2;F8VYR5	Q96EL2	28S ribosomal pr	MRPS24	6	6	167	0	66.322	1.0404	0.82895	7.31E+08
O75400-2;O7540	O75400-2;O7540	Pre-mRNA-proces	PRPF40A	3	3	930	0	12.995	1.0403	1.6759	3.41E+08
O43347;H0YHB7	O43347;H0YHB7	RNA-binding prot	MSI1	11	10	362	0	93.968	1.0397	0.90825	2.86E+09
P06737-2;P0673	P06737-2;P0673	Glycogen phosph	PYGL	46	38	813	0	323.31	1.0397	1.0392	1.90E+10
Q96L92;Q96L92-	Q96L92;Q96L92-	Sorting nexin-27	SNX27	18	18	541	0	92.671	1.0394	NaN	1.77E+09
K7EKE6;K7EJE8;P	K7EKE6;K7EJE8;P	Lon protease hon	LONP1	40	40	845	0	323.31	1.0393	0.878	1.23E+10
P49959;F8W7U8	P49959;F8W7U8	Double-strand br	MRE11A	21	21	708	0	153.74	1.0392	0.96891	2.80E+09
A0A0G2JQX1;A0/	A0A0G2JQX1;A0/	Gamma-tubulin c	TUBGCP5	3	3	1024	0	41.515	1.0383	0.6476	1.65E+08
Q9Y2H6-2;Q9Y2H	Q9Y2H6-2;Q9Y2H	Fibronectin type-	FNDC3A	6	6	1142	0	57.938	1.0382	2.1094	2.65E+08
Q9NVI7-2;Q9NVI7	Q9NVI7-2;Q9NVI7	ATPase family AA/	ATAD3A	36	9	586	0	312.51	1.0381	0.86759	8.22E+09
Q5T9A4;Q5T9A4-	Q5T9A4;Q5T9A4-	ATPase family AA/	ATAD3B	31	6	648	0	153.35	1.0378	1.1021	5.45E+08
J3QS41;P42694;I	J3QS41;P42694;I	Probable helicase	HELZ	18	18	1943	0	99.083	1.0376	0.78673	8.43E+08
Q5JQP3;Q5JQP4;	Q5JQP3;Q5JQP4;	DNA polymerase I	POLL	2	2	218	0	9.9537	1.0375	NaN	3.53E+07
O14949	O14949	Cytochrome b-c1	UQCRQ	9	9	82	0	34.619	1.0363	0.63836	3.00E+09
Q14643-4;Q1464	Q14643-4;Q1464	Inositol 1,4,5-tris	ITPR1	4	2	2695	0	7.6089	1.0361	0.67736	5.12E+07
O43684-2;O4368	O43684-2;O4368	Mitotic checkpoi	BUB3	15	15	326	0	196.82	1.0352	0.91656	1.05E+10
P51116;I3L1Z2	P51116	Fragile X mental r	FXR2	6	4	673	0	31.67	1.0346	0.75254	3.33E+08
P82675;P82675-	P82675	28S ribosomal pr	MRPS5	5	5	430	0	22.023	1.0346	1.262	4.29E+08
Q9UMS4;F5GY56	Q9UMS4;F5GY56	Pre-mRNA-proces	PRPF19	16	16	504	0	298.9	1.0346	1.0175	6.05E+09
W0S4B9;P16591	W0S4B9;P16591	Tyrosine-protein	Pe1Fe10;FER	4	4	411	0	5.0797	1.0341	3.6303	1.96E+08
Q96P47;Q96P47·	Q96P47;Q96P47·	Arf-GAP with GTP	AGAP3	11	11	875	0	112.01	1.034	0.7876	1.65E+09
Q8NCW5-2;Q8NC	Q8NCW5-2;Q8NC	NAD(P)H-hydrate	APOA1BP	5	5	185	0	16.7	1.0339	1.1199	2.94E+08
Q6P9B6;H3BM75	Q6P9B6;H3BM75	TLD domain-cont	TLDC1	6	6	456	0	87.366	1.0338	1.237	1.04E+09
Q96EY1;Q96EY1-;	Q96EY1;Q96EY1-;	DnaJ homolog sul	DNAJA3	8	8	480	0	51.072	1.0332	1.2336	2.24E+09
P12956;B1AHC9;	P12956;B1AHC9;	X-ray repair cross	XRCC6	42	42	609	0	323.31	1.0331	0.94035	3.28E+10
I3L0N3;P46459;I	I3L0N3;P46459;I	Vesicle-fusing ATP	NSF	47	47	739	0	323.31	1.0329	0.9601	1.33E+10
O95140;O95140·	O95140	Mitofusin-2	MFN2	12	12	757	0	75.405	1.0328	0.74371	1.00E+09
Q86W42;Q86W4	Q86W42;Q86W4	THO complex sub	THOC6	13	13	341	0	240.7	1.0326	0.96578	3.61E+09
Q92526;Q92526·	Q92526;Q92526·	T-complex protei	CCT6B	9	2	530	0	14.485	1.0324	NaN	1.40E+08
P08133;P08133-	P08133;P08133-	Annexin A6;Anne	ANXA6	9	9	673	0	67.143	1.032	NaN	5.89E+08
P60891;P60891-	P60891;P60891-	Ribose-phosphat	PRPS1	23	9	318	0	302.77	1.032	0.92137	1.52E+10

Q9UNS2;Q9UNS2	Q9UNS2;Q9UNS2	COP9 signalosom	COPS3	5	5	423	0	36.873	1.032	1.1291	9.40E+08
A0A0C4DFX4;Q6Z	A0A0C4DFX4;Q6Z	Helicase SRCAP	SRCAP	12	11	3053	0	57.489	1.0317	0.80992	4.19E+08
Q9UPR3	Q9UPR3	Protein SMG5	SMG5	5	5	1016	0	14.646	1.0315	1.7129	1.36E+08
A0A087WVF7;Q9	A0A087WVF7;Q9	Intersectin-2;Inte	ITSN2;ITSN1	2	2	1680	0	4.1708	1.0312	0.70352	6.85E+07
A0A0D9SEJ5;F5G	A0A0D9SEJ5;F5G	Constitutive coac	FAM120B	7	7	922	0	51.779	1.0312	1.1205	6.31E+08
Q9BW92;U3KQG	Q9BW92;U3KQG	Threonine--tRNA l	TARS2	21	21	718	0	166.4	1.0311	0.82946	2.30E+09
Q5SQP8;P56545;	Q5SQP8;P56545;	C-terminal-bindir	CTBP2	16	11	513	0	156.57	1.0308	0.8645	6.90E+09
O60725	O60725	Protein-S-isopren	ICMT	4	4	284	0	15.726	1.0306	0.8535	8.02E+08
F8VY35;F5H4R6;I	F8VY35;F5H4R6;I	Nucleosome asser	NAP1L1	13	11	264	0	323.31	1.0304	1.0586	9.27E+09
P49588;P49588-	P49588;P49588-	Alanine--tRNA lig	AARS	45	45	968	0	323.31	1.0303	0.94672	9.59E+09
Q8NCM8;Q8NCM	Q8NCM8;Q8NCM	Cytoplasmic dyne	DYNC2H1	34	34	4307	0	131.85	1.0303	1.0588	1.50E+09
O43660;O43660·	O43660;O43660·	Pleiotropic regul	PLRG1	14	14	514	0	165.03	1.0301	1.109	8.52E+08
Q9Y6A9	Q9Y6A9	Signal peptidase c	SPCS1	1	1	102	0	5.5555	1.0299	NaN	1.08E+08
O00178;F5H716;	O00178;F5H716	GTP-binding prot	GTPBP1	5	5	669	0	24.161	1.0298	1.1378	7.45E+08
P24752;H0YEL7;I	P24752	Acetyl-CoA acetyl	ACAT1	22	22	427	0	237.45	1.0292	0.87075	1.83E+10
Q8N2K0-3;Q8N2I	Q8N2K0-3;Q8N2I	Monoacylglycero	ABHD12	5	5	360	0	10.873	1.0291	0.99554	2.80E+08
Q9UM13;D6RA92	Q9UM13;D6RA92	Anaphase-promo	ANAPC10	3	3	185	0	23.798	1.0291	0.92889	2.55E+08
O95861-4;O9586	O95861-4;O9586	3(2),5-bisphosph	BPNT1	9	9	272	0	72.231	1.0287	1.1145	7.98E+08
P07814;V9GYZ6;'	P07814;V9GYZ6	Bifunctional glut	EPRS	96	96	1512	0	323.31	1.0287	0.90462	3.54E+10
Q9NPD3;E9PPI9;I	Q9NPD3;E9PPI9;I	Exosome comple	EXOSC4	4	4	245	0	15.129	1.0285	1.0873	3.40E+08
Q93008-1;Q9300	Q93008-1;Q9300	Probable ubiquiti	USP9X	58	58	2554	0	323.31	1.0278	1.0044	7.08E+09
Q7KZ85;Q7KZ85-	Q7KZ85	Transcription elo	SUPT6H	38	38	1726	0	323.31	1.0276	0.90241	2.97E+09
Q16352;A0A087\	Q16352;A0A087\	Alpha-internexin	INA	9	7	499	0	64.013	1.0275	NaN	3.88E+08
P78346;P78346-	P78346;P78346-	Ribonuclease P pr	RPP30	17	17	268	0	238.74	1.0271	0.4419	3.60E+09
O00629;H7C4F6	O00629	Importin subunit	KPNA4	15	8	521	0	111.6	1.026	NaN	3.57E+08
P55735;A0A0C4I	P55735;A0A0C4I	Protein SEC13 ho	SEC13	12	12	322	0	182.39	1.0256	0.79645	4.53E+09
O43172-2;O4317	O43172-2;O4317	U4/U6 small nucl	PRPF4	16	16	521	0	184.4	1.0255	NaN	2.14E+09
Q7Z3K3-5;Q7Z3K	Q7Z3K3-5;Q7Z3K	Pogo transposabl	POGZ	19	19	1315	0	147.37	1.0255	0.80484	2.10E+09
P23246;P23246-	P23246;P23246-	Splicing factor, pr	SFPQ	30	28	707	0	323.31	1.0254	0.94944	1.50E+10
P11142;E9PKE3;I	P11142;E9PKE3;I	Heat shock cogna	HSPA8	48	32	646	0	323.31	1.0252	1.2019	9.83E+10
P48507;P48507-	P48507;P48507-	Glutamate--cystei	GCLM	8	8	274	0	92.687	1.0246	0.95272	1.86E+09
P08238;Q58FF7	P08238	Heat shock protei	HSP90AB1	58	29	724	0	323.31	1.0242	0.98648	2.51E+11
G8JLB6;P31943;I	G8JLB6;P31943;I	Heterogeneous nu	HNRNPH1	22	12	472	0	323.31	1.0241	0.97115	6.45E+10
P05388;F8VWS0;	P05388;F8VWS0;	60S acidic riboso	RPLP0	23	23	317	0	323.31	1.0241	0.92063	4.97E+10
O60502;O60502·	O60502;O60502·	Bifunctional prot	MGEA5	16	16	916	0	186.51	1.0239	0.96992	2.82E+09
Q15018	Q15018	BRISC complex su	FAM175B	14	14	415	0	92.294	1.0239	0.88079	1.72E+09
Q8NBM4;X6R5E5	Q8NBM4;X6R5E5	Ubiquitin-associa	UBAC2	4	4	344	0	37.133	1.0237	0.65007	2.17E+08
H0YF29;Q6P1X6·	H0YF29;Q6P1X6·	UPF0598 protein	C8orf82	5	5	261	0	36.993	1.0236	0.73812	1.34E+08
P51649;P51649-	P51649;P51649-	Succinate-semial	ALDH5A1	17	17	535	0	138.35	1.0234	0.83902	1.70E+09
P16152;E9PQ63;	P16152;E9PQ63;	Carbonyl reducta	CBR1	20	16	277	0	294.52	1.0231	1.0504	2.29E+10
P62906	P62906	60S ribosomal pr	RPL10A	18	18	217	0	188.65	1.0231	0.51793	1.70E+10
Q9UIA9;E7ESC6;E	Q9UIA9;E7ESC6	Exportin-7	XPO7	12	12	1087	0	51.304	1.0229	0.67841	4.56E+08
Q15654;A0A0D9	Q15654;A0A0D9	Thyroid receptor-	TRIP6	6	6	476	0	86.414	1.0228	0.46934	6.64E+08
Q13131;Q13131·	Q13131;Q13131·	5-AMP-activated	PRKAA1	4	3	559	0	14.398	1.0225	NaN	2.18E+08
P60842;J3KT12;F	P60842;J3KT12;F	Eukaryotic initiat	EIF4A1	36	18	406	0	323.31	1.0224	1.0464	1.17E+11
Q8IWV8-4;Q8IW\	Q8IWV8-4;Q8IW\	E3 ubiquitin-prot	UBR2	12	12	1755	0	34.043	1.0224	0.96937	3.78E+08
Q9BUF5;K7ESM5;	Q9BUF5;K7ESM5	Tubulin beta-6 ch	TUBB6	25	11	446	0	289.64	1.022	1.0055	1.63E+10
Q9HAV4;H0Y9I3;I	Q9HAV4	Exportin-5	XPO5	23	23	1204	0	244.72	1.022	0.90148	3.12E+09
P37802;P37802-	P37802;P37802-	Transgelin-2	TAGLN2	7	7	199	0	38.558	1.0217	0.99813	3.54E+08
P83731;C9JXB8;(	P83731;C9JXB8;(	60S ribosomal pr	RPL24	12	12	157	0	42.322	1.0217	0.536	7.96E+09
Q5VWZ2;Q5VWZ	Q5VWZ2;Q5VWZ	Lysophospholipa	LYPLAL1	10	10	237	0	121.93	1.0217	0.94677	2.21E+09
O94925-3;H7BZD	O94925-3	Glutaminase kidn	GLS	18	3	598	0	49.36	1.0216	1.376	5.24E+08
P29218;P29218-	P29218;P29218-	Inositol monoph	IMPA1	6	6	277	0	68.48	1.0215	0.69861	9.05E+08
Q12797-10;Q127	Q12797-10;Q127	Aspartyl/asparagi	ASPH	8	8	729	0	43.906	1.0215	1.3064	6.56E+08
Q6NUK1;Q6NUK1	Q6NUK1;Q6NUK1	Calcium-binding	SLC25A24	23	23	477	0	102.17	1.0207	0.84356	3.38E+09
Q8N122;Q8N122	Q8N122;Q8N122	Regulatory-associ	RPTOR	25	25	1335	0	190.04	1.0205	0.9351	2.45E+09
P46736-2;P4673	P46736-2;P4673	Lys-63-specific de	BRCC3	10	10	291	0	75.702	1.0203	0.92331	1.79E+09
Q9BYE7-3;Q9BYE	Q9BYE7-3;Q9BYE	Polycomb group	PCGF6	1	1	275	0	9.6945	1.0202	1.3892	1.98E+07
O75534-2;O7553	O75534-2;O7553	Cold shock domai	CSDE1	38	38	767	0	323.31	1.0201	0.92501	8.72E+09
P25788-2;P2578	P25788-2;P2578	Proteasome subu	PSMA3	9	9	248	0	63.957	1.02	1.0468	2.59E+09
P50991;P50991-	P50991;P50991-	T-complex protei	CCT4	39	39	539	0	323.31	1.02	0.86044	5.06E+10
Q9Y4R8;H3BRS3;	Q9Y4R8	Telomere length r	TELO2	13	13	837	0	42.082	1.0197	0.92513	6.14E+08
Q8NHH9-3;Q8NH	Q8NHH9-3;Q8NH	Atlastin-2	ATL2	4	4	412	0	33.156	1.0196	NaN	3.00E+08
Q6NXE6-2;Q6NXE	Q6NXE6-2;Q6NXE	Armadillo repeat-	ARMC6	16	16	476	0	169.45	1.0195	1.0475	3.57E+09
P26196;Q8IV96	P26196	Probable ATP-dep	DDX6	19	19	483	0	323.31	1.0194	0.8444	1.47E+10
Q96TA2-3;Q96TA	Q96TA2-3;Q96TA	ATP-dependent zi	YME1L1	8	8	683	0	127.39	1.0193	NaN	7.83E+08
Q92890;Q92890·	Q92890;Q92890·	Ubiquitin fusion d	UFD1L	11	11	307	0	114.94	1.0192	0.93526	1.87E+09
Q8IYI6	Q8IYI6	Exocyst complex	EXOC8	8	8	725	0	57.377	1.0191	1.4806	4.88E+08
O15379;O15379·	O15379;O15379·	Histone deacetyla	HDAC3	4	3	428	0	9.5631	1.0188	0.85472	2.48E+08
Q9UBT2;Q9UBT2·	Q9UBT2;Q9UBT2·	SUMO-activating	UBA2	17	17	640	0	231.17	1.0188	0.99418	1.12E+09
Q8IX18-3;Q8IX18	Q8IX18-3;Q8IX18	Probable ATP-dep	DHX40	16	16	722	0	66.694	1.0187	0.88893	1.71E+09
P27144;D3DQ64	P27144;D3DQ64	Adenylate kinase	AK4	9	9	223	0	70.442	1.0185	0.85763	2.19E+09
Q58FF8	Q58FF8	Putative heat sho	HSP90AB2P	14	2	381	0	41.333	1.0183	1.0051	7.82E+09
F8WBE2;C9J8K7;	F8WBE2;C9J8K7;	Cytochrome P45(	CYP20A1	3	3	208	0	8.0377	1.0182	1.1157	7.23E+07
Q0VDF9;H7C2A1;	Q0VDF9	Heat shock 70 kD	HSPA14	16	16	509	0	78.866	1.0181	0.92148	2.65E+09
Q68CZ2-2;Q68CZ	Q68CZ2-2;Q68CZ	Tensin-3	TNS3	4	4	1205	0	23.264	1.018	0.87115	2.02E+08
P12081-3;P1208	P12081-3;P1208	Histidine--tRNA li	HARS	5	2	449	0	33.135	1.0179	1.4424	6.62E+08
Q5JY65;Q9BZJ0-2	Q5JY65;Q9BZJ0-2	Crooked neck-like	CRNKL1	13	13	836	0	66.892	1.0177	0.87249	9.01E+08
O75844	O75844	CAAX prenyl prot	ZMPSTE24	13	13	475	0	103.24	1.0173	1.0007	2.14E+09
P27694;I3L4R8;I	P27694;I3L4R8	Replication prote	RPA1	29	29	616	0	323.31	1.0173	0.62261	1.21E+10
P36551;H0YA22;	P36551	Oxygen-depender	CPOX	4	4	454	0	13.136	1.0173	1.2028	3.10E+08
J3QRV5;Q6P1M3	J3QRV5;Q6P1M3	Lethal(2) giant lar	SPATS2;LLGL2;ST.	2	2	1019	0.003786	2.5725	1.0172	NaN	1.76E+07
Q7L3T8	Q7L3T8	Probable proline-	PARS2	6	6	475	0	52.92	1.0172	0.92581	4.28E+08
A0A0C4DG89;Q7	A0A0C4DG89;Q7	Probable ATP-dep	DDX46	33	33	1032	0	186.1	1.0166	0.95573	3.60E+09
Q07065	Q07065	Cytoskeleton-assc	CKAP4	6	6	602	0	83.71	1.0165	NaN	2.08E+08
Q9BZH6;S4R3Z0;'	Q9BZH6	WD repeat-contai	WDR11	22	22	1224	0	232.18	1.0164	0.80409	2.42E+09
Q6PKG0;A0A0B4.	Q6PKG0;A0A0B4.	La-related protein	LARP1	9	9	1096	0	47.085	1.0162	1.0502	5.28E+08
Q9UI30;F5GX77;I	Q9UI30;F5GX77;I	Multifunctional n	TRMT112	7	7	125	0	56.692	1.0157	0.95461	2.02E+09
A0A0A0MRP6;B7	A0A0A0MRP6;B7	Probable global t	SMARCA1	23	8	1058	0	55.149	1.0156	1.193	3.20E+08
Q71RC2-5;Q71RC	Q71RC2-5;Q71RC	La-related protein	LARP4	11	10	653	0	70.139	1.0156	0.90263	2.61E+09
P50748;E7ES84;I	P50748;E7ES84	Kinetochore-asso	KNTC1	40	40	2209	0	202.28	1.0154	1.1045	2.06E+09
Q8IZQ1-2;Q8IZQ1	Q8IZQ1-2;Q8IZQ1	WD repeat and FY	WDFY3	4	4	3509	0	7.9155	1.0153	NaN	4.23E+07
P08243-2;P0824	P08243-2;P0824	Asparagine synthe	ASNS	29	29	540	0	249.27	1.015	1.1312	1.07E+10
Q8IU60-2;Q8IU6(	Q8IU60-2;Q8IU6(	m7GpppN-mRNA	DCP2	3	3	385	0	8.8488	1.015	1.0559	1.78E+08
A0A0C4DGQ8;Q6	A0A0C4DGQ8;Q6	Dehydrogenase/r	DHRS7B	11	11	310	0	62.485	1.0147	0.74462	1.50E+09
O94806;C9JKP8;I	O94806;C9JKP8;I	Serine/threonine	PRKD3;PRKD1	2	2	890	0	5.6444	1.0144	0.68248	1.13E+08
H3BLV9;Q5R363;	H3BLV9;Q5R363;	SRSF protein kina	SRPK1	12	11	671	0	158	1.014	0.99055	1.90E+09
Q9NRX1;F8WBJ6	Q9NRX1;F8WBJ6	RNA-binding prot	PNO1	10	10	252	0	35.598	1.014	0.92719	1.20E+09
C9JJ19;P82930;A	C9JJ19;P82930;A	28S ribosomal pr	MRPS34	8	8	225	0	49.106	1.0136	1.0949	1.58E+09
Q9GZZ9;E7EQ61;I	Q9GZZ9;E7EQ61;I	Ubiquitin-like mc	UBA5	5	5	404	0	61.233	1.0136	1.2734	9.08E+08
Q99426;Q99426·	Q99426;Q99426·	Tubulin-folding c	TBCB	13	13	244	0	185.02	1.0135	0.76061	1.42E+09
Q8TB61-5;Q8TB6	Q8TB61-5;Q8TB6	Adenosine 3-phos	SLC35B2	2	2	299	0	5.1265	1.0134	NaN	2.46E+08
Q13509;A0A0B4J	Q13509;A0A0B4J	Tubulin beta-3 ch	TUBB3	23	3	450	0	104	1.0133	1.1028	2.03E+09
O43395;O43395·	O43395	U4/U6 small nucl	PRPF3	9	9	683	0	161.33	1.0132	1.0415	6.26E+08

Q14152;Q14152·	Q14152;Q14152·	Eukaryotic transl	EIF3A	43	43	1382	0	237.83	1.0129	0.92458	1.02E+10
Q9UG01;Q9UG01	Q9UG01;Q9UG01	Intraflagellar tran	IFT172	14	14	1749	0	64.019	1.0129	0.96111	4.51E+08
O75874;C9J4N6;	O75874;C9J4N6	Isocitrate dehydr	IDH1	8	6	414	0	23.534	1.0128	0.78255	2.59E+08
O95163;F5H2T0;	O95163;F5H2T0	Elongator compl	IKBKAP	40	40	1332	0	323.31	1.0126	0.96044	6.44E+09
Q9UIG0-2;Q9UIG	Q9UIG0-2;Q9UIG	Tyrosine-protein	BAZ1B	25	25	1479	0	127.39	1.0125	1.3717	1.29E+09
Q9Y5B9;G3V5A4;	Q9Y5B9	FACT complex sul	SUPT16H	56	56	1047	0	323.31	1.0124	0.99788	2.18E+10
P51570;P51570·	P51570;P51570·	Galactokinase	GALK1	20	20	392	0	210.26	1.0123	0.88215	7.71E+09
F6SS63;Q8N5C8·:	F6SS63;Q8N5C8·:	TGF-beta-activate	TAB3	1	1	608	0.0061501	2.2092	1.0122	NaN	5.35E+07
O75152;E9PQ61;	O75152;E9PQ61;	Zinc finger CCCH	ZC3H11A	16	16	810	0	71.525	1.012	0.86737	1.41E+09
Q15648-3;Q1564	Q15648-3;Q1564	Mediator of RNA	MED1	1	1	556	0.0027954	2.6934	1.012	0.91679	7.55E+07
O15144;C9JTV5;(	O15144	Actin-related pro	ARPC2	8	8	300	0	71.799	1.0118	1.0086	7.42E+08
A8DPD7;Q9C0D3	A8DPD7;Q9C0D3	Protein zyg-11 ho	ZYG11B	4	4	566	0	15.985	1.0114	NaN	2.26E+08
Q9H900;Q9H900	Q9H900;Q9H900	Protein zwilch ho	ZWILCH	6	6	591	0	55.915	1.0114	NaN	2.19E+08
Q92620;Q92620·	Q92620	Pre-mRNA-splicin	DHX38	11	11	1227	0	41.977	1.0112	0.98456	5.06E+08
Q8WXF1-2;Q8W>	Q8WXF1-2;Q8W>	Paraspeckle comp	PSPC1	15	13	393	0	203.76	1.011	1.0272	2.35E+09
E9PN51;F8W9K7	E9PN51;F8W9K7	NADH dehydroge	NDUFS8	4	4	110	0	15.342	1.0106	0.82252	3.45E+08
P26368-2;P2636	P26368-2;P2636	Splicing factor U2	U2AF2	17	17	471	0	231.14	1.0102	1.0732	3.96E+09
P42765;A0A0B4J	P42765;A0A0B4J	3-ketoacyl-CoA th	ACAA2	20	20	397	0	323.31	1.0101	0.81288	4.29E+09
P78371;F5GWF6	P78371;F5GWF6	T-complex protei	CCT2	35	35	535	0	323.31	1.01	0.99585	1.79E+10
Q14966-4;Q1496	Q14966-4;Q1496	Zinc finger protei	ZNF638	8	8	1139	0	32.463	1.01	1.0353	2.75E+08
Q53H96;A0A0A0I	Q53H96;A0A0A0I	Pyrroline-5-carbo	PYCRL	10	10	274	0	56.424	1.0099	0.73648	9.61E+08
Q13907;Q13907·	Q13907;Q13907·	Isopentenyl-diph	IDI1	12	12	227	0	83.758	1.0092	0.75045	2.59E+09
D6RF48;Q9P2W9	D6RF48;Q9P2W9	Syntaxin-18	STX18	7	7	308	0	39.164	1.009	0.98007	5.97E+08
M0R0F0;P46782;	M0R0F0;P46782;	40S ribosomal pr	RPS5	10	10	200	0	109.52	1.009	0.95362	3.84E+08
A0A0C4DFP4;Q9(	A0A0C4DFP4;Q9(	Peptide-N(4)-(N-a	NGLY1	5	5	633	0	16.17	1.0086	NaN	1.03E+08
P42695;G3V1A9;	P42695;G3V1A9;	Condensin-2 com	NCAPD3	30	30	1498	0	194.65	1.0084	0.94336	2.14E+09
F5H8F7;Q9UBL3·	F5H8F7;Q9UBL3·	Set1/Ash2 histon	ASH2L	10	10	489	0	101.94	1.0081	0.38741	1.01E+09
O43678;O43678·	O43678;O43678·	NADH dehydroge	NDUFA2	2	2	99	0	38.056	1.0078	0.73552	1.08E+08
Q13322-3;Q1332	Q13322-3;Q1332	Growth factor rec	GRB10	5	5	536	0	8.1965	1.0078	NaN	1.53E+08
P53007;B4DP62	P53007;B4DP62	Tricarboxylate tra	SLC25A1	12	12	311	0	91.87	1.0076	0.84311	5.89E+09
P50502;A0A087>	P50502;A0A087>	Hsc70-interactin	ST13;ST13P4;ST1	8	8	369	0	64.758	1.0074	1.0812	2.48E+09
Q5T160;H0Y450	Q5T160	Probable arginine	RARS2	6	6	578	0	36.191	1.0072	NaN	4.20E+08
B4DLN1;P52815;	B4DLN1		MRPL12	18	4	442	0	315.23	1.0068	0.7316	5.81E+09
Q9NWK9-2;Q9NV	Q9NWK9-2;Q9NV	Box C/D snoRNA	ZNHIT6	5	5	431	0	29.05	1.0068	NaN	2.16E+08
A0A087WY71;Q9	A0A087WY71;Q9	AP-2 complex sub	AP2M1	19	19	434	0	94.93	1.0067	0.80766	2.12E+09
G5EA36;I3L394;F	G5EA36		CDC27	20	1	823	0	164.63	1.0067	0.91994	3.32E+09
Q9BSF4;K7ENF5	Q9BSF4	Uncharacterized	C19orf52	6	6	260	0	65.087	1.0067	0.95007	1.43E+09
P18754;P18754·	P18754;P18754·	Regulator of chro	RCC1	13	13	421	0	267.46	1.0065	0.91097	8.87E+09
P62258;P62258·	P62258;P62258·	14-3-3 protein ep	YWHAE	22	19	255	0	168.29	1.0059	0.82956	7.19E+09
P08574	P08574	Cytochrome c1, h	CYC1	10	10	325	0	91.454	1.0056	0.88389	2.90E+09
X6R6D0;P29353·	X6R6D0;P29353·	SHC-transforming	SHC1	4	4	354	0	21.19	1.0055	1.1498	3.10E+08
A0A096LPI6;A0A	A0A096LPI6;A0A	ES1 protein homc	C21orf33	13	9	279	0	216.83	1.0052	0.29638	4.41E+09
O75155-2;O7515	O75155-2;O7515	Cullin-associated	CAND2	16	10	1119	0	63.763	1.0051	0.88392	1.17E+09
Q9H0A8;A0A0B4.	Q9H0A8;A0A0B4.	COMM domain-co	COMMD4	6	6	199	0	108.46	1.0051	0.46208	1.12E+09
Q5JWT2;Q9ULK4	Q5JWT2;Q9ULK4	Mediator of RNA	MED23	22	22	1374	0	126.44	1.0047	0.94815	2.16E+09
G3XAG1;Q96ME7	G3XAG1;Q96ME7	Zinc finger protei	ZNF512	3	3	566	0	13.033	1.0046	0.33615	8.52E+07
J3QL56;O75880	J3QL56;O75880	Protein SCO1 hon	SCO1	3	3	270	0	27.144	1.0046	1.0277	8.48E+08
P61077;P61077·	P61077;P61077·	Ubiquitin-conjug	UBE2D3;UBE2D2	2	2	147	0	6.5846	1.004	NaN	4.09E+08
H3BSW6;Q2VPK5	H3BSW6;Q2VPK5	Cytoplasmic tRNA	CTU2	4	4	586	0	21.102	1.0039	NaN	2.43E+08
P42345;B1AKP8;	P42345	Serine/threonine·	MTOR	19	19	2549	0	146.76	1.0039	0.97016	1.16E+09
Q8TD30;Q8TD30·	Q8TD30;Q8TD30·	Alanine aminotra	GPT2	4	4	523	0	17.471	1.0037	1.1689	1.96E+08
B1ANM7;Q9UNN!	B1ANM7;Q9UNN!	FAS-associated fa	FAF1	2	2	490	0	6.2151	1.0036	NaN	3.43E+07
Q9BYB4;Q9BYB4·	Q9BYB4;Q9BYB4·	Guanine nucleoti	GNB1L	10	10	327	0	51.515	1.0036	0.81224	1.05E+09
Q9Y223;Q9Y223·	Q9Y223;Q9Y223·	Bifunctional UDP	GNE	12	12	722	0	57.675	1.0033	1.5398	1.32E+09
Q13951-2;J3KRT(	Q13951-2	Core-binding fact	CBFB	9	3	187	0	90.962	1.0029	1.0141	1.07E+09
Q14318;Q14318·	Q14318;Q14318·	Peptidyl-prolyl ci	FKBP8	11	11	412	0	75.241	1.0029	0.92508	1.17E+09
O60343-2;O6034	O60343-2;O6034	TBC1 domain fam	TBC1D4	23	21	1235	0	172.4	1.0028	1.137	2.20E+09
Q8NE71-2;Q8NE7	Q8NE71-2;Q8NE7	ATP-binding casse	ABCF1	20	20	807	0	188.18	1.0028	1.0526	2.38E+09
Q9Y6X3;V9GYS3;'	Q9Y6X3;V9GYS3;'	MAU2 chromatid	MAU2	5	5	613	0	16.39	1.0027	NaN	1.54E+08
P45974-2;P4597	P45974-2;P4597	Ubiquitin carbox	USP5	26	24	835	0	218.06	1.0023	0.99075	5.20E+09
Q15208	Q15208	Serine/threonine·	STK38	3	3	465	0	11.071	1.0023	NaN	9.11E+07
Q15291;Q15291·	Q15291;Q15291·	Retinoblastoma-b	RBBP5	9	9	538	0	85.179	1.0022	NaN	7.25E+08
P31146;H3BRY3;	P31146;H3BRY3	Coronin-1A;Coro	CORO1A	5	5	461	0	11.085	1.002	0.55672	1.94E+07
Q00587-2;Q0058	Q00587-2;Q0058	Cdc42 effector pr	CDC42EP1	7	7	384	0	29.951	1.0016	0.81066	4.10E+08
A0A087X0Q1;Q7:	A0A087X0Q1;Q7:	YTH domain-cont	YTHDF3	9	4	583	0	35.513	1.0012	NaN	3.62E+08
A0A087X211;Q8'	A0A087X211;Q8'	Protein CIP2A	KIAA1524	6	6	906	0	26.806	1.0007	0.78483	2.74E+08
Q9H9Y6;Q9H9Y6·	Q9H9Y6;Q9H9Y6·	DNA-directed RN	POLR1B	21	21	1135	0	106.47	1.0003	0.89529	1.65E+09
E9PMS3;E9PQW0	E9PMS3;E9PQW0	Peroxisomal mem	PEX16	1	1	52	0.00079386	3.3462	1.0001	1.3104	3.02E+07
P33991;E5RG31;	P33991	DNA replication li	MCM4	46	46	863	0	323.31	0.99979	0.94487	2.71E+10
Q9NZL9-4;Q9NZL	Q9NZL9-4;Q9NZL	Methionine aden	MAT2B	5	5	306	0	32.692	0.99926	1.0307	6.36E+08
Q92882	Q92882	Osteoclast-stimul	OSTF1	2	2	214	0	6.5629	0.99897	NaN	9.79E+07
P25685;P25685·	P25685;P25685·	DnaJ homolog sul	DNAJB1	9	9	340	0	27.741	0.99879	1.027	2.99E+08
O94966-7;O9496	O94966-7;O9496	Ubiquitin carbox	USP19	14	14	1372	0	86.847	0.99875	0.8233	8.26E+08
Q8TAG9;E7EW84	Q8TAG9;E7EW84	Exocyst complex	EXOC6	8	8	804	0	36.705	0.99857	0.69147	2.67E+08
Q5HYK3;F8VVX6;	Q5HYK3;F8VVX6;	2-methoxy-6-pol	COQ5	6	6	327	0	79.207	0.9985	1.0036	6.78E+08
Q16891-2;Q1689	Q16891-2;Q1689	MICOS complex s	IMMT	38	38	747	0	323.31	0.99819	0.91914	5.21E+09
O14654;H3BTC1	O14654	Insulin receptor s	IRS4	51	51	1257	0	323.31	0.99734	0.87848	1.11E+10
P07196;A0A087>	P07196;A0A087>	Neurofilament lig	NEFL	10	8	543	0	54.279	0.99722	NaN	5.08E+08
Q6PJ69;H0YG27;	Q6PJ69;H0YG27;	Tripartite motif-c	TRIM65	4	4	517	0	31.07	0.99709	NaN	1.23E+08
O94776;O94776·	O94776;O94776·	Metastasis-associ	MTA2	14	10	668	0	88.301	0.99707	0.76787	1.19E+09
P56937-3;P5693	P56937-3;P5693	3-keto-steroid rec	HSD17B7	4	4	306	0	15.634	0.99705	NaN	2.30E+08
P68366-2;P6836	P68366-2;P6836	Tubulin alpha-4A	TUBA4A	32	3	433	0	10.84	0.99691	0.81809	5.99E+08
Q15717;Q15717·	Q15717;Q15717·	ELAV-like protein	ELAVL1	19	17	326	0	223.65	0.99627	1.2931	1.85E+10
Q99570;D6RJ98;	Q99570	Phosphoinositide	PIK3R4	23	23	1358	0	145.05	0.99621	0.9365	2.13E+09
Q96I59;Q96I59-2	Q96I59;Q96I59-2	Probable asparagi	NARS2	13	13	477	0	177.01	0.99591	0.81292	2.59E+09
O75419-2;O7541	O75419-2;O7541	Cell division cont	CDC45	13	13	520	0	78.402	0.99565	NaN	6.76E+08
Q9P035;H3BS72;	Q9P035;H3BS72;	Very-long-chain (3	PTPLAD1	14	14	362	0	201.26	0.99495	0.98949	8.30E+09
P49189;P49189·	P49189;P49189·	4-trimethylamino	ALDH9A1	23	23	494	0	199.12	0.99461	0.90398	1.62E+10
Q5T8C6;Q13042·	Q5T8C6;Q13042·	Cell division cycle	CDC16	6	6	475	0	22.423	0.99446	NaN	2.10E+08
E9PHH8;Q9Y6X2	E9PHH8;Q9Y6X2	E3 SUMO-protein	PIAS3	2	2	593	0	8.3705	0.99419	NaN	4.90E+07
E9PC15;Q53H12;	E9PC15;Q53H12;	Acylglycerol kina	AGK	12	12	394	0	191.19	0.99414	0.79539	5.92E+09
M0R0N4;M0QYZ2	M0R0N4;M0QYZ2	AP-2 complex sub	AP2S1	6	6	144	0	36.665	0.99393	0.9625	1.85E+09
Q9BPX3;D6RA93;	Q9BPX3	Condensin compl	NCAPG	26	26	1015	0	198.34	0.99373	0.96203	3.89E+09
Q6P4A7;Q6P4A7·	Q6P4A7;Q6P4A7·	Sideroflexin-4	SFXN4	9	9	337	0	99.361	0.99291	0.96159	7.18E+08
Q75QN2-2;Q75Q	Q75QN2-2;Q75Q	Integrator compl	INTS8	8	7	978	0	162.72	0.99269	0.73116	7.40E+08
A0A087X1N2;Q0:	A0A087X1N2;Q0:	CCAAT/enhancer-	CEBPZ	20	20	998	0	180.01	0.99219	1.1233	1.04E+09
Q96GW9	Q96GW9	Methionine--tRN	MARS2	4	4	593	0	19.81	0.99205	NaN	2.66E+08
O60783	O60783	28S ribosomal pr	MRPS14	3	3	128	0	21.797	0.99149	0.99362	1.02E+09
Q9UBI1;R4GMW(	Q9UBI1;R4GMW(	COMM domain-co	COMMD3;COMM	6	6	195	0	41.286	0.99148	1	4.94E+08
P15170-2;P1517	P15170-2;P1517	Eukaryotic peptid	GSPT1	26	26	636	0	217.99	0.99131	0.9199	3.95E+09
Q8WUA4;H0Y4Q(	Q8WUA4;H0Y4Q(	General transcrip	GTF3C2	8	8	911	0	58.637	0.99125	0.71823	3.39E+08
Q5T447;Q5T447·	Q5T447	E3 ubiquitin-prot	HECTD3	8	8	861	0	48.682	0.99119	0.46503	5.59E+08
Q9NQT4;M0R050	Q9NQT4;M0R050	Exosome comple	EXOSC5	3	3	235	0	5.081	0.99104	0.53706	2.45E+08
A8MU39;H0YDU8	A8MU39;H0YDU8	Serine/threonine·	PPP5C	3	3	371	0	10.546	0.9897	NaN	1.56E+06

Q9Y678;H0Y8X7;	Q9Y678	Coatomer subuni	COPG1	46	42	874	0	323.31	0.98956	0.95314	1.86E+10
P29590-4;P2959	P29590-4;P2959	Protein PML	PML	2	2	560	0	18.365	0.98955	NaN	7.52E+07
P05141	P05141	ADP/ATP transloc	SLC25A5	37	18	298	0	274.99	0.9888	0.831	9.33E+10
Q9Y5R8;I3L3S0;I	Q9Y5R8;I3L3S0	Trafficking protei	TRAPPC1	3	3	145	0	9.5087	0.98879	0.92056	4.41E+08
O60216;E5RJW1;	O60216	Double-strand-br	RAD21	16	16	631	0	69.126	0.98855	1.0557	1.04E+09
Q92621;U3KPX2;	Q92621	Nuclear pore com	NUP205	68	68	2012	0	323.31	0.98851	0.94173	1.54E+10
Q92696;H0YLH3;	Q92696;H0YLH3	Geranylgeranyl tr	RABGGTA	13	13	567	0	84.818	0.98842	NaN	7.81E+08
Q6P2E9;Q6P2E9-	Q6P2E9;Q6P2E9-	Enhancer of mRN	EDC4	26	26	1401	0	161.6	0.98829	0.75847	3.13E+09
F5H365;Q15436;	F5H365;Q15436;	Protein transport	SEC23A	17	14	736	0	228.04	0.98811	1.0157	4.00E+09
Q96I25;Q5W012	Q96I25;Q5W012	Splicing factor 45	RBM17	7	7	401	0	38.346	0.98811	0.66007	2.34E+08
F8VWT9;J3KPF0;I	F8VWT9;J3KPF0;I	Probable E3 ubiq	HECTD4	4	4	4284	0	23	0.98773	0.97997	1.14E+08
U3KQC1;A0A0A0I	U3KQC1;A0A0A0I	WD repeat-contai	WDR18	11	11	394	0	73.322	0.98754	0.95095	2.69E+09
P50579-3;P5057	P50579-3;P5057	Methionine amin	METAP2	5	5	455	0	56.835	0.98752	NaN	1.37E+08
Q9H871	Q9H871	Protein RMD5 ho	RMND5A	2	2	391	0	8.3353	0.987	0.89549	2.41E+08
Q9Y265;Q9Y265-	Q9Y265;Q9Y265-	RuvB-like 1	RUVBL1	31	31	456	0	323.31	0.98699	0.94791	1.86E+10
Q9Y3I0	Q9Y3I0	tRNA-splicing liga	RTCB	34	34	505	0	323.31	0.98695	1.0449	3.36E+10
P37198;M0QXN5	P37198;M0QXN5	Nuclear pore glyc	NUP62	5	5	522	0	57.28	0.98603	NaN	1.60E+08
Q15645;H0YAL2;	Q15645	Pachytene checkp	TRIP13	18	18	432	0	184.49	0.98599	0.87133	5.92E+09
Q86VV8;Q86VV8-	Q86VV8;Q86VV8-	Rotatin	RTTN	4	4	2226	0	11.809	0.98592	0.88198	7.05E+08
A0PJW6	A0PJW6	Transmembrane p	TMEM223	2	2	202	0	18.181	0.98571	NaN	7.89E+07
Q15477;H7C5N0	Q15477	Helicase SKI2W	SKIV2L	28	28	1246	0	200.59	0.9857	1.0893	2.15E+09
P63244;J3KPE3;H	P63244;J3KPE3;H	Guanine nucleoti	GNB2L1	13	9	317	0	101.75	0.98559	1.3149	2.65E+09
P33993;P33993-	P33993;P33993-	DNA replication li	MCM7	45	45	719	0	323.31	0.98533	0.96054	3.79E+10
A0A0A0MRJ0;Q5	A0A0A0MRJ0;Q5	Serine/threonine-	CDC42BPA	13	10	1699	0	54.617	0.98532	1.0961	2.92E+08
Q9UBB6-2;Q9UBI	Q9UBB6-2;Q9UBI	Neurochondrin	NCDN	4	4	712	0	11.633	0.98528	NaN	1.13E+08
O43318-2;O4331	O43318-2;O4331	Mitogen-activate	MAP3K7;DKFZp5	5	5	579	0	92.337	0.98517	NaN	1.47E+08
Q12792;Q12792-	Q12792;Q12792-	Twinfilin-1	TWF1	7	6	350	0	75.793	0.98517	0.97516	1.24E+09
O95168;C9JXQ9;	O95168;C9JXQ9;	NADH dehydroge	NDUFB4	4	4	129	0	29.87	0.98505	0.76938	3.02E+08
P62308;A8MWD9	P62308;A8MWD9	Small nuclear ribo	SNRPG;SNRPGP1	5	5	76	0	26.8	0.98462	0.83118	3.07E+09
A2A3N6	A2A3N6	Putative PIP5K1A	PIPSL	8	0	862	0	34.439	0.984	NaN	1.40E+08
Q96P70	Q96P70	Importin-9	IPO9	21	21	1041	0	292.57	0.98363	0.90783	5.35E+09
O00257-3;O0025	O00257-3;O0025	E3 SUMO-protein	CBX4	2	2	290	0	5.6341	0.98354	NaN	5.67E+07
P14324-2;P1432	P14324-2;P1432	Farnesyl pyropho	FDPS	9	9	353	0	139.84	0.98336	0.97063	9.99E+09
E9PS17;Q96KG9-	E9PS17;Q96KG9-	N-terminal kinase	SCYL1	16	16	775	0	199.03	0.98314	0.71296	1.27E+09
Q96S55-2;Q96S5	Q96S55-2;Q96S5	ATPase WRNIP1	WRNIP1	10	10	640	0	44.618	0.98307	1.1261	9.89E+08
Q04837;A0A0G2	Q04837;A0A0G2	Single-stranded D	SSBP1	9	9	148	0	98.293	0.98305	0.91817	1.81E+09
P61026;H0YLJ8;H	P61026	Ras-related protei	RAB10	6	4	200	0	17.257	0.98272	1.131	3.32E+08
Q9UHD2	Q9UHD2	Serine/threonine-	TBK1	11	11	729	0	120.1	0.98243	0.72226	9.44E+08
J3QLE5;A8MT02;I	J3QLE5;A8MT02;I	Small nuclear ribo	SNRPN;SNRPB	9	9	169	0	50.169	0.98231	1.0318	7.87E+09
P61221;D6R9I9;I	P61221;D6R9I9	ATP-binding casse	ABCE1	21	21	599	0	196.7	0.9823	0.36921	3.88E+09
P09874;Q5VX84;	P09874	Poly [ADP-ribose]	PARP1	68	68	1014	0	323.31	0.98215	1.1324	6.45E+10
Q9UBF2;Q9UBF2	Q9UBF2;Q9UBF2	Coatomer subuni	COPG2	32	28	871	0	323.31	0.98209	1.0568	5.98E+09
A8MTY9;O14972	A8MTY9;O14972	Down syndrome c	DSCR3	4	4	249	0	23.958	0.98189	0.9397	5.12E+08
P10768;X6RA14;	P10768;X6RA14;	S-formylglutathio	ESD	11	11	282	0	214.64	0.98172	0.90887	5.72E+09
Q14204;H0YJ21	Q14204	Cytoplasmic dyne	DYNC1H1	244	244	4646	0	323.31	0.98123	1.0274	6.22E+10
I3L0E3;Q9Y2R5;E	I3L0E3;Q9Y2R5;E	28S ribosomal pr	MRPS17	6	6	225	0	45.277	0.98083	1.102	1.07E+09
P40763-3;P4076	P40763-3;P4076	Signal transducer	STAT3	9	9	722	0	99.448	0.98068	0.8993	9.39E+08
Q14999;Q14999	Q14999;Q14999	Cullin-7	CUL7	6	6	1698	0	50.242	0.98051	1.9422	2.61E+08
H0Y760;Q9Y4B4	H0Y760;Q9Y4B4	Helicase ARIP4	RAD54L2	6	6	1296	0	45.026	0.98047	1.103	2.64E+08
Q9UJS0;Q9UJS0-	Q9UJS0;Q9UJS0-	Calcium-binding	SLC25A13	29	22	675	0	303.81	0.98024	0.94891	1.17E+10
Q15910-3;Q1591	Q15910-3;Q1591	Histone-lysine N-r	EZH2	4	4	707	0	28.379	0.98006	1.0855	3.51E+08
Q9NVH0-2;Q9NVI	Q9NVH0-2;Q9NVI	Exonuclease 3-5 d	EXD2	8	8	496	0	24.429	0.97989	NaN	4.17E+08
P55010;H0YLZ1;I	P55010	Eukaryotic transl	EIF5	6	6	431	0	13.902	0.97948	1.0467	4.25E+08
P46199;H7C213	P46199	Translation initia	MTIF2	5	5	727	0	14.78	0.97909	0.94595	3.28E+08
Q13043-2;Q1304	Q13043-2;Q1304	Serine/threonine-	STK4	4	3	462	0	11.886	0.97875	NaN	1.22E+08
B4DTS2;Q9BZL6;(	B4DTS2;Q9BZL6;(	Serine/threonine-	PRKD2	3	3	888	0	43.644	0.97857	0.96859	2.89E+08
Q9NUQ9;E5RI16;	Q9NUQ9;E5RI16;	Protein FAM49B	FAM49B	4	4	324	0	21.773	0.97856	0.95424	3.65E+08
O00116;B8ZZ81	O00116	Alkyldihydroxyac	AGPS	25	25	658	0	261.19	0.97827	1.3266	3.56E+09
Q92547;H0Y8I7	Q92547	DNA topoisomera	TOPBP1	9	9	1522	0	24.726	0.97802	0.87814	1.53E+08
Q14566	Q14566	DNA replication li	MCM6	49	49	821	0	323.31	0.9778	0.95364	2.25E+10
O95782-2;O9578	O95782-2;O9578	AP-2 complex sub	AP2A1	28	16	955	0	156.62	0.97767	0.89121	2.45E+09
K7ENL9;Q96DM3	K7ENL9;Q96DM3	Uncharacterized p	C18orf8	2	2	609	0	10.79	0.97694	NaN	8.27E+07
P12235;V9GYG0;	P12235;V9GYG0	ADP/ATP transloc	SLC25A4	26	8	298	0	57.011	0.9767	1.1235	2.34E+09
Q8IUF8;Q8IUF8-4	Q8IUF8;Q8IUF8-4	Bifunctional lysin	MINA	14	14	465	0	230.4	0.97653	0.82536	2.60E+09
Q8WVM8;Q8WVI	Q8WVM8;Q8WVI	Sec1 family doma	SCFD1	24	24	642	0	314.9	0.97643	NaN	2.58E+09
H3BSW3;H3BQF1	H3BSW3;H3BQF1	Adenine phospho	APRT	4	4	63	0	19.564	0.97633	1.0366	4.87E+08
C9JVN9;Q9H9P8-	C9JVN9;Q9H9P8-	L-2-hydroxyglutar	L2HGDH	9	9	441	0	48.95	0.97618	0.91975	1.60E+09
Q9UBV2;G3V3B3	Q9UBV2;G3V3B3	Protein sel-1 hom	SEL1L	2	2	794	0	10.52	0.97579	0.85972	7.07E+07
Q9HAV7	Q9HAV7	GrpE protein hom	GRPEL1	4	4	217	0	15.337	0.97574	0.43318	2.25E+08
E7EM64;Q7L5N1;	E7EM64;Q7L5N1	COP9 signalosom	COPS6	6	6	326	0	57.857	0.97509	0.8616	1.20E+09
Q9P2I0;H0YJF4;G	Q9P2I0	Cleavage and poly	CPSF2	17	17	782	0	199.42	0.97488	0.99532	1.55E+09
O14776-2;O1477	O14776-2;O1477	Transcription elor	TCERG1	5	5	1077	0	19.358	0.97445	0.78759	2.09E+08
F5H7S7;Q13576;	F5H7S7;Q13576;	Ras GTPase-activa	IQGAP2	24	22	1525	0	204.28	0.97336	0.95786	1.17E+09
H0Y7P7;Q9UG56	H0Y7P7;Q9UG56	Phosphatidylserir	PISD	3	3	362	0	11.716	0.9732	1.3932	2.29E+08
F5H170;Q8WW2	F5H170;Q8WW2	DnaJ homolog sul	DNAJA4	1	1	219	0.0063694	2.1619	0.9731	0.94918	6.98E+07
O43242;O43242	O43242;O43242	26S proteasome r	PSMD3	37	37	534	0	248.78	0.97292	0.84113	1.22E+10
P05091;P05091-	P05091;P05091-	Aldehyde dehydr	ALDH2	14	12	517	0	47.231	0.97292	1.0008	9.96E+08
Q6P2P2;Q6P2P2	Q6P2P2;Q6P2P2	Putative protein a	PRMT9	9	9	845	0	25.065	0.97256	1.2708	4.14E+08
O00303;H0YDT6;	O00303	Eukaryotic transl	EIF3F	16	16	357	0	230.98	0.97251	1.0015	2.72E+10
P50990;P50990-	P50990;P50990-	T-complex protei	CCT8	46	46	548	0	323.31	0.97207	0.8608	3.82E+10
C9JKF1;Q5K651	C9JKF1;Q5K651	Sterile alpha moti	SAMD9	3	3	1283	0	9.6446	0.97195	1.54	7.65E+07
Q9BYN8	Q9BYN8	28S ribosomal pr	MRPS26	10	10	205	0	25.72	0.9717	0.9764	4.53E+08
B4E2Q0;P98194-	B4E2Q0;P98194-	Calcium-transpor	ATP2C1	5	5	953	0	32.773	0.97165	1.0705	2.36E+08
D6RGI3;D6RER5;I	D6RGI3;D6RER5;I	Septin-11	11-Sep	6	3	425	0	17.986	0.97164	1.2276	1.65E+08
A0A0U1RQC9;P0	A0A0U1RQC9;P0	Cellular tumor an	TP53	18	18	410	0	98.041	0.97163	1.2122	2.60E+09
Q9UNE7;Q9UNE7	Q9UNE7;Q9UNE7	E3 ubiquitin-prot	STUB1	15	15	303	0	111.29	0.97163	0.93283	3.06E+09
P23368;P23368-	P23368;P23368-	NAD-dependent n	ME2	2	2	584	0	26.952	0.97151	NaN	6.68E+07
Q99653;H0YNG9	Q99653;H0YNG9	Calcineurin B hon	CHP1	8	8	195	0	80.578	0.97125	0.67656	4.54E+08
Q99497;K7ELW0	Q99497;K7ELW0	Protein DJ-1	PARK7	11	11	189	0	48.098	0.97111	0.783	1.49E+09
P55210;P55210-	P55210;P55210-	Caspase-7;Caspas	CASP7	9	5	303	0	144.79	0.97103	0.85424	1.05E+09
P19447;H7C309	P19447	TFIIH basal transc	ERCC3	8	8	782	0	114.91	0.97088	1.0828	1.15E+09
P25705;P25705-	P25705;P25705-	ATP synthase sub	ATP5A1	37	37	553	0	323.31	0.9705	0.91854	5.01E+10
O95757;E9PDE8;	O95757;E9PDE8;	Heat shock 70 kD	HSPA4L	12	9	839	0	58.239	0.97019	1.1857	1.04E+09
C9JQ72;Q9Y4P1-I	C9JQ72;Q9Y4P1-I	Cysteine protease	ATG4B	8	8	266	0	84.143	0.97007	1.0018	1.54E+09
Q13535-2;Q1353	Q13535-2;Q1353	Serine/threonine-	ATR	12	12	2580	0	41.72	0.96985	0.70681	2.54E+08
P35580;P35580-	P35580;P35580-	Myosin-10	MYH10	91	66	1976	0	323.31	0.96974	1.127	1.54E+10
Q86X10;Q86X10-	Q86X10;Q86X10-	Ral GTPase-activa	RALGAPB	10	10	1494	0	105.28	0.96962	1.073	8.80E+08
E9PJN0;O14734;I	E9PJN0;O14734;I	Acyl-coenzyme A	ACOT8	4	4	226	0	42.353	0.96945	0.97169	4.50E+08
P13984	P13984	General transcrip	GTF2F2	7	7	249	0	84.769	0.96919	0.79433	9.70E+08
R4GNB2;R4GN35	R4GNB2;R4GN35	DENN domain-co	DENND4C	5	5	1909	0	45.108	0.96894	1.049	3.05E+08
Q9UK61-3;Q9UK(	Q9UK61-3;Q9UK(	Protein FAM208A	FAM208A	12	12	1512	0	40.154	0.9686	0.94078	4.66E+08
P12814;P12814-	P12814;P12814-	Alpha-actinin-1	ACTN1	30	1	892	0	231.85	0.96845	1.3317	2.20E+09
H7BXZ6;Q8IXI2-4	H7BXZ6;Q8IXI2-4	Mitochondrial Rh	TMEM91;RHOT1	7	6	597	0	60.608	0.96832	1.0732	2.98E+08
A6NJD9;A8MVT4;	A6NJD9;A8MVT4;	39S ribosomal pr	MRPL23	3	3	163	0	15.422	0.96803	1.3186	4.25E+08

O60701;O60701·	O60701;O60701·	UDP-glucose 6-de	UGDH	19	19	494	0	219.07	0.96782	0.8789	6.22E+09
Q1KMD3;H3BQZ7	Q1KMD3;H3BQZ7	Heterogeneous nu	HNRNPUL2;HNRN	10	10	747	0	41.43	0.96778	1.7322	7.34E+08
F6RFD5;P60981;I	F6RFD5;P60981;I	Destrin	DSTN	5	4	135	0	24.885	0.96722	0.64999	2.01E+09
Q9NXE4;Q9NXE4·	Q9NXE4;Q9NXE4·	Sphingomyelin ph	SMPD4	15	1	827	0	114.34	0.96721	1.1185	1.97E+09
Q14C86-2;Q14C8	Q14C86-2;Q14C8	GTPase-activating	GAPVD1	25	25	1460	0	215.3	0.967	0.644	1.60E+09
P62487;E9PIU7;I	P62487	DNA-directed RN/	POLR2G	5	5	172	0	34.911	0.9665	1.3523	3.18E+08
Q86W50;I3L362;	Q86W50;I3L362;	Methyltransferase	METTL16	3	3	562	0	9.5242	0.96629	NaN	1.04E+08
K7ES31;K7ERF1;C	K7ES31;K7ERF1;C	Eukaryotic transl	EIF3K	5	5	137	0	24.418	0.96626	0.75235	2.77E+08
D6R938;E9PBG7;	D6R938;E9PBG7;	Calcium/calmodu	CAMK2D	17	12	498	0	198.55	0.966	1.0632	2.86E+09
O60256;O60256·	O60256;O60256·	Phosphoribosyl p	PRPSAP2	19	17	369	0	181.84	0.96586	1.0525	8.28E+09
P09960;P09960·	P09960;P09960·	Leukotriene A-4 h	LTA4H	21	21	611	0	215.89	0.96558	NaN	1.75E+09
G5E953;Q13615·	G5E953;Q13615·	Myotubularin-rel	MTMR3	5	5	1062	0	13.152	0.96545	0.73384	1.38E+08
C9J2P0;P51965;I	C9J2P0;P51965;I	Ubiquitin-conjug	UBE2E1	4	2	147	0	11.214	0.96534	1.0748	8.37E+08
O75191;O75191·	O75191;O75191·	Xylulose kinase	XYLB	5	5	536	0	26.787	0.9644	1.1038	2.59E+08
P61011;P61011·	P61011;P61011·	Signal recognitio	SRP54	29	29	504	0	323.31	0.96416	1.0279	5.78E+09
Q9BZX2;Q9BZX2·	Q9BZX2	Uridine-cytidine k	UCK2	8	7	261	0	112.59	0.96406	0.67065	3.63E+09
Q86YS7;Q86YS7·;	Q86YS7;Q86YS7·;	C2 domain-conta	C2CD5	3	3	1000	0	20.276	0.96385	1.562	1.93E+08
P29372-5;P2937	P29372-5;P2937	DNA-3-methylade	MPG	6	6	281	0	51.621	0.9638	1.081	1.40E+09
Q07021;I3L3Q7;I	Q07021;I3L3Q7;I	Complement com	C1QBP	10	10	282	0	148.28	0.96373	1.196	9.27E+09
P51809-3;P5180	P51809-3;P5180	Vesicle-associatec	VAMP7	5	5	179	0	21.338	0.96364	0.88142	3.18E+08
A0A0A0MTS7;Q8'	A0A0A0MTS7;Q8'	Titin	TTN	2	2	35991	0.0051916	2.3083	0.96348	0.75175	2.35E+09
Q9NSE4	Q9NSE4	Isoleucine--tRNA l	IARS2	34	34	1012	0	231.9	0.96317	1.0273	5.56E+09
Q8N142;G3V5D8	Q8N142	Adenylosuccinate	ADSSL1	5	2	457	0	8.3254	0.96271	0.94443	2.50E+07
P33176;Q12840;	P33176	Kinesin-1 heavy cl	KIF5B	37	30	963	0	323.31	0.96266	0.9037	5.40E+09
P17152	P17152	Transmembrane p	TMEM11	3	3	192	0	15.978	0.9623	0.89068	1.49E+09
B7ZM99;A0A087'	B7ZM99;A0A087'	Monofunctional C	MTHFD1L	36	35	979	0	199.46	0.96227	0.9951	6.92E+09
Q5T4S7-3;Q5T4S7	Q5T4S7-3;Q5T4S7	E3 ubiquitin-prot	UBR4	88	88	5159	0	323.31	0.96175	1.0438	1.06E+10
B5MC22;Q9UDX5	B5MC22;Q9UDX5	Mitochondrial fis	MTFP1	3	3	143	0	16.757	0.96168	1.323	3.59E+08
B8ZZW5;Q8NBF6	B8ZZW5;Q8NBF6	Late secretory pat	AVL9	4	4	630	0	15.141	0.96162	NaN	1.16E+08
Q15084-3;Q1508	Q15084-3;Q1508	Protein disulfide-	PDIA6	17	17	437	0	219.3	0.96099	1.0217	1.40E+10
P45954;P45954·	P45954;P45954·	Short/branched c	ACADSB	9	9	432	0	72.771	0.96095	0.80762	1.79E+09
D6RGK9;H0Y9C1;	D6RGK9;H0Y9C1;	CCR4-NOT transcr	CNOT6L	3	1	163	0	9.2514	0.96074	NaN	9.40E+07
P56537;P56537·	P56537;P56537·	Eukaryotic transl	EIF6	5	5	245	0	167.52	0.96073	0.93516	2.14E+09
Q9H0A0;Q9H0A0	Q9H0A0;Q9H0A0	N-acetyltransfera	NAT10	32	32	1025	0	210.74	0.96073	1.3838	3.84E+09
P62851	P62851	40S ribosomal pr	RPS25	6	6	125	0	36.295	0.96068	1.2576	5.92E+09
P43686;P43686·	P43686;P43686·	26S protease regu	PSMC4	37	37	418	0	323.31	0.96024	0.85529	2.55E+10
P08670;B0YJC4;I	P08670;B0YJC4	Vimentin	VIM	55	51	466	0	323.31	0.96008	2.0121	5.57E+10
Q07666-2;Q0766	Q07666-2;Q0766	KH domain-conta	KHDRBS1	7	7	418	0	35.272	0.9596	NaN	2.60E+08
P55036;H0Y3Y9	P55036	26S proteasome r	PSMD4	14	2	377	0	182.42	0.9594	0.8258	4.78E+09
Q8N201;H7C582	Q8N201	Integrator compl	INTS1	16	16	2190	0	61.14	0.95935	1.1253	9.00E+08
Q8TC12;Q8TC12·	Q8TC12;Q8TC12·	Retinol dehydrog	RDH11	11	11	318	0	92.914	0.95931	1.0528	2.97E+09
P31040;P31040·	P31040;P31040·	Succinate dehydr	SDHA	17	17	664	0	154.66	0.9593	NaN	1.27E+09
O94906;O94906·	O94906;O94906·	Pre-mRNA-proces	PRPF6	38	38	941	0	221.14	0.95925	0.89814	2.90E+09
O14874-2;O1487	O14874-2;O1487	[3-methyl-2-oxob	BCKDK	3	3	335	0	11.928	0.95916	1.4106	2.77E+08
P43487-2;P4348	P43487-2;P4348	Ran-specific GTPa	RANBP1	10	10	200	0	139.17	0.95902	0.89296	1.52E+10
Q9Y230;Q9Y230·	Q9Y230;Q9Y230·	RuvB-like 2	RUVBL2	35	35	463	0	323.31	0.95836	0.99734	3.18E+10
Q9Y512	Q9Y512	Sorting and assen	SAMM50	16	16	469	0	126.77	0.95732	0.956	1.64E+09
Q96ME1-2;Q96M	Q96ME1-2;Q96M	F-box/LRR-repeat	FBXL18	8	8	668	0	70.457	0.95726	NaN	4.92E+08
J3KS15;Q14197;J	J3KS15;Q14197	Peptidyl-tRNA hy	ICT1	3	3	192	0	36.658	0.95712	1.2855	3.64E+08
Q6NVU6	Q6NVU6	Inactive Ufm1-spe	UFSP1	2	2	142	0	8.6656	0.95694	0.81182	1.13E+08
P21397-2;P2139	P21397-2;P2139	Amine oxidase [fl	MAOA;MAOB	2	2	394	0	5.9424	0.95692	NaN	7.79E+06
P84085;C9J1Z8;F	P84085;C9J1Z8	ADP-ribosylation	ARF5	11	7	180	0	64.805	0.95683	0.90919	3.74E+08
Q9NRF8;H0Y5S6	Q9NRF8	CTP synthase 2	CTPS2	22	18	586	0	138.03	0.95654	NaN	2.19E+09
O95573;F5GWH2	O95573	Long-chain-fatty-a	ACSL3	21	19	720	0	129.82	0.95634	0.98825	4.46E+09
P51587	P51587	Breast cancer typ	BRCA2	6	6	3418	0	27.666	0.9559	0.91399	1.08E+08
Q9UNX3;E5RIT6;I	Q9UNX3;E5RIT6	60S ribosomal pr	RPL26L1	13	2	145	0	4.665	0.95585	NaN	6.50E+06
Q9UJX2;Q9UJX2·	Q9UJX2;Q9UJX2·	Cell division cycle	CDC23	8	8	597	0	38.311	0.95527	NaN	2.65E+08
Q6PML9;D6R9M(	Q6PML9	Zinc transporter 9	SLC30A9	8	8	568	0	67.167	0.95522	1.0866	6.40E+08
Q12769;G3V198;	Q12769;G3V198;	Nuclear pore com	NUP160	38	38	1436	0	323.31	0.95521	0.97743	6.27E+09
A5YKK6-2;A5YKK(	A5YKK6-2;A5YKK(	CCR4-NOT transcr	CNOT1	44	44	2371	0	279.39	0.95518	1.0292	4.95E+09
O43707;O43707·	O43707;O43707·	Alpha-actinin-4	ACTN4	50	37	911	0	323.31	0.9551	1.4173	1.98E+10
Q99615;Q99615·	Q99615;Q99615·	DnaJ homolog sul	DNAJC7	18	18	494	0	100.42	0.95492	NaN	3.69E+08
P49593;P49593·	P49593;P49593·	Protein phosphat	PPM1F	19	19	454	0	323.31	0.95458	0.90632	7.40E+09
A0A087X0W7;A0	A0A087X0W7;A0	Acyl-coenzyme A t	ACOT1;ACOT2	16	16	421	0	127.64	0.95408	0.96032	1.89E+09
Q9H9T3-2;Q9H9T	Q9H9T3-2;Q9H9T	Elongator comple	ELP3	13	13	533	0	54.557	0.95402	NaN	6.12E+08
P54619-2;P5461	P54619-2;P5461	5-AMP-activated p	PRKAG1	11	11	299	0	93.222	0.9536	0.98376	8.55E+08
P61009	P61009	Signal peptidase c	SPCS3	4	4	180	0	20.712	0.95352	0.93905	8.41E+08
Q14181;Q14181·	Q14181;Q14181·	DNA polymerase a	POLA2	9	9	598	0	43.681	0.95343	NaN	6.42E+08
F5H0C4;Q9BRP4·	F5H0C4;Q9BRP4·	Proteasomal ATPa	PAAF1	5	3	393	0	13.946	0.95328	0.72794	2.40E+08
C9JBG0;A8MYQ9;	C9JBG0;A8MYQ9;	Ras-related protei	RAB34	4	4	211	0	12.139	0.95293	0.91462	2.31E+08
P62875	P62875	DNA-directed RN/	POLR2L	2	2	67	0	8.7562	0.95281	0.91764	5.52E+08
P30566;A0A0A6\	P30566;A0A0A6\	Adenylosuccinate	ADSL	26	23	484	0	323.31	0.95278	0.86776	1.95E+10
P51149;C9J8S3;(	P51149;C9J8S3;(	Ras-related protei	RAB7A	10	10	207	0	107.49	0.95223	1.0171	1.53E+09
Q06587;Q06587·	Q06587;Q06587·	E3 ubiquitin-prot	RING1	7	6	406	0	136.46	0.95221	1.0028	9.79E+08
Q9BQA1;Q9BQA1	Q9BQA1;Q9BQA1	Methylosome pro	WDR77	7	7	342	0	41.602	0.95147	1.1784	1.55E+09
Q9HD33-2;Q9HD	Q9HD33-2;Q9HD	39S ribosomal pr	MRPL47	6	6	230	0	11.588	0.95138	0.96756	1.55E+08
O96008;O96008·	O96008;O96008·	Mitochondrial im	TOMM40	12	12	361	0	323.31	0.95134	1.1623	4.82E+09
P35606-2;P3560	P35606-2;P3560	Coatomer subuni	COPB2	42	42	877	0	323.31	0.95123	0.96389	1.24E+10
P35611;P35611·	P35611;P35611·	Alpha-adducin	ADD1	18	16	737	0	125	0.9511	0.99245	2.45E+09
O00505;H0Y4S9	O00505	Importin subunit	KPNA3	17	10	521	0	113.99	0.95095	NaN	2.23E+09
G5EA19;U3KQS5;	G5EA19;U3KQS5;	Putative deoxyrib	TATDN1	2	2	207	0	3.9711	0.95046	0.58409	6.21E+07
K7EMM8;Q49A2(	K7EMM8;Q49A2(	Putative oxidorec	GLYR1	9	9	524	0	64.541	0.95036	NaN	4.02E+08
F5H8D7;P18887;	F5H8D7;P18887	DNA repair protei	FOXH1;XRCC1	10	10	602	0	23.846	0.95025	0.6618	6.04E+08
O75691	O75691	Small subunit pro	UTP20	30	30	2785	0	197.93	0.94974	1.1505	1.89E+09
Q9Y3D0;J3KS95;I	Q9Y3D0;J3KS95	Mitotic spindle-a	FAM96B	8	8	163	0	129.77	0.94933	0.96906	1.51E+09
Q9P258	Q9P258	Protein RCC2	RCC2	6	6	522	0	35.979	0.9489	NaN	1.19E+08
Q9Y4B6-2;Q9Y4B	Q9Y4B6-2;Q9Y4B	Protein VPRBP	VPRBP	19	19	1506	0	83.358	0.9484	1.0286	6.43E+08
O95433;O95433·	O95433;O95433·	Activator of 90 kD	AHSA1	19	19	338	0	323.31	0.94831	0.85825	1.34E+10
Q8IYU2-2;Q8IYU2	Q8IYU2-2;Q8IYU2	E3 ubiquitin-prot	HACE1	2	2	318	0	4.6238	0.94796	NaN	7.52E+07
Q8N4C6-10;Q8N4	Q8N4C6-10;Q8N4	Ninein	NIN	2	2	2116	0.0027961	2.6934	0.94792	NaN	3.37E+08
O14980;C9JKM9;	O14980	Exportin-1	XPO1	36	36	1071	0	323.31	0.94785	1.0979	1.42E+10
P38919;I3L3H2	P38919	Eukaryotic initiat	EIF4A3	31	25	411	0	174.46	0.94727	1.1031	2.12E+10
Q96D53-2;Q96D5	Q96D53-2;Q96D5	AarF domain-con	ADCK4	4	4	503	0	46.373	0.94717	0.87945	4.15E+08
P19388;A0A087\	P19388;A0A087\	DNA-directed RN/	POLR2E	8	8	210	0	69.908	0.94661	0.98358	9.91E+08
A0A087WYR0;P0	A0A087WYR0;P0	Signal recognitio	SRP19	3	3	120	0	11.609	0.94652	0.77496	2.25E+08
O94763-2;O9476	O94763-2;O9476	Unconventional p	URI1	1	1	459	0.001821	3.0489	0.94603	NaN	9.37E+06
P11586;F5H2F4;'	P11586;F5H2F4	C-1-tetrahydrofol	MTHFD1	62	61	935	0	323.31	0.9459	1.0422	4.57E+10
F2Z2W7;Q8IZ69-;	F2Z2W7;Q8IZ69-;	tRNA (uracil-5-)-m	TRMT2A	6	6	643	0	23.662	0.94586	NaN	1.34E+08
O94925;B7Z509;	O94925	Glutaminase kidn	GLS	19	4	669	0	209.91	0.94557	2.1146	1.74E+09
Q9NU22;Q5T795	Q9NU22	Midasin	MDN1	90	90	5596	0	323.31	0.94521	1.0374	7.75E+09
Q9NWX5;F6TX30	Q9NWX5;F6TX30	Ankyrin repeat an	ASB6	5	5	421	0	18.923	0.94474	0.84573	4.48E+08
Q9UN37;I3L4J1	Q9UN37;I3L4J1	Vacuolar protein	VPS4A	15	8	437	0	74.496	0.9446	1.0161	2.91E+09
I3L2W9;I3L2N2;(	I3L2W9;I3L2N2;(	Segment polarity	DVL2	3	3	363	0	10.522	0.94455	NaN	2.00E+08
Q6UVY6-2;Q6UV\	Q6UVY6-2;Q6UV\	DBH-like monoox	MOXD1	2	2	545	0.0037936	2.6027	0.94448	NaN	3.34E+07

Q92538-3;Q9253	Q92538-3;Q9253	Golgi-specific bre	GBF1	27	27	1855	0	201.56	0.94401	1.0861	1.72E+09
Q9Y221;Q9Y221-	Q9Y221;Q9Y221-	60S ribosome sub	NIP7	5	5	180	0	47.434	0.94368	1.6511	1.07E+09
Q8N2F6-4;Q8N2F	Q8N2F6-4;Q8N2F	Armadillo repeat-	ARMC10	3	3	249	0	16.724	0.9436	NaN	5.17E+07
H7BZN3;Q5UIP0-	H7BZN3;Q5UIP0-	Telomere-associa	RIF1	2	2	845	0	9.1708	0.94309	0.62166	7.17E+07
Q15054;Q15054-	Q15054;Q15054-	DNA polymerase (	POLD3	8	8	466	0	75.45	0.9429	NaN	4.47E+08
Q9Y2L5;J3QQJ5;(	Q9Y2L5;J3QQJ5;(	Trafficking protei	TRAPPC8	37	37	1435	0	323.31	0.94225	0.86801	2.34E+09
H0Y630;B4DR80;	H0Y630;B4DR80;	Serine/threonine-	STK24	7	1	369	0	15.256	0.94217	1.8173	1.14E+08
P60604;P60604-	P60604;P60604-	Ubiquitin-conjug	UBE2G2	3	3	165	0	70.15	0.94205	0.94125	4.62E+08
Q8IVW6-4;Q8IVW	Q8IVW6-4;Q8IVW	AT-rich interactiv	ARID3B;ARID3A	2	2	560	0	5.3569	0.94186	NaN	5.47E+07
O14976-2;O1497	O14976-2;O1497	Cyclin-G-associat	GAK	9	9	1232	0	168.89	0.94144	1.6298	5.23E+08
O60264	O60264	SWI/SNF-related r	SMARCA5	50	35	1052	0	310.38	0.94131	1.2191	7.78E+09
Q9H0S4;Q9H0S4	Q9H0S4;Q9H0S4	Probable ATP-dep	DDX47	17	17	455	0	170.24	0.94129	1.0121	3.33E+09
P10155-3;P1015	P10155-3;P1015	60 kDa SS-A/Ro ril	TROVE2	15	15	518	0	187.31	0.94118	1.8148	2.60E+09
J9JID7;Q03252	J9JID7;Q03252	Lamin-B2	LMNB2	15	11	620	0	33.623	0.94113	1.3585	5.10E+08
H7BXI1;A0FGR8-;	H7BXI1;A0FGR8-;	Extended synapto	ESYT2	17	17	884	0	141.61	0.94111	0.93773	2.19E+09
P24390-2;P2439	P24390-2;P2439	ER lumen protein	KDELR1;KDELR2	3	3	150	0	12.936	0.94109	0.5281	1.28E+08
O43175;Q5SZU1	O43175;Q5SZU1	D-3-phosphoglyc	PHGDH	27	27	533	0	323.31	0.9408	1.0734	6.82E+10
O75843;H0YJ08;(	O75843	AP-1 complex sub	AP1G2	7	7	785	0	21.476	0.94074	0.82062	7.59E+08
O75643;O75643-	O75643	U5 small nuclear r	SNRNP200	104	103	2136	0	323.31	0.9407	1.1291	2.63E+10
Q6SZW1;Q6SZW1	Q6SZW1;Q6SZW1	Sterile alpha and	SARM1	12	12	724	0	54.041	0.94007	NaN	5.51E+08
Q16658;C9JFC0;/	Q16658	Fascin	FSCN1	22	22	493	0	181.37	0.94002	0.71961	6.20E+09
Q08945;E9PMD4	Q08945	FACT complex sut	SSRP1	33	33	709	0	323.31	0.93992	0.97781	1.94E+10
O00148;O00148-	O00148;O00148-	ATP-dependent RI	DDX39A	25	6	427	0	189.81	0.93984	1.0471	4.45E+09
Q9BQ67;M0QX71	Q9BQ67	Glutamate-rich W	GRWD1	15	15	446	0	158.48	0.93977	0.97553	1.46E+10
D6RH30;P19838;	D6RH30;P19838;	Nuclear factor NF	NFKB1	3	3	198	0	21.542	0.93951	1.0628	1.38E+08
Q9BUE0	Q9BUE0	Mediator of RNA p	MED18	2	2	208	0	6.2263	0.93932	NaN	5.70E+07
Q8WVC2;P63220	Q8WVC2;P63220	40S ribosomal pr	RPS21	5	5	81	0	68.346	0.93925	1.1915	8.50E+08
Q01167-2;Q0116	Q01167-2;Q0116	Forkhead box pro	FOXK2	3	3	614	0	32.988	0.93917	0.9471	1.52E+08
P68371;M0R2D3	P68371	Tubulin beta-4B c	TUBB4B	36	1	445	0	323.31	0.93915	1.0972	3.92E+11
Q9UFC0;H7C5S6;	Q9UFC0;H7C5S6	Leucine-rich repe	LRWD1	11	11	647	0	149.62	0.93909	NaN	1.05E+09
P82663;E7EPW2;	P82663;E7EPW2;	28S ribosomal pr	MRPS25	9	9	173	0	36.067	0.93903	1.1335	6.79E+08
P17655;P17655-	P17655;P17655-	Calpain-2 catalyti	CAPN2	16	16	700	0	122.48	0.93861	0.96021	1.43E+09
O43143	O43143	Putative pre-mRN	DHX15	35	34	795	0	219.44	0.93853	1.1743	1.18E+10
P22102;P22102-	P22102;P22102-	Trifunctional puri	GART	54	54	1010	0	323.31	0.93823	0.97018	3.68E+10
P30085;Q5T0D2;	P30085;Q5T0D2;	UMP-CMP kinase	CMPK1	7	7	196	0	79.475	0.93816	0.96325	5.41E+08
Q96SK2-3;Q96SK	Q96SK2-3;Q96SK	Transmembrane p	TMEM209	7	7	519	0	62.834	0.93801	NaN	4.56E+08
P56385	P56385	ATP synthase sub	ATP5I	4	4	69	0	14.231	0.93762	1.9119	7.32E+08
Q00839-2;Q5RI1	Q00839-2	Heterogeneous nu	HNRNPU	38	1	806	0	323.31	0.93715	1.3922	4.72E+10
Q5JRX3;Q5JRX3-;	Q5JRX3;Q5JRX3-;	Presequence prot	PITRM1	37	37	1037	0	323.31	0.93709	0.99797	7.24E+09
Q99956;F8VW29	Q99956	Dual specificity p	DUSP9	7	7	384	0	39.999	0.93691	0.94876	5.18E+08
P08237;P08237-	P08237;P08237-	ATP-dependent 6-	PFKM	30	26	780	0	323.31	0.93619	1.002	1.02E+10
Q13188;Q13188-	Q13188;Q13188-	Serine/threonine-	STK3	4	3	491	0	18.313	0.93604	NaN	1.21E+08
A0A087WZ13;E9I	A0A087WZ13;E9I	Ribonucleoprotei	RAVER1	15	15	739	0	163.45	0.93588	0.70076	2.35E+09
Q9NV88-3;Q9NV	Q9NV88-3;Q9NV	Integrator compl	INTS9	5	5	634	0	20.282	0.93546	NaN	2.89E+08
J3KN66;Q5JTV8-;	J3KN66;Q5JTV8-;	Torsin-1A-interac	TOR1AIP1	8	8	599	0	78.242	0.93535	0.87686	5.74E+08
Q96IU4;B4DQJ4;I	Q96IU4;B4DQJ4;I	Alpha/beta hydro	ABHD14B	9	9	210	0	111.96	0.93535	0.88456	3.77E+09
Q7Z3U7-2;Q7Z3U	Q7Z3U7-2;Q7Z3U	Protein MON2 ho	MON2	12	12	1675	0	39.945	0.93534	0.99394	8.10E+08
Q9Y5Q8;Q9Y5Q8	Q9Y5Q8;Q9Y5Q8	General transcrip	GTF3C5	13	13	519	0	65.651	0.93505	NaN	1.50E+09
C9JXC3;C9JNE2;(	C9JXC3;C9JNE2;(	O-acetyl-ADP-ribo	OARD1	6	6	113	0	21.594	0.93502	0.99167	3.99E+08
Q9NX46	Q9NX46	Poly(ADP-ribose)	ADPRHL2	4	4	363	0	15.487	0.93451	0.80496	3.70E+08
Q6NSI4;Q6NSI4-4	Q6NSI4;Q6NSI4-4	Uncharacterized p	CXorf57	4	4	855	0	24.942	0.93392	1.1982	2.03E+08
Q9UHI6;E9PJ60;(	Q9UHI6	Probable ATP-dep	DDX20	23	23	824	0	237.53	0.93374	1.1887	3.54E+09
P16615;P16615-	P16615;P16615-	Sarcoplasmic/enc	ATP2A2	41	41	1042	0	323.31	0.93337	1.049	2.58E+10
Q9UDW1;Q9NZY	Q9UDW1;Q9NZY	Cytochrome b-c1	UQCR10	3	3	63	0	10.717	0.93322	0.89658	6.87E+08
Q6DKI1;R4GMU7	Q6DKI1;R4GMU7	60S ribosomal pr	RPL7L1	8	8	246	0	34.303	0.93315	1.5444	2.65E+09
O95671-2;O9567	O95671-2;O9567	N-acetylserotonir	ASMTL	4	4	605	0	28.357	0.93313	NaN	2.07E+08
Q05397-7;Q0539	Q05397-7;Q0539	Focal adhesion kir	PTK2	9	9	1006	0	72.157	0.93296	0.97019	9.07E+08
I3L2C7;P57678;I	I3L2C7;P57678	Gem-associated p	GEMIN4	23	23	1047	0	182.07	0.93293	1.0393	3.83E+09
Q13155;A8MU58	Q13155;A8MU58	Aminoacyl tRNA s	AIMP2	13	13	320	0	267.46	0.93286	0.92125	6.30E+09
Q9NWT1	Q9NWT1	p21-activated pro	PAK1IP1	4	4	392	0	9.3944	0.93275	1.059	1.98E+08
Q9Y2H2;Q9Y2H2	Q9Y2H2	Phosphatidylinos	INPP5F	3	3	1132	0	7.1	0.93252	0.81349	1.19E+08
O75746;O75746	O75746;O75746	Calcium-binding r	SLC25A12	22	15	678	0	125.88	0.93228	NaN	2.12E+09
A0A0A6YYL4;P57	A0A0A6YYL4;P57	Coronin-7	CORO7	15	15	1048	0	171.26	0.93224	0.85504	1.57E+09
A0A087WVQ6;Q(	A0A087WVQ6;Q(	Clathrin heavy ch	CLTC	104	83	1679	0	323.31	0.93221	1.0388	1.45E+11
Q14974;Q14974-	Q14974;Q14974-	Importin subunit	KPNB1	35	35	876	0	323.31	0.9321	1.1218	2.74E+10
Q9UJX3-2;Q9UJX	Q9UJX3-2;Q9UJX	Anaphase-promo	ANAPC7	8	8	537	0	59.628	0.93191	NaN	3.49E+08
Q5SRN1;O60508	Q5SRN1;O60508	Pre-mRNA-proces	CDC40	4	4	539	0	35.123	0.93184	NaN	1.35E+08
Q7Z4R8	Q7Z4R8	UPF0669 protein	C6orf120	2	2	191	0	62.118	0.93175	0.79673	3.77E+08
P55884;P55884-	P55884;P55884-	Eukaryotic transl	EIF3B	34	34	814	0	323.31	0.93103	1.0347	1.27E+10
Q6PGP7;D6RCE2;	Q6PGP7	Tetratricopeptide	TTC37	31	31	1564	0	291.47	0.93086	0.9918	2.85E+09
Q9NYY8-2;Q9NYY	Q9NYY8-2;Q9NYY	FAST kinase doma	FASTKD2	12	12	648	0	59.769	0.93064	NaN	9.13E+08
P35998;P35998-	P35998;P35998-	26S protease regu	PSMC2	33	33	433	0	297.51	0.93028	0.89308	1.90E+10
P62266;D6RD47;	P62266;D6RD47;	40S ribosomal pr	RPS23	6	6	143	0	19.407	0.92913	1.3668	3.36E+09
A0A087WWS7;Q	A0A087WWS7;Q	Syntaxin-binding	STXBP2;ZNF14	9	9	579	0	85.496	0.92908	NaN	4.68E+08
Q9Y2X0-2;Q9Y2X	Q9Y2X0-2;Q9Y2X	Mediator of RNA p	MED16	6	6	841	0	28.026	0.92905	0.90272	5.69E+08
A0A0A0MQR1;Q9	A0A0A0MQR1;Q9	Mitogen-activate	MAP4K5	9	9	846	0	69.192	0.92884	0.91486	6.24E+08
Q15738;C9JDR0	Q15738;C9JDR0	Sterol-4-alpha-ca	NSDHL	8	8	373	0	101.69	0.92877	0.89785	1.38E+09
Q96EK4	Q96EK4	THAP domain-cor	THAP11	3	3	314	0	5.7717	0.92796	0.9158	1.97E+08
O60341;O60341	O60341;O60341	Lysine-specific his	KDM1A	16	16	852	0	81.785	0.92792	1.083	1.89E+09
Q9UJU6;Q9UJU6	Q9UJU6;Q9UJU6	Drebrin-like prote	DBNL	12	12	430	0	217.22	0.9278	0.57684	1.03E+09
B0QY89;Q9Y262-	B0QY89;Q9Y262-	Eukaryotic transl	EIF3L	17	17	607	0	244.83	0.92772	NaN	3.02E+09
Q9NXX6;Q9NXX6	Q9NXX6;Q9NXX6	Non-structural m	NSMCE4A	6	6	385	0	19.795	0.92771	1.0509	2.08E+08
Q9NUQ7;D6RGX2	Q9NUQ7;D6RGX2	Ufm1-specific pro	UFSP2	16	16	469	0	122.41	0.92721	1.1956	2.99E+09
Q8TED0-3;Q8TED	Q8TED0-3;Q8TED	U3 small nucleola	UTP15	10	10	499	0	67.551	0.92692	1.0063	8.74E+08
Q9BZF1-3;Q9BZF	Q9BZF1-3;Q9BZF	Oxysterol-bindin	OSBPL8	12	12	847	0	102.19	0.92685	0.9037	7.76E+08
Q6PL18;Q6PL18-	Q6PL18;Q6PL18-	ATPase family AA	ATAD2	2	2	1390	0	10.446	0.92666	NaN	6.79E+07
Q9NVH2-3;Q9NVI	Q9NVH2-3;Q9NVI	Integrator compl	INTS7	20	20	942	0	149.17	0.92646	0.85735	2.29E+09
C9JG97;C9JEH3;(	C9JG97;C9JEH3;(	Angio-associated	AAMP	8	8	415	0	112.95	0.92636	1.1743	2.90E+09
A0A087WZ30;O9	A0A087WZ30;O9	ATP-dependent D	RECQL4	3	3	1208	0	7.802	0.92635	0.64673	3.81E+07
P30050;P30050-	P30050;P30050-	60S ribosomal pr	RPL12	12	12	165	0	160.64	0.92619	1.2097	1.51E+10
A0A0A0MT33;O9	A0A0A0MT33;O9	Splicing factor, ar	SCAF4;SCAF8	1	1	1349	0	3.6507	0.926	NaN	1.18E+08
P49419-2;P4941	P49419-2;P4941	Alpha-aminoadip	ALDH7A1	21	21	511	0	323.31	0.9256	1.0369	7.40E+09
Q8IWB1	Q8IWB1	Inositol 1,4,5-tris	ITPRIP	3	3	547	0	5.7014	0.92559	NaN	6.68E+07
Q14165;F5H1S8;	Q14165;F5H1S8;	Malectin	MLEC	4	4	292	0	31.645	0.92548	1.0859	2.80E+08
Q96EN8	Q96EN8	Molybdenum cof	MOCOS	3	3	888	0	18.24	0.92542	1.1928	1.50E+08
P62191;P62191-	P62191;P62191-	26S protease regu	PSMC1	26	26	440	0	323.31	0.92538	0.95468	1.17E+10
P57088;D6RAA6;	P57088;D6RAA6	Transmembrane p	TMEM33	10	10	247	0	68.793	0.92537	1.0002	7.87E+09
Q5QNZ2;P24539	Q5QNZ2;P24539	ATP synthase F(0)	ATP5F1	10	10	195	0	104.91	0.92465	0.77623	7.90E+08
O43149;O43149-	O43149	Zinc finger ZZ-typ	ZZEF1	12	12	2961	0	79.147	0.92426	1.1269	5.35E+08
Q9NVX2;A0A0A0I	Q9NVX2;A0A0A0I	Notchless protein	NLE1	16	16	485	0	186.21	0.92418	0.95607	3.30E+09
P22307-7;P2230	P22307-7;P2230	Non-specific lipid	SCP2	7	7	503	0	36.178	0.92416	0.84687	6.55E+08
O75592-2;O7559	O75592-2;O7559	E3 ubiquitin-prot	MYCBP2	30	30	4637	0	207.88	0.92413	0.9173	1.68E+09
Q8WWC4;H7C0V	Q8WWC4;H7C0V	Uncharacterized p	C2orf47	6	6	291	0	33.464	0.92356	0.78508	1.41E+09
Q6PIW4-2;Q6PIW	Q6PIW4-2;Q6PIW	Fidgetin-like prot	FIGNL1	3	2	563	0	20.767	0.92335	NaN	8.26E+07

Q92900-2;Q9290	Q92900-2;Q9290	Regulator of nons	UPF1	52	52	1118	0	323.31	0.92282	1.0916	1.52E+10
Q93100-4;Q9310	Q93100-4;Q9310	Phosphorylase b k	PHKB	7	7	1086	0	21.809	0.92277	1.0741	4.62E+08
P62244;I3L3P7;I	P62244;I3L3P7;I	40S ribosomal pr	RPS15A	13	7	130	0	123.36	0.92254	1.1001	1.85E+10
Q86WJ1;Q86WJ1	Q86WJ1;Q86WJ1	Chromodomain-h	CHD1L	14	2	897	0	122.46	0.92196	1.0543	9.70E+08
Q10567-3;Q1056	Q10567-3;Q1056	AP-1 complex sub	AP1B1	20	9	939	0	50.19	0.92182	1.2712	7.92E+08
P52907	P52907	F-actin-capping p	CAPZA1	12	10	286	0	145.9	0.92175	0.70347	3.92E+09
E9PER6;O15530-	E9PER6;O15530-	3-phosphoinositi	PDPK1;PDPK2	5	5	529	0	31.752	0.92174	NaN	3.63E+08
Q96RF0-2;Q96RF	Q96RF0-2;Q96RF	Sorting nexin-18	SNX18	6	6	624	0	19.526	0.9217	NaN	2.15E+08
Q32P28-4;Q32P2	Q32P28-4;Q32P2	Prolyl 3-hydroxyl	LEPRE1	3	3	697	0	15.672	0.92155	1.4782	2.53E+08
P63010;P63010-	P63010;P63010-	AP-2 complex sub	AP2B1	27	16	937	0	234.48	0.92154	0.97683	5.07E+09
O15397;O15397-	O15397;O15397-	Importin-8	IPO8	14	13	1037	0	65.656	0.92131	0.96981	1.10E+09
C9J0J7;G5E9Q6;F	C9J0J7;G5E9Q6;F	Profilin;Profilin-2	PFN2	7	2	91	0	36.731	0.92119	0.78863	6.09E+08
A6NJA2;P54578-;	A6NJA2;P54578-;	Ubiquitin carbox	USP14	16	16	448	0	132.5	0.92118	0.80275	2.39E+09
Q7L5D6;Q7L5D6	Q7L5D6;Q7L5D6	Golgi to ER traffic	GET4	9	9	327	0	66.429	0.92115	1.0483	1.87E+09
P10398;Q96II5;P	P10398;Q96II5	Serine/threonine	ARAF	8	7	606	0	19.479	0.92111	5.2201	6.67E+08
C9J3L8;C9J5W0;I	C9J3L8;C9J5W0;I	Translocon-associ	SSR1	2	2	265	0	25.042	0.9211	1.3303	9.85E+08
Q96J02-2;Q96J0	Q96J02-2;Q96J0	E3 ubiquitin-prot	ITCH	13	13	862	0	80.46	0.92095	0.82292	1.17E+09
Q8IYQ7	Q8IYQ7	Threonine syntha	THNSL1	5	5	743	0	47.913	0.9204	NaN	1.54E+08
O43156	O43156	TELO2-interacting	TTI1	4	4	1089	0	33.313	0.92038	1.0967	3.15E+08
Q9Y295;F8WEE0	Q9Y295	Developmentally	DRG1	11	11	367	0	83.293	0.92036	1.1885	1.48E+09
A0A0A0MSH8;E9I	A0A0A0MSH8;E9I	Tetratricopeptide	TTC39A	3	3	227	0	6.5771	0.92018	NaN	3.40E+07
Q9BW27-3;Q9BW	Q9BW27-3;Q9BW	Nuclear pore com	NUP85	15	15	610	0	147.9	0.92008	NaN	1.88E+09
Q9BVS4-2;Q9BVS	Q9BVS4-2;Q9BVS	Serine/threonine	RIOK2	2	2	474	0	23.92	0.92004	NaN	6.04E+07
Q96HR8-2;Q96HI	Q96HR8-2;Q96HI	H/ACA ribonuclec	NAF1;TMX1	2	2	389	0	21.064	0.92003	NaN	1.23E+08
Q9HC35;B5MBZ0	Q9HC35;B5MBZ0	Echinoderm micr	EML4	30	30	981	0	241.39	0.91994	1.1081	1.77E+09
O94808;E5RJP4	O94808	Glutamine--fructo	GFPT2	12	7	682	0	25.217	0.91947	NaN	2.19E+08
O95373;E9PLJ0;E	O95373	Importin-7	IPO7	25	24	1038	0	323.31	0.91946	1.0961	7.80E+09
O75607	O75607	Nucleoplasmin-3	NPM3	6	6	178	0	143.1	0.91944	0.95247	7.75E+09
Q12904;Q12904	Q12904;Q12904	Aminoacyl tRNA s	AIMP1	20	20	312	0	263.58	0.919	1.0764	7.88E+09
K7EIG1	K7EIG1		CLUH	44	0	1251	0	323.31	0.91876	0.93328	6.97E+09
Q8TEQ6	Q8TEQ6	Gem-associated p	GEMIN5	34	34	1508	0	323.31	0.91826	1.0752	4.79E+09
O43379-4;O4337	O43379-4;O4337	WD repeat-contai	WDR62	8	8	1523	0	39.949	0.91824	0.91629	1.84E+08
P48651;J3KNR6;I	P48651	Phosphatidylserir	PTDSS1	3	3	473	0	6.93	0.91824	0.63091	3.34E+08
B1AMS2;Q14141	B1AMS2;Q14141	Septin-6	06-Sep	5	2	431	0	85.512	0.91822	1.064	5.11E+08
Q8NBY1;B4E0Y9;I	Q8NBY1;B4E0Y9;I	Serine/threonine	RBM4B;MST4	10	4	392	0	39.802	0.91821	1.1723	1.28E+09
F5H5V6;F5H6S1;I	F5H5V6;F5H6S1;I	Lysine-specific de	KDM6A;UTY	4	4	1269	0	33.259	0.91798	0.94091	5.24E+07
Q9BVJ6-3;Q9BVJ	Q9BVJ6-3;Q9BVJ	U3 small nucleola	UTP14A	10	10	719	0	100	0.9172	0.79381	8.02E+08
Q13564-3;Q1356	Q13564-3;Q1356	NEDD8-activating	NAE1	3	3	445	0	32.831	0.91715	NaN	1.13E+08
Q16512;Q16512	Q16512;Q16512	Serine/threonine	PKN1	12	11	942	0	63.431	0.91715	0.89412	9.78E+08
Q15046;Q15046	Q15046;Q15046	Lysine--tRNA ligas	KARS	32	32	597	0	323.31	0.91712	0.97507	7.06E+09
Q9P0M9;D6RAN8	Q9P0M9;D6RAN8	39S ribosomal pr	MRPL27	5	5	148	0	18.369	0.91706	0.385	2.10E+08
Q9UQ13-2;Q9UQ	Q9UQ13-2;Q9UQ	Leucine-rich repe	SHOC2	4	4	536	0	35.799	0.91697	NaN	2.86E+08
A2IDC6;Q13084;/	A2IDC6;Q13084;/	39S ribosomal pr	MRPL28	4	4	240	0	9.6021	0.91696	1.1425	8.60E+07
E7ES33;E7EPK1;C	E7ES33;E7EPK1;C	Septin-7	07-Sep	12	12	417	0	83.471	0.91686	1.1792	1.88E+09
Q9UPN7;K7EM28	Q9UPN7	Serine/threonine	PPP6R1	7	7	881	0	61.714	0.91643	1.0562	2.63E+08
Q8N3U4;Q8N3U4	Q8N3U4;Q8N3U4	Cohesin subunit S	STAG2	11	11	1231	0	30.912	0.91636	0.91671	2.50E+08
O75131;A0A087\	O75131;A0A087\	Copine-3	CPNE3	20	19	537	0	193.84	0.91619	1.0482	5.05E+09
Q9P0J0;Q9P0J0-;	Q9P0J0;Q9P0J0-;	NADH dehydroge	NDUFA13	9	8	144	0	57.262	0.91589	0.6982	1.95E+09
P68104;Q5VTE0;/	P68104;Q5VTE0;/	Elongation factor	EEF1A1;EEF1A1P5	32	16	462	0	323.31	0.91584	1.1002	1.32E+11
Q06210-2;Q0621	Q06210-2;Q0621	Glutamine--fructo	GFPT1	30	25	681	0	260.32	0.91525	0.84748	6.51E+09
Q13637;O14966;	Q13637	Ras-related protei	RAB32	5	5	225	0	29.167	0.91522	0.93082	2.38E+08
P31689;P31689-	P31689;P31689-	DnaJ homolog sul	DNAJA1	16	16	397	0	182.39	0.91495	1.0106	4.83E+09
Q8N8L6	Q8N8L6	ADP-ribosylation	ARL10	2	2	244	0.00078989	3.2586	0.91495	0.7217	9.81E+07
P51648;P51648-	P51648;P51648-	Fatty aldehyde de	ALDH3A2	11	10	485	0	31.541	0.91488	0.87031	6.26E+08
Q13257;Q13257	Q13257	Mitotic spindle as	MAD2L1	7	7	205	0	74.072	0.91474	0.99512	2.05E+09
Q9Y2Z4;H0YHS6	Q9Y2Z4;H0YHS6	Tyrosine--tRNA lig	YARS2	12	12	477	0	146.56	0.91468	1.032	9.45E+08
Q9BTT6;Q5T0G3;	Q9BTT6;Q5T0G3;	Leucine-rich repe	LRRC1	4	3	524	0	24.36	0.91456	NaN	4.36E+08
Q96NB2;R4GMR9	Q96NB2;R4GMR9	Sideroflexin-2	SFXN2	8	8	322	0	23.486	0.91455	1.7619	4.83E+08
Q8NB90;Q8NB90	Q8NB90;Q8NB90	Spermatogenesis-	SPATA5	14	13	893	0	238	0.91451	0.90548	8.31E+08
P61962;A0A087\	P61962;A0A087\	DDB1- and CUL4-;	DCAF7	8	8	342	0	71.59	0.91437	0.98341	2.06E+09
Q9NVC6;E9PJZ4;I	Q9NVC6	Mediator of RNA	MED17	3	3	651	0	15.161	0.91403	1.3685	1.87E+08
J3QRU1;P07947;	J3QRU1;P07947;	Tyrosine-protein	YES1;FYN;SRC	4	3	548	0	11.395	0.91358	1.1417	2.72E+08
Q09161;X6R941;	Q09161	Nuclear cap-bindi	NCBP1	23	23	790	0	193.57	0.91352	0.95976	4.99E+09
E9PLL6;P46776;E	E9PLL6;P46776;E	60S ribosomal pr	RPL27A	5	5	108	0	22.558	0.91315	1.7399	5.37E+09
P18085;C9JAK5;(	P18085;C9JAK5;(	ADP-ribosylation	ARF4	11	8	180	0	35.904	0.91286	2.7106	1.30E+09
Q6DD88;F5H6I7;	Q6DD88;F5H6I7;	Atlastin-3	ATL3	8	8	541	0	69.984	0.91275	1.0193	1.16E+09
Q5TH30;Q9UGV2	Q5TH30;Q9UGV2	Protein NDRG3	NDRG3	6	6	388	0	76.811	0.91257	0.65499	8.15E+08
P09110;C9JDE9;I	P09110;C9JDE9;I	3-ketoacyl-CoA th	ACAA1	6	6	424	0	34.037	0.91203	0.81478	4.18E+08
F8WCF6;P59998;	F8WCF6;P59998;	Actin-related prot	ARPC4-TTLL3;ARP	7	7	181	0	21.994	0.91167	1.0155	2.86E+09
Q86X55-1;Q86X5	Q86X55-1;Q86X5	Histone-arginine	CARM1	16	16	585	0	113.52	0.91159	1.031	2.06E+09
Q9NPQ8-4;Q9NP	Q9NPQ8-4;Q9NP	Synembryn-A	RIC8A	13	12	530	0	117.59	0.9109	NaN	1.49E+09
P46940;H0YLE8;/	P46940;H0YLE8;/	Ras GTPase-activa	IQGAP1	49	47	1657	0	323.31	0.91067	1.4184	1.07E+10
Q9Y696;A6PVS0;I	Q9Y696	Chloride intracell	CLIC4	17	17	253	0	258.15	0.91053	0.89217	4.50E+09
I3L2B0	I3L2B0		CLUH	38	2	1236	0	4.3349	0.91051	NaN	9.34E+06
Q9BXW7-2;Q9BX	Q9BXW7-2;Q9BX	Cat eye syndrome	CECR5	13	13	393	0	199.38	0.91037	0.99205	4.40E+09
Q92769-3;Q9276	Q92769-3;Q9276	Histone deacetyla	HDAC2	11	7	458	0	93.638	0.91024	NaN	5.88E+08
B1AH87;P30536	B1AH87;P30536	Translocator prot	TSPO	2	2	107	0	3.8388	0.90981	0.97641	1.02E+08
Q8N8A6	Q8N8A6	ATP-dependent RI	DDX51	7	7	666	0	29.579	0.90926	1.0296	4.28E+08
F8W930;Q9Y6M1	F8W930;Q9Y6M1	Insulin-like growt	IGF2BP2	10	8	605	0	64.113	0.90921	NaN	5.00E+08
O76003	O76003	Glutaredoxin-3	GLRX3	11	11	335	0	92.771	0.90888	0.81783	5.12E+09
Q8NFH4;F8VTY2	Q8NFH4;F8VTY2	Nucleoporin Nup	NUP37	8	8	326	0	66.304	0.90886	1.3591	1.65E+09
I3L4X2;P33527-6	I3L4X2;P33527-6	Multidrug resista	ABCC1	14	14	1440	0	82.676	0.90847	1.3108	8.49E+08
P17812;P17812-	P17812;P17812-	CTP synthase 1	CTPS1	26	22	591	0	254.51	0.90816	0.89109	9.14E+09
Q9NZL4;Q9NZL4-	Q9NZL4;Q9NZL4-	Hsp70-binding pr	HSPBP1	4	4	362	0	14.198	0.90813	1.3883	6.10E+08
P51153;A0A087\	P51153	Ras-related protei	RAB13	10	7	203	0	51.91	0.90777	0.98066	1.54E+09
P11387;Q969P6-	P11387	DNA topoisomera	TOP1	30	30	765	0	224.65	0.90748	1.3514	7.79E+09
J3KPT4;Q9H4I3-2	J3KPT4;Q9H4I3-2	TraB domain-con	TRABD	3	3	379	0	9.7607	0.90719	1.0461	2.99E+08
Q13547;Q5TEE2;I	Q13547;Q5TEE2	Histone deacetyla	HDAC1	12	8	482	0	119.13	0.90702	NaN	2.95E+09
Q14697;Q14697-	Q14697;Q14697-	Neutral alpha-glu	GANAB	31	31	944	0	297.93	0.90647	1.0668	5.18E+09
A0A087WY61;Q1	A0A087WY61;Q1	Nuclear mitotic a	NUMA1	8	8	2099	0	65.838	0.90595	1.1684	2.59E+08
Q6YHU6;Q6YHU6	Q6YHU6;Q6YHU6	Thyroid adenoma	THADA	19	19	1953	0	97.84	0.90589	1.1307	9.24E+08
J3QSE8;Q9BX63-;	J3QSE8;Q9BX63-;	Fanconi anemia g	BRIP1	3	3	994	0	10.208	0.90581	NaN	3.86E+07
O00442;O00442	O00442;O00442	RNA 3-terminal pl	RTCA	15	15	366	0	155.2	0.90566	1.0924	4.44E+09
Q9NZ01;Q9NZ01	Q9NZ01	Very-long-chain e	TECR	17	17	308	0	89.148	0.90553	0.75701	5.48E+09
Q9H583;Q5T3Q7	Q9H583;Q5T3Q7	HEAT repeat-cont	HEATR1	57	57	2144	0	323.31	0.9054	1.2719	9.84E+09
Q86YV9	Q86YV9	Hermansky-Pudla	HPS6	4	4	775	0	12.03	0.90537	0.99706	2.94E+08
Q5JP53;P07437;I	Q5JP53;P07437;I	Tubulin beta chai	TUBB	34	5	426	0	323.31	0.90521	1.1635	1.53E+11
J3KN10;P42356;I	J3KN10;P42356	Phosphatidylinos	PI4KA	30	30	2102	0	163.74	0.9051	1.018	1.70E+09
P20290-2;P2029	P20290-2;P2029	Transcription fact	BTF3	5	5	162	0	90.747	0.90501	1.8296	8.47E+08
Q9H300;F8WCQ4	Q9H300;F8WCQ4	Presenilins-associ	PARL	4	4	379	0	13.586	0.90469	0.76029	2.21E+08
Q96GM8;Q96GM	Q96GM8;Q96GM	Target of EGR1 pr	TOE1	6	6	510	0	25.663	0.90409	NaN	3.08E+08
Q9ULC4-2;Q9ULC	Q9ULC4-2;Q9ULC	Malignant T-cell-a	MCTS1	8	8	169	0	105.7	0.90406	0.78871	2.90E+09
Q9H845;H0Y8Z9	Q9H845;H0Y8Z9	Acyl-CoA dehydro	ACAD9	13	13	621	0	46.063	0.90346	NaN	1.40E+09
P34896-2;P3489	P34896-2;P3489	Serine hydroxyme	SHMT1	13	12	444	0	105.22	0.90342	0.73904	1.69E+09

P26640;A0A1401	P26640;A0A1401	Valine--tRNA ligas	VARS	50	50	1264	0	323.31	0.90332	0.96256	1.75E+10
Q8N163-2;Q8N1(	Q8N163-2;Q8N1(	Cell cycle and apo	CCAR2	21	21	923	0	202.31	0.9033	1.0684	4.95E+09
H0Y4B0;O43414-	H0Y4B0;O43414-	ERI1 exoribonucl	ERI3	4	4	204	0	11.177	0.90326	NaN	3.11E+07
P13861-2;P1386	P13861-2;P1386	cAMP-dependent	PRKAR2A	16	13	382	0	102.46	0.90253	0.97764	1.69E+09
Q96T76;Q96T76-	Q96T76;Q96T76-	MMS19 nucleotic	MMS19	31	31	1030	0	323.31	0.90249	1.2062	9.44E+09
Q9H061;E9PI90;(	Q9H061;E9PI90;(	Transmembrane p	TMEM126A	4	4	195	0	14.76	0.90225	1.7341	4.75E+08
Q9UIV1-2;Q9UIV:	Q9UIV1-2;Q9UIV:	CCR4-NOT transcr	CNOT7	4	4	244	0	45.202	0.90107	0.95463	4.73E+08
Q7L523;Q5VZM2	Q7L523;Q5VZM2	Ras-related GTP-b	RRAGA;RRAGB	6	6	313	0	27.512	0.90096	2.1119	7.38E+08
O95758-1;O9575	O95758-1;O9575	Polypyrimidine tr	PTBP3	6	3	521	0	31.134	0.90084	1.121	1.30E+08
P49736;H0Y8E6;I	P49736;H0Y8E6	DNA replication li	MCM2	36	36	904	0	323.31	0.90079	1.1777	9.86E+09
P19367;P19367-	P19367;P19367-	Hexokinase-1	HK1	54	50	917	0	323.31	0.90025	1.0767	1.80E+10
O43447;C9JQD4;	O43447;C9JQD4;	Peptidyl-prolyl ci	PPIH	12	12	177	0	105.52	0.90009	1.2096	5.25E+09
Q9BUK6-3;Q9BUI	Q9BUK6-3;Q9BUI	Protein misato ho	MSTO1	7	6	558	0	20.773	0.90008	NaN	5.30E+08
E9PGW7;Q5T8T7	E9PGW7;Q5T8T7	Mediator of RNA p	MED22	2	2	111	0	4.7881	0.89922	NaN	3.55E+07
P0DN79;P35520;	P0DN79;P35520;	Cystathionine bet	CBS	25	25	551	0	169.38	0.89886	0.79834	3.06E+09
O95251-4;O9525	O95251-4;O9525	Histone acetyltra	KAT7	7	7	581	0	50.185	0.89868	1.0085	3.63E+08
P60866;P60866-	P60866;P60866-	40S ribosomal pr	RPS20	11	11	119	0	72.458	0.89825	1.0092	2.21E+10
J3KPS3;P04075;F	J3KPS3;P04075;F	Fructose-bisphos	ALDOA	26	23	368	0	323.31	0.89824	1.1614	8.15E+09
A0A0C4DFR8;Q9I	A0A0C4DFR8;Q9I	Protein UXT	UXT	3	3	169	0	12.422	0.89814	1.4681	1.47E+08
O75794;X6RKY7;	O75794;X6RKY7;	Cell division cycle	CDC123	5	5	336	0	15.863	0.89787	1.0599	4.20E+08
F5GYQ1;P61421;	F5GYQ1;P61421;	V-type proton ATI	ATP6V0D1	3	3	392	0	16.399	0.89782	4.4514	7.24E+08
Q8TCX1-3;Q8TCX	Q8TCX1-3;Q8TCX	Cytoplasmic dyne	DYNC2LI1	3	3	334	0	9.5106	0.89777	1.4933	1.43E+08
K7ESP4;Q8WVC6	K7ESP4;Q8WVC6	Dephospho-CoA k	DCAKD	10	10	209	0	46.953	0.89752	0.67846	5.94E+08
A0A0U1RRH6;O9	A0A0U1RRH6;O9	PHD finger protei	PHF14	3	3	948	0	5.525	0.8973	0.99908	5.28E+07
Q8IYB7;H7C440;(	Q8IYB7;H7C440;(	DIS3-like exonucl	DIS3L2	8	8	885	0	32.863	0.89693	1.0631	5.30E+08
B7WPG3;C9IYN3;	B7WPG3;C9IYN3;	Heterogeneous nu	HNRPLL;HNRNPLI	13	12	508	0	96.557	0.89673	NaN	1.35E+09
Q15437;Q5QPE1;	Q15437	Protein transport	SEC23B	18	15	767	0	244.76	0.89673	0.97305	2.19E+09
Q13885	Q13885	Tubulin beta-2A c	TUBB2A	34	2	445	0	229.97	0.89672	1.075	1.53E+10
O60884;A0A087\	O60884	DnaJ homolog sul	DNAJA2	19	19	412	0	279.48	0.89601	1.1816	5.04E+09
Q9BZE9;Q9BZE9-;	Q9BZE9;Q9BZE9-;	Tether containing	ASPSCR1	5	5	553	0	45.96	0.89538	NaN	1.78E+08
Q15459;Q15459-	Q15459;Q15459-	Splicing factor 3A	SF3A1	6	6	793	0	28.031	0.89483	1.5057	2.17E+08
Q9UN86-2;Q9UN	Q9UN86-2;Q9UN	Ras GTPase-activa	G3BP2	12	10	449	0	107.42	0.89467	0.22331	1.23E+09
Q96T58;H0Y5U7;	Q96T58;H0Y5U7;	Msx2-interacting	SPEN	2	2	3664	0	5.8419	0.89453	1.0443	9.81E+06
C9J2Y9;P30876;(	C9J2Y9;P30876;(	DNA-directed RN/	POLR2B	41	41	1167	0	323.31	0.89436	1.2828	8.73E+09
Q9NYH9;J3KRR8	Q9NYH9	U3 small nucleola	UTP6	11	11	597	0	108.5	0.89417	NaN	7.59E+08
Q9BU02;G3V5Q5	Q9BU02;G3V5Q5	Thiamine-triphos	THTPA	6	6	230	0	14.972	0.8941	0.98361	2.93E+08
A0A0C4DGS1;P3!	A0A0C4DGS1;P3!	Dolichyl-diphosp	DDOST	13	13	439	0	210.02	0.89396	1.3471	6.81E+09
Q14558-2;Q1455	Q14558-2;Q1455	Phosphoribosyl p	PRPSAP1	11	4	385	0	109.21	0.89336	1.0039	2.91E+09
Q96RG2;Q96RG2	Q96RG2;Q96RG2	PAS domain-cont	PASK	7	7	1323	0	46.143	0.89334	0.88331	4.09E+08
A0A0A0MTR7;A0/	A0A0A0MTR7;A0/	E3 ubiquitin-prot	RNF213	38	37	5207	0	197.26	0.89314	0.86386	1.82E+09
P56282-3;P5628	P56282-3;P5628	DNA polymerase e	POLE2	5	5	502	0	37.89	0.89301	1.0974	2.29E+08
Q5VV89;O14880;	Q5VV89;O14880	Microsomal gluta	MGST2	4	4	166	0	42.515	0.89291	1.1699	8.12E+08
P23743;G3V4E1;	P23743;G3V4E1	Diacylglycerol kin	DGKA	3	3	735	0	14.317	0.8929	NaN	1.26E+08
O60333-3	O60333-3	Kinesin-like prote	KIF1B	16	4	1153	0	72.622	0.89268	1.3203	2.54E+08
Q99504-5;Q9950	Q99504-5;Q9950	Eyes absent homo	EYA3	2	2	527	0	24.118	0.89258	NaN	1.15E+08
E9PKL7;Q5HYI5;P	E9PKL7;Q5HYI5;P	Ras-related protei	RAB2A;DKFZp313	3	3	181	0	6.8899	0.89245	NaN	1.06E+08
J3KQ61;O95696;	J3KQ61;O95696;	Bromodomain-co	BRD1	1	1	509	0.0047346	2.402	0.89228	NaN	2.23E+07
P60983;G3V4P8;	P60983;G3V4P8	Glia maturation fa	GMFB	7	7	142	0	62.479	0.892	0.99933	1.03E+09
P16435;H0Y4R2;	P16435;H0Y4R2;	NADPH--cytochro	POR	5	5	677	0	21.19	0.8919	NaN	2.57E+08
M0R0Y2;P54920;	M0R0Y2;P54920;	Alpha-soluble NS	NAPA	6	6	256	0	56.176	0.89126	0.68214	3.73E+08
Q9H9A5-4;Q9H9/	Q9H9A5-4;Q9H9/	CCR4-NOT transcr	CNOT10	12	12	695	0	65.433	0.89122	0.80699	1.03E+09
Q14146;Q5VYD0	Q14146	Unhealthy riboso	URB2	29	29	1524	0	122.05	0.89023	1.0652	2.36E+09
D6RIY6;Q06265;(	D6RIY6;Q06265;(	Exosome comple	EXOSC9	4	4	423	0	14.955	0.89006	NaN	7.63E+08
P49903;P49903-	P49903;P49903-	Selenide, water di	SEPHS1	7	7	392	0	129.74	0.89003	1.1802	1.09E+09
Q00013-2;Q0001	Q00013-2;Q0001	55 kDa erythrocyt	MPP1	4	4	436	0	17.62	0.88978	1.0785	2.36E+08
Q13472-3;Q1347	Q13472-3;Q1347	DNA topoisomera	TOP3A	4	4	906	0	7.622	0.88978	NaN	3.48E+08
F8VVA0;F8VQD9;	F8VVA0;F8VQD9;	Autophagy-relate	ATG101	1	1	141	0	4.2762	0.88933	0.87893	3.50E+07
P28072;A0A087\	P28072;A0A087\	Proteasome subu	PSMB6	6	6	239	0	19.826	0.88903	0.68105	2.32E+08
Q13015	Q13015	Protein AF1q	MLLT11	4	4	90	0	128.74	0.88884	0.97043	2.02E+08
Q96A33;Q96A33-	Q96A33;Q96A33-	Coiled-coil domai	CCDC47	10	10	483	0	81.808	0.88882	NaN	3.72E+08
Q96BY7	Q96BY7	Autophagy-relate	ATG2B	6	6	2078	0	65.253	0.88841	1.1392	1.67E+08
V9GYX7;Q9NZ32;	V9GYX7;Q9NZ32;	Actin-related pro	ACTR10	5	5	302	0	42.417	0.88816	1.1626	5.99E+08
P31483-2;C9JTN:	P31483-2;C9JTN:	Nucleolysin TIA-1	TIA1	7	0	375	0	26.701	0.88779	1.8973	3.00E+08
Q86V85	Q86V85	Integral membra	GPR180	2	2	440	0	11.542	0.88779	0.77165	7.32E+07
A3KFL1;A3KFL5;A	A3KFL1;A3KFL5;A	Exosome comple	EXOSC2	2	2	200	0	6.7518	0.88744	NaN	1.37E+08
P61978-3;Q5T6W	P61978-3;Q5T6W	Heterogeneous nu	HNRNPK	34	2	440	0	9.8937	0.88711	1.7273	1.16E+09
Q09028-3;Q0902	Q09028-3;Q0902	Histone-binding p	RBBP4	14	7	410	0	257.49	0.88708	1.2422	7.61E+09
Q709F0;Q709F0-	Q709F0;Q709F0-	Acyl-CoA dehydro	ACAD11	13	13	780	0	104.28	0.88668	0.78425	1.31E+09
P51398-2;P5139	P51398-2;P5139	28S ribosomal pr	DAP3	9	9	357	0	64.648	0.88666	1.3855	1.66E+09
P14868;P14868-	P14868;P14868-	Aspartate--tRNA li	DARS	29	29	501	0	228.98	0.88611	0.96973	5.98E+09
Q8N6R0;Q8N6R0	Q8N6R0;Q8N6R0	Methyltransferas	METTL13	18	18	699	0	98.904	0.88606	0.92495	1.34E+09
Q92995-2;Q9299	Q92995-2;Q9299	Ubiquitin carbox	USP13	5	3	798	0	30.314	0.88564	1.0647	2.73E+08
Q9ULX3;H3BUR4	Q9ULX3	RNA-binding prot	NOB1	17	17	412	0	99.418	0.8855	1.0044	2.51E+09
G5E9W7;G5E9V5	G5E9W7;G5E9V5	28S ribosomal pr	MRPS22	13	13	319	0	86.119	0.88396	0.90325	3.42E+09
P86791;P86790;	P86791;P86790	Vacuolar fusion p	CCZ1;CCZ1B	5	5	482	0	28.55	0.88359	0.87148	2.64E+08
Q14676-3;Q1467	Q14676-3;Q1467	Mediator of DNA	MDC1	10	10	1802	0	82.739	0.88337	1.0717	4.99E+08
Q8TCE6-2;Q8TCE(	Q8TCE6-2;Q8TCE(	Protein FAM45A;I	FAM45A;FAM45B	6	6	349	0	24.923	0.88335	1.0075	4.71E+08
Q9H2C0	Q9H2C0	Gigaxonin	GAN	9	9	597	0	40.052	0.88335	NaN	5.02E+08
Q9UDY8;Q9UDY8	Q9UDY8;Q9UDY8	Mucosa-associate	MALT1	3	3	824	0	58.554	0.88315	1.0892	2.50E+08
P61313;E7EQV9;I	P61313;E7EQV9;I	60S ribosomal pr	RPL15	14	14	204	0	79.4	0.88297	1.2494	3.93E+09
Q13838;Q13838-	Q13838;Q13838-	Spliceosome RNA	DDX39B	28	9	428	0	282.17	0.8829	1.1765	3.02E+10
Q96EL3	Q96EL3	39S ribosomal pr	MRPL53	1	1	112	0	19.807	0.8828	1.0428	1.01E+08
Q9NRX4;Q9NRX4	Q9NRX4	14 kDa phosphoh	PHPT1	5	5	125	0	59.684	0.88268	0.78926	4.63E+08
P60510;H3BTA2;	P60510;H3BTA2;	Serine/threonine-	PPP4C	7	6	307	0	26.317	0.88252	0.87879	2.14E+08
Q9H0U4;E9PLD0;	Q9H0U4;E9PLD0;	Ras-related protei	RAB1B;RAB1C	9	4	201	0	119.02	0.88239	1.1202	7.82E+08
P57772;P57772-	P57772;P57772-	Selenocysteine-sp	EEFSEC	14	14	596	0	48.789	0.88235	NaN	4.87E+08
Q96CX2;Q68DU8	Q96CX2	BTB/POZ domain-	KCTD12	10	10	325	0	63.699	0.88205	0.6738	1.64E+09
Q08209-2;Q0820	Q08209-2;Q0820	Serine/threonine-	PPP3CA;PPP3CB	6	6	511	0	15.576	0.88172	NaN	3.38E+08
A1L0T0;M0R026;	A1L0T0;M0R026	Acetolactate synt	ILVBL	9	9	632	0	83.361	0.88119	NaN	5.53E+08
Q16576;E9PC52;	Q16576;E9PC52;	Histone-binding p	RBBP7	16	9	425	0	323.31	0.88077	1.1176	1.19E+10
Q5T8U5;O15260-	Q5T8U5;O15260-	Surfeit locus prot	SURF4	4	4	186	0	24.198	0.88062	1.1565	1.53E+08
P35270	P35270	Sepiapterin reduc	SPR	8	8	261	0	122.67	0.88049	1.1625	2.92E+09
F8VVA7;P61923;I	F8VVA7;P61923;I	Coatomer subuni	COPZ1	6	6	198	0	76.799	0.88003	0.95066	2.95E+09
H0YGV7;H0YG20;	H0YGV7;H0YG20;	Endoplasmic retic	MAN1B1	2	2	550	0	6.7358	0.87934	NaN	6.90E+07
Q9BST9;Q9BST9-;	Q9BST9;Q9BST9-;	Rhotekin	RTKN	2	2	563	0	9.8263	0.87917	NaN	1.19E+08
P25490;H0YJV7;I	P25490;H0YJV7	Transcriptional re	YY1	7	7	414	0	26.148	0.87904	0.41018	1.38E+08
Q7Z392;Q7Z392-	Q7Z392;Q7Z392-	Trafficking protei	TRAPPC11	10	10	1133	0	48.512	0.87876	0.98179	4.29E+08
A0A0C4DG33;O4	A0A0C4DG33;O4	Peroxisome biogé	PEX1	9	9	1226	0	28.379	0.87854	0.85579	2.39E+08
Q14739;C9JXK0;I	Q14739;C9JXK0	Lamin-B receptor	LBR	17	17	615	0	165.04	0.87833	1.2421	6.07E+09
P47897;P47897-	P47897;P47897-	Glutamine--tRNA	QARS	43	43	775	0	323.31	0.87791	1.0264	1.43E+10
Q15021;E7EN77;	Q15021;E7EN77	Condensin compl	NCAPD2	36	36	1401	0	223.7	0.87763	1.1129	4.71E+09
Q8IU81	Q8IU81	Interferon regulat	IRF2BP1	5	5	584	0	10.375	0.87713	NaN	1.56E+08
Q5VW36	Q5VW36	Focadhesin	FOCAD	16	5	1801	0	50.82	0.87712	1.1583	9.71E+08
Q05639	Q05639	Elongation factor	EEF1A2	20	4	463	0	71.454	0.87691	1.0824	1.10E+09

Q6L8Q7-2;Q6L8C	Q6L8Q7-2;Q6L8C	2,5-phosphodiest	PDE12	17	17	535	0	160.11	0.87691	3.8514	2.26E+09
E7EQY4;E7EV10;C	E7EQY4;E7EV10;C	Metastasis-associ	MTA3	8	2	514	0	8.9506	0.87668	NaN	6.86E+07
Q9BTE3-2;Q9BTE:	Q9BTE3-2;Q9BTE:	Mini-chromosom	MCMBP	10	10	640	0	32.396	0.87624	NaN	5.62E+08
Q16531;F5GY55;	Q16531;F5GY55;	DNA damage-binc	DDB1	23	23	1140	0	155.26	0.8762	0.93149	2.84E+09
O95816;O95816·	O95816;O95816·	BAG family molec	BAG2	8	8	211	0	30.514	0.87605	0.8975	4.92E+08
Q6YP21-3;Q6YP2	Q6YP21-3;Q6YP2	Kynurenine--oxog	CCBL2	9	9	420	0	59.275	0.87567	0.76116	2.38E+09
Q92734-2;Q9273	Q92734-2;Q9273	Protein TFG	TFG	2	2	396	0	8.6998	0.87563	NaN	5.95E+07
Q8TEA1;U3KQU2	Q8TEA1;U3KQU2	Putative methyltr	NSUN6	5	5	469	0	9.5669	0.87554	0.6276	2.33E+08
Q7Z3T8	Q7Z3T8	Zinc finger FYVE d	ZFYVE16	5	5	1539	0	25.457	0.87511	0.86356	1.94E+08
P42858;H0YA07	P42858	Huntingtin	HTT	32	32	3142	0	311.99	0.87503	1.1044	2.67E+09
P13807-2;P1380	P13807-2;P1380	Glycogen [starch]	GYS1	18	18	673	0	170.09	0.87462	0.95948	5.85E+09
Q9UIC8-3;Q9UIC	Q9UIC8-3;Q9UIC	Leucine carboxyl	LCMT1	7	7	279	0	30.014	0.87461	1.1724	9.54E+08
E7EN32;O00255-	E7EN32;O00255-	Menin	MEN1	5	5	555	0	41.709	0.87423	NaN	1.28E+08
H0Y9G6;E7ETU7;I	H0Y9G6;E7ETU7;I	39S ribosomal pr	MRPL3	3	3	363	0	9.9789	0.87386	1.3223	7.40E+07
Q16698-2;Q1669	Q16698-2;Q1669	2,4-dienoyl-CoA r	DECR1	6	6	326	0	36.067	0.87337	1.2167	5.70E+08
Q9H2W6;A0A087	Q9H2W6	39S ribosomal pr	MRPL46	5	5	279	0	18.88	0.87283	1.2137	2.16E+08
Q8IUR0	Q8IUR0	Trafficking protei	TRAPPC5	2	2	188	0	4.0625	0.87229	NaN	1.28E+08
P07900;P07900-	P07900;P07900-	Heat shock protei	HSP90AA1	57	36	732	0	323.31	0.87226	1.133	4.71E+10
Q99714;Q5H928	Q99714;Q5H928	3-hydroxyacyl-Co	HSD17B10	4	4	261	0	87.962	0.87216	0.91399	3.27E+08
A0A087WT20;Q9	A0A087WT20;Q9	DDB1- and CUL4-i	DCAF13	10	10	597	0	35.631	0.87178	1.6345	6.58E+08
E9PN17;O75964	E9PN17;O75964	ATP synthase sub	ATP5L	5	5	76	0	41.246	0.87117	0.9305	1.98E+09
P35232;C9JW96;	P35232;C9JW96;	Prohibitin	PHB	17	17	272	0	210.71	0.87111	1.117	1.87E+10
Q14669-4;Q1466	Q14669-4;Q1466	E3 ubiquitin-prot	TRIP12	21	21	1722	0	92.778	0.87103	0.94588	1.54E+09
Q9BQ69	Q9BQ69	O-acetyl-ADP-ribc	MACROD1	6	6	325	0	36.922	0.87052	1.4147	1.12E+09
O00425;O00425·	O00425	Insulin-like growt	IGF2BP3	22	19	579	0	194.23	0.87043	NaN	2.07E+09
Q99707;Q99707·	Q99707;Q99707·	Methionine synth	MTR	21	21	1265	0	154.23	0.87042	1.1154	1.97E+09
E9PN81;Q8TDP1-	E9PN81;Q8TDP1-	Ribonuclease H2 s	RNASEH2C	5	5	247	0	26.097	0.87023	1.0376	3.47E+08
J3QS39;J3QTR3;F	J3QS39;J3QTR3;F	Ubiquitin-60S rib	UBB;RPS27A;UBC	11	4	93	0	224.6	0.86999	1.525	1.39E+11
Q7Z7K6;Q7Z7K6-	Q7Z7K6	Centromere prote	CENPV	5	1	275	0	52.796	0.86948	2.5436	6.54E+08
P62330	P62330	ADP-ribosylation	ARF6	5	5	175	0	34.941	0.86903	1.2066	1.06E+09
A0A0C4DGY8;D6I	A0A0C4DGY8;D6I	Enolase-phosphat	ENOPH1	3	3	149	0	16.044	0.86896	0.94156	1.38E+08
O60318;O60318·	O60318	Germinal-center a	MCM3AP	16	16	1980	0	164.11	0.8685	0.5475	9.45E+08
P51991	P51991	Heterogeneous nu	HNRNPA3	23	4	378	0	233.29	0.86849	0.99804	8.10E+09
Q96GA3;A0A075I	Q96GA3	Protein LTV1 hom	LTV1	7	7	475	0	127.18	0.86844	NaN	3.92E+08
R4GNB1;Q4L235·	R4GNB1;Q4L235·	Acyl-CoA synthet	AASDH	3	3	945	0	4.6174	0.86802	1.2332	4.96E+07
Q9BZE4;Q9BZE4-;	Q9BZE4;Q9BZE4-;	Nucleolar GTP-bir	GTPBP4	19	19	634	0	100.17	0.86801	2.6359	1.30E+09
Q96EM0;D6RC46	Q96EM0;D6RC46	Trans-L-3-hydroxy	L3HYPDH	5	5	354	0	12.992	0.86761	0.8615	2.09E+08
C9J6D1;C9JZI7;Q	C9J6D1;C9JZI7;Q	Nucleosome asse	NAP1L4	7	5	178	0	68.776	0.86689	1.2676	3.93E+08
K7EP06;O43148;	K7EP06;O43148;	mRNA cap guanin	RNMT	2	2	298	0	10.62	0.8667	NaN	1.45E+08
Q969X5-2;Q969X	Q969X5-2;Q969X	Endoplasmic retic	ERGIC1	4	4	198	0	11.333	0.86669	1.2115	5.02E+08
A0A0A0MT60;Q5	A0A0A0MT60;Q5	FK506-binding pr	FKBP15	5	5	1244	0	22.579	0.86665	0.48446	1.83E+08
D6R9P3;D6RD18	D6R9P3;D6RD18	Heterogeneous nu	HNRNPAB	16	15	280	0	107.67	0.86662	1.4597	6.40E+09
Q9HAD4;H0YAA3	Q9HAD4;H0YAA3	WD repeat-contai	WDR41	10	10	459	0	182.74	0.86613	1.0648	1.41E+09
Q676U5;E7EVC7;	Q676U5;E7EVC7;	Autophagy-relate	ATG16L1	3	3	607	0	56.097	0.86609	NaN	1.61E+08
Q9P2D3-3;Q9P2I	Q9P2D3-3;Q9P2I	HEAT repeat-cont	HEATR5B	16	16	1982	0	98.049	0.86533	0.91138	4.86E+08
A6NMN0;P46020	A6NMN0;P46020	Phosphorylase b k	PHKA1	10	9	1240	0	55.266	0.86517	1.0674	4.35E+08
Q9BVI4;F5H303	Q9BVI4	Nucleolar comple	NOC4L	6	6	516	0	23.19	0.86492	1.0991	4.09E+08
P42025	P42025	Beta-centractin	ACTR1B	9	3	376	0	21.678	0.86486	0.80559	1.56E+09
A0A087X295;Q9I	A0A087X295;Q9I	WD repeat-contai	WDR6	13	13	1151	0	121.23	0.86455	1.1442	2.24E+09
Q9BUQ8;H0YI52;	Q9BUQ8	Probable ATP-dep	DDX23	18	18	820	0	77.088	0.86392	1.0957	2.18E+09
P54646;A0A087\	P54646;A0A087\	5-AMP-activated	PRKAA2	3	2	552	0	6.1431	0.86388	NaN	5.41E+07
Q8WVD3;Q8WVE	Q8WVD3;Q8WVE	E3 ubiquitin-prot	RNF138	4	4	245	0	46.202	0.86376	0.90854	2.24E+08
Q5T2E6;Q5T2E6-;	Q5T2E6;Q5T2E6-;	UPF0668 protein	C10orf76	5	5	689	0	50.149	0.8631	NaN	1.63E+08
H0YNG3;P67812·	H0YNG3;P67812·	Signal peptidase c	SEC11A	8	8	163	0	35.05	0.86251	1.012	3.32E+09
O75396;A0A087)	O75396	Vesicle-trafficking	SEC22B	7	7	215	0	51.016	0.86225	1.2898	1.36E+09
Q9Y676;A0A0G2J	Q9Y676;A0A0G2J	28S ribosomal pr	MRPS18B	4	4	258	0	53.92	0.86204	1.2078	3.14E+08
I6L894;Q01484;(	I6L894;Q01484;(	Ankyrin-2	ANK2	6	4	3924	0	22.213	0.86198	1.1929	1.42E+08
O00330-3;O0033	O00330-3;O0033	Pyruvate dehydro	PDHX	11	11	486	0	32.683	0.86161	0.93598	6.78E+08
Q5QPM7;Q9253(	Q5QPM7;Q9253(	Proteasome inhib	PSMF1	5	5	263	0	42.533	0.86142	0.67304	8.79E+08
P38606-2;P3860	P38606-2;P3860	V-type proton ATI	ATP6V1A	3	3	584	0	10.867	0.86136	NaN	7.47E+07
P41240;H3BUM9	P41240	Tyrosine-protein I	CSK	21	21	450	0	162.87	0.86135	1.0275	4.60E+09
Q13085;Q13085·	Q13085;Q13085·	Acetyl-CoA carbo	ACACA	54	47	2346	0	323.31	0.86132	1.1618	5.28E+09
Q6P1M0;Q6P1MI	Q6P1M0	Long-chain fatty a	SLC27A4	14	12	643	0	75.071	0.86094	NaN	7.61E+08
R4GNH3;E9PKD5	R4GNH3;E9PKD5;	E9PN50;E9PMD8	PSMC3	29	1	423	0	323.31	0.86046	0.95747	1.48E+10
B4E1G1;Q9BUN8	B4E1G1;Q9BUN8	Derlin-1	DERL1	4	4	151	0	15.662	0.86035	0.97666	6.43E+08
Q8NEZ5;Q8NEZ5-	Q8NEZ5;Q8NEZ5-	F-box only protei	FBXO22	7	7	403	0	38.56	0.8603	1.0649	7.17E+08
Q10570;A0A087)	Q10570	Cleavage and poly	CPSF1	38	38	1443	0	253.76	0.86025	1.1449	4.85E+09
Q9H1A4;H0Y564;	Q9H1A4;H0Y564	Anaphase-promo	ANAPC1	24	24	1944	0	202.14	0.85975	1.0297	1.63E+09
Q9NS69	Q9NS69	Mitochondrial im	TOMM22	5	5	142	0	156.34	0.85971	1.0281	3.53E+09
Q6PCE3	Q6PCE3	Glucose 1,6-bisp	PGM2L1	5	5	622	0	20.669	0.85954	NaN	3.02E+08
Q86XI2;Q86XI2-2	Q86XI2;Q86XI2-2	Condensin-2 com	NCAPG2	26	26	1143	0	130.42	0.8595	1.038	1.34E+09
Q8WZ82	Q8WZ82	Ovarian cancer-as	OVCA2	2	2	227	0	12.531	0.85938	0.90191	1.40E+08
Q15424-2;Q1542	Q15424-2;Q1542	Scaffold attachme	SAFB	2	2	848	0	11.32	0.85937	NaN	3.86E+07
P14866;M0QXS5	P14866;M0QXS5	Heterogeneous nu	HNRNPL	35	22	589	0	323.31	0.85921	0.86802	2.30E+10
P49005;F8W8R3	P49005;F8W8R3	DNA polymerase d	POLD2	16	16	469	0	152.14	0.85903	0.99525	3.87E+09
O15042-3;O1504	O15042-3;O1504	U2 snRNP-associa	U2SURP	6	6	620	0	19.464	0.85828	1.0192	5.26E+08
F8W1B9;O95619	F8W1B9;O95619	YEATS domain-co	YEATS4	4	4	211	0	12.175	0.85807	0.64046	1.07E+08
A0A0C4DFL7;Q1(	A0A0C4DFL7;Q1(	Lanosterol 14-alp	CYP51A1	8	8	509	0	34.153	0.85797	0.9373	4.87E+08
J9JIE6;Q9UM00-2	J9JIE6;Q9UM00-2	Transmembrane a	TMCO1	4	4	239	0	31.933	0.85796	0.64849	5.79E+08
Q7LGA3-3;Q7LGA	Q7LGA3-3;Q7LGA	Heparan sulfate 2	HS2ST1	2	2	229	0	3.7472	0.85787	NaN	3.20E+08
F8VZJ2;F8W0W4	F8VZJ2;F8W0W4	Nascent polypept	NACA	6	6	136	0	106.51	0.85777	0.85434	5.18E+09
A0A0A0MQW0;A(	A0A0A0MQW0;A(	Myelin expressior	MYEF2	5	5	576	0	25.105	0.85669	NaN	1.84E+08
Q9Y679-2;Q9Y67	Q9Y679-2;Q9Y67	Ancient ubiquito	AUP1	10	10	410	0	48.52	0.85646	0.97294	7.96E+08
H0Y6T7;Q92542-	H0Y6T7;Q92542-	Nicastrin	NCSTN	2	2	275	0.0018182	3.0355	0.85567	NaN	5.75E+07
P51659;E7EWE5;	P51659;E7EWE5;	Peroxisomal mult	HSD17B4	21	21	736	0	250.44	0.85539	1.074	4.91E+09
Q6P2Q9;I3L0J9;I	Q6P2Q9	Pre-mRNA-proces	PRPF8	112	112	2335	0	323.31	0.8553	1.2348	2.42E+10
Q96DB5-2;Q96DI	Q96DB5-2;Q96DI	Regulator of micr	RMDN1	4	4	284	0	7.8141	0.85424	0.43389	2.39E+08
P07199	P07199	Major centromer	CENPB	2	2	599	0	13.229	0.85415	1.0332	8.65E+07
Q8NB37;Q8NB37	Q8NB37;Q8NB37	Parkinson disease	PDDC1	3	3	220	0	17.713	0.85407	0.93573	4.89E+08
Q92973-2;Q9297	Q92973-2;Q9297	Transportin-1	TNPO1	7	4	890	0	22.508	0.85397	1.1192	8.97E+08
Q9UJA5;Q9UJA5-	Q9UJA5;Q9UJA5-	tRNA (adenine(58	TRMT6	7	7	497	0	13.593	0.85373	NaN	5.39E+07
P61163;R4GMT0	P61163;R4GMT0	Alpha-centractin	ACTR1A	18	12	376	0	323.31	0.8537	1.0804	1.59E+10
P35813-2;P3581	P35813-2;P3581	Protein phosphat	PPM1A	4	4	324	0	31.993	0.85369	0.91127	2.89E+08
P50583	P50583	Bis(5-nucleosyl)-t	NUDT2	2	2	147	0	19.46	0.8536	1.0798	2.88E+08
P50416-2;P5041	P50416-2;P5041	Carnitine O-palmi	CPT1A	10	10	756	0	41.288	0.85288	1.0833	1.24E+09
Q8WYP5;Q8WYP!	Q8WYP5;Q8WYP!	Protein ELYS	AHCTF1	11	11	2266	0	68.394	0.85281	1.5091	5.82E+08
Q3ZCQ8;Q3ZCQ8·	Q3ZCQ8;Q3ZCQ8·	Mitochondrial im	TIMM50	10	10	353	0	133.78	0.85257	0.93522	4.44E+09
O15270;H0YJV2	O15270;H0YJV2	Serine palmitoylt	SPTLC2	5	5	562	0	26.637	0.85227	NaN	2.47E+08
Q9BT22;Q9BT22-	Q9BT22;Q9BT22-	Chitobiosyldipho	ALG1	6	6	464	0	26.616	0.85219	1.2208	9.46E+08
Q8N335;C9K0P5;	Q8N335	Glycerol-3-phosp	GPD1L	5	5	351	0	18.49	0.85179	1.1144	2.18E+08
E7ET49;Q8NCG7-	E7ET49;Q8NCG7-	Sn1-specific diacy	DAGLB	2	2	631	0	6.0528	0.85165	NaN	1.07E+07
Q9NRK6;A0A0G2	Q9NRK6	ATP-binding casse	ABCB10	3	3	738	0	20.206	0.85163	NaN	9.84E+07
Q9UNX4;Q6PDA5	Q9UNX4	WD repeat-contai	WDR3	31	31	943	0	236.66	0.85157	1.5039	3.86E+09
Q9P0J7;C9J3I2	Q9P0J7	E3 ubiquitin-prot	KCMF1	5	5	381	0	98.328	0.85152	1.3037	1.16E+09

O60244;H7C3E5;	O60244	Mediator of RNA ;	MED14		16	16	1454	0	90.762	0.85145	1.0787	8.18E+08
O00264;O00264·	O00264;O00264·	Membrane-associ	PGRMC1		8	8	195	0	35.165	0.85131	0.82996	6.25E+08
O95831-3;O9583	O95831-3;O9583	Apoptosis-induci	AIFM1		30	30	609	0	207.46	0.85103	0.75128	6.95E+09
Q9NZQ3-4;Q9NZ(	Q9NZQ3-4;Q9NZ(	NCK-interacting p	NCKIPSD		3	1	651	0	6.9653	0.85053	1.1518	9.03E+07
Q53GT1-3;Q53GT	Q53GT1-3;Q53GT	Kelch-like protein	KLHL22		1	1	491	0	13.414	0.85049	NaN	1.09E+07
Q00796;H0YLA4;	Q00796;H0YLA4	Sorbitol dehydro	SORD		10	10	357	0	60.131	0.85012	1.064	2.84E+09
Q7KZF4;H7C597	Q7KZF4	Staphylococcal n	SND1		53	53	910	0	323.31	0.84992	1.1252	2.65E+10
P46778;G3V1B3;	P46778;G3V1B3;	60S ribosomal pr	RPL21		12	12	160	0	75.044	0.84987	1.2656	7.16E+09
P10586-2;P1058	P10586-2;P1058	Receptor-type tyr	PTPRF		12	10	1898	0	92.912	0.84922	0.85635	4.82E+08
Q14126;J3KSI6	Q14126	Desmoglein-2	DSG2		12	12	1118	0	62.765	0.84869	1.0676	3.43E+08
P30101	P30101	Protein disulfide-	PDIA3		3	2	505	0	5.4847	0.84854	NaN	5.86E+06
A0A0A0MTR2;Q8	A0A0A0MTR2;Q8	Prolyl 3-hydroxyl	OGFOD1		4	4	499	0	27.371	0.84835	NaN	1.27E+08
Q9NZD8;Q9NZD8	Q9NZD8;Q9NZD8	Maspardin	SPG21		5	5	308	0	22.204	0.84815	1.1165	4.11E+08
A0A087WTA5;E7I	A0A087WTA5;E7I	Translation initia	EIF2B4		13	13	520	0	68.745	0.84796	NaN	6.01E+08
Q9UKF6;G5E9W3	Q9UKF6;G5E9W3	Cleavage and poly	CPSF3		12	12	684	0	46.655	0.84785	1.0176	1.36E+09
P21912;A0A087\	P21912;A0A087\	Succinate dehydr	SDHB		6	6	280	0	27.244	0.84782	1.0127	6.13E+08
Q96GA7;F8VYZ3;I	Q96GA7;F8VYZ3;I	Serine dehydratas	SDSL		5	5	329	0	58.397	0.84713	1.1767	4.16E+08
I3L496;I3L2P4;Q	I3L496;I3L2P4;Q	SET and MYND do	SMYD4		1	1	177	0	12.214	0.8471	NaN	1.36E+08
P10606	P10606	Cytochrome c oxi	COX5B		5	5	129	0	12.02	0.84653	0.49494	2.71E+08
A0A087WXP7;Q9	A0A087WXP7;Q9	Diphthine syntha	DPH5		9	9	243	0	59.327	0.84638	1.1293	1.19E+09
Q14139;Q14139·	Q14139;Q14139·	Ubiquitin conjug	UBE4A		4	4	1066	0	23.686	0.84603	1.1903	3.77E+08
B1AHR1;Q9UH03	B1AHR1;Q9UH03	Neuronal-specific		03-Sep	6	6	294	0	20.068	0.84591	0.80877	2.88E+08
O95486;O95486·	O95486	Protein transport	SEC24A		9	9	1093	0	58.852	0.8454	1.2348	7.67E+08
P22234;E9PBS1;I	P22234;E9PBS1;I	Multifunctional p	PAICS		24	24	425	0	323.31	0.84515	1.2458	1.56E+10
P52294;C9JYI4;C	P52294;C9JYI4	Importin subunit	KPNA1		14	6	538	0	77.739	0.84461	NaN	5.49E+08
B4DGL8;O75027;	B4DGL8;O75027;	ATP-binding casse	ABCB7		9	9	702	0	72.474	0.8443	NaN	2.81E+08
P62314;J3QLI9;J	P62314;J3QLI9	Small nuclear ribo	SNRPD1		5	5	119	0	81.644	0.84358	1.3965	5.07E+09
Q5SWX8-4;Q5SW	Q5SWX8-4;Q5SW	Protein odr-4 hor	ODR4		8	8	422	0	34.832	0.84355	0.45436	1.16E+09
P62820;E7END7;	P62820;E7END7;	Ras-related protei	RAB1A		8	3	205	0	25.702	0.84333	1.3051	1.55E+08
Q9UBM7;E9PM0(	Q9UBM7;E9PM0(	7-dehydrocholest	DHCR7		8	8	475	0	52.974	0.84323	1.0169	2.36E+09
A0A0A0MS52;Q1	A0A0A0MS52;Q1	Calcium/calmodu	CAMK2G		13	7	539	0	89.382	0.84302	1.0207	8.27E+08
P51114-2;P5111	P51114-2;P5111	Fragile X mental r	FXR1		15	13	539	0	84.671	0.84264	0.89349	1.79E+09
Q9BUR4;E9PMG4	Q9BUR4;E9PMG4	Telomerase Cajal	WRAP53		4	4	548	0	59.047	0.84249	NaN	1.29E+08
A0A096LP25;Q62	A0A096LP25;Q62	Uncharacterized	protein FLJ45252		2	2	511	0	12.005	0.84238	NaN	6.81E+07
E9PCY5;Q02880-;	E9PCY5;Q02880-;	DNA topoisomera	TOP2B		27	14	1150	0	66.874	0.84232	1.7124	1.14E+09
B4DKY1;P49589-	B4DKY1;P49589-	Cysteine--tRNA lig	CARS		10	10	739	0	30.862	0.84219	0.89599	9.38E+08
P30520;G3V232	P30520	Adenylosuccinate	ADSS		25	22	456	0	295.91	0.84189	1.0865	2.20E+10
O43819;C9JBU1	O43819	Protein SCO2 hon	SCO2		3	3	266	0	11.038	0.84188	NaN	1.08E+08
Q96EY7;B8ZZQ4;I	Q96EY7	Pentatricopeptid	PTCD3		7	7	689	0	59.511	0.84185	NaN	5.10E+08
H0YK95;H0YL95;I	H0YK95;H0YL95;I	AP-4 complex sub	AP4E1		2	2	321	0	5.6972	0.84164	NaN	3.80E+07
O75083;O75083·	O75083;O75083·	WD repeat-contai	WDR1		22	22	606	0	323.31	0.84136	0.88353	8.45E+09
Q96F86;H3BSQ0;	Q96F86	Enhancer of mRN	EDC3		15	15	508	0	65.098	0.84105	NaN	1.02E+09
Q8WWL2-3;Q8W	Q8WWL2-3;Q8W	Protein spire hom	SPIRE2		1	1	666	0.0030434	2.6393	0.84061	NaN	2.45E+08
O75530-3;O7553	O75530-3;O7553	Polycomb protei	EED		4	4	400	0	9.0758	0.8405	1.1388	1.97E+08
Q8TED1;J3KNB5;I	Q8TED1;J3KNB5;I	Probable glutathi	GPX8		3	3	209	0	10.042	0.83965	NaN	2.00E+08
Q12906-5;Q1290	Q12906-5;Q1290	Interleukin enhan	ILF3		34	30	690	0	323.31	0.83945	1.2575	1.26E+10
Q9BYC8	Q9BYC8	39S ribosomal pr	MRPL32		1	1	188	0	76.791	0.83911	NaN	2.74E+08
Q9UDR5;F8WAH:	Q9UDR5;F8WAH:	Alpha-aminoadip	AASS		11	11	926	0	70.458	0.83903	0.82412	6.19E+08
Q8NEM2	Q8NEM2	SHC SH2 domain-	SHCBP1		3	3	672	0	10.121	0.83896	1.5266	1.11E+08
Q9UJT0;S4R3K3;/	Q9UJT0;S4R3K3	Tubulin epsilon cl	TUBE1		6	6	475	0	38.402	0.83885	1.0026	4.18E+08
Q9HD20-2;Q9HD	Q9HD20-2;Q9HD	Manganese-trans	ATP13A1		5	5	1086	0	14.904	0.83861	1.0515	2.52E+08
A0A087X0Q9;Q9I	A0A087X0Q9;Q9I	Selenoprotein O	SELO		6	6	668	0	19.855	0.83804	NaN	3.69E+08
A0A0A0MRK6;Q1	A0A0A0MRK6;Q1	Metaxin-1	MTX1		5	5	466	0	28.745	0.83788	1.0142	3.67E+08
Q9NY61;A0A087\	Q9NY61	Protein AATF	AATF		6	6	560	0	50.399	0.83736	0.99885	6.80E+08
O95239-2;O9523	O95239-2;O9523	Chromosome-ass	KIF4A		9	9	1127	0	48.795	0.83706	1.0686	3.61E+08
Q05823;Q05823·	Q05823;Q05823·	2-5A-dependent r	RNASEL		4	3	741	0	5.3252	0.83695	NaN	9.40E+07
Q8NFF5-3;Q8NFF	Q8NFF5-3;Q8NFF	FAD synthase;Mol	FLAD1		12	12	446	0	98.739	0.83679	0.96515	1.57E+09
Q8N0X7	Q8N0X7	Spartin	SPG20		13	13	666	0	160.37	0.8367	1.3048	1.83E+09
Q9UGP8;A6PVC9	Q9UGP8	Translocation pro	SEC63		8	8	760	0	30.388	0.83654	1.0871	9.44E+08
P63151;P63151-	P63151;P63151-	Serine/threonine·	PPP2R2A		5	5	447	0	32.538	0.83637	1.1124	2.53E+08
P84077;P61204;	P84077;P61204;	ADP-ribosylation	ARF1;ARF3		12	8	181	0	205.56	0.83613	1.3705	1.23E+10
P62495;B7Z7P8;I	P62495;B7Z7P8;I	Eukaryotic peptid	ETF1		7	7	437	0	38.09	0.83601	1.3081	8.09E+08
Q9BV44;H7C3J3;	Q9BV44;H7C3J3;	THUMP domain-c	THUMPD3		8	8	507	0	30.964	0.83595	NaN	4.75E+08
O43542;G3V3H9	O43542;G3V3H9	DNA repair protei	XRCC3		5	5	346	0	9.0886	0.83579	1.5937	2.63E+08
Q3SXM5;Q3SXM5	Q3SXM5;Q3SXM5	Inactive hydroxys	HSDL1		10	10	330	0	36.814	0.83534	1.1222	1.11E+09
Q13347;Q5TFK1	Q13347	Eukaryotic transl	EIF3I		15	15	325	0	172.68	0.83507	1.1472	7.05E+09
Q5R3B4;O95563	Q5R3B4;O95563	Mitochondrial py	MPC2		4	4	105	0	9.3841	0.83495	0.5824	1.33E+08
Q147X3;Q147X3·	Q147X3;Q147X3·	N-alpha-acetyltra	NAA30		5	5	362	0	40.873	0.83494	1.2443	2.51E+08
A0A0C4DGA6;Q1	A0A0C4DGA6;Q1	Helicase-like tran	HLTF		10	10	1008	0	75.484	0.83474	0.9622	5.44E+08
P84090;G3V279	P84090;G3V279	Enhancer of rudin	ERH		2	2	104	0	18.122	0.8342	0.78704	1.02E+09
O00483	O00483	Cytochrome c oxi	NDUFA4		3	3	81	0	10.821	0.83378	1.1233	1.62E+09
Q5R3I4;H7C089;/	Q5R3I4	Tetratricopeptide	TTC38		5	5	469	0	18.548	0.83376	0.91433	4.93E+08
Q99717;D6RIZ9;I	Q99717	Mothers against d	SMAD5		6	6	465	0	31.222	0.83355	0.60102	2.66E+08
Q5T760;Q05519·	Q5T760;Q05519·	Serine/arginine-ri	SRSF11		4	4	389	0	20.774	0.83347	1.0943	4.91E+08
Q9BQ39;A0A087'	Q9BQ39;A0A087'	ATP-dependent RI	DDX50		9	7	737	0	44.574	0.83321	0.99971	1.11E+09
P11388;P11388-	P11388;P11388-	DNA topoisomera	TOP2A		60	47	1531	0	323.31	0.83288	1.5014	8.72E+09
G3V529;Q9GZR7;	G3V529;Q9GZR7;	ATP-dependent RI	DDX24		10	10	816	0	93.007	0.83245	1.7248	6.11E+08
Q6KC79-2;Q6KC7	Q6KC79-2;Q6KC7	Nipped-B-like pro	NIPBL		8	8	2697	0	46.103	0.8324	1.144	2.16E+08
Q9UJZ1;A0A087V	Q9UJZ1;A0A087V	Stomatin-like pro	STOML2		20	20	356	0	323.31	0.83137	1.0599	1.07E+10
Q96LJ7;H0YNC2	Q96LJ7;H0YNC2	Dehydrogenase/r	DHRS1		2	2	313	0	5.6878	0.83114	NaN	2.44E+07
Q9BU61;Q9BU61	Q9BU61	NADH dehydroge	NDUFAF3		3	3	184	0	14.907	0.8305	NaN	8.89E+07
P00387-2;P0038	P00387-2;P0038	NADH-cytochrom	CYB5R3		11	11	278	0	161.48	0.83033	1.0779	2.39E+09
F5H442;Q99816;	F5H442;Q99816;	Tumor susceptibi	TSG101		6	6	365	0	27.498	0.83011	0.28233	2.03E+08
Q9HD45;Q5TB53	Q9HD45;Q5TB53	Transmembrane !	TM9SF3		8	8	589	0	55.799	0.83	0.99433	1.55E+09
C9J266;Q5XPI4;C	C9J266;Q5XPI4;C	E3 ubiquitin-prot	RNF123		5	5	762	0	15.839	0.82958	0.704	1.36E+08
E9PFN5;Q9Y2Q3-	E9PFN5;Q9Y2Q3-	Glutathione S-tra	GSTK1		3	3	190	0	26.349	0.82925	0.92468	4.01E+08
H0Y8C4;E9PFR3;(	H0Y8C4;E9PFR3;(	Serine/threonine·	PPP2R5D		2	2	504	0	5.1909	0.82899	NaN	4.95E+07
Q9Y232-3;Q9Y23	Q9Y232-3;Q9Y23	Chromodomain Y	CDYL		1	1	309	0	3.6714	0.82872	NaN	3.90E+07
O14929;O14929·	O14929;O14929·	Histone acetyltra	HAT1		8	8	419	0	151.31	0.82829	1.0507	3.03E+09
Q00653-4;Q0065	Q00653-4;Q0065	Nuclear factor NF	NFKB2		5	5	899	0	23.585	0.82817	0.96073	2.32E+08
Q9HA77;H0YFF0;	Q9HA77	Probable cysteine	CARS2		8	8	564	0	27.523	0.82812	0.9077	5.51E+08
F6SL11;O95258-;	F6SL11;O95258-;	Brain mitochondr	SLC25A14		5	3	290	0	10.272	0.82799	0.3705	1.86E+08
Q8WU90;H7C46(	Q8WU90;H7C46(	Zinc finger CCCH	ZC3H15		2	2	426	0	14.931	0.82754	NaN	1.37E+08
P28066;P28066-	P28066;P28066-	Proteasome subu	PSMA5		7	7	241	0	82.046	0.82738	1.3993	1.64E+09
Q9Y6G9;E9PHI6;(	Q9Y6G9;E9PHI6	Cytoplasmic dyne	DYNC1LI1		10	10	523	0	103.06	0.82695	NaN	3.77E+08
Q13595-4;Q1359	Q13595-4;Q1359	Transformer-2 pr	TRA2A		4	4	180	0	16.104	0.82649	2.4649	4.75E+08
O00410;H0Y8C6;	O00410;H0Y8C6;	Importin-5	IPO5		11	10	1097	0	76.147	0.82617	1.0033	1.08E+09
Q8IZ73;Q8IZ73-2	Q8IZ73;Q8IZ73-2	RNA pseudouridy	RPUSD2		4	4	545	0	6.3831	0.82518	NaN	1.03E+08
Q06203;D6RCC8;	Q06203;D6RCC8	Amidophosphorib	PPAT		4	4	517	0	34.297	0.82469	NaN	1.93E+08
Q9H3P7	Q9H3P7	Golgi resident pro	ACBD3		12	12	528	0	220.28	0.82463	NaN	7.05E+08
O60271-4;A0A08	O60271-4;A0A08	C-Jun-amino-terr	SPAG9		24	24	1307	0	140.65	0.82422	1.1183	7.89E+08
O60763;O60763·	O60763;O60763·	General vesicular	USO1		27	27	962	0	323.31	0.82394	1.1599	4.25E+09
J3KMZ7;Q9H0H0	J3KMZ7;Q9H0H0	Integrator compl	INTS2		5	5	1196	0	41.397	0.82333	1.4743	5.46E+08
Q9BRR6-2;Q9BRR	Q9BRR6-2;Q9BRR	ADP-dependent g	ADPGK		3	3	496	0	13.593	0.82323	1.1179	7.69E+07

Q9BY44;Q9BY44-	Q9BY44;Q9BY44-	Eukaryotic transl	EIF2A		18	18	585	0	211.62	0.8231	NaN	2.47E+09
Q5XUX1-3;Q5XUX	Q5XUX1-3;Q5XUX	F-box/WD repeat	FBXW9		3	3	458	0	31.282	0.82299	1.3258	1.22E+08
E7ETK0;A0A087W	E7ETK0;A0A087W	40S ribosomal pr	RPS24		7	7	131	0	29.07	0.82297	1.1467	3.33E+09
Q96FX7;H0Y2Q1	Q96FX7;H0Y2Q1	tRNA (adenine(58	TRMT61A		5	5	289	0	57.244	0.82272	1.2276	4.02E+08
A0A140TA86;Q5X	A0A140TA86;Q5X	Protein QIL1	QIL1;C19orf70		4	4	140	0	67.587	0.82264	1.3881	3.61E+08
P46977;P46977-	P46977;P46977-	Dolichyl-diphosp	STT3A		12	12	705	0	65.747	0.82259	1.0673	3.29E+09
C9JA28;Q9UNL2;	C9JA28;Q9UNL2;	Translocon-associ	SSR3		2	2	174	0	28.74	0.82233	1.182	1.23E+09
P10809;E7ESH4;I	P10809	60 kDa heat shock	HSPD1		41	41	573	0	323.31	0.82221	1.0604	1.37E+10
P31939;P31939-	P31939;P31939-	Bifunctional puri	ATIC		13	13	592	0	143.87	0.82198	NaN	8.75E+08
A0A0C4DGZ0;P2	A0A0C4DGZ0;P2	DNA-directed RN	POLR2A		54	54	1970	0	323.31	0.82192	1.2369	4.17E+09
J3KPP4;O95232;I	J3KPP4;O95232;I	Luc7-like protein	LUC7L3		4	4	489	0	29.809	0.82071	1.0622	2.48E+08
P17858;P17858-	P17858;P17858-	ATP-dependent 6	PFKL		30	25	780	0	323.31	0.82038	1.1991	8.50E+09
P36957;P36957-	P36957;P36957-	Dihydrolipoyllysi	DLST		9	9	453	0	50.245	0.82004	1.5782	1.23E+09
P54136;P54136-	P54136;P54136-	Arginine--tRNA lig	RARS		43	43	660	0	310.06	0.81926	1.6576	9.77E+09
Q6P158;H7C109;	Q6P158;H7C109	Putative ATP-dep	DHX57		19	18	1386	0	117.13	0.81915	1.3531	6.81E+08
C9JYM0;O75817	C9JYM0;O75817	Ribonuclease P pr	POP7		4	4	137	0	12.68	0.81907	3.5549	4.33E+08
F5H619;Q86XA9;	F5H619;Q86XA9;	HEAT repeat-cont	HEATR5A		6	6	2046	0	22.564	0.81902	1.2677	2.57E+08
Q96T21-2;Q96T2	Q96T21-2;Q96T2	Selenocysteine in	SECISBP2		3	3	781	0	13.104	0.81868	NaN	1.07E+08
A0A087WZT2;Q6	A0A087WZT2;Q6	Methyltransferas	METTL7B		2	2	276	0.0037869	2.5752	0.81867	NaN	7.49E+07
O14744;O14744-	O14744;O14744-	Protein arginine	PRMT5		13	13	637	0	92.422	0.81831	NaN	1.11E+09
G3V1C3;Q9BZZ5-	G3V1C3;Q9BZZ5-	Apoptosis inhibit	API5		2	2	510	0	63.072	0.81732	NaN	8.60E+07
Q9Y291;C9JBY7	Q9Y291;C9JBY7	28S ribosomal pr	MRPS33		3	3	106	0	8.3013	0.81678	1.3782	1.80E+08
U3KPU7;U3KQS2	U3KPU7;U3KQS2	Glucose-6-phosph	SLC37A4		1	1	429	0	4.6554	0.81677	1.4818	3.21E+08
Q53GS9;B9A018;	Q53GS9;B9A018;	U4/U6.U5 tri-snR	USP39		13	13	565	0	114.6	0.8167	NaN	1.31E+09
Q969V3-2;Q969V	Q969V3-2;Q969V	Nicalin	NCLN		22	22	562	0	281.17	0.8162	1.1629	3.50E+09
Q00577	Q00577	Transcriptional ac	PURA		2	2	322	0	107.19	0.81594	1.3565	5.39E+08
Q86U42-2;Q86U4	Q86U42-2;Q86U4	Polyadenylate-bir	PABPN1		2	2	296	0	11.282	0.81521	NaN	1.60E+08
Q9BVQ7-2;Q9BVC	Q9BVQ7-2;Q9BVC	Spermatogenesis-	SPATA5L1		3	3	620	0	26.041	0.81517	1.1789	3.31E+08
P11172;P11172-	P11172;P11172-	Uridine 5-monop	UMPS		24	24	480	0	146.91	0.81516	1.1558	5.54E+09
P82673;H0YG82;	P82673;H0YG82;	28S ribosomal pr	MRPS35		5	5	323	0	63.567	0.81488	0.18951	7.20E+08
A0A087X2H1;Q9	A0A087X2H1;Q9	E3 ubiquitin-prot	HECTD1		36	36	2614	0	278.17	0.81469	1.2016	2.16E+09
O94829;Q5T4X2	O94829	Importin-13	IPO13		6	6	963	0	19.507	0.81461	1.2688	2.65E+08
P49642;H0YIP2;F	P49642	DNA primase sma	PRIM1		7	7	420	0	46.04	0.81417	1.2813	4.03E+08
Q8N1B4;Q8N1B4	Q8N1B4;Q8N1B4	Vacuolar protein	VPS52		14	14	723	0	115.7	0.81372	0.74434	6.87E+08
F5H039;Q9NQX3	F5H039;Q9NQX3	Gephyrin;Molybd	GPHN		8	8	782	0	32.253	0.81362	1.3998	6.90E+08
P56589;Q7Z6V3	P56589;Q7Z6V3	Peroxisomal biog	PEX3		6	6	373	0	40.878	0.81356	0.77498	7.01E+07
Q9Y478;F5H2X8;	Q9Y478;F5H2X8	5-AMP-activated	PRKAB1		3	3	270	0	43.598	0.81348	0.93657	2.23E+08
Q8IZ83-3;Q8IZ83	Q8IZ83-3;Q8IZ83	Aldehyde dehydr	ALDH16A1		9	9	751	0	71.562	0.81342	1.0543	1.09E+09
Q92572;F5H459	Q92572	AP-3 complex sub	AP3S1		7	7	193	0	25.683	0.81237	0.77746	1.21E+09
P15121;E9PCX2;I	P15121;E9PCX2;I	Aldose reductase	AKR1B1		5	5	316	0	75.969	0.81214	0.99823	4.35E+08
Q9BTX1-3;Q9BTX	Q9BTX1-3;Q9BTX	Nucleoporin NDC	NDC1		2	2	557	0	21.727	0.8121	NaN	1.55E+08
Q13112	Q13112	Chromatin assem	CHAF1B		8	8	559	0	20.583	0.81151	NaN	2.53E+08
Q86Y07-4;Q86Y0	Q86Y07-4;Q86Y0	Serine/threonine	VRK2		2	2	390	0	5.4196	0.8107	NaN	3.77E+07
Q9P2K8-2;Q9P2K	Q9P2K8-2;Q9P2K	Eukaryotic transl	EIF2AK4		10	10	1621	0	49.225	0.81067	1.2988	6.04E+08
B1AHD1;P55769	B1AHD1;P55769	NHP2-like protein	NHP2L1		3	3	132	0	16.047	0.81062	NaN	5.70E+08
P46019	P46019	Phosphorylase b k	PHKA2		4	3	1235	0	5.7305	0.81051	NaN	1.41E+08
A0A0G2JNZ2;A0A	A0A0G2JNZ2;A0A	Protein scribble h	SCRIB		11	10	1630	0	77.369	0.80988	0.85187	8.20E+08
Q6PI78	Q6PI78	Transmembrane p	TMEM65		2	2	240	0	8.1667	0.80988	NaN	1.05E+08
Q9HCS7	Q9HCS7	Pre-mRNA-splicin	XAB2		10	10	855	0	54.457	0.80979	0.94508	4.82E+08
Q7Z2Z2-2;Q7Z2Z	Q7Z2Z2-2;Q7Z2Z	Elongation factor	EFTUD1		23	23	1069	0	235.78	0.80973	1.1232	1.25E+09
Q9Y3T9	Q9Y3T9	Nucleolar comple	NOC2L		22	22	749	0	91.058	0.80909	1.2425	4.20E+09
Q05DH4	Q05DH4	Protein FAM160A	FAM160A1		1	1	1040	0.008037	2.0723	0.80882	NaN	9.16E+07
A0A087WVR3;A0	A0A087WVR3;A0	E3 ubiquitin-prot	UHRF1		10	10	806	0	31.362	0.80876	1.31	5.73E+08
F5H0F9;Q9UJX4;I	F5H0F9;Q9UJX4;I	Anaphase-promo	ANAPC5		10	10	742	0	46.999	0.8085	0.81476	4.80E+08
P0DMV9;P0DMV	P0DMV9;P0DMV8;A0A0G2JIW1;P0		HSPA1A		50	26	641	0	323.31	0.80843	1.4583	1.39E+11
P35219	P35219	Carbonic anhydra	CA8		3	3	290	0	20.227	0.8084	1.0199	3.20E+08
O75351;K7EL71;I	O75351	Vacuolar protein	VPS4B		12	5	444	0	88.499	0.80836	1.3773	8.32E+08
P50453	P50453	Serpin B9	SERPINB9		5	5	376	0	15.511	0.80787	0.72496	3.01E+08
Q69YN4;Q69YN4	Q69YN4;Q69YN4	Protein virilizer h	KIAA1429		16	16	1812	0	74.785	0.80761	1.5012	6.09E+08
Q92604	Q92604	Acyl-CoA:lysopho	LPGAT1		2	2	370	0	3.7654	0.80668	1.0999	2.33E+08
Q9BSC4-2;Q9BSC	Q9BSC4-2;Q9BSC	Nucleolar protein	NOL10		2	2	638	0	7.3611	0.80624	0.98571	1.82E+08
P15374;A0A087\	P15374;A0A087\	Ubiquitin carboxy	UCHL3		8	8	230	0	37.598	0.80613	1.0635	8.30E+08
Q9UHD8-7;Q9UH	Q9UHD8-7;Q9UH	Septin-9	09-Sep		27	27	567	0	236.8	0.80595	1.0803	3.31E+09
O00258;B7Z1T1;I	O00258;B7Z1T1;I	Tail-anchored pro	WRB		4	4	174	0	8.7221	0.80592	NaN	1.21E+08
J3KQS6;Q9NWV8	J3KQS6;Q9NWV8	BRISC and BRCA1	BABAM1		5	5	254	0	149.5	0.80579	1.1347	3.96E+08
F8WBW1;Q86X8:	F8WBW1;Q86X8:	COMM domain-co	COMMD2		2	2	135	0	9.4244	0.80568	NaN	2.09E+08
P61160;P61160-	P61160;P61160-	Actin-related pro	ACTR2		11	11	394	0	116.11	0.80552	1.0439	2.93E+09
Q14012;C9JES6;I	Q14012;C9JES6;I	Calcium/calmod	CAMK1		2	2	370	0	4.1925	0.80537	0.8125	6.75E+07
Q12788;J3KNP2;	Q12788;J3KNP2	Transducin beta-l	TBL3		23	23	808	0	213.03	0.80506	1.3427	4.09E+09
Q8TBQ9	Q8TBQ9	Protein kish-A	TMEM167A		2	2	72	0	4.3149	0.80421	1.1424	5.97E+08
O15294;O15294-	O15294;O15294-	UDP-N-acetylgluc	OGT		10	10	1046	0	64.815	0.80369	1.1252	8.73E+08
Q9BWH6-2;Q9BV	Q9BWH6-2;Q9BV	RNA polymerase I	RPAP1		16	16	1315	0	146.06	0.80351	1.225	1.05E+09
Q9GZT4;V9GYE8;I	Q9GZT4;V9GYE8	Serine racemase	SRR		7	7	340	0	76.264	0.80337	1.274	4.54E+08
Q9H7D7-2;Q9H7I	Q9H7D7-2;Q9H7I	WD repeat-contai	WDR26		3	3	645	0	10.534	0.80311	NaN	2.05E+08
Q9ULE6	Q9ULE6	Paladin	PALD1		8	8	856	0	62.96	0.8027	1.0537	8.67E+08
P30041	P30041	Peroxiredoxin-6	PRDX6		9	9	224	0	46.867	0.80169	1.1151	1.04E+09
O14735;B3KY94;	O14735;B3KY94;	CDP-diacylglycer	CDIPT		6	6	213	0	28.894	0.80141	1.1409	2.12E+09
P49327;A0A0U1I	P49327;A0A0U1I	Fatty acid synthas	FASN		138	138	2511	0	323.31	0.80139	1.1938	1.88E+11
H3BRE4;H3BNQ5	H3BRE4;H3BNQ5	Dual specificity p	CLK3		1	1	190	0	9.806	0.80133	NaN	5.85E+07
P13639	P13639	Elongation factor	EEF2		60	59	858	0	323.31	0.80123	1.2933	5.82E+10
Q8IXB1;Q8IXB1-2	Q8IXB1;Q8IXB1-2	DnaJ homolog sul	DNAJC10		3	3	793	0	11.666	0.80074	1.7581	1.13E+08
Q6PI48	Q6PI48	Aspartate--tRNA li	DARS2		25	25	645	0	304.43	0.80073	0.8692	5.56E+09
H3BMQ0;P49815	H3BMQ0;P49815	Tuberin	TSC2		18	18	1751	0	129.5	0.80009	1.122	1.14E+09
Q9BX10-2;Q9BX1	Q9BX10-2;Q9BX1	GTP-binding prot	GTPBP2		3	3	514	0	5.9485	0.80009	NaN	3.14E+07
Q9H936;E9PJH7;	Q9H936;E9PJH7;	Mitochondrial gl	SLC25A22		13	13	323	0	170	0.80006	1.2625	2.73E+09
P09972;K7EKH5;	P09972;K7EKH5;	Fructose-bisphos	ALDOC		5	2	364	0	85.15	0.79976	1.0686	2.01E+09
C9JLU1;P52434;I	C9JLU1;P52434;I	DNA-directed RN	POLR2H		8	8	149	0	111.53	0.7995	1.1033	1.35E+09
P34897-3;P3489	P34897-3;P3489	Serine hydroxyme	SHMT2		14	13	483	0	80.473	0.79905	1.3063	1.91E+09
Q9UPY3-2;Q9UPY	Q9UPY3-2;Q9UPY	Endoribonuclease	DICER1		13	13	1829	0	122.87	0.79884	1.1966	3.32E+08
E9PEB5;Q96AE4;(	E9PEB5;Q96AE4;(	Far upstream elen	FUBP1		10	6	655	0	85.114	0.79874	NaN	2.80E+08
A0A0G2JIS2;Q96I	A0A0G2JIS2;Q96I	Histone-lysine N-r	EHMT2		8	8	1176	0	22.858	0.79846	1.3491	1.58E+08
Q13033-2;Q1303	Q13033-2;Q1303	Striatin-3	STRN3		4	4	713	0	15.611	0.79845	0.59114	3.47E+08
P39019;M0R2L9;	P39019;M0R2L9;	40S ribosomal pr	RPS19		14	14	145	0	58.543	0.79843	1.491	3.13E+09
Q68E01-2;Q68E0	Q68E01-2;Q68E0	Integrator compl	INTS3		14	14	1042	0	130.38	0.79792	1.0214	9.41E+08
P49755;G3V2K7	P49755;G3V2K7	Transmembrane e	TMED10		6	6	219	0	31.832	0.7978	1.1137	1.63E+09
Q13546-2;Q1354	Q13546-2;Q1354	Receptor-interact	RIPK1		6	6	625	0	22.118	0.79775	NaN	2.08E+08
O15504;C9JYA1;(	O15504;C9JYA1;(	Nucleoporin-like	NUPL2		2	2	423	0	21.887	0.79767	0.78752	2.97E+08
O15355	O15355	Protein phosphat	PPM1G		10	10	546	0	59.888	0.79764	NaN	8.35E+08
F8WJN3;Q16630	F8WJN3;Q16630	Cleavage and poly	CPSF6		3	3	478	0	73.741	0.7968	NaN	9.50E+07
A0A087WW77;Q	A0A087WW77;Q	Lethal(2) giant lar	LLGL1		12	12	1056	0	55.34	0.79631	1.243	1.15E+09
Q96DI7;Q9NSS8;I	Q96DI7;Q9NSS8;I	U5 small nuclear	SNRNP40;DKFZp4		5	5	357	0	103.68	0.79625	1.2156	2.29E+09
P78406;E9PPG9;	P78406	mRNA export fact	RAE1		5	5	368	0	14.415	0.79595	0.93862	1.72E+08
Q9BQS8;Q9BQS8-	Q9BQS8;Q9BQS8-	FYVE and coiled-c	FYCO1		2	2	1478	0	23.013	0.79588	1.6039	1.35E+08
Q8IZL8;I3L445;C9	Q8IZL8;I3L445;C9	Proline-, glutamic	PELP1		3	3	1130	0	28.876	0.79535	1.1039	2.53E+08

Q5TA45-2;Q5TA4	Q5TA45-2;Q5TA4	Integrator compl	CPSF3L	9	9	499	0	51.128	0.79524	NaN	3.41E+08
Q6P9B9	Q6P9B9	Integrator compl	INTS5	5	5	1019	0	20.292	0.79492	1.5459	3.91E+08
I1E4Y6;Q6Y7W6	I1E4Y6;Q6Y7W6	PERQ amino acid-	GIGYF2	2	2	1321	0	4.9959	0.7949	NaN	2.35E+07
P28074;P28074-	P28074;P28074-	Proteasome subu	PSMB5	7	7	263	0	43.904	0.79489	1.2073	4.05E+08
O75529;O75529	O75529;O75529	TAF5-like RNA pol	TAF5L	3	3	589	0	7.8436	0.79474	NaN	4.42E+07
O75955;A0A140	O75955;A0A140	Flotillin-1	FLOT1	11	11	427	0	93.374	0.79442	1.2723	1.00E+09
Q96CS3;D6RBG6	Q96CS3	FAS-associated fa	FAF2	21	21	445	0	323.31	0.79418	1.2767	1.23E+10
J3QQW9;Q15022	J3QQW9;Q15022	Polycomb protei	SUZ12	5	5	716	0	80.533	0.79406	1.4543	4.25E+08
P05455;E9PGX9;	P05455	Lupus La protein	SSB	8	8	408	0	19.599	0.79397	0.89587	4.29E+08
Q9H6R4-4;Q9H6	Q9H6R4-4;Q9H6	Nucleolar protein	NOL6	13	13	1143	0	90.508	0.79371	1.5709	1.14E+09
P62304;A6NHK2	P62304	Small nuclear ribo	SNRPE	3	3	92	0	28.318	0.79362	1.4856	4.50E+09
Q8WU76-2;Q8W	Q8WU76-2;Q8W	Sec1 family doma	SCFD2	3	3	639	0	14.291	0.7932	NaN	1.22E+08
O75533;H7C341	O75533	Splicing factor 3B	SF3B1	37	36	1304	0	276.47	0.79262	1.1025	5.59E+09
A0A087WUZ3;Q0	A0A087WUZ3;Q0	Spectrin beta cha	SPTBN1	12	11	2366	0	43.504	0.79252	1.0609	4.34E+08
Q9Y5J1;J3KSR7;J	Q9Y5J1	U3 small nucleola	UTP18	7	7	556	0	18.946	0.79231	NaN	5.07E+08
Q9UKZ1;H7C0C7	Q9UKZ1;H7C0C7	CCR4-NOT transcr	CNOT11	4	4	510	0	44.881	0.79175	1.3807	4.91E+08
P06576;H0YH81;	P06576;H0YH81;	ATP synthase subu	ATP5B	24	24	529	0	323.31	0.79122	1.1663	1.91E+10
Q8TEX9;Q8TEX9	Q8TEX9;Q8TEX9	Importin-4	IPO4	23	23	1081	0	323.31	0.7912	1.3872	5.69E+09
P19387;H3BRR2	P19387	DNA-directed RN	POLR2C	7	7	275	0	37.911	0.791	1.5561	7.75E+08
Q3LIE7;Q15392	Q3LIE7;Q15392	Delta(24)-sterol r	Nbla03646;DHCR	13	13	427	0	58.715	0.79075	1.2122	1.03E+09
Q9Y6C9	Q9Y6C9	Mitochondrial ca	MTCH2	9	2	303	0	128.01	0.79045	1.465	4.69E+09
O75489;E9PS48	O75489	NADH dehydroge	NDUFS3	15	15	264	0	88.884	0.78988	0.96029	2.21E+09
P35269;M0R0Z3	P35269;M0R0Z3	General transcrip	GTF2F1	3	3	517	0	38.402	0.78955	NaN	9.79E+07
Q9H223;A0A087	Q9H223;A0A087	EH domain-conta	EHD4	14	10	541	0	55.16	0.78955	NaN	8.62E+08
Q9BSJ8;Q9BSJ8-2	Q9BSJ8;Q9BSJ8-2	Extended synapto	ESYT1	15	15	1104	0	111.58	0.78858	1.4868	2.05E+09
Q9BPU6;E7EWB4	Q9BPU6	Dihydropyrimidir	DPYSL5	17	17	564	0	156.48	0.78815	NaN	1.38E+09
M0R0F9;Q15642	M0R0F9;Q15642	Cdc42-interactin	TRIP10	2	2	437	0	4.9818	0.78766	NaN	4.22E+07
B7Z7F3;Q9H6Z4	B7Z7F3;Q9H6Z4	Ran-binding prot	ZNF8;RANBP3	4	4	494	0	33.799	0.78664	NaN	8.47E+07
Q15029-2;Q1502	Q15029-2;Q1502	116 kDa U5 small	EFTUD2	45	30	937	0	323.31	0.7854	1.1734	1.29E+10
P51665;H3BNT7;	P51665;H3BNT7;	26S proteasome r	PSMD7	5	5	324	0	38.012	0.78488	1.1193	6.84E+08
J3KQN4;P83881;	J3KQN4;P83881;	60S ribosomal pr	RPL36A;RPL36A-I	10	2	142	0	22.058	0.78442	0.60217	3.64E+08
P52209-2;P5220	P52209-2;P5220	6-phosphogluco	PGD	27	27	470	0	323.31	0.78397	1.154	1.62E+10
O60287	O60287	Nucleolar pre-rib	URB1	24	24	2271	0	211.28	0.78336	1.1487	2.43E+09
Q9Y3U8;J3QSB5	Q9Y3U8;J3QSB5	60S ribosomal pr	RPL36	6	6	105	0	21.072	0.78329	1.1912	1.31E+09
P04843;B7Z4L4;I	P04843;B7Z4L4	Dolichyl-diphosp	RPN1	30	30	607	0	313.98	0.78246	1.0475	7.10E+09
A0A087WY88;Q8	A0A087WY88;Q8	Protein jagunal h	JAGN1	3	3	181	0	8.956	0.78242	1.4522	1.61E+08
Q9H9B4;D6RFI0;	Q9H9B4;D6RFI0;	Sideroflexin-1	SFXN1	16	15	322	0	323.31	0.78069	1.054	1.62E+10
O60506-3;O6050	O60506-3;O6050	Heterogeneous nu	SYNCRIP	18	13	562	0	197.21	0.77981	1.6842	4.31E+09
P56192;P56192-	P56192;P56192-	Methionine--tRN	MARS	42	42	900	0	323.31	0.77933	1.2215	2.31E+10
P52292;J3QLL0;J	P52292;J3QLL0;J	Importin subunit	KPNA2;POU2F2	14	14	529	0	185	0.77923	0.96736	3.32E+09
A0A087WTP3;Q9	A0A087WTP3;Q9	Far upstream elen	KHSRP	8	6	711	0	21.244	0.77879	1.1689	2.04E+08
H0Y8R1;F5H5I6;I	H0Y8R1;F5H5I6;I	G-rich sequence f	GRSF1	15	15	417	0	149.78	0.77868	1.0523	3.38E+09
Q8IX12-2;Q8IX12	Q8IX12-2;Q8IX12	Cell division cycle	CCAR1	19	19	1135	0	139.97	0.77838	1.1399	2.38E+09
Q86X76-2;Q86X7	Q86X76-2;Q86X7	Nitrilase homolo	NIT1	4	4	291	0	8.4012	0.77833	0.52879	1.98E+08
F8VPD4;P27708;	F8VPD4;P27708	CAD protein;Glut	CAD	103	99	2162	0	323.31	0.77816	1.3363	4.22E+10
Q13200;Q13200	Q13200;Q13200	26S proteasome r	PSMD2	42	42	908	0	323.31	0.7775	1.1663	1.64E+10
Q8NF37;A0A0G2	Q8NF37;A0A0G2	Lysophosphatidyl	LPCAT1	11	11	534	0	42.432	0.77745	1.1524	5.01E+08
P51790-4;P5179	P51790-4;P5179	H(+)/Cl(-) exchang	CLCN3;CLCN4;CL	2	2	791	0.00026709	3.5394	0.77741	NaN	6.47E+07
S4R400;S4R3N8;	S4R400		FOCAD	12	1	1237	0	5.6076	0.77681	NaN	1.83E+08
Q96IJ6;Q96IJ6-2	Q96IJ6;Q96IJ6-2	Mannose-1-phos	GMPPA	9	9	420	0	103.96	0.77675	1.372	9.30E+08
Q9BYJ9	Q9BYJ9	YTH domain-cont	YTHDF1	8	3	559	0	31.016	0.77544	NaN	1.05E+08
Q9NZ08;Q9NZ08	Q9NZ08;Q9NZ08	Endoplasmic retic	ERAP1	2	2	941	0.00079072	3.2785	0.77523	NaN	4.87E+07
S4R3D6;Q96GX9	S4R3D6;Q96GX9	Methylthioribulo	APIP	2	2	195	0.0020576	2.8789	0.77476	NaN	1.13E+07
Q9BYC9;I3L2X1;C	Q9BYC9;I3L2X1;C	39S ribosomal pr	MRPL20	2	2	149	0	4.9359	0.77454	1.1257	1.03E+08
Q9NS86	Q9NS86	LanC-like protein	LANCL2	5	5	450	0	35.267	0.77443	1.429	3.01E+08
P21281;H0YC04;	P21281;H0YC04	V-type proton ATI	ATP6V1B2	5	5	511	0	17.763	0.7744	1.5199	3.30E+08
Q6SPF0;E9PIW9;I	Q6SPF0;E9PIW9	Atherin	SAMD1	6	6	538	0	15.221	0.77349	NaN	2.57E+08
E9PLK3;P55786;I	E9PLK3;P55786;I	Puromycin-sensit	NPEPPS	27	27	915	0	196.99	0.77264	1.2851	6.73E+09
E9PIR7;F8W809;;	E9PIR7;F8W809;;	Thioredoxin redu	GML;TXNRD1	8	8	482	0	49.2	0.77248	1.2936	1.48E+09
P53396;P53396-	P53396;P53396-	ATP-citrate synth	ACLY	64	64	1101	0	323.31	0.77148	1.1353	5.87E+10
Q96TC7;H0YMB1	Q96TC7;H0YMB1	Regulator of micr	RMDN3	6	6	470	0	69.063	0.77056	NaN	2.96E+08
P32189-1;P3218	P32189-1;P3218	Glycerol kinase;P	GK;GK3P	2	2	524	0	10.771	0.77017	NaN	2.38E+07
P00492	P00492	Hypoxanthine-gu	HPRT1	7	7	218	0	26.344	0.7699	1.4304	2.96E+09
P14735;P14735-	P14735;P14735-	Insulin-degrading	IDE	14	14	1019	0	61.602	0.76884	0.95679	1.28E+09
Q8TCS8;H7C3C5	Q8TCS8	Polyribonucleoti	PNPT1	3	3	783	0	14.374	0.76847	0.81853	1.41E+08
B5MCF9;O00541	B5MCF9;O00541	Pescadillo homol	PES1	17	17	571	0	66.908	0.7682	3.4744	9.19E+08
J3QR09;J3KTE4;P	J3QR09;J3KTE4;P	Ribosomal protei	RPL19	14	14	193	0	61.63	0.76817	2.0125	2.45E+09
Q5VTU3;P63172	Q5VTU3;P63172	Dynein light chai	DYNLT1	3	3	92	0	167.9	0.76811	1.1183	1.24E+09
O00299	O00299	Chloride intracell	CLIC1	17	17	241	0	319.37	0.76766	1.0395	6.91E+09
Q15751;H0YNB1	Q15751	Probable E3 ubiq	HERC1	4	4	4861	0	9.6125	0.76715	NaN	3.15E+07
P51148;P51148-	P51148;P51148-	Ras-related protei	RAB5C	6	6	216	0	44.633	0.76714	1.0357	6.34E+08
P49406;S4R3W9	P49406;S4R3W9	39S ribosomal pr	MRPL19	4	4	292	0	10.916	0.76693	1.2607	2.51E+08
Q14657	Q14657	EKC/KEOPS comp	LAGE3	3	3	143	0	20.695	0.7669	0.45515	5.99E+07
O95336;M0R261	O95336;M0R261	6-phosphogluco	PGLS	11	11	258	0	142.72	0.76689	0.81786	5.15E+09
Q8IXI1;H3BST5;I	Q8IXI1;H3BST5;I	Mitochondrial Rh	RHOT2	9	8	618	0	145.19	0.76655	NaN	9.79E+08
Q7Z494;Q7Z494	Q7Z494;Q7Z494	Nephrocystin-3	NPHP3	10	10	1330	0	40.564	0.7665	2.317	3.90E+08
Q8TCJ2	Q8TCJ2	Dolichyl-diphosp	STT3B	5	5	826	0	13.756	0.76589	NaN	3.55E+08
J3QLK5;Q86UE8	J3QLK5;Q86UE8	Serine/threonine	TLK2;TLK1	3	3	601	0	9.9461	0.76488	0.72529	1.38E+08
P00338;P00338	P00338;P00338	L-lactate dehydro	LDHA	20	20	332	0	202.47	0.76483	1.0153	5.23E+09
P36871;P36871	P36871;P36871	Phosphoglucomu	PGM1	17	17	562	0	106.69	0.76375	1.0382	1.50E+09
P10515;H0YDD4;	P10515;H0YDD4	Dihydrolipoyllysi	DLAT	13	13	647	0	77.727	0.76318	1.2183	1.97E+09
Q9BWD1;Q9BWD	Q9BWD1;Q9BWD	Acetyl-CoA acetyl	ACAT2	14	14	397	0	194.43	0.7624	1.11	6.38E+09
Q8TDZ2-2;Q8TDZ	Q8TDZ2-2;Q8TDZ	Protein-methioni	MICAL1	3	3	981	0	16.095	0.76184	NaN	1.17E+08
H0Y6Y8;B1AL05;(	H0Y6Y8;B1AL05;(	39S ribosomal pr	MRPL43	4	4	169	0	9.4073	0.76147	1.5401	1.82E+08
O75947;O75947	O75947;O75947	ATP synthase subu	ATP5H	4	4	161	0	16.892	0.76058	0.69325	1.64E+08
X6RGJ2;Q5SSJ5;C	X6RGJ2;Q5SSJ5;C	Heterochromatin	HP1BP3	7	7	327	0	25.088	0.76038	2.9008	3.74E+08
Q9BQG0;Q9BQG	Q9BQG0;Q9BQG	Myb-binding prot	MYBBP1A	37	37	1328	0	231.04	0.76028	1.5007	3.69E+09
Q9P0I2;Q9P0I2-2	Q9P0I2;Q9P0I2-2	ER membrane pro	EMC3	4	4	261	0	28.628	0.75997	0.88503	2.71E+08
G5E9S8;G3V2E7;I	G5E9S8;G3V2E7;I	Kinesin light chai	KLC1	4	4	549	0	18.117	0.75962	NaN	1.17E+08
Q99808;Q99808	Q99808;Q99808	Equilibrative nucl	SLC29A1	2	2	456	0	5.8282	0.75932	0.65364	1.42E+07
J3KNN3;P15735	J3KNN3;P15735	Phosphorylase b k	PHKG2	4	4	410	0	21.878	0.75922	1.1241	2.48E+08
Q13283;E5RIZ6;E	Q13283	Ras GTPase-activa	G3BP1	13	11	466	0	166.02	0.75904	0.96326	2.38E+09
Q9Y3B7;Q9Y3B7	Q9Y3B7;Q9Y3B7	39S ribosomal pr	MRPL11	5	5	192	0	41.481	0.75848	1.2831	3.48E+08
B1ANR0;Q13310	B1ANR0;Q13310	Polyadenylate-bi	PABPC4	10	4	615	0	9.4531	0.75782	NaN	3.06E+08
Q15008;Q15008	Q15008;Q15008	26S proteasome r	PSMD6	13	13	389	0	79.183	0.75732	1.2235	2.63E+09
E7EPT4;P19404	E7EPT4;P19404	NADH dehydroge	NDUFV2	3	3	252	0	11.76	0.75718	1.0846	2.17E+08
Q5SRE5;Q5SRE5	Q5SRE5;Q5SRE5	Nucleoporin NUP	NUP188	36	36	1749	0	255.01	0.75587	1.1786	3.70E+09
Q9UBQ7;U3KQ56	Q9UBQ7;U3KQ56	Glyoxylate reduct	GRHPR	14	14	328	0	209.71	0.75579	1.0984	7.33E+09
Q13724-2;Q1372	Q13724-2;Q1372	Mannosyl-oligosa	MOGS	4	4	731	0	27.464	0.75544	3.5786	2.11E+08
A0A087X0S7;A0A	A0A087X0S7;A0A	Leucine-rich repe	LRRC41	4	4	521	0	18.634	0.75371	1.0959	2.04E+08
Q8N2G8-3;Q8N2	Q8N2G8-3;Q8N2	GH3 domain-con	GHDC	3	3	491	0	8.6059	0.75271	NaN	4.80E+07
Q6P996-4;Q6P99	Q6P996-4;Q6P99	Pyridoxal-depend	PDXDC1	17	17	760	0	161.12	0.7523	1.2344	1.61E+09
P48553	P48553	Trafficking protei	TRAPPC10	1	1	1259	0.00079239	3.306	0.75221	NaN	5.02E+07
Q9NY12-2;Q9NY1	Q9NY12-2;Q9NY1	H/ACA ribonuclec	GAR1	3	3	199	0	4.103	0.75214	2.0913	1.47E+08

P42575;A0A087\	P42575;A0A087\	Caspase-2;Caspas	CASP2	2	2	452	0	9.6788	0.75188	NaN	1.60E+08
Q15397;S4R3K8	Q15397	Pumilio domain-c	KIAA0020	6	6	648	0	27.535	0.7515	NaN	1.05E+08
Q15048;E9PP40;	Q15048;E9PP40	Leucine-rich repe	LRRC14	6	6	493	0	45.71	0.75146	1.1576	3.14E+08
Q5QJE6;J3KP30;E	Q5QJE6;J3KP30	Deoxynucleotidyl	DNTTIP2	4	4	756	0	25.691	0.75131	1.2515	2.44E+08
P46777;Q5T7N0	P46777	60S ribosomal pr	RPL5	16	16	297	0	78.685	0.75106	1.7135	1.69E+09
Q92922;F8WE13	Q92922	SWI/SNF complex	SMARCC1	10	10	1105	0	56.048	0.75021	1.0803	2.83E+08
Q15428;K7EMT0	Q15428;K7EMT0	Splicing factor 3A	SF3A2	5	5	464	0	16.784	0.74837	NaN	4.53E+07
O43396;K7ER96;	O43396;K7ER96;	Thioredoxin-like p	TXNL1	10	10	289	0	108.24	0.74825	1.0762	2.75E+09
Q96DV4;Q96DV4	Q96DV4	39S ribosomal pr	MRPL38	4	4	380	0	16.594	0.74806	1.4819	1.26E+09
Q96C19;H0Y4Y4	Q96C19	EF-hand domain-c	EFHD2	3	3	240	0	12.258	0.74804	0.92272	7.26E+07
P62917;E9PKZ0;I	P62917;E9PKZ0;I	60S ribosomal pr	RPL8	17	17	257	0	146.07	0.74778	1.652	5.15E+09
P22570-5;P2257	P22570-5;P2257	NADPH:adrenodo	FDXR	4	4	483	0	15.098	0.74723	0.76395	8.10E+07
P52306-4;P5230	P52306-4;P5230	Rap1 GTPase-GDP	RAP1GDS1	7	7	607	0	43.415	0.74723	NaN	4.26E+08
Q68CQ4	Q68CQ4	Digestive organ e	DIEXF	3	3	756	0	8.2522	0.74719	1.5013	1.11E+08
Q02543;M0R3D6	Q02543;M0R3D6	60S ribosomal pr	RPL18A	13	13	176	0	67.734	0.74717	1.9141	2.51E+09
A0A024R4M0;P4	A0A024R4M0;P4	40S ribosomal pr	RPS9	21	21	194	0	61.452	0.74689	1.7169	1.46E+10
Q96P48-3;Q96P4	Q96P48-3;Q96P4	Arf-GAP with Rho	ARAP1	11	11	1439	0	55.029	0.7468	0.81393	7.42E+08
Q9Y4E6-2;Q9Y4E	Q9Y4E6-2;Q9Y4E	WD repeat-contai	WDR7	4	4	1457	0	15.11	0.74656	1.2128	1.49E+08
Q9Y2R0;K7EPV0	Q9Y2R0;K7EPV0	Cytochrome c oxi	COA3	2	2	106	0.0010485	3.1683	0.74638	NaN	4.86E+07
Q9NRP0;A0A087	Q9NRP0;A0A087	Oligosaccharyltra	OSTC	2	2	149	0	16.39	0.74474	1.5173	2.33E+08
Q86UT6;Q86UT6	Q86UT6;Q86UT6	NLR family memb	NLRX1	6	6	975	0	15.608	0.74451	1.0769	4.16E+08
Q9BQC6	Q9BQC6	Ribosomal protei	MRPL57	1	1	102	0	13.249	0.74366	NaN	1.62E+08
B0QXZ6;O95503	B0QXZ6;O95503	Chromobox prote	CBX6	2	2	394	0	10.765	0.74363	NaN	2.36E+07
P09496-2;P0949	P09496-2;P0949	Clathrin light cha	CLTA	5	5	218	0	97.081	0.74231	0.72805	1.25E+08
P14174	P14174	Macrophage migr	MIF	4	4	115	0	25.747	0.74212	2.3623	2.55E+09
J3KN36;A0A0G2J	J3KN36;A0A0G2J	Nodal modulator	NOMO3;NOMO2;	8	8	1267	0	39.075	0.74164	1.4263	4.83E+08
Q04760-2;Q0476	Q04760-2;Q0476	Lactoylglutathior	GLO1	5	5	169	0	14.525	0.74142	1.0136	5.23E+08
E9PNK6;E9PPQ1;	E9PNK6;E9PPQ1;	Tumor protein D5	TPD52L1	2	2	166	0	4.9894	0.74088	NaN	6.18E+07
H0YLI7;P59780;C	H0YLI7;P59780;C	AP-3 complex sub	AP3S2	3	3	205	0	4.9765	0.74026	0.94196	1.38E+08
E9PC44;E9PDM8;	E9PC44;E9PDM8;	Protein transport	SEC24D	6	6	393	0	25.825	0.73977	1.069	8.73E+08
O76094;O76094·	O76094;O76094·	Signal recognitior	SRP72	12	12	671	0	110.57	0.7396	2.0573	9.25E+08
E9PL17;Q92989;I	E9PL17;Q92989;I	Polyribonucleotid	CLP1	4	4	436	0	6.692	0.73953	2.2838	3.75E+08
P49257	P49257	Protein ERGIC-53	LMAN1	10	10	510	0	52.166	0.73888	0.61051	1.17E+09
F5H269;Q9Y485	F5H269;Q9Y485	DmX-like protein	DMXL1	2	2	3048	0	9.2225	0.73861	0.93	5.27E+07
H3BMH2;H3BSC1	H3BMH2;H3BSC1	Ras-related protei	RAB11A;RAB11B	6	6	155	0	19.214	0.73849	1.3055	6.79E+08
S4R3Q9;J3KNA0;I	S4R3Q9;J3KNA0;I	Mitochondrial in	OXA1L	3	3	435	0	10.295	0.73772	1.5537	3.79E+07
A0A0G2JQK5;Q6I	A0A0G2JQK5;Q6I	Nucleoredoxin	NXN	3	3	120	0	29.912	0.73752	0.93829	1.09E+08
Q96CU9-3;Q96CU	Q96CU9-3;Q96CU	FAD-dependent o	FOXRED1	4	4	472	0	19.977	0.73732	1.2249	5.85E+08
Q15036;Q15036·	Q15036;Q15036·	Sorting nexin-17	SNX17	9	9	470	0	83.758	0.73701	1.2507	9.53E+08
E7EPF2;E7ETU5;F	E7EPF2;E7ETU5;F	RNA-binding mot	RBMS1;RBMS3;RI	2	2	128	0	6.6895	0.73674	NaN	1.46E+08
Q9H3K6;A0A087	Q9H3K6;A0A087	BolA-like protein	BOLA2	3	3	86	0	47.009	0.7365	1.4405	1.04E+09
P43007;P43007·	P43007;P43007·	Neutral amino aci	SLC1A4	4	4	532	0	33.844	0.73649	NaN	1.50E+08
A0A088AWN3;A0	A0A088AWN3;A0	Dedicator of cyto	DOCK9	6	5	2079	0	20.112	0.73648	0.9183	1.90E+08
Q8N138-4;Q8N1	Q8N138-4;Q8N1	ORM1-like protei	ORMDL3	3	2	137	0	5.1653	0.73609	NaN	1.06E+08
Q9NPE3;H0YM60	Q9NPE3	H/ACA ribonuclec	NOP10	4	4	64	0	16.402	0.73487	2.322	1.70E+08
P62854;Q5JNZ5	P62854;Q5JNZ5	40S ribosomal pr	RPS26;RPS26P11	4	4	115	0	13.018	0.7338	1.6705	2.90E+09
Q5T6H7;Q9NQW	Q5T6H7;Q9NQW	Xaa-Pro aminope	XPNPEP1	2	2	552	0	12.404	0.73303	NaN	3.29E+08
Q9Y3B4	Q9Y3B4	Splicing factor 3B	SF3B6	4	4	125	0	17.768	0.73237	1.2024	1.11E+09
O43809;H3BND3	O43809;H3BND3	Cleavage and poly	NUDT21	7	7	227	0	28.101	0.73235	4.4929	5.17E+08
Q9H8Y5;B8ZZS4;(	Q9H8Y5;B8ZZS4	Ankyrin repeat an	ANKZF1	3	3	726	0	30.118	0.73193	3.115	3.86E+08
Q9BR76;F5H0D2;	Q9BR76	Coronin-1B	CORO1B	5	5	489	0	56.414	0.73043	1.3173	6.80E+08
A6NNK5;Q12888	A6NNK5;Q12888	Tumor suppresso	TP53BP1	3	3	1927	0	10.259	0.72984	1.1937	2.77E+08
P52788-2;P5278	P52788-2;P5278	Spermine synthas	SMS	5	5	313	0	112.95	0.72984	1.3703	1.32E+09
A6NEM2;P51610	A6NEM2;P51610	Host cell factor 1;	HCFC1	17	17	2080	0	79.35	0.72931	1.2734	1.63E+09
P62277;J3KMX5;	P62277;J3KMX5	40S ribosomal pr	RPS13	15	15	151	0	99.211	0.72885	1.4767	1.50E+10
O95396	O95396	Adenylyltransfera	MOCS3	12	12	460	0	111.91	0.72881	1.2369	1.02E+09
J3KPG2;E9PJF7;C	J3KPG2;E9PJF7;C	Translationally-cc	TPT1	2	2	160	0.0010493	3.1848	0.72808	NaN	2.52E+07
P68133;P68032;	P68133;P68032;	Actin, alpha skele	ACTA1;ACTC1;AC	16	1	377	0	69.288	0.728	1.4021	1.67E+10
P27105;F8VSL7;F	P27105;F8VSL7;F	Erythrocyte band	STOM	2	2	288	0	40.587	0.72698	0.95179	8.04E+07
P60763;J3KSC4;J	P60763;J3KSC4;J	Ras-related C3 bo	RAC3;RAC1	3	2	192	0	4.1956	0.72528	NaN	5.27E+07
P62753;A2A3R5;	P62753;A2A3R5	40S ribosomal pr	RPS6	13	13	249	0	120.99	0.72485	2.128	4.53E+09
G3XAN4;Q15629	G3XAN4;Q15629	Translocating cha	TRAM1	2	2	288	0	4.5626	0.72456	0.95908	2.34E+08
Q8N5N7;Q8N5N7	Q8N5N7;Q8N5N7	39S ribosomal pr	MRPL50	2	2	158	0	23.941	0.72435	1.4743	1.87E+08
P11413;P11413·	P11413;P11413·	Glucose-6-phospl	G6PD	10	10	515	0	56.839	0.72432	1.3968	7.87E+08
O75616;J3QSB2;.	O75616;J3QSB2;.	GTPase Era, mitoc	ERAL1	5	5	437	0	25.393	0.72306	0.89943	5.68E+08
Q12768;E7EQI7;E	Q12768;E7EQI7	WASH complex su	KIAA0196	12	12	1159	0	57.889	0.72225	1.2618	8.70E+08
E9PEC3;E7EUY3;E	E9PEC3;E7EUY3;E	Propionyl-CoA ca	PCCB	4	4	423	0	14.173	0.7216	NaN	1.57E+08
O96007	O96007	Molybdopterin sy	MOCS2	5	5	188	0	28.388	0.72126	0.91631	3.14E+08
P60953;P60953·	P60953;P60953·	Cell division cont	CDC42	6	5	191	0	92.254	0.72072	0.90374	6.57E+08
E9PMY3;E9PML8;	E9PMY3;E9PML8;	Protein tyrosine p	PTP4A2;PTP4A1	2	2	63	0.0047417	2.4134	0.72052	NaN	8.72E+07
Q9H8M7;X6R9S5	Q9H8M7	Protein FAM188A	FAM188A	4	4	445	0	9.222	0.71828	1.0401	2.72E+08
O43913;O43913·	O43913;O43913·	Origin recognitio	ORC5	6	6	435	0	35.105	0.71761	1.6022	1.06E+09
Q9BVP2-2;Q9BVP	Q9BVP2-2;Q9BVP	Guanine nucleoti	GNL3	8	8	537	0	41.987	0.71617	NaN	8.58E+08
J3KR97;Q9BTW9;	J3KR97;Q9BTW9;	Tubulin-specific c	TBCD	22	22	1230	0	203.79	0.71601	1.2643	3.43E+09
Q9UKE5-8;Q9UKE	Q9UKE5-8;Q9UKE	TRAF2 and NCK-in	TNIK;MINK1	9	2	1268	0	8.2789	0.71561	NaN	3.10E+07
Q8N766-4;Q8N7(	Q8N766-4;Q8N7(	ER membrane pro	EMC1	7	7	971	0	38.491	0.71524	1.3333	5.29E+08
Q969S3	Q969S3	Zinc finger protei	ZNF622	2	2	477	0	7.6961	0.71395	NaN	1.03E+08
Q8N442	Q8N442	Translation factor	GUF1	4	4	669	0	9.1355	0.71391	NaN	4.17E+08
O95197-3;O9519	O95197-3;O9519	Reticulon-3	RTN3	1	1	236	0	4.4684	0.71359	NaN	6.94E+07
F8VPF2;Q96K12-:	F8VPF2;Q96K12-:	Fatty acyl-CoA rec	FAR2	1	1	44	0.0020672	2.9422	0.71305	1.164	1.89E+07
P31942-2;P3194	P31942-2;P3194	Heterogeneous nu	HNRNPH3	7	6	331	0	33.999	0.71305	1.4773	9.56E+08
Q9UKD2	Q9UKD2	mRNA turnover p	MRTO4	15	15	239	0	118.91	0.71162	0.8855	1.55E+09
Q9UBW8;F5H7C6	Q9UBW8;F5H7C6	COP9 signalosom	COPS7A	4	4	275	0	47.06	0.71055	1.0491	3.10E+08
P06748;P06748·	P06748;P06748·	Nucleophosmin	NPM1	18	18	294	0	323.31	0.71048	1.2615	2.62E+10
B7Z683;A0A0G2J	B7Z683;A0A0G2J	Active breakpoint	ABR	3	2	641	0	11.033	0.71026	NaN	7.75E+07
P00403	P00403	Cytochrome c oxi	MT-CO2	6	6	227	0	51.516	0.70975	1.1079	1.34E+09
Q9NRG9;Q9NRG9	Q9NRG9;Q9NRG9	Aladin	AAAS	11	11	546	0	65.909	0.70915	1.4198	1.62E+09
Q5TDH0;Q5TDH0	Q5TDH0;Q5TDH0	Protein DDI1 hon	DDI2	8	8	399	0	67.424	0.70895	1.356	2.83E+09
Q9NYJ8;Q9NYJ8-:	Q9NYJ8;Q9NYJ8-:	TGF-beta-activate	TAB2	5	5	693	0	49.473	0.70803	1.6854	1.82E+08
Q14674;Q14674·	Q14674;Q14674·	Separin	ESPL1	9	9	2120	0	28.757	0.70795	1.1531	1.44E+08
A6NLH6;Q9P003	A6NLH6;Q9P003	Protein cornichoi	CNIH4	1	1	137	0	47.73	0.7076	1.3597	4.52E+09
Q96K37;H7C1I0;	Q96K37;H7C1I0	Solute carrier fam	SLC35E1	4	4	410	0	37.357	0.70676	0.95115	1.52E+08
K7ELQ0;K7ES61;I	K7ELQ0;K7ES61;I	39S ribosomal pr	MRPL4	4	4	220	0	26.235	0.70606	NaN	3.16E+08
Q7KZN9-2;Q7KZN	Q7KZN9-2;Q7KZN	Cytochrome c oxi	COX15	7	7	388	0	24.207	0.70592	1.4215	6.82E+08
B4DR61;P61619;	B4DR61;P61619;	Protein transport	SEC61A1;SEC61A	14	14	482	0	115.66	0.70518	1.4272	1.28E+09
Q13561;Q13561·	Q13561;Q13561·	Dynactin subunit	DCTN2	2	2	401	0	7.6391	0.70455	NaN	1.14E+08
Q8WTT2	Q8WTT2	Nucleolar comple	NOC3L	8	8	800	0	90.874	0.70409	0.81146	1.59E+09
B1AKV4;F6UTR7;I	B1AKV4;F6UTR7;I	Ubiquinol-cytoch	UQCC1	2	2	219	0	56.846	0.70334	4.5327	2.62E+08
H0YI50;A0A087\	H0YI50;A0A087\	Endoplasmic retic	RLN3;ERGIC2	3	3	209	0	10.54	0.70319	0.97136	3.75E+07
Q10469	Q10469	Alpha-1,6-manno	MGAT2	4	4	447	0	7.1922	0.70287	NaN	7.32E+08
Q969M3;Q969M:	Q969M3;Q969M:	Protein YIPF5	YIPF5	2	2	257	0	5.64	0.70274	0.79906	7.52E+08
Q9BYD1;E5RJI7;H	Q9BYD1;E5RJI7	39S ribosomal pr	MRPL13	9	9	178	0	35.754	0.70218	1.2911	4.40E+08
P39023;G5E9G0;	P39023;G5E9G0;	60S ribosomal pr	RPL3	27	27	403	0	203.07	0.70197	1.8443	8.09E+09
Q8WV93;H0Y5F4	Q8WV93;H0Y5F4	Lactation elevate	LACE1	3	3	481	0	4.7015	0.7012	NaN	7.68E+07

P38646;D6RJI2;[	P38646	Stress-70 protein,	HSPA9	37	36	679	0	323.31	0.70093	1.7906	9.64E+09
P04844-2;P0484	P04844-2;P0484	Dolichyl-diphosp	RPN2	17	17	615	0	300.23	0.69958	1.138	3.54E+09
O43251-6;O4325	O43251-6;O4325	RNA binding prot	RBFOX2;RBFOX1	11	11	450	0	65.674	0.69813	0.92973	5.18E+08
P13797;P13797-	P13797;P13797-	Plastin-3	PLS3	17	17	630	0	115.16	0.69813	NaN	1.40E+09
Q9UKM9-2;Q9UK	Q9UKM9-2;Q9UK	RNA-binding prot	RALY	11	11	290	0	64.88	0.69806	1.477	1.79E+09
P51572;P51572-	P51572;P51572-	B-cell receptor-as	BCAP31	5	5	246	0	32.482	0.69783	1.0989	3.93E+08
H0YK01;P49770	H0YK01;P49770	Translation initia	EIF2B2	1	1	71	0	4.0342	0.6977	1.6581	1.56E+07
Q10713;Q10713-	Q10713	Mitochondrial-pr	PMPCA	8	8	525	0	70.934	0.69655	0.99715	5.22E+08
Q92889;Q92889-	Q92889	DNA repair endon	ERCC4	5	5	916	0	24.762	0.69653	1.488	2.01E+08
Q6AI08;K7EIX2;A	Q6AI08;K7EIX2;A	HEAT repeat-cont	HEATR6	11	11	1181	0	98.57	0.69651	1.7089	7.71E+08
Q13416	Q13416	Origin recognitio	ORC2	2	2	577	0	6.9376	0.69638	NaN	5.04E+07
P06733;P06733-	P06733;P06733-	Alpha-enolase;En	ENO1	19	19	434	0	197.48	0.69592	1.5313	3.06E+09
Q7Z417;Q7Z417-	Q7Z417	Nuclear fragile X r	NUFIP2	5	5	695	0	74.257	0.69526	0.83621	1.58E+08
Q9Y276;C9J8G3;(	Q9Y276;C9J8G3	Mitochondrial ch	BCS1L	5	5	419	0	28.939	0.69453	1.5463	2.88E+08
P16403	P16403	Histone H1.2	HIST1H1C	16	5	213	0	60.122	0.69449	0.60699	2.92E+09
Q7Z2W9-2;Q7Z2\	Q7Z2W9-2;Q7Z2\	39S ribosomal pr	MRPL21	4	4	120	0	14.266	0.6944	1.1846	2.85E+08
O95352;O95352-	O95352;O95352-	Ubiquitin-like mo	ATG7	5	5	703	0	18.535	0.69431	NaN	1.47E+08
P00367;P00367-	P00367;P00367-	Glutamate dehyd	GLUD1;GLUD2	14	14	558	0	47.877	0.69429	1.3859	1.32E+09
P08240-2;P0824	P08240-2;P0824	Signal recognitio	SRPR	12	12	610	0	58.177	0.69272	NaN	6.88E+08
B7Z6R6;A0AVF1-;	B7Z6R6;A0AVF1-;	Tetratricopeptide	TTC26	5	5	447	0	84.982	0.6908	NaN	2.44E+08
Q14498-3;Q1449	Q14498-3;Q1449	RNA-binding prot	RBM39	19	16	508	0	157.31	0.69047	2.191	4.18E+09
J3QLD9;E7EMK3;	J3QLD9;E7EMK3;	Flotillin-2	FLOT2	10	10	428	0	42.026	0.69041	1.709	5.11E+08
G3V5Z7;P60900;	G3V5Z7;P60900;	Proteasome subu	PSMA6	7	7	252	0	29.058	0.69039	1.2582	1.05E+09
Q15813;Q15813-	Q15813;Q15813-	Tubulin-specific c	TBCE	14	13	527	0	66.644	0.69016	NaN	9.02E+08
E9PH70;Q9ULH0-	E9PH70;Q9ULH0-	Kinase D-interacti	KIDINS220	7	7	1305	0	20.854	0.69002	2.2994	2.23E+08
Q00403;B1APE1;	Q00403	Transcription init	GTF2B	7	7	316	0	45.527	0.69	0.97179	1.71E+08
P52789;E9PB90;(	P52789;E9PB90	Hexokinase-2	HK2	31	27	917	0	162.4	0.68893	1.3924	3.15E+09
P10412;Q02539;	P10412;Q02539	Histone H1.4;Hist	HIST1H1E;HIST1H	13	2	219	0.0023036	2.795	0.68849	0.68233	1.05E+07
E9PIF2;Q13206	E9PIF2;Q13206	Probable ATP-dep	DDX10	4	4	835	0	29.182	0.68803	1.2504	1.20E+08
Q9BWJ5	Q9BWJ5	Splicing factor 3B	SF3B5	4	4	86	0	39.19	0.68792	0.91811	2.75E+08
A0A0B4J2A0;Q9L	A0A0B4J2A0;Q9L	Sedoheptulokina	SHPK	6	6	478	0	31.252	0.68787	1.4805	4.66E+08
Q9UBB4-2;Q9UBI	Q9UBB4-2;Q9UBI	Ataxin-10	ATXN10	16	16	411	0	110.51	0.68752	1.3029	2.05E+09
B4DWR3;P61758	B4DWR3;P61758	Prefoldin subunit	VBP1	5	5	192	0	10.911	0.68716	1.0862	1.73E+08
Q13405;H0YDP7;	Q13405;H0YDP7	39S ribosomal pr	MRPL49	3	3	166	0	29.021	0.68554	1.9738	4.50E+08
Q12874	Q12874	Splicing factor 3A	SF3A3	3	3	501	0	6.1122	0.68544	NaN	2.98E+07
Q8NFJ9;Q8NFJ9-;	Q8NFJ9;Q8NFJ9-;	Bardet-Biedl synd	BBS1	2	2	593	0	10.58	0.68507	NaN	4.44E+07
F2Z2Y8;Q9H0E2;I	F2Z2Y8;Q9H0E2;I	Toll-interacting p	TOLLIP	2	2	213	0	8.7719	0.68433	1.2	2.42E+08
E7EN86;P52747-;	E7EN86;P52747-;	Zinc finger protei	ZNF143	3	3	610	0	18.668	0.68401	NaN	4.24E+07
Q9Y3P9;Q9Y3P9-	Q9Y3P9;Q9Y3P9-	Rab GTPase-activ	RABGAP1	4	4	1069	0	15.43	0.68367	2.7503	1.30E+08
H0Y5D5;Q9BTG3;	H0Y5D5;Q9BTG3;	Cip1-interacting z	CIZ1	1	1	820	0	15.505	0.68344	NaN	2.15E+07
Q96JJ7;B4DIE3;Q	Q96JJ7;B4DIE3;Q	Protein disulfide-	TMX3	2	2	454	0	5.1156	0.68234	NaN	7.07E+07
Q99536;K7ER81;	Q99536;K7ER81;	Synaptic vesicle n	VAT1	2	2	393	0	8.6955	0.68052	NaN	1.45E+08
Q9BZE1;S4R369;/	Q9BZE1;S4R369;/	39S ribosomal pr	MRPL37	4	4	423	0	8.6704	0.68019	0.95789	2.23E+08
M0R3A4;M0QYA2	M0R3A4;M0QYA2	PIH1 domain-con	PIH1D1	2	2	183	0	9.4537	0.67985	2.3161	2.73E+08
Q15125;C9J719;(	Q15125;C9J719;(	3-beta-hydroxyst	EBP	2	2	230	0	10.789	0.67945	1.1029	3.43E+08
A0A0J9YYL3;A0A(	A0A0J9YYL3;A0A(	Poly(U)-binding-s	PUF60	16	16	505	0	158.51	0.67848	0.90497	1.25E+09
Q6ZXV5-2;Q6ZXV	Q6ZXV5-2;Q6ZXV	Transmembrane a	TMTC3	2	2	914	0	15.076	0.67838	NaN	1.09E+08
O14828-2;O1482	O14828-2;O1482	Secretory carrier-	SCAMP3	3	3	321	0	22.924	0.67768	1.9617	1.07E+08
Q5JTH9-2;Q5JTH9	Q5JTH9-2;Q5JTH9	RRP12-like protei	RRP12	11	11	1197	0	67.838	0.67694	1.7857	3.87E+08
Q9Y333	Q9Y333	U6 snRNA-associa	LSM2	1	1	95	0	17.461	0.67615	NaN	1.04E+08
B0QYW5;F6RTR7;	B0QYW5;F6RTR7;	Peroxisomal mem	SLC25A17	3	3	225	0	16.798	0.67608	0.90283	7.12E+08
Q9Y3I1;Q9Y3I1-3	Q9Y3I1;Q9Y3I1-3	F-box only protei	FBXO7	4	4	522	0	21.398	0.67591	NaN	2.14E+08
Q9H6U6-2;Q9H6I	Q9H6U6-2;Q9H6I	Breast carcinoma	BCAS3	7	7	913	0	88.009	0.67478	1.6154	5.50E+08
P22314-2;P2231	P22314-2;P2231	Ubiquitin-like mo	UBA1	25	25	1018	0	323.31	0.67442	1.3543	5.49E+09
A0A0U1RRM4;P2	A0A0U1RRM4;P2	Polypyrimidine tr	PTBP1	14	11	588	0	147.04	0.67428	1.3107	4.61E+09
Q8TB37;H0YHR7;	Q8TB37;H0YHR7;	Iron-sulfur protei	NUBPL	2	2	319	0	64.26	0.67246	0.80929	1.55E+08
Q9Y4J8-13;Q9Y4J	Q9Y4J8-13;Q9Y4J	Dystrobrevin alph	DTNA	7	4	683	0	148.21	0.67139	0.62784	5.20E+08
O43301;K7ELE6	O43301	Heat shock 70 kD	HSPA12A	4	4	675	0	22.024	0.67119	NaN	1.71E+08
Q6IA86-4;Q6IA86	Q6IA86-4;Q6IA86	Elongator comple	ELP2	7	7	705	0	70.73	0.66985	1.1175	7.32E+08
A2A2V2;P42696;	A2A2V2;P42696	RNA-binding prot	RBM34	3	3	408	0	8.4888	0.66938	NaN	4.75E+07
Q96GK7;Q6P2I3;	Q96GK7;Q6P2I3;	Fumarylacetoace	FAHD2A;FAHD2B	5	5	314	0	66.516	0.66933	0.7815	4.48E+08
E5RHW4;O94905	E5RHW4;O94905	Erlin-2	ERLIN2	14	11	338	0	98.489	0.66909	1.606	4.11E+09
Q8TDD1;Q8TDD1	Q8TDD1;Q8TDD1	ATP-dependent RI	DDX54	8	8	881	0	24.394	0.66871	1.5192	4.91E+08
P09211;A8MX94	P09211;A8MX94	Glutathione S-tra	GSTP1	7	7	210	0	190.99	0.66844	1.1261	3.31E+09
P30419-2;P3041	P30419-2;P3041	Glycylpeptide N-t	NMT1;NMT2	2	2	416	0	4.933	0.66765	NaN	1.63E+08
P52739-2;P5273	P52739-2;P5273	Zinc finger protei	ZNF131	3	3	589	0	37.701	0.66544	0.68594	1.58E+08
Q9H3G5;H7C0X5	Q9H3G5;H7C0X5	Probable serine c	CPVL	7	7	476	0	20.526	0.66429	2.7352	6.91E+08
K7EM09;K7EPR0;	K7EM09;K7EPR0;	Transmembrane p	TMEM205	2	2	120	0	14.217	0.66366	1.0853	3.16E+08
Q14137-2;Q1413	Q14137-2;Q1413	Ribosome biogen	BOP1	13	13	634	0	107.3	0.66361	1.3081	1.19E+09
P61353;K7ELC7;I	P61353;K7ELC7;I	60S ribosomal pr	RPL27	10	10	136	0	49.757	0.66293	0.62897	9.74E+09
A0A024RA52;P2	A0A024RA52;P2	Proteasome subu	PSMA2	5	5	234	0	23.201	0.66259	1.4012	2.16E+08
Q9NQT8;E7ERX9	Q9NQT8;E7ERX9	Kinesin-like prote	KIF13B	2	2	1826	0	4.875	0.66232	NaN	1.94E+08
A8MSZ8;A6NN50	A8MSZ8;A6NN50	Obscurin-like pro	OBSL1	1	1	612	0	3.8103	0.66124	1.1021	3.49E+07
P61956-2;P6195	P61956-2;P6195	Small ubiquitin-r	SUMO2	3	3	71	0	40.783	0.66111	1.2511	3.96E+08
Q13423;E9PCX7;	Q13423;E9PCX7	NAD(P) transhydr	NNT	13	13	1086	0	90.191	0.66097	1.49	1.10E+09
Q8TAE8	Q8TAE8	Growth arrest an	GADD45GIP1	3	3	222	0	6.9471	0.66054	NaN	6.65E+07
A0A0D9SF54;A0A	A0A0D9SF54;A0A	Spectrin alpha ch	SPTAN1	6	6	2457	0	34.958	0.65997	1.3301	2.97E+08
Q9NR30;Q9NR30	Q9NR30;Q9NR30	Nucleolar RNA he	DDX21	52	50	783	0	323.31	0.65901	1.5909	3.16E+10
O14818;O14818-	O14818;O14818-	Proteasome subu	PSMA7	12	12	248	0	126.83	0.65781	1.1902	4.17E+09
P24386	P24386	Rab proteins gera	CHM	4	4	653	0	13.857	0.65778	1.103	1.91E+08
S4R3G0;Q13242;	S4R3G0;Q13242;	Serine/arginine-ri	SRSF9	4	3	119	0	12.068	0.65737	1.9581	3.29E+08
A0A087WUV8;A0	A0A087WUV8;A0	Basigin	BSG	4	4	189	0	12.888	0.65649	2.4809	3.93E+08
P05023-4;P0502	P05023-4;P0502	Sodium/potassiu	ATP1A1	49	31	1023	0	323.31	0.65503	1.4648	2.26E+10
E5RJR5;P63208;E	E5RJR5;P63208;E	S-phase kinase-as	SKP1	4	4	163	0	24.549	0.65499	2.0552	1.47E+08
Q9GZN8;Q9GZN8	Q9GZN8;Q9GZN8	UPF0687 protein	C20orf27	3	3	174	0	10.892	0.65451	1.5512	1.65E+08
Q9Y4C2;Q9Y4C2-	Q9Y4C2;Q9Y4C2-	Protein FAM115A	FAM115A	11	11	921	0	38.824	0.65239	1.3574	8.49E+08
P18077;C9K025;	P18077;C9K025;	60S ribosomal pr	RPL35A	12	12	110	0	31.311	0.6522	1.6206	4.06E+09
P27824;P27824-	P27824;P27824-	Calnexin	CANX	14	14	592	0	69.943	0.65148	1.3348	4.94E+09
Q9UEW8-2;Q9UE	Q9UEW8-2;Q9UE	STE20/SPS1-relat	STK39	8	6	526	0	20.956	0.65135	NaN	4.76E+08
A0A0B4J220;E9P	A0A0B4J220;E9PLD3;E9PRG8		LOC102288414	2	2	123	0	8.9966	0.65087	NaN	1.87E+08
H0Y2Y8;Q15942;	H0Y2Y8;Q15942;	Zyxin	ZYX	6	6	540	0	11.586	0.64984	0.48585	1.40E+08
P28070	P28070	Proteasome subu	PSMB4	3	3	264	0	19.391	0.64974	1.1214	2.41E+08
Q16643;Q16643-	Q16643;Q16643-	Drebrin	DBN1	4	4	649	0	33.762	0.64807	1.3906	4.84E+08
Q15750;Q15750-	Q15750;Q15750-	TGF-beta-activate	TAB1	9	9	504	0	54.874	0.64744	NaN	6.16E+08
Q9UNF1;Q5H909	Q9UNF1;Q5H909	Melanoma-associ	MAGED2	17	15	606	0	250.33	0.64727	1.1333	1.92E+09
J3QQ67;Q07020;	J3QQ67;Q07020;	60S ribosomal pr	RPL18	11	11	190	0	86.939	0.64612	1.8543	8.09E+09
Q6UWP7-3;Q6UV	Q6UWP7-3;Q6UV	Lysocardiolipin a	LCLAT1	3	3	376	0	7.1474	0.64543	1.2992	9.90E+07
Q05209;H0YC15;	Q05209;H0YC15;	Tyrosine-protein	PTPN12	2	2	780	0	7.0448	0.6453	NaN	3.95E+07
Q9HCC0-2;Q9HC	Q9HCC0-2;Q9HC	Methylcrotonoyl-	MCCC2	4	4	525	0	18.051	0.64377	NaN	8.92E+07
A0A0U1RR27;Q7;	A0A0U1RR27;Q7;	C-myc promoter-l	DENND4A	4	4	1916	0	18.018	0.64373	2.9762	2.10E+08
Q9Y2S7;B4DEM9	Q9Y2S7;B4DEM9	Polymerase delta	POLDIP2	3	3	368	0	9.1433	0.64356	NaN	1.72E+08
Q9BYG3;C9J6C5;(	Q9BYG3;C9J6C5;(	MKI67 FHA doma	NIFK	6	6	293	0	60.69	0.64226	2.2244	7.89E+08
Q92522	Q92522	Histone H1x	H1FX	5	5	213	0	21.614	0.64104	2.3067	8.96E+08
Q9Y3A4	Q9Y3A4	Ribosomal RNA-p	RRP7A	3	3	280	0	7.1722	0.64098	0.94107	1.37E+08

P49711;P49711-	P49711	Transcriptional re	CTCF	5	5	727	0	101.28	0.64079	1.6502	3.63E+08
P51812;B1AXG1;	P51812;B1AXG1	Ribosomal protei	RPS6KA3	3	2	740	0	10.338	0.63971	1.6096	2.78E+08
Q9NW13;Q9NW1	Q9NW13;Q9NW1	RNA-binding prot	RBM28	10	10	759	0	38.172	0.63966	1.7276	6.35E+08
Q5QPR4;J3QR29;	Q5QPR4;J3QR29;	Cyclin-dependent	CDK11A;CDK11B;	5	3	746	0	8.0441	0.63955	1.343	1.17E+08
O43390;O43390·	O43390;O43390·	Heterogeneous nu	HNRNPR	18	13	633	0	117.96	0.6392	1.7358	3.17E+09
O60294	O60294	tRNA wybutosine	LCMT2	4	4	686	0	20.716	0.63919	NaN	2.76E+08
E9PPY3;O43159	E9PPY3;O43159	Ribosomal RNA-p	RRP8	3	3	306	0	5.4833	0.63787	NaN	3.48E+07
A0A087X0U3;A0/	A0A087X0U3;A0/	Excitatory amino	SLC1A3	2	2	430	0	16.038	0.63726	NaN	2.18E+08
Q9Y2P8;Q5VZU3;	Q9Y2P8;Q5VZU3	RNA 3-terminal pl	RCL1	11	11	373	0	75.359	0.63684	1.6117	1.41E+09
F8W726;Q14157	F8W726;Q14157	Ubiquitin-associa	UBAP2L	6	6	1079	0	29.696	0.63586	1.3779	3.64E+08
P40926;P40926-	P40926;P40926-	Malate dehydroge	MDH2	6	6	338	0	40.729	0.63534	1.5717	4.91E+08
Q9NP92;A0A087	Q9NP92;A0A087	28S ribosomal pr	MRPS30	6	6	439	0	21.633	0.63456	1.5352	2.85E+08
B9A062;P13995;	B9A062;P13995;	Bifunctional meth	MTHFD2	2	2	222	0	13.333	0.6335	2.1094	6.20E+08
Q14694;Q14694·	Q14694;Q14694·	Ubiquitin carboxy	USP10	10	10	798	0	48.918	0.63316	1.1064	9.80E+08
A0A0A0MRP2;O1	A0A0A0MRP2;O1	Fucose-1-phosph	FPGT;FPGT-TNNI3	2	2	607	0	6.7273	0.63239	NaN	6.98E+07
B4DJV5;Q13610	B4DJV5;Q13610	Periodic tryptoph	PWP1	2	2	439	0	21.337	0.63232	NaN	1.51E+08
P51692;K7EIF9;C	P51692;K7EIF9;C	Signal transducer	STAT5B;STAT5A	2	2	787	0	23.182	0.63219	NaN	6.98E+07
Q9NP97;B1AKR6;	Q9NP97;B1AKR6;	Dynein light chair	DYNLRB1;DYNLRE	4	4	96	0	32.738	0.63183	1.2737	6.17E+08
F8W6I7;P09651-	F8W6I7;P09651-	Heterogeneous nu	HNRNPA1;HNRNF	22	20	307	0	323.31	0.63166	1.6768	1.81E+10
A1L020	A1L020	RNA-binding prot	MEX3A	1	1	520	0.0015649	3.0861	0.63082	NaN	1.55E+07
P50454;E9PR70;I	P50454;E9PR70;I	Serpin H1	SERPINH1	15	15	418	0	201.85	0.63063	1.5622	7.91E+09
P62241;Q5JR95	P62241;Q5JR95	40S ribosomal pr	RPS8	14	14	208	0	160.39	0.62785	2.0073	1.20E+10
Q9NPI6-2;Q9NPI(	Q9NPI6-2;Q9NPI(	mRNA-decapping	DCP1A	6	6	544	0	190.01	0.62646	NaN	6.07E+08
P11940;P11940-	P11940;P11940-	Polyadenylate-bir	PABPC1	23	17	636	0	227.55	0.62608	1.0758	3.77E+09
B5MDF5;P62826	B5MDF5;P62826	GTP-binding nucl	RAN	11	11	233	0	124.22	0.6258	1.3759	4.89E+09
P22626;P22626-	P22626;P22626-	Heterogeneous nu	HNRNPA2B1	25	24	353	0	323.31	0.62567	1.4933	1.15E+10
E9PHS0;O43813;	E9PHS0;O43813;	LanC-like protein	LANCL1	6	6	196	0	28.492	0.62515	1.6301	5.71E+08
C9JQV3;Q8N1F8;	C9JQV3;Q8N1F8	Serine/threonine·	STK11IP	3	3	1088	0	5.8005	0.62474	1.6606	2.67E+07
R9WNI0;A8MQB8	R9WNI0;A8MQB8	Fragile X mental r	FMR1	3	2	544	0	14.247	0.62394	NaN	2.50E+07
P04406;P04406-	P04406;P04406-	Glyceraldehyde-3	GAPDH	20	20	335	0	273.45	0.62359	1.6522	1.39E+10
P10644;K7EPB2;I	P10644;K7EPB2;I	cAMP-dependent	PRKAR1A	6	6	381	0	38.605	0.62359	1.1313	2.57E+08
G5E9V4;Q969F9-	G5E9V4;Q969F9-	Hermansky-Pudla	HPS3	3	3	839	0	7.6572	0.6234	1.7497	1.55E+08
Q8IWF6	Q8IWF6	Protein DENND6A	DENND6A	2	2	608	0	7.9039	0.6232	NaN	5.24E+07
A0A0A0MRK1;E9I	A0A0A0MRK1;E9I	G patch domain-c	GPATCH4	2	2	370	0	18.241	0.62298	NaN	7.73E+07
O75369-2;O7536	O75369-2;O7536	Filamin-B	FLNB	56	48	2578	0	323.31	0.62218	1.4843	4.96E+09
O00151	O00151	PDZ and LIM dom	PDLIM1	3	3	329	0	19.681	0.6211	0.7027	1.30E+08
B8ZZJ0;B9A032;E	B8ZZJ0;B9A032;E	Small ubiquitin-re	SUMO1	1	1	58	0	3.7341	0.6198	1.26	1.17E+08
P18124;A8MUD9	P18124;A8MUD9	60S ribosomal pr	RPL7	18	18	248	0	103.62	0.6191	1.8472	1.25E+10
A0A0B4J203;Q6L	A0A0B4J203;Q6L	Pre-mRNA 3-end-p	FIP1L1	4	4	849	0	55.831	0.61852	NaN	2.10E+08
Q8IWA0	Q8IWA0	WD repeat-contai	WDR75	12	12	830	0	128.61	0.61842	1.5685	2.51E+09
Q5MNZ6;I3L4L8;I	Q5MNZ6	WD repeat domai	WDR45B	3	3	344	0	7.3	0.61816	NaN	2.15E+08
P07195;C9J7H8;/	P07195;C9J7H8;/	L-lactate dehydro	LDHB	10	10	334	0	85.398	0.61812	0.87835	4.99E+09
P62899;H7C2W9	P62899;H7C2W9	60S ribosomal pr	RPL31	11	11	125	0	57.999	0.61777	2.0015	2.25E+09
J3QS48;I3L295;J:	J3QS48;I3L295;J:	Mannose-P-dolicl	MPDU1;HBEBP2E	2	2	101	0	4.9211	0.61751	1.0932	1.03E+08
P25789;H0YN18;	P25789;H0YN18;	Proteasome subu	PSMA4	7	7	261	0	24.352	0.61705	1.0293	1.91E+09
Q9HCN8	Q9HCN8	Stromal cell-deriv	SDF2L1	3	3	221	0	23.196	0.61692	1.4231	4.99E+08
Q9UII4;E9PBL0	Q9UII4	E3 ISG15--protein	HERC5	5	5	1024	0	18.211	0.61668	0.90439	1.68E+08
F5GZ90;Q9NZJ0-;	F5GZ90;Q9NZJ0-;	Denticleless prote	DTL	2	2	688	0	5.0652	0.61663	NaN	4.36E+06
Q9UBS4;H7C2Y5	Q9UBS4	DnaJ homolog sul	DNAJB11	5	5	358	0	24.934	0.61627	1.9804	9.78E+08
K7EJU3;K7EN86;(	K7EJU3;K7EN86;(	Protein unc-119 h	UNC119;UNC119	1	1	125	0.0051954	2.3158	0.61609	0.90377	1.03E+08
F5H5U2;Q8NHQ9	F5H5U2;Q8NHQ9	ATP-dependent RI	DDX55	2	2	569	0	54.093	0.61538	NaN	8.34E+07
Q7Z7F7;Q7Z7F7-;	Q7Z7F7;Q7Z7F7-;	39S ribosomal pr	MRPL55	2	2	128	0	4.5797	0.61298	NaN	6.96E+07
K7ENI6;K7ERE1;C	K7ENI6;K7ERE1;C	Transmembrane p	TMEM256	3	3	41	0	7.7385	0.61179	1.2725	4.44E+08
P61513;C9J4Z3;(	P61513;C9J4Z3;(	60S ribosomal pr	RPL37A	6	6	92	0	60.243	0.6102	0.50088	3.77E+09
J3KNN7;Q7Z569;	J3KNN7;Q7Z569;	BRCA1-associated	BRAP	2	2	562	0.00026695	3.5184	0.61	NaN	3.52E+07
Q5JR04;Q9HCE1;	Q5JR04;Q9HCE1;	Putative helicase	MOV10	10	10	947	0	82.183	0.6086	1.8331	5.87E+08
P63092-3;P6309	P63092-3;P6309	Guanine nucleoti	GNAS	10	9	379	0	37.773	0.60681	1.4846	1.17E+09
Q9NYP9	Q9NYP9	Protein Mis18-alp	MIS18A	2	2	233	0	25.912	0.60619	0.37567	3.50E+08
Q9NZJ9-2;Q9NZJ	Q9NZJ9-2;Q9NZJ	Diphosphoinositc	NUDT4	3	2	181	0	12.677	0.60614	1.7481	2.16E+10
P47914;F8WF43;	P47914	60S ribosomal pr	RPL29	4	4	159	0	9.2263	0.60608	1.998	8.90E+07
Q8WVX9;E9PNW	Q8WVX9;E9PNW	Fatty acyl-CoA rec	FAR1	14	14	515	0	56.629	0.60469	1.3772	1.53E+09
R4GMR5;P48556	R4GMR5;P48556	26S proteasome r	PSMD8	5	5	287	0	21.344	0.60409	1.1343	2.40E+08
A2AE48;Q12899;	A2AE48;Q12899;	Tripartite motif-c	TRIM26	2	2	248	0	5.445	0.60393	NaN	3.67E+07
O00567;H0YDU4	O00567	Nucleolar protein	NOP56	25	25	594	0	213.44	0.60204	2.2633	4.56E+09
Q8TEM1;Q8TEM1	Q8TEM1;Q8TEM1	Nuclear pore mem	NUP210	30	30	1887	0	238.58	0.60193	1.5591	2.86E+09
P07305;P07305-	P07305;P07305-	Histone H1.0;Hist	H1F0	4	4	194	0	14.323	0.60084	1.9388	1.17E+08
Q9NQ50	Q9NQ50	39S ribosomal pr	MRPL40	2	2	206	0	5.654	0.60076	1.7597	1.73E+08
P30480;P30460;	P30480;P30460;	HLA class I histoc	HLA-B;HLA-C;HLA	4	0	362	0	27.23	0.60067	0.88666	3.48E+08
Q8NBF2;Q8NBF2·	Q8NBF2;Q8NBF2·	NHL repeat-conta	NHLRC2	4	4	726	0	19.332	0.59921	1.0342	1.76E+08
F5GZS6;J3KPF3;P	F5GZS6;J3KPF3;P	4F2 cell-surface a	SLC3A2	22	22	599	0	308.14	0.59838	1.8208	1.17E+10
Q96H55;Q96H55	Q96H55;Q96H55	Unconventional r	MYO19	4	4	970	0	10.913	0.5978	2.5895	1.75E+08
A0A087WV73;P4	A0A087WV73;P4	Probable 28S rRN	NOP2	21	21	855	0	95.683	0.59668	1.6943	3.74E+09
Q9Y3D6	Q9Y3D6	Mitochondrial fis	FIS1	3	3	152	0	16.275	0.59483	1.5824	1.12E+08
C9J7X6;A4D1U4	C9J7X6;A4D1U4	Protein LCHN	KIAA1147;LCHN	2	2	351	0	6.4511	0.59475	NaN	3.81E+07
Q8IY81	Q8IY81	pre-rRNA processi	FTSJ3	2	2	847	0	6.3885	0.59468	2.7209	1.83E+08
Q969Z0;C9J7P5;(	Q969Z0;C9J7P5;(	Protein TBRG4	TBRG4	7	7	631	0	30.901	0.5943	NaN	3.41E+08
Q6P1L8	Q6P1L8	39S ribosomal pr	MRPL14	3	3	145	0	21.16	0.59366	1.1685	2.35E+08
Q96KP4;Q96KP4·	Q96KP4;Q96KP4·	Cytosolic non-spe	CNDP2	9	8	475	0	33.157	0.58982	2.7823	7.70E+08
D6RD24;Q7Z6J8;	D6RD24;Q7Z6J8;	E3 ubiquitin-prot	UBE3D	2	2	284	0	15.537	0.5898	0.79481	1.05E+08
P36578;H3BM89	P36578;H3BM89	60S ribosomal pr	RPL4	25	25	427	0	234.93	0.58787	2.5945	2.02E+10
Q04637-5;Q0463	Q04637-5;Q0463	Eukaryotic transl	EIF4G1	23	23	1435	0	113.84	0.58722	1.3526	1.50E+09
Q15393;Q15393·	Q15393	Splicing factor 3B	SF3B3	35	35	1217	0	323.31	0.5856	1.6718	1.09E+10
P51571;A6NLM8	P51571;A6NLM8	Translocon-associ	SSR4	7	7	173	0	50.023	0.58509	1.6016	2.84E+09
A0A087WT84;Q9	A0A087WT84;Q9	JmjC domain-con	JMJD4	3	3	417	0	15.102	0.58366	1.5917	1.71E+08
Q96ER9;C9JSW8;	Q96ER9;C9JSW8;	Coiled-coil domai	CCDC51	4	4	411	0	13.809	0.58237	0.63573	2.69E+07
A0A024R4E5;Q0(	A0A024R4E5;Q0(	Vigilin	HDLBP	31	31	1268	0	253.46	0.58111	2.07	2.95E+09
Q9BX68	Q9BX68	Histidine triad nu	HINT2	3	3	163	0	28.296	0.58078	1.7442	1.93E+08
P11802-2;P1180	P11802-2;P1180	Cyclin-dependent	CDK4	3	2	183	0.00401	2.4572	0.58063	1.018	6.68E+07
P40429;M0QYS1;	P40429;M0QYS1;	60S ribosomal pr	RPL13A;RPL13a	10	10	203	0	37.143	0.58026	2.132	3.68E+09
Q9HCU5;B5MC9{	Q9HCU5;B5MC9{	Prolactin regulat	PREB	4	4	417	0	31.933	0.58025	1.0931	1.76E+08
Q8NFQ8	Q8NFQ8	Torsin-1A-interac	TOR1AIP2	2	2	470	0	7.5339	0.57922	NaN	5.59E+07
Q9H8H0;J3QR28	Q9H8H0;J3QR28	Nucleolar protein	NOL11	15	15	719	0	68.94	0.57726	2.0154	1.81E+09
Q9NR31;Q9NR31	Q9NR31;Q9NR31	GTP-binding prot	SAR1A;SAR1B	8	8	198	0	24.531	0.57723	2.3458	1.17E+09
Q9NVP1;H7C452	Q9NVP1	ATP-dependent RI	DDX18	14	14	670	0	48.286	0.5769	2.2431	1.06E+09
Q9H2Y7;U3KQH7	Q9H2Y7;U3KQH7	Zinc finger protei	ZNF106	2	2	1883	0	9.3048	0.57634	NaN	3.10E+07
H0YNU5;P54132	H0YNU5;P54132	Bloom syndrome	BLM	3	3	1286	0	6.2066	0.57631	NaN	9.68E+07
A0A0A0MTB8;Q8	A0A0A0MTB8;Q8	WD repeat-contai	WDR36	12	12	895	0	117.02	0.57588	2.0571	1.24E+09
A0A0U1RQT9;C9J	A0A0U1RQT9;C9J	Synaptophysin-lil	SYPL1	1	1	135	0.0037927	2.6006	0.57587	NaN	1.84E+08
P28838-2;P2883	P28838-2;P2883	Cytosol aminopep	LAP3	8	8	488	0	32.442	0.5738	1.3595	4.09E+08
Q9NX58	Q9NX58	Cell growth-regul	LYAR	6	6	379	0	34	0.57324	2.3155	2.97E+08
Q8IZD4;F5H4R4;I	Q8IZD4;F5H4R4;I	mRNA-decapping	DCP1B	3	3	617	0	9.1251	0.57234	NaN	1.70E+08
Q00059;H7BYN3;	Q00059;H7BYN3;	Transcription fact	TFAM	2	2	246	0	5.9237	0.57199	NaN	8.76E+07
Q08380	Q08380	Galectin-3-bindin	LGALS3BP	2	2	585	0	18.064	0.57041	NaN	5.75E+07
P07237;H7BZ94;	P07237;H7BZ94;	Protein disulfide-	P4HB	16	16	508	0	145.04	0.56864	0.62438	1.53E+09

A0A087WUL2;P4	A0A087WUL2;P4	Proteasome subu	PSMB3	3	3	145	0	18.122	0.56822	1.164	4.29E+08
Q9UBQ0;F8VXU5	Q9UBQ0;F8VXU5	Vacuolar protein	VPS29	6	6	182	0	61.095	0.56799	1.5785	1.78E+09
Q8NFH3;B4E301;	Q8NFH3	Nucleoporin Nup	NUP43	3	3	380	0	23.628	0.56569	1.7198	4.74E+08
P62937;F8WE65;	P62937;F8WE65;	Peptidyl-prolyl ci	PPIA	14	14	165	0	163.62	0.56545	1.343	1.18E+10
O15511;O15511·	O15511;O15511·	Actin-related pro	ARPC5	3	3	151	0	11.768	0.56396	1.8711	4.38E+08
O60493-2;O6049	O60493-2;O6049	Sorting nexin-3	SNX3	4	4	130	0	8.2737	0.5635	1.1479	1.31E+08
P08621;P08621-	P08621;P08621-	U1 small nuclear	SNRNP70	11	11	437	0	32.142	0.56337	NaN	6.73E+08
Q96GM5-2;Q96G	Q96GM5-2;Q96G	SWI/SNF-related	SMARCD1	5	3	474	0	17.034	0.56332	NaN	7.10E+07
Q9Y2X3;H7BZ72;	Q9Y2X3	Nucleolar protein	NOP58	21	21	529	0	287.45	0.56256	2.264	7.57E+09
O95747;C9JIG9;I	O95747;C9JIG9	Serine/threonine-	OXSR1	13	11	527	0	82.379	0.56136	NaN	1.24E+09
P50914;E7EPB3	P50914;E7EPB3	60S ribosomal pr	RPL14	9	9	215	0	35.108	0.56088	2.1281	4.42E+09
P84103-2;P8410	P84103-2;P8410	Serine/arginine-ri	SRSF3	5	4	124	0	36.737	0.55747	1.2692	1.86E+09
P05387;H0YDD8	P05387	60S acidic riboso	RPLP2	8	8	115	0	172.25	0.55726	0.77795	8.66E+09
D6RC52;D6RCB9;	D6RC52;D6RCB9;	H/ACA ribonuclec	NHP2	2	2	132	0	59.524	0.5571	1.6238	2.62E+08
Q15031;E9PHM2	Q15031;E9PHM2	Probable leucine-	LARS2	5	5	903	0	24.412	0.55622	1.4159	9.61E+08
B7Z879;A0A087V	B7Z879;A0A087V	Vacuolar protein	VPS11	6	6	931	0	15.389	0.55587	0.97545	1.93E+08
P62995-3;P6299	P62995-3;P6299	Transformer-2 pr	TRA2B	3	3	188	0	17.511	0.55578	2.2415	3.13E+08
Q9NR09;H7C094	Q9NR09	Baculoviral IAP re	BIRC6	33	32	4857	0	294.47	0.55524	1.5953	2.22E+09
E9PR30;P62861	E9PR30;P62861	40S ribosomal pr	FAU	3	3	98	0	10.178	0.55474	2.142	1.64E+09
A0A087WVD4;Q9	A0A087WVD4;Q9	Arsenite methyltr	AS3MT	6	6	338	0	37.76	0.5541	1.405	8.92E+08
P22087;M0QXL5	P22087;M0QXL5	rRNA 2-O-methylt	FBL	12	11	321	0	99.764	0.55398	1.6267	7.61E+09
Q13247-3;Q1324	Q13247-3;Q1324	Serine/arginine-ri	SRSF6	5	5	335	0	7.9122	0.55378	1.9407	8.59E+07
H3BT71;P38159;	H3BT71;P38159;	RNA-binding mot	RBMX;RBMXL1	11	11	296	0	39.773	0.55118	1.8217	1.29E+09
Q9H9J2	Q9H9J2	39S ribosomal pr	MRPL44	3	3	332	0	8.3403	0.55117	NaN	9.78E+07
O60832;O60832·	O60832;O60832·	H/ACA ribonuclec	DKC1	14	14	514	0	122.25	0.551	3.5834	1.11E+09
F8VX04;Q9H2H9	F8VX04;Q9H2H9	Sodium-coupled	SLC38A1	2	2	503	0.00078802	3.2108	0.55054	NaN	5.06E+07
P19338;H7BY16;	P19338;H7BY16	Nucleolin	NCL	40	40	710	0	323.31	0.55052	2.3569	3.13E+10
H3BPE7;P35637-	H3BPE7;P35637-	RNA-binding prot	FUS	2	2	527	0	5.5338	0.54896	NaN	8.81E+07
O96013-2;O9601	O96013-2;O9601	Serine/threonine-	PAK4	3	3	426	0	30.234	0.54871	NaN	1.27E+08
E9PF16;Q96CM8·	E9PF16;Q96CM8·	Acyl-CoA synthet	ACSF2	3	3	572	0	23.537	0.54773	NaN	1.33E+08
P63261;I3L3I0;I3	P63261;I3L3I0;I3	Actin, cytoplasmi	ACTG1	22	1	375	0	323.31	0.54637	1.636	5.71E+10
Q16763;K7EPJ1;I	Q16763;K7EPJ1	Ubiquitin-conjug	UBE2S	5	5	222	0	24.192	0.54621	1.2182	7.60E+07
H3BSH7;Q969X6;	H3BSH7;Q969X6;	Cirhin	CIRH1A	9	9	700	0	85.766	0.54596	NaN	9.09E+08
Q12834	Q12834	Cell division cycle	CDC20	7	7	499	0	57.392	0.54504	1.124	2.48E+08
P20618	P20618	Proteasome subu	PSMB1	6	6	241	0	36.24	0.54368	1.3385	5.73E+08
P31948;P31948-	P31948;P31948-	Stress-induced-ph	STIP1	15	15	543	0	43.721	0.53925	NaN	4.68E+08
P55011-3;P5501	P55011-3;P5501	Solute carrier fam	SLC12A2	2	2	1196	0	3.8669	0.53924	NaN	8.03E+07
Q13232;H3BPR2;	Q13232	Nucleoside dipho	NME3	8	8	169	0	37.711	0.53831	1.4089	9.74E+08
Q9UMY1;H7C2B1	Q9UMY1;H7C2B1	Nucleolar protein	NOL7	4	4	257	0	9.5681	0.53569	0.57202	3.49E+07
Q15181;Q5SQT6	Q15181;Q5SQT6	Inorganic pyroph	PPA1	10	10	289	0	173	0.53533	2.0605	4.68E+09
Q9NY93-2;Q9NY9	Q9NY93-2;Q9NY9	Probable ATP-dep	DDX56	3	3	507	0	4.8078	0.53533	NaN	2.99E+07
Q99460-2;Q9946	Q99460-2;Q9946	26S proteasome r	PSMD1	39	39	922	0	323.31	0.53406	1.7493	1.33E+10
P54577;A0A0C4I	P54577;A0A0C4I	Tyrosine--tRNA lig	YARS	5	5	528	0	15.666	0.53363	NaN	1.99E+08
A8MV53;A0A0A6	A8MV53;A0A0A6	Suppressor of SW	PPAN	2	2	420	0	3.9078	0.53345	NaN	2.82E+07
Q13823;H0YG10	Q13823	Nucleolar GTP-bir	GNL2	3	3	731	0	12.74	0.53291	2.0665	2.03E+08
P21333-2;P2133	P21333-2;P2133	Filamin-A	FLNA	63	55	2639	0	323.31	0.53201	1.909	5.31E+09
A0A0B4J2E5;Q15	A0A0B4J2E5;Q15	Periodic tryptoph	PWP2	22	18	919	0	168.4	0.53057	1.6815	4.53E+09
A0A024R571;Q9I	A0A024R571;Q9I	EH domain-conta	EHD1	15	8	548	0	95.364	0.52825	NaN	8.21E+08
H3BUV4;Q9NWV	H3BUV4;Q9NWV	Ceroid-lipofuscin	CLN6	4	4	213	0	22.688	0.52716	1.0793	1.38E+09
P53999	P53999	Activated RNA po	SUB1	2	2	127	0	7.2306	0.5253	1.1468	1.96E+08
Q96A35;X6RJ73;:	Q96A35	39S ribosomal pr	MRPL24	5	5	216	0	15.453	0.52501	1.8002	2.75E+08
Q14680-3;Q1468	Q14680-3;Q1468	Maternal embryo	MELK	2	2	457	0	4.9051	0.52278	NaN	1.66E+07
Q8IUI8;Q8IUI8-2;	Q8IUI8;Q8IUI8-2	Cytokine recepto	CRLF3	5	5	442	0	33.121	0.52268	2.0847	2.38E+08
Q15758;M0QXM·	Q15758;M0QXM·	Neutral amino aci	SLC1A5	12	12	541	0	75.775	0.52202	1.2513	2.38E+09
P11021	P11021	78 kDa glucose-re	HSPA5	44	42	654	0	323.31	0.5216	1.739	1.17E+10
Q8NAT1	Q8NAT1	Protein O-linked-I	POMGNT2	2	2	580	0	8.0538	0.51963	NaN	6.46E+07
Q9UHV9	Q9UHV9	Prefoldin subunit	PFDN2	3	3	154	0	20.712	0.51941	1.875	3.80E+08
Q9H307-2;Q9H3(	Q9H307-2;Q9H3(	Pinin	PNN	3	3	584	0	6.9502	0.51767	1.6451	9.33E+07
Q13601;Q13601·	Q13601;Q13601·	KRR1 small subun	KRR1	5	5	381	0	17.824	0.51724	1.6351	2.93E+08
Q02878;F8VZ45;I	Q02878	60S ribosomal pr	RPL6	16	16	288	0	203.79	0.51551	2.4759	5.88E+09
F2Z2V0;B0QZ18;(	F2Z2V0;B0QZ18;(	Copine-1	CPNE1	10	10	533	0	79.012	0.51395	NaN	1.01E+09
X6R700;Q9Y3Y2-;	X6R700;Q9Y3Y2-;	Chromatin target	CHTOP	3	3	223	0	15.365	0.51365	1.2437	9.22E+07
Q96BN8;H0Y9T0	Q96BN8	Ubiquitin thioest	OTULIN	3	3	352	0	9.5717	0.51332	0.57678	1.98E+08
F5H6N1;Q96A72;	F5H6N1;Q96A72	Protein mago nas	MAGOHB	4	1	90	0	21.156	0.51324	1.4025	4.07E+08
B2R4S9;U3KQK0;	B2R4S9;U3KQK0;	Histone H2B;Hist	HIST1H2BC;HIST1	10	0	126	0.0037812	2.563	0.5126	1.7307	1.74E+08
Q71UI9;P0C0S5;(	Q71UI9;P0C0S5;(	Histone H2A.V;Hi	H2AFV;H2AFZ	5	3	128	0	27.273	0.51257	1.4215	1.73E+09
K7ER15;Q9H0R4;	K7ER15;Q9H0R4;	Haloacid dehalog	HDHD2	5	5	204	0	23.51	0.5109	0.78532	4.00E+08
A0A140T9L0;A0A	A0A140T9L0;A0A	WD repeat-contai	WDR46	6	6	322	0	80.618	0.5098	NaN	3.06E+08
K7EN97;Q96S52	K7EN97;Q96S52	GPI transamidase	PIGS	1	1	116	0	3.8005	0.50883	NaN	4.81E+06
P30048-2;P3004	P30048-2;P3004	Thioredoxin-depe	PRDX3	4	4	238	0	11.467	0.50806	2.6507	3.63E+08
Q02809;Q02809·	Q02809;Q02809·	Procollagen-lysin	PLOD1	3	3	727	0	13.474	0.5054	1.6047	2.40E+08
Q01650;A0A0C4I	Q01650	Large neutral ami	SLC7A5	5	5	507	0	16.251	0.50289	1.5976	6.25E+08
Q9Y5S9-2;Q9Y5S	Q9Y5S9-2;Q9Y5S	RNA-binding prot	RBM8A	2	2	173	0	13.394	0.50165	NaN	5.60E+07
Q14684;Q14684·	Q14684;Q14684·	Ribosomal RNA p	RRP1B	5	5	758	0	14.918	0.49955	4.6649	2.64E+08
Q14692	Q14692	Ribosome biogen	BMS1	9	9	1282	0	54.373	0.49909	2.5234	4.90E+08
D6RGE2;Q96CN7	D6RGE2;Q96CN7	Isochorismatase c	ISOC1	2	2	188	0	7.3003	0.49733	2.1113	1.73E+08
Q14964;C9JB90;I	Q14964	Ras-related protei	RAB39A	5	4	217	0	25.957	0.49373	1.401	1.04E+09
Q13162;H7C3T4;	Q13162;H7C3T4	Peroxiredoxin-4	PRDX4	8	5	271	0	23.646	0.49199	1.9381	4.55E+08
Q12986-2;Q1298	Q12986-2;Q1298	Transcriptional re	NFX1	4	4	1024	0	70.5	0.49082	NaN	5.55E+07
Q32Q12;P22392·	Q32Q12;P22392·	Nucleoside dipho	NME1-NME2;NMI	13	5	292	0	71.824	0.48783	1.4241	2.85E+09
Q92759	Q92759	General transcrip	GTF2H4	2	2	462	0	7.4428	0.48535	NaN	1.48E+08
A0A0B4J1R6;P29	A0A0B4J1R6;P29	Transketolase	TKT	5	5	457	0	44.605	0.485	NaN	3.39E+08
P03886	P03886	NADH-ubiquinon	MT-ND1	3	3	318	0	25.723	0.48371	NaN	1.75E+08
Q8TDN6	Q8TDN6	Ribosome biogen	BRIX1	6	6	353	0	38.7	0.48277	2.6365	7.66E+08
K7EK07;Q71DI3;(	K7EK07;Q71DI3;(	Histone H3;Histo	H3F3B;HIST2H3A	6	2	132	0	23.265	0.48196	2.118	1.05E+10
E9PMR6;Q9NZN5	E9PMR6;Q9NZN5	Rho guanine nucl	ARHGEF12	7	7	1441	0	18.33	0.47854	0.64158	2.43E+08
Q9Y366	Q9Y366	Intraflagellar tran	IFT52	4	4	437	0	14.318	0.47546	0.69319	1.37E+08
A0A087WUT6;O6	A0A087WUT6;O6	Eukaryotic transl	EIF5B	7	7	1220	0	61.689	0.47276	1.6642	1.06E+09
P08579	P08579	U2 small nuclear	SNRPB2	4	3	225	0	6.417	0.47275	1.3429	2.93E+08
Q8NC51-4;Q8NC	Q8NC51-4;Q8NC	Plasminogen acti	SERBP1	4	4	387	0	31.56	0.47251	2.7766	5.28E+07
Q06830;A0A0A0I	Q06830;A0A0A0I	Peroxiredoxin-1	PRDX1	12	8	199	0	35.638	0.47224	2.3395	4.59E+09
Q92598-2;Q9259	Q92598-2;Q9259	Heat shock protei	HSPH1	32	29	814	0	287.37	0.47175	2.1273	6.03E+09
Q9Y3B9	Q9Y3B9	RRP15-like protei	RRP15	2	2	282	0	4.6848	0.46954	1.9611	1.69E+08
P17066;P48741	P17066	Heat shock 70 kD	HSPA6	26	13	643	0	50.116	0.46915	1.2571	2.17E+09
Q5TEC6	Q5TEC6	Histone H3	HIST2H3PS2	5	1	136	0.00026759	3.5832	0.46845	2.1454	1.84E+09
Q9H6R0;I3L1L6;(	Q9H6R0	Putative ATP-dep	DHX33	3	3	707	0	7.0445	0.46578	2.0793	2.10E+08
Q9Y3D3;A6ND22	Q9Y3D3;A6ND22	28S ribosomal pr	MRPS16	3	3	137	0	9.6555	0.46282	0.97227	7.40E+08
B7Z6D5;Q96GQ7	B7Z6D5;Q96GQ7	Probable ATP-dep	DDX27	8	8	765	0	27.995	0.46046	2.3707	7.84E+08
O76021;J3QSV6;I	O76021;J3QSV6;I	Ribosomal L1 dor	RSL1D1	15	15	490	0	54.018	0.46039	NaN	1.14E+09
F6S8N6;A0A0A0I	F6S8N6;A0A0A0I	Protein-L-isoaspa	PCMT1	7	7	250	0	43.514	0.45993	0.84006	8.51E+08
Q92793-2;Q9279	Q92793-2;Q9279	CREB-binding pro	CREBBP	14	6	2404	0	134.27	0.45789	0.59051	6.96E+08
P55072;C9JUP7;I	P55072	Transitional endo	VCP	41	41	806	0	323.31	0.45412	2.1296	1.63E+10
Q04323;E9PJ81;I	Q04323;E9PJ81;I	UBX domain-cont	UBXN1	9	9	297	0	148.11	0.4499	1.9049	2.42E+09
Q96E14;I3L2E0	Q96E14;I3L2E0	RecQ-mediated ge	RMI2	2	2	147	0	6.4373	0.44771	NaN	2.36E+08

O75477;B0QZ43	O75477;B0QZ43	Erlin-1	ERLIN1	9	6	346	0	23.355	0.44524	1.8751	3.61E+08
P00374-2;P0037	P00374-2;P0037	Dihydrofolate red	DHFR	2	2	135	0	24.03	0.44406	2.7654	2.37E+08
M0QXH0;Q99757	M0QXH0;Q99757	Thioredoxin, mitc	TXN2	2	2	64	0	9.0202	0.44387	0.76682	2.62E+08
Q15061;C9JEE7;(	Q15061	WD repeat-contai	WDR43	13	13	677	0	78.219	0.43936	1.951	9.55E+08
Q9H7B2;Q5VXN0	Q9H7B2;Q5VXN0	Ribosome produc	RPF2	4	4	306	0	14.652	0.43861	2.7166	2.07E+08
Q13895;F8WBL2	Q13895;F8WBL2	Bystin	BYSL	5	5	437	0	34.013	0.43852	1.6912	1.70E+08
P12277;H0YJG0;I	P12277;H0YJG0	Creatine kinase B-	CKB	5	5	381	0	31.69	0.43837	1.6131	5.01E+08
E9PHY5;O43491-	E9PHY5;O43491-	Band 4.1-like pro	EPB41L2	37	0	935	0.001049	3.1803	0.43744	NaN	7.61E+06
A0A0A6YYA0;Q86	A0A0A6YYA0;Q86	Transmembrane e	TMED7	1	1	188	0.0020645	2.9301	0.43742	NaN	1.39E+08
P38432	P38432	Coilin	COIL	5	5	576	0	15.029	0.43405	NaN	3.06E+08
O43237-2;O4323	O43237-2;O4323	Cytoplasmic dyne	DYNC1LI2	2	2	415	0	35.059	0.42459	NaN	1.52E+08
Q7Z628-2;Q7Z62	Q7Z628-2;Q7Z62	Neuroepithelial c	NET1	2	2	542	0	12.008	0.4218	NaN	3.19E+07
Q9Y281;Q9Y281-	Q9Y281;Q9Y281-	Cofilin-2	CFL2	7	3	166	0	102.37	0.41935	0.6615	2.50E+08
P02786;G3V0E5;	P02786;G3V0E5	Transferrin recept	TFRC	17	17	760	0	85.634	0.4189	2.5975	2.18E+09
G3V4W0;B4DY08	G3V4W0;B4DY08	Heterogeneous nu	HNRNPC	22	2	262	0	174.82	0.41737	1.0097	2.08E+10
P57053	P57053	Histone H2B type	H2BFS	10	1	126	0	65.942	0.41483	1.9694	1.91E+10
P62805	P62805	Histone H4	HIST1H4A	14	14	103	0	106.98	0.41173	2.0334	4.42E+10
Q9P0M6;Q5SQT3	Q9P0M6	Core histone mac	H2AFY2	8	7	372	0	57.323	0.41164	2.2301	1.05E+09
O75367-2;O7536	O75367-2;O7536	Core histone mac	H2AFY	7	6	369	0	118.23	0.40802	2.2277	2.78E+09
H0Y307;Q9H1H9	H0Y307;Q9H1H9	Kinesin-like prote	KIF13A	2	2	889	0.0030418	2.6341	0.40575	NaN	7.21E+07
Q93077;Q7L7L0;	Q93077;Q7L7L0;	Histone H2A type	HIST1H2AC;HIST3	7	2	130	0	146.35	0.40472	2.1258	3.22E+10
P23284	P23284	Peptidyl-prolyl ci	PPIB	2	2	216	0	5.3938	0.40097	2.2106	2.81E+08
A0A087X1A5;O9	A0A087X1A5;O9	Double-stranded	STAU1	7	7	493	0	35.361	0.39461	NaN	4.78E+08
Q8WXX5	Q8WXX5	DnaJ homolog sul	DNAJC9	2	2	260	0	30.751	0.39267	1.4129	2.56E+08
P49773;D6RC06;	P49773;D6RC06;	Histidine triad nu	HINT1	2	2	126	0	31.141	0.38997	2.6223	6.17E+08
Q9UNS1-2;Q9UN	Q9UNS1-2;Q9UN	Protein timeless h	TIMELESS	3	3	1207	0	6.6335	0.38905	NaN	6.94E+07
P09382	P09382	Galectin-1	LGALS1	3	3	135	0	11.429	0.38837	3.2174	3.40E+08
H0Y4R1;P12268;	H0Y4R1;P12268	Inosine-5-monop	IMPDH2	10	9	470	0	43.772	0.38812	2.5699	6.93E+08
Q9HCJ3-2;Q9HCJ	Q9HCJ3-2;Q9HCJ	Ribonucleoprotei	RAVER2	2	2	678	0	12.236	0.3864	NaN	1.04E+08
P62879;C9JXA5;I	P62879;C9JXA5;I	Guanine nucleoti	GNB2;GNB4	10	4	340	0	15.788	0.38404	0.90754	1.75E+09
Q86TB9-4;Q86TB	Q86TB9-4;Q86TB	Protein PAT1 hon	PATL1	8	8	703	0	49.37	0.37322	0.82526	3.45E+08
P00505;P00505-	P00505;P00505-	Aspartate aminot	GOT2	3	3	430	0	11.46	0.3708	3.8837	3.20E+08
A0A087WYS3;H7	A0A087WYS3;H7	Protein kinase C-t	ZMYND8	3	3	1087	0	8.6363	0.36771	NaN	5.81E+07
Q69YN2;Q69YN2	Q69YN2;Q69YN2	CWF19-like prote	CWF19L1	12	12	538	0	83.734	0.36562	NaN	6.62E+08
G3V393;G3V5M2	G3V393;G3V5M2	Purine nucleosid	PNP	2	2	61	0	8.4682	0.36406	2.2774	7.05E+07
P60174-1;P6017	P60174-1;P6017	Triosephosphate i	TPI1	12	12	249	0	99.071	0.36	2.7076	1.02E+09
P18669;P15259;	P18669;P15259;	Phosphoglycerate	PGAM1;PGAM2;P	4	4	254	0	20.07	0.35288	1.8898	1.70E+08
P11166	P11166	Solute carrier fam	SLC2A1	1	1	492	0.004008	2.4512	0.35175	1.4654	4.78E+07
Q04656-5;Q0465	Q04656-5;Q0465	Copper-transport	ATP7A	3	3	1422	0	8.0315	0.3461	1.4106	1.06E+08
J3QRG6;P42771;	J3QRG6;P42771;	Cyclin-dependent	CDKN2A	4	4	138	0	28.755	0.34238	3.8365	9.97E+08
G3V2Q1;P07910;	G3V2Q1;P07910;	Heterogeneous nu	HNRNPC	21	1	305	0	134.09	0.34166	1.6683	7.00E+08
P27797;K7EJB9	P27797;K7EJB9	Calreticulin	CALR	6	6	417	0	22.931	0.3325	1.6712	9.10E+07
Q04864-2;Q0486	Q04864-2;Q0486	Proto-oncogene c	REL	2	2	587	0	7.0672	0.32509	NaN	3.72E+07
F8VYE8;P36873;F	F8VYE8;P36873;F	Serine/threonine	PPP1CC	21	3	304	0	64.566	0.32257	0.79792	2.54E+09
P07355;H0YKS4;I	P07355;H0YKS4;I	Annexin A2;Anne	ANXA2;ANXA2P2	6	6	339	0	37.998	0.31706	3.2557	6.93E+08
M0R0X9;M0QXC	M0R0X9;M0QXC	Interferon regulat	IRF3	2	2	106	0	20.994	0.31516	NaN	2.22E+08
A0A0J9YXP8;A0A	A0A0J9YXP8;A0A	Glucose-6-phosp	GPI	2	2	268	0	5.9754	0.31354	NaN	5.94E+07
Q9UJC3-2;Q9UJC	Q9UJC3-2;Q9UJC	Protein Hook hon	HOOK1	5	5	686	0	34.047	0.31127	0.93112	1.24E+08
P11717	P11717	Cation-independe	IGF2R	2	2	2491	0	3.8964	0.30142	6.3148	6.25E+08
P09661;H0YMA0	P09661;H0YMA0	U2 small nuclear	SNRPA1	25	25	255	0	323.31	0.29551	3.7613	1.87E+10
Q92625;Q92625-	Q92625;Q92625-	Ankyrin repeat an	ANKS1A	6	6	1134	0	18.269	0.29444	0.75749	9.01E+07
Q8IZV5;E5RK48	Q8IZV5;E5RK48	Retinol dehydrog	RDH10	3	3	341	0	4.7014	0.27577	NaN	2.86E+08
A0A024RCR6;A0/	A0A024RCR6;A0/	Large proline-rich	BAT3;BAG6	11	11	1126	0	55.42	0.26208	5.3189	9.70E+08
P32119;A6NIW5;	P32119;A6NIW5	Peroxiredoxin-2	PRDX2	15	14	198	0	75.421	0.26034	3.5967	5.86E+09
O95372;Q5QPQ1	O95372;Q5QPQ1	Acyl-protein thio	LYPLA2	6	6	231	0	40.192	0.25039	0.67836	2.52E+08
M0R116;A0A0A0	M0R116;A0A0A0	Sodium/potassiu	ATP1A3	20	2	983	0	7.7882	0.24613	NaN	7.24E+07
A0A087WYB2;A0	A0A087WYB2;A0	RUN and SH3 dom	RUSC1;DKFZp761	2	2	225	0	6.5812	0.23448	NaN	1.37E+08
P00918;E5RID5;I	P00918;E5RID5;I	Carbonic anhydra	CA2	2	2	260	0	16.315	0.23144	2.6344	3.05E+08
F2Z2K0;Q9UNZ2-	F2Z2K0;Q9UNZ2-	NSFL1 cofactor p4	NSFL1C	2	2	274	0	4.6805	0.2022	4.3483	3.17E+07
P63173;J3KT73;J	P63173;J3KT73;J	60S ribosomal pr	RPL38	8	8	70	0	65.954	0.18922	0.15476	2.37E+10
Q13255-2;Q1325	Q13255-2;Q1325	Metabotropic glu	GRM1	2	2	906	0.0020581	2.8827	0.1045	NaN	1.21E+08
Q8N5U6;Q8N5U6	Q8N5U6;Q8N5U6	RING finger prote	RNF10	3	3	811	0	30.562	0.095838	0.88191	4.61E+09
K7ELU5;Q7Z3V5	K7ELU5;Q7Z3V5	Zinc finger protei	ZNF571	1	1	84	0.0047076	2.3321	0.094262	NaN	8.04E+09
M0QY31;M0R2A2	M0QY31;M0R2A2	Pregnancy-specifi	PSG4;PSG1;PSG3	1	1	244	0.0023095	2.8339	0.0089702	NaN	1.96E+08

6.8. Paper: Shieldin complex promotes DNA end-joining and counters homologous recombination in BRCA1-null cells (2018)

ARTICLES
https://doi.org/10.1038/s41556-018-0140-1
nature cell biology

Shieldin complex promotes DNA end-joining and counters homologous recombination in BRCA1-null cells

Harveer Dev[1,2], Ting-Wei Will Chiang[1,12], Chloe Lescale[3,12], Inge de Krijger[4,12], Alistair G. Martin[5], Domenic Pilger[1], Julia Coates[1], Matylda Sczaniecka-Clift[1], Wenming Wei[3], Matthias Ostermaier[6], Mareike Herzog[1], Jonathan Lam[1], Abigail Shea[5], Mukerrem Demir[1], Qian Wu[7], Fengtang Yang[8], Beiyuan Fu[8], Zhongwu Lai[9], Gabriel Balmus[1,8], Rimma Belotserkovskaya[1], Violeta Serra[10], Mark J. O'Connor[11], Alejandra Bruna[5], Petra Beli[6], Luca Pellegrini[7], Carlos Caldas[5], Ludovic Deriano[3*], Jacqueline J. L. Jacobs[4*], Yaron Galanty[1*] and Stephen P. Jackson[1*]

BRCA1 deficiencies cause breast, ovarian, prostate and other cancers, and render tumours hypersensitive to poly(ADP-ribose) polymerase (PARP) inhibitors. To understand the resistance mechanisms, we conducted whole-genome CRISPR–Cas9 synthetic-viability/resistance screens in BRCA1-deficient breast cancer cells treated with PARP inhibitors. We identified two previously uncharacterized proteins, C20orf196 and FAM35A, whose inactivation confers strong PARP-inhibitor resistance. Mechanistically, we show that C20orf196 and FAM35A form a complex, 'Shieldin' (SHLD1/2), with FAM35A interacting with single-stranded DNA through its C-terminal oligonucleotide/oligosaccharide-binding fold region. We establish that Shieldin acts as the downstream effector of 53BP1/RIF1/MAD2L2 to promote DNA double-strand break (DSB) end-joining by restricting DSB resection and to counteract homologous recombination by antagonizing BRCA2/RAD51 loading in BRCA1-deficient cells. Notably, Shieldin inactivation further sensitizes BRCA1-deficient cells to cisplatin, suggesting how defining the SHLD1/2 status of BRCA1-deficient tumours might aid patient stratification and yield new treatment opportunities. Highlighting this potential, we document reduced SHLD1/2 expression in human breast cancers displaying intrinsic or acquired PARP-inhibitor resistance.

DNA double-strand breaks (DSBs) are highly cytotoxic cellular lesions that must be effectively and accurately repaired to maintain genome stability and prevent premature aging, neurodegeneration, immunodeficiency, cancer and other diseases[1–3]. In response to DSB detection, the apical kinases ATM, ATR and PRKDC (DNA-dependent protein kinase catalytic subunit) become activated and phosphorylate numerous substrates to initiate the cellular DNA damage response (DDR)[4]. The ensuing cascade of molecular DDR events, which are promoted by various post-translational modifications including protein phosphorylation, ubiquitylation, sumoylation and poly (ADP-ribosyl)ation, impacts on a myriad of cellular components, among other things leading to the assembly of DDR factors at DNA-damage sites, arrest or slowing of cell-cycle progression, and activation of DNA repair mechanisms[4,5]. The two main types of DSB-repair pathway are non-homologous end-joining (NHEJ), which is active throughout the cell cycle, and homologous recombination (HR), which normally requires a sister chromatid as a template and hence only operates in the S and G2 phases of the cell cycle. DSB-repair pathway choice is partly determined by functional antagonism between the HR-promoting factor BRCA1 and NHEJ-promoting proteins such as TP53BP1 (53BP1), RIF1 and MAD2L2 (REV7)[6–13].

Inherited or acquired mutations in the *BRCA1* or *BRCA2* genes that result in protein loss or a mutant BRCA1/2 protein cause breast, ovarian, prostate and other cancers, and render tumours hypersensitive to poly(ADP-ribose) polymerase (PARP)-inhibitor drugs such as olaparib[14–17]. Unfortunately, intrinsic or acquired PARP-inhibitor resistance frequently leads to a lack of response or to patient relapse and tumour regrowth[15,18]. In the clinic, the most common PARP-inhibitor resistance mechanisms reported to date are restoration of BRCA1/2 expression or function. Notably, 53BP1 expression is lost in various triple-negative breast cancers[7], which may account for certain clinically relevant examples of PARP-inhibitor resistance. Nevertheless, the mechanisms driving PARP-inhibitor resistance in a large proportion of BRCA1/2-deficient tumours remain unexplained[18,19].

[1]The Wellcome Trust/Cancer Research UK Gurdon Institute and Department of Biochemistry, University of Cambridge, Cambridge, UK. [2]Academic Urology Group, Department of Surgery, Cambridge University Hospitals NHS Foundation Trust, Addenbrooke's Hospital, Cambridge, UK. [3]Genome Integrity, Immunity and Cancer Unit, Department of Immunology, Department of Genomes and Genetics, Institut Pasteur, Paris, France. [4]Division of Oncogenomics, The Netherlands Cancer Institute, Plesmanlaan , Amsterdam, the Netherlands. [5]Department of Oncology and Cancer Research UK Cambridge Institute, Li Ka Shing Centre, University of Cambridge, Cambridge, UK. [6]Institute of Molecular Biology (IMB), Mainz, Germany. [7]Department of Biochemistry, University of Cambridge, Cambridge, UK. [8]Wellcome Trust Sanger Institute, Hinxton, UK. [9]AstraZeneca, Waltham, MA, USA. [10]Vall d'Hebron Institute of Oncology, Barcelona, Spain. [11]AstraZeneca, Cambridge, UK. [12]These authors contributed equally: Ting-Wei Will Chiang, Chloe Lescale, Inge de Krijger. *e-mail: ludovic.deriano@pasteur.fr; j.jacobs@nki.nl; y.galanty@gurdon.cam.ac.uk; s.jackson@gurdon.cam.ac.uk

To systematically survey for genetic mechanisms of PARP-inhibitor resistance, we conducted whole-genome CRISPR–Cas9 synthetic-viability/resistance screens in human BRCA1-deficient breast cancer cells treated with PARP inhibitors. In addition to identifying known resistance factors such as 53BP1, RIF1 and MAD2L2 loss[6–13], we identified two previously uncharacterized proteins, C20orf196 and FAM35A, whose inactivation confers PARP-inhibitor resistance to BRCA1-deficient cells. Our ensuing work led us to define the 'Shieldin' (SHLD1^{C20orf196}/SHLD2^{FAM35A}) complex, which promotes NHEJ by serving as the downstream effector of 53BP1, RIF1 and MAD2L2, restricts DSB resection, and counteracts HR in BRCA1-deficient cells by antagonizing replacement of replication protein A (RPA) with BRCA2 and RAD51 on resected single-stranded DNA (ssDNA). Finally, we report that SHLD1^{C20orf196}/SHLD2^{FAM35A} loss confers hypersensitivity to the DNA-crosslinking agent cisplatin, and that reduced SHLD1^{C20orf196} or SHLD2^{FAM35A} expression is associated with evolution of PARP-inhibitor resistance in a patient-derived BRCA1-deficient breast cancer xenograft model and in BRCA1-mutant cancers displaying intrinsic PARP-inhibitor resistance.

Results

FAM35A or C20orf196 loss suppresses PARP-inhibitor sensitivity of *BRCA1*-mutant cells. To systematically explore genetic mechanisms imparting PARP-inhibitor resistance, we carried out genome-wide CRISPR–Cas9 gene-inactivation screens with the GeCKO library[20] in the *BRCA1*-mutant breast cancer cell line SUM149PT treated in parallel with the PARP inhibitors olaparib, talazoparib (BMN673) or AZD2461 (Fig. 1a,b and Supplementary Fig. 1a–c). In addition to identifying the known resistance genes *TP53BP1*, *RIF1* and *MAD2L2*, whose products form a complex[21], we identified several new suppressor candidates (Supplementary Table 1 and Supplementary Fig. 1d,e). These included DYNLL1, a known 53BP1 interaction partner[22], and TEN1, a component of the CST telomere-capping complex (CTC1/STN1/TEN1) that also promotes telomere DNA replication[23]. In our ensuing studies, however, we focused on the uncharacterized proteins FAM35A and C20orf196, which collectively received the highest scores from our screens (Fig. 1b and Supplementary Table 1). Thus, by carrying out short-interfering RNA (siRNA) mediated mRNA silencing in non-transformed, human telomerase reverse transcriptase-immortalized retinal pigment epithelial 1 (RPE1) cells (Supplementary Fig. 1f), we established that, as for 53BP1 loss[7], depletion of FAM35A or C20orf196 markedly suppressed PARP-inhibitor sensitivity caused by BRCA1 inactivation while having no discernible effect in BRCA1-proficient cells (Fig. 1c and Supplementary Fig. 1g). This conclusion was independently confirmed by de novo CRISPR–Cas9 gene editing, with FAM35A or C20orf196 inactivation alleviating the olaparib hypersensitivity of BRCA1-deficient cells in a manner counteracted by the re-introduction of wild-type FAM35A or C20orf196 (Fig. 1d,e and Supplementary Fig. 1h; as shown in Supplementary Fig. 1i, these effects did not reflect altered cell-cycle profiles).

FAM35A/C20orf196 complex interacts with and acts downstream of 53BP1/RIF1/MAD2L2. Sequence analyses indicated that FAM35A and C20orf196 are well conserved in vertebrates. Moreover, structure prediction modelling (RaptorX; http://raptorx.uchicago.edu/) revealed that FAM35A harbours a disordered N terminus and an ordered C-terminal region containing three oligonucleotide/oligosaccharide-binding (OB) folds, with the last C-terminal OB fold/FAM domain containing a CXXC-type zinc finger motif (Fig. 2a). Notably, this organization is highly similar to those of the RPA1 subunit of ssDNA binding protein RPA and the CTC1 subunit of the CST complex that also binds ssDNA[23]. In this regard, we noted that while the C20orf196 N terminus (residues 1–70) is predicted to be intrinsically disordered, its C-terminal part is more structured and may harbour one- or two-winged helix (WH) domains (Fig. 2a) similar to those in the yeast CST subunit Stn1[23,24], suggesting that C20orf196 and Stn1 might play analogous or complementary roles.

By combining cellular co-localization and co-immunoprecipitation experiments, we established that FAM35A and C20orf196 directly interact in a manner that is mainly, but not exclusively, mediated by the FAM35A OB3/FAM domain (Fig. 2b,c and Supplementary Fig. 2a,b). Because loss of FAM35A or C20orf196 had similar effects to loss of 53BP1/RIF1/MAD2L2 in BRCA1-deficient cells, we tested for possible interactions between these factors. Thus, via co-immunoprecipitation and mass spectrometry (MS) studies, we found that both C20orf196 and FAM35A interact with MAD2L2, the most distal factor of the 53BP1/RIF1/MAD2L2 axis mediating PARP-inhibitor sensitivity in BRCA1-deficient cells[6–13] (Fig. 2d and Supplementary Fig. 2c).

Many DDR proteins accumulate at DSB sites within ionizing radiation (IR)-induced nuclear foci (IRIF)[5]. We established that both FAM35A and C20orf196 formed IRIF, and by live-cell imaging studies found that the proteins were also recruited to localized DNA-damage sites induced by laser micro-irradiation (Supplementary Fig. 2d). Furthermore, we determined by confocal and super-resolution microscopy that FAM35A co-localized with the established DSB markers phosphorylated histone H2AFX[25] (γH2AX) and 53BP1[26] (Fig. 2e,f and Supplementary Fig. 2e). Notably, siRNA/shRNA-depletion experiments established that while 53BP1 IRIF and MAD2L2 levels and IRIF were not significantly impaired by FAM35A or C20orf196 depletion (Supplementary Fig. 2f–h), IRIF formation by FAM35A and C20orf196 required 53BP1, RIF1 and MAD2L2 but not PTIP (Fig. 2e and Supplementary Fig. 3a–c; note that the total levels of green fluorescent protein (GFP)-tagged FAM35A/C20orf196 were minimally affected by 53BP1/RIF1/MAD2L2 depletion). We also established that C20orf196 IRIF were almost totally abrogated by FAM35A depletion, while C20orf196 depletion reduced but did not abolish FAM35A IRIF (Fig. 2e). In addition, FAM35A formed nuclear foci when cells were treated with the DNA topoisomerase I inhibitor camptothecin (CPT; Supplementary Fig. 3d). Significantly, the FAM35A N terminus was necessary and sufficient for its IRIF formation; these IRIF depended on 53BP1, RIF1, MAD2L2 and C20orf196, and this region could be co-immunoprecipitated with MAD2L2 (Fig. 2f,g and Supplementary Fig. 3e,f). Collectively, these findings indicated that FAM35A and C20orf196 act as downstream components of 53BP1/RIF1/MAD2L2 molecular assembly[21] at DSB sites.

FAM35A and C20orf196 promote NHEJ. As 53BP1, RIF1 and MAD2L2 promote NHEJ[6–13], we tested whether FAM35A and C20orf196 fulfil a similar role. Indeed, as for depletion of the NHEJ factor XRCC4, siRNA depletion of 53BP1, FAM35A or C20orf196 impaired NHEJ, as measured by random integration of plasmid DNA into chromosomes[27] (Fig. 3a). In addition, FAM35A or C20orf196 depletion conferred IR hypersensitivity to both human and mouse cells (Fig. 3b and Supplementary Fig. 4a). 53BP1 and associated factors promote NHEJ-mediated class-switch recombination (CSR) at the immunoglobulin heavy-chain locus, a process that allows B lymphocytes to change antibody production from one type to another[28]. By CRISPR–Cas9 gene editing in mouse CH12F3 (CH12) B lymphocytes[29], we established that, as for 53BP1/RIF1/MAD2L2 inactivation[6,8,10–12,30,31], loss of FAM35A or C20orf196 markedly reduced CSR (Fig. 3c,d and Supplementary Fig. 4b–d). Furthermore, analysis of metaphase chromosomal spreads of such cells revealed that FAM35A or C20orf196 inactivation led to chromosomal breaks and translocations symptomatic of aberrant CSR[32] (Fig. 3e,f; note from Supplementary Fig. 4e,f that CSR effects were not associated with defects in cell proliferation, or in Aid or germline Sα switch region transcription).

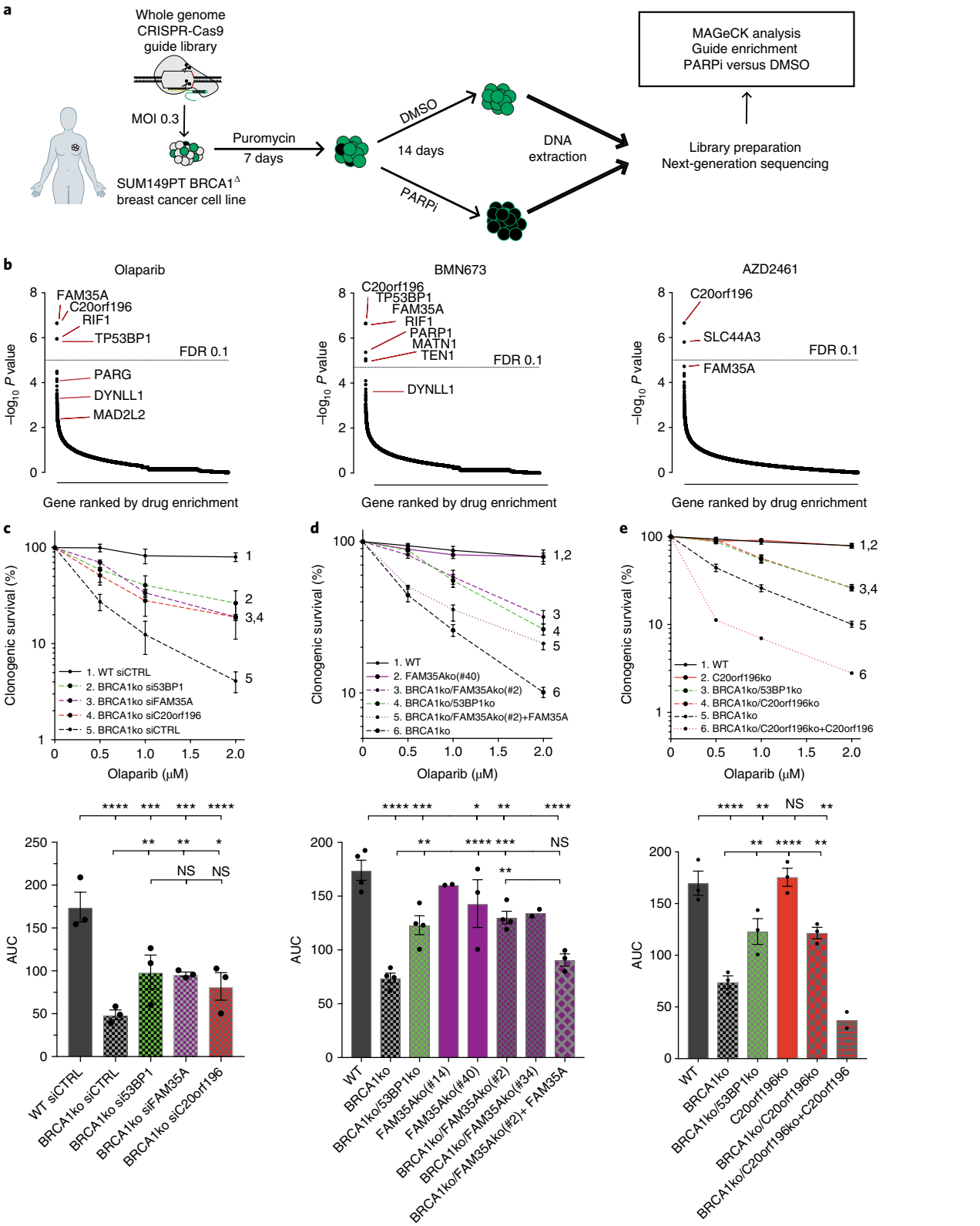

Fig. 1 | CRISPR–Cas9 screens identify suppressors of PARP-inhibitor sensitivity in *BRCA1*-mutant cells. a, Schematic of screen procedure. MOI, multiplicity of infection; PARPi, PARP-inhibitor. **b**, MAGeCK analysis of guide enrichments following specified drug treatments; false discovery rate (FDR) of 0.1 indicated by dotted line; $n=3$ technical replicates per drug treatment. **c**, siRNA-mediated verification of hits in clonogenic survival assays; lower panels show area under the curve (AUC); $n=3$ independent experiments. **d**, De novo Cas9-mediated knockout (ko) verification and complementation for FAM35A in clonogenic survival assays (multiple ko clones are shown in AUC); $n=4$ independent experiments except FAM35Ako(#14) ($n=2$), FAM35Ako(#40) ($n=3$), BRCA1ko/FAM35Ako(#34) ($n=2$) and BRCA1ko/FAM35Ako(#2) + FAM35A ($n=3$). **e**, As in **d** but for C20orf196; $n=3$ independent experiments except BRCA1ko/C20orf196ko + C20orf196 ($n=2$). In **c**–**e**, bars represent mean ± s.e.m., one-way analysis of variance (ANOVA); $^{*}P<0.05$, $^{**}P<0.01$, $^{***}P<0.001$, $^{****}P<0.0001$, NS, not significant ($P\geq0.05$). Individual data points are plotted over bars, and statistical source data including the precise P values are provided in Supplementary Table 5.

FAM35A and C20orf196 antagonize DNA-end resection. To explore FAM35A and C20orf196 function further, we carried out assays in mouse cells harbouring a temperature-sensitive allele of the telomere-associated factor TRF2 (TRF2ts). TRF2ts inactivation at higher temperatures results in deprotected chromosome ends and causes NHEJ-mediated telomere fusions (Fig. 4a)[6,33]. Strikingly, through the use of short-hairpin RNA (shRNA) mediated mRNA silencing, we found that such chromosome fusions were diminished by FAM35A or C20orf196 depletion, like that elicited by MAD2L2 depletion (Fig. 4b and Supplementary Fig. 5a,b).

The impacts of 53BP1, RIF1 or MAD2L2 depletion in the TRF2ts system are connected to these factors counteracting DSB resection[6–13,34]. We thus explored whether FAM35A and C20orf196 might also have this function. Indeed, as for 53BP1/RIF1/MAD2L2 inactivation[6–13,35], loss of FAM35A or C20orf196 in human cells enhanced DSB-resection, as measured by RPA and ssDNA staining intensity in pre-extracted nuclei after treatment with CPT (Fig. 4c–e; RPA1 kinetics at DNA damage sites induced by laser micro-irradiation were not altered by FAM35A or C20orf196 depletion, Supplementary Fig. 5c). In line with this resection being mediated by canonical pathways, it was diminished by depletion of the resection promoting factors RBBP8 (CtIP) or BLM (bloom syndrome RecQ-like helicase, Fig. 4f). Furthermore, we established that recruitment of BLM to sites of laser micro-irradiation was enhanced by FAM35A or C20orf196 depletion (Fig. 4g). Similarly, as shown for 53BP1 depletion in mouse cells[6], FAM35A or C20orf196 depletion in such cells led to higher levels of the DNA-end resection marker, Ser4/8 phosphorylated RPA2, after IR treatment (Fig. 4d). Together with our other findings, these data established FAM35A and C20orf196 as crucial components of 53BP1/RIF1/MAD2L2-mediated chromosomal NHEJ, and suggested that their pro-NHEJ function is connected to limiting DSB resection.

FAM35A OB fold region interacts with ssDNA and promotes IR survival. Consistent with our prediction of structural similarity between FAM35A and RPA1, the FAM35A C terminus could be retrieved from cell extracts via interaction with a ssDNA oligonucleotide (Fig. 5a). Sequence alignment to RPA1 and structural modelling of FAM35A identified two Trp (W) residues predicted to be at the protein–ssDNA interface, based on analogous residues critical for RPA binding to ssDNA (Fig. 5b and Supplementary Fig. 5d). In accord with this prediction, we found, via electrophoretic gel-mobility shift assays (EMSAs), that the bacterially expressed, purified FAM35A C-terminal region bound preferentially to ssDNA rather than double-stranded DNA (Fig. 5c and Supplementary Fig. 5e), and ssDNA binding was reduced when the two Trp residues were mutated to Ala (W489/W640A; Fig. 5c). Furthermore, while full-length FAM35A bearing these mutations (FAM35A$^{W489/W640A}$) still interacted with C20orf196 (Supplementary Fig. 5f) and formed IRIF in cells, these IRIF were consistently less pronounced than those of the wild-type FAM35A protein (Fig. 5d). This suggested that, following IRIF recruitment via its N-terminal region, the FAM35A C-terminal ssDNA binding region may allow further FAM35A recruitment, retention and/or stabilization. In addition, unlike the wild-type protein, FAM35A$^{W489/W640A}$ did not confer significant IR resistance when reintroduced into FAM35A null cells (Fig. 5e). In parallel studies, expression of the FAM35A C terminus did not complement the IR hypersensitivity of FAM35A null cells. Moreover, expression of the FAM35A N terminus rendered cells IR-hypersensitive, irrespective of whether they expressed endogenous FAM35A, implying that the N-terminal IRIF-forming domain of FAM35A may have a dominant-negative effect on NHEJ (Fig. 5f; overexpression of these FAM35A derivatives did not affect olaparib sensitivity in a wild-type background, Supplementary Fig. 5g).

FAM35A and C20orf196 antagonize HR in BRCA1-deficient cells. PARP inhibitors generate replication-associated DNA lesions that require BRCA1-mediated HR for their effective repair[19], and loss of 53BP1/RIF1/MAD2L2 partly restores the ability of BRCA1-deficient cells to repair such lesions[6–13]. This has led to a model in which BRCA1 and 53BP1/RIF1/MAD2L2 play antagonistic roles in channelling DSBs towards HR or NHEJ, respectively. We thus speculated that BRCA1 might antagonize FAM35A/C20orf196 action. Accordingly, both FAM35A and C20orf196 IRIF, but not 53BP1 IRIF, were significantly enhanced in number and intensity following BRCA1 but not BRCA2 depletion (Fig. 6a,b and Supplementary Fig. 6a,b).

Collectively, our results suggested that FAM35A/C20orf196 act at the interface between the opposing functions of BRCA1 and 53BP1/RIF1/MAD2L2 to regulate DSB-repair pathway choice. Although this action could operate at least in part through control of DSB resection, which is misregulated and of slower kinetics in BRCA1-deficient cells[11,36], we reasoned that FAM35A/C20orf196 might also contribute to the severe defect in BRCA2-mediated RAD51 loading at DNA-damage sites in BRCA1-deficient cells[11,35,37]. Indeed, as for 53BP1 inactivation, loss of FAM35A or C20orf196 restored RAD51 IRIF formation in *BRCA1*-null cells (Fig. 6c). While exploring the mechanism for this effect, we found that elevated resection levels in FAM35A and C20orf196 knockout cells, as measured by RPA recruitment at DNA-damage sites, were still maintained in the absence of BRCA1 (Supplementary Fig. 6c,d). Furthermore, FAM35A/C20orf196 depletion also alleviated the impaired recruitment of BRCA2 to DNA-damage sites in BRCA1-deficient cells (Fig. 6d and Supplementary Fig. 6e). Accordingly, studies with a cell-based chromosomal traffic light reporter (TLR) HR system[38,39] established that FAM35A or C20orf196 depletion in BRCA1-deficient cells restored HR to levels similar to those acquired following 53BP1 depletion in this setting (Fig. 6e and Supplementary 6f). In addition, removing FAM35A or C20orf196 rescued the spontaneous genomic instability phenotype of BRCA1 knockout cells (Fig. 6f). Building on our findings that the FAM35A N-terminal region largely mediates its localization to IRIF (Fig. 2f and Supplementary Fig. 3e,f), introducing the FAM35A N terminus, but not the C terminus, enhanced PARP-inhibitor sensitivity of BRCA1/FAM35A null cells (Fig. 6g and Supplementary Fig. 6g). Furthermore, FAM35A inactivation was epistatic to 53BP1 inactivation in relation to conferring PARP-inhibitor resistance in BRCA1 knockout cells (Supplementary Fig. 6h). Considering our findings together, we propose that C20orf196 and FAM35A be named SHLD1 and SHLD2, respectively, or collectively as the 'Shieldin complex' because it shields DSBs from inappropriate activities and promotes appropriate modes of DSB repair.

FAM35A/C20orf196 loss correlates with PARP-inhibitor resistance in cancers. Having identified SHLD1^{C20orf196} and SHLD2^{FAM35A} as mediating the PARP-inhibitor sensitivity of a BRCA1-deficient breast cancer cell line, we speculated that this might also apply in more physiological settings. Consequently, we employed a patient-derived xenograft (PDX) model of BRCA1-deficient breast cancer propagated in mice in the presence (cohort 2) or absence (cohort 1) of olaparib (Fig. 7a). The resistant tumour was further serially passaged into new hosts that were treated in the presence (cohort 4) or absence (cohort 3) of olaparib to confirm and sustain drug resistance (Fig. 7a; see also Supplementary Fig. 7a). The tumours were then harvested and subjected to whole-genome RNA-sequencing. Notably, our analyses revealed that in contrast to the other cohorts, nearly all resistant tumours after chronic olaparib treatment (cohort 4) correlated with reduced mRNA expression of SHLD1^{C20orf196}, SHLD2^{FAM35A}, 53BP1 and/or PARP1 (Fig. 7a; each heatmap column represents one tumour/mouse sample).

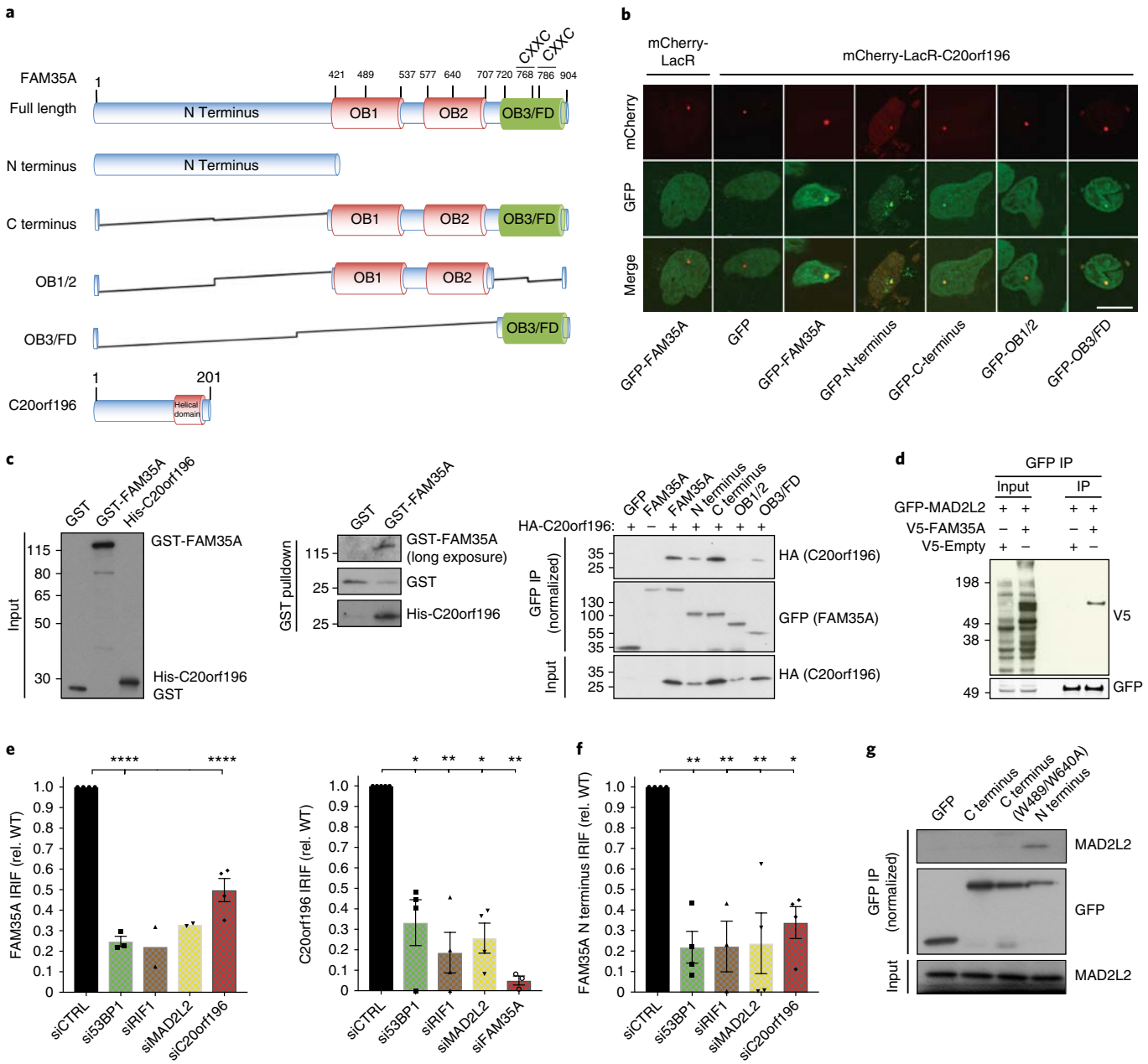

Fig. 2 | FAM35A and C20orf196 domains, interactions and IRIF formation. a, FAM35A and C20orf196 predicted domains and variants used, OB fold (OB) and FAM domain (OB3/FD). **b**, Recruitment of FAM35A/derivatives GFP-fusions to a chromosomal Lac-operator array via mCherry-LacR-C20orf196. Data represent three experiments, with quantifications as shown in Supplementary Fig. 2a. Scale bar, 10 µm. **c**, Left and middle, Purified recombinant GST-FAM35A directly interacts with recombinant His-C20orf196. Right, Cell extracts expressing GFP-FAM35A/derivatives and HA-C20orf196 analysed by co-immunoprecipitation and immunoblotting. **d**, V5-FAM35A co-immunoprecipitates with GFP-MAD2L2; the interaction with C20orf196 is shown in Supplementary Fig. 2c. **e**, Quantification of inducible GFP-FAM35A (left) and GFP-C20orf196 (right) IRIF in γH2AX-positive cells 5 h after IR (5 Gy) treated with indicated siRNAs. $n=4$ independent experiments except (left) si53BP1 ($n=3$), siRIF1 and siMAD2L2 ($n=2$) and (right) siCTRL ($n=5$), siRIF1($n=3$) and siFAM35A ($n=3$). **f**, As in **e** but for inducible GFP-FAM35A N terminus; $n=4$ independent experiments except siRIF1 ($n=3$). **g**, Endogenous MAD2L2 co-immunoprecipitates with GFP-FAM35A N terminus. In **e**,**f**, bars represent mean ± s.e.m. (relative to wild type), one-way ANOVA; $^{*}P<0.05$, $^{**}P<0.01$, $^{****}P<0.0001$; NS, not significant ($P\geq0.05$); individual data points plotted over bars. Statistical source data including precise P values are shown in Supplementary Table 5. All immunoblots are representative of two independent experiments; unprocessed scans of immunoblots are shown in Supplementary Fig. 8.

Because this tumour model is polyclonal[40], our data suggested that olaparib resistance mechanisms might arise through parallel evolutionary trajectories converging on loss of Shieldin activity. Furthermore, when we stratified a cohort of BRCA1-deficient PDX tumours by SHLD1/2 expression, ensuing analyses indicated that low SHLD1^{C20orf196} transcript levels correlated with intrinsic olaparib resistance (Fig. 7b). One of the olaparib-resistant models (PDX127) demonstrated concomitant loss of both SHLD1^{C20orf196} and SHLD2^{FAM35A}, while two other resistant models exhibiting normal SHLD1/2 transcript levels harboured deleterious 53BP1 mutations. Notably, several of these resistant PDX models also display BRCA1 nuclear foci[41], suggesting the presence of multiple mechanisms of resistance, due to tumour heterogeneity and/or mechanistic cooperation.

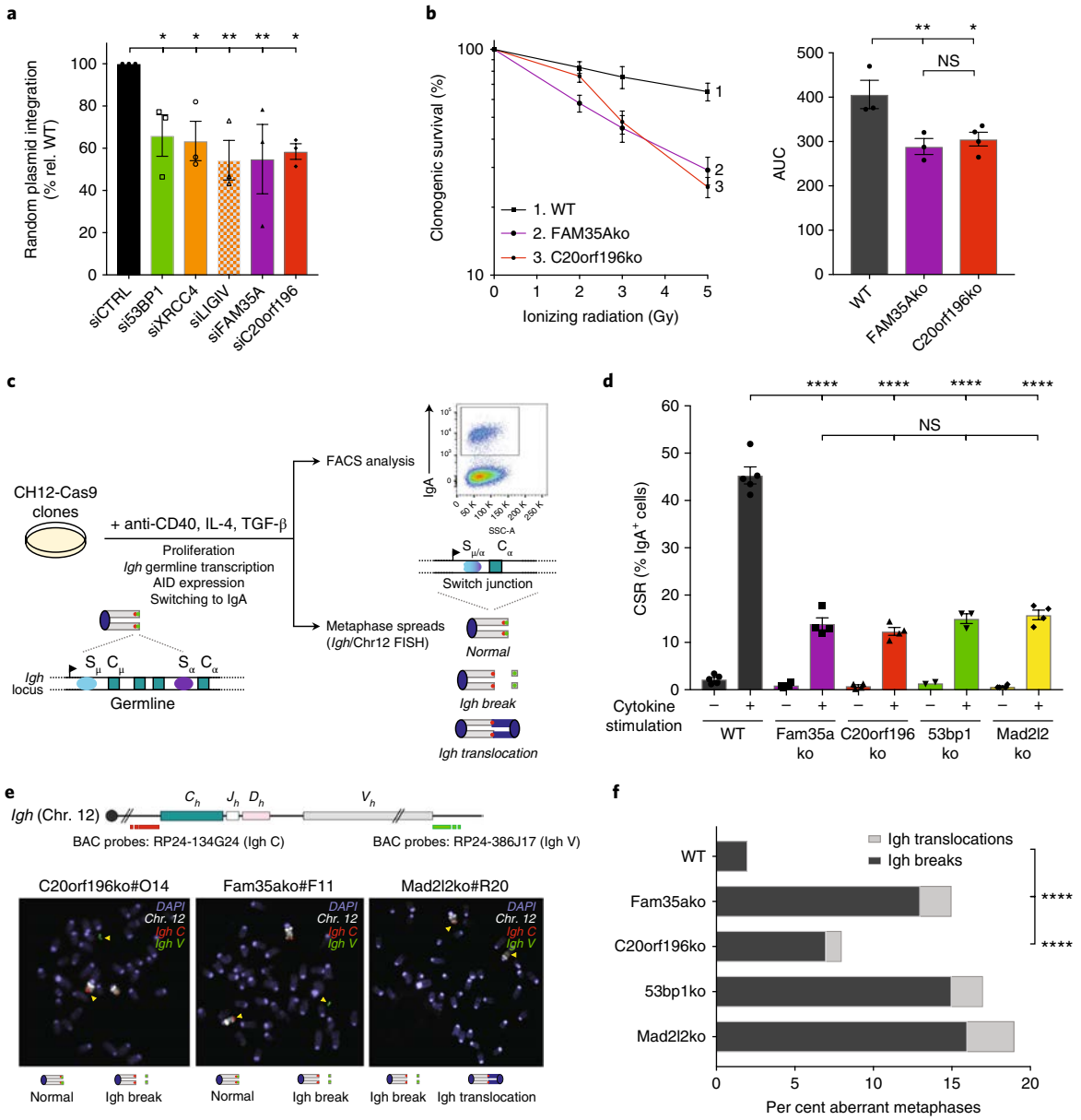

Fig. 3 | FAM35A and C20orf196 promote NHEJ and immunoglobulin CSR. a, Random plasmid integration assay. **b**, FAM35Ako and C20orf196ko cells were treated with IR and analysed for clonogenic survival. Right, AUC. In **a**,**b**, Bars represent mean ± s.e.m., one-way ANOVA; $n = 3$ independent experiments, except C20orf196ko in **b** ($n = 4$), with individual data points plotted over bars; statistical source data are provided in Supplementary Table 5. **c**, Schematic representation of CSR and chromosomal instability in murine IgM$^+$ B cells (germline configuration with C_μ transcription) induced to express AID and undergo CSR to IgA (switch configuration with C_α transcription) on addition of anti-CD40, interleukin-4 (IL-4) and transforming growth factor beta (TGF-β). CSR levels were measured as percent of IgA-positive cells after 72 h cytokine stimulation, and DNA fluorescence in situ hybridization (FISH) was performed using a chromosome 12-specific paint (grey chromosome) and *Igh* locus-specific probes (red and green spots) for the measurement of chromosomal instability at the *Igh* locus on induction of CSR. **d**, CSR levels in Fam35Ako and C20orf196ko CH12-Cas9 cells are reduced compared with wild-type (WT) CH12-Cas9 cells. Bars represent mean ± s.e.m., one-way ANOVA. $n = 4$ independent experiments of three clones except 53bp1ko + cytokine where $n = 3$ of two clones, and 53bp1ko-cytokine where $n = 2$ of two clones; individual data points are plotted over bars. **e**, Representative images of *Igh* translocation and breaks in aberrant metaphases, as quantified in **f**. **f**, Quantification of *Igh* breaks and translocations in metaphases of the indicated CH12-Cas9 cells. Horizontal bars represent means, Fisher's exact test; $n = 2$ independent experiments except Fam35ako and C20orf196ko where $n = 3$. For **a**, **b**, **d** and **f**, $^*P < 0.05$, $^{**}P < 0.01$, $^{****}P < 0.0001$; NS, not significant ($P \geq 0.05$); statistical source data including precise *P* values are provided in Supplementary Table 5.

Finally, we found that in contrast to 53BP1 deficiency[42], SHLD1^{C20orf196} or SHLD2^{FAM35A} loss increased the sensitivity of BRCA1-proficient and BRCA1-null cells to IR, and even more markedly enhanced their sensitivity to the DNA crosslinking agent cisplatin (Fig. 7c,d and Supplementary Fig. 7b,c). Furthermore, enhanced cisplatin sensitivity following SHLD1^{C20orf196} or SHLD2^{FAM35A} inactivation was associated with increased DNA-damage focus formation by the FANCD2 protein that is involved in the detection and repair of DNA crosslinks (Fig. 7e and Supplementary Fig. 7d). These findings therefore suggested that, if loss/reduced expression of SHLD1/2 occurs in patients, it may provide collateral therapeutic vulnerabilities that could be exploited clinically.

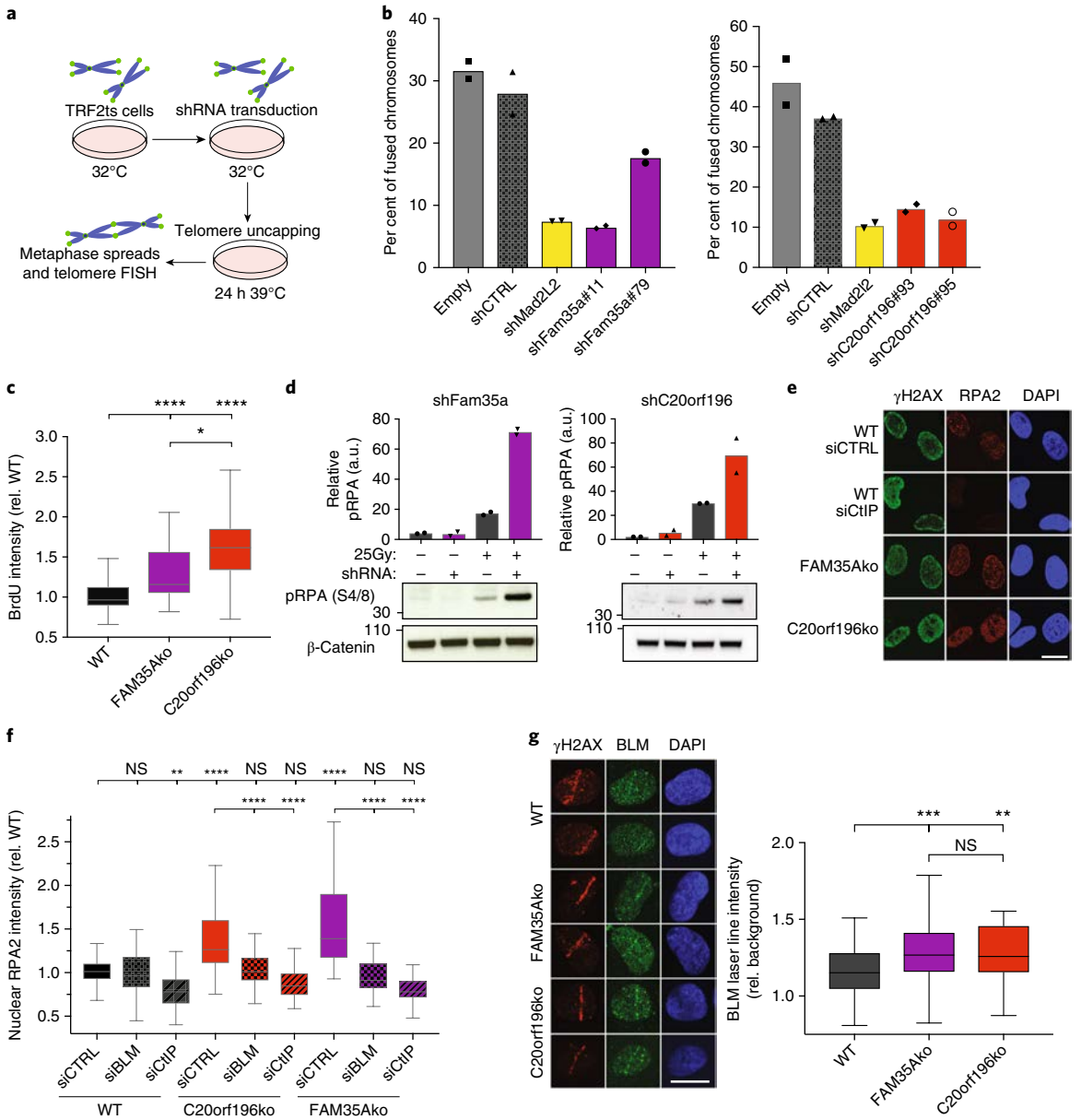

Fig. 4 | FAM35A and C20orf196 promote telomere-mediated fusions and limit DNA-end resection. a, Schematic of TRF2ts experimental set-up. **b**, shRNA depletion of FAM35A (left) or C20orf196 (right) reduces uncapped telomere-mediated chromosome fusions. Bars represent means. Experiments were performed twice with ≥1,300 chromosomes counted per condition, and individual data points are plotted over bars; source data are provided in Supplementary Table 5. **c**, FAM35Ako and C20orf196ko RPE1 cells labelled with BrdU (10 μM) for 48 h then treated with 1 μM camptothecin (CPT) for 1 h, pre-extracted, fixed and stained for BrdU under non-denaturing conditions to visualize ssDNA. Box and whisker plot with centre line at median, box limits at 25th/75th centiles and whiskers ±1.5× interquartile range (IQR); one-way ANOVA; $n = 3$ independent experiments. **d**, IR-induced pRPA(S4/8) is enhanced in MEFs due to Fam35a or C20orf196 silencing. Bars represent means. Experiments were performed twice. Individual data points are plotted over bars; source data are provided in Supplementary Table 5. **e**, RPE1-FAM35Ako or -C20orf196ko cells display hyper DNA-end resection (cells treated with 1 μM CPT for 1 h). Representative images from three independent experiments. Scale bar, 10 μm. **f**, RPE1-FAM35Ako or -C20orf196ko cells display BLM- and CtIP-dependent markers of excessive DNA-end resection. Box and whisker plot with centre line at median, box limits at 25th/75th centiles and whiskers ±1.5× IQR; one-way ANOVA; $n = 3$ independent experiments. **g**, Enhanced BLM accrual in FAM35Ako and C20orf196ko compared with wild-type (WT) RPE1 cells fixed and stained 2 h after laser micro-irradiation. Left, Representative images. Right, Quantification. Scale bar, 10 μm. Box and whisker plot with centre line at median, box limits at 25th/75th centiles and whiskers ±1.5× IQR; one-way ANOVA; $n = 3$ independent experiments. a.u., arbitrary units. For **c**, **f** and **g**, $^{*}P < 0.05$, $^{**}P < 0.01$, $^{***}P < 0.001$, $^{****}P < 0.0001$; NS, not significant ($P \geq 0.05$); statistical source data including precise P values are provided in Supplementary Table 5.

Discussion

Over the past two decades, it has become evident that eukaryotic cells have evolved multiple mechanisms of DNA DSB repair that are regulated in complex and sophisticated ways to optimize genome stability. In particular, much attention has focused on how cells strategically employ the two prime modes of DSB repair—NHEJ and HR—which antagonize one another, operate optimally in different contexts and whose relative usage is regulated by factors such as chromatin structure and cell-cycle stage. In addition to being of academic interest, work on such subjects is also of clinical relevance,

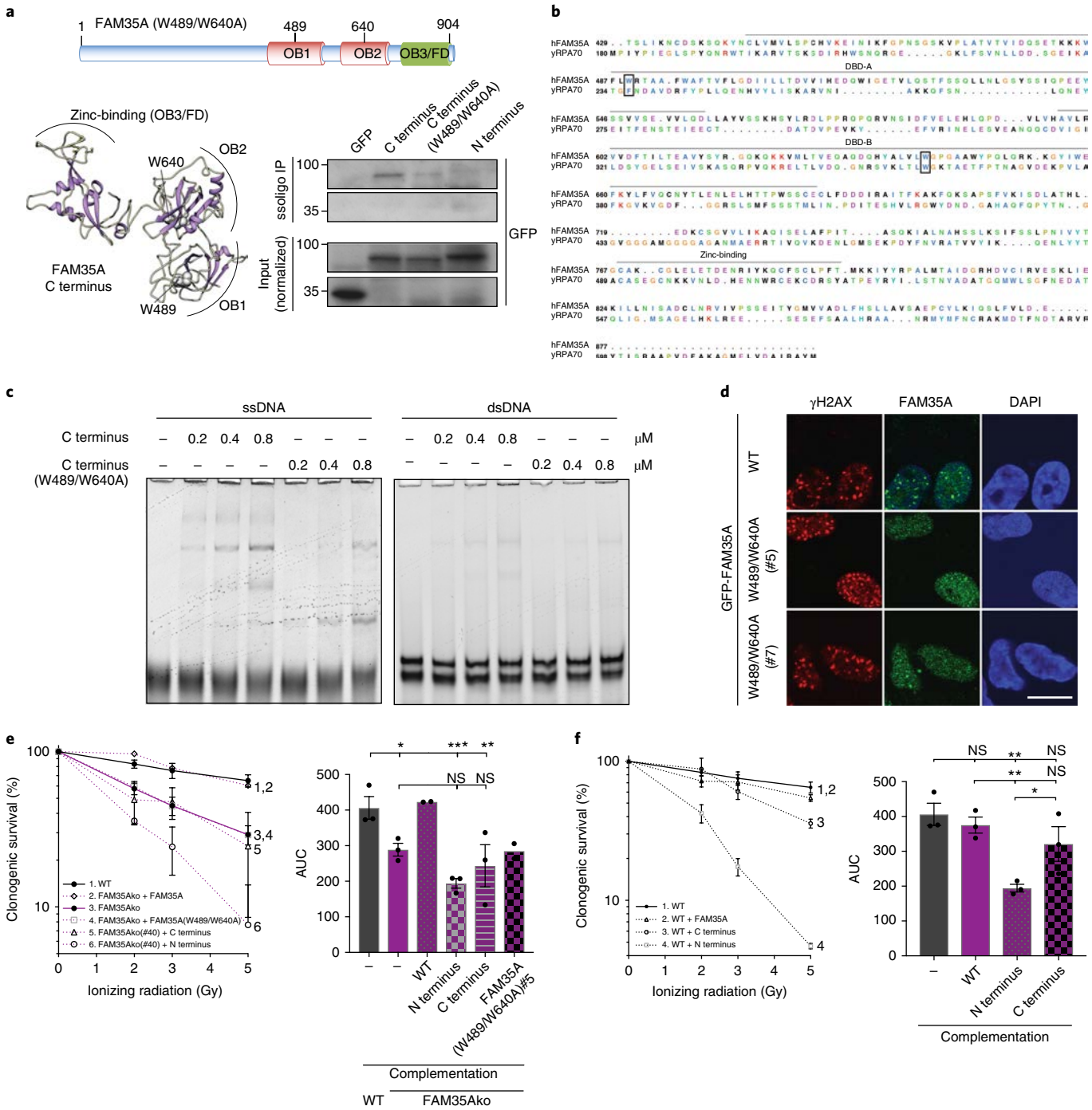

Fig. 5 | FAM35A OB folds mediate ssDNA interaction and are required for IR resistance. a, Schematic of FAM35A with residues W489/W640 mutated to A (top). Predicted 3D structure of wild-type FAM35A with W489 and W640 positions (lower left). FAM35A W489/W640 promote efficient ssDNA binding in cellular extracts (lower right). **b**, Alignment of yRPA1 with FAM35A C terminus; amino acids critical for yRPA1 ssDNA binding and the corresponding amino acid residues in FAM35A are boxed. **c**, EMSAs on native (non-denaturing) gels with 10 nM ssDNA or dsDNA, and the indicated purified, bacterially expressed FAM35A C terminus or W489/W640A mutant (in μM). **d**, Inducible GFP-FAM35A W489/W640A fails to efficiently form IRIF (12 h after 5 Gy of IR). Scale bar, 10 μm. Representative images from three independent experiments. **e**, FAM35Ako RPE1 cells complemented with FAM35A derivatives in clonogenic survival assays. Right, AUC. **f**, Overexpression of FAM35A N terminus but not the C terminus or full-length FAM35A sensitizes wild-type cells to IR in clonogenic assays. Right, AUC. In **e**,**f**, bars represent mean ± s.e.m., one-way ANOVA; $^{*}P < 0.05$, $^{**}P < 0.01$, $^{***}P < 0.001$; NS, not significant ($P \geq 0.05$); $n = 3$ independent experiments except Groups 2 and 4 in **e** ($n = 2$). Individual data points are plotted over bars; statistical source data including precise P values are provided in Supplementary Table 5. All immunoblots are representative of two independent experiments; unprocessed scans of immunoblots are shown in Supplementary Fig. 8.

particularly in cancer therapy where DSB-inducing chemotherapeutic agents are frequently used, and molecularly targeted drugs such as PARP inhibitors are being increasingly employed in specific settings. Intrinsic or arising PARP-inhibitor resistance in patients with *BRCA1/2* mutations is nevertheless an increasing clinical problem. Using whole-genome CRISPR–Cas9 synthetic-viability/

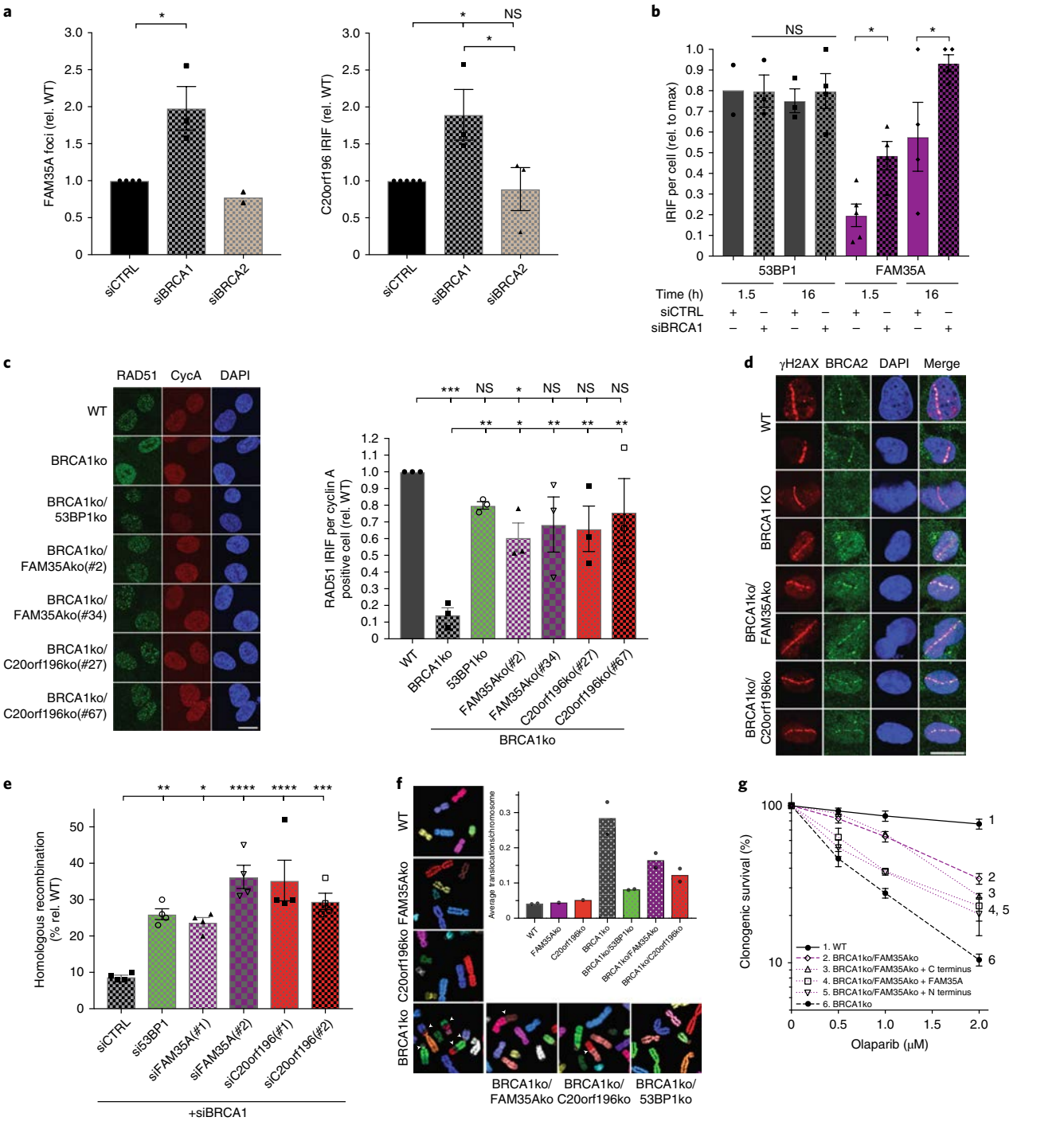

Fig. 6 | FAM35A or C20orf196 loss restores HR in BRCA1-deficient cells. a, Quantification of GFP-FAM35A (left) and GFP-C20orf196 (right) IRIF in U2OS cells after BRCA1 or BRCA2 depletion (5 h after 5 Gy). Bars represent mean ± s.e.m., one-way ANOVA; $n = 3$ independent experiments, except FAM35A siCTRL ($n = 4$), FAM35A siBRCA2 ($n = 2$) and C20orf196 siCTRL ($n = 5$). Individual data points are plotted over bars. **b**, Quantification of 53BP1 and inducible GFP-FAM35A IRIF in U2OS cells with or without BRCA1 depletion (5 Gy, indicated time points). Bars represent mean ± s.e.m., one-way ANOVA; $n = 4$ independent experiments, except 53BP1, 1.5 h siCTRL ($n = 2$); 53BP1, 1.5 h siBRCA1 and 53BP1, 16 h siCTRL ($n = 3$); FAM35A, 1.5 h siCTRL ($n = 5$). Individual data points are plotted over bars. **c**, Representative images (left) and quantification (right) of RAD51 IRIF (5.5 h after 5 Gy) in Cyclin A (CycA) positive RPE1ko cell lines as indicated. Bars represent mean ± s.e.m., one-way ANOVA; $n = 3$ independent experiments. Individual data points are plotted over bars. Scale bar, 10 μm. **d**, FAM35A/C20orf196 loss restore BRCA2 recruitment 2 h after laser-induced DNA-damage sites in *BRCA1*-null cells (for quantification see Supplementary Fig. 6e). Scale bar, 10 μm. **e**, HR assay in U2OS-TLR cells treated with indicated siRNAs (for gating strategy see Supplementary Fig. 6f). Bars represent mean ± s.e.m., one-way ANOVA; $n = 4$ independent experiments. Individual data points are plotted over bars. **f**, Formation of spontaneous chromosomal aberrations in BRCA1ko cells is alleviated by FAM35A/C20orf196 inactivation. Representative images of metaphase spreads are shown and quantified; bars represent means, $n = 2$ independent experiments except FAM35Ako and C20orf196ko ($n = 1$). Individual data points are plotted over bars. **g**, Olaparib clonogenic survival assay with indicated RPE1ko and complemented cell lines. Bars represent mean ± s.e.m., one-way ANOVA; $n = 4$ independent experiments, except Groups 4 and 5 ($n = 3$) and Group 3 ($n = 2$); AUC is shown in Supplementary Fig. 6g. For **a**–**c**,**e**, $^{*}P < 0.05$, $^{**}P < 0.01$, $^{***}P < 0.001$, $^{****}P < 0.0001$; NS, not significant ($P \geq 0.05$); statistical source data including precise P values are provided in Supplementary Table 5.

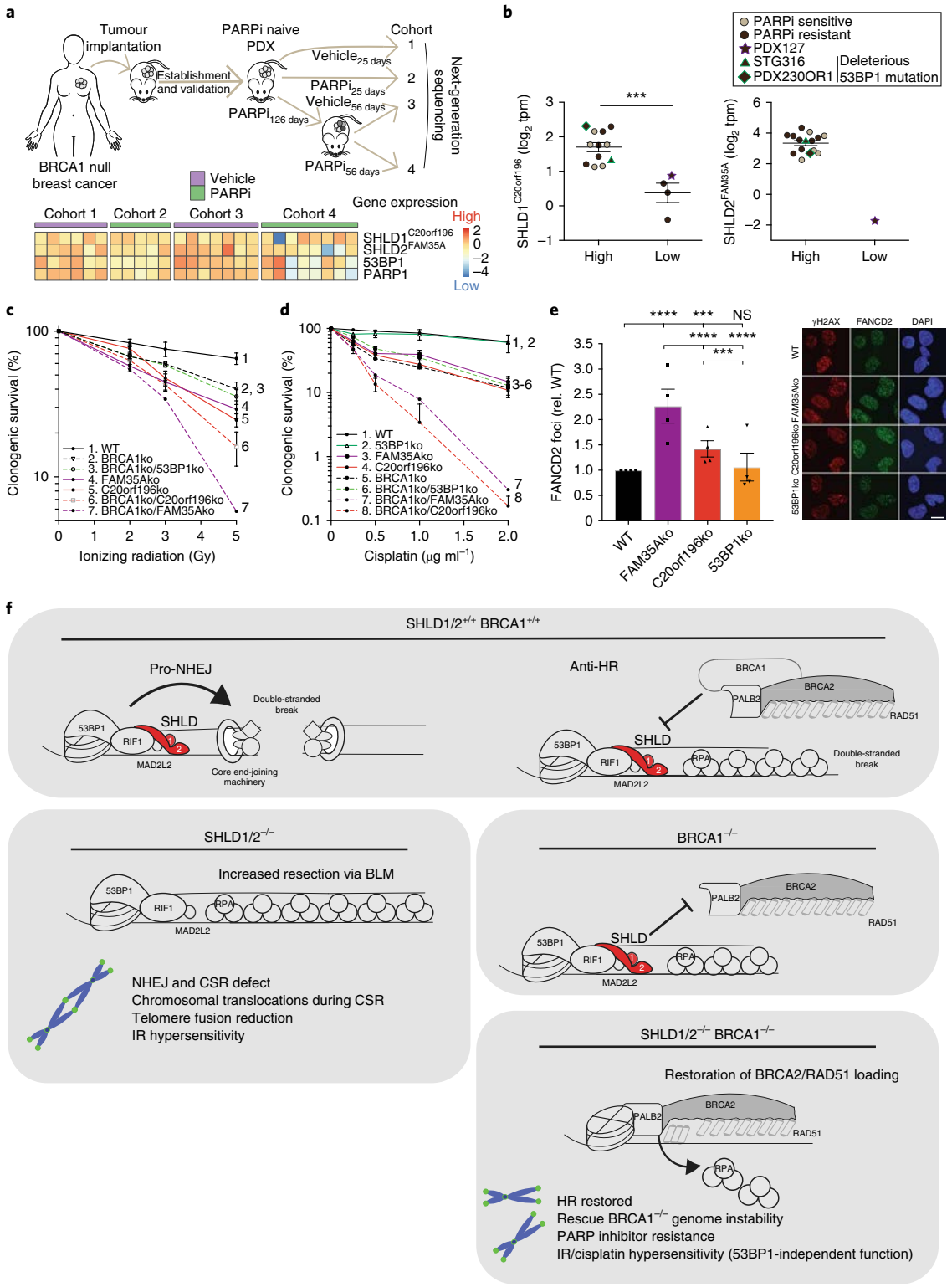

Fig. 7 | FAM35A or C20orf196 loss correlates with PARP-inhibitor resistance in cancers. a, Top, Schematic of in vivo PDX study. Bottom, Heatmap generated from mRNA sequencing showing scaled expression levels of indicated genes from corresponding PDX samples; $n = 6, 5, 7, 8$ mice for cohorts 1–4, respectively. **b**, Expression of C20orf196/FAM35A in breast and ovarian cancer PDXs derived from BRCA1-deficient tumours. *y* axis: $\log_2$ transcript per million (tpm). Lines represent mean ± s.e.m.; $n = 12, 4, 15, 1$ for SHLD1-high, SHLD1-low, SHLD2-high, SHLD2-low groups, respectively; two-tailed unpaired Student's *t*-test; ***$P = 0.0003$. Statistical source data for PDXs are provided in Supplementary Table 5 and the Methods. **c**,**d**, Clonogenic survival assay after IR (**c**) or cisplatin treatment (**d**) in the indicated RPE1ko cell lines (AUC shown in Supplementary Fig. 7b,c, respectively). Data shown represent mean ± s.e.m. ($n = 3$ independent experiments except for Group 7 in **c** and Group 7 in **d** where $n = 2$). **e**, Loss of FAM35A/C20orf196 leads to increased cisplatin-induced FANCD2 foci. Bars represent mean ± s.e.m., one-way ANOVA; ***$P < 0.001$, ****$P < 0.0001$; NS, not significant ($P \geq 0.05$); $n = 4$ independent experiments, with individual data points plotted over bars; statistical source data are provided in Supplementary Table 5. Scale bar, 10 μm. **f**, Proposed model for the action of SHLD1/2 in DSB repair in the presence or absence of functional BRCA1.

resistance screens, we have uncovered two, previously uncharacterized proteins—SHLD1^{C20orf196} and SHLD2^{FAM35A}—whose loss mediates PARP-inhibitor resistance and which we have shown act as the most distal factors of the 53BP1/RIF1/MAD2L2 molecular axis to promote NHEJ and restrict HR in BRCA1-deficient settings. Our screens have also identified additional candidate PARP-inhibitor resistance factors that await validation in future studies.

Mechanistically, we have shown that SHLD1^{C20orf196} and SHLD2^{FAM35A} form a complex, termed 'Shieldin', with SHLD1^{C20orf196} recruitment to DNA-damage sites via its interactions with SHLD2^{FAM35A} and other factors, and SHLD2^{FAM35A} interacting with single-stranded DNA via its C-terminal OB fold region. Moreover, we have established that SHLD1^{C20orf196} and SHLD2^{FAM35A} promote NHEJ in a manner that may be mediated via their effects on restricting DNA-end resection, and serve as a barrier to HR by antagonizing the replacement of RPA with BRCA2/RAD51 on resected ssDNA in a manner counteracted by BRCA1. Our work is in line with a recent report[43] that independently identified SHLD1^{C20orf196} and SHLD2^{FAM35A} as NHEJ-promoting factors and antagonists of HR in BRCA1-defective cells. This study also identified a third component, RINN1/SHLD3$^{CTC-534A2.2}$, which is proposed to serve as a molecular bridge from RIF1 to MAD2L2 and SHLD1/2.

Although it seems possible that Shieldin loss contributes to HR restoration in BRCA1-deficient cells through effects on both resection and BRCA2/RAD51 loading, the relative importance of these mechanisms needs further investigation. We note that more extensive and possibly faster resection in the absence of Shieldin might enhance BRCA2/RAD51 loading. Alternatively, or in addition, Shieldin might serve as a physical barrier to BRCA2/RAD51 loading at dsDNA/ssDNA junctions in BRCA1-deficient cells—perhaps through it being tethered to DSB-flanking chromatin via the 53BP1/RIF1/MAD2L2 complex allowing interactions between the C terminus of distal SHLD2^{FAM35A} and ssDNA (see Fig. 7f for a model and Supplementary Fig. 7e for SHLD2^{FAM35A} domain function summary). Nevertheless, we found that overexpression of the SHLD2^{FAM35A} N terminus but not the C terminus confers olaparib hypersensitivity to *BRCA1/FAM35A* double knockout cells, suggesting that at least in this context, chromatin binding by SHLD2^{FAM35A} plays a dominant role in restricting HR. By contrast, we found that both the SHLD2^{FAM35A} N and C termini are important for IR resistance (in BRCA1-proficient cells). As IR sensitivity in Shieldin-deficient cells probably reflects impaired NHEJ, we speculate that Shieldin potentiates NHEJ by restricting DSB resection as well as by assembling with other NHEJ-promoting factors to tether DSB ends together to facilitate their juxtaposition and repair.

Notably, we have found that SHLD1^{C20orf196} or SHLD2^{FAM35A} inactivation confers enhanced cisplatin sensitivity to BRCA1-null or BRCA1-proficient cells. Such sensitivity probably does not reflect the roles for Shieldin in promoting NHEJ, restricting DNA-end resection or antagonizing BRCA1-mediated BRCA2/RAD51 loading because, in our hands, 53BP1 loss does not have pronounced effects on cisplatin sensitivity. Intra-strand DNA crosslinks (ICLs) generated by cisplatin and other compounds are detected and repaired by the Fanconi anaemia (FA) pathway, with a key FA protein being FANCD2, which forms foci at sites of these lesions[44]. We have observed that, following cisplatin treatment, FANCD2 foci were more pronounced in cells in which SHLD1^{C20orf196} or SHLD2^{FAM35A} was inactivated. It will thus be of interest to determine if Shieldin—like MAD2L2, which (with REV3L) functions as a regulatory subunit of the trans-lesion DNA synthesis (TLS) polymerase Pol zeta, and whose biallelic inactivation has been associated with FA[45–47]—might also promote ICL repair via TLS mechanisms.

Finally, based on our findings, it will be interesting to evaluate SHLD1/2 expression in tumour biopsies from patients, establish whether this information can be used in patient stratification for PARP-inhibitor therapies, and determine whether SHLD1/2 expression changes arise in patients whose BRCA1-deficient cancers develop resistance after PARP-inhibitor treatment. In this regard, we note that if downregulation of Shieldin components in BRCA1-deficient cancers does confer clinical resistance, this might allow alternative treatments, such as ones based on platinum compounds.

Methods

Methods, including statements of data availability and any associated accession codes and references, are available at https://doi.org/10.1038/s41556-018-0140-1.

Received: 27 April 2018; Accepted: 11 June 2018;
Published online: 18 July 2018

References

1. Goldstein, M. & Kastan, M. B. The DNA damage response: implications for tumor responses to radiation and chemotherapy. *Annu. Rev. Med.* **66**, 129–143 (2015).
2. Jackson, S. P. & Bartek, J. The DNA-damage response in human biology and disease. *Nature* **461**, 1071–1078 (2009).
3. Schwertman, P., Bekker-Jensen, S. & Mailand, N. Regulation of DNA double-strand break repair by ubiquitin and ubiquitin-like modifie s. *Nat. Rev. Mol. Cell Biol.* **17**, 379–394 (2016).
4. Blackford, A. N. & Jackson, S. P. ATM, ATR, and DNA-PK: the trinity at the heart of the DNA damage response. *Mol. Cell* **66**, 801–817 (2017).
5. Bekker-Jensen, S. & Mailand, N. Assembly and function of DNA double-strand break repair foci in mammalian cells. *DNA Repair (Amst.)* **9**, 1219–1228 (2010).
6. Boersma, V. et al. MAD2L2 controls DNA repair at telomeres and DNA breaks by inhibiting 5′ end resection. *Nature* **521**, 537–540 (2015).
7. Bunting, S. F. et al. 53BP1 inhibits homologous recombination in Brca1-deficie t cells by blocking resection of DNA breaks. *Cell* **141**, 243–254 (2010).
8. Chapman, J. R. et al. RIF1 is essential for 53BP1-dependent nonhomologous end joining and suppression of DNA double-strand break resection. *Mol. Cell* **49**, 858–871 (2013).
9. Daley, J. M. & Sung, P. RIF1 in DNA break repair pathway choice. *Mol. Cell* **49**, 840–841 (2013).
10. Di Virgilio, M. et al. Rif1 prevents resection of DNA breaks and promotes immunoglobulin class switching. *Science* **339**, 711–715 (2013).
11. Escribano-Diaz, C. et al. A cell cycle-dependent regulatory circuit composed of 53BP1-RIF1 and BRCA1-CtIP controls DNA repair pathway choice. *Mol. Cell* **49**, 872–883 (2013).
12. Xu, G. et al. REV7 counteracts DNA double-strand break resection and affects PARP inhibition. *Nature* **521**, 541–544 (2015).
13. Zimmermann, M., Lottersberger, F., Buonomo, S. B., Sfeir, A. & de Lange, T. 53BP1 regulates DSB repair using Rif1 to control 5′ end resection. *Science* **339**, 700–704 (2013).
14. Capoluongo, E. et al. Guidance statement on BRCA1/2 tumor testing in ovarian cancer patients. *Semin. Oncol.* **44**, 187–197 (2017).
15. Lord, C. J. & Ashworth, A. PARP inhibitors: synthetic lethality in the clinic. *Science* **355**, 1152–1158 (2017).
16. Bryant, H. E. et al. Specific killing of BRCA2-deficie t tumours with inhibitors of poly(ADP-ribose) polymerase. *Nature* **434**, 913–917 (2005).
17. Farmer, H. et al. Targeting the DNA repair defect in BRCA mutant cells as a therapeutic strategy. *Nature* **434**, 917–921 (2005).
18. Lord, C. J., & Ashworth, A. Mechanisms of resistance to therapies targeting BRCA-mutant cancers. *Nat. Med.* **19**, 1381–1388 (2013).
19. Basu, B., Sandhu, S. K. & de Bono, J. S. PARP inhibitors: mechanism of action and their potential role in the prevention and treatment of cancer. *Drugs* **72**, 1579–1590 (2012).
20. Shalem, O. et al. Genome-scale CRISPR–Cas9 knockout screening in human cells. *Science* **343**, 84–87 (2014).
21. Simonetta, M. et al. H4K20me2 distinguishes pre-replicative from post-replicative chromatin to appropriately direct DNA repair pathway choice by 53BP1-RIF1-MAD2L2. *Cell Cycle* **17**, 124–136 (2018).
22. Lo, K. W. et al. The 8-kDa dynein light chain binds to p53-binding protein 1 and mediates DNA damage-induced p53 nuclear accumulation. *J. Biol. Chem.* **280**, 8172–8179 (2005).
23. Giraud-Panis, M. J., Teixeira, M. T., Geli, V. & Gilson, E. CST meets shelterin to keep telomeres in check. *Mol. Cell* **39**, 665–676 (2010).
24. Sun, J. et al. Stn1-Ten1 is an Rpa2-Rpa3-like complex at telomeres. *Genes Dev.* **23**, 2900–2914 (2009).
25. Scully, R. & Xie, A. Double strand break repair functions of histone H2AX. *Mutat. Res.* **750**, 5–14 (2013).
26. Kakarougkas, A. & Jeggo, P. A. DNA DSB repair pathway choice: an orchestrated handover mechanism. *Br. J. Radiol.* **87**, 20130685 (2014).

27. Galanty, Y. et al. Mammalian SUMO E3-ligases PIAS1 and PIAS4 promote responses to DNA double-strand breaks. *Nature* **462**, 935–939 (2009).
28. Feldman, S. et al. 53BP1 contributes to *Igh* locus chromatin topology during class switch recombination. *J. Immunol.* **198**, 2434–2444 (2017).
29. Nakamura, M. et al. High frequency class switching of an IgM$^+$ B lymphoma clone CH12F3 to IgA$^+$ cells. *Int Immunol.* **8**, 193–201 (1996).
30. Manis, J. P. et al. 53BP1 links DNA damage-response pathways to immunoglobulin heavy chain class-switch recombination. *Nat. Immunol.* **5**, 481–487 (2004).
31. Ward, I. M. et al. 53BP1 is required for class switch recombination. *J. Cell Biol.* **165**, 459–464 (2004).
32. Lieber, M. R. Mechanisms of human lymphoid chromosomal translocations. *Nat. Rev. Cancer* **16**, 387–398 (2016).
33. Konishi, A. & de Lange, T. Cell cycle control of telomere protection and NHEJ revealed by a ts mutation in the DNA-binding domain of TRF2. *Genes Dev.* **22**, 1221–1230 (2008).
34. Dimitrova, N., Chen, Y. C., Spector, D. L. & de Lange, T. 53BP1 promotes non-homologous end joining of telomeres by increasing chromatin mobility. *Nature* **456**, 524–528 (2008).
35. Ochs, F. et al. 53BP1 fosters fid lity of homology-directed DNA repair. *Nat. Struct. Mol. Biol.* **23**, 714–721 (2016).
36. Cruz-Garcia, A., Lopez-Saavedra, A. & Huertas, P. BRCA1 accelerates CtIP-mediated DNA-end resection. *Cell Rep.* **9**, 451–459 (2014).
37. Gudmundsdottir, K. & Ashworth, A. The roles of BRCA1 and BRCA2 and associated proteins in the maintenance of genomic stability. *Oncogene* **25**, 5864–5874 (2006).
38. Certo, M. T. et al. Tracking genome engineering outcome at individual DNA breakpoints. *Nat. Methods* **8**, 671–676 (2011).
39. Schmidt, C. K. et al. Systematic E2 screening reveals a UBE2D-RNF138-CtIP axis promoting DNA repair. *Nat. Cell Biol.* **17**, 1458–1470 (2015).
40. Bruna, A. et al. A biobank of breast cancer explants with preserved intra-tumor heterogeneity to screen anticancer compounds. *Cell* **167**, 260–274 (2016).
41. Cruz, C. et al. RAD51 foci as a functional biomarker of homologous recombination repair and PARP inhibitor resistance in germline BRCA mutated breast cancer. *Ann. Oncol.* **29**, 1203–1210 (2018).
42. Bunting, S. F. et al. BRCA1 functions independently of homologous recombination in DNA interstrand crosslink repair. *Mol. Cell* **46**, 125–135 (2012).
43. Gupta, R. et al. DNA repair network analysis reveals Shieldin as a key regulator of NHEJ and PARP inhibitor sensitivity. *Cell* **173**, 972–988 (2018).
44. Ceccaldi, R., Sarangi, P. & D'Andrea, A. D. The Fanconi anaemia pathway: new players and new functions. *Nat. Rev. Mol. Cell Biol.* **17**, 337–349 (2016).
45. Makarova, A. V. & Burgers, P. M. Eukaryotic DNA polymerase zeta. *DNA Repair (Amst.)* **29**, 47–55 (2015).
46. Tomida, J. et al. REV7 is essential for DNA damage tolerance via two REV3L binding sites in mammalian DNA polymerase zeta. *Nucleic Acids Res.* **43**, 1000–1011 (2015).
47. Bluteau, D. et al. Biallelic inactivation of REV7 is associated with Fanconi anemia. *J. Clin. Invest.* **126**, 3580–3584 (2016).

Acknowledgements

The authors thank all S.P.J. laboratory members for support and advice, and Cambridge colleagues N. Lawrence for OMX super-resolution microscopy support and R. Butler for help with computational image analyses and programming. The authors also thank S. Selivanova and S. Hough for help with plasmid amplification, sample preparation and tissue culture maintenance, K. Dry for extensive editorial assistance, F. Muñoz-Martinez for assistance with CRISPR–Cas9 knockout generation, L. Radu for assistance with protein purification, C. Lord (Institute of Cancer Research, London) for SUM149PT cells, D. Durocher (University of Toronto, Canada) for U2OS LacSceIII cells, F. Alt (Harvard University, USA) for CH12F3 cells and *53bp1* knockout CH12F3 cell clones, T. Honjo (Kyoto University, Japan) for permission to use the CH12F3 cell line, and J. Serrat in the Jacobs lab for technical assistance. The SPJ lab is largely funded by a Cancer Research UK (CRUK) Program Grant, C6/A18796, and a Wellcome Trust (WT) Investigator Award, 206388/Z/17/Z. Core infrastructure funding was provided by CRUK grant C6946/A24843 and WT grant WT203144. S.P.J. receives a salary from the University of Cambridge. H.D. is funded by WT Clinical Fellowship 206721/Z/17/Z. TWC was supported by a Cambridge International Scholarship. D.P. is funded by Cancer Research UK studentship C6/A21454. The P.B. lab is supported by the Emmy Noether Program (BE 5342/1-1) from the German Research Foundation and a Marie Curie Career Integration Grant from the European Commission (630763). The L.P. lab is funded by the WT (investigator award 104641/Z/14/Z) and the Medical Research Council (project grant MR/N000161/1). The C.C. lab was supported with funding from CRUK. The J.J. lab was supported by the European Research Council grant ERC-StG 311565, The Dutch Cancer Society (KWF) grant KWF 10999, and the Netherlands Organization for Scientific Research (NWO) as part of the National Roadmap Large-scale Research Facilities of the Netherlands, Proteins@Work (project no. 184.032.201 to the Proteomics Facility of the Netherlands Cancer Institute). The L.D. lab is funded by the Institut Pasteur, the Institut National du Cancer (no. PLBIO16-181) and the European Research Council (starting grant agreement no. 310917). W.W. is part of the Pasteur–Paris University (PPU) International PhD program and this project received funding from the CNBG company, China. Q.W. is funded by the Wellcome Trust (200814/Z/16/Z). The V.S. lab work was funded by the Instituto de Salud Carlos III (ISCIII), an initiative of the Spanish Ministry of Economy and Innovation partially supported by European Regional Development FEDER Funds (PI17-01080 to VS), the European Research Area-NET, Transcan-2 (AC15/00063), a non-commercial research agreement with AstraZeneca UK, and structural funds from the Agència de Gestió d'Ajuts Universitaris i de Recerca (AGAUR, 2017 SGR 540) and the Orozco Family. V.S. received a salary and travel support to C.C.'s lab from ISCIII (CP14/00228, MV15/00041) and the FERO Foundation.

Author contributions

T.W.C. and S.P.J. conceived the project and T.W.C. initiated the project by performing the CRISPR–Cas9 screens, with M.H. doing the bioinformatic analyses. L.D. supervised, and C.L. and W.W. performed CSR and *Igh* locus instability experiments. J.J. supervised, and I.K. performed recombinant MAD2L2 co-IPs, MAD2L2 IRIF/IB, pS4/8-RPA2 IB and telomere fusion experiments. M.O. and P.B. performed mass spectrometry. J.C. performed and analysed clonogenic survival experiments and random plasmid integration assay. M.D. and M.S. generated human knockout cell lines and M.S. performed in vitro pulldown experiments. J.L. carried out oligonucleotide interaction studies. D.P. performed end-resection assays. T.W.C. and R.B. generated RPE1 p53ko, RPE1 p53ko/BRCAko and p53ko/BRCA1ko/53BP1ko cell lines. Y.G. and S.P.J. supervised the above. G.B. performed IR survivals in mouse cells, mouse sgRNA cloning, and FISH with F.Y. and B.F. L.P. performed structural analysis and FAM35A modelling. Q.W. performed purification of bacterially expressed recombinant FAM35A proteins and EMSA. A.M., A.S., A.B. and C.C. performed patient-derived xenograft experiments on PARPi-induced resistance. V.S., M.O'C. and Z.L. established, performed, analysed and characterized PDXs in the experiments on intrinsic PARPi resistance. H.D. assisted with many of the above, and devised and performed all other experiments. H.D., Y.G. and S.P.J. wrote the manuscript with input from all others. L.D., J.J., Y.G. and S.P.J. supervised the project.

Competing interests

S.P.J. receives some research funding from AstraZeneca and is a named inventor on patents describing the use of PARP inhibitors in cancer therapy. V.S.'s laboratory receives research funding support from AstraZeneca. M.O. and Z.L. are employees and shareholders of AstraZeneca.

Additional information

Supplementary information is available for this paper at https://doi.org/10.1038/s41556-018-0140-1.

Reprints and permissions information is available at www.nature.com/reprints.

Correspondence and requests for materials should be addressed to L.D. or J.J.L.J. or Y.G. or S.P.J.

Publisher's note: Springer Nature remains neutral with regard to jurisdictional claims in published maps and institutional affiliations.

Methods

CRISPR–Cas9 screen. CRISPR–Cas9 was performed using genome-scale (GeCKO) v2.0[20]. SUM149PT cells were transduced at a multiplicity of infection of 0.3 and 250-fold coverage of the library. Cells were then selected with puromycin for 7 days before treatment with three different PARPi (PARP inhibitor) for a further 14 days. ICs used were Olaparib IC95–2 μM, BMN673 IC95–5 nM, AZD2461 IC70–4 μM. Surviving clones from each condition were collected, and genomic DNA (gDNA) was isolated (Blood & Cell Culture DNA Midi Kit, Qiagen) and subjected to PCR with Illumina-compatible primers, followed by Illumina sequencing. Genes enriched or depleted in the inhibitor-treated samples were determined with software package MAGeCK version 0.5.5 (see commands in the Code availability section).

Cell culture. U2OS, U2OS-derived, HEK293 and HEK293T-LentiX cells were cultured as in ref. [39]. RPE1 p53 null FRT[48] and RPE1 p53 null FRT-derived cells were cultured in F12 (Ham's F12; Sigma-Aldrich) supplemented with 17 ml $NaHCO_3$ 7.5% per 500 ml (Sigma-Aldrich). All media were supplemented with 10% (vol/vol) fetal bovine serum (FBS; BioSera), 100 U ml^{-1} penicillin, 100 μg ml^{-1} streptomycin (Sigma-Aldrich) and 2 mM l -glutamine. SUM149PT cells were cultured in Ham's F12 Nutrient Mixture (ThermoFisher) supplemented with 5% (vol/vol) FBS (BioSera), 10 mM HEPES, 1 μg ml^{-1} hydrocortisone, 5 μg ml^{-1} insulin, and antibiotic as described above. For maintenance and selection of RPE1 FRT p53 null or U20S Trex cells stably expressing GFP or GFP-tagged constructs, 2 μg ml^{-1} blasticidin (Sigma-Aldrich) and 0.5 mg ml^{-1} G418 (Invitrogen) were used. U2OS-TLR were cultured as in ref. [39]. In addition to RPE1 p53 null FRT-derived cells, U20S Trex cells stably expressing inducible constructs were cultured with 1 μg ml^{-1} doxycycline (Sigma-Aldrich) for 24–48 h to induce expression of GFP constructs. All cells were originally obtained from the ATCC cell repository and routinely tested to be mycoplasma free. The U2OS and RPE1 cell lines were recently authenticated using Affymetrix SNP6 copy number analysis. *Trf2*$^{-/-}$;*p53*$^{-/-}$;TRF2(Ile468Ala) MEFs (TRF2ts MEFs) were as described previously[33,49]. CH12F3 (CH12)[29] and CH12-Cas9 cell lines were cultured in RPMI 1640 supplemented with 10% FBS, 100 U ml^{-1} penicillin, 100 μg ml^{-1} streptomycin, 50 μM 2-mercaptoethanol, 1× MEM non-essential amino acids, 1 mM sodium pyruvate and 10 mM HEPES.

Generation of human stable cell lines and knockouts. U2OS Trex or RPE1 p53 null FRT-derived cells stably expressing inducible GFP-tagged constructs were generated by transfection of pcDNA5/FRT/TO-neo containing the GFP-tagged construct and pOG44 (1:4, respectively). Selection began at 48 h using 0.5 mg ml^{-1} G418 (Invitrogen). Knockouts were generated in RPE1 p53 null cells by transfecting an 'All-in-one' plasmid[48]. Single-cell sorting by GFP expression was done using MoFlo (Beckman Coulter). Single clones were expanded, genomic DNA extracted and screened by PCR, TOPO-cloning and sequencing. Validated mouse embryonic stem cell (mESC) knockouts of Fam35a and C20orf196 were obtained from Haplobank (www.haplobank.at).

Plasmids and cloning. See Supplementary Table 3.

siRNA and plasmid transfection. siRNAs were obtained from MWG or IDT and transfected using Lipofectamine RNAiMAX (Invitrogen) according to the manufacturer's protocol. Plasmid transfections were carried out using TransIT-LT1 (Mirus Bio) according to the manufacturer's protocol. For siRNA and DNA co-transfections, plasmids were transfected 8 h after siRNA treatment. See Supplementary Table 4.

Random plasmid integration assay. The assay was performed as described in ref. [27].

DNA-damage induction using chemical agents, ionizing radiation and laser micro-irradiation. These processes were performed as described in ref. [39].

FRAP and association kinetics. FRAP (fluorescence recovery after photobleaching) and association kinetics were performed as described in ref. [50].

TLR assays. The TLR assay and the constructs used herein are described in detail in refs [38,39].

Cell cycle profiling. Cell cycle profiling was performed as described in ref. [39].

Clonogenic survival assays. Survival assays were performed as described in refs [27,39].

Whole cell extracts and immunoblotting. Whole cell extracts and immunoblotting were performed as described in ref. [39]. For detection of phospho-RPA (pS4/S8-RPA2), lysates were prepared by scraping cells in 2× SDS buffer followed by SDS–PAGE using 4–12% Bis-Tris gel (Invitrogen), and immunoblotting was carried out using SuperSignal West Pico PLUS (Thermo Scientific). IRDye800CW- and IRDye680-labelled secondary antibody were used for detection on an Odyssey infrared imager (LI-COR). Quantification of blots was performed using ImageJ. All protein concentrations were determined using a BCA assay (Pierce). All antibodies are listed in Supplementary Table 2.

Immunoprecipitation. All immunoprecipitation procedures were performed twice as described in ref. [39]. For the co-immunoprecipitation shown in Fig. 2d (FAM35A), 293T cells were co-transfected with pMSCV-blas-eGFP-MAD2L2 and either pLX304-blast-V5-Empty or pLX304-V5-FAM35A. At 72 h post-transfection, cells were exposed to 25 Gy IR followed by 3 h recovery. GFP-Trap_MA beads (ChromoTek) were used, and immunoprecipitation was performed according to the manufacturer's protocol. For C20orf196 (Supplementary Fig. 2c), 293T cells were co-transfected with pMSCV-blas-3xFlag-hMAD2L2 and either pcDNA5.1-GFP or pcDNA5.1-GFP-C20orf196. At 72 h post-transfection, cells were exposed to 25 Gy IR followed by 3 h recovery. After washing with cold PBS, cells were lysed in 1 ml lysis buffer (50 mM Tris HCl pH 7.4; 150 mM NaCl; 1 mM EDTA; 1% Triton X-100) supplemented with the same inhibitors as above. After 30 min incubation on ice followed by centrifugation (16,000*g*), anti-Flag M2 Magnetic Beads (M8823, Sigma-Aldrich) pre-washed with TBS (50 mM Tris HCl, 150 mM NaCl pH 7.4), were added to the lysate and rotated overnight at 4 °C. Immune complexes were eluted by 5 min boiling.

DNA pulldown experiments. Procedures are described in detail in ref. [39], using oligos with the sequence:

5′BiosG/ATCGCATTGGCATTGGCAATGCGATACGACTGATCGAGG-GTACTCAGCTAGCTGATTCCGATCGGCTTATTCCGTGTACATACATCG GAT-3′ (IDT).

In vitro GST pulldown. Gluathione sepharose beads (GE Healthcare) were washed with ice-cold PBS and blocked for 30 min with PBS supplemented with 10% bacterial lysate (non-induced BL21 cells, lysed using PBS/lysozyme) then resuspended in binding buffer (10 mM Tris pH 7.5, 150 mM NaCl, 0.5% NP40, 0.5 mM EDTA, 0.5% BSA). Purified GST (glutathione-*S*-transferase, bacterial expression), GST-FAM35A (Novus Biologicals) and His-C20orf196 (Creative BioMart) were added to the beads at 2 pmol and incubated for 30 min at 4 °C. Beads were washed five times with 10 mM Tris, pH 7.5, 250 mM NaCl, 0.5% NP40, 0.5 mM EDTA and eluted with 100 mM Tris pH 8, 20 mM reduced glutathione, 120 mM NaCl for 15 min rotating at 4 °C. The eluates were boiled for 5 min, loaded on 4–12% Bis-Tris gel (Invitrogen) and subjected to western blotting. The blots were probed with the indicated antibodies.

Recombinant protein purifications and electrophoretic mobility shift assays. Wild-type and mutant FAM35A C-terminal domains were purified using the same method. Harvested cells were lysed by sonication in 50 mM Tris pH 8.0, 5% glycerol, 150 mM NaCl, 2 mM β-mercaptoethanol, 10 mM imidazole, protease inhibitor (Roche) and 40 g ml^{-1} deoxyribonuclease I (Sigma). After centrifugation at 30,000*g* for 30 min, supernatant was loaded onto a gravity column containing Ni-NTA affinity resin (Qiagen) pre-equilibrated with 50 mM Tris pH 8.0, 5% glycerol, 150 mM NaCl, 2 mM β-mercaptoethanol and 10 mM imidazole. After washing beads with the same buffer for 10× column volume, protein was eluted using 50 mM Tris pH 8.0, 5% glycerol, 150 mM NaCl, 2 mM β-mercaptoethanol and 100 mM imidazole. The eluate was dialysed with Q column (GE healthcare) buffer A (20 mM Tris pH 8.0, 50 mM NaCl, 5% glycerol and 2 mM β-mercaptoethanol) and loaded onto a 5 ml Q column. Protein was eluted in a gradient against buffer B (20 mM Tris pH 8.0, 1 M NaCl, 5% glycerol and 2 mM β-mercaptoethanol). Fractions containing FAM35A protein were collected and further purified by running through a Superdex 200 10/300 column (GE Healthcare) equilibrated in buffer GF (gel-filtration, 20 mM Tris pH 8, 150 mM NaCl, 5% glycerol and 5 mM dithiothreitol). Protein samples during each step of purification were analysed on 4–12% Bis-Tris gels (Invitrogen). Final purified samples were concentrated and stored at −80 °C. Both forward and reverse 90-base DNA oligos (IDT) (F: 6-FAM (6-carboxyfluorescein)-ATCGC ATTGGCATTGGCAATGCGATACGACTGATCGAGGGTACTCAGCTAG CTGATTCCGATCGGCTTATTCCGTGTACATACATCGGAT; R:6-FAM-ATCCGATGTATGTACACGGAATAAGCCGATCGGAATCAGCTAGCT GAGTACCCTCGATCAGTCGTATCGCATTGCCAATGCCAATGCGAT) were dissolved in annealing buffer (10 mM Tris pH 8.0, 50 mM NaCl and 1 mM EDTA) to a final concentration of 100 μM. DNA oligo F was used as ssDNA for electrophoretic mobility shift assay (EMSA). Equal volumes of DNA oligo F and R were mixed and annealed (heated to 95 °C for 2 min and cooled to 25 °C over 45 min) to generate dsDNA. Each 20 μl of EMSA reaction contained 10 nM of ssDNA/dsDNA incubated with different concentrations of proteins in 20 mM Tris HCl pH 7.5, 50 mM KCl, 5% (vol/vol) glycerol, 100 μM dithiothreitol, 10 μ g ml^{-1} BSA. Samples were incubated at 37 °C for 15 min and applied onto a 5% polyacrylamide native gel in 0.5× TBE buffer for electrophoresis at 4 °C. DNA was visualized by Typhoon 9000 (GE Healthcare).

GFP-Trap pulldown for mass spectrometry. HEK293T cells were cultured in SILAC medium containing either l -arginine and l -lysine, or l -arginine [$^{13}C_6$, $^{15}N_4$] and l -lysine [$^{13}C_6$, $^{15}N_2$] (Cambridge Isotope Laboratories) as described previously[51]. Cells were lysed 48 h post-transfection in modified RIPA buffer (50 mM Tris pH 7.5, 150 mM NaCl, 1 mM EDTA, 1% NP-40, 0.1% sodium deoxycholate) supplemented with protease, phosphatase inhibitors and *N*-ethylmaleimide. Lysates were cleared by centrifugation at 16,000*g* for 15 min at

4 °C and protein concentrations were estimated using QuickStart Bradford Protein assay (BioRad). Per SILAC condition, 20 µl of pre-equilibrated GFP-Trap-A beads (ChromoTek) were added to 2 mg of lysate and incubated 1 h at 4 °C while rotating, followed by three washes with modified RIPA buffer. Bound proteins were eluted in NuPAGE LDS Sample Buffer (Life Technologies) supplemented with 1 mM dithiothreitol, heated at 70 °C for 10 min and alkylated with 5.5 mM chloroacetamide at RT. Samples were loaded onto 4–12% gradient SDS–PAGE gels, and proteins were stained using a Colloidal Blue Staining Kit (Life Technologies) and digested in gel using trypsin. Peptides were extracted from the gel and desalted on reversed-phase C18 StageTips[52].

Mass spectrometry analysis. Peptide fractions were analysed on a quadrupole Orbitrap mass spectrometer (Q Exactive Plus, Thermo Scientific) equipped with an EASY-nLC 1000 (Thermo Scientific) as described in ref. [53]. Peptide samples were loaded onto C18 reversed-phase columns and eluted with a linear gradient from 8 to 40% acetonitrile containing 0.1% formic acid for 2 h. The mass spectrometer was operated in data-dependent mode, automatically switching between MS and MS2 acquisition. Survey full-scan MS spectra (m/z 300–1,650) were acquired in the Orbitrap. The ten most intense ions were sequentially isolated and fragmented using HCD (higher-energy C-trap dissociation)[54]. Fragment spectra were acquired in the Orbitrap mass analyser. Raw data files were analysed using MaxQuant (development version 1.5.2.8)[55]. Parent ion and MS2 spectra were searched against a database containing 92,578 human protein sequences obtained from UniProtKB, released in December 2016, using the Andromeda search engine[56]. Spectra were searched with a mass tolerance of 6 ppm in the MS mode, 20 ppm in HCD MS2 mode, strict trypsin specificity and allowing up to three miscleavages. Cysteine carbamidomethylation was searched as a fixed modification, whereas protein N-terminal acetylation, methionine oxidation, *N*-ethylmaleimide modification of cysteines were searched as variable modifications. The data set was filtered based on posterior error probability to arrive at a false discovery rate below 1% estimated using a target-decoy approach[57].

Immunofluorescence and microscopy imaging. Confocal imaging for γH2AX, RAD51, RPA, ssDNA (BrdU), BLM, BRCA2, FANCD2, Cyclin A and GFP (FAM35A and C20orf196) was performed as described in ref. [39]; for RAD51 and Cyclin A the pre-extraction step was omitted and cells were permeabilized for 15 min in 0.2% Triton X-100 (Sigma) in PBS after fixation. Super-resolution images were acquired using a Deltavision OMX 3D-SIM System V3 BLAZE (Applied Precision, a GE Healthcare company) equipped with three sCMOS (scientific complementary metal-oxide semiconductor) cameras, 405, 488 and 592.5 nm diode laser illumination, an Olympus Plan Apo N ×60, 1.42 NA oil objective, and standard excitation and emission filter sets. Imaging of each channel was done sequentially using three angles and five phase shifts of the illumination pattern, as described in ref. [58]. Sections were acquired at 0.125 µm z steps. Raw OMX data were reconstructed and channel registered in SoftWoRx software version 6.5.2 (Applied Precision, a GE Healthcare company). Voxelwise nearest-neighbour distances were measured for the GFP-FAM35A signal relative to the 53BP1 signal using a custom script (Butler R) for Fiji (https://github.com/gurdon-institute/OMX-Spatial-Analysis). The script maps signal volumes using Kapur's maximum entropy thresholding method[59] and measures distances using the exact signed 3D Euclidean distance transform with internal distances set to zero for display on the histogram. For all images, scale bars represent 10 µm.

Multiplex fluorescence in situ hybridization. Human 24-colour multiplex fluorescence in situ hybridization (M-FISH) probe preparation and slide treatment was carried out as in ref. [60]. For each human cell sample, 10–30 metaphases were karyotyped based on the M-FISH classification and DAPI-banding pattern. FISH on metaphase spreads using BAC probes was performed as previously described[61] and counted manually. For CSR assays, DNA FISH on metaphase spreads was performed as previously described[61] and counted manually. At least 470 metaphases were evaluated per genotype, using at least two independent clones for each condition. For telomere uncapping, cell harvesting, preparation of metaphase spreads and telomere FISH with an Alexa488-(CCCTAA repeat) peptide nucleic acid custom probe (PN-TC060-005, Panagene/Eurogentec), metaphase chromosome analysis was done as described previously[6]. The data represent two independent experiments, with ≥1,300 chromosomes for each condition, counted manually after blinding the genotypes.

Telomere fusion assays and MEFs viral transduction. Cells were transduced as in ref. [49] with pLKO-puro shRNA lentiviruses obtained from the MISSION shRNA library (Sigma), against mouse genes as described or left untransduced ('empty'). For assessment of telomere NHEJ, TRF2ts MEFs were grown for 24 h at the non-permissive temperature of 39 °C to inactivate TRF2 and induce NHEJ-dependent chromosome end-to-end fusions because of telomere uncapping.

CSR assays for CH12 and CH12-Cas9 cell lines. The CH12-Cas9 cell line was generated by transducing CH12-Cas9 cells made using spin-infect with lentivirus particles packaged in HEK293T. Plasmids: pKLV2-EF1aBsd2Acas9-W, pxPAX2 (Addgene #12260), VSV-G and pMD2.G (Addgene #12259). Blasticidin selection (10 µg ml^{-1}) started 48 h after transduction for one week. In sgRNA expression plasmids for CSR assays, sgRNAs were used to target Fam35a, C20orf196 and Mad2l2/Rev7 mouse genes (two sgRNAs per target gene; sequences listed in Supplementary Table 4). sgRNAs were cloned into pKLV-flipped U6gRNA_CCDB_PB_BbsI_PGKpuro2ABFP vector[62]. For the generation of wild-type and knockout CH12-Cas9 cell clones, 53bp1 null CH12 cell clones (gift from F. Alt) were as previously described[63]. 12 million CH12-Cas9 cells were nucleofected with 2.2 µg each of sgRNA-1 and sgRNA-2 and 0.6 µg of piggyBac transposase expression vector[64], using an Amaxa Nucleofector, Nucleofector Kit V solution (Lonza) and program X-001. Two days later, BFP-positive/puromycin-resistant CH12-Cas9 cells were selected with 3 µg ml^{-1} puromycin for one week. Cells were then single cell diluted into 96-well plates, further cultured and screened by PCR, and Sanger sequenced using PCR primers (listed in Supplementary Table 4). For CSR and cell proliferation assays, CH12 cells were plated at 50,000 cells per ml in complete RPMI supplemented with anti-CD40 antibody (1 µg ml^{-1}, Miltenyi), IL-4 (20 ng ml^{-1}, Miltenyi) and TGF-β (1 ng ml^{-1}, R&D Biotech) to induce IgM to IgA switching. After 3 days, cells were assayed for class-switching by flow cytometry using an IgA-PE antibody (eBiosciences) and a Canto II analyser (BD Biosciences). Viable cells were counted using a Casy cell counter (Roche). CSR and proliferation assays were done on 3× wild-type (WT), 3× Fam35a knockout (Fam35a), 3× C20orf196 knockout (C20orf196), 2× 53bp1 knockout (53bp1) and 3× Mad2l2 knockout (Mad2l2) cell lines in three independent experiments. For RT–PCR analysis, *Igh*, *α* germ-line transcripts (*αGLT*) and *Aid* mRNA were quantified as previously described[12]. Primers are listed in Supplementary Table 4.

Patient-derived tumour xenografts. PDXs were generated and established from breast or ovarian cancer patients' samples (with consent) as previously described[40]. The research was done with appropriate approval by the National Research Ethics Service, Cambridgeshire 2 REC (REC reference number: 08/H0308/178), and by the Vall d'Hebron Hospital Clinical Investigation Ethical Committee (PR(AG)183/2012). STG201, the PDX model used in this study, is a BRCA-null model featuring BRCA1 promoter methylation, loss of BRCA1 mRNA and protein expression. We have previously shown its sensitivity in vivo and in PDX-derived cells to PARP inhibitors, including olaparib. STG201 is also linked to deep molecular and drug sensitivity annotation[40] (http://caldaslab.cruk.cam.ac.uk/bcape/). All other PDXs were derived from breast or ovarian tumours from *BRCA1*-mutation carriers or *BRCA1* epigenetic silencing due to promoter hypermethylation[41]. PDX127 did not show any co-expression of BRCA1 but it was low in both FAM35A and C20orf196 expression. None of the five PARPi-sensitive PDXs exhibited low levels of C20orf196, FAM35A or 53BP1 loss nor BRCA1 hypomorphs. The study was compliant with all relevant ethical regulations regarding research involving animal use and human participants.

Generation of acquired drug resistance in vivo. AZD2281 (Olaparib/Lynparza) as a PARP inhibitor was administered to immunocompromised tumour-bearing mice following randomization, as previously described (50 mg kg^{-1}, 5 days per week)[40]. To classify the response of the subcutaneous implants we modified the RECIST (response evaluation criteria in solid tumours) criteria to be based on the percent tumour volume change following continuous olaparib treatment: complete response (CR); best response, ≤−95%; partial response (PR), −95% < best response ≤ −30%; stable disease (SD), −30% < best response ≤ +20%; progressive disease (PD), % tumour volume change at day 21 of treatment > + 20%. PARPi-resistant PDXs exhibited PD while PARPi-sensitive models exhibited SD, PR or CR. For STG201, time-matched vehicle- and olaparib-treated samples were collected 25 days after treatment (PARPi naive PDX) and processed for RNA extractions and sequencing. A couple of mice in the study were left with continued exposure to olaparib until tumour regrowth. One of these resistant tumours was serially passaged 126 days after treatment into new host mice (PARPi-resistant PDX) and treated with further vehicle or olaparib. At 58 days after treatment, the resistance phenotype was confirmed and samples were collected and processed for RNA-sequencing. Growth curves show average and standard deviation of at least five independent tumour volumes per trial arm. All experimental procedures were approved by the University of Cambridge Animal Welfare and Ethical Review Committee and by the Vall d'Hebron Hospital Clinical Investigation Ethical Committee and Animal Use Committee. For RNA-sequencing, RNA was extracted from all samples using the Qiagen miRNeasy or RNeasy Mini kit (cat. ID 217004 or 74104) according to the manufacturer's instructions. Libraries for Illumina sequencing were prepared using a TruSeq Stranded mRNA HT kit or Total RNA Library Prep kit with Ribo-Zero Gold (cat. ID, RS-122-2103 or RS-122-2301, Illumina). 500 ng of total RNA with RNA integrity numbers (RINs) above 8 was used for library preparation. Samples were processed following the manufacturer's HS (High-Sample) instructions (part no. 15031048 Rev. E, Illumina) with 12 or 15 cycles of PCR used at the Enrichment of DNA Fragments step. All libraries were quantified using KAPA Library Quantification Kit Illumina ROX Low (Cat ID, KK4873, KAPA Biosystems) and normalized. Libraries were pooled in equal volumes and pools were used for clustering on a HiSeq4000 sequencing flow cell following the manufacturer's instructions. Sequencing was performed using 150 bp or 100 bp paired-end run types for dual-indexed libraries. Before alignment, the sequencing quality of the reads was enforced using Trim Galore!

(v0.4.2; http://www.bioinformatics.babraham.ac.uk/projects/trim_galore/). Then, as described in refs [65,66], reads were aligned to a combined human (hg19) and mouse (mm10) reference genome using STAR (v2.5.2b)[66,67]. Counts were assigned to genome features using featureCounts (v1.5.2), whereby the alignment score is used to discern accurately between reads sourced from human and mouse[68]. Counts from multiple sequencing runs were merged and then normalized using the edgeR package[69,70].

Statistics and reproducibility. Unless stated otherwise, Prism v7.0b (GraphPad Software) was used to generate graphs, perform statistical tests and calculate *P* values. Error bars, statistical tests and number of independent repeats (*n*) are indicated in the figure legends, and statistical source data including precise *P* values are provided in Supplementary Table 5. Statistical tests included two-tailed Student's *t*-tests, Fisher's exact test, and one-way analysis of variance (ANOVA), the latter all being corrected as recommended for multiple comparisons. Microscopy image analyses were performed using ImageJ/FIJI or Volocity 6.3 (Perkin-Elmer). CRISPR screens were performed with three clones per drug treatment. Mass spectrometry of GFP-FAM35A and GFP-C20orf196 was performed in two independent experiments. RNA-sequencing was performed as three replicates for each trial arm, due to sequencing across multiple lanes (which were merged before any further analysis). This was performed for the following number of independent biological samples: six PDXs in cohort 1, five PDXs in cohort 2, seven PDXs in cohort 3 and eight PDXs in cohort 4. For the SHLD1 high and low expression cohorts, 12 and 4 independent PDXs were evaluated, respectively. All immunofluorescence assay quantification data represent mean ± s.e.m. of three independent biological repeats and $n \geq 30$ cells per condition unless otherwise specified. All immunoblots are representative of two independent experiments, with unprocessed scans of immunoblots shown in Supplementary Fig. 8.

Reporting summary. Further information on experimental design is available in the Nature Research Reporting Summary linked to this article.

Code availability. A custom FIJI script used in OMX analysis is available at https://github.com/gurdon-institute/OMX-Spatial-Analysis.

The MAGeCK commands used for CRISPR–Cas9 screens were mageck test -k counts.csv -c DMSO -t WC_2461 -n WC_2461 mageck test -k counts.csv -c DMSO -t WC-673 -n WC-673 mageck test -k counts.csv -c DMSO -t WC-2281 -n WC-2281

Data availability. The raw data files for the whole-genome CRISPR–Cas9 screen in SUM149 cells are available from the NIH Sequence Read Archive (SRA) via accession no. PRJNA471892. Raw data files for the PDX RNA sequencing are available from the NIH SRA via accession no. PRJNA473981. Raw data files for mass spectrometry are available via the ProteomeXchange Consortium on the PRIDE partner repository with data set identifier PXD009830. Source data for figures are provided in Supplementary Table 5. All other data supporting the findings of this study are available from the corresponding authors on reasonable request.

References

48. Chiang, T. W., le Sage, C., Larrieu, D., Demir, M. & Jackson, S. P. CRISPR–Cas9(D10A) nickase-based genotypic and phenotypic screening to enhance genome editing. *Sci. Rep.* **6**, 24356 (2016).
49. Peuscher, M. H. & Jacobs, J. J. DNA-damage response and repair activities at uncapped telomeres depend on RNF8. *Nat. Cell Biol.* **13**, 1139–1145 (2011).
50. Galanty, Y., Belotserkovskaya, R., Coates, J. & Jackson, S. P. RNF4, a SUMO-targeted ubiquitin E3 ligase, promotes DNA double-strand break repair. *Genes Dev.* **26**, 1179–1195 (2012).
51. Ong, S. E. et al. Stable isotope labeling by amino acids in cell culture, SILAC, as a simple and accurate approach to expression proteomics. *Mol. Cell Proteom.* **1**, 376–386 (2002).
52. Rappsilber, J., Mann, M. & Ishihama, Y. Protocol for micro-purifi ation, enrichment, pre-fractionation and storage of peptides for proteomics using StageTips. *Nat. Protoc.* **2**, 1896–1906 (2007).
53. Michalski, A. et al. Mass spectrometry-based proteomics using Q Exactive, a high-performance benchtop quadrupole Orbitrap mass spectrometer. *Mol. Cell Proteom.* **10**, M111 011015 (2011).
54. Olsen, J. V. et al. Higher-energy C-trap dissociation for peptide modifi ation analysis. *Nat. Methods* **4**, 709–712 (2007).
55. Cox, J. & Mann, M. MaxQuant enables high peptide identifi ation rates, individualized p.p.b.-range mass accuracies and proteome-wide protein quantifi ation. *Nat. Biotechnol.* **26**, 1367–1372 (2008).
56. Cox, J. et al. Andromeda: a peptide search engine integrated into the MaxQuant environment. *J. Proteome Res.* **10**, 1794–1805 (2011).
57. Elias, J. E. & Gygi, S. P. Target-decoy search strategy for increased confide ce in large-scale protein identifi ations by mass spectrometry. *Nat. Methods* **4**, 207–214 (2007).
58. Gustafsson, M. G. et al. Th ee-dimensional resolution doubling in wide-fi ld fluorescence microscopy by structured illumination. *Biophys. J.* **94**, 4957–4970 (2008).
59. Kapur, J. N., Sahoo, P. K. & Wong, A. K. C. A new method for gray-level picture thresholding using the entropy of the histogram. *Comput. Vision. Graph* **29**, 273–285 (1985).
60. Agu, C. A. et al. Successful generation of human induced pluripotent stem cell lines from blood samples held at room temperature for up to 48 hr. *Stem Cell Rep.* **5**, 660–671 (2015).
61. Lescale, C. et al. RAG2 and XLF/Cernunnos interplay reveals a novel role for the RAG complex in DNA repair. *Nat. Commun.* **7**, 10529 (2016).
62. Metzakopian, E. et al. Enhancing the genome editing toolbox: genome wide CRISPR arrayed libraries. *Sci. Rep.* **7**, 2244 (2017).
63. Panchakshari, R. A. et al. DNA double-strand break response factors influence end-joining features of IgH class switch and general translocation junctions. *Proc. Natl Acad. Sci. USA* **115**, 762–767 (2018).
64. Yusa, K., Zhou, L., Li, M. A., Bradley, A. & Craig, N. L. A hyperactive piggyBac transposase for mammalian applications. *Proc. Natl Acad. Sci. USA* **108**, 1531–1536 (2011).
65. Ahdesmaki, M. J., Gray, S. R., Johnson, J. H. & Lai, Z. Disambiguate: an open-source application for disambiguating two species in next generation sequencing data from grafted samples. *F1000Research* **5**, 2741 (2016).
66. Callari, M. et al. Computational approach to discriminate human and mouse sequences in patient-derived tumour xenografts. *BMC Genom.* **19**, 19 (2018).
67. Casper, J. et al. The UCSC Genome Browser database: 2018 update. *Nucleic Acids Res.* **46**, D762–D769 (2018).
68. Liao, Y., Smyth, G. K. & Shi, W. featureCounts: an effici t general purpose program for assigning sequence reads to genomic features. *Bioinformatics* **30**, 923–930 (2014).
69. McCarthy, D. J., Chen, Y. & Smyth, G. K. Differential expression analysis of multifactor RNA-Seq experiments with respect to biological variation. *Nucleic Acids Res.* **40**, 4288–4297 (2012).
70. Robinson, M. D., McCarthy, D. J. & Smyth, G. K. edgeR: a Bioconductor package for differential expression analysis of digital gene expression data. *Bioinformatics* **26**, 139–140 (2010).

nature cell biology

SUPPLEMENTARY INFORMATION

https://doi.org/10.1038/s41556-018-0140-1

In the format provided by the authors and unedited.

Shieldin complex promotes DNA end-joining and counters homologous recombination in BRCA1-null cells

Harveer Dev[1,2], Ting-Wei Will Chiang[1,12], Chloe Lescale[3,12], Inge de Krijger[4,12], Alistair G. Martin[5], Domenic Pilger[1], Julia Coates[1], Matylda Sczaniecka-Clift[1], Wenming Wei[3], Matthias Ostermaier[6], Mareike Herzog[1], Jonathan Lam[1], Abigail Shea[5], Mukerrem Demir[1], Qian Wu[7], Fengtang Yang[8], Beiyuan Fu[8], Zhongwu Lai[9], Gabriel Balmus[1,8], Rimma Belotserkovskaya[1], Violeta Serra[10], Mark J. O'Connor[11], Alejandra Bruna[5], Petra Beli[6], Luca Pellegrini[7], Carlos Caldas[5], Ludovic Deriano[3]*, Jacqueline J. L. Jacobs[4]*, Yaron Galanty[1]* and Stephen P. Jackson[1]*

[1]The Wellcome Trust/Cancer Research UK Gurdon Institute and Department of Biochemistry, University of Cambridge, Cambridge, UK. [2]Academic Urology Group, Department of Surgery, Cambridge University Hospitals NHS Foundation Trust, Addenbrooke's Hospital, Cambridge, UK. [3]Genome Integrity, Immunity and Cancer Unit, Department of Immunology, Department of Genomes and Genetics, Institut Pasteur, Paris, France. [4]Division of Oncogenomics, The Netherlands Cancer Institute, Plesmanlaan , Amsterdam, the Netherlands. [5]Department of Oncology and Cancer Research UK Cambridge Institute, Li Ka Shing Centre, University of Cambridge, Cambridge, UK. [6]Institute of Molecular Biology (IMB), Mainz, Germany. [7]Department of Biochemistry, University of Cambridge, Cambridge, UK. [8]Wellcome Trust Sanger Institute, Hinxton, UK. [9]AstraZeneca, Waltham, MA, USA. [10]Vall d'Hebron Institute of Oncology, Barcelona, Spain. [11]AstraZeneca, Cambridge, UK. [12]These authors contributed equally: Ting-Wei Will Chiang, Chloe Lescale, Inge de Krijger. *e-mail: ludovic.deriano@pasteur.fr; j.jacobs@nki.nl; y.galanty@gurdon.cam.ac.uk; s.jackson@gurdon.cam.ac.uk**

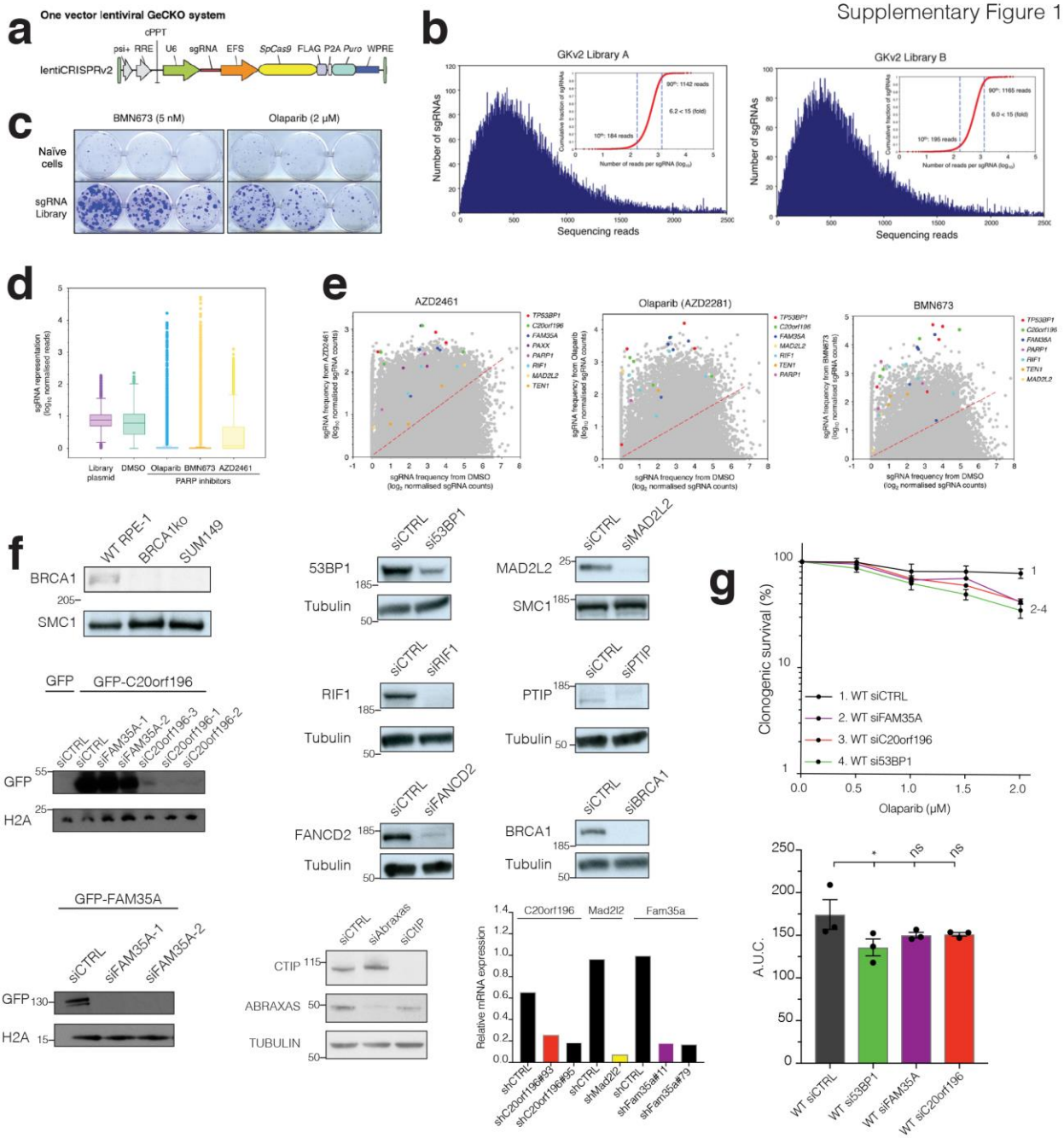

Clone reference	Genotype	Allele 1	Allele 2	Allele 3
27_14_NF	p53- FAM35A-	+5bp	+362bp/-54bp	
27_40_NF	p53- FAM35A-	-1bp	-5bp	
33FAM_2	p53- BRCA1-FAM35A-	-10bp	+1bp	-29bp
33FAM_34	p53- BRCA1-FAM35A-	+1bp	-20bp	-317bp
24FAM_46	p53- BRCA1- 53BP1- FAM35A-	-5bp	-1bp/STOP/+1bp	
27_14NC	p53- c20orf196	+313bp	-25bp	-9bp/+20bp
33C20_27	p53- BRCA1-c20orf196	+1bp		
33C20_67	p53- BRCA1-c20orf196	+2bp	+1bp	

Genotypes of knockouts confirmed by topo-clone sequencing

Supplementary Figure 1

Whole Genome CRISPR screen data and validation studies

a, Schematic of the one vector lentiviral GeCKOv2 system. **b,** Histograms of sgRNA representation of GeCKOv2 (GKv2) library A (left panel) and B (right panel). Inset: cumulative distribution of sequencing reads. The number of sequencing reads for the 10^{th} and 90^{th} sgRNA percentiles are indicated by the dashed vertical blue lines and text labels. The representation of sgRNAs is indicated by the fold-difference between the 10^{th} and 90^{th} percentile. **c,** Representative surviving clones after treatment with PARP inhibitors, representative of 2 independent experiments. Top panel: naïve, un-transduced SUM149PT cells; bottom panel: GeCKOv2 library-transduced cells. **d,** Distributions of sgRNA frequencies arising in different conditions; Box and whisker plot with centre line at median, box limits at 25^{th}/75^{th} centiles and whiskers ±1.5xIQR; n=3 technical replicates. **e,** sgRNA enrichments after treatments with the indicated drugs; each dot represents one sgRNA, with coloured dots representing the indicated target genes. **f,** Verification of BRCA1 mutant SUM149PT, BRCA1ko RPE1 and siRNAs and shRNAs used in this paper, by immunoblot or RT-qPCR (bars represent means; one experiment performed in triplicates). **g,** Clonogenic survival assay using the indicated siRNAs in BRCA1-proficient cells (WT); lower panel shows AUC. Bars represent mean ± SEM, one-way Anova; *p<0.05, **p<0.01, ***p<0.001, ****p<0.0001, ns=not significant (p≥0.05); n=3 independent experiments, with individual data points plotted over bars; statistical source data including the precise p values can be found in Supplementary Table 5. **h,** Genotypes of human knockout clones used in this work confirmed by Topo-cloning and Sanger sequencing. **i,** Cell cycle profiles of cells transfected with the indicated siRNAs used in this work (bars represent means derived from two independent experiments). All immunoblots are representative of two independent experiments; unprocessed scans of immunoblots are shown in Supplementary Fig 8.

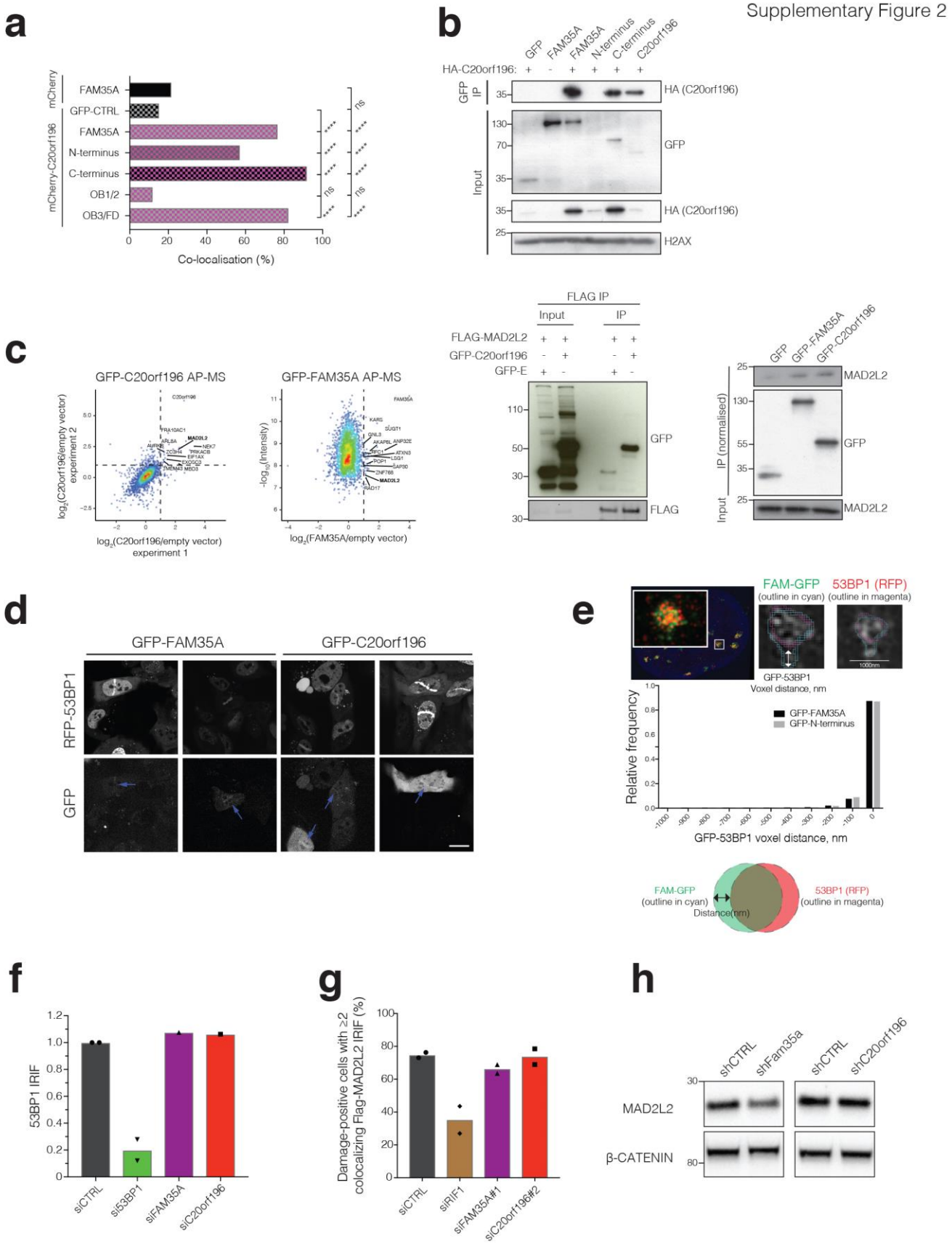
a
mCherry
FAM35A
GFP-CTRL
mCherry-C20orf196
FAM35A
N-terminus
C-terminus
OB1/2
OB3/FD
****
ns
0
20
40
60
80
100
Co-localisation (%)
b
GFP
FAM35A
FAM35A
N-terminus
C-terminus
C20orf196
HA-C20orf196: + - + + + +
GFP IP
35
HA (C20orf196)
Input
130
70
35
GFP
35
HA (C20orf196)
25
H2AX
FLAG IP
Input
IP
FLAG-MAD2L2 + + + +
GFP-C20orf196 - + - +
GFP-E + - + -
110
50
30
GFP
30
FLAG
GFP
GFP-FAM35A
GFP-C20orf196
25
MAD2L2
IP (normalised)
130
55
35
GFP
Input
25
MAD2L2
c
GFP-C20orf196 AP-MS
log2(C20orf196/empty vector) experiment 2
log2(C20orf196/empty vector) experiment 1
GFP-FAM35A AP-MS
-log10(Intensity)
log2(FAM35A/empty vector)
d
GFP-FAM35A
GFP-C20orf196
RFP-53BP1
GFP
e
FAM-GFP (outline in cyan)
53BP1 (RFP) (outline in magenta)
1000nm
GFP-53BP1 Voxel distance, nm
Relative frequency
GFP-FAM35A
GFP-N-terminus
GFP-53BP1 voxel distance, nm
FAM-GFP (outline in cyan)
53BP1 (RFP) (outline in magenta)
Distance(nm)
f
53BP1 IRIF
siCTRL
si53BP1
siFAM35A
siC20orf196
g
Damage-positive cells with ≥2 colocalizing Flag-MAD2L2 IRIF (%)
siCTRL
siRIF1
siFAM35A#1
siC20orf196#2
h
shCTRL
shFam35a
shCTRL
shC20orf196
MAD2L2
β-CATENIN
30
80

Supplementary Figure 2

C20orf196/FAM35A interactions and localisation to DNA damage sites

a, Co-localisation quantification of FAM35A/derivatives GFP-fusions with mCherry-LacR-C20orf196. Horizontal bars represent means, one-way Anova; *p<0.05, **p<0.01, ***p<0.001, ****p<0.0001, ns=not significant (p≥0.05); n=3 independent experiments; statistical source data including the precise p values can be found in Supplementary Table 5. **b,** C-terminus of FAM35A interacts with C20orf196 in cells (without normalisation). **c,** Immunoprecipitation-mass spectrometric analysis of protein interactors of GFP-C20orf196 or GFP-FAM35A (MAD2L2 is detected in both; far left and middle left panels). GFP-C20orf196 co-immunoprecipitates with Flag-MAD2L2 in HEK293 cells (middle right IB panel). Endogenous MAD2L2 co-immunoprecipitates with GFP-FAM35A and GFP-C20orf196 (far right IB panel) in HEK293 cells. **d,** Live-cell imaging of GFP-FAM35A or GFP-C20orf196 transiently expressed in U2OS cells stably expressing RFP-53BP1. Recruitment of GFP-FAM35A and GFP-C20orf196 to laser tracks was visible 30 min after laser micro-irradiation; representative image from 3 independent experiments. **e,** GFP-FAM35A and GFP-FAM35A N-terminus co-localise with 53BP1 in IRIF by super-resolution microscopy; histogram of n=11 cells per condition. **f,** Depletion of FAM35A or C20orf196 does not affect 53BP1 IRIF (U2OS cells). **g,** as in f but for MAD2L2 IRIF. Bars represent means derived from 2 independent experiments, with individual data points plotted over bars. **h,** Depletion of FAM35A or C20orf196 does not affect MAD2L2 protein levels. All immunoblots are representative of two independent experiments; unprocessed scans of immunoblots are shown in Supplementary Fig 8.

Supplementary Figure 3

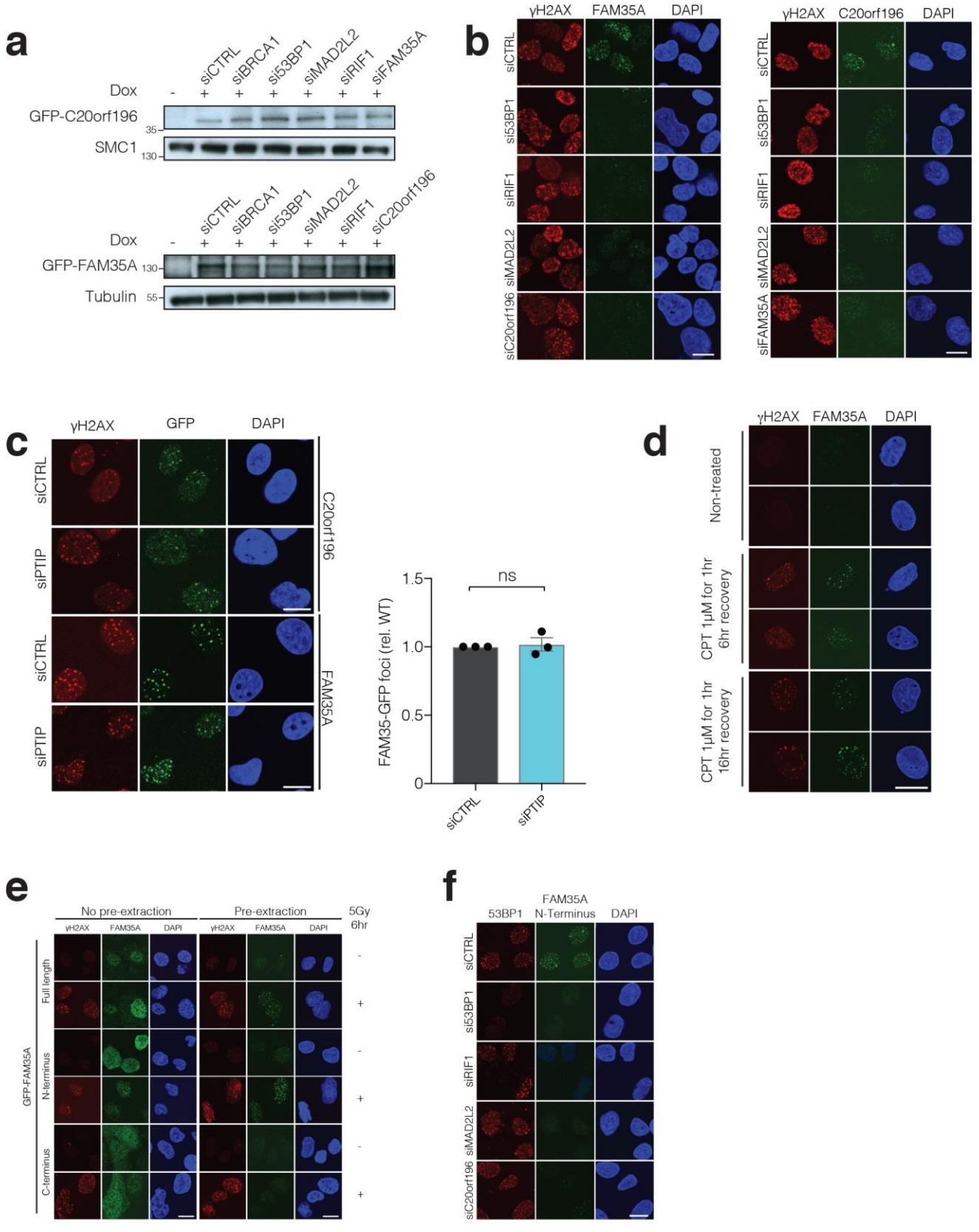

Supplementary Figure 3

DNA damage response and IRIF factor dependencies of FAM35A and C20orf196

a, Minimal variation of doxycycline induced GFP-FAM35A (U2OS) and GFP-C20orf196 (RPE1) in cells treated with the indicated siRNAs. Immunoblots shown are representative of two independent experiments with unprocessed scans of immunoblots in Supplementary Fig 8. **b,** Representative images of GFP-FAM35A (left panel) and GFP-C20orf196 (right panel) IRIF in γH2AX positive cells quantified in Fig 2e. Scale bar 10μm. **c,** Depletion of PTIP does not affect GFP-C20orf196 or GFP-FAM35A IRIF. Bars represent mean ± SEM, one-way Anova; ns=not significant ($p \geq 0.05$); n=3 independent experiments, with individual data points plotted over bars; statistical source data can be found in Supplementary Table 5. Scale bar 10μm. **d,** Camptothecin induced GFP-FAM35A foci. Scale bar 10μm. **e,** Representative images of GFP-FAM35A derivatives with/without pre-extraction ±IR; d-e representative of 2 independent experiments. Scale bar 10μm. **f,** Representative images of GFP-FAM35A N-terminus IRIF dependencies quantified in Fig 2f. Scale bar 10μm.

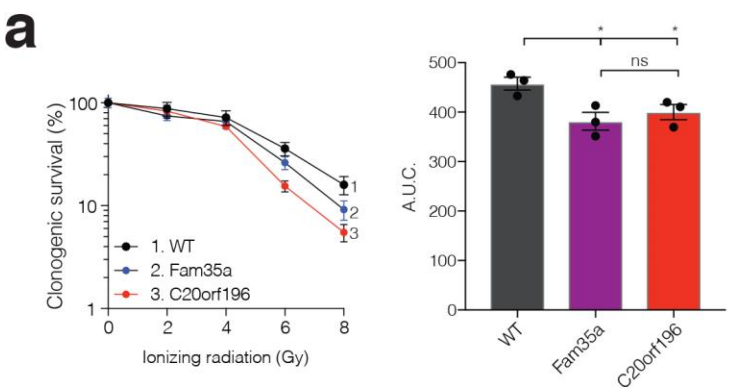

b

CH12 cell clone reference	Genotype	Allele 1	Allele 2	Allele 3	Allele 4
F10	*Fam35a-*	-5bp	-1bp	-171bp	-166bp
F11	*Fam35a-*	-1bp	-18bp		
F12	*Fam35a-*	-33bp/+8b	-1bp		
O1	*c20orf196-*	-58bp			
O6	*c20orf196-*	-17bp			
O12	*c20orf196-*	-25bp	-186bp		
R13	*Mad2l2-*	-7bp/+4bp			
R14	*Mad2l2-*	-1bp	-4bp		
R20	*Mad2l2-*	-1bp	-10bp		

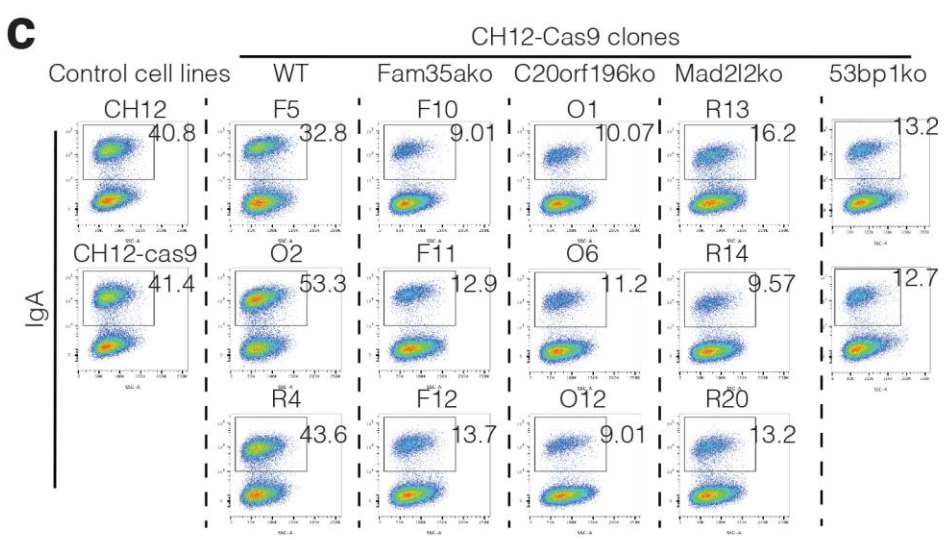

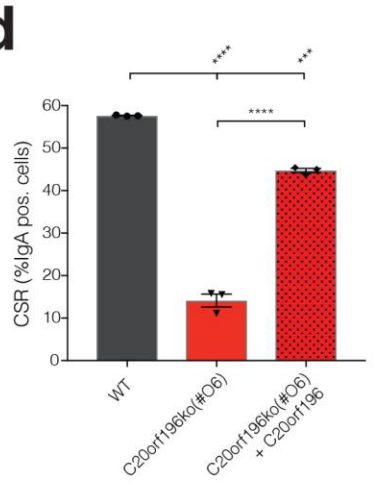

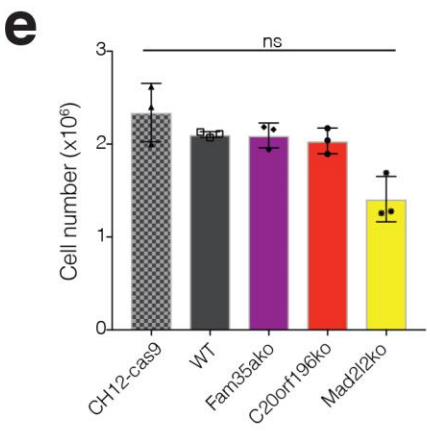

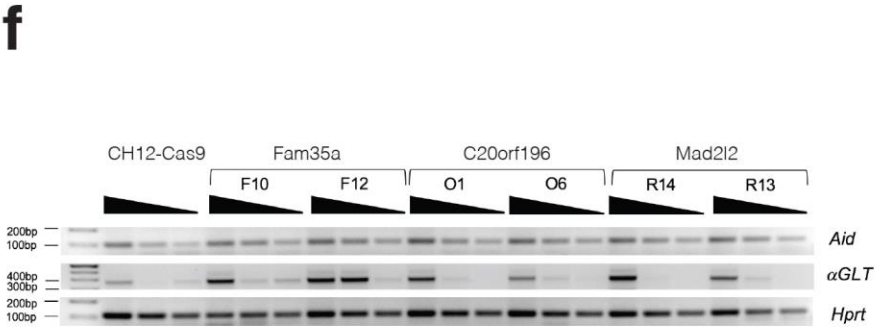

Supplementary Figure 4

FAM35A and C20orf196 directly affect class switch recombination

a, Clonogenic survival assay following IR treatment using wild-type, Fam35ako or C20orf196ko mouse ES cells (right panel shows AUC). Bars represent means ± SEM, one-way Anova; n=3 independent experiments, with individual data points plotted over bars. **b,** Genotypes of CH12-Cas9 cell knockout clones used CSR assays confirmed by Topo-cloning and Sanger sequencing. **c,** Flow cytometry profiles showing the percentage of IgA^+ cells for indicated CH12-Cas9 cell clones (genotypes) after 3 days stimulation with anti-CD40, IL-4 and TGF-β. Cell clone numbers are indicated; representative of 3 independent experiments. **d,** CSR assay in C20orf196ko cells complemented with C20orf196. Bars represent means ± SEM, one-way Anova; n=3 independent experiments, with individual data points plotted over bars. **e,** CH12-Cas9 clones were plated at 50,000 cells/ml and counted after 3 days stimulation with anti-CD40, IL4, and TGF-β. Bars represent means ± SEM, one-way Anova; n=3 independent experiments, with individual data points plotted over bars. For a, d and e, *p<0.05, ***p<0.001, ****p<0.0001, ns=not significant (p≥0.05); statistical source data including the precise p values can be found in Supplementary Table 5. **f,** *Igh*, α germ-line transcripts (αGLT) and *Aid* mRNA were quantified by semi-quantitative RT–PCR using 2.5-fold serial dilutions of cDNA made from CH12-Cas9 cells and indicated CH12-Cas9 knockout cell clones after 2 days stimulation with anti-CD40, IL4, and TGF-β. *Hprt* was used as a control for transcript expression. Immunoblots are representative of two independent experiments with unprocessed scans of immunoblots in Supplementary Fig 8.

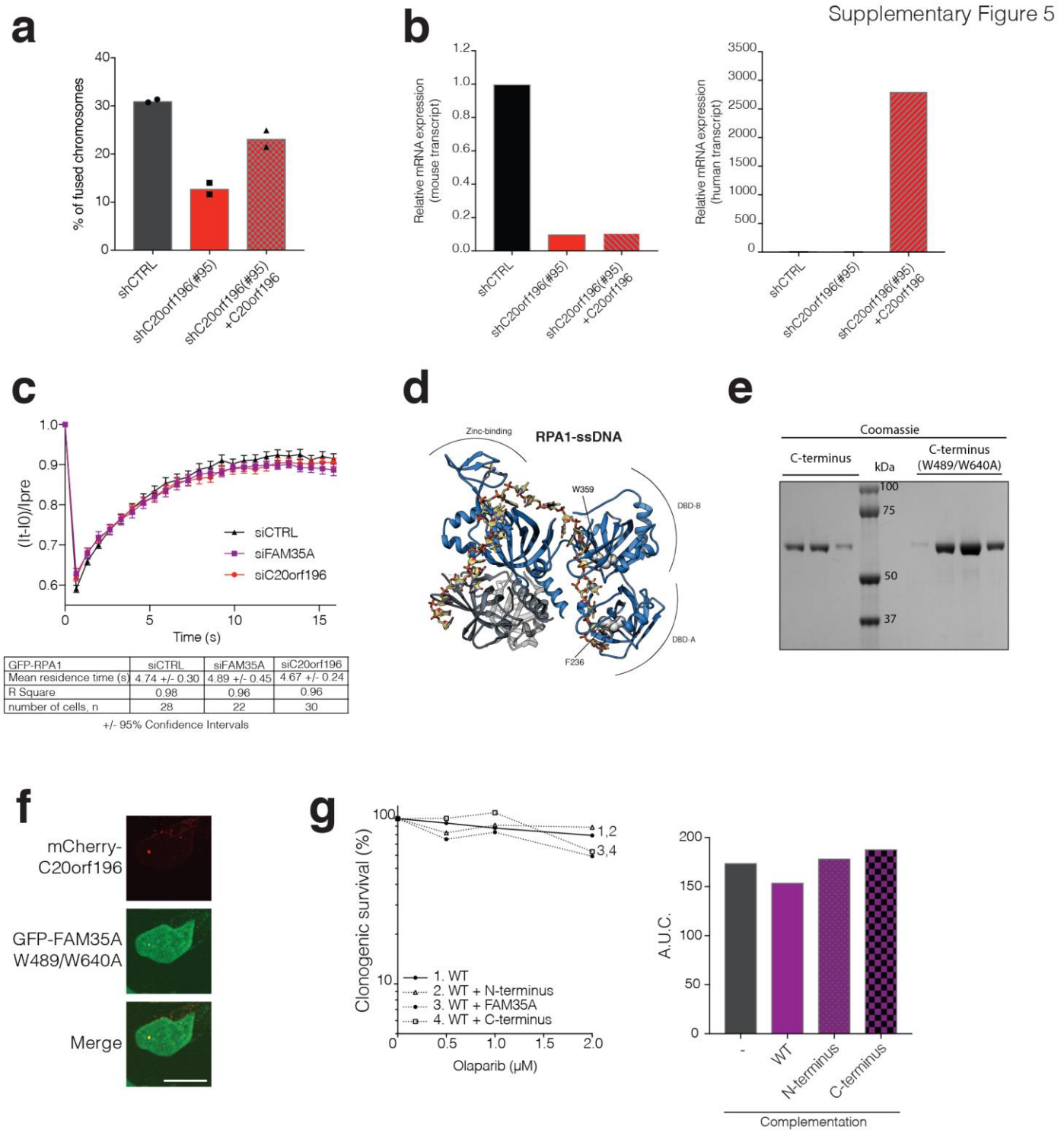

Supplementary Figure 5

Effects of FAM35A and C20orf196 on telomere fusions, DNA binding and DNA-end resection

a, Telomere fusion assay as shown in Fig 4b but complemented with shRNA resistant human C20orf196. Bars represent means derived from 2 independent experiments with ≥1300 chromosomes counted per

condition, and individual data points plotted over bars; source data can be found in Supplementary Table 5. **b,** qRT-PCR of mouse (left) and human (right) transcripts in MEFs. Bars represent means from one experiment performed in triplicates. **c,** FRAP of GFP-RPA1 in stably expressing U2OS cells, depleted of FAM35A or C20orf196. Points represent mean ± 95% confidence intervals; residence time calculated as previously described[50]; n=28 independent experiments (siCTRL), n=22 (siFAM35A) and n=30 (siC20orf196). **d,** Structure of yeast RPA1 (yRPA1) with ssDNA. **e,** Coomassie stained SDS-PAGE gel showing the bacterial purified FAM35A variants used in EMSAs. Immunoblots are representative of two independent experiments with unprocessed scans of immunoblots in Supplementary Fig 8. **f,** GFP-FAM35A W489/W640A is able to interact with mCherry-LacR-C20orf196 in cells; representative of two independent experiments, scale bar 10μm. **g,** Overexpression of FAM35A or derivatives does not sensitise wild-type cells to olaparib, adjacent panel shows AUC. Bars represent means from one experiment performed in triplicates.

Supplementary Figure 6

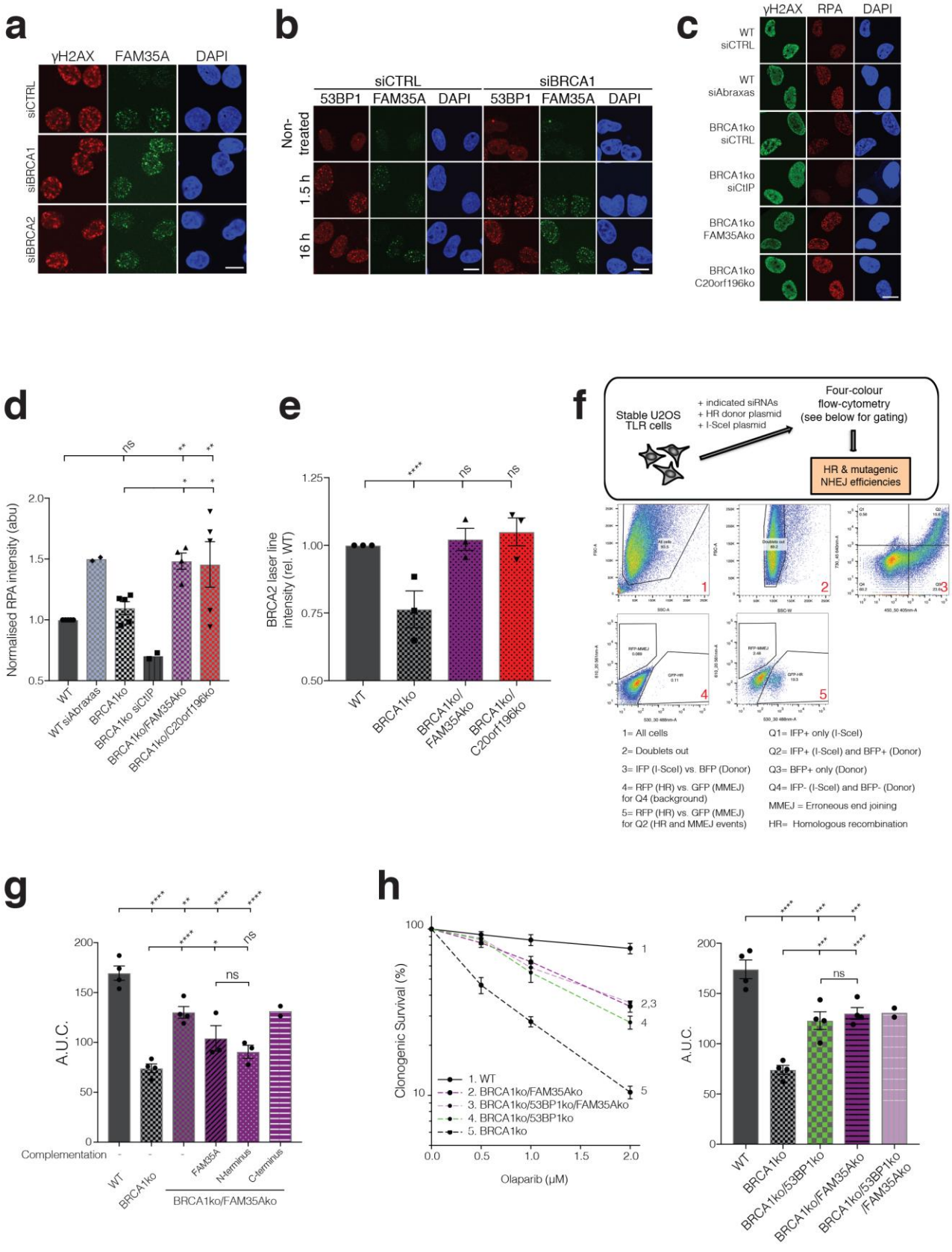

Supplementary Figure 6

FAM35A and C20orf196 functions relating to homologous recombination

a, Representative images for quantifications of GFP-FAM35A presented in Fig 6a; scale bar 10μm. **b,** Representative images for quantifications presented in Fig 6b; scale bar 10μm. **c**, Representative images of FAM35A and C20orf196 effects on DNA-end resection in wild-type and BRCA1ko cells as measured by RPA nuclear intensity (after pre-extraction) following camptothecin treatment in the indicated genotypes, quantified in Supplementary Fig 6d; scale bar 10μm. **d,** Quantification of nuclear RPA intensity; n=5 independent experiments, except WT siAbraxas and BRCA1ko siCtIP (n=2) and BRCA1ko/FAM35Ako (n=4), with individual data points plotted over bars. **e,** Quantification of BRCA2 accrual at laser micro-irradiated RPE1 cells with the indicated genotypes for the representative images presented in Fig 6d. n=3 independent experiments, with individual data points plotted over bars. **f,** Gating strategy employed for TLR assay. **g,** AUC for clonogenic survival assay presented in Fig 6g. N=4 independent experiments, except BRCA1ko/FAM35Ako +FAM35A and +N-terminus where n=3, and +C-terminus where n=2; with individual data points plotted over bars. **h,** FAM35A and 53BP1 effects on olaparib resistance in BRCA1ko cells are not additive as measured by clonogenic survival assay (left panel), AUC (right panel). N=4 independent experiments, except BRCA1ko/53BP1ko/FAM35Ako where n=2; with individual data points plotted over bars. In d, e, g and h, bars represent mean ± SEM, one-way Anova; *p<0.05, **p<0.01, ***p<0.001, ****p<0.0001, ns=not significant (p≥0.05); statistical source data including the precise p values can be found in Supplementary Table 5.

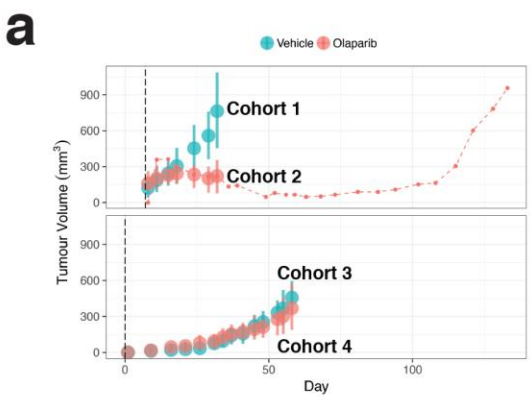
a
Vehicle
Olaparib
Cohort 1
Cohort 2
Cohort 3
Cohort 4
Tumour Volume (mm3)
Day

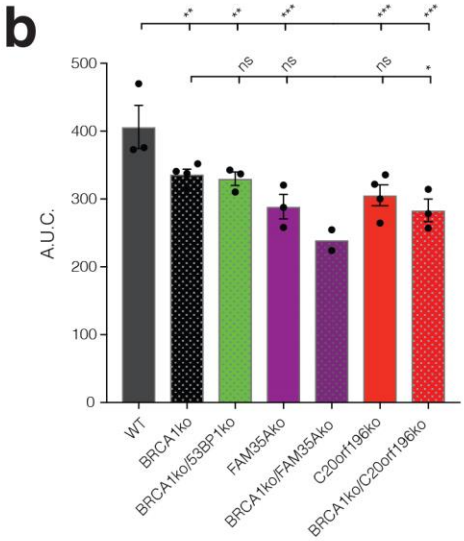
b
A.U.C.
WT
BRCA1ko
BRCA1ko/53BP1ko
FAM35Ako
BRCA1ko/FAM35Ako
C20orf196ko
BRCA1ko/C20orf196ko

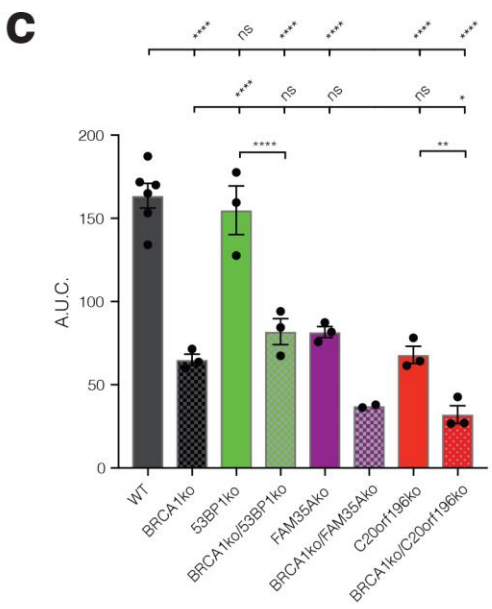
c
A.U.C.
WT
BRCA1ko
53BP1ko
BRCA1ko/53BP1ko
FAM35Ako
BRCA1ko/FAM35Ako
C20orf196ko
BRCA1ko/C20orf196ko

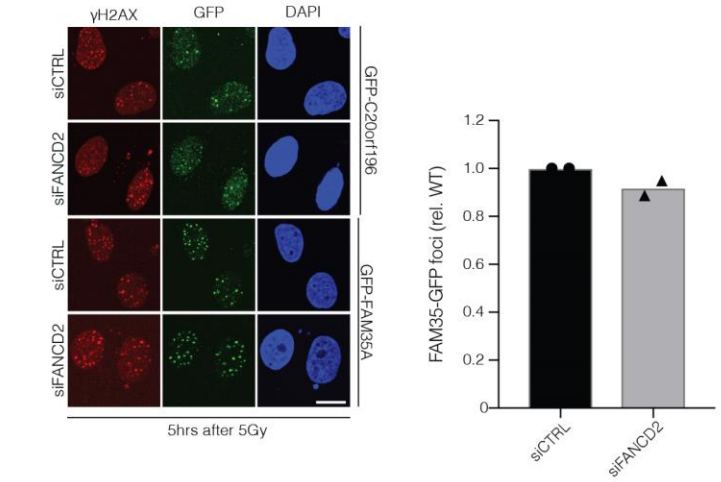
d
γH2AX
GFP
DAPI
siCTRL
siFANCD2
GFP-C20orf196
GFP-FAM35A
5hrs after 5Gy
FAM35-GFP foci (rel. WT)

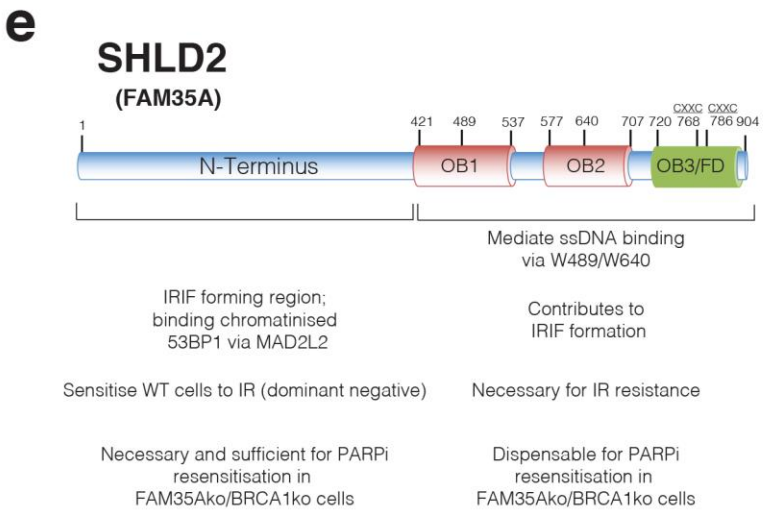
e
SHLD2
(FAM35A)
N-Terminus
OB1
OB2
OB3/FD
CXXC
CXXC
Mediate ssDNA binding via W489/W640
IRIF forming region; binding chromatinised 53BP1 via MAD2L2
Contributes to IRIF formation
Sensitise WT cells to IR (dominant negative)
Necessary for IR resistance
Necessary and sufficient for PARPi resensitisation in FAM35Ako/BRCA1ko cells
Dispensable for PARPi resensitisation in FAM35Ako/BRCA1ko cells

Supplementary Figure 7

Tumour growth curves in mice and cell sensitivities of SHLD mutant cells to DNA damaging agents

a, Tumour growth curves of PDX mice cohorts treated with vehicle or olaparib in Fig 7a; points are means, with lines representing s.d. for each of cohorts 1-4. **b,** AUC for clonogenic survival assay presented in Fig 7c. N=3 independent experiments except BRCA1ko and C20orf196ko where n=4, and BRCA1ko/FAM35Ako where n=2. **c,** AUC for clonogenic survival assay presented in Fig 7d. N=3 independent experiments except WT where n=6 and BRCA1ko/FAM35Ako where n=2. **b-c** Bars represent mean ± SEM, one-way Anova; *p<0.05, **p<0.01, ***p<0.001, ****p<0.0001, ns=not significant (p≥0.05). Individual data points plotted over bars; statistical source data including the precise p values can be found in Supplementary Table 5. **d,** GFP-FAM35A foci are not affected by depletion of FANCD2; representative images (left panel) and quantification (right panel). Bars represent means from 2 independent experiments, with individual data points plotted over bars. Scale bar 10μm. **e,** Graphical summary of SHLD2^{FAM35A} domains and their function.

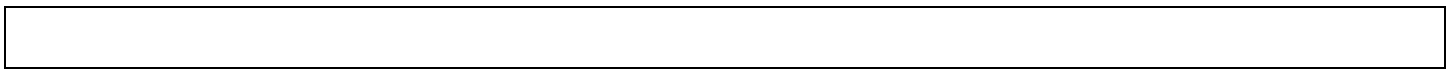

Fig 2c (left panel)

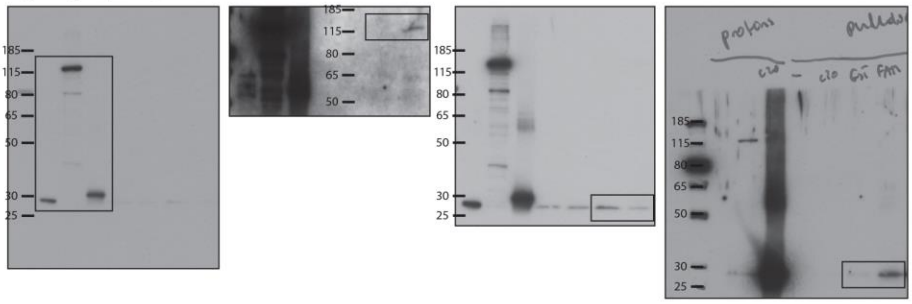

Fig 2c (right panel)

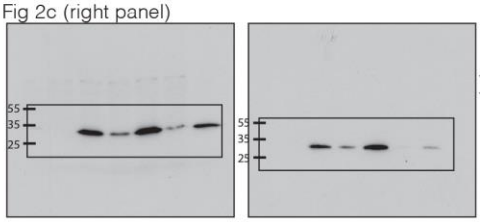

Fig 2d

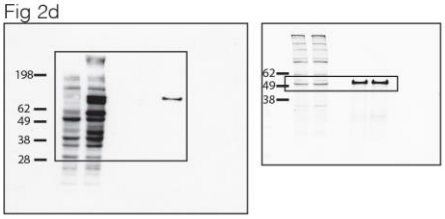

Fig 2g

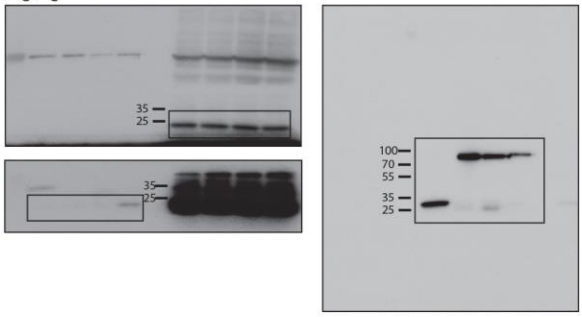

Fig 5a

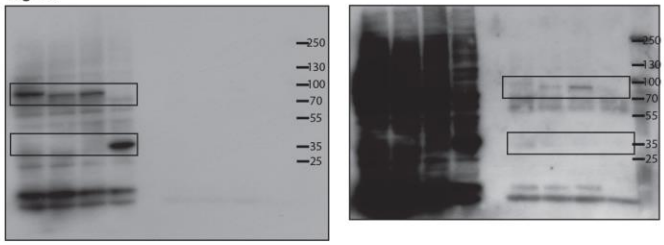

Fig 5c (native polyacrylamide gel)

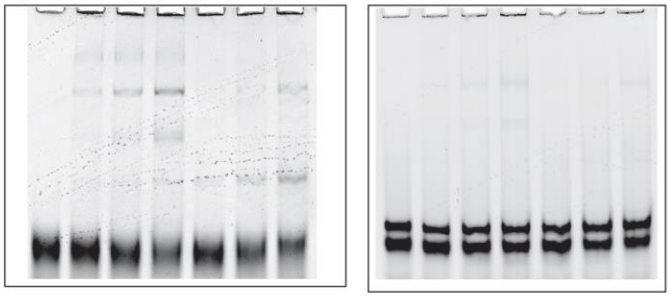

Supplementary Fig 1f (BRCA1)

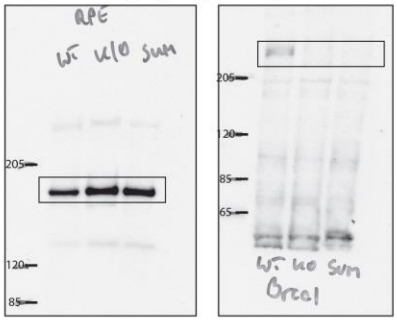

(si53BP1) (siMAD2L2) (siPTIP) (siBRCA1) (siRIF1) (siFANCD2) (siCTIP) (siABRAXAS)

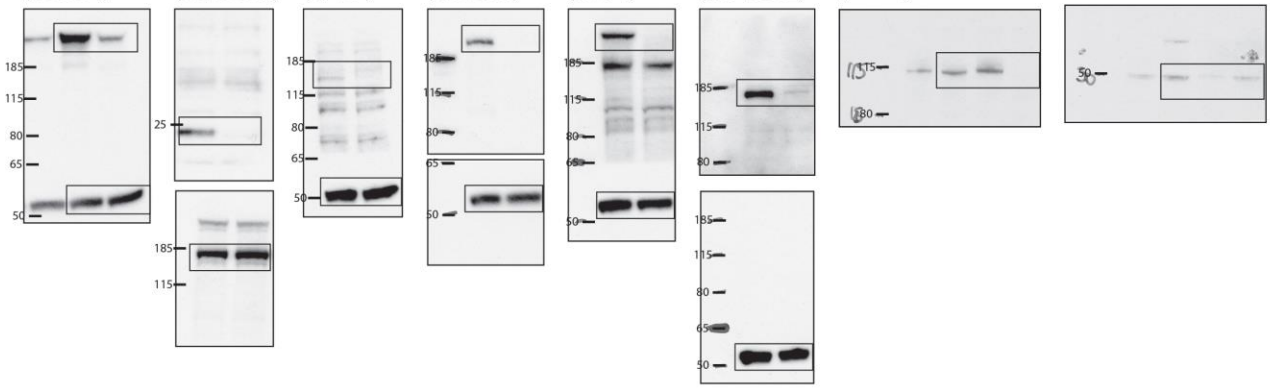

Supplementary Figure 8

Uncropped blots

Supplementary Fig1f (GFP-C20orf196)

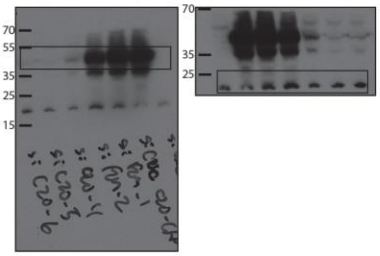

(GFP-FAM35A)

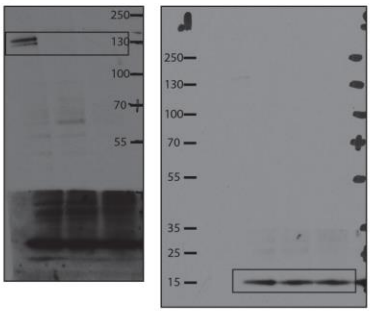

Supplementary Fig 2b

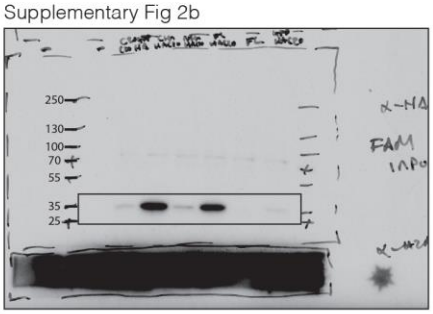

Supplementary Fig 2b

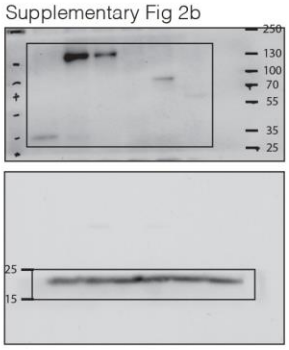

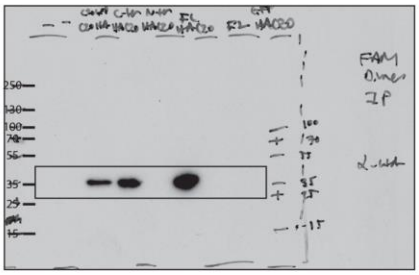

Supplementary Fig 2c

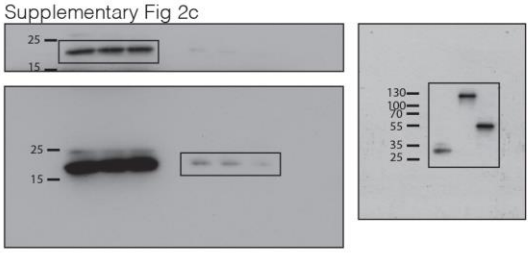

Supplementary Fig 2c

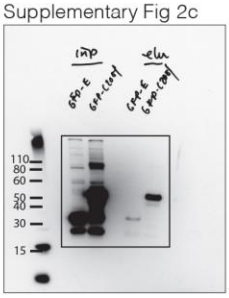

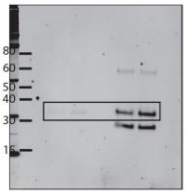

Supplementary Fig 3a (GFP-C20orf196)

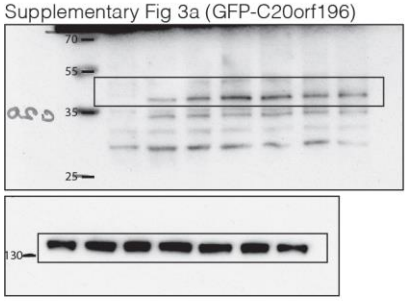

(GFP-FAM35A)

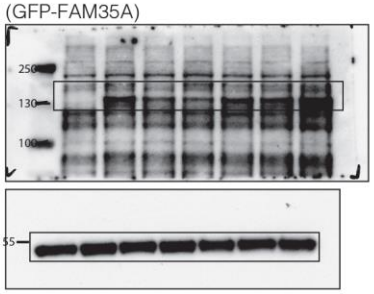

Supplementary Fig 2h

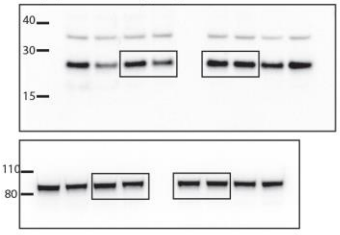

Supplementary Fig 4f

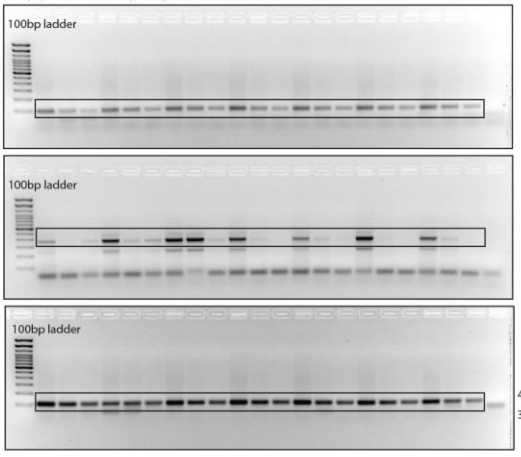

Fig 4d

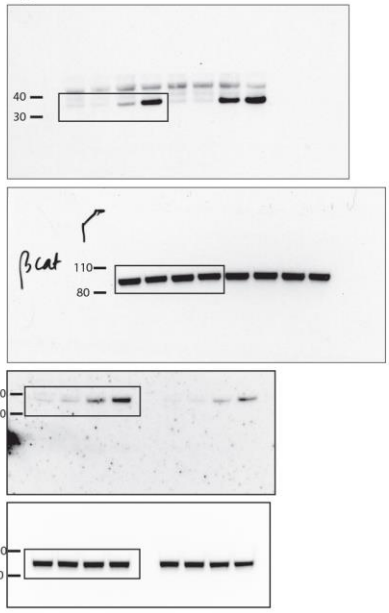

Supplementary Fig 5e

Supplementary Figure 8 continued
Uncropped blots

Supplementary Table 1. CRISPR-Cas9 screen results
Supplementary Table 2. Antibodies
Supplementary Table 3. Plasmids
Supplementary Table 4. Oligos, siRNA/shRNA, CRISPR-cas9 sgRNAs sequences
Supplementary Table 5. Statistics source data

7. References

AARTS, M., SHARPE, R., GARCIA-MURILLAS, I., GEVENSLEBEN, H., HURD, M. S., SHUMWAY, S. D., TONIATTI, C., ASHWORTH, A. & TURNER, N. C. 2012. Forced mitotic entry of S-phase cells as a therapeutic strategy induced by inhibition of WEE1. *Cancer Discov,* 2**,** 524-39.

ADIMOOLAM, S., SIRISAWAD, M., CHEN, J., THIEMANN, P., FORD, J. M. & BUGGY, J. J. 2007. HDAC inhibitor PCI-24781 decreases RAD51 expression and inhibits homologous recombination. *Proc Natl Acad Sci U S A,* 104**,** 19482-7.

AN, L., DONG, C., LI, J., CHEN, J., YUAN, J., HUANG, J., CHAN, K. M., YU, C. H. & HUEN, M. S. Y. 2018. RNF169 limits 53BP1 deposition at DSBs to stimulate single-strand annealing repair. *Proc Natl Acad Sci U S A,* 115**,** E8286-E8295.

ANAND, R., RANJHA, L., CANNAVO, E. & CEJKA, P. 2016. Phosphorylated CtIP Functions as a Co-factor of the MRE11-RAD50-NBS1 Endonuclease in DNA End Resection. *Mol Cell,* 64**,** 940-950.

ARNOULT, N., CORREIA, A., MA, J., MERLO, A., GARCIA-GOMEZ, S., MARIC, M., TOGNETTI, M., BENNER, C. W., BOULTON, S. J., SAGHATELIAN, A. & KARLSEDER, J. 2017. Regulation of DNA repair pathway choice in S and G2 phases by the NHEJ inhibitor CYREN. *Nature,* 549**,** 548-552.

AYMARD, F., BUGLER, B., SCHMIDT, C. K., GUILLOU, E., CARON, P., BRIOIS, S., IACOVONI, J. S., DABURON, V., MILLER, K. M., JACKSON, S. P. & LEGUBE, G. 2014. Transcriptionally active chromatin recruits homologous recombination at DNA double-strand breaks. *Nat Struct Mol Biol,* 21**,** 366-74.

BALMUS, G., PILGER, D., COATES, J., DEMIR, M., SCZANIECKA-CLIFT, M., BARROS, A. C., WOODS, M., FU, B., YANG, F., CHEN, E., OSTERMAIER, M., STANKOVIC, T., PONSTINGL, H., HERZOG, M., YUSA, K., MARTINEZ, F. M., DURANT, S. T., GALANTY, Y., BELI, P., ADAMS, D. J., BRADLEY, A., METZAKOPIAN, E., FORMENT, J. V. & JACKSON, S. P. 2019. ATM orchestrates the DNA-damage response to counter toxic non-homologous end-joining at broken replication forks. *Nat Commun,* 10**,** 87.

BARAZAS, M., ANNUNZIATO, S., PETTITT, S. J., DE KRIJGER, I., GHEZRAOUI, H., ROOBOL, S. J., LUTZ, C., FRANKUM, J., SONG, F. F., BROUGH, R., EVERS, B., GOGOLA, E., BHIN, J., VAN DE VEN, M., VAN GENT, D. C., JACOBS, J. J. L., CHAPMAN, R., LORD, C. J., JONKERS, J. & ROTTENBERG, S. 2018. The CST Complex Mediates End Protection at Double-Strand Breaks and Promotes PARP Inhibitor Sensitivity in BRCA1-Deficient Cells. *Cell Rep,* 23**,** 2107-2118.

BARAZAS, M., GASPARINI, A., HUANG, Y., KUCUKOSMANOGLU, A., ANNUNZIATO, S., BOUWMAN, P., SOL, W., KERSBERGEN, A., PROOST, N., DE KORTE-GRIMMERINK, R., VAN DE VEN, M., JONKERS, J., BORST, G. R. & ROTTENBERG, S. 2019.

Radiosensitivity Is an Acquired Vulnerability of PARPi-Resistant BRCA1-Deficient Tumors. *Cancer Res,* 79**,** 452-460.

BARTON, O., NAUMANN, S. C., DIEMER-BIEHS, R., KUNZEL, J., STEINLAGE, M., CONRAD, S., MAKHARASHVILI, N., WANG, J., FENG, L., LOPEZ, B. S., PAULL, T. T., CHEN, J., JEGGO, P. A. & LOBRICH, M. 2014. Polo-like kinase 3 regulates CtIP during DNA double-strand break repair in G1. *J Cell Biol,* 206**,** 877-94.

BASS, T. E., LUZWICK, J. W., KAVANAUGH, G., CARROLL, C., DUNGRAWALA, H., GLICK, G. G., FELDKAMP, M. D., PUTNEY, R., CHAZIN, W. J. & CORTEZ, D. 2016. ETAA1 acts at stalled replication forks to maintain genome integrity. *Nat Cell Biol,* 18**,** 1185-1195.

BECKER, J. R., CUELLA-MARTIN, R., BARAZAS, M., LIU, R., OLIVEIRA, C., OLIVER, A. W., BILHAM, K., HOLT, A. B., BLACKFORD, A. N., HEIERHORST, J., JONKERS, J., ROTTENBERG, S. & CHAPMAN, J. R. 2018. The ASCIZ-DYNLL1 axis promotes 53BP1-dependent non-homologous end joining and PARP inhibitor sensitivity. *Nat Commun,* 9**,** 5406.

BETERMIER, M., BERTRAND, P. & LOPEZ, B. S. 2014. Is non-homologous end-joining really an inherently error-prone process? *PLoS Genet,* 10**,** e1004086.

BETOUS, R., GLICK, G. G., ZHAO, R. & CORTEZ, D. 2013. Identification and characterization of SMARCAL1 protein complexes. *PLoS One,* 8**,** e63149.

BEUCHER, A., BIRRAUX, J., TCHOUANDONG, L., BARTON, O., SHIBATA, A., CONRAD, S., GOODARZI, A. A., KREMPLER, A., JEGGO, P. A. & LOBRICH, M. 2009. ATM and Artemis promote homologous recombination of radiation-induced DNA double-strand breaks in G2. *EMBO J,* 28**,** 3413-27.

BHARGAVA, R., ONYANGO, D. O. & STARK, J. M. 2016. Regulation of Single-Strand Annealing and its Role in Genome Maintenance. *Trends Genet,* 32**,** 566-575.

BHAT, K. P., KRISHNAMOORTHY, A., DUNGRAWALA, H., GARCIN, E. B., MODESTI, M. & CORTEZ, D. 2018. RADX Modulates RAD51 Activity to Control Replication Fork Protection. *Cell Rep,* 24**,** 538-545.

BHOWMICK, R., MINOCHERHOMJI, S. & HICKSON, I. D. 2016. RAD52 Facilitates Mitotic DNA Synthesis Following Replication Stress. *Mol Cell,* 64**,** 1117-1126.

BIEHS, R., STEINLAGE, M., BARTON, O., JUHASZ, S., KUNZEL, J., SPIES, J., SHIBATA, A., JEGGO, P. A. & LOBRICH, M. 2017. DNA Double-Strand Break Resection Occurs during Non-homologous End Joining in G1 but Is Distinct from Resection during Homologous Recombination. *Mol Cell,* 65**,** 671-684 e5.

BLACKFORD, A. N. & JACKSON, S. P. 2017. ATM, ATR, and DNA-PK: The Trinity at the Heart of the DNA Damage Response. *Mol Cell,* 66**,** 801-817.

BLACKFORD, A. N., NIEMINUSZCZY, J., SCHWAB, R. A., GALANTY, Y., JACKSON, S. P. & NIEDZWIEDZ, W. 2015. TopBP1 interacts with BLM to maintain genome stability but is dispensable for preventing BLM degradation. *Mol Cell,* 57**,** 1133-1141.

BOERSMA, V., MOATTI, N., SEGURA-BAYONA, S., PEUSCHER, M. H., VAN DER TORRE, J., WEVERS, B. A., ORTHWEIN, A., DUROCHER, D. & JACOBS, J. J. L. 2015. MAD2L2 controls DNA repair at telomeres and DNA breaks by inhibiting 5' end resection. *Nature,* 521**,** 537-540.

BOTHMER, A., ROBBIANI, D. F., DI VIRGILIO, M., BUNTING, S. F., KLEIN, I. A., FELDHAHN, N., BARLOW, J., CHEN, H. T., BOSQUE, D., CALLEN, E., NUSSENZWEIG, A. & NUSSENZWEIG, M. C. 2011. Regulation of DNA end joining, resection, and immunoglobulin class switch recombination by 53BP1. *Mol Cell,* 42**,** 319-29.

BOTHMER, A., ROBBIANI, D. F., FELDHAHN, N., GAZUMYAN, A., NUSSENZWEIG, A. & NUSSENZWEIG, M. C. 2010. 53BP1 regulates DNA resection and the choice between classical and alternative end joining during class switch recombination. *J Exp Med,* 207**,** 855-65.

BOTUYAN, M. V., CUI, G., DRANE, P., OLIVEIRA, C., DETAPPE, A., BRAULT, M. E., PARNANDI, N., CHAUBEY, S., THOMPSON, J. R., BRAGANTINI, B., ZHAO, D., CHAPMAN, J. R., CHOWDHURY, D. & MER, G. 2018. Mechanism of 53BP1 activity regulation by RNA-binding TIRR and a designer protein. *Nat Struct Mol Biol,* 25**,** 591-600.

BOUWMAN, P., ALY, A., ESCANDELL, J. M., PIETERSE, M., BARTKOVA, J., VAN DER GULDEN, H., HIDDINGH, S., THANASOULA, M., KULKARNI, A., YANG, Q., HAFFTY, B. G., TOMMISKA, J., BLOMQVIST, C., DRAPKIN, R., ADAMS, D. J., NEVANLINNA, H., BARTEK, J., TARSOUNAS, M., GANESAN, S. & JONKERS, J. 2010. 53BP1 loss rescues BRCA1 deficiency and is associated with triple-negative and BRCA-mutated breast cancers. *Nat Struct Mol Biol,* 17**,** 688-95.

BRITTON, S., COATES, J. & JACKSON, S. P. 2013. A new method for high-resolution imaging of Ku foci to decipher mechanisms of DNA double-strand break repair. *J Cell Biol,* 202**,** 579-95.

BRYANT, H. E., SCHULTZ, N., THOMAS, H. D., PARKER, K. M., FLOWER, D., LOPEZ, E., KYLE, S., MEUTH, M., CURTIN, N. J. & HELLEDAY, T. 2005. Specific killing of BRCA2-deficient tumours with inhibitors of poly(ADP-ribose) polymerase. *Nature,* 434**,** 913-7.

BUISSON, R., NIRAJ, J., RODRIGUE, A., HO, C. K., KREUZER, J., FOO, T. K., HARDY, E. J., DELLAIRE, G., HAAS, W., XIA, B., MASSON, J. Y. & ZOU, L. 2017. Coupling of Homologous Recombination and the Checkpoint by ATR. *Mol Cell,* 65**,** 336-346.

BUNTING, S. F., CALLEN, E., WONG, N., CHEN, H. T., POLATO, F., GUNN, A., BOTHMER, A., FELDHAHN, N., FERNANDEZ-CAPETILLO, O., CAO, L., XU, X., DENG, C. X., FINKEL, T., NUSSENZWEIG, M., STARK, J. M. & NUSSENZWEIG, A. 2010. 53BP1 inhibits homologous recombination in Brca1-deficient cells by blocking resection of DNA breaks. *Cell,* 141**,** 243-54.

BUONOMO, S. B., WU, Y., FERGUSON, D. & DE LANGE, T. 2009. Mammalian Rif1 contributes to replication stress survival and homology-directed repair. *J Cell Biol,* 187**,** 385-98.

BURRELL, R. A., MCCLELLAND, S. E., ENDESFELDER, D., GROTH, P., WELLER, M. C., SHAIKH, N., DOMINGO, E., KANU, N., DEWHURST, S. M., GRONROOS, E., CHEW, S. K., ROWAN, A. J., SCHENK, A., SHEFFER, M., HOWELL, M., KSCHISCHO, M., BEHRENS, A., HELLEDAY, T., BARTEK, J., TOMLINSON, I. P. & SWANTON, C. 2013. Replication stress links structural and numerical cancer chromosomal instability. *Nature,* 494**,** 492-496.

BYRUM, A. K., CARVAJAL-MALDONADO, D., MUDGE, M. C., VALLE-GARCIA, D., MAJID, M. C., PATEL, R., SOWA, M. E., GYGI, S. P., HARPER, J. W., SHI, Y., VINDIGNI, A. & MOSAMMAPARAST, N. 2019. Mitotic regulators TPX2 and Aurora A protect DNA forks during replication stress by counteracting 53BP1 function. *J Cell Biol,* 218**,** 422-432.

CALLEN, E., DI VIRGILIO, M., KRUHLAK, M. J., NIETO-SOLER, M., WONG, N., CHEN, H. T., FARYABI, R. B., POLATO, F., SANTOS, M., STARNES, L. M., WESEMANN, D. R., LEE, J. E., TUBBS, A., SLECKMAN, B. P., DANIEL, J. A., GE, K., ALT, F. W., FERNANDEZ-CAPETILLO, O., NUSSENZWEIG, M. C. & NUSSENZWEIG, A. 2013. 53BP1 mediates productive and mutagenic DNA repair through distinct phosphoprotein interactions. *Cell,* 153**,** 1266-80.

CARIDI, C. P., D'AGOSTINO, C., RYU, T., ZAPOTOCZNY, G., DELABAERE, L., LI, X., KHODAVERDIAN, V. Y., AMARAL, N., LIN, E., RAU, A. R. & CHIOLO, I. 2018. Nuclear F-actin and myosins drive relocalization of heterochromatic breaks. *Nature,* 559**,** 54-60.

CARREIRA, A. & KOWALCZYKOWSKI, S. C. 2011. Two classes of BRC repeats in BRCA2 promote RAD51 nucleoprotein filament function by distinct mechanisms. *Proc Natl Acad Sci U S A,* 108**,** 10448-53.

CECCALDI, R., LIU, J. C., AMUNUGAMA, R., HAJDU, I., PRIMACK, B., PETALCORIN, M. I., O'CONNOR, K. W., KONSTANTINOPOULOS, P. A., ELLEDGE, S. J., BOULTON, S. J., YUSUFZAI, T. & D'ANDREA, A. D. 2015. Homologous-recombination-deficient tumours are dependent on Poltheta-mediated repair. *Nature,* 518**,** 258-62.

CECCALDI, R., RONDINELLI, B. & D'ANDREA, A. D. 2016a. Repair Pathway Choices and Consequences at the Double-Strand Break. *Trends Cell Biol,* 26**,** 52-64.

CECCALDI, R., SARANGI, P. & D'ANDREA, A. D. 2016b. The Fanconi anaemia pathway: new players and new functions. *Nat Rev Mol Cell Biol,* 17**,** 337-49.

CESCUTTI, R., NEGRINI, S., KOHZAKI, M. & HALAZONETIS, T. D. 2010. TopBP1 functions with 53BP1 in the G1 DNA damage checkpoint. *EMBO J,* 29**,** 3723-32.

CHAN, K. L. & HICKSON, I. D. 2009. On the origins of ultra-fine anaphase bridges. *Cell Cycle,* 8**,** 3065-6.

CHAN, K. L., PALMAI-PALLAG, T., YING, S. & HICKSON, I. D. 2009. Replication stress induces sister-chromatid bridging at fragile site loci in mitosis. *Nat Cell Biol,* 11**,** 753-60.

CHANDRAMOULY, G., KWOK, A., HUANG, B., WILLIS, N. A., XIE, A. & SCULLY, R. 2013. BRCA1 and CtIP suppress long-tract gene conversion between sister chromatids. *Nat Commun,* 4**,** 2404.

CHANG, H. H., WATANABE, G., GERODIMOS, C. A., OCHI, T., BLUNDELL, T. L., JACKSON, S. P. & LIEBER, M. R. 2016. Different DNA End Configurations Dictate Which NHEJ Components Are Most Important for Joining Efficiency. *J Biol Chem,* 291**,** 24377-24389.

CHANG, H. H. Y., PANNUNZIO, N. R., ADACHI, N. & LIEBER, M. R. 2017. Non-homologous DNA end joining and alternative pathways to double-strand break repair. *Nat Rev Mol Cell Biol,* 18**,** 495-506.

CHAPMAN, J. R., BARRAL, P., VANNIER, J. B., BOREL, V., STEGER, M., TOMAS-LOBA, A., SARTORI, A. A., ADAMS, I. R., BATISTA, F. D. & BOULTON, S. J. 2013. RIF1 is essential for 53BP1-dependent nonhomologous end joining and suppression of DNA double-strand break resection. *Mol Cell,* 49**,** 858-71.

CHAPMAN, J. R., SOSSICK, A. J., BOULTON, S. J. & JACKSON, S. P. 2012. BRCA1-associated exclusion of 53BP1 from DNA damage sites underlies temporal control of DNA repair. *J Cell Sci,* 125**,** 3529-34.

CHEN, H., LISBY, M. & SYMINGTON, L. S. 2013. RPA coordinates DNA end resection and prevents formation of DNA hairpins. *Mol Cell,* 50**,** 589-600.

CHEN, L., NIEVERA, C. J., LEE, A. Y. & WU, X. 2008. Cell cycle-dependent complex formation of BRCA1.CtIP.MRN is important for DNA double-strand break repair. *J Biol Chem,* 283**,** 7713-20.

CHEN, S. & PARMIGIANI, G. 2007. Meta-analysis of BRCA1 and BRCA2 penetrance. *J Clin Oncol,* 25**,** 1329-33.

CHIOLO, I., MINODA, A., COLMENARES, S. U., POLYZOS, A., COSTES, S. V. & KARPEN, G. H. 2011. Double-strand breaks in heterochromatin move outside of a dynamic HP1a domain to complete recombinational repair. *Cell,* 144**,** 732-44.

CHOI, E., PARK, P. G., LEE, H. O., LEE, Y. K., KANG, G. H., LEE, J. W., HAN, W., LEE, H. C., NOH, D. Y., LEKOMTSEV, S. & LEE, H. 2012. BRCA2 fine-tunes the spindle assembly checkpoint through reinforcement of BubR1 acetylation. *Dev Cell,* 22**,** 295-308.

CICCIA, A. & ELLEDGE, S. J. 2010. The DNA damage response: making it safe to play with knives. *Mol Cell,* 40**,** 179-204.

CLOUAIRE, T. & LEGUBE, G. 2019. A Snapshot on the Cis Chromatin Response to DNA Double-Strand Breaks. *Trends Genet,* 35**,** 330-345.

CLOUAIRE, T., ROCHER, V., LASHGARI, A., ARNOULD, C., AGUIRREBENGOA, M., BIERNACKA, A., SKRZYPCZAK, M., AYMARD, F., FONGANG, B., DOJER, N., IACOVONI, J. S., ROWICKA, M., GINALSKI, K., COTE, J. & LEGUBE, G. 2018. Comprehensive Mapping of Histone Modifications at DNA Double-Strand Breaks Deciphers Repair Pathway Chromatin Signatures. *Mol Cell,* 72**,** 250-262 e6.

COSTANTINO, L., SOTIRIOU, S. K., RANTALA, J. K., MAGIN, S., MLADENOV, E., HELLEDAY, T., HABER, J. E., ILIAKIS, G., KALLIONIEMI, O. P. & HALAZONETIS, T. D. 2014. Break-induced replication repair of damaged forks induces genomic duplications in human cells. *Science,* 343**,** 88-91.

CRUZ, C., CASTROVIEJO-BERMEJO, M., GUTIERREZ-ENRIQUEZ, S., LLOP-GUEVARA, A., IBRAHIM, Y. H., GRIS-OLIVER, A., BONACHE, S., MORANCHO, B., BRUNA, A., RUEDA, O. M., LAI, Z., POLANSKA, U. M., JONES, G. N., KRISTEL, P., DE BUSTOS, L., GUZMAN, M., RODRIGUEZ, O., GRUESO, J., MONTALBAN, G., CARATU, G., MANCUSO, F., FASANI, R., JIMENEZ, J., HOWAT, W. J., DOUGHERTY, B., VIVANCOS, A., NUCIFORO, P., SERRES-CREIXAMS, X., RUBIO, I. T., OAKNIN, A., CADOGAN, E., BARRETT, J. C., CALDAS, C., BASELGA, J., SAURA, C., CORTES, J., ARRIBAS, J., JONKERS, J., DIEZ, O., O'CONNOR, M. J., BALMANA, J. & SERRA, V. 2018. RAD51 foci as a functional biomarker of homologous recombination repair and PARP inhibitor resistance in germline BRCA-mutated breast cancer. *Ann Oncol,* 29**,** 1203-1210.

CRUZ-GARCIA, A., LOPEZ-SAAVEDRA, A. & HUERTAS, P. 2014. BRCA1 accelerates CtIP-mediated DNA-end resection. *Cell Rep,* 9**,** 451-9.

CUELLA-MARTIN, R., OLIVEIRA, C., LOCKSTONE, H. E., SNELLENBERG, S., GROLMUSOVA, N. & CHAPMAN, J. R. 2016. 53BP1 Integrates DNA Repair and p53-Dependent Cell Fate Decisions via Distinct Mechanisms. *Mol Cell,* 64**,** 51-64.

D'ANDREA, A. D. 2018. Mechanisms of PARP inhibitor sensitivity and resistance. *DNA Repair (Amst),* 71**,** 172-176.

DANIELS, M. J., WANG, Y., LEE, M. & VENKITARAMAN, A. R. 2004. Abnormal cytokinesis in cells deficient in the breast cancer susceptibility protein BRCA2. *Science,* 306**,** 876-9.

DEHE, P. M. & GAILLARD, P. H. 2017. Control of structure-specific endonucleases to maintain genome stability. *Nat Rev Mol Cell Biol,* 18**,** 315-330.

DENG, S. K., GIBB, B., DE ALMEIDA, M. J., GREENE, E. C. & SYMINGTON, L. S. 2014. RPA antagonizes microhomology-mediated repair of DNA double-strand breaks. *Nat Struct Mol Biol,* 21**,** 405-12.

DENSHAM, R. M., GARVIN, A. J., STONE, H. R., STRACHAN, J., BALDOCK, R. A., DAZA-MARTIN, M., FLETCHER, A., BLAIR-REID, S., BEESLEY, J., JOHAL, B., PEARL, L. H., NEELY, R., KEEP, N. H., WATTS, F. Z. & MORRIS, J. R. 2016. Human BRCA1-BARD1 ubiquitin ligase activity counteracts chromatin barriers to DNA resection. *Nat Struct Mol Biol,* 23**,** 647-55.

DEV, H., CHIANG, T. W., LESCALE, C., DE KRIJGER, I., MARTIN, A. G., PILGER, D., COATES, J., SCZANIECKA-CLIFT, M., WEI, W., OSTERMAIER, M., HERZOG, M., LAM, J., SHEA, A., DEMIR, M., WU, Q., YANG, F., FU, B., LAI, Z., BALMUS, G., BELOTSERKOVSKAYA, R., SERRA, V., O'CONNOR, M. J., BRUNA, A., BELI, P., PELLEGRINI, L., CALDAS, C., DERIANO, L., JACOBS, J. J. L., GALANTY, Y. & JACKSON, S. P. 2018. Shieldin complex

promotes DNA end-joining and counters homologous recombination in BRCA1-null cells. *Nat Cell Biol,* 20**,** 954-965.

DI VIRGILIO, M., CALLEN, E., YAMANE, A., ZHANG, W., JANKOVIC, M., GITLIN, A. D., FELDHAHN, N., RESCH, W., OLIVEIRA, T. Y., CHAIT, B. T., NUSSENZWEIG, A., CASELLAS, R., ROBBIANI, D. F. & NUSSENZWEIG, M. C. 2013. Rif1 prevents resection of DNA breaks and promotes immunoglobulin class switching. *Science,* 339**,** 711-5.

DIFILIPPANTONIO, S., GAPUD, E., WONG, N., HUANG, C. Y., MAHOWALD, G., CHEN, H. T., KRUHLAK, M. J., CALLEN, E., LIVAK, F., NUSSENZWEIG, M. C., SLECKMAN, B. P. & NUSSENZWEIG, A. 2008. 53BP1 facilitates long-range DNA end-joining during V(D)J recombination. *Nature,* 456**,** 529-33.

DIMITROVA, N., CHEN, Y. C., SPECTOR, D. L. & DE LANGE, T. 2008. 53BP1 promotes non-homologous end joining of telomeres by increasing chromatin mobility. *Nature,* 456**,** 524-8.

DRANE, P., BRAULT, M. E., CUI, G., MEGHANI, K., CHAUBEY, S., DETAPPE, A., PARNANDI, N., HE, Y., ZHENG, X. F., BOTUYAN, M. V., KALOUSI, A., YEWDELL, W. T., MUNCH, C., HARPER, J. W., CHAUDHURI, J., SOUTOGLOU, E., MER, G. & CHOWDHURY, D. 2017. TIRR regulates 53BP1 by masking its histone methyl-lysine binding function. *Nature,* 543**,** 211-216.

DUBBURY, S. J., BOUTZ, P. L. & SHARP, P. A. 2018. CDK12 regulates DNA repair genes by suppressing intronic polyadenylation. *Nature,* 564**,** 141-145.

DUBOIS, J. C., YATES, M., GAUDREAU-LAPIERRE, A., CLEMENT, G., CAPPADOCIA, L., GAUDREAU, L., ZOU, L. & MARECHAL, A. 2017. A phosphorylation-and-ubiquitylation circuitry driving ATR activation and homologous recombination. *Nucleic Acids Res,* 45**,** 8859-8872.

DUNGRAWALA, H., BHAT, K. P., LE MEUR, R., CHAZIN, W. J., DING, X., SHARAN, S. K., WESSEL, S. R., SATHE, A. A., ZHAO, R. & CORTEZ, D. 2017. RADX Promotes Genome Stability and Modulates Chemosensitivity by Regulating RAD51 at Replication Forks. *Mol Cell,* 67**,** 374-386 e5.

DUNGRAWALA, H., ROSE, K. L., BHAT, K. P., MOHNI, K. N., GLICK, G. G., COUCH, F. B. & CORTEZ, D. 2015. The Replication Checkpoint Prevents Two Types of Fork Collapse without Regulating Replisome Stability. *Mol Cell,* 59**,** 998-1010.

EDWARDS, S. L., BROUGH, R., LORD, C. J., NATRAJAN, R., VATCHEVA, R., LEVINE, D. A., BOYD, J., REIS-FILHO, J. S. & ASHWORTH, A. 2008. Resistance to therapy caused by intragenic deletion in BRCA2. *Nature,* 451**,** 1111-5.

ESCRIBANO-DIAZ, C., ORTHWEIN, A., FRADET-TURCOTTE, A., XING, M., YOUNG, J. T., TKAC, J., COOK, M. A., ROSEBROCK, A. P., MUNRO, M., CANNY, M. D., XU, D. & DUROCHER, D. 2013. A cell cycle-dependent regulatory circuit composed of 53BP1-RIF1 and BRCA1-CtIP controls DNA repair pathway choice. *Mol Cell,* 49**,** 872-83.

FALCK, J., FORMENT, J. V., COATES, J., MISTRIK, M., LUKAS, J., BARTEK, J. & JACKSON, S. P. 2012. CDK targeting of NBS1 promotes DNA-end resection, replication restart and homologous recombination. *EMBO Rep,* 13**,** 561-8.

FARMER, H., MCCABE, N., LORD, C. J., TUTT, A. N., JOHNSON, D. A., RICHARDSON, T. B., SANTAROSA, M., DILLON, K. J., HICKSON, I., KNIGHTS, C., MARTIN, N. M., JACKSON, S. P., SMITH, G. C. & ASHWORTH, A. 2005. Targeting the DNA repair defect in BRCA mutant cells as a therapeutic strategy. *Nature,* 434**,** 917-21.

FENG, L., FONG, K. W., WANG, J., WANG, W. & CHEN, J. 2013. RIF1 counteracts BRCA1-mediated end resection during DNA repair. *J Biol Chem,* 288**,** 11135-43.

FENG, W. & JASIN, M. 2017. BRCA2 suppresses replication stress-induced mitotic and G1 abnormalities through homologous recombination. *Nat Commun,* 8**,** 525.

FINDLAY, S., HEATH, J., LUO, V. M., MALINA, A., MORIN, T., COULOMBE, Y., DJERIR, B., LI, Z., SAMIEI, A., SIMO-CHEYOU, E., KARAM, M., BAGCI, H., RAHAT, D., GRAPTON, D., LAVOIE, E. G., DOVE, C., KHALED, H., KUASNE, H., MANN, K. K., KLEIN, K. O., GREENWOOD, C. M., TABACH, Y., PARK, M., COTE, J. F., MASSON, J. Y., MARECHAL, A. & ORTHWEIN, A. 2018. SHLD2/FAM35A co-operates with REV7 to coordinate DNA double-strand break repair pathway choice. *EMBO J,* 37.

FRADET-TURCOTTE, A., CANNY, M. D., ESCRIBANO-DIAZ, C., ORTHWEIN, A., LEUNG, C. C., HUANG, H., LANDRY, M. C., KITEVSKI-LEBLANC, J., NOORDERMEER, S. M., SICHERI, F. & DUROCHER, D. 2013. 53BP1 is a reader of the DNA-damage-induced H2A Lys 15 ubiquitin mark. *Nature,* 499**,** 50-4.

FRANCIA, S., MICHELINI, F., SAXENA, A., TANG, D., DE HOON, M., ANELLI, V., MIONE, M., CARNINCI, P. & D'ADDA DI FAGAGNA, F. 2012. Site-specific DICER and DROSHA RNA products control the DNA-damage response. *Nature,* 488**,** 231-5.

GALANTY, Y., BELOTSERKOVSKAYA, R., COATES, J. & JACKSON, S. P. 2012. RNF4, a SUMO-targeted ubiquitin E3 ligase, promotes DNA double-strand break repair. *Genes Dev,* 26**,** 1179-95.

GALANTY, Y., BELOTSERKOVSKAYA, R., COATES, J., POLO, S., MILLER, K. M. & JACKSON, S. P. 2009. Mammalian SUMO E3-ligases PIAS1 and PIAS4 promote responses to DNA double-strand breaks. *Nature,* 462**,** 935-9.

GALLINA, I., CHRISTIANSEN, S. K., PEDERSEN, R. T., LISBY, M. & OESTERGAARD, V. H. 2016. TopBP1-mediated DNA processing during mitosis. *Cell Cycle,* 15**,** 176-83.

GAO, S., FENG, S., NING, S., LIU, J., ZHAO, H., XU, Y., SHANG, J., LI, K., LI, Q., GUO, R. & XU, D. 2018. An OB-fold complex controls the repair pathways for DNA double-strand breaks. *Nat Commun,* 9**,** 3925.

GHEZRAOUI, H., OLIVEIRA, C., BECKER, J. R., BILHAM, K., MORALLI, D., ANZILOTTI, C., FISCHER, R., DEOBAGKAR-LELE, M., SANCHIZ-CALVO, M., FUEYO-MARCOS, E., BONHAM, S., KESSLER, B. M., ROTTENBERG, S., CORNALL, R. J., GREEN, C. M. &

CHAPMAN, J. R. 2018. 53BP1 cooperation with the REV7-shieldin complex underpins DNA structure-specific NHEJ. *Nature,* 560**,** 122-127.

GIUNTA, S., BELOTSERKOVSKAYA, R. & JACKSON, S. P. 2010. DNA damage signaling in response to double-strand breaks during mitosis. *J Cell Biol,* 190**,** 197-207.

GIUNTA, S. & JACKSON, S. P. 2011. Give me a break, but not in mitosis: the mitotic DNA damage response marks DNA double-strand breaks with early signaling events. *Cell Cycle,* 10**,** 1215-21.

GLOVER, T. W., BERGER, C., COYLE, J. & ECHO, B. 1984. DNA polymerase alpha inhibition by aphidicolin induces gaps and breaks at common fragile sites in human chromosomes. *Hum Genet,* 67**,** 136-42.

GOGOLA, E., DUARTE, A. A., DE RUITER, J. R., WIEGANT, W. W., SCHMID, J. A., DE BRUIJN, R., JAMES, D. I., GUERRERO LLOBET, S., VIS, D. J., ANNUNZIATO, S., VAN DEN BROEK, B., BARAZAS, M., KERSBERGEN, A., VAN DE VEN, M., TARSOUNAS, M., OGILVIE, D. J., VAN VUGT, M., WESSELS, L. F. A., BARTKOVA, J., GROMOVA, I., ANDUJAR-SANCHEZ, M., BARTEK, J., LOPES, M., VAN ATTIKUM, H., BORST, P., JONKERS, J. & ROTTENBERG, S. 2018. Selective Loss of PARG Restores PARylation and Counteracts PARP Inhibitor-Mediated Synthetic Lethality. *Cancer Cell,* 33**,** 1078-1093 e12.

GONG, Z., CHO, Y. W., KIM, J. E., GE, K. & CHEN, J. 2009. Accumulation of Pax2 transactivation domain interaction protein (PTIP) at sites of DNA breaks via RNF8-dependent pathway is required for cell survival after DNA damage. *J Biol Chem,* 284**,** 7284-93.

GRABARZ, A., GUIROUILH-BARBAT, J., BARASCU, A., PENNARUN, G., GENET, D., RASS, E., GERMANN, S. M., BERTRAND, P., HICKSON, I. D. & LOPEZ, B. S. 2013. A role for BLM in double-strand break repair pathway choice: prevention of CtIP/Mre11-mediated alternative nonhomologous end-joining. *Cell Rep,* 5**,** 21-8.

GRAHAM, T. G., WALTER, J. C. & LOPARO, J. J. 2016. Two-Stage Synapsis of DNA Ends during Non-homologous End Joining. *Mol Cell,* 61**,** 850-8.

GRAHAM, T. G. W., CARNEY, S. M., WALTER, J. C. & LOPARO, J. J. 2018. A single XLF dimer bridges DNA ends during nonhomologous end joining. *Nat Struct Mol Biol,* 25**,** 877-884.

GUPTA, R., SOMYAJIT, K., NARITA, T., MASKEY, E., STANLIE, A., KREMER, M., TYPAS, D., LAMMERS, M., MAILAND, N., NUSSENZWEIG, A., LUKAS, J. & CHOUDHARY, C. 2018. DNA Repair Network Analysis Reveals Shieldin as a Key Regulator of NHEJ and PARP Inhibitor Sensitivity. *Cell,* 173**,** 972-988 e23.

HAAHR, P., HOFFMANN, S., TOLLENAERE, M. A., HO, T., TOLEDO, L. I., MANN, M., BEKKER-JENSEN, S., RASCHLE, M. & MAILAND, N. 2016. Activation of the ATR kinase by the RPA-binding protein ETAA1. *Nat Cell Biol,* 18**,** 1196-1207.

HALAZONETIS, T. D., GORGOULIS, V. G. & BARTEK, J. 2008. An oncogene-induced DNA damage model for cancer development. *Science,* 319**,** 1352-5.

HANAHAN, D. & WEINBERG, R. A. 2011. Hallmarks of cancer: the next generation. *Cell,* 144**,** 646-74.

HANZLIKOVA, H., KALASOVA, I., DEMIN, A. A., PENNICOTT, L. E., CIHLAROVA, Z. & CALDECOTT, K. W. 2018. The Importance of Poly(ADP-Ribose) Polymerase as a Sensor of Unligated Okazaki Fragments during DNA Replication. *Mol Cell,* 71**,** 319-331 e3.

HARRIGAN, J. A., BELOTSERKOVSKAYA, R., COATES, J., DIMITROVA, D. S., POLO, S. E., BRADSHAW, C. R., FRASER, P. & JACKSON, S. P. 2011. Replication stress induces 53BP1-containing OPT domains in G1 cells. *J Cell Biol,* 193**,** 97-108.

HE, Y. J., MEGHANI, K., CARON, M. C., YANG, C., RONATO, D. A., BIAN, J., SHARMA, A., MOORE, J., NIRAJ, J., DETAPPE, A., DOENCH, J. G., LEGUBE, G., ROOT, D. E., D'ANDREA, A. D., DRANE, P., DE, S., KONSTANTINOPOULOS, P. A., MASSON, J. Y. & CHOWDHURY, D. 2018. DYNLL1 binds to MRE11 to limit DNA end resection in BRCA1-deficient cells. *Nature,* 563**,** 522-526.

HER, J. & BUNTING, S. F. 2018. How cells ensure correct repair of DNA double-strand breaks. *J Biol Chem,* 293**,** 10502-10511.

HER, J., RAY, C., ALTSHULER, J., ZHENG, H. & BUNTING, S. F. 2018. 53BP1 Mediates ATR-Chk1 Signaling and Protects Replication Forks under Conditions of Replication Stress. *Mol Cell Biol,* 38.

HSIAO, K. Y. & MIZZEN, C. A. 2013. Histone H4 deacetylation facilitates 53BP1 DNA damage signaling and double-strand break repair. *J Mol Cell Biol,* 5**,** 157-65.

HU, Q., BOTUYAN, M. V., CUI, G., ZHAO, D. & MER, G. 2017. Mechanisms of Ubiquitin-Nucleosome Recognition and Regulation of 53BP1 Chromatin Recruitment by RNF168/169 and RAD18. *Mol Cell,* 66**,** 473-487 e9.

HU, Y., SCULLY, R., SOBHIAN, B., XIE, A., SHESTAKOVA, E. & LIVINGSTON, D. M. 2011. RAP80-directed tuning of BRCA1 homologous recombination function at ionizing radiation-induced nuclear foci. *Genes Dev,* 25**,** 685-700.

HUERTAS, P., CORTES-LEDESMA, F., SARTORI, A. A., AGUILERA, A. & JACKSON, S. P. 2008. CDK targets Sae2 to control DNA-end resection and homologous recombination. *Nature,* 455**,** 689-92.

HUERTAS, P. & JACKSON, S. P. 2009. Human CtIP mediates cell cycle control of DNA end resection and double strand break repair. *J Biol Chem,* 284**,** 9558-65.

HUSTEDT, N. & DUROCHER, D. 2016. The control of DNA repair by the cell cycle. *Nat Cell Biol,* 19**,** 1-9.

IBRAHIM, Y. H., GARCIA-GARCIA, C., SERRA, V., HE, L., TORRES-LOCKHART, K., PRAT, A., ANTON, P., COZAR, P., GUZMAN, M., GRUESO, J., RODRIGUEZ, O., CALVO, M. T., AURA, C., DIEZ, O., RUBIO, I. T., PEREZ, J., RODON, J., CORTES, J., ELLISEN, L. W., SCALTRITI, M. & BASELGA, J. 2012. PI3K inhibition impairs BRCA1/2 expression and

sensitizes BRCA-proficient triple-negative breast cancer to PARP inhibition. *Cancer Discov,* 2**,** 1036-47.

ISMAIL, I. H., GAGNE, J. P., GENOIS, M. M., STRICKFADEN, H., MCDONALD, D., XU, Z., POIRIER, G. G., MASSON, J. Y. & HENDZEL, M. J. 2015. The RNF138 E3 ligase displaces Ku to promote DNA end resection and regulate DNA repair pathway choice. *Nat Cell Biol,* 17**,** 1446-57.

JACKSON, S. P. & BARTEK, J. 2009. The DNA-damage response in human biology and disease. *Nature,* 461**,** 1071-8.

JOHNSON, N., JOHNSON, S. F., YAO, W., LI, Y. C., CHOI, Y. E., BERNHARDY, A. J., WANG, Y., CAPELLETTI, M., SAROSIEK, K. A., MOREAU, L. A., CHOWDHURY, D., WICKRAMANAYAKE, A., HARRELL, M. I., LIU, J. F., D'ANDREA, A. D., MIRON, A., SWISHER, E. M. & SHAPIRO, G. I. 2013. Stabilization of mutant BRCA1 protein confers PARP inhibitor and platinum resistance. *Proc Natl Acad Sci U S A,* 110**,** 17041-6.

JOHNSON, N., LI, Y. C., WALTON, Z. E., CHENG, K. A., LI, D., RODIG, S. J., MOREAU, L. A., UNITT, C., BRONSON, R. T., THOMAS, H. D., NEWELL, D. R., D'ANDREA, A. D., CURTIN, N. J., WONG, K. K. & SHAPIRO, G. I. 2011. Compromised CDK1 activity sensitizes BRCA-proficient cancers to PARP inhibition. *Nat Med,* 17**,** 875-82.

JOWSEY, P. A., DOHERTY, A. J. & ROUSE, J. 2004. Human PTIP facilitates ATM-mediated activation of p53 and promotes cellular resistance to ionizing radiation. *J Biol Chem,* 279**,** 55562-9.

KABECHE, L., NGUYEN, H. D., BUISSON, R. & ZOU, L. 2018. A mitosis-specific and R loop-driven ATR pathway promotes faithful chromosome segregation. *Science,* 359**,** 108-114.

KACHHAP, S. K., ROSMUS, N., COLLIS, S. J., KORTENHORST, M. S., WISSING, M. D., HEDAYATI, M., SHABBEER, S., MENDONCA, J., DEANGELIS, J., MARCHIONNI, L., LIN, J., HOTI, N., NORTIER, J. W., DEWEESE, T. L., HAMMERS, H. & CARDUCCI, M. A. 2010. Downregulation of homologous recombination DNA repair genes by HDAC inhibition in prostate cancer is mediated through the E2F1 transcription factor. *PLoS One,* 5**,** e11208.

KAIS, Z., RONDINELLI, B., HOLMES, A., O'LEARY, C., KOZONO, D., D'ANDREA, A. D. & CECCALDI, R. 2016. FANCD2 Maintains Fork Stability in BRCA1/2-Deficient Tumors and Promotes Alternative End-Joining DNA Repair. *Cell Rep,* 15**,** 2488-99.

KAKAROUGKAS, A., ISMAIL, A., KLEMENT, K., GOODARZI, A. A., CONRAD, S., FREIRE, R., SHIBATA, A., LOBRICH, M. & JEGGO, P. A. 2013. Opposing roles for 53BP1 during homologous recombination. *Nucleic Acids Res,* 41**,** 9719-31.

KANAKKANTHARA, A., JEGANATHAN, K. B., LIMZERWALA, J. F., BAKER, D. J., HAMADA, M., NAM, H. J., VAN DEURSEN, W. H., HAMADA, N., NAYLOR, R. M., BECKER, N. A., DAVIES, B. A., VAN REE, J. H., MER, G., SHAPIRO, V. S., MAHER, L. J., 3RD, KATZMANN, D. J. & VAN DEURSEN, J. M. 2016. Cyclin A2 is an RNA binding protein that controls Mre11 mRNA translation. *Science,* 353**,** 1549-1552.

KENT, T., MATEOS-GOMEZ, P. A., SFEIR, A. & POMERANTZ, R. T. 2016. Polymerase theta is a robust terminal transferase that oscillates between three different mechanisms during end-joining. *Elife,* 5.

KITEVSKI-LEBLANC, J., FRADET-TURCOTTE, A., KUKIC, P., WILSON, M. D., PORTELLA, G., YUWEN, T., PANIER, S., DUAN, S., CANNY, M. D., VAN INGEN, H., ARROWSMITH, C. H., RUBINSTEIN, J. L., VENDRUSCOLO, M., DUROCHER, D. & KAY, L. E. 2017. The RNF168 paralog RNF169 defines a new class of ubiquitylated histone reader involved in the response to DNA damage. *Elife,* 6.

KOTSANTIS, P., PETERMANN, E. & BOULTON, S. J. 2018. Mechanisms of Oncogene-Induced Replication Stress: Jigsaw Falling into Place. *Cancer Discov,* 8**,** 537-555.

LABUN, K., MONTAGUE, T. G., KRAUSE, M., TORRES CLEUREN, Y. N., TJELDNES, H. & VALEN, E. 2019. CHOPCHOP v3: expanding the CRISPR web toolbox beyond genome editing. *Nucleic Acids Res*.

LAI, X., BRODERICK, R., BERGOGLIO, V., ZIMMER, J., BADIE, S., NIEDZWIEDZ, W., HOFFMANN, J. S. & TARSOUNAS, M. 2017. MUS81 nuclease activity is essential for replication stress tolerance and chromosome segregation in BRCA2-deficient cells. *Nat Commun,* 8**,** 15983.

LANGELIER, M. F., PLANCK, J. L., ROY, S. & PASCAL, J. M. 2012. Structural basis for DNA damage-dependent poly(ADP-ribosyl)ation by human PARP-1. *Science,* 336**,** 728-32.

LEE, D. H., ACHARYA, S. S., KWON, M., DRANE, P., GUAN, Y., ADELMANT, G., KALEV, P., SHAH, J., PELLMAN, D., MARTO, J. A. & CHOWDHURY, D. 2014. Dephosphorylation enables the recruitment of 53BP1 to double-strand DNA breaks. *Mol Cell,* 54**,** 512-25.

LEIMBACHER, P. A., JONES, S. E., SHORROCKS, A. K., DE MARCO ZOMPIT, M., DAY, M., BLAAUWENDRAAD, J., BUNDSCHUH, D., BONHAM, S., FISCHER, R., FINK, D., KESSLER, B. M., OLIVER, A. W., PEARL, L. H., BLACKFORD, A. N. & STUCKI, M. 2019. MDC1 Interacts with TOPBP1 to Maintain Chromosomal Stability during Mitosis. *Mol Cell,* 74**,** 571-583 e8.

LEMAITRE, C., GRABARZ, A., TSOUROULA, K., ANDRONOV, L., FURST, A., PANKOTAI, T., HEYER, V., ROGIER, M., ATTWOOD, K. M., KESSLER, P., DELLAIRE, G., KLAHOLZ, B., REINA-SAN-MARTIN, B. & SOUTOGLOU, E. 2014. Nuclear position dictates DNA repair pathway choice. *Genes Dev,* 28**,** 2450-63.

LI, W., XU, H., XIAO, T., CONG, L., LOVE, M. I., ZHANG, F., IRIZARRY, R. A., LIU, J. S., BROWN, M. & LIU, X. S. 2014. MAGeCK enables robust identification of essential genes from genome-scale CRISPR/Cas9 knockout screens. *Genome Biol,* 15**,** 554.

LIM, K. S., LI, H., ROBERTS, E. A., GAUDIANO, E. F., CLAIRMONT, C., SAMBEL, L. A., PONNIENSELVAN, K., LIU, J. C., YANG, C., KOZONO, D., PARMAR, K., YUSUFZAI, T., ZHENG, N. & D'ANDREA, A. D. 2018. USP1 Is Required for Replication Fork Protection in BRCA1-Deficient Tumors. *Mol Cell,* 72**,** 925-941 e4.

LIU, Y., NIELSEN, C. F., YAO, Q. & HICKSON, I. D. 2014. The origins and processing of ultra fine anaphase DNA bridges. *Curr Opin Genet Dev,* 26**,** 1-5.

LOK, B. H., CARLEY, A. C., TCHANG, B. & POWELL, S. N. 2013. RAD52 inactivation is synthetically lethal with deficiencies in BRCA1 and PALB2 in addition to BRCA2 through RAD51-mediated homologous recombination. *Oncogene,* 32**,** 3552-8.

LORD, C. J. & ASHWORTH, A. 2016. BRCAness revisited. *Nat Rev Cancer,* 16**,** 110-20.

LORD, C. J. & ASHWORTH, A. 2017. PARP inhibitors: Synthetic lethality in the clinic. *Science,* 355**,** 1152-1158.

LUIJSTERBURG, M. S., ACS, K., ACKERMANN, L., WIEGANT, W. W., BEKKER-JENSEN, S., LARSEN, D. H., KHANNA, K. K., VAN ATTIKUM, H., MAILAND, N. & DANTUMA, N. P. 2012. A new non-catalytic role for ubiquitin ligase RNF8 in unfolding higher-order chromatin structure. *EMBO J,* 31**,** 2511-27.

LUKAS, C., SAVIC, V., BEKKER-JENSEN, S., DOIL, C., NEUMANN, B., PEDERSEN, R. S., GROFTE, M., CHAN, K. L., HICKSON, I. D., BARTEK, J. & LUKAS, J. 2011. 53BP1 nuclear bodies form around DNA lesions generated by mitotic transmission of chromosomes under replication stress. *Nat Cell Biol,* 13**,** 243-53.

LUO, J., SOLIMINI, N. L. & ELLEDGE, S. J. 2009. Principles of cancer therapy: oncogene and non-oncogene addiction. *Cell,* 136**,** 823-37.

MARTINEZ, P., FLORES, J. M. & BLASCO, M. A. 2012. 53BP1 deficiency combined with telomere dysfunction activates ATR-dependent DNA damage response. *J Cell Biol,* 197**,** 283-300.

MATEO, J., CARREIRA, S., SANDHU, S., MIRANDA, S., MOSSOP, H., PEREZ-LOPEZ, R., NAVA RODRIGUES, D., ROBINSON, D., OMLIN, A., TUNARIU, N., BOYSEN, G., PORTA, N., FLOHR, P., GILLMAN, A., FIGUEIREDO, I., PAULDING, C., SEED, G., JAIN, S., RALPH, C., PROTHEROE, A., HUSSAIN, S., JONES, R., ELLIOTT, T., MCGOVERN, U., BIANCHINI, D., GOODALL, J., ZAFEIRIOU, Z., WILLIAMSON, C. T., FERRALDESCHI, R., RIISNAES, R., EBBS, B., FOWLER, G., RODA, D., YUAN, W., WU, Y. M., CAO, X., BROUGH, R., PEMBERTON, H., A'HERN, R., SWAIN, A., KUNJU, L. P., EELES, R., ATTARD, G., LORD, C. J., ASHWORTH, A., RUBIN, M. A., KNUDSEN, K. E., FENG, F. Y., CHINNAIYAN, A. M., HALL, E. & DE BONO, J. S. 2015. DNA-Repair Defects and Olaparib in Metastatic Prostate Cancer. *N Engl J Med,* 373**,** 1697-708.

MATEOS-GOMEZ, P. A., GONG, F., NAIR, N., MILLER, K. M., LAZZERINI-DENCHI, E. & SFEIR, A. 2015. Mammalian polymerase theta promotes alternative NHEJ and suppresses recombination. *Nature,* 518**,** 254-7.

MATTIROLI, F., VISSERS, J. H., VAN DIJK, W. J., IKPA, P., CITTERIO, E., VERMEULEN, W., MARTEIJN, J. A. & SIXMA, T. K. 2012. RNF168 ubiquitinates K13-15 on H2A/H2AX to drive DNA damage signaling. *Cell,* 150**,** 1182-95.

MAYA-MENDOZA, A., MOUDRY, P., MERCHUT-MAYA, J. M., LEE, M., STRAUSS, R. & BARTEK, J. 2018. High speed of fork progression induces DNA replication stress and genomic instability. *Nature,* 559**,** 279-284.

MENGWASSER, K. E., ADEYEMI, R. O., LENG, Y., CHOI, M. Y., CLAIRMONT, C., D'ANDREA, A. D. & ELLEDGE, S. J. 2019. Genetic Screens Reveal FEN1 and APEX2 as BRCA2 Synthetic Lethal Targets. *Mol Cell,* 73**,** 885-899 e6.

MINOCHERHOMJI, S., YING, S., BJERREGAARD, V. A., BURSOMANNO, S., ALELIUNAITE, A., WU, W., MANKOURI, H. W., SHEN, H., LIU, Y. & HICKSON, I. D. 2015. Replication stress activates DNA repair synthesis in mitosis. *Nature,* 528**,** 286-90.

MIRMAN, Z., LOTTERSBERGER, F., TAKAI, H., KIBE, T., GONG, Y., TAKAI, K., BIANCHI, A., ZIMMERMANN, M., DUROCHER, D. & DE LANGE, T. 2018. 53BP1-RIF1-shieldin counteracts DSB resection through CST- and Polalpha-dependent fill-in. *Nature,* 560**,** 112-116.

MOHIUDDIN, M., RAHMAN, M. M., SALE, J. E. & PEARSON, C. E. 2019. CtIP-BRCA1 complex and MRE11 maintain replication forks in the presence of chain terminating nucleoside analogs. *Nucleic Acids Res,* 47**,** 2966-2980.

MOORE, K., COLOMBO, N., SCAMBIA, G., KIM, B. G., OAKNIN, A., FRIEDLANDER, M., LISYANSKAYA, A., FLOQUET, A., LEARY, A., SONKE, G. S., GOURLEY, C., BANERJEE, S., OZA, A., GONZALEZ-MARTIN, A., AGHAJANIAN, C., BRADLEY, W., MATHEWS, C., LIU, J., LOWE, E. S., BLOOMFIELD, R. & DISILVESTRO, P. 2018. Maintenance Olaparib in Patients with Newly Diagnosed Advanced Ovarian Cancer. *N Engl J Med,* 379**,** 2495-2505.

MORALES, J. C., XIA, Z., LU, T., ALDRICH, M. B., WANG, B., ROSALES, C., KELLEMS, R. E., HITTELMAN, W. N., ELLEDGE, S. J. & CARPENTER, P. B. 2003. Role for the BRCA1 C-terminal repeats (BRCT) protein 53BP1 in maintaining genomic stability. *J Biol Chem,* 278**,** 14971-7.

MORENO, A., CARRINGTON, J. T., ALBERGANTE, L., AL MAMUN, M., HAAGENSEN, E. J., KOMSELI, E. S., GORGOULIS, V. G., NEWMAN, T. J. & BLOW, J. J. 2016. Unreplicated DNA remaining from unperturbed S phases passes through mitosis for resolution in daughter cells. *Proc Natl Acad Sci U S A,* 113**,** E5757-64.

MUNOZ, I. M., JOWSEY, P. A., TOTH, R. & ROUSE, J. 2007. Phospho-epitope binding by the BRCT domains of hPTIP controls multiple aspects of the cellular response to DNA damage. *Nucleic Acids Res,* 35**,** 5312-22.

MURAI, J., HUANG, S. Y., DAS, B. B., RENAUD, A., ZHANG, Y., DOROSHOW, J. H., JI, J., TAKEDA, S. & POMMIER, Y. 2012. Trapping of PARP1 and PARP2 by Clinical PARP Inhibitors. *Cancer Res,* 72**,** 5588-99.

NACSON, J., KRAIS, J. J., BERNHARDY, A. J., CLAUSEN, E., FENG, W., WANG, Y., NICOLAS, E., CAI, K. Q., TRICARICO, R., HUA, X., DIMARCANTONIO, D., MARTINEZ, E., ZONG, D., HANDORF, E. A., BELLACOSA, A., TESTA, J. R., NUSSENZWEIG, A., GUPTA, G. P.,

SYKES, S. M. & JOHNSON, N. 2018. BRCA1 Mutation-Specific Responses to 53BP1 Loss-Induced Homologous Recombination and PARP Inhibitor Resistance. *Cell Rep,* 24**,** 3513-3527 e7.

NAIM, V. & ROSSELLI, F. 2009. The FANC pathway and BLM collaborate during mitosis to prevent micro-nucleation and chromosome abnormalities. *Nat Cell Biol,* 11**,** 761-8.

NAIM, V., WILHELM, T., DEBATISSE, M. & ROSSELLI, F. 2013. ERCC1 and MUS81-EME1 promote sister chromatid separation by processing late replication intermediates at common fragile sites during mitosis. *Nat Cell Biol,* 15**,** 1008-15.

NAKAMURA, K., SAREDI, G., BECKER, J. R., FOSTER, B. M., NGUYEN, N. V., BEYER, T. E., CESA, L. C., FAULL, P. A., LUKAUSKAS, S., FRIMURER, T., CHAPMAN, J. R., BARTKE, T. & GROTH, A. 2019. H4K20me0 recognition by BRCA1-BARD1 directs homologous recombination to sister chromatids. *Nat Cell Biol,* 21**,** 311-318.

NIEDERNHOFER, L. J., GARINIS, G. A., RAAMS, A., LALAI, A. S., ROBINSON, A. R., APPELDOORN, E., ODIJK, H., OOSTENDORP, R., AHMAD, A., VAN LEEUWEN, W., THEIL, A. F., VERMEULEN, W., VAN DER HORST, G. T., MEINECKE, P., KLEIJER, W. J., VIJG, J., JASPERS, N. G. & HOEIJMAKERS, J. H. 2006. A new progeroid syndrome reveals that genotoxic stress suppresses the somatotroph axis. *Nature,* 444**,** 1038-43.

NIK-ZAINAL, S., VAN LOO, P., WEDGE, D. C., ALEXANDROV, L. B., GREENMAN, C. D., LAU, K. W., RAINE, K., JONES, D., MARSHALL, J., RAMAKRISHNA, M., SHLIEN, A., COOKE, S. L., HINTON, J., MENZIES, A., STEBBINGS, L. A., LEROY, C., JIA, M., RANCE, R., MUDIE, L. J., GAMBLE, S. J., STEPHENS, P. J., MCLAREN, S., TARPEY, P. S., PAPAEMMANUIL, E., DAVIES, H. R., VARELA, I., MCBRIDE, D. J., BIGNELL, G. R., LEUNG, K., BUTLER, A. P., TEAGUE, J. W., MARTIN, S., JONSSON, G., MARIANI, O., BOYAULT, S., MIRON, P., FATIMA, A., LANGEROD, A., APARICIO, S. A., TUTT, A., SIEUWERTS, A. M., BORG, A., THOMAS, G., SALOMON, A. V., RICHARDSON, A. L., BORRESEN-DALE, A. L., FUTREAL, P. A., STRATTON, M. R., CAMPBELL, P. J. & BREAST CANCER WORKING GROUP OF THE INTERNATIONAL CANCER GENOME, C. 2012. The life history of 21 breast cancers. *Cell,* 149**,** 994-1007.

NOON, A. T., SHIBATA, A., RIEF, N., LOBRICH, M., STEWART, G. S., JEGGO, P. A. & GOODARZI, A. A. 2010. 53BP1-dependent robust localized KAP-1 phosphorylation is essential for heterochromatic DNA double-strand break repair. *Nat Cell Biol,* 12**,** 177-84.

NOORDERMEER, S. M., ADAM, S., SETIAPUTRA, D., BARAZAS, M., PETTITT, S. J., LING, A. K., OLIVIERI, M., ALVAREZ-QUILON, A., MOATTI, N., ZIMMERMANN, M., ANNUNZIATO, S., KRASTEV, D. B., SONG, F., BRANDSMA, I., FRANKUM, J., BROUGH, R., SHERKER, A., LANDRY, S., SZILARD, R. K., MUNRO, M. M., MCEWAN, A., GOULLET DE RUGY, T., LIN, Z. Y., HART, T., MOFFAT, J., GINGRAS, A. C., MARTIN, A., VAN ATTIKUM, H., JONKERS, J., LORD, C. J., ROTTENBERG, S. & DUROCHER, D. 2018. The shieldin complex mediates 53BP1-dependent DNA repair. *Nature,* 560**,** 117-121.

NOWSHEEN, S., AZIZ, K., AZIZ, A., DENG, M., QIN, B., LUO, K., JEGANATHAN, K. B., ZHANG, H., LIU, T., YU, J., DENG, Y., YUAN, J., DING, W., VAN DEURSEN, J. M. & LOU, Z. 2018.

L3MBTL2 orchestrates ubiquitin signalling by dictating the sequential recruitment of RNF8 and RNF168 after DNA damage. *Nat Cell Biol,* 20**,** 455-464.

O'CONNOR, M. J. 2015. Targeting the DNA Damage Response in Cancer. *Mol Cell,* 60**,** 547-60.

OCHI, T., BLACKFORD, A. N., COATES, J., JHUJH, S., MEHMOOD, S., TAMURA, N., TRAVERS, J., WU, Q., DRAVIAM, V. M., ROBINSON, C. V., BLUNDELL, T. L. & JACKSON, S. P. 2015. DNA repair. PAXX, a paralog of XRCC4 and XLF, interacts with Ku to promote DNA double-strand break repair. *Science,* 347**,** 185-188.

OCHS, F., SOMYAJIT, K., ALTMEYER, M., RASK, M. B., LUKAS, J. & LUKAS, C. 2016. 53BP1 fosters fidelity of homology-directed DNA repair. *Nat Struct Mol Biol,* 23**,** 714-21.

OKSENYCH, V., ALT, F. W., KUMAR, V., SCHWER, B., WESEMANN, D. R., HANSEN, E., PATEL, H., SU, A. & GUO, C. 2012. Functional redundancy between repair factor XLF and damage response mediator 53BP1 in V(D)J recombination and DNA repair. *Proc Natl Acad Sci U S A,* 109**,** 2455-60.

ORTHWEIN, A., FRADET-TURCOTTE, A., NOORDERMEER, S. M., CANNY, M. D., BRUN, C. M., STRECKER, J., ESCRIBANO-DIAZ, C. & DUROCHER, D. 2014. Mitosis inhibits DNA double-strand break repair to guard against telomere fusions. *Science,* 344**,** 189-93.

ORTHWEIN, A., NOORDERMEER, S. M., WILSON, M. D., LANDRY, S., ENCHEV, R. I., SHERKER, A., MUNRO, M., PINDER, J., SALSMAN, J., DELLAIRE, G., XIA, B., PETER, M. & DUROCHER, D. 2015. A mechanism for the suppression of homologous recombination in G1 cells. *Nature,* 528**,** 422-6.

PALM, W. & DE LANGE, T. 2008. How shelterin protects mammalian telomeres. *Annu Rev Genet,* 42**,** 301-34.

PANIER, S. & BOULTON, S. J. 2014. Double-strand break repair: 53BP1 comes into focus. *Nat Rev Mol Cell Biol,* 15**,** 7-18.

PANIER, S., ICHIJIMA, Y., FRADET-TURCOTTE, A., LEUNG, C. C., KAUSTOV, L., ARROWSMITH, C. H. & DUROCHER, D. 2012. Tandem protein interaction modules organize the ubiquitin-dependent response to DNA double-strand breaks. *Mol Cell,* 47**,** 383-95.

PATEL, A. G., SARKARIA, J. N. & KAUFMANN, S. H. 2011. Nonhomologous end joining drives poly(ADP-ribose) polymerase (PARP) inhibitor lethality in homologous recombination-deficient cells. *Proc Natl Acad Sci U S A,* 108**,** 3406-11.

PEDERSEN, R. T., KRUSE, T., NILSSON, J., OESTERGAARD, V. H. & LISBY, M. 2015. TopBP1 is required at mitosis to reduce transmission of DNA damage to G1 daughter cells. *J Cell Biol,* 210**,** 565-82.

PELLEGRINO, S., MICHELENA, J., TELONI, F., IMHOF, R. & ALTMEYER, M. 2017. Replication-Coupled Dilution of H4K20me2 Guides 53BP1 to Pre-replicative Chromatin. *Cell Rep,* 19**,** 1819-1831.

PETTITT, S. J., KRASTEV, D. B., BRANDSMA, I., DREAN, A., SONG, F., ALEKSANDROV, R., HARRELL, M. I., MENON, M., BROUGH, R., CAMPBELL, J., FRANKUM, J., RANES, M., PEMBERTON, H. N., RAFIQ, R., FENWICK, K., SWAIN, A., GUETTLER, S., LEE, J. M., SWISHER, E. M., STOYNOV, S., YUSA, K., ASHWORTH, A. & LORD, C. J. 2018. Genome-wide and high-density CRISPR-Cas9 screens identify point mutations in PARP1 causing PARP inhibitor resistance. *Nat Commun,* 9**,** 1849.

POLATO, F., CALLEN, E., WONG, N., FARYABI, R., BUNTING, S., CHEN, H. T., KOZAK, M., KRUHLAK, M. J., RECZEK, C. R., LEE, W. H., LUDWIG, T., BAER, R., FEIGENBAUM, L., JACKSON, S. & NUSSENZWEIG, A. 2014. CtIP-mediated resection is essential for viability and can operate independently of BRCA1. *J Exp Med,* 211**,** 1027-36.

PRYOR, J. M., CONLIN, M. P., CARVAJAL-GARCIA, J., LUEDEMAN, M. E., LUTHMAN, A. J., SMALL, G. W. & RAMSDEN, D. A. 2018. Ribonucleotide incorporation enables repair of chromosome breaks by nonhomologous end joining. *Science,* 361**,** 1126-1129.

PRZETOCKA, S., PORRO, A., BOLCK, H. A., WALKER, C., LEZAJA, A., TRENNER, A., VON AESCH, C., HIMMELS, S. F., D'ANDREA, A. D., CECCALDI, R., ALTMEYER, M. & SARTORI, A. A. 2018. CtIP-Mediated Fork Protection Synergizes with BRCA1 to Suppress Genomic Instability upon DNA Replication Stress. *Mol Cell,* 72**,** 568-582 e6.

QIN, B., YU, J., NOWSHEEN, S., WANG, M., TU, X., LIU, T., LI, H., WANG, L. & LOU, Z. 2019. UFL1 promotes histone H4 ufmylation and ATM activation. *Nat Commun,* 10**,** 1242.

RAY CHAUDHURI, A., CALLEN, E., DING, X., GOGOLA, E., DUARTE, A. A., LEE, J. E., WONG, N., LAFARGA, V., CALVO, J. A., PANZARINO, N. J., JOHN, S., DAY, A., CRESPO, A. V., SHEN, B., STARNES, L. M., DE RUITER, J. R., DANIEL, J. A., KONSTANTINOPOULOS, P. A., CORTEZ, D., CANTOR, S. B., FERNANDEZ-CAPETILLO, O., GE, K., JONKERS, J., ROTTENBERG, S., SHARAN, S. K. & NUSSENZWEIG, A. 2016. Replication fork stability confers chemoresistance in BRCA-deficient cells. *Nature,* 535**,** 382-7.

RAY CHAUDHURI, A., HASHIMOTO, Y., HERRADOR, R., NEELSEN, K. J., FACHINETTI, D., BERMEJO, R., COCITO, A., COSTANZO, V. & LOPES, M. 2012. Topoisomerase I poisoning results in PARP-mediated replication fork reversal. *Nat Struct Mol Biol,* 19**,** 417-23.

RAY CHAUDHURI, A. & NUSSENZWEIG, A. 2017. The multifaceted roles of PARP1 in DNA repair and chromatin remodelling. *Nat Rev Mol Cell Biol,* 18**,** 610-621.

REYNOLDS, J. J., BICKNELL, L. S., CARROLL, P., HIGGS, M. R., SHAHEEN, R., MURRAY, J. E., PAPADOPOULOS, D. K., LEITCH, A., MURINA, O., TARNAUSKAITE, Z., WESSEL, S. R., ZLATANOU, A., VERNET, A., VON KRIEGSHEIM, A., MOTTRAM, R. M., LOGAN, C. V., BYE, H., LI, Y., BREAN, A., MADDIREVULA, S., CHALLIS, R. C., SKOULOUDAKI, K., ALMOISHEER, A., ALSAIF, H. S., AMAR, A., PRESCOTT, N. J., BOBER, M. B., DUKER, A., FAQEIH, E., SEIDAHMED, M. Z., AL TALA, S., ALSWAID, A., AHMED, S., AL-AAMA, J. Y., ALTMULLER, J., AL BALWI, M., BRADY, A. F., CHESSA, L., COX, H., FISCHETTO, R., HELLER, R., HENDERSON, B. D., HOBSON, E., NURNBERG, P., PERCIN, E. F., PERON, A., SPACCINI, L., QUIGLEY, A. J., THAKUR, S., WISE, C. A., YOON, G.,

ALNEMER, M., TOMANCAK, P., YIGIT, G., TAYLOR, A. M., REIJNS, M. A., SIMPSON, M. A., CORTEZ, D., ALKURAYA, F. S., MATHEW, C. G., JACKSON, A. P. & STEWART, G. S. 2017. Mutations in DONSON disrupt replication fork stability and cause microcephalic dwarfism. *Nat Genet,* 49**,** 537-549.

RIEDER, C. L. & COLE, R. W. 1998. Entry into mitosis in vertebrate somatic cells is guarded by a chromosome damage checkpoint that reverses the cell cycle when triggered during early but not late prophase. *J Cell Biol,* 142**,** 1013-22.

ROBERT, I., DANTZER, F. & REINA-SAN-MARTIN, B. 2009. Parp1 facilitates alternative NHEJ, whereas Parp2 suppresses IgH/c-myc translocations during immunoglobulin class switch recombination. *J Exp Med,* 206**,** 1047-56.

ROBSON, M., IM, S. A., SENKUS, E., XU, B., DOMCHEK, S. M., MASUDA, N., DELALOGE, S., LI, W., TUNG, N., ARMSTRONG, A., WU, W., GOESSL, C., RUNSWICK, S. & CONTE, P. 2017. Olaparib for Metastatic Breast Cancer in Patients with a Germline BRCA Mutation. *N Engl J Med,* 377**,** 523-533.

RODRIGUEZ, A. & D'ANDREA, A. 2017. Fanconi anemia pathway. *Curr Biol,* 27**,** R986-R988.

RONDINELLI, B., GOGOLA, E., YUCEL, H., DUARTE, A. A., VAN DE VEN, M., VAN DER SLUIJS, R., KONSTANTINOPOULOS, P. A., JONKERS, J., CECCALDI, R., ROTTENBERG, S. & D'ANDREA, A. D. 2017. EZH2 promotes degradation of stalled replication forks by recruiting MUS81 through histone H3 trimethylation. *Nat Cell Biol,* 19**,** 1371-1378.

SAKAI, W., SWISHER, E. M., KARLAN, B. Y., AGARWAL, M. K., HIGGINS, J., FRIEDMAN, C., VILLEGAS, E., JACQUEMONT, C., FARRUGIA, D. J., COUCH, F. J., URBAN, N. & TANIGUCHI, T. 2008. Secondary mutations as a mechanism of cisplatin resistance in BRCA2-mutated cancers. *Nature,* 451**,** 1116-20.

SARBAJNA, S., DAVIES, D. & WEST, S. C. 2014. Roles of SLX1-SLX4, MUS81-EME1, and GEN1 in avoiding genome instability and mitotic catastrophe. *Genes Dev,* 28**,** 1124-36.

SARBAJNA, S. & WEST, S. C. 2014. Holliday junction processing enzymes as guardians of genome stability. *Trends Biochem Sci,* 39**,** 409-19.

SAREDI, G., HUANG, H., HAMMOND, C. M., ALABERT, C., BEKKER-JENSEN, S., FORNE, I., REVERON-GOMEZ, N., FOSTER, B. M., MLEJNKOVA, L., BARTKE, T., CEJKA, P., MAILAND, N., IMHOF, A., PATEL, D. J. & GROTH, A. 2016. H4K20me0 marks post-replicative chromatin and recruits the TONSL-MMS22L DNA repair complex. *Nature,* 534**,** 714-718.

SARTORI, A. A., LUKAS, C., COATES, J., MISTRIK, M., FU, S., BARTEK, J., BAER, R., LUKAS, J. & JACKSON, S. P. 2007. Human CtIP promotes DNA end resection. *Nature,* 450**,** 509-14.

SCHLACHER, K., CHRIST, N., SIAUD, N., EGASHIRA, A., WU, H. & JASIN, M. 2011. Double-strand break repair-independent role for BRCA2 in blocking stalled replication fork degradation by MRE11. *Cell,* 145**,** 529-42.

SCHLACHER, K., WU, H. & JASIN, M. 2012. A distinct replication fork protection pathway connects Fanconi anemia tumor suppressors to RAD51-BRCA1/2. *Cancer Cell,* 22**,** 106-16.

SCHMIDT, C. K., GALANTY, Y., SCZANIECKA-CLIFT, M., COATES, J., JHUJH, S., DEMIR, M., CORNWELL, M., BELI, P. & JACKSON, S. P. 2015. Systematic E2 screening reveals a UBE2D-RNF138-CtIP axis promoting DNA repair. *Nat Cell Biol,* 17**,** 1458-1470.

SCHMIDT, L., WIEDNER, M., VELIMEZI, G., PROCHAZKOVA, J., OWUSU, M., BAUER, S. & LOIZOU, J. I. 2014. ATMIN is required for the ATM-mediated signaling and recruitment of 53BP1 to DNA damage sites upon replication stress. *DNA Repair (Amst),* 24**,** 122-30.

SCHUBERT, L., HO, T., HOFFMANN, S., HAAHR, P., GUERILLON, C. & MAILAND, N. 2017. RADX interacts with single-stranded DNA to promote replication fork stability. *EMBO Rep,* 18**,** 1991-2003.

SCHWERTMAN, P., BEKKER-JENSEN, S. & MAILAND, N. 2016. Regulation of DNA double-strand break repair by ubiquitin and ubiquitin-like modifiers. *Nat Rev Mol Cell Biol,* 17**,** 379-94.

SETIAPUTRA, D. & DUROCHER, D. 2019. Shieldin - the protector of DNA ends. *EMBO Rep,* 20.

SIMONETTA, M., DE KRIJGER, I., SERRAT, J., MOATTI, N., FORTUNATO, D., HOEKMAN, L., BLEIJERVELD, O. B., ALTELAAR, A. F. M. & JACOBS, J. J. L. 2018. H4K20me2 distinguishes pre-replicative from post-replicative chromatin to appropriately direct DNA repair pathway choice by 53BP1-RIF1-MAD2L2. *Cell Cycle,* 17**,** 124-136.

SPIES, J., LUKAS, C., SOMYAJIT, K., RASK, M. B., LUKAS, J. & NEELSEN, K. J. 2019. 53BP1 nuclear bodies enforce replication timing at under-replicated DNA to limit heritable DNA damage. *Nat Cell Biol,* 21**,** 487-497.

SUN, J., YU, E. Y., YANG, Y., CONFER, L. A., SUN, S. H., WAN, K., LUE, N. F. & LEI, M. 2009. Stn1-Ten1 is an Rpa2-Rpa3-like complex at telomeres. *Genes Dev,* 23**,** 2900-14.

TANG, J., CHO, N. W., CUI, G., MANION, E. M., SHANBHAG, N. M., BOTUYAN, M. V., MER, G. & GREENBERG, R. A. 2013. Acetylation limits 53BP1 association with damaged chromatin to promote homologous recombination. *Nat Struct Mol Biol,* 20**,** 317-25.

THORSLUND, T., RIPPLINGER, A., HOFFMANN, S., WILD, T., UCKELMANN, M., VILLUMSEN, B., NARITA, T., SIXMA, T. K., CHOUDHARY, C., BEKKER-JENSEN, S. & MAILAND, N. 2015. Histone H1 couples initiation and amplification of ubiquitin signalling after DNA damage. *Nature,* 527**,** 389-93.

TKAC, J., XU, G., ADHIKARY, H., YOUNG, J. T. F., GALLO, D., ESCRIBANO-DIAZ, C., KRIETSCH, J., ORTHWEIN, A., MUNRO, M., SOL, W., AL-HAKIM, A., LIN, Z. Y., JONKERS, J., BORST, P., BROWN, G. W., GINGRAS, A. C., ROTTENBERG, S., MASSON, J. Y. & DUROCHER, D. 2016. HELB Is a Feedback Inhibitor of DNA End Resection. *Mol Cell,* 61**,** 405-418.

TOLEDO, L., NEELSEN, K. J. & LUKAS, J. 2017. Replication Catastrophe: When a Checkpoint Fails because of Exhaustion. *Mol Cell,* 66**,** 735-749.

TOLEDO, L. I., ALTMEYER, M., RASK, M. B., LUKAS, C., LARSEN, D. H., POVLSEN, L. K., BEKKER-JENSEN, S., MAILAND, N., BARTEK, J. & LUKAS, J. 2013. ATR prohibits replication catastrophe by preventing global exhaustion of RPA. *Cell,* 155**,** 1088-103.

TOMIDA, J., TAKATA, K. I., BHETAWAL, S., PERSON, M. D., CHAO, H. P., TANG, D. G. & WOOD, R. D. 2018. FAM35A associates with REV7 and modulates DNA damage responses of normal and BRCA1-defective cells. *EMBO J,* 37.

WANG, X., TAKENAKA, K. & TAKEDA, S. 2010. PTIP promotes DNA double-strand break repair through homologous recombination. *Genes Cells,* 15**,** 243-54.

WARD, I. M., REINA-SAN-MARTIN, B., OLARU, A., MINN, K., TAMADA, K., LAU, J. S., CASCALHO, M., CHEN, L., NUSSENZWEIG, A., LIVAK, F., NUSSENZWEIG, M. C. & CHEN, J. 2004. 53BP1 is required for class switch recombination. *J Cell Biol,* 165**,** 459-64.

WILLIAMS, R. S., WILLIAMS, J. S. & TAINER, J. A. 2007. Mre11-Rad50-Nbs1 is a keystone complex connecting DNA repair machinery, double-strand break signaling, and the chromatin template. *Biochem Cell Biol,* 85**,** 509-20.

WILLIS, N. A., FROCK, R. L., MENGHI, F., DUFFEY, E. E., PANDAY, A., CAMACHO, V., HASTY, E. P., LIU, E. T., ALT, F. W. & SCULLY, R. 2017. Mechanism of tandem duplication formation in BRCA1-mutant cells. *Nature,* 551**,** 590-595.

WOOD, R. D. & DOUBLIE, S. 2016. DNA polymerase theta (POLQ), double-strand break repair, and cancer. *DNA Repair (Amst),* 44**,** 22-32.

XU, D., MUNIANDY, P., LEO, E., YIN, J., THANGAVEL, S., SHEN, X., II, M., AGAMA, K., GUO, R., FOX, D., 3RD, MEETEI, A. R., WILSON, L., NGUYEN, H., WENG, N. P., BRILL, S. J., LI, L., VINDIGNI, A., POMMIER, Y., SEIDMAN, M. & WANG, W. 2010. Rif1 provides a new DNA-binding interface for the Bloom syndrome complex to maintain normal replication. *EMBO J,* 29**,** 3140-55.

XU, G., CHAPMAN, J. R., BRANDSMA, I., YUAN, J., MISTRIK, M., BOUWMAN, P., BARTKOVA, J., GOGOLA, E., WARMERDAM, D., BARAZAS, M., JASPERS, J. E., WATANABE, K., PIETERSE, M., KERSBERGEN, A., SOL, W., CELIE, P. H. N., SCHOUTEN, P. C., VAN DEN BROEK, B., SALMAN, A., NIEUWLAND, M., DE RINK, I., DE RONDE, J., JALINK, K., BOULTON, S. J., CHEN, J., VAN GENT, D. C., BARTEK, J., JONKERS, J., BORST, P. & ROTTENBERG, S. 2015. REV7 counteracts DNA double-strand break resection and affects PARP inhibition. *Nature,* 521**,** 541-544.

YANG, G., LIU, C., CHEN, S. H., KASSAB, M. A., HOFF, J. D., WALTER, N. G. & YU, X. 2018. Super-resolution imaging identifies PARP1 and the Ku complex acting as DNA double-strand break sensors. *Nucleic Acids Res,* 46**,** 3446-3457.

YAZINSKI, S. A., COMAILLS, V., BUISSON, R., GENOIS, M. M., NGUYEN, H. D., HO, C. K., TODOROVA KWAN, T., MORRIS, R., LAUFFER, S., NUSSENZWEIG, A., RAMASWAMY, S., BENES, C. H., HABER, D. A., MAHESWARAN, S., BIRRER, M. J. & ZOU, L. 2017. ATR inhibition disrupts rewired homologous recombination and fork

protection pathways in PARP inhibitor-resistant BRCA-deficient cancer cells. *Genes Dev,* 31**,** 318-332.

YIN, Y., SEIFERT, A., CHUA, J. S., MAURE, J. F., GOLEBIOWSKI, F. & HAY, R. T. 2012. SUMO-targeted ubiquitin E3 ligase RNF4 is required for the response of human cells to DNA damage. *Genes Dev,* 26**,** 1196-208.

YING, S., MINOCHERHOMJI, S., CHAN, K. L., PALMAI-PALLAG, T., CHU, W. K., WASS, T., MANKOURI, H. W., LIU, Y. & HICKSON, I. D. 2013. MUS81 promotes common fragile site expression. *Nat Cell Biol,* 15**,** 1001-7.

YOUSEFZADEH, M. J., WYATT, D. W., TAKATA, K., MU, Y., HENSLEY, S. C., TOMIDA, J., BYLUND, G. O., DOUBLIE, S., JOHANSSON, E., RAMSDEN, D. A., MCBRIDE, K. M. & WOOD, R. D. 2014. Mechanism of suppression of chromosomal instability by DNA polymerase POLQ. *PLoS Genet,* 10**,** e1004654.

YU, A. M. & MCVEY, M. 2010. Synthesis-dependent microhomology-mediated end joining accounts for multiple types of repair junctions. *Nucleic Acids Res,* 38**,** 5706-17.

ZELLWEGER, R., DALCHER, D., MUTREJA, K., BERTI, M., SCHMID, J. A., HERRADOR, R., VINDIGNI, A. & LOPES, M. 2015. Rad51-mediated replication fork reversal is a global response to genotoxic treatments in human cells. *J Cell Biol,* 208**,** 563-79.

ZHANG, H., LIU, H., CHEN, Y., YANG, X., WANG, P., LIU, T., DENG, M., QIN, B., CORREIA, C., LEE, S., KIM, J., SPARKS, M., NAIR, A. A., EVANS, D. L., KALARI, K. R., ZHANG, P., WANG, L., YOU, Z., KAUFMANN, S. H., LOU, Z. & PEI, H. 2016. A cell cycle-dependent BRCA1-UHRF1 cascade regulates DNA double-strand break repair pathway choice. *Nat Commun,* 7**,** 10201.

ZHAO, W., STEINFELD, J. B., LIANG, F., CHEN, X., MARANON, D. G., JIAN MA, C., KWON, Y., RAO, T., WANG, W., SHENG, C., SONG, X., DENG, Y., JIMENEZ-SAINZ, J., LU, L., JENSEN, R. B., XIONG, Y., KUPFER, G. M., WIESE, C., GREENE, E. C. & SUNG, P. 2017. BRCA1-BARD1 promotes RAD51-mediated homologous DNA pairing. *Nature,* 550**,** 360-365.

ZHOU, Y., CARON, P., LEGUBE, G. & PAULL, T. T. 2014. Quantitation of DNA double-strand break resection intermediates in human cells. *Nucleic Acids Res,* 42**,** e19.

ZIMMER, J., TACCONI, E. M. C., FOLIO, C., BADIE, S., PORRU, M., KLARE, K., TUMIATI, M., MARKKANEN, E., HALDER, S., RYAN, A., JACKSON, S. P., RAMADAN, K., KUZNETSOV, S. G., BIROCCIO, A., SALE, J. E. & TARSOUNAS, M. 2016. Targeting BRCA1 and BRCA2 Deficiencies with G-Quadruplex-Interacting Compounds. *Mol Cell,* 61**,** 449-460.

ZIMMERMANN, M. & DE LANGE, T. 2014. 53BP1: pro choice in DNA repair. *Trends Cell Biol,* 24**,** 108-17.

ZIMMERMANN, M., LOTTERSBERGER, F., BUONOMO, S. B., SFEIR, A. & DE LANGE, T. 2013. 53BP1 regulates DSB repair using Rif1 to control 5' end resection. *Science,* 339**,** 700-4.

ZIMMERMANN, M., MURINA, O., REIJNS, M. A. M., AGATHANGGELOU, A., CHALLIS, R., TARNAUSKAITE, Z., MUIR, M., FLUTEAU, A., AREGGER, M., MCEWAN, A., YUAN, W., CLARKE, M., LAMBROS, M. B., PANEESHA, S., MOSS, P., CHANDRASHEKHAR, M., ANGERS, S., MOFFAT, J., BRUNTON, V. G., HART, T., DE BONO, J., STANKOVIC, T., JACKSON, A. P. & DUROCHER, D. 2018. CRISPR screens identify genomic ribonucleotides as a source of PARP-trapping lesions. *Nature,* 559**,** 285-289.

ZIRKLE, R. E. & BLOOM, W. 1953. Irradiation of parts of individual cells. *Science,* 117**,** 487-93.

ZONG, D., ADAM, S., WANG, Y., SASANUMA, H., CALLEN, E., MURGA, M., DAY, A., KRUHLAK, M. J., WONG, N., MUNRO, M., RAY CHAUDHURI, A., KARIM, B., XIA, B., TAKEDA, S., JOHNSON, N., DUROCHER, D. & NUSSENZWEIG, A. 2019. BRCA1 Haploinsufficiency Is Masked by RNF168-Mediated Chromatin Ubiquitylation. *Mol Cell,* 73**,** 1267-1281 e7.